



**Chemical Constituents from the Roots and Fruits of *Diospyros wallichii*
and the Roots and Twigs of *Premna obtusifolia*
and Their Biological Activities**

Abdulwahab Salae

**A Thesis Submitted in Fulfillment of the Requirements for the Degree of
Doctor of Philosophy in Organic Chemistry
Prince of Songkla University
2012
Copyright of Prince of Songkla University**

T

เลขที่	QK495.E25 A22 2012
Bib Key	869860
	3 31.0. 2556

Thesis Title Chemical Constituents from the Roots and Fruits of *Diospyros wallichii* and the Roots and Twigs of *Premna obtusifolia* and Their Biological Activities

Author Mr. Abdulwahab Salae

Major Program Organic Chemistry

Major Advisor :

C. Karalai

 (Assoc. Prof. Dr. Chatchanok Karalai)

Co-advisor :

C. Ponglimanont

 (Assoc. Prof. Chanita Ponglimanont)

Examining Committee :

K. Chantapromma
Chairperson
 (Assoc. Prof. Dr. Kan Chantapromma)

C. Karalai
Committee
 (Assoc. Prof. Dr. Chatchanok Karalai)

C. Ponglimanont
Committee
 (Assoc. Prof. Chanita Ponglimanont)

S. Tewtrakul
Committee
 (Assoc. Prof. Dr. Supinya Tewtrakul)

The Graduate School, Prince of Songkla University, has approved this thesis as fulfillment of the requirements for the Doctor of Philosophy in Organic Chemistry

A. Phongdara

 (Prof. Dr. Amornrat Phongdara)
 Dean of Graduate School

This is to certify that the work here submitted is the result of the candidate's own investigations. Due acknowledgement has been made of any assistance received.

C. Karalai

Signature

(Assoc. Prof. Dr. Chatchanok Karalai)

Major Advisor

Abdulwahab Salae

Signature

(Mr. Abdulwahab Salae)

Candidate

I hereby certify that this work has not already been accepted in substance for any degree, and is not being concurrently submitted in candidature for any degree.

Abdulwahab Salae. Signature

(Mr. Abdulwahab Salae)

Candidate

ชื่อวิทยานิพนธ์	องค์ประกอบทางเคมีจากราก และ ผล ต้นตำตะโก และ ราก และ กิ่ง ต้นอัคคีทวารทะเล และ ฤทธิ์ทางชีวภาพ
ผู้เขียน	นายอับดุลวาฮาบ สาแล๊ะ
สาขาวิชา	เคมีอินทรีย์
ปีการศึกษา	2555

บทคัดย่อ

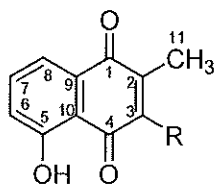
ตอนที่ 1 องค์ประกอบทางเคมีจากรากและผลต้นตำตะโก

การศึกษาองค์ประกอบทางเคมีจากส่วนสกัด เฮกเซน และไดคลอโรมีเทน จาก ส่วนราก และ ผล ของต้นตำตะโก สามารถแยกสารใหม่ได้ 3 สาร ซึ่งประกอบด้วยสารประเภท อนุพันธ์แนฟโทควิโนน 1 สาร (DW9), อนุพันธ์แนฟทาลีน 2 สาร (DW11 และ DW12) และ ยังสามารถแยกสารประกอบที่มีการรายงานแล้ว 18 สาร คือ สารประเภทอนุพันธ์แนฟโทควิโนน 9 สาร (DW1-DW7, DW8 และ DW10), อนุพันธ์คูมาริน 1 สาร (DW13), ไตรเทอร์พีนอยด์ 6 สาร (DW14-DW19) และ สารผสมสเตอรอยด์ (DW20 และ DW21) โครงสร้าง ของสารประกอบเหล่านี้สามารถวิเคราะห์โดยใช้ข้อมูลทางสเปกโทรสโกปี และเปรียบเทียบกับสาร ที่มีรายงานวิจัยแล้ว นอกจากนี้ยังมีการทดสอบฤทธิ์ต้านเชื้อแบคทีเรีย และ ต้านมะเร็ง พบว่า สารประกอบ DW8 และ DW9 มีฤทธิ์ต้านเซลล์มะเร็งเต้านม ที่ค่า $IC_{50} = 0.06$ และ $0.09 \mu M$ ตามลำดับ

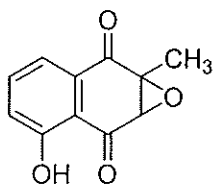
ตอนที่ 2 องค์ประกอบทางเคมีจากรากและกิ่งต้นอัคคีทวารทะเล

การศึกษาองค์ประกอบทางเคมีจากส่วนสกัด เฮกเซน และไดคลอโรมีเทน จาก ส่วน ราก และ กิ่ง ต้นอัคคีทวารทะเล สามารถแยกสารใหม่ได้ 11 สาร ประกอบด้วย สารประกอบ ไอโซพิมาเรนไดเทอร์พีนอยด์ 2 สาร (PO1 และ PO2), โรเซนไดเทอร์พีนอยด์ 1 สาร (PO3), อะบีเทนไดเทอร์พีนอยด์ 4 สาร (PO4, PO5, PO18 และ PO19), ไอทีเซนได เทอร์พีนอยด์ 4 สาร (PO23-PO26) และยังสามารถแยกสารประกอบที่มีการรายงานแล้ว 18 สาร (PO6, PO7, PO8-PO15, PO16, PO17, PO20-PO22 และ PO27-PO29) โครงสร้างของสารประกอบเหล่านี้สามารถวิเคราะห์โดยใช้ข้อมูลทางสเปกโทรสโกปี และเปรียบเทียบกับสารที่มีรายงานวิจัยแล้ว และสำหรับสารประกอบ PO10, PO11, PO13, PO20, PO22 และ PO25 ใช้ข้อมูลทางเอกซ์เรย์ประกอบการพิสูจน์โครงสร้างอีกด้วย

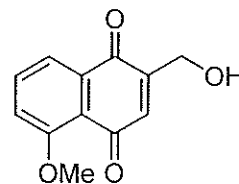
นอกจากนี้ยังมีการทดสอบฤทธิ์ต้านเชื้อแบคทีเรีย และ ต้านการอักเสบ พบว่า สารประกอบ PO24 มีฤทธิ์ต้านการอักเสบ ที่ค่า $IC_{50} = 1.7 \mu M$.



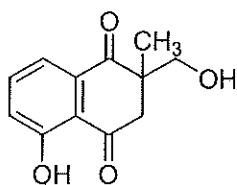
R= H, **DW1**: Plumbagin
R= OH, **DW2**: Droserone



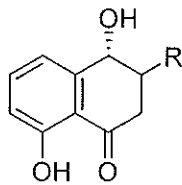
DW3: 2,3-Epoxyplumbagin



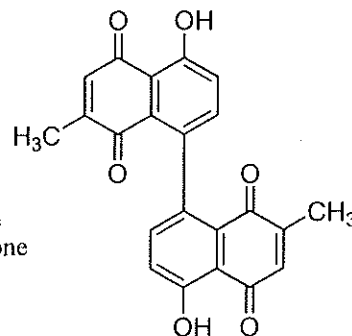
DW4: 2-Hydroxymethyl-5-methoxy-1,4-naphthoquinone



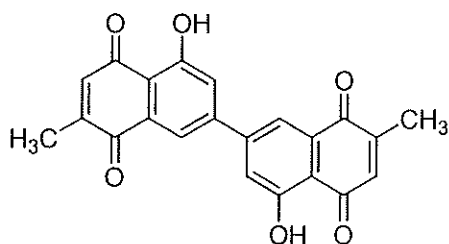
DW5: Diomuscinone



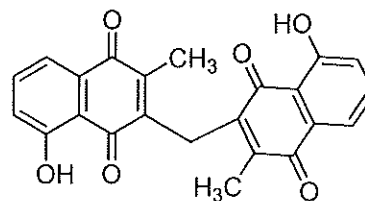
R= ---CH_3 , **DW6**: *iso*-Shinanolone
R= ---CH_3 , **DW7**: *epi*-Isoshinanolone



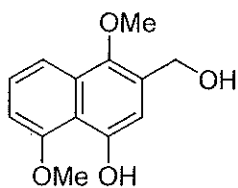
DW8: Maritinone



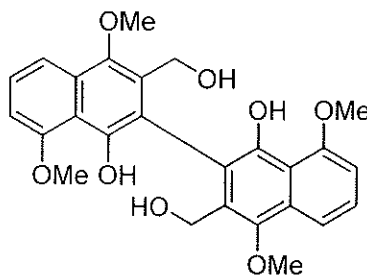
DW9: 5,5'-Dihydroxy-2,2'-dimethyl-7,7'-binaphthalen-1,1',4,4'-tetraone



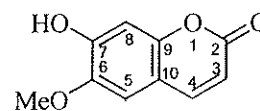
DW10: Methylene-3,3'-biplumbagin



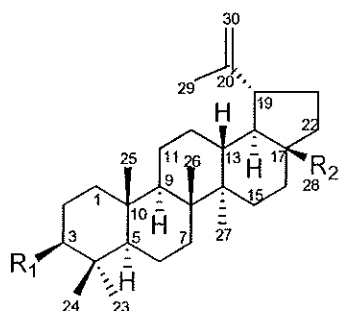
DW11: 2-Hydroxy-methyl-1,5-dimethoxynaphthalen-4-ol



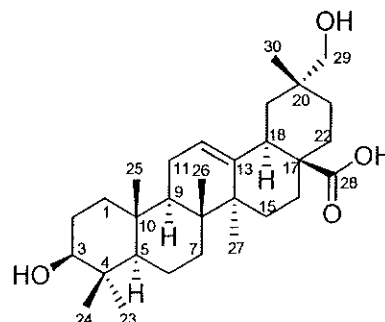
DW12: 2,2'-bis-Hydroxymethyl-1,1',5,5'-tetramethoxy-3,3'-binaphthalen-4,4'-diol



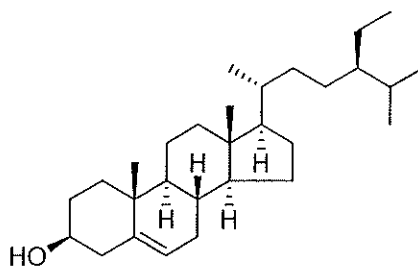
DW13: Scopoletin



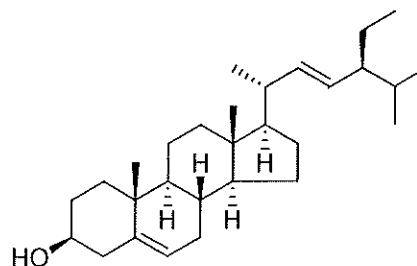
- $R_1 = \text{OH}$, $R_2 = \text{CH}_3$, **DW14**: Lupeol
 $R_1 = =\text{O}$, $R_2 = \text{CH}_3$, **DW15**: Lupenone
 $R_1 = \text{OH}$, $R_2 = \text{CH}_2\text{OH}$, **DW16**: Betulin
 $R_1 = \text{OH}$, $R_2 = \text{CHO}$, **DW17**: Betulinaldehyde
 $R_1 = \text{OH}$, $R_2 = \text{CO}_2\text{H}$, **DW18**: Betulinic acid



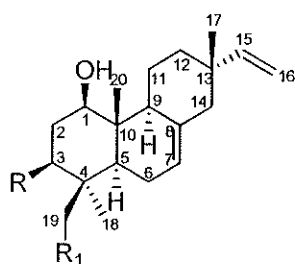
DW19: 3,29-Dihydroxyolean-12-en-28-oic acid



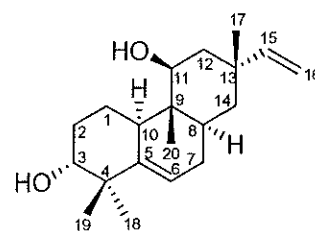
DW20: β -Sitosterol



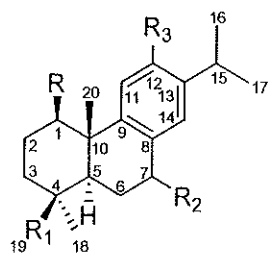
DW21: Stigmasterol



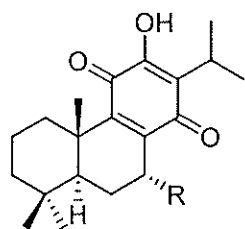
- $R = \text{OH}$, $R_1 = \text{H}$, **PO1**: Isopimara-7,15-dien-1 β ,3 β -diol
 $R = \text{H}$, $R_1 = \text{OH}$, **PO2**: Isopimara-7,15-dien-1 β ,19-diol



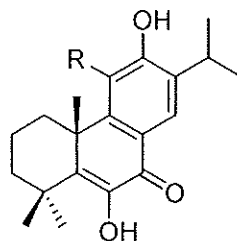
PO3: 13-*epi*-5,15-Rosadien-3 α ,11 β -diol



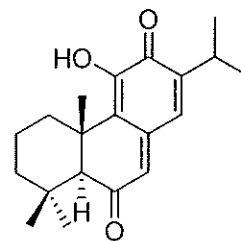
- $R = \text{OH}$, $R_1, R_2, R_3 = \text{H}$, **PO4**: Abietatrien-1 β -ol
 $R, R_3 = \text{OH}$, $R_1, R_2 = \text{H}$, **PO5**: Abietatrien-1 β ,12-diol
 $R, R_1, R_2 = \text{H}$, $R_3 = \text{OH}$, **PO6**: Ferruginol
 $R, R_1, R_2 = \text{H}$, $R_3 = \text{OCH}_3$, **PO7**: *O*-Methyl ferruginol
 $R, R_2 = \text{H}$, $R_1 = \text{CO}_2\text{H}$, $R_3 = \text{OH}$, **PO8**: Lambertic acid
 $R, R_1, R_3 = \text{H}$, $R_2 = =\text{O}$, **PO9**: Sugiol



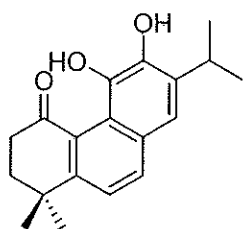
R = H, **PO10**: Royleanone
R = OH, **PO11**: Horminone



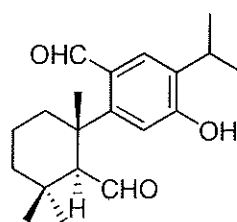
R = H, **PO12**: Montbretrol
R = OH, **PO13**: 14-Deoxycoleon



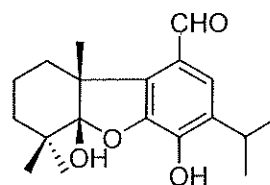
PO14: Taxodion



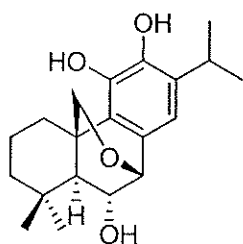
PO15: Arucadiol



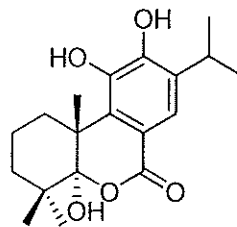
PO16: 12-Hydroxy-6,7-seco
abieta-8,11,13-triene-6,7-dial



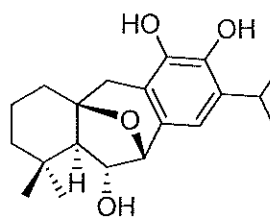
PO17: Salvicanaraldehyde



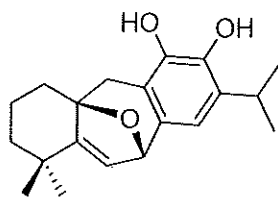
PO18: 6 α ,11,12-Trihydroxy-7 β ,
20-epoxy-8,11,13-abietatriene



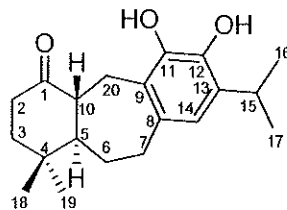
PO19: 5 α ,11,12-Trihydroxy-6-
oxa-abieta-8,11,13-trien-7-one



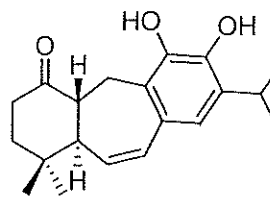
PO20: 5,6-Dihydro-6 α -
hydroxysalviasperanol



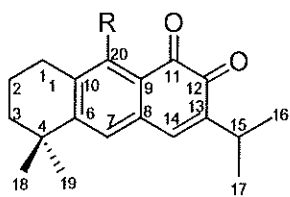
PO21: Salviasperanol



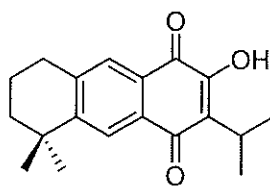
PO22: 11,12-Dihydroxy-8,
11,13-icetexatrien-1-one



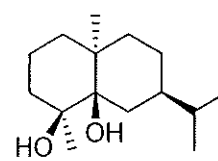
PO23: 11,12-Dihydroxy-6,8,
11,13-icetexatetraen-1-one



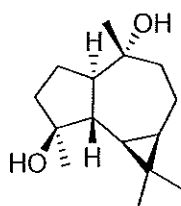
R = OH, **PO24**: Obtusinone A
R = H, **PO25**: Obtusinone B



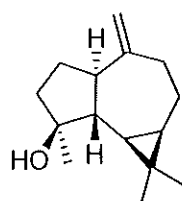
PO26: Obtusinone C



PO27: 4 β ,5 β -Dihydroxy-
10-*epi*-eudesmane



PO28: 4 β ,10 β -Dihydroxy
aromadendrane



PO29: Spathulenol

Thesis Title	Chemical Constituents from the roots and fruits of <i>Diospyros wallichii</i> and the roots and twigs of <i>Premna obtusifolia</i> and their Biological activities.
Author	Mr. Abdulwahab Salae
Major Program	Organic Chemistry
Academic Year	2012

ABSTRACT

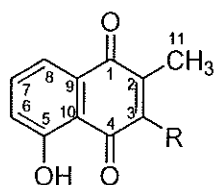
Part I Chemical constituents from the roots and fruits of Diospyros wallichii

Phytochemical investigation of the hexane and CH₂Cl₂ extracts of the roots and fruits of *D. wallichii*, afforded three new compounds as one binaphthoquinone (**DW9**) and two naphthalene derivatives (**DW11** and **DW12**), together with eighteen known compounds including nine naphthoquinones (**DW1-DW7**, **DW8** and **DW10**), one coumarin (**DW13**), six triterpenoids (**DW14-DW19**) and a mixture of steroids (**DW20-DW21**). Their structures were elucidated by spectroscopic methods and comparison with those reported in the literature. The antibacterial and cytotoxic activities of the isolates were also evaluated. Compound **DW8** and **DW9** showed significant cytotoxic activity against human cancer cell line MCF-7 with IC₅₀ values of 0.06 and 0.09 μM, respectively.

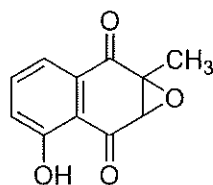
Part II Chemical constituents from the roots and twigs of Premna obtusifolia

Phytochemical investigation of the hexane and CH₂Cl₂ extracts of the roots and twigs of *P. obtusifolia* led to the isolation and characterization of eleven new compounds as two isopimarane diterpenoids (**PO1** and **PO2**), one rosane diterpenoid (**PO3**), four abietane diterpenoids (**PO4**, **PO5**, **PO18** and **PO19**), four icetexane diterpenoids (**PO23-PO26**), along with eighteen known compounds (**PO6**, **PO7**, **PO8-PO15**, **PO16**, **PO17**, **PO20- PO22** and **PO27- PO29**). Their structures were elucidated by spectroscopic methods and comparison with those reported in the literature. The structures of **PO10**, **PO11**, **PO13**, **PO20**, **PO22** and **PO25** were additionally confirmed by X-ray diffraction analysis. The antibacterial and anti-

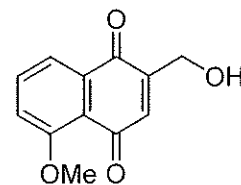
inflammatory activities of the isolates were also evaluated. Compound **PO24** exhibited potential anti-inflammatory activity with the IC_{50} value of 1.7 μ M.



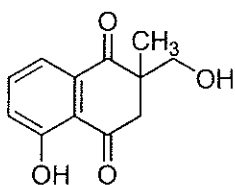
R= H, **DW1**: Plumbagin
R= OH, **DW2**: Droserone



DW3: 2,3-Epoxyplumbagin



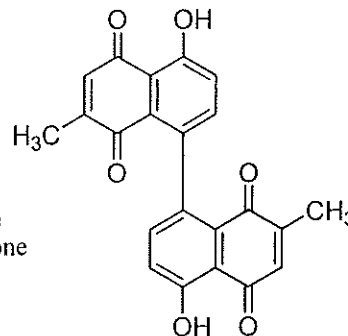
DW4: 2-Hydroxymethyl-5-methoxy-1,4-naphthoquinone



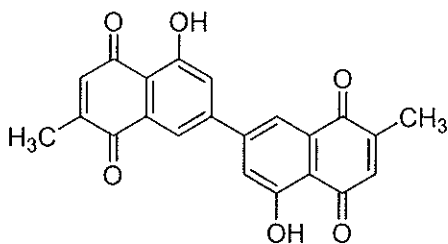
DW5: Diomuscinone



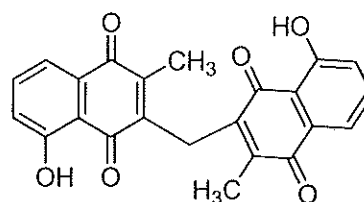
R= ---CH_3 , **DW6**: *iso*-Shinanolone
R= ---CH_3 , **DW7**: *epi*-Isoshinanolone



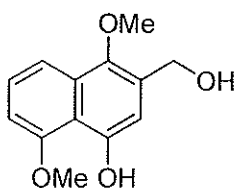
DW8: Maritinone



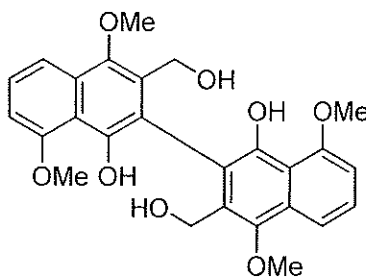
DW9: 5,5'-Dihydroxy-2,2'-dimethyl-7,7'-binaphthalen-1,1',4,4'-tetraone



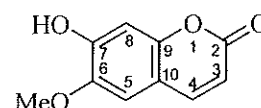
DW10: Methylene-3,3'-biplumbagin



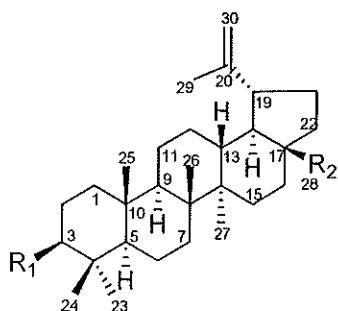
DW11: 2-Hydroxy-methyl-1,5-dimethoxynaphthalen-4-ol



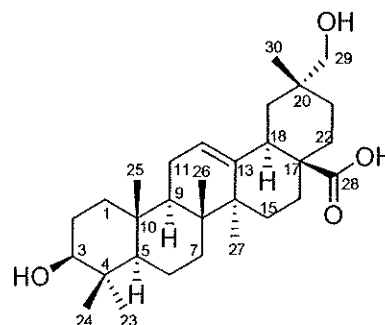
DW12: 2,2'-bis-Hydroxymethyl-1,1',5,5'-tetramethoxy-3,3'-binaphthalen-4,4'-diol



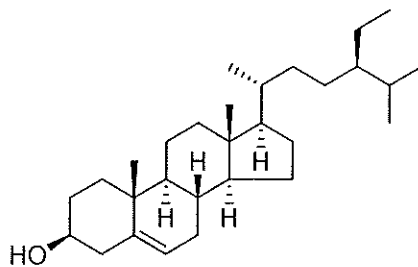
DW13: Scopoletin



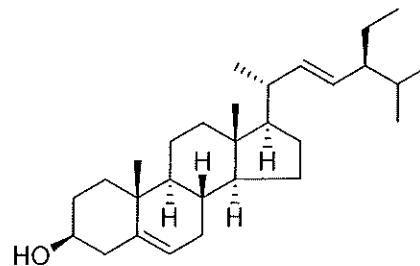
- $R_1 = \text{OH}$, $R_2 = \text{CH}_3$, **DW14**: Lupeol
 $R_1 = =\text{O}$, $R_2 = \text{CH}_3$, **DW15**: Lupenone
 $R_1 = \text{OH}$, $R_2 = \text{CH}_2\text{OH}$, **DW16**: Betulin
 $R_1 = \text{OH}$, $R_2 = \text{CHO}$, **DW17**: Betulinaldehyde
 $R_1 = \text{OH}$, $R_2 = \text{CO}_2\text{H}$, **DW18**: Betulinic acid



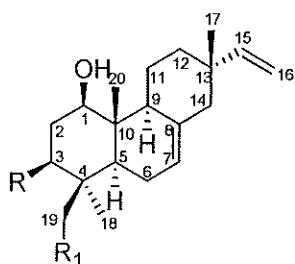
DW19: 3,29-Dihydroxyolean-12-en-28-oic acid



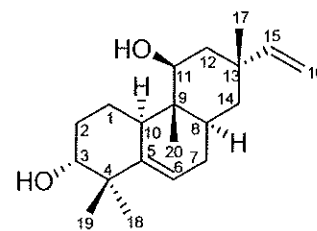
DW20: β -Sitosterol



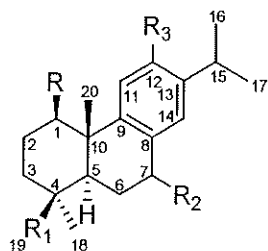
DW21: Stigmasterol



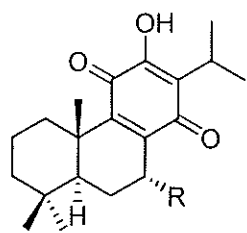
- $R = \text{OH}$, $R_1 = \text{H}$, **PO1**: Isopimara-7,15-dien-1 β ,3 β -diol
 $R = \text{H}$, $R_1 = \text{OH}$, **PO2**: Isopimara-7,15-dien-1 β ,19-diol



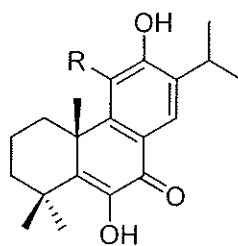
PO3: 13-*epi*-5,15-Rosadien-3 α ,11 β -diol



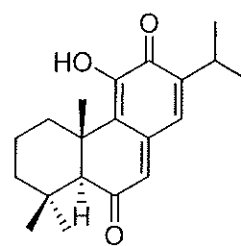
- $R = \text{OH}$, $R_1, R_2, R_3 = \text{H}$, **PO4**: Abietatrien-1 β -ol
 $R, R_3 = \text{OH}$, $R_1, R_2 = \text{H}$, **PO5**: Abietatrien-1 β ,12-diol
 $R, R_1, R_2 = \text{H}$, $R_3 = \text{OH}$, **PO6**: Ferruginol
 $R, R_1, R_2 = \text{H}$, $R_3 = \text{OCH}_3$, **PO7**: *O*-Methyl ferruginol
 $R, R_2 = \text{H}$, $R_1 = \text{CO}_2\text{H}$, $R_3 = \text{OH}$, **PO8**: Lambertic acid
 $R, R_1, R_3 = \text{H}$, $R_2 = =\text{O}$, **PO9**: Sugiol



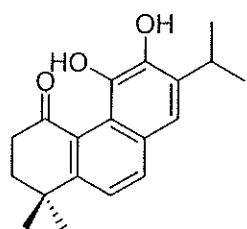
R = H, **PO10**: Royleanone
R = OH, **PO11**: Horminone



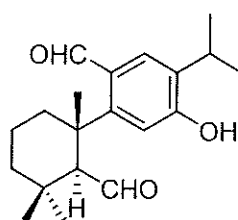
R = H, **PO12**: Montbretrol
R = OH, **PO13**: 14-Deoxycoleon



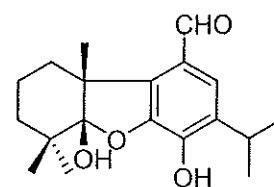
PO14: Taxodion



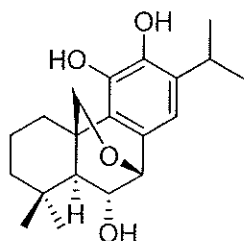
PO15: Arucadiol



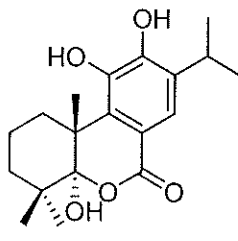
PO16: 12-Hydroxy-6,7-seco-
abieta-8,11,13-triene-6,7-dial



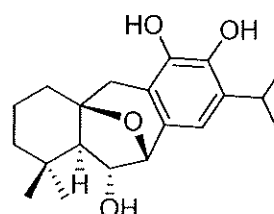
PO17: Salvicanaraldehyde



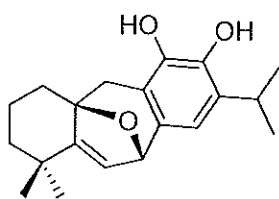
PO18: 6 α ,11,12-Trihydroxy-7 β ,
20-epoxy-8,11,13-abietatriene



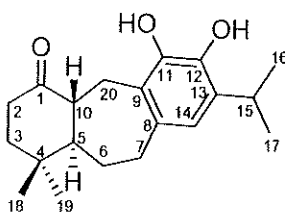
PO19: 5 α ,11,12-Trihydroxy-6-
oxa-abieta-8,11,13-trien-7-one



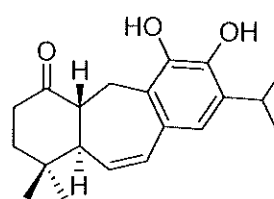
PO20: 5,6-Dihydro-6 α -
hydroxysalviasperanol



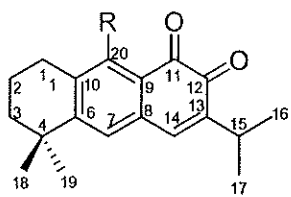
PO21: Salviasperanol



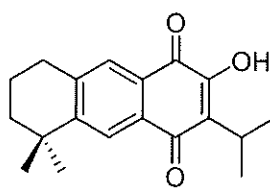
PO22: 11,12-Dihydroxy-8,
11,13-icetaxatrien-1-one



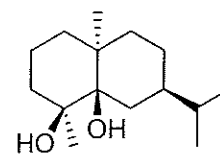
PO23: 11,12-Dihydroxy-6,8,
11,13-icetexatetraen-1-one



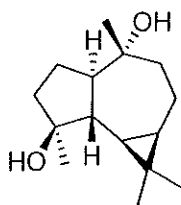
R = OH, **PO24**: Obtusinone A
R = H, **PO25**: Obtusinone B



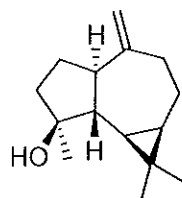
PO26: Obtusinone C



PO27: 4 β ,5 β -Dihydroxy-
10-*epi*-eudesmane



PO28: 4 β ,10 β -Dihydroxy
aromadendrane



PO29: Spathulenol

ACKNOWLEDGEMENT

I wish to express my sincere thanks to Associate Professor Dr. Chatchanok Karalai, my major advisor for his constant guidance, useful suggestions, appreciation, sincere advice and kindness. This was a great motivator for me and will remain to be deep-rooted in my heart.

My sincere thanks are expressed to Associate Professor Chanita Ponglimanont my co-advisor for her kindness and valuable advices and also to Associate Professor Dr. Suchada Chantrapromma for her kindness, valuable advices and structure determination by single X-ray diffraction. I am very thankful to Associate Professor Dr. Uma Prawat and Miss Nareerat Thongtip, School of Science, Phuket Rajabhat University for their valuable advices and for recording NMR spectral data. Special thanks are addressed to Professor Dr. Hoong-Kun Fun and Associate Professor Dr. Abdul Razak Ibrahim, X-ray Crystallography Unit, School of Physics, Universiti Sains Malaysia, Malaysia for structure determination by single X-ray diffraction and partial financial support during the period of short training and also to Dr. Melati Khairuddean, School of Chemical Science, Universiti Sains Malaysia, Malaysia for her kindness and support during the period of training. I would like to offer thanks to Professor Dr. Puangpen Sirirugsa and Associate Professor Dr. Kitichate Sridith for plant identification. I am very thankful to Associate Professor Dr. Supinya Tewtrakul, Assistant Professor Dr. Akkharawit Kanjana-Opas, and Assistant Professor Dr. Supreeya Yuenyongsawad for bioactivity test.

I wish to express my appreciation to the staffs of the Department of Chemistry, Faculty of Science, Prince of Songkla University for making this thesis possible.

This research was supported by a scholarship from the Center for Innovation in Chemistry (PERCH-CIC), Commission on Higher Education, Ministry of Education. I would like to acknowledge the Faculty of Science Research Fund and the Graduated School, Prince of Songkla University for partial financial support.

Abdulwahab Salae

THE RELEVANCE OF THE RESEARCH WORK TO THAILAND

The purpose of this research is to investigate the chemical constituents of *Diospyros wallichii* and *Premna obtusifolia*. They are parts of the basic research on the utilization of the Thai medicinal plants. Chemical investigation of constituents from the roots and fruits of *D. wallichii* and the roots and twigs of *P. obtusifolia* led to isolation of fourteen new compounds (**DW9**, **DtW11**, **DW12**, **PO1-PO5**, **PO18**, **PO19**, and **PO23-PO26**), together with thirty-six known compounds. Some of the compounds exhibited significant cytotoxic activity against MCF-7 cell line (Human breast adenocarcinoma), antibacterial and anti-inflammatory activities. Hence they have potential to be developed into drug.

CONTENTS (Continued)

	Page
2.3.2.1 Investigation of the crude CH ₂ Cl ₂ extract from the twigs of <i>P. obtusifolia</i>	128
2.4 Bioassays	134
2.4.1 Cytotoxic assay	134
2.4.2 Antibacterial assay	134
2.4.3 Anti-inflammatory assay	135
2.5 X-ray crystallographic studies of compounds (PO23) and (PO24)	136
CHAPTER 3 RESULTS AND DISCUSSION	138
3.1 Structure elucidation of compounds from the roots and fruits of <i>D. wallichii</i>	138
3.1.1 Compound DW1	139
3.1.2 Compound DW2	142
3.1.3 Compound DW3	145
3.1.4 Compound DW4	148
3.1.5 Compound DW5	150
3.1.6 Compound DW6	153
3.1.7 Compound DW7	156
3.1.8 Compound DW8	159
3.1.9 Compound DW9	162
3.1.10 Compound DW10	165
3.1.11 Compound DW11	168
3.1.12 Compound DW12	170
3.1.13 Compound DW13	172
3.1.14 Compound DW14	174
3.1.15 Compound DW15	178
3.1.16 Compound DW16	182
3.1.17 Compound DW17	186

CONTENTS (Continued)

	Page
3.1.18 Compound DW18	190
3.1.19 Compound DW19	195
3.1.20 Compounds DW20 and DW21	198
3.2 Structure elucidation of compounds from the roots and twigs of <i>P. obtusifolia</i>	199
3.2.1 Compound PO1	200
3.2.2 Compound PO2	203
3.2.3 Compound PO3	206
3.2.4 Compound PO4	209
3.2.5 Compound PO5	212
3.2.6 Compound PO6	215
3.2.7 Compound PO7	218
3.2.8 Compound PO8	221
3.2.9 Compound PO9	223
3.2.10 Compound PO10	226
3.2.11 Compound PO11	230
3.2.12 Compound PO12	234
3.2.13 Compound PO13	237
3.2.14 Compound PO14	240
3.2.15 Compound PO15	244
3.2.16 Compound PO16	246
3.2.10 Compound PO17	249
3.2.11 Compound PO18	252
3.2.12 Compound PO19	255
3.2.13 Compound PO20	258
3.2.14 Compound PO21	262
3.2.15 Compound PO22	265

CONTENTS (Continued)

	Page
3.2.16 Compound PO23	269
3.2.16 Compound PO24	272
3.2.10 Compound PO25	275
3.2.11 Compound PO26	278
3.2.12 Compound PO27	282
3.2.13 Compound PO28	285
3.2.14 Compound PO29	288
3.3 Biological activities of isolated compounds from <i>D. wallichii</i> and <i>P. obtusifolia</i>	291
3.3.1 Activity of isolated compounds from <i>D. wallichii</i> on antibacterial and cytotoxic activities	291
3.3.2 Activity of isolated compounds from <i>P. obtusifolia</i> on antibacterial and anti-inflammatory activities	294
CHAPTER 4 CONCLUSION	298
REFERENCES	301
APPENDIX	326
VITAE	376

LIST OF TABLES

Table	Page
1 Compounds from plant of <i>Diospyros</i> genus	2
2 Compounds from plant of <i>Premna</i> genus	74
3 ¹ H, ¹³ C NMR, DEPT and HMBC spectral data of compound DW1	140
4 Comparison of ¹ H and ¹³ C NMR spectral data of compounds DW1 and plumbagin	141
5 ¹ H, ¹³ C NMR, DEPT and HMBC spectral data of compound DW2 and ¹³ C NMR of droserone (R)	143
6 Comparison of ¹ H NMR spectral data of compounds DW1, DW2 and droserone	144
7 ¹ H, ¹³ C NMR, DEPT and HMBC spectral data of compound DW3 and ¹³ C NMR of 2,3-epoxyplumbagin (R)	146
8 Comparison of ¹ H NMR spectral data of compounds DW1, DW3 and 2,3-epoxyplumbagin	147
9 ¹ H, ¹³ C NMR, DEPT and HMBC spectral data of compound DW4	149
10 ¹ H, ¹³ C NMR, DEPT and HMBC spectral data of compound DW5 and ¹³ C NMR of diomuscine (R)	151
11 Comparison of ¹ H NMR spectral data of compounds DW1, DW5 and diomuscine	152
12 ¹ H, ¹³ C NMR, DEPT and HMBC spectral data of compound DW6 and ¹³ C NMR of isoshinanolone (R)	154
13 Comparison of ¹ H NMR spectral data of compounds DW1, DW6 and isoshinanolone	155
14 ¹ H, ¹³ C NMR, DEPT and HMBC spectral data of compound DW7 and ¹³ C NMR of <i>epi</i> -isoshinanolone (R)	157
15 Comparison of ¹ H NMR spectral data of compounds DW6, DW7 and <i>epi</i> -isoshinanolone	158

LIST OF TABLES (Continued)

Table	Page
16 ¹ H, ¹³ C NMR, DEPT and HMBC spectral data of compound DW8 and ¹³ C NMR of Maritinone (R)	160
17 Comparison of ¹ H NMR spectral data of compounds DW1, DW8 and maritinone	161
18 ¹ H, ¹³ C NMR, DEPT and HMBC spectral data of compound DW9	163
19 Comparison of ¹ H and ¹³ C NMR spectral data of compounds DW1 and DW9	164
20 ¹ H, ¹³ C NMR, DEPT and HMBC spectral data of compound DW10	166
21 Comparison of ¹ H NMR spectral data of compounds DW1, DW10 and methylene-3,3'-biplumbagin (R)	167
22 Comparison of ¹³ C NMR spectral data of compounds DW1-DW10	167
23 ¹ H, ¹³ C NMR, DEPT and HMBC spectral data of compounds DW11	169
24 Comparison of ¹ H and ¹³ C NMR spectral data of compounds DW11 and DW12	171
25 ¹ H, ¹³ C NMR, DEPT and HMBC spectral data of compound DW13 and comparison of ¹ H and ¹³ C NMR of DW13 and scopoletin (R)	173
26 ¹ H, ¹³ C NMR, DEPT and HMBC spectral data of compound DW14 and ¹³ C NMR of lupeol (R)	175
27 Comparison of ¹ H NMR spectral data of compounds DW14 and lupeol and ¹³ C NMR of 2,3-epoxyplumbagin (R)	177
28 ¹ H, ¹³ C NMR, DEPT and HMBC spectral data of compound DW15 and ¹³ C NMR of lupenone (R)	179
29 Comparison of ¹ H NMR spectral data of compounds DW14, DW15 and lupenone	180
30 ¹ H, ¹³ C NMR, DEPT and HMBC spectral data of compound DW16 and ¹³ C NMR of betulin (R)	183

LIST OF TABLES (Continued)

Table	Page
31 Comparison of ^1H NMR spectral data of compounds DW14, DW16 and betulin	184
32 ^1H , ^{13}C NMR, DEPT and HMBC spectral data of compound DW17 and ^{13}C NMR of betulinaldehyde (R)	187
33 Comparison of ^1H NMR spectral data of compounds DW14, DW17 and betulinaldehyde	188
34 ^1H , ^{13}C NMR, DEPT and HMBC spectral data of compound DW18 and ^{13}C NMR of betulinic acid (R)	191
35 Comparison of ^1H NMR spectral data of compounds DW14, DW18 and betulinic acid	192
36 Comparison of ^{13}C NMR spectral data of compounds DW14-DW18	193
37 ^1H , ^{13}C NMR, DEPT and HMBC spectral data of compounds DW19 and ^{13}C NMR of 3 β ,29-dihydroxyolean-12-en-28-oic acid (R)	196
38 ^1H , ^{13}C NMR, DEPT and HMBC spectral data of compound PO1	202
39 ^1H , ^{13}C NMR, DEPT and HMBC spectral data of compound PO2	204
40 Comparison of ^1H and ^{13}C NMR spectral data of compounds PO1 and PO2	205
41 ^1H , ^{13}C NMR and HMBC spectral data of compound PO3	208
42 ^1H , ^{13}C NMR, DEPT and HMBC spectral data of compound PO4	211
43 ^1H , ^{13}C NMR, DEPT and HMBC spectral data of compound PO5	213
44 Comparison of ^1H and ^{13}C NMR spectral data of compounds PO4 and PO5	214
45 ^1H , ^{13}C NMR, DEPT and HMBC spectral data of compound PO6 and ^{13}C NMR of ferruginol (R)	216
46 Comparison of ^1H NMR spectral data of compounds PO5, PO6 and ferruginol	218

LIST OF TABLES (Continued)

Table	Page
47 ^1H , ^{13}C NMR, DEPT and HMBC spectral data of compound PO7 and ^{13}C NMR of <i>O</i> -methyl ferruginol (R)	219
48 Comparison of ^1H NMR spectral data of compounds PO6 , PO7 and <i>O</i> -methyl ferruginol	220
49 ^1H , ^{13}C NMR, DEPT and HMBC spectral data of compound PO8	222
50 ^1H , ^{13}C NMR, DEPT and HMBC spectral data of compound PO9 and ^{13}C NMR of sugiol (R)	224
51 Comparison of ^1H NMR spectral data of compounds PO6 , PO9 and sugiol	225
52 ^1H , ^{13}C NMR, DEPT and HMBC spectral data of compound PO10 and ^{13}C NMR of royleanone (R)	228
53 Comparison of ^1H NMR spectral data of compounds PO6 , PO10 and royleanone	229
54 ^1H , ^{13}C NMR, DEPT and HMBC spectral data of compound PO11 and ^{13}C NMR of horminone (R)	231
55 Comparison of ^1H NMR spectral data of compounds PO10 , PO11 and royleanone	232
56 Comparison of ^{13}C NMR spectral data of compounds PO4-PO9	233
57 ^1H , ^{13}C NMR, DEPT and HMBC spectral data of compound PO12 and ^{13}C NMR of montbretrol (R)	235
58 Comparison of ^1H NMR spectral data of compounds PO9 , PO12 and montbretrol	236
59 ^1H , ^{13}C NMR, DEPT and HMBC spectral data of compound PO13 and ^{13}C NMR of 14-deoxycoleon (R)	238
60 Comparison of ^1H NMR spectral data of compounds PO12 , PO13 and 14-deoxycoleon (R)	239

LIST OF TABLES (Continued)

Table	Page
61 ¹ H, ¹³ C NMR, DEPT and HMBC spectral data of compound PO14 and ¹³ C NMR of taxodione (R)	242
62 Comparison of ¹ H NMR spectral data of compounds PO14 and taxodione	243
63 ¹ H, ¹³ C NMR, DEPT and HMBC spectral data of compound PO15	245
64 ¹ H, ¹³ C NMR, DEPT and HMBC spectral data of compound PO16 and ¹³ C NMR of 12-hydroxy-6,7-secoabieta-8,11,13-triene-6,7-dial (R)	247
65 Comparison of ¹ H NMR spectral data of compounds PO16 and 12-hydroxy-6,7-secoabieta-8,11,13-triene-6,7-dial	248
66 ¹ H, ¹³ C NMR, DEPT and HMBC spectral data of compound PO17 and ¹³ C NMR of salvicanaraldehyde (R)	250
67 Comparison of ¹ H NMR spectral data of compounds PO16 , PO17 and salvicanaraldehyde	251 219
68 ¹ H, ¹³ C NMR, DEPT and HMBC spectral data of compound PO18	254
69 ¹ H, ¹³ C NMR, DEPT and HMBC spectral data of compound PO19	257
70 ¹ H, ¹³ C NMR, DEPT and HMBC spectral data of compound PO20 and ¹³ C NMR of 5,6-dihydro-6 α -hydroxysalviasperanol (R)	260
71 Comparison of ¹ H NMR spectral data of compounds PO20 and 5,6-dihydro-6 α -hydroxysalviasperanol	261
72 ¹ H, ¹³ C NMR, DEPT and HMBC spectral data of compound PO21 and ¹³ C NMR of salviasperanol (R)	263
73 Comparison of ¹ H NMR spectral data of compounds PO20 , PO21 and salviasperanol	264
74 ¹ H, ¹³ C NMR, DEPT and HMBC spectral data of compound PO22 (300 (¹ H NMR) and 75 (¹³ C NMR) MHz, CDCl ₃) and ¹³ C NMR of 11,12-dihydroxy-8,11,13-icetexatrien-1-one (100 MHz, CDCl ₃)	267

LIST OF TABLES (Continued)

Table	Page
75 Comparison of ^1H spectrum data of compounds PO22 and 11,12-dihydroxy-8,11,13-icetexatrien-1-one (R)	268
76 ^1H , ^{13}C NMR, DEPT and HMBC spectral data of compound PO23	271
77 ^1H , ^{13}C NMR, DEPT and HMBC spectral data of compound PO24	274
78 ^1H , ^{13}C NMR, DEPT and HMBC spectral data of compound PO25	276
79 Comparison of ^1H and ^{13}C NMR spectral data of compounds PO24 and PO25	277
80 ^1H , ^{13}C NMR, DEPT and HMBC spectral data of compound PO26	280
81 Comparison of ^1H and ^{13}C NMR spectral data of compounds PO25 and PO26	281
82 ^1H , ^{13}C NMR, DEPT and HMBC spectral data of compound PO27 and ^{13}C NMR of 4 β ,5 β -dihydroxy-10- <i>epi</i> -eudesmane (R)	283
83 Comparison of ^1H NMR spectral data of compounds PO27 and 4 β ,5 β -dihydroxy-10- <i>epi</i> -eudesmane	284
84 ^1H , ^{13}C NMR, DEPT and HMBC spectral data of compound PO28 and ^{13}C NMR of 4 β ,10 β -dihydroxy aromadendrane (R)	286
85 Comparison of ^1H NMR spectral data of compounds PO28 and 4 β ,10 β -dihydroxy aromadendrane	287
86 ^1H , ^{13}C NMR, DEPT and HMBC spectral data of compound PO29 and ^{13}C NMR of spathulenol (R)	289
87 Comparison of ^1H NMR spectral data of compounds PO29 and spathulenol	290
88 Antibacterial activities against gram-positive bacteria of compounds DW1-DW6 , DW8 , DW9 , DW11 and DW12 from <i>D. wallichii</i>	292

LIST OF TABLES (Continued)

Table	Page
89 Antibacterial activities against gram-negative bacteria and cytotoxicity against MCF-7 cell line of compounds DW1-DW6, DW8, DW9, DW11 and DW12 from <i>D. wallichii</i>	293
90 Antibacterial activities against gram-positive bacteria of compounds PO4, PO11, PO13, PO15-PO22, PO24, PO25 and PO27 from <i>P. obtusifolia</i>	295
91 Antibacterial activities against gram-negative bacteria of compounds PO4, PO11, PO13, PO15-PO22, PO24, PO25 and PO27 from <i>P. obtusifolia</i>	296
92 Inhibitory effects on NO production ^c of compounds PO3-PO7, PO11-PO15, PO17-PO25, PO27 and PO28 from <i>P. obtusifolia</i>	297

LIST OF ILLUSTRATIONS

Schemes	Page
1 Extraction of the roots of <i>D. wallichii</i>	117
2 Isolation of compounds DW1, DW6-DW7, DW9, DW15, DW17 and DW20-DW21 from the hexane extract	118
3 Isolation of compounds DW2, DW5, DW11-DW14 and DW16 from the CH ₂ Cl ₂ extract	119
4 Isolation of compounds DW3-DW4, DW8, DW10, DW18 and DW19 from the CH ₂ Cl ₂ extract	120
5 Extraction of the roots of <i>P. obtusifolia</i>	124
6 Isolation of compounds PO6, PO7, PO10, PO11, PO14, PO15, PO19, PO23-PO26 and PO29 from the hexane extract	125
7 Isolation of compounds PO4, PO5, PO9, PO12, PO13, PO16-PO18, PO20-PO22 and PO27-PO28 from the CH ₂ Cl ₂ extract	
8 Isolation of compounds PO1-PO3 and PO8 from the CH ₂ Cl ₂ extract	
Figures	
1 <i>Diospyros wallichii</i>	1
2 <i>Premna obtusifolia</i>	73
3 Major HMBC correlations of DW1	140
4 Major HMBC correlations of DW2	142
5 Major HMBC correlations of DW3	145
6 Major HMBC correlations of DW4	148
7 Major HMBC correlations of DW5	150
8 Major HMBC correlations of DW6	153
9 Major HMBC correlations of DW8	159
10 Major HMBC correlations of DW9	163
11 Major HMBC correlations of DW10	166

LIST OF ILLUSTRATIONS (Continued)

Figures	Page
12 Selected HMBC correlations (A) and NOESY correlations (B) for DW11	169
13 Major HMBC and NOESY correlations of DW13	173
14 Major HMBC correlations of DW14	175
15 Major HMBC correlations of DW19	196
16 Selected HMBC correlations (A) and NOESY correlations (B) for PO1	201
17 Selected HMBC correlations (A) and NOESY correlations (B) for PO3	207
18 Selected HMBC correlations (A) and NOESY correlations (B) for PO4	210
19 Selected HMBC correlations for PO6	215
20 Selected HMBC correlations of PO10	227
21 <i>ORTEP</i> drawing of PO10	227
22 <i>ORTEP</i> drawing of PO11	230
23 <i>ORTEP</i> drawing of PO13	237
24 Major selected HMBC correlations of PO14	241
25 Major selected HMBC correlations of PO17	249
26 Selected HMBC correlations (A) and NOESY correlations (B) for PO18	253
27 Major selected HMBC correlations of PO19	256
28 Major selected HMBC correlations of PO20	259
29 <i>ORTEP</i> drawing of PO20	259
30 Major selected HMBC correlations of PO22	266
31 <i>ORTEP</i> drawing of PO22	266
32 Major selected HMBC correlations of PO24	272
33 <i>ORTEP</i> drawing of PO24	272

LIST OF ILLUSTRATIONS (Continued)

Figures	Page
34 Major selected HMBC correlations of PO25	274
35 Major selected HMBC correlations of PO26	278
36 Selected HMBC correlations (A) and NOESY correlations (B) for PO27	282
37 Selected HMBC correlations (A) and NOESY correlations (B) for PO28	285
38 ¹ H NMR (300 MHz) (CDCl ₃) spectrum of compound DW1	327
39 ¹³ C NMR (75 MHz) (CDCl ₃) spectrum of compound DW1	327
40 ¹ H NMR (300 MHz) (CDCl ₃) spectrum of compound DW2	328
41 ¹³ C NMR (75 MHz) (CDCl ₃) spectrum of compound DW2	328
42 ¹ H NMR (300 MHz) (CDCl ₃) spectrum of compound DW3	329
43 ¹³ C NMR (75 MHz) (CDCl ₃) spectrum of compound DW3	329
44 ¹ H NMR (400 MHz) (CDCl ₃) spectrum of compound DW4	330
45 ¹³ C NMR (100 MHz) (CDCl ₃) spectrum of compound DW4	330
46 ¹ H NMR (300 MHz) (CDCl ₃) spectrum of compound DW5	331
47 ¹³ C NMR (75 MHz) (CDCl ₃) spectrum of compound DW5	331
48 ¹ H NMR (300 MHz) (CDCl ₃) spectrum of compound DW6	332
49 ¹³ C NMR (75 MHz) (CDCl ₃) spectrum of compound DW6	332
50 ¹ H NMR (300 MHz) (CDCl ₃) spectrum of compound DW7	333
51 ¹³ C NMR (75 MHz) (CDCl ₃) spectrum of compound DW7	333
52 ¹ H NMR (300 MHz) (CDCl ₃) spectrum of compound DW8	334
53 ¹³ C NMR (75 MHz) (CDCl ₃) spectrum of compound DW8	334
54 ¹ H NMR (300 MHz) (CDCl ₃) spectrum of compound DW9	335
55 ¹³ C NMR (75 MHz) (CDCl ₃) spectrum of compound DW9	335
56 ¹ H NMR (300 MHz) (CDCl ₃) spectrum of compound DW10	336
57 ¹³ C NMR (75 MHz) (CDCl ₃) spectrum of compound DW10	336
58 ¹ H NMR (400 MHz) (CDCl ₃) spectrum of compound DW11	337

LIST OF ILLUSTRATIONS (Continued)

Figures	Page
59 ^{13}C NMR (100 MHz) (CDCl_3) spectrum of compound DW11	337
60 ^1H NMR (300 MHz) (CDCl_3) spectrum of compound DW12	338
61 ^{13}C NMR (75 MHz) (CDCl_3) spectrum of compound DW12	338
62 ^1H NMR (300 MHz) (CDCl_3) spectrum of compound DW13	339
63 ^{13}C NMR (75 MHz) (CDCl_3) spectrum of compound DW13	339
64 ^1H NMR (300 MHz) (CDCl_3) spectrum of compound DW14	340
65 ^{13}C NMR (75 MHz) (CDCl_3) spectrum of compound DW14	340
66 ^1H NMR (300 MHz) (CDCl_3) spectrum of compound DW15	341
67 ^{13}C NMR (75 MHz) (CDCl_3) spectrum of compound DW15	341
68 ^1H NMR (300 MHz) (CDCl_3) spectrum of compound DW16	342
69 ^{13}C NMR (75 MHz) (CDCl_3) spectrum of compound DW16	342
70 ^1H NMR (300 MHz) (CDCl_3) spectrum of compound DW17	343
71 ^{13}C NMR (75 MHz) (CDCl_3) spectrum of compound DW17	343
72 ^1H NMR (300 MHz) ($\text{CDCl}_3+\text{CD}_3\text{OD}$) spectrum of compound DW18	344
73 ^{13}C NMR (75 MHz) ($\text{CDCl}_3+\text{CD}_3\text{OD}$) spectrum of compound DW18	344
74 ^1H NMR (300 MHz) (CDCl_3) spectrum of compound DW19	345
75 ^{13}C NMR (75 MHz) (CDCl_3) spectrum of compound DW19	345
76 ^1H NMR (300 MHz) (CDCl_3) spectrum of compound DW20 and DW21	346
77 ^1H NMR (300 MHz) (CDCl_3) spectrum of compound PO1	347
78 ^{13}C NMR (75 MHz) (CDCl_3) spectrum of compound PO1	347
79 ^1H NMR (300 MHz) ($\text{CDCl}_3+\text{CD}_3\text{OD}$) spectrum of compound PO2	348
80 ^{13}C NMR (75 MHz) ($\text{CDCl}_3+\text{CD}_3\text{OD}$) spectrum of compound PO2	348
81 ^1H NMR (300 MHz) (CDCl_3) spectrum of compound PO3	349
82 ^{13}C NMR (75 MHz) (CDCl_3) spectrum of compound PO3	349
83 ^1H NMR (300 MHz) (CDCl_3) spectrum of compound PO4	350
84 ^{13}C NMR (75 MHz) (CDCl_3) spectrum of compound PO4	350

LIST OF ILLUSTRATIONS (Continued)

Figures	Page
85 ^1H NMR (400 MHz) (CDCl_3) spectrum of compound PO5	351
86 ^{13}C NMR (100 MHz) (CDCl_3) spectrum of compound PO5	351
87 ^1H NMR (300 MHz) (CDCl_3) spectrum of compound PO6	352
88 ^{13}C NMR (75 MHz) (CDCl_3) spectrum of compound PO6	352
89 ^1H NMR (300 MHz) (CDCl_3) spectrum of compound PO7	353
90 ^{13}C NMR (75 MHz) (CDCl_3) spectrum of compound PO7	353
91 ^1H NMR (300 MHz) ($\text{CDCl}_3+\text{CD}_3\text{OD}$) spectrum of compound PO8	354
92 ^{13}C NMR (75 MHz) ($\text{CDCl}_3+\text{CD}_3\text{OD}$) spectrum of compound PO8	354
93 ^1H NMR (300 MHz) (CDCl_3) spectrum of compound PO9	355
94 ^{13}C NMR (75 MHz) (CDCl_3) spectrum of compound PO9	355
95 ^1H NMR (300 MHz) (CDCl_3) spectrum of compound PO10	356
96 ^{13}C NMR (75 MHz) (CDCl_3) spectrum of compound PO10	356
97 ^1H NMR (300 MHz) (CDCl_3) spectrum of compound PO11	357
98 ^{13}C NMR (75 MHz) (CDCl_3) spectrum of compound PO11	357
99 ^1H NMR (300 MHz) (CDCl_3) spectrum of compound PO12	358
100 ^{13}C NMR (75 MHz) (CDCl_3) spectrum of compound PO12	358
101 ^1H NMR (300 MHz) (CDCl_3 CD_3OD) spectrum of compound PO13	359
102 ^{13}C NMR (75 MHz) (CDCl_3 CD_3OD) spectrum of compound PO13	359
103 ^1H NMR (400 MHz) (CDCl_3) spectrum of compound PO14	360
104 ^{13}C NMR (100 MHz) (CDCl_3) spectrum of compound PO14	360
105 ^1H NMR (300 MHz) (CDCl_3) spectrum of compound PO15	361
106 ^{13}C NMR (75 MHz) (CDCl_3) spectrum of compound PO15	361
107 ^1H NMR (300 MHz) (CDCl_3) spectrum of compound PO16	362
108 ^{13}C NMR (75 MHz) (CDCl_3) spectrum of compound PO16	362
109 ^1H NMR (400 MHz) (CDCl_3) spectrum of compound PO17	363
110 ^{13}C NMR (100 MHz) (CDCl_3) spectrum of compound PO17	363
111 ^1H NMR (400 MHz) ($\text{CDCl}_3+\text{CD}_3\text{OD}$) spectrum of compound PO18	364

LIST OF ILLUSTRATIONS (Continued)

Figures	Page
112 ^{13}C NMR (100 MHz) ($\text{CDCl}_3+\text{CD}_3\text{OD}$) spectrum of compound PO18	364
113 ^1H NMR (300 MHz) (CDCl_3) spectrum of compound PO19	365
114 ^{13}C NMR (75 MHz) (CDCl_3) spectrum of compound PO19	365
115 ^1H NMR (400 MHz) ($\text{CDCl}_3+\text{CD}_3\text{OD}$) spectrum of compound PO20	366
116 ^{13}C NMR (100 MHz) ($\text{CDCl}_3+\text{CD}_3\text{OD}$) spectrum of compound PO20	366
117 ^1H NMR (400 MHz) ($\text{CDCl}_3+\text{CD}_3\text{OD}$) spectrum of compound PO21	367
118 ^{13}C NMR (100 MHz) ($\text{CDCl}_3+\text{CD}_3\text{OD}$) spectrum of compound PO21	367
119 ^1H NMR (400 MHz) (CDCl_3) spectrum of compound PO22	368
120 ^{13}C NMR (100 MHz) (CDCl_3) spectrum of compound PO22	368
121 ^1H NMR (300 MHz) (CDCl_3) spectrum of compound PO23	369
122 ^{13}C NMR (75 MHz) (CDCl_3) spectrum of compound PO23	369
123 ^1H NMR (300 MHz) (CDCl_3) spectrum of compound PO24	370
124 ^{13}C NMR (75 MHz) (CDCl_3) spectrum of compound PO24	370
125 ^1H NMR (400 MHz) (CDCl_3) spectrum of compound PO25	371
126 ^{13}C NMR (100 MHz) (CDCl_3) spectrum of compound PO25	371
127 ^1H NMR (300 MHz) (CDCl_3) spectrum of compound PO26	372
128 ^{13}C NMR (75 MHz) (CDCl_3) spectrum of compound PO26	372
129 ^1H NMR (300 MHz) (CDCl_3) spectrum of compound PO27	373
130 ^{13}C NMR (75 MHz) (CDCl_3) spectrum of compound PO27	373
131 ^1H NMR (400 MHz) (CDCl_3) spectrum of compound PO28	374
132 ^{13}C NMR (100 MHz) (CDCl_3) spectrum of compound PO28	374
133 ^1H NMR (300 MHz) (CDCl_3) spectrum of compound PO29	375
134 ^{13}C NMR (75 MHz) (CDCl_3) spectrum of compound PO29	375

LIST OF ABBREVIATIONS AND SYMBOLS

s	=	singlet
d	=	doublet
t	=	triplet
q	=	quartet
m	=	multiplet
dd	=	doublet of doublet
dt	=	doublet of triplet
br s	=	broad singlet
br d	=	broad doublet
qd	=	quartet of doublet
g	=	Gram
nm	=	Nanometer
m.p.	=	Melting point
cm ⁻¹	=	Reciprocal centimeter (wave number)
δ	=	Chemical shift relative to TMS
<i>J</i>	=	Coupling constant
$[\alpha]_D$	=	Specific rotation
λ_{\max}	=	Maximum wavelength
ν	=	Absorption frequencies
ϵ	=	Molar extinction coefficient
m/z	=	A value of mass divided by charge
°C	=	Degree celcius
MHz	=	Megahertz
ppm	=	Part per million
<i>C</i>	=	Concentration
FT-IR	=	Fourier Transform Infrared
UV-Vis	=	Ultraviolet-Visible

LIST OF ABBREVIATIONS AND SYMBOLS (Continued)

HREIMS	=	High Resolution Chemical Impact Mass Spectrometry
EIMS	=	Electron Impact Mass Spectrometry
HREIMS	=	High Resolution Electron Impact Mass Spectrometry
NMR	=	Nuclear Magnetic Resonance
1D NMR	=	One Dimensional Nuclear Magnetic Resonance
2D NMR	=	Two Dimensional Nuclear Magnetic Resonance
COSY	=	Correlation Spectroscopy
DEPT	=	Distortionless Enhancement by Polarization Transfer
HMBC	=	Heteronuclear Multiple Bond Correlation
HMQC	=	Heteronuclear Multiple Quantum Coherence
NOESY	=	Nuclear Overhauser Effect Correlation Spectroscopy
CC	=	Column Chromatography
VLC	=	Vacuum liquid Chromatography
DCM	=	Dichloromethane
TMS	=	Tetramethylsilane
CDCl ₃	=	Deuteriochloroform
CD ₃ OD	=	Deuteromethanol
CO ₂	=	Carbon dioxide
HCl	=	Hydrochloric acid
DMSO	=	Dimethyl sulfoxide
CAPE	=	Caffeic acid phenylester
MCF-7	=	Human breast adenocarcinoma
µg/ml	=	Microgram per milliliter
IC ₅₀	=	The half maximal inhibitory concentration
NO	=	Nitric oxide

CHAPTER 1

INTRODUCTION

1.1 Chemical constituents from *Diospyros wallichii* King&Gamble

1.1.1 Introduction

The genus *Diospyros* (Family Ebenaceae), includes about 400 species. In Thailand, 60 *Diospyros* species have been described by Phengklai. Many of them are distributed in the forest throughout the country. Their fine and hard wood is of high value, and the leaves, bark and fruit of some species have been used as medicinal herbs, such as the fruit of *D. Montana* is used to treat hiccups, ulcers, urinary diseases and dysentery. The fruit of *D. decandra* and *D. malabarica* is used as an emmenagogue in Vietnam and leukorrhea in India, respectively (Utsunomiya *et al.*, 1998). *Diospyros wallichii* is known in Thailand as “damtako (ตำตะโก)”. This plant is grown to about 10-20 m in height. It has small white flower. The round fruits are poisonous and used for fishing.



Figure 1 Parts of *Diospyros wallichii*

1.1.2 Review of literatures

Chemical constituents isolated from seventeen species of *Diospyros* genus were summarized in **Table 1**. Information from the Scifinder Scholar copyright in 2012 will be presented and they can be classified into groups as follows: alkaloid, benzenoids, betulide, carotenoids, coumarins, diterpenoids, fatty acids, flavonoids, hydrocarbons, lignans, naphthalenes, phenolics, quinones, sesquiterpenoid, steroids, sugars, triterpenoids, miscellaneous terpenoids and vitamin

Table 1 Compounds from plants of *Diospyros* genus.

a: alkaloid	h: flavonoids	o: steroids
b: benzenoids	i: hydrocabons	p: sugars
c: betenolide	j: lignans	q: triterpenoids
d: carotenoids	k: naphthalenes	r: terpenoids
e: coumarins	l: phenolics	s: vitamin
f: diterpenoids	m: quinones	
g: fatty acids	n: sesquiterpenoid	

Plant	part	Compound	Bibliography
<i>D. angustifolia</i>	Stem barks	Diospyrosonaphthoside, 99k Diospyrososide, 105l Lupeol, 215q Betulinic acid, 219q β -Amyrin, 246q 3 β -Hydroxy-28,19 β -oleanolide, 303q Diospyrosooleanolide, 310q Friedelin, 315q	Pathak <i>et al.</i> , 2004

Table 1 (continued)

Plant	part	Compound	Bibliography
<i>D. assimilis</i>	Roots	5-Hydroxy-4-methoxy-2-naphthaldehyde, 93k	Ganapaty <i>et al.</i> , 2006
		4-Hydroxy-3,5-dimethoxy-2-naphthaldehyde, 94k 4-Hydroxy-5-methoxy-2-naphthaldehyde, 95k Plumbagin, 112m Diospyrin, 145m 8'-Hydroxyisodiospyrin, 150m Hydroxyisodiospyrin, 162m	
<i>D. batocana</i>	Root barks	7-Methyljuglone, 113m 2-Methylnaphthazarin, 115m Diospyrin, 145m Isodiospyrin, 152m Rotundiquinone, 164m Biramentaceone, 165m Mamegakinone, 167m Diosquinone, 170m Batocanone, 171m	Alves <i>et al.</i> , 1983
<i>D. blancoi</i>	Leaves	Isoarborinol methyl ether, 224q α -Amyrin palmitate, 250q α -Amyrin palmitoleate, 252q β -Amyrin palmitate, 293q β -Amyrin palmitoleate, 294q	Ragasa <i>et al.</i> , 2009
<i>D. buxifolia</i>	Wood	Diosindigo A, 173m	Musgrave <i>et al.</i> , 1970
<i>D. canaliculata</i>	Stem barks	Gerberinol, 33e	Tangmouo <i>et al.</i> , 2005

Table 1 (continued)

Plant	part	Compound	Bibliography
<i>D. canaliculata</i>	Stem barks	Plumbagin, 112m Canaliculatin, 179m Diospyrone, 190m Betulinic acid, 219q Lupenone, 221q	Tangmouo <i>et al.</i> , 2005
<i>D. cauliflora</i>	Roots	Tetralone, 132m	Auamcharoen <i>et al.</i> , 2009
<i>D. celebica</i>	Heartwoods	Macassar II, 77k Macassar III, 78k Dihydrodiosindigo B, 98k 8-Methoxy-6-methyl-1,2-naphthoquinone, 111m Diomelquinone, 124m Diosindigo B, 174m Diosindigo B ₁ , 175m Diosindigo B ₂ , 176m Celebaquinone, 177m Isocelebaquinone, 178m Betulinic acid, 219q	Maiti <i>et al.</i> , 1986, 1990
<i>D. chamaethamnus</i>	Root barks	2-Methyl naphthazarin, 115m 7-Methyljuglone, 113m Biramantaceone, 165m Mamegakinone, 177m Xylospyrin, 191m Diospyrin, 145m Diosquinone, 170m Isodiospyrin, 152m	Costa <i>et al.</i> , 1998

Table 1 (continued)

Plant	part	Compound	Bibliography
<i>D. chloroxylon</i>	Roots	2-Methyl-3,6-dihydroxy-4,5-dimethoxynaphthalene, 79k 2-Methyl-3,4,5,6-tetramethoxynaphthalene, 80k	Sidhu <i>et al.</i> , 1967
<i>D. costata</i>	Fruits	Lycopene, 22d α -Carotene, 23d β -Carotene, 24d Cryptoxanthin, 25d Zeaxanthin, 26d Violaxanthin, 27d	Karl, 1935
<i>D. crassiflora</i>	Stem barks	Gerberinol, 33e Plumbagin, 112m Crassiflorone, 184m Cyclocanaliculatin, 185m Lupeol, 215q Betulinic acid, 219q Luponone, 220q	Tangmouo <i>et al.</i> , 2006
	Leaves	Diosfeboside A, 36e Diosfeboside B, 37e Kaempferol 3-O- α -L-rhamnopyranosyl-(1 \rightarrow 2)- β -D-glucopyranoside, 65h Stigmasterol, 200o Stigmasterol 3-O- β -D-glucopyranoside, 206o Betulinic acid, 219q Ursolic acid, 247q	Akak <i>et al.</i> , 2010

Table 1 (continued)

Plant	part	Compound	Bibliography
<i>D. decandra</i>	Stem barks	Diospyric acid A, 258q Diospyric acid B, 259q Diospyric acid C, 260q Diospyric acid D, 261q Diospyric acid E, 262q	Nareeboon <i>et al.</i> , 2006
	Barks	Vismiaefolic acid, 273q Dimethyl-2 α ,3 β -di- <i>O</i> -acetyl-19- <i>nor</i> -20-dimethyl-11-oxo urs-12-en-24,28-dioate, 276q Dimethyl-2 α ,3 β -di- <i>O</i> -acetyl-18,19- <i>seco</i> -19-oxours-11,13(18)-dien-24,28-dioate, 277q Dimethyl-2 α ,3 β -di- <i>O</i> -acetyl-19 α -hydroxy-11-oxours-12-en-24,28-dioate, 278q 2 α ,3 β ,2',3',4',6'-Hexa- <i>O</i> -acetyl-24-methyl-28-1'- β -D-glucopyranosyl-19 α -hydroxy urs-12-en-24,28-dioate, 283q 24-Methyl-2 α ,3 β ,2',3',4',2'',3'',4'',6''-nona- <i>O</i> -acetyl-28-1'- β -D-[glucopyranosyl-(1'' \rightarrow 6')-glucopyranosyl]-19 α -hydroxy urs-12-en-24,28-dioate, 284q	Sutthivaiyakit <i>et al.</i> , 2012
<i>D. dendo</i>	Leaves	3 β - <i>O</i> - <i>cis</i> - <i>p</i> -Coumaroyl-20 β -hydroxy-12-ursen-28-oic acid, 311q	Hu <i>et al.</i> , 2006

Table 1 (continued)

Plant	part	Compound	Bibliography
<i>D. dendo</i>	Leaves	3 β - <i>O</i> - <i>trans</i> - <i>p</i> -Coumaroyl-2 α -hydroxy-12-ursen-28-oic acid, 312q 3 β - <i>O</i> - <i>cis</i> - <i>p</i> -Coumaroyl-2 α -hydroxy-12-ursen-28-oic acid, 313q 3 β - <i>O</i> - <i>trans</i> -Feruloyl-2 α -hydroxy-12-ursen-28-oic acid, 314q Ursolic acid, 247q	Hu <i>et al.</i> , 2006
<i>D. discolor</i>	Stem barks	Aglycone, 196m 1,3,5-Trihydroxy-6-methoxy-2-methylantraquinone-8- <i>O</i> - β -D-glucopyranoside, 197m	Srivastava <i>et al.</i> , 1985
	Roots	Diospyrin, 145m 8'-Hydroxyisodiospyrin, 163m Habibone, 168m	Ganapaty <i>et al.</i> , 2005
	Twigs	Betunaldehyde, 218q Betulinic acid methyl ester, 219q Ursaldehyde, 289q 24-Ethyl-3 β -methoxylanost-9(11)-en-25-ol, 317q 3 β -Methoxy-24-methylenelanost-9(11)-en-25-ol, 318q 3 β -Methoxy-25-methyl-24-methylenelanost-9(11)-en-21-ol, 319q	Chen <i>et al.</i> , 2007

Table 1 (continued)

Plant	part	Compound	Bibliography
<i>D. discolor</i>	Twigs	3 β -Methoxy-24-methylanost-9(11),25-dien-24-ol, 320q	Chen <i>et al.</i> , 2007
	Fruits	D-Galactose, 207d D-Galacturonic acid, 208d D-Glucose, 209p L-Arabinose, 210p D-Xylose, 211p L-Rhamnose, 212p β -D-Glucopyranose pentaacetate, 213p D-Fructose, 214p	Haq <i>et al.</i> , 1984
<i>D. ebenum</i>	Stem barks	Elliptinone, 136m Ebenone, 186m Ellagic acid, 35e 6-Hydroxy-4,5-dimethoxy-2-naphthoic acid, 83k β -Sitosterol, 199o Stigmasterol, 200o Betulin, 216q Betulinic acid, 219q α -Amyrin, 246q Ursolic acid, 247q α -Amyrenone, 251q Baurenol, 254q	Sankaram <i>et al.</i> , 1984 Sharma <i>et al.</i> , 1985
	Heartwoods	6-Hydroxy-4,5-dimethoxy-2-naphthaldehyde, 81k 4,5,6-Trimethoxy-2-naphthaldehyde, 82k	Brown <i>et al.</i> , 1965

Table 1 (continued)

Plant	part	Compound	Bibliography
<i>D. ebenum</i>	Heartwoods	Betulinic acid, 223q	Brown <i>et al.</i> , 1965
		6-Hydroxy-4,5-dimethoxy-2-naphthoic acid, 83k	Gupta <i>et al.</i> , 1969
<i>D. ehretioides</i>	Wood	Ehretione, 164m	Lillie <i>et al.</i> , 1976
	Fruits	Palmarumycins JC, 101k Palmarumycins JC2, 102k Isodiospyrin, 151m Isodiospyrol A, 172m	Prajoubklang <i>et al.</i> , 2005
<i>D. eriantha</i>	bark	(+)-Syringaresinol, 75j β -Sitosterol, 199o Lupeol, 215q Betulin, 216q Betulinaldehyde, 218q Betulinic acid, 219q 3 β -Acetoxypurs-11-en-28,13-olide, 274q 3 β -Acetoxyoleanolic acid, 292q Friedelin, 315q	Chen <i>et al.</i> , 1992
	Heartwoods	Syringic acid, 7b 3,4,5-Trimethoxyphenol, 103l 2,6-Dimethoxy-1,4-benzoquinone, 109m 2-Methoxy-7-methyljuglone, 127m	Chen <i>et al.</i> , 1994

Table 1 (continued)

Plant	part	Compound	Bibliography
<i>D. eriantha</i>	Heartwoods	3-Methoxy-7-methyljuglone, 128m Stigmast-4-en-3-one, 201o Stigmast-4-ene-3,6-dione, 203o 3 β -Hydroxystigmast-5-en-7- one, 204o Lupeol, 215q Betulin, 216q Betulinaldehyde, 218q Betulinic acid, 219q Friedelin, 315q	Chen <i>et al.</i> , 1994
<i>D. ferrea</i>	Fruits	Isodiospyrin, 152m 8'-Hydroxyisodiospyrin, 163q β -Sitosterol, 199o Stigmasterol, 200o Betulin, 216q Lupenone, 221q Lupeol, 215q Lup-20(29)-en-3 β ,30-diol, 226q Friedelin, 315q β -Friedelinol, 316q	Kau <i>et al.</i> , 1997
<i>D. glandulosa</i>	Stems	Lupeol, 215q Betulin, 216q Ursolic acid, 247q β -Amyrin, 285q Oleanolic acid, 290q	Thanakijcharo enpath <i>et al.</i> , 2005

Table 1 (continued)

Plant	part	Compound	Bibliography
<i>D. greeniwayi</i>	Stem barks	Plumbagin, 112m 7-Methyljuglone, 113m 3,8'-Biplumbagin, 134m Isodiospyrin, 152m Ehretione, 164m Habibone, 168m Neodiospyrin, 169m	Khan <i>et al.</i> , 1998
<i>D. hallierii</i>	Root bark, Stem barks, and Leaves	Isoxylopyrin, 192m 7-Methyljuglone, 113m Lupeol, 215q	Khan <i>et al.</i> , 1999
<i>D. ismailii</i>	Root bark	Canaliculatin, 179m Ismailin, 189m	Jeffreys <i>et al.</i> , 1983
	Wood	4-Hydroxy-5-methyl coumarin, 28e	Zakaria, 1989
<i>D. japonica</i>	Roots	7-Methyljuglone, 113m Shinanolone, 129m Isodiospyrin, 152m Bisisodiospyrin, 188m Lupeol, 215q Betulin, 216q Betulinic acid, 219q Taraxerol, 305q	Kuroyanagi <i>et al.</i> , 1971
<i>D. kaki</i>	Roots	Gerberinol, 33e 11-Methylgerberinol, 34e	Paknikar <i>et al.</i> , 1996
	Leaves	Tatarine C, 1a Kakispyrone, 20b Kampferol, 47h	Chen <i>et al.</i> , 2005, 2007

Table 1 (continued)

Plant	part	Compound	Bibliography
<i>D. kaki</i>	Leaves	Quercetin, 48h	Chen <i>et al.</i> , 2005, 2007
		Myricetin, 49h	
		Annulatin, 50h	
		Astragalin, 52h	
		Trifolin, 53h	
		Hyperin, 55h	
		Isorhamnetin-3- <i>O</i> - β -D- glucopyranoside, 56h	
		Isoquercetin, 57h	
		Vitexin, 62h	
		2''- <i>O</i> -Rhamnosylvitexin, 63h	
		Kakispyrol, 106l	Thuong <i>et al.</i> , 2008
		4,4'-Dihydroxy- α -truxillic acid, 107l	
		Pomolic acid, 256q	
		24-Hydroxyursolic acid, 264q	
		Rotungenic acid, 265q	
		Coussaric acid, 267q	
		Barbinervic acid, 268q	
		3 α , 19 α -Dihydroxyurs-12,20 (30)-dien-24,28-dioic acid, 270q	
		3 α , 19 α -Dihydroxyurs-12-en- 24,28-dioic acid, 271q	
		Kakisaponin A, 279q	
Ursolic acid, 247q	Thuong <i>et al.</i> , 2008		
24-Hydroxy-3- <i>epi</i> -ursolic acid, 263q			

Table 1 (continued)

Plant	part	Compound	Bibliography
<i>D. kaki</i>	Leaves	19,24-Dihydroxyurs-12-en-3-on-28-oic acid, 266q Oleanolic acid, 290q 24-Hydroxy-3- <i>epi</i> -oleanolic acid, 299q Spathodic acid, 300q Kaempferol-3- <i>O</i> - α -L-rhamno pyranoside, 54h Myricetin-3- <i>O</i> - α -L-rhamno pyranoside, 58h Myricetin-3- <i>O</i> - β -D-glucopyranoside, 59h 2''- <i>O</i> -rhamnosylvitexin, 63h 8-C-[α -L-rhamnopyranosyl-(1 \rightarrow 4)]- α -D-glucopyranosyl apigenin, 66h Kakidiol, 269q Kakisaponin B, 280q Kakisaponin C, 281q Rosamultin, 282q Byzantionoside B, 321r Blumeol C glucoside, 322r	Thuong <i>et al.</i> , 2008 Chen <i>et al.</i> , 2009
	Fruits	α -Carotene, 23d β -Carotene, 24d Gallic acid, 6b α -Cryptoxanthin, 25d Zeaxanthin, 26d Neolutein, 205o	Daood <i>et al.</i> , 1992

Table 1 (continued)

Plant	part	Compound	Bibliography
<i>D. kaki</i>	Fruits	D-Glucose, 209p D-Fructose, 214p	Daood <i>et al.</i> , 1992
<i>D. leucomelas</i>	Leaves	Betulin, 216q Betulinic acid, 219q Ursolic acid, 247q	Recio <i>et al.</i> , 1995
<i>D. lotus</i>	Roots	7-Methyljuglone, 113m Isodiospyrin, 152m Memegakinone, 167m Bisisodiospyrin, 188m Betulinic acid, 219q Oxyallobetulin, 302q Tetraxerol, 304q	Yoshihira <i>et al.</i> , 1971
	Leaves	Gallic acid, 6b Methyl gallate, 9b Ellagic acid, 35e Kaempferol, 47h Quercetin, 48h Myricetin, 49h Myricetin 3- <i>O</i> - α -rhamnoside, 60h Myricetin 3- <i>O</i> - β -glucuronide, 61h	Said <i>et al.</i> , 2009
	Fruits	Gallic acid, 6b Methyl gallate, 9b Ellagic acid, 35e Kaempferol, 47h Quercetin, 48h Myricetin, 49h	Loizzo <i>et al.</i> , 2009

Table 1 (continued)

Plant	part	Compound	Bibliography
<i>D. lotus</i>	Fruits	Myricetin 3- <i>O</i> - β -glucuronide, 59h Myricetin 3- <i>O</i> - α -rhamnoside, 60h	Loizzo <i>et al.</i> , 2009
<i>D. lycioides</i>	Twigs	1',2-Binaphthalen-4-one-2',3-dimethyl-1,8'-epoxy-1,4',5,5',8,8'-hexahydroxy-8- <i>O</i> - β -glucopyranosyl-5'- <i>O</i> - β -xylopyranosyl -(1 \rightarrow 6)- β -glucopyranoside, 194m	Li <i>et al.</i> , 1998
<i>D. mafeinsis</i>	Stem barks	Isodiospyrin, 152m Diosquinone, 170m 6",8'-Bisdiosquinone, 193m	Khan <i>et al.</i> , 1999
<i>D. malanonilau</i>	Heartwood	<i>n</i> -Hexacosanol, 71i <i>n</i> -Nonacosane, 72i β -Sitosterol, 199o Betulin, 216q Betulic acid, 219q Ursolic acid, 247q Oleanolic acid, 290q Morolic acid, 298q	Singh <i>et al.</i> , 1988
<i>D. maritima</i>	Stems	3-Ethoxy-1-(4-hydroxy-3-methoxyphenyl)-1-propanone, 10b Maritolide, 21c Plumbagin, 112m Isodiospyrin, 152m	Kuo <i>et al.</i> , 1997, 1998

Table 1 (continued)

Plant	part	Compound	Bibliography
<i>D. maritima</i>	Stems	(<i>E</i>)-3-(4-Acetyloxy-3,5-dimethoxyphenyl)-2-propenal, 14b 5-Hydroxy-2-methylchromanone, 31e 5,7-Dihydroxy-2-methylchomanone, 32e Butylmethyl succinate, 73i 4-Ketopinoresinol, 76j <i>bis</i> (6-Hydroxy-2,3,4-trimethoxyphen-1-yl)methane, 104l Diomelquinone, 124m <i>epi</i> -Isoshinanolone, 131m 2-Ethoxy-8'-hydroxyisodiospyrin, 160m 3-Ethoxy-8'-hydroxyisodiospyrin, 161m Bisisodiospyrin, 188m Lupeol, 215q Betulin, 216q Betulin-28-acetate, 217q Betulinaldehyde, 218q Betulinic acid, 219q 3-Oxo-20(29)-lupen-28-oic acid, 222q Betulic acid acetate, 227q 3-(<i>E</i>)-Coumaroyllupeol, 228q	Chang <i>et al.</i> , 1998, 1999, 2007, 2009

Table 1 (continued)

Plant	part	Compound	Bibliography
<i>D. maritima</i>	Stems	3-(Z)-Coumaroyllupeol, 229q 3-(E)-Coumaroyl betulinal dehyde, 230q Lupeol caffeate, 233q 3-O-Betulinic acid <i>p</i> -coumarate, 234q (E)-Betulin-3 β - <i>p</i> -coumarate, 235q 3-(E)-Coumaroyl-28-palmi toylbetulin, 240q (Z)-Betulin-3 β - <i>p</i> -coumarate, 241q 3-(Z)-Coumaroyl-28-palmi toylbetulin, 242q 3-(E)-Feruloyl-28-palmitoyl betulin, 243q 3 β -Acetoxy- urs-12-en-28-oic Acid, 249q 3 β -Hydroxyurs-12-en-28,13- olide, 273q 3-O-Palmitoylerythrodiol, 287q 28-O-Acetylerythrodiol, 288q 3 β -Acetoxyoleanolic acid, 292q 3 β -Hydroxytaraxastan-28,20 β - olide, 309q α -Tocopherol, 323s	Chang <i>et al.</i> , 1998, 1999, 2007, 2009
<i>D. maritima</i>	Barks	7,8-Dimethoxy-6-hydroxy coumarin, 30e	Gu <i>et al.</i> , 2004

Table 1 (continued)

Plant	part	Compound	Bibliography
<i>D. maritima</i>	Barks	Plumbagin, 112m 7-Methyljuglone, 113m 2-Methoxy-7-methyljuglone, 127m 3-Methoxy-7-methyljuglone, 128m Shinanolone, 129m Maritinone, 135m Chitranone, 139m Zeylanone, 138m	Gu <i>et al.</i> , 2004
	Heartwood	3-(<i>E</i>)-Coumaroylbetulin-28-yl ethylsuccinate, 237q 3-(<i>E</i>)-Coumaroylbetulin-28-yl ethyl (2 <i>R</i>)-2-hydroxy succinate, 238q 3-(<i>E</i>)-Coumaroylbetulin-28-yl ethyl nonanedioate, 239q Diospyrolide, 244q Diospyrolidone, 245q	Kou <i>et al.</i> , 2000
	Fresh fruits	Vanillin, 5b Scopoletin, 29e Abbeokutone, 38f 3 α ,16 α ,17-Trihydroxy kaurane, 39f Plumbagin, 112m 2,3-Epoxyplumbagin, 116m 3-Bromoplumbagin, 117m 3-Chloroplumbagin, 118m	Higa <i>et al.</i> , 1987, 1988, 1998, 2002

Table 1 (continued)

Plant	part	Compound	Bibliography
<i>D. maritima</i>	Fresh fruits	Droserone, 119m 3-Methylplumbagin, 120m 3-(2-hydroxyethyl) plumbagin, 121m 6-(1-Ethoxyethyl) plumbagin, 122m 3,3'-Biplumbagin, 133m 3,8'-Biplumbagin, 134m Maritinone, 135m Elliptinone, 136m Isozeylanone, 138m Chitranone, 139m Methylene-3,3'-biplumbagin, 141m Ethylidene-3,3'-biplumbagin, 142m Ethylidene-3,6'-biplumbagin, 143m Ethyllidene-6,6'-biplumbagin, 144m Lupeol, 215q Betulin, 216q Betulinic acid, 219q Lupenone, 221q β -Amyrin, 285q Oleanolic acid, 290q Glutinol, 304q Friedelin, 315q	Higa <i>et al.</i> , 1987, 1988, 1998, 2002

Table 1 (continued)

Plant	part	Compound	Bibliography
<i>D. melanoxylon</i>	Leaves	Jacoumaric acid methyl ester, 275q Maslinic acid methyl ester, 297q Gallic acid, 6b Piotoaitechuic acid methyl ester, 8b 5,7-Dihydroxy-3- <i>O</i> - β -D-glucopyranosyl-1'''' \rightarrow 6'' glucopyranoside-2-(4-hydroxyphenyl)-4 <i>H</i> -benzopyran-4-one, 67h 4,6-Dihydroxy-2-(4-hydroxyphenyl) hydroxymethylene-3(2 <i>H</i>)-benzofuranone, 68h Selin-4(15)-en-1 β ,11-diol, 198n β -Sitosterol, 199o α -Amyrin, 246q Ursolic acid, 247q Uvaol, 248q Corsolic acid, 255q Pomolic acid methyl ester, 257q Jacoumaric acid methyl ester, 275q β -Amyrin, 285q	Mallavadhani <i>et al.</i> , 1998, 2001, 2005

Table 1 (continued)

Plant	part	Compound	Bibliography
<i>D. melanoxylon</i>	Leaves	Oleanolic acid, 290q Maslinic acid methyl ester, 297q	Mallavadhani <i>et al.</i> , 1998, 2001, 2005
<i>D. mespiliformis</i>	Seed	Myristic acid, 40g Palmitic acid, 41g Stearic acid, 42g Arachidic acid, 43g Myristoleic acid, 44g Palmitoleic acid, 45g Linoleic acid, 46g	Chivandi <i>et al.</i> , 2009
<i>D. mollis</i>	leaves	3-Methyl-naphthalene-1,8-diol, 89k Diospyrol , 97k Diospyrol-8,8'-di- <i>O</i> -(6- β -D- apio furanosyl- β -D- glucopyranoside), 100k	Mongkolsuk <i>et al.</i> , 1965 Paphassarang <i>et al.</i> , 1984
<i>D. montana</i>	Bark	Tetrahydrodiospyrin, 151m	Pardhasaradhi <i>et al.</i> , 1979
	Seeds	8-Hydroxyoctadec-10(<i>Z</i>)-enoic acid, 70i	Rauf <i>et al.</i> , 1987
<i>D. montana</i>	Heartwood Stem bark, Bark	7-Methyljuglone, 113m Diospyrin, 145m 2'-Chlorodiospyrin, 147m 3'-Chlorodiospyrin, 148m 3'-Chloro-2'-hydroxy diospyrin, 149m Isodiospyrin, 152m 8'-Hydroxydiospyrin, 163m	Lillie <i>et al.</i> , 1976

Table 1 (continued)

Plant	part	Compound	Bibliography
<i>D. montana</i>	Heartwood	Biramentacene, 165m	Lillie <i>et al.</i> , 1976
	Stem bark,	Mamegakinone, 167m	
	Bark	Diosquinone, 170m	
		Cyclodiospyrin, 178m	
		Chromenone acid, 180m	
		Chromenone ester, 181m	
		β -Sitosterol, 199o	
		Lupeol , 215q	
		Betulin, 216q	
		Betulinic acid, 219q	
	Allobetulin, 301q		
	Oxyallobetulin , 302q		
<i>D. morrisiana</i>	Stems	Isodiospyrin, 152m	Yan <i>et al.</i> , 1989
		β -Amyrin, 285q	
		Olean-12-en-3-one, 295q	
		β -Amyrin acetate, 291q	
	Heartwoods	3-Methoxyjuglone, 114m	Chen <i>et al.</i> , 1987
		Shinanolone, 129m	
		Isodiospyrin, 152m	
		3'-Methoxy isodiospyrin, 154m	
		3,3'-Dimethoxy isodiospyrin, 157m	
		β -Sitosterol, 199o	
		Sitosterol 3-O- β -D- glucopyrano side, 206o	
		Lupeol , 215q	
		Betulinic acid, 219q	

Table 1 (continued)

Plant	part	Compound	Bibliography
<i>D. morrisiana</i>	Heartwoods	2'-Methoxy isodiospyrin, 153m 2,2'-Dimethoxy isodiospyrin, 154m 2,3'-Dimethoxy isodiospyrin, 156m 8'-Hydroxy-3-methoxy isodiospyrin, 158m 2'-Chloro-3,3'-dimethoxy isodiospyrin, 159m β -D-Dlucopyranose pentaacetate, 213p	Chen <i>et al.</i> , 1987
<i>D. nigra</i>	Aerial parts	Diospyrodin, 74i	Dinda <i>et al.</i> , 2006
<i>D. peregrina</i>	Roots	5,7,3,5'-Tetrahydroxy-3'-methoxy flavanone, 4'-O- α -L-rhamnopyranoside, 64h	Chauhan <i>et al.</i> , 1979
	Stems	Nonadecan-7-ol-2-one, 69i	Chauhan <i>et al.</i> , 1980
	Fruits	Peregrinol, 223q Ferano-(2'',3'',7,8)-3',5'-dimethoxy-5-hydroxyflavone, 51h Marsformosanone, 253q	Jain <i>et al.</i> , 1994, 1997 Bhaumik <i>et al.</i> , 1981
<i>D. quaesita</i>	Leaves	Betulinic acid 3-caffeate, 231q Diospyrosin, 108l	Ma <i>et al.</i> , 2008
<i>D. quiloensis</i>	Heartwoods	5-Hydroxy-4,6,8-trimethoxy naphthaldehyde, 71k	Harper <i>et al.</i> , 1970

Table 1 (continued)

Plant	part	Compound	Bibliography
<i>D. quiloensis</i>	Heartwoods	4,5,6,8-Tetramethoxy naphthalene, 79k 4,5-Dimethoxy naphthaldehyde, 91k 4,5,6-Trimethoxy naphthaldehyde, 92k 5-Hydroxy-4-methoxy-2-naphthaldehyde, 93k	Harper <i>et al.</i> , 1970
<i>D. rhodocalyx</i>	Barks	T β -Sitosterol, 199o Lupeol, 215q Betulin, 216q Stigma-4-en-3-one, 201o Betulinic acid, 219q Lupenone, 221q Taraxerol, 305q Taraxeryl acetate, 307q Araxerone, 308q	Sutthivaiyakit <i>et al.</i> , 1995
<i>D. samoensis</i>	leaves	Plumbagin, 112m <i>iso</i> -Shinanolone, 130m Maritinone, 135m Elliptinone, 136m	Richomme <i>et al.</i> , 1991
<i>D. sanza-minika</i>	Stem barks	Norbergenin, 15b 11- <i>O-p</i> -Hydroxybenzoyl norbergenin, 16b 4- <i>O</i> -Galloylnorbergenin, 17b 4- <i>O</i> -(3'-Methylgalloyl) norbergenin, 18b	Tangmouo <i>et al.</i> , 2009

Table 1 (continued)

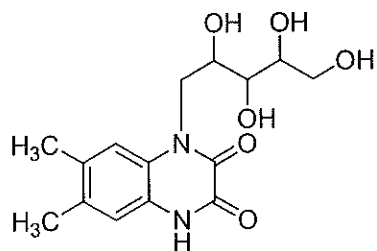
Plant	part	Compound	Bibliography
<i>D. sanza-minika</i>	Stem barks	4- <i>O</i> -Syringoylnorbergenin, 19b	Tangmouo <i>et al.</i> , 2009
<i>D. sylvatica</i>	Roots	Plumbagin, 112m Diospyrin, 145m Isodiospyrin, 152m Diosindigo A, 173m Microphyllone, 187m 2-Methyl-anthraquinone, 195m	Ganapaty <i>et al.</i> , 2004
<i>D. tricolor</i>	Roots	Diosquinone, 170m	Alake, 1994
<i>D. usambarensis</i>	Stem barks	Diosindigo A, 173m Diosindigo B, 174m 7-Methyljuglone, 113m Mamegakinone, 167m Bisisodiospyrin, 188m	Khan, <i>et al.</i> , 1989
<i>D. verrucosa</i>	Root barks	7-Methyljuglone, 113m Isodiospyrin, 152m Diosquinone, 170m Diosindigo A, 173m Betulin , 216q Betulinic acid, 219q	Khan, <i>et al.</i> , 1987
<i>D. virginiana</i>	Roots	4-Hydroxy-5,6-dimethoxy naphthalene-2-carbaldehyde, 96k 7-Methyljuglone, 113m Shinanolone, 129m Diospyrin, 145m	Wang <i>et al.</i> , 2011

Table 1 (continued)

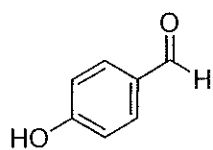
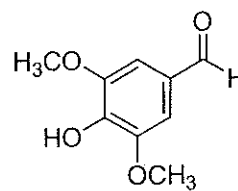
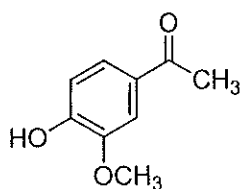
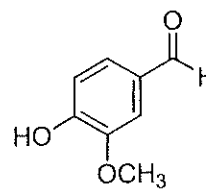
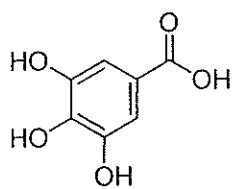
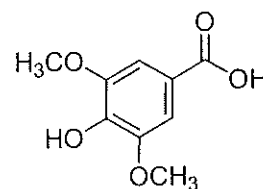
Plant	part	Compound	Bibliography
<i>D. virginiana</i>	Roots	Isodiospyrin, 152m Lupeol, 215q Betulin, 216q Betulinaldehyde, 218q Betulinic acid, 219q 12,13-Dehydro-20,29-dihydro betulin, 225q Ursolic acid, 247q	Wang <i>et al.</i> , 2011
<i>D. villosiuscula</i>	Roots and Stem barks	Diosindigo A, 173m Diosindigo B, 174m Taraxerol methyl ether, 306q	Khan, <i>et al.</i> , 1999

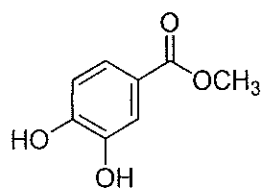
Structures

a: alkaloid

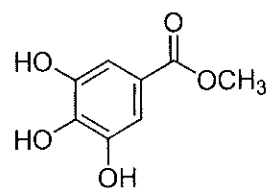
**1a:** Tatarine C

b: benzenoids

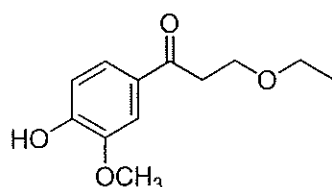
**2b:** 4-Hydroxybenzaldehyde**3b:** 4-Hydroxy-3,5-dimethoxy-
benzaldehyde**4b:** Acetovanillone**5b:** Vanillin**6b:** Gallic acid**7b:** Syringic acid



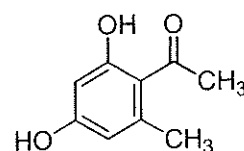
8b: Piotoaitechuic acid methyl ester



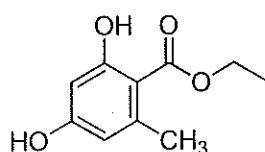
9b: Methyl gallate



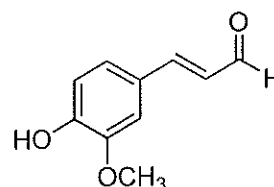
10b: 3-Ethoxy-1-(4-hydroxy-3-methoxyphenyl)-1-propanone



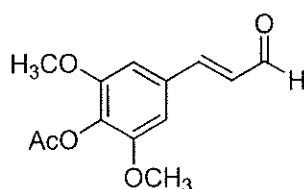
11b: 1-(4,6-Dihydroxy-2-methylphenyl)ethanone



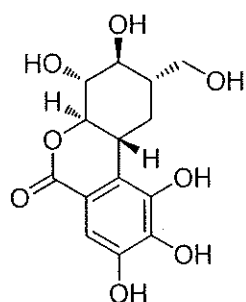
12b: Ethyl 2,4-dihydroxy-6-methylbenzoate



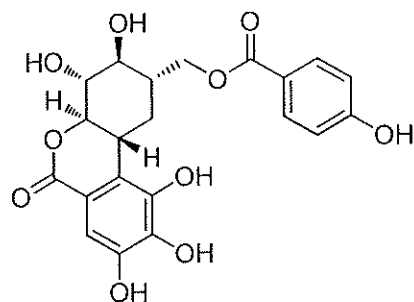
13b: *trans*-Coniferylaldehyde



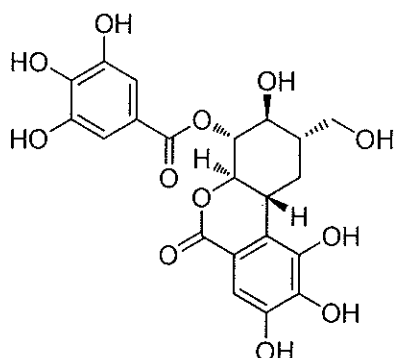
14b: (*E*)-3-(4-Acetyloxy-3,5-dimethoxyphenyl)-2-propenal



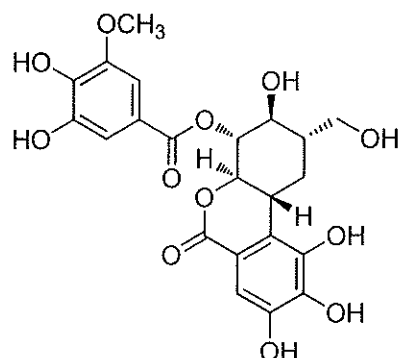
15b: Norbergenin



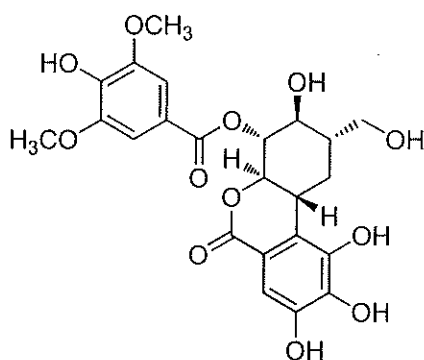
16b: 11-*O*-*p*-Hydroxybenzoyl norbergenin



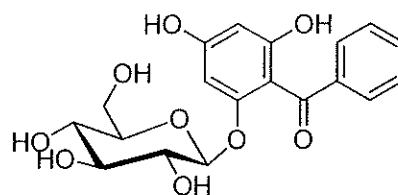
17b: 4-*O*-Galloylnorbergenin



18b: 4-*O*-(3'-Methylgalloyl) norbergenin

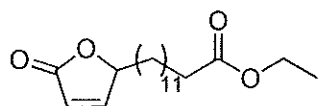


19b: 4-*O*-Syringoylnorbergenin



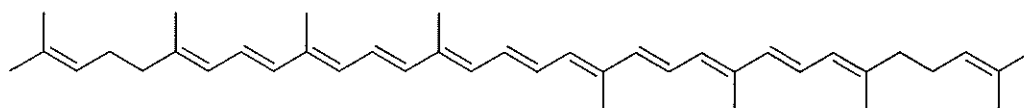
20b: Kakispyrone

c: betenolide

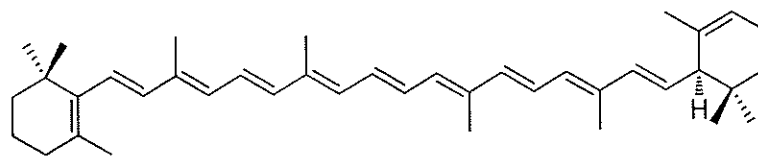
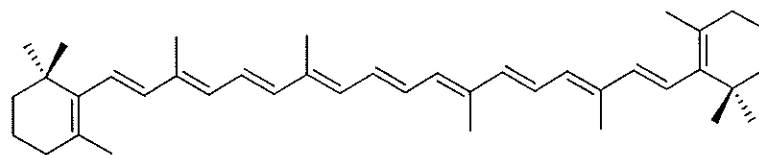
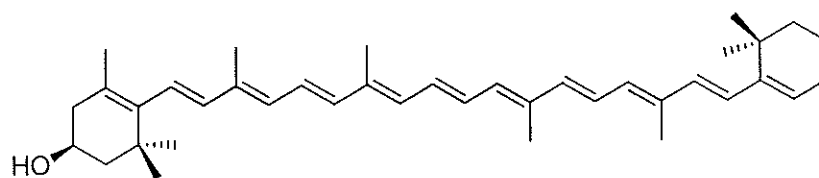


21c: Maritolide

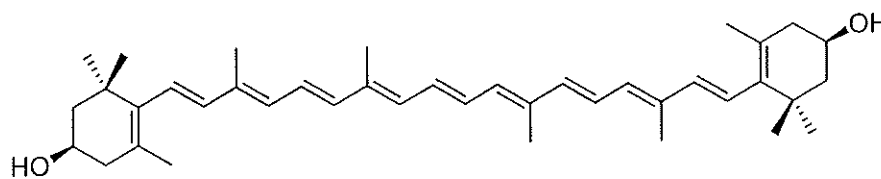
d: carotenoids



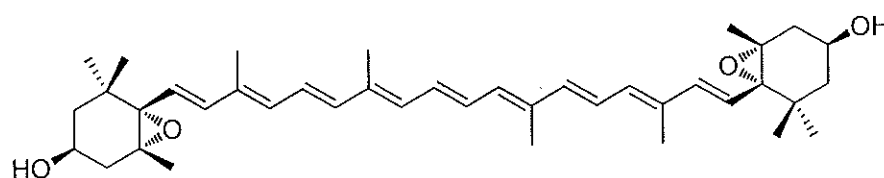
22d: Lycopene

23d: α -Carotene24d: β -Carotene

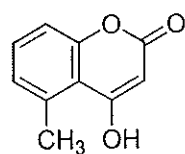
25d: Cryptoxanthin



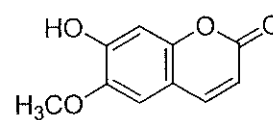
26d: Zeaxanthin



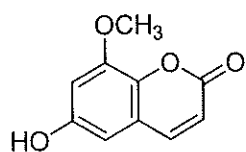
27d: Violaxanthin

e: coumarins

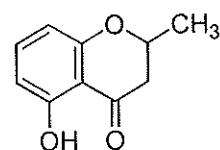
28e: 4-Hydroxy-5-methylcoumarin



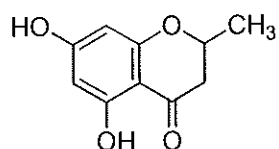
29e: Scopoletin



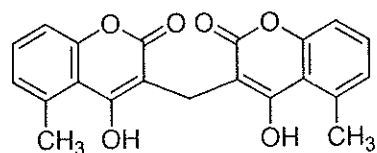
30e: 7,8-Dimethoxy-6-hydroxycoumarin



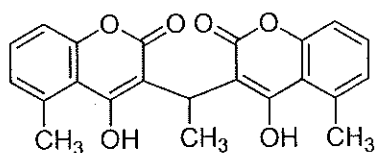
31e: 5-Hydroxy-2-methylchromanone



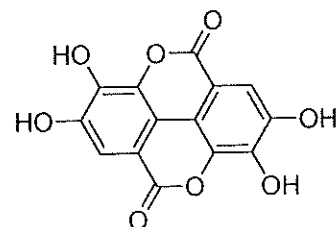
32e: 5,7- Dihydroxy-2-methyl chromanone



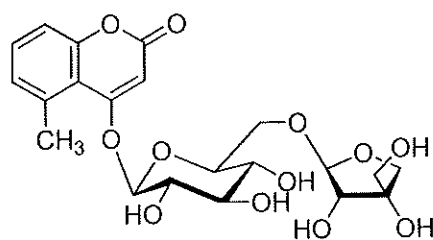
33e: Gerberinol



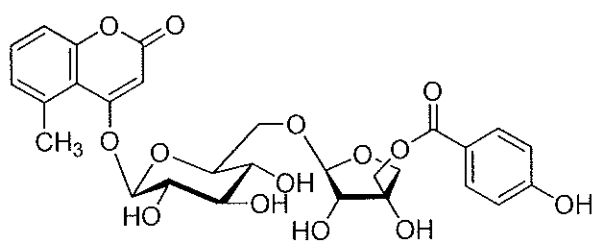
34e: 11-Methylgerberinol



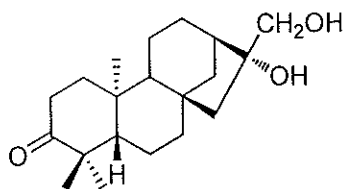
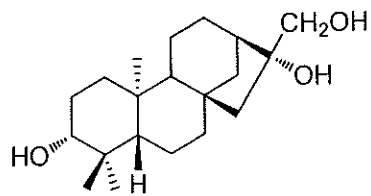
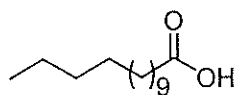
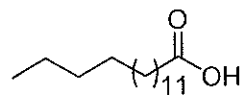
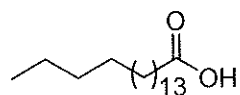
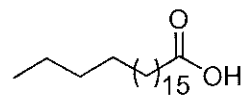
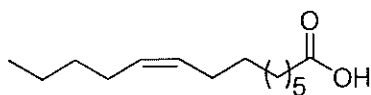
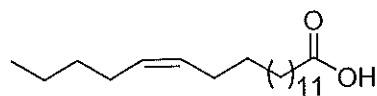
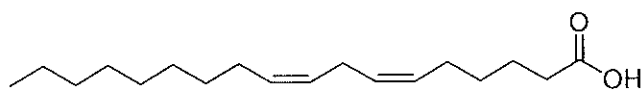
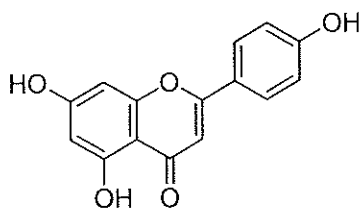
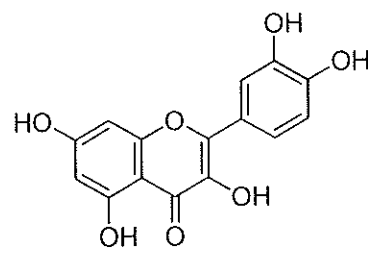
35e: Ellagic acid

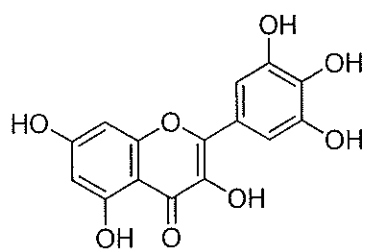
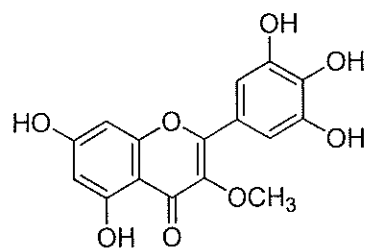
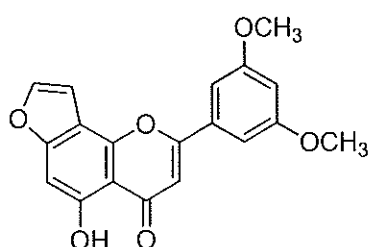
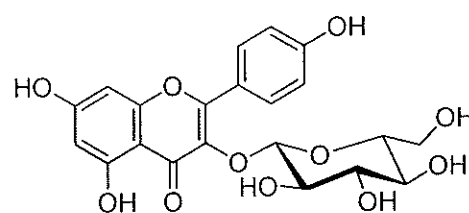
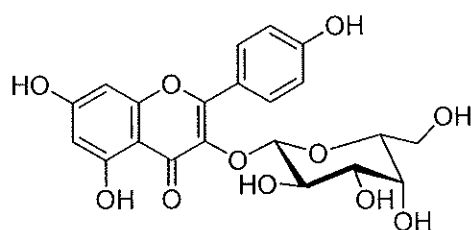
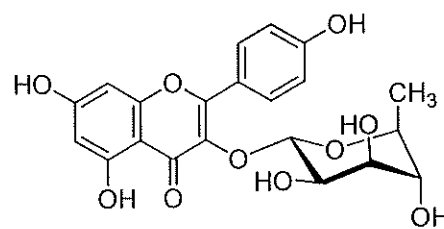
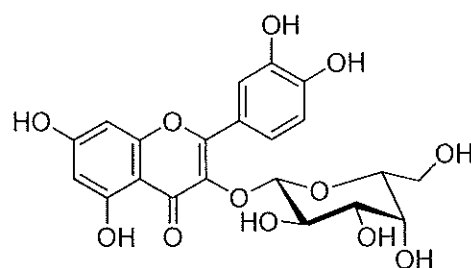
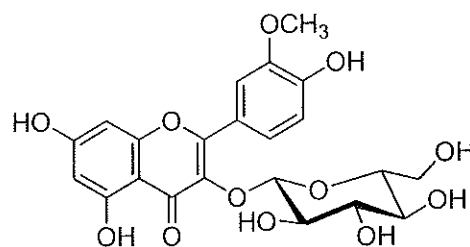


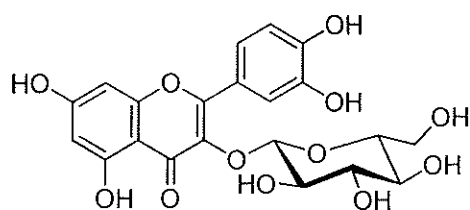
36e: Diosfeboside A



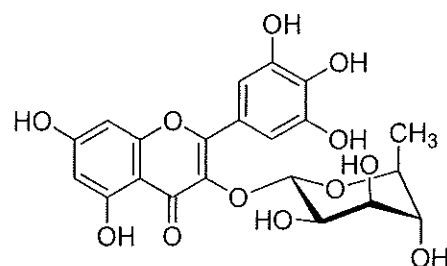
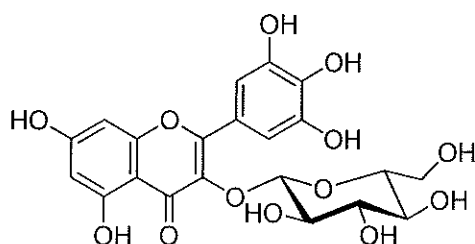
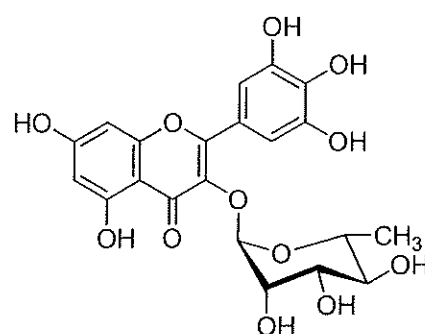
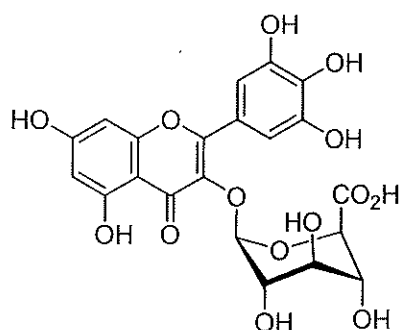
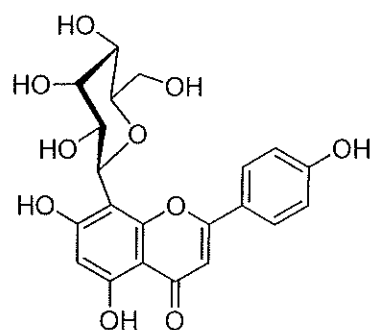
37e: Diosfeboside B

f: diterpenoids**38f:** Abbeokutone**39f:** 3 α ,16 α ,17-Trihydroxykaurane**g: fatty acids****40g:** Myristic acid**41g:** Palmitic acid**42g:** Stearic acid**43g:** Arachidic acid**44g:** Myristoleic acid**45g:** Palmitoleic acid**46g:** Linoleic acid**h: flavonoids****47h:** Kaempferol**48h:** Quercetin

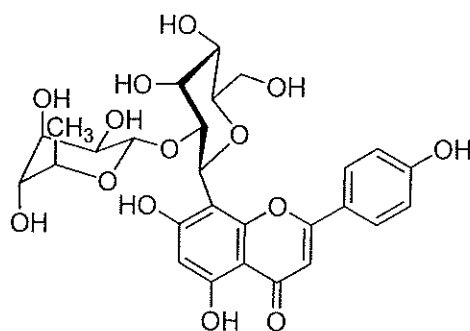
**49h:** Myricetin**50h:** Annulatin**51h:** Ferano-(2'',3'',7,8)-3',5'-dimethoxy-5-hydroxyflavone**52h:** Astragalin**53h:** Trifolin**54h:** Kampferol-3-O- α -L-rhamnopyranoside**55h:** Hyperin**56h:** Isorhamnetin-3-O- β -D-glucopyranoside



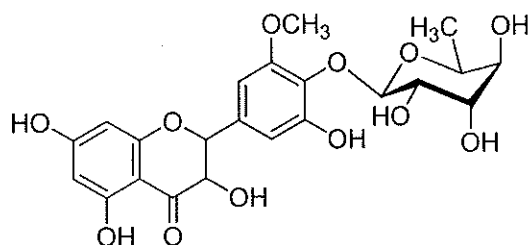
57h: Isoquercetin

58h: Myricetin-3-O- α -L-rhamnopyranoside59h: Myricetin-3-O- β -D-glucopyranoside60h: 56h: Myricetin 3-O- α -rhamnoside61h: Myricetin 3-O- β -glucuronide

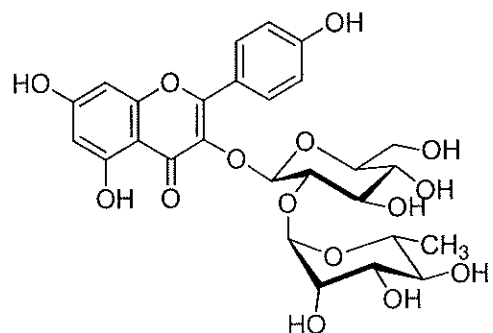
62h: Vitexin



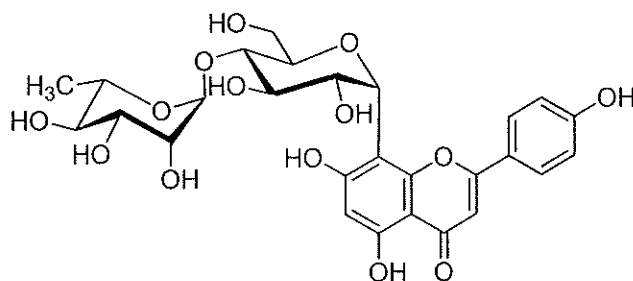
63h: 2''-O-Rhamnosyl vitexin



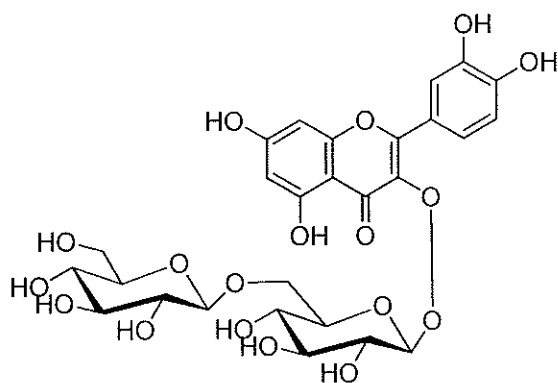
64h: 5,7,3,5'-Tetrahydroxy-3'-methoxyflavanone, 4'-O- α -L-rhamnopyranoside



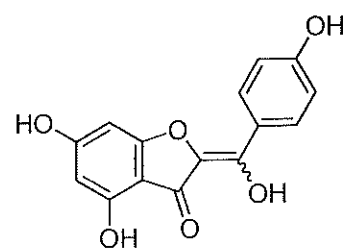
65h: kaempferol 3-O- α -L-rhamnopyranosyl-(1 \rightarrow 2)- β -D-glucopyranoside



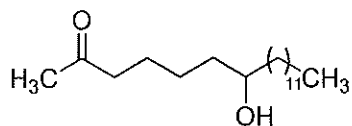
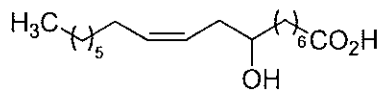
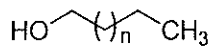
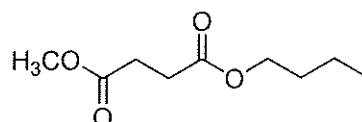
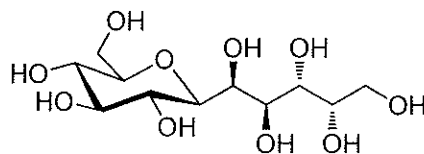
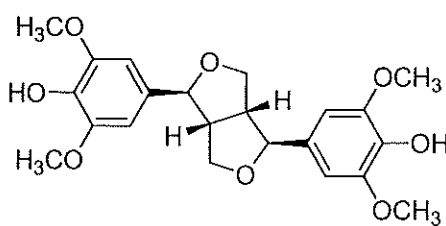
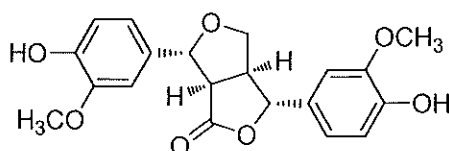
66h: 8-C-[α -L-Rhamnopyranosyl-(1 \rightarrow 4)]- α -D-glucopyranosyl apigenin

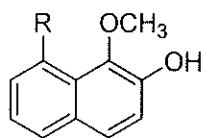
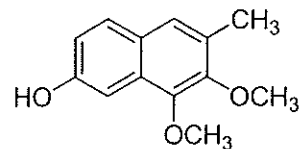
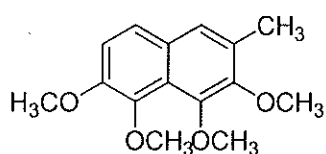
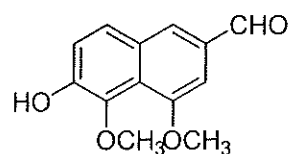
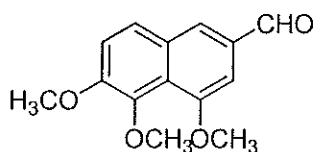
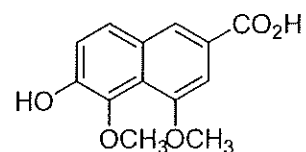
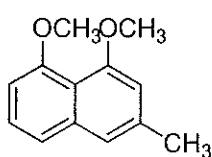
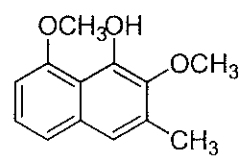
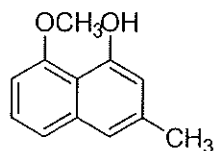
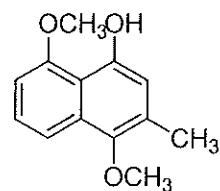


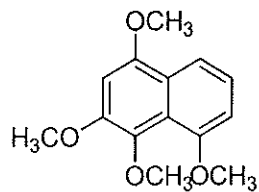
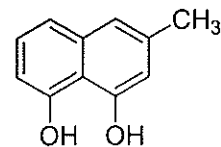
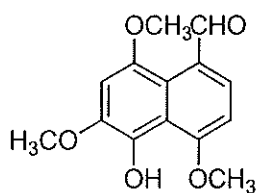
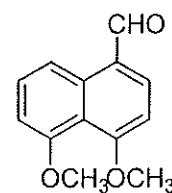
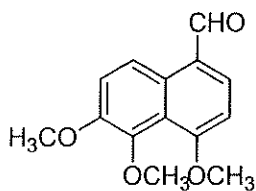
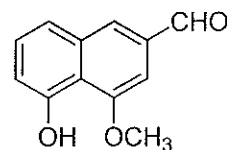
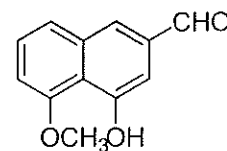
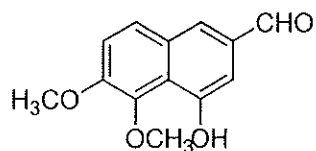
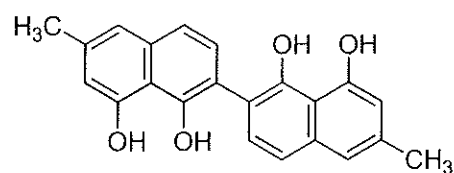
67h: 5,7-Dihydroxy-3-O- β -D-glucopyranosyl-1''' \rightarrow 6''glucopyranoside-2-{4-hydroxyphenyl}-4H-benzopyran-4-one

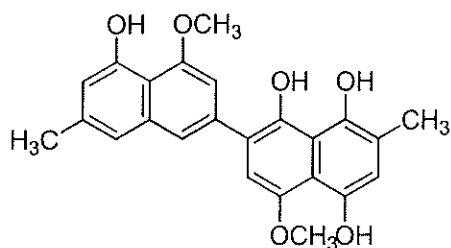


68h: 4,6-Dihydroxy-2-(4-hydroxyphenyl)hydroxymethylene-3(2H)-benzofuranone

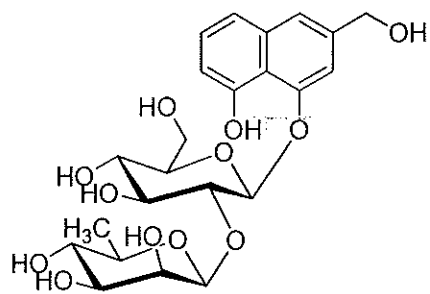
i: hydrocabons**69i:** Nonadecan-7-ol-2-one**70i:** 8-Hydroxyoctadec-10(Z)-enoic acid**71i:** n=22; *n*-Hexacosanol**72i:** n= 24; *n*-Nonacosane**73i:** Butylmethyl succinate**74i:** Diospyrodin**j: lignans****75j:** (+)-Syringaresinol**76j:** 4-Ketopinoresinol

k: naphthalenes**77k:** R= OH; Macassar II**78k:** R= OCH₃; Macassar III**79k:** 2-Methyl-3,6-dihydroxy-4,5-dimethoxynaphthalene**80k:** 2-Methyl-3,4,5,6-tetramethoxy naphthalene**81k:** 6-Hydroxy-4,5-dimethoxy-2-naphthaldehyde**82k:** 4,5,6-Trimethoxy-2-naphthaldehyde**83k:** 6-Hydroxy-4,5-dimethoxy-2-naphthoic acid**84k:** 3-Methyl-1,8-dimethoxynaphthalene**85k:** 3-Methyl-2,8-dimethoxy-1-naphthol**86k:** 3-Methyl-8-methoxy-1-naphthol**87k:** 3-Methyl-4,8-dimethoxy-1-naphthol

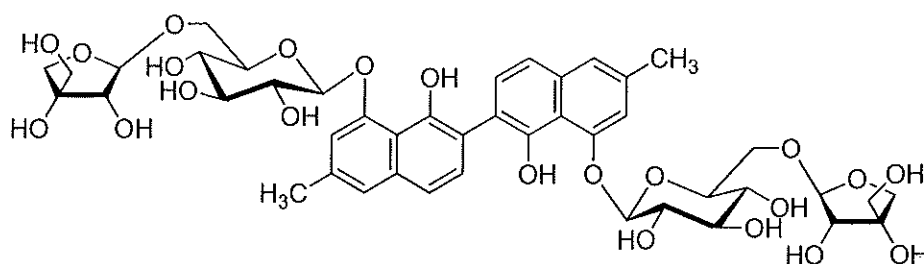
**88k:** 4,5,6,8-Tetramethoxy naphthalene**89k:** 3-Methyl-naphthalene-1,8-diol**90k:** 5-Hydroxy-4,6,8-trimethoxynaphthaldehyde**91k:** 4,5-Dimethoxy naphthaldehyde**92k:** 4,5,6-Trimethoxynaphthaldehyde**93k:** 5-Hydroxy-4-methoxy-2-naphthaldehyde**94k:** 4-Hydroxy-3,5-dimethoxy-2-naphthaldehyde**95k:** 4-Hydroxy-5-methoxy-2-naphthaldehyde**96k:** 4-Hydroxy-5,6-dimethoxy naphthalene-2-carbaldehyde**97k:** Diospyrol



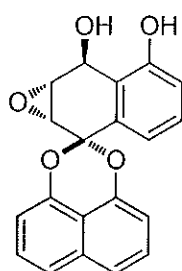
98k: Dihydrodiosindigo B



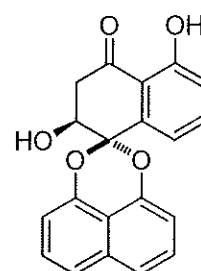
99k: Diospyronaphthoside



100k: Diospyrol-8,8'-di-O-(6- β -D-apiofuranosyl- β -D-glucopyranoside)

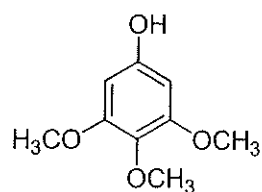


101k: Palmarumycins JC1

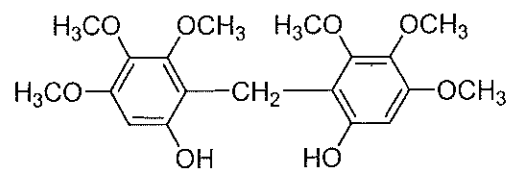


102k: Palmarumycins JC2

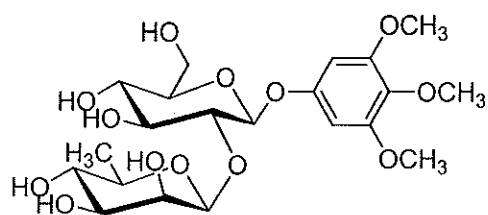
I: phenolics



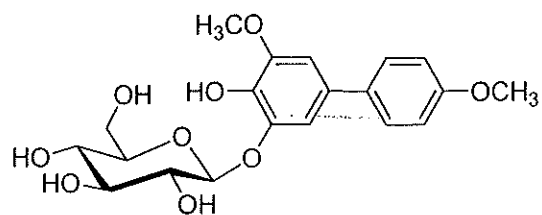
103l: 3,4,5-Trimethoxyphenol



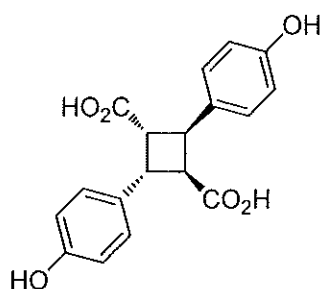
104l: *bis* (6-Hydroxy-2,3,4-trimethoxyphen-1-yl)methane



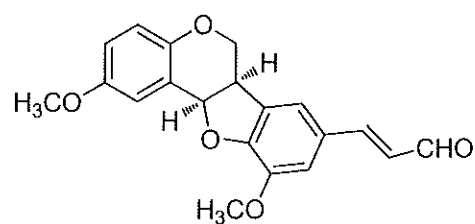
105l: Diospyrososide



106l: Kakispyrol

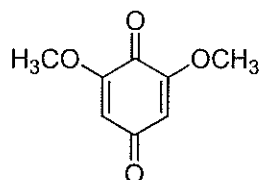


107l: 4,4'-Dihydroxy- α -truxillic acid

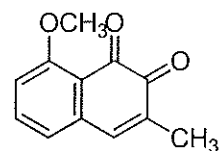


108l: Diospyrosin

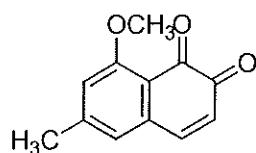
m: quinones



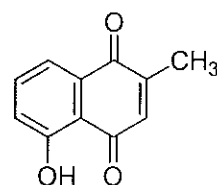
109m: 2,6-Dimethoxy-1,4-benzoquinone



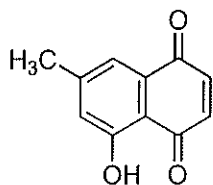
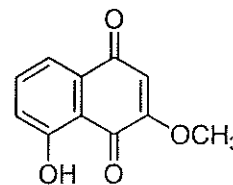
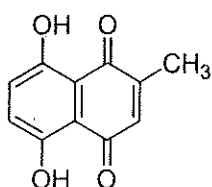
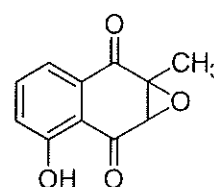
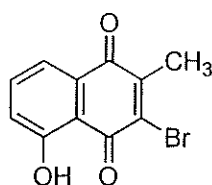
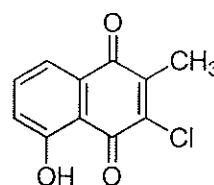
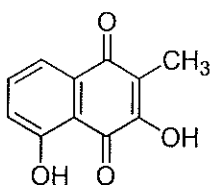
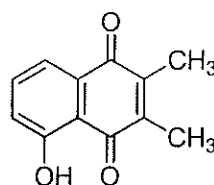
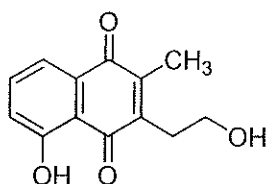
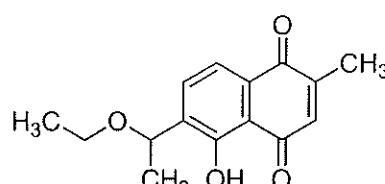
110m: 3-Methyl-8-methoxy-1,2-naphthoquinone

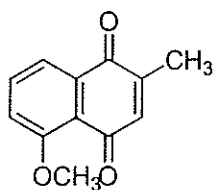


111m: 8-Methoxy-6-methyl-1,2-naphthoquinone

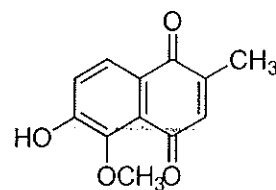


112m: Plumbagin

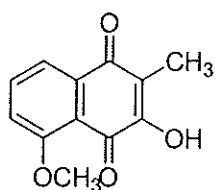
**113m:** 7-Methyljuglone**114m:** 3-Methoxyjuglone**115m:** 2-Methyl naphthazarine**116m:** 2,3-Epoxyplumbagin**117m:** 3-Bromoplumbagin**118m:** 3-Chloroplumbagin**119m:** Droserone**120m:** 3-Methylplumbagin**121m:** 3-(2-Hydroxyethyl) plumbagin**122m:** 6-(1-Ethoxyethyl) plumbagin



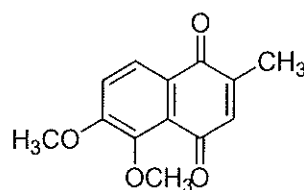
123m: 2-Methyl-5-methoxy-1,4-naphthoquinone



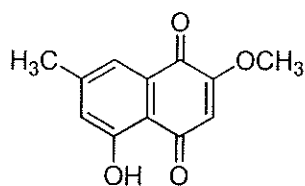
124m: Diomelquinone



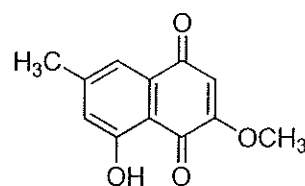
125m: 2-Methyl-3-hydroxy-5-methoxy-1,4-naphthoquinone



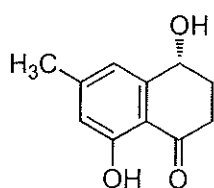
126m: 2-Methyl-5,6-dimethoxy-1,4-naphthoquinone



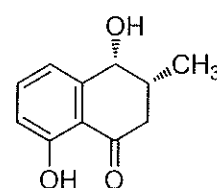
127m: 2-Methoxy-7-methyljuglone



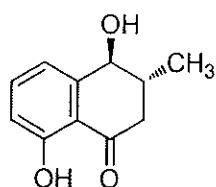
128m: 3-Methoxy-7-methyljuglone



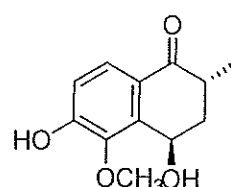
129m: Shinanolone



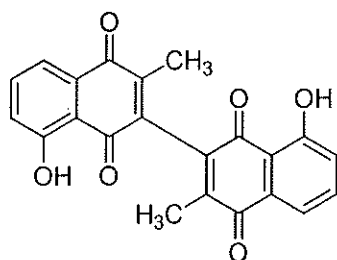
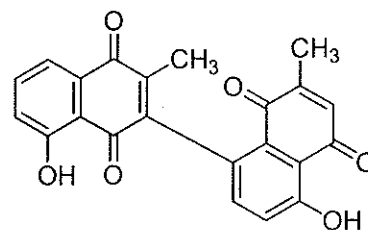
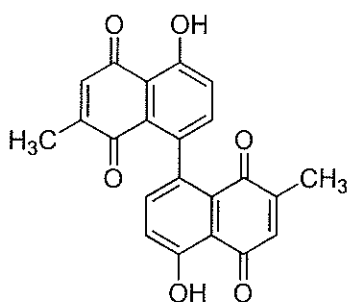
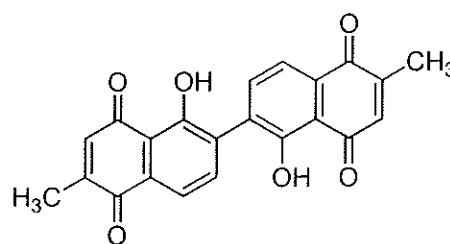
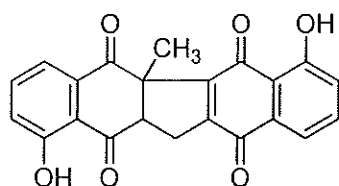
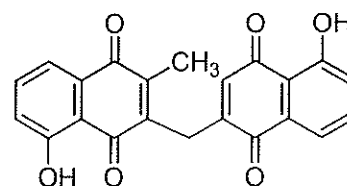
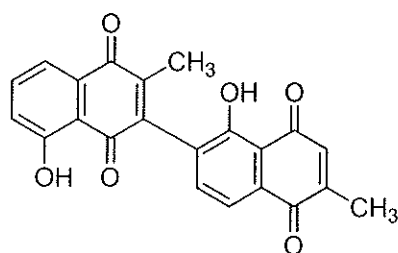
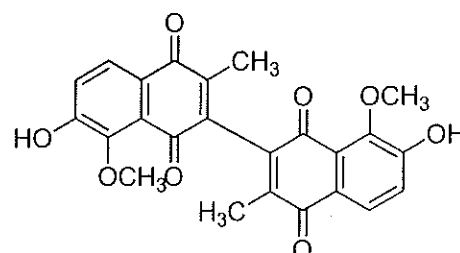
130m: *iso*-Shinanolone

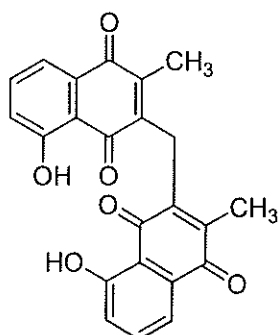


131m: *epi*-Isoshinanolone

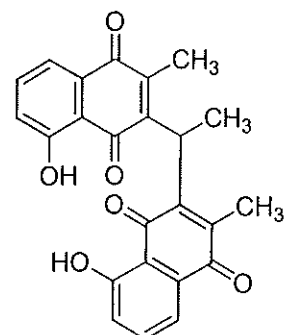


132m: Tetralone

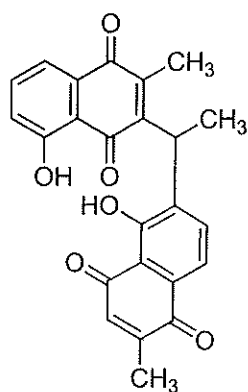
**133m:** 3,3'-Biplumbagin**134m:** 3,8'-Biplumbagin**135m:** Maritinone**136m:** Elliptinone**137m:** Zeylanone**138m:** Isozeylanone**139:** Chitrone**140m:** 3,3'-Dimer-6-hydroxy-5-methoxy-
2-methyl naphthoquinone



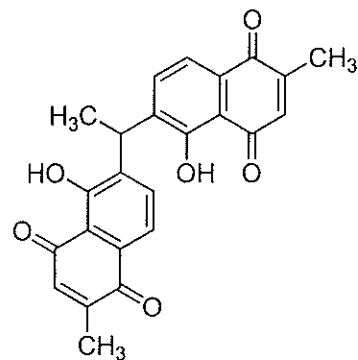
141m: Methylene-3,3'-biplumbagin



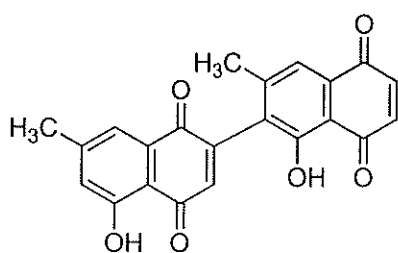
142m: Ethylidene-3,3'-biplumbagin



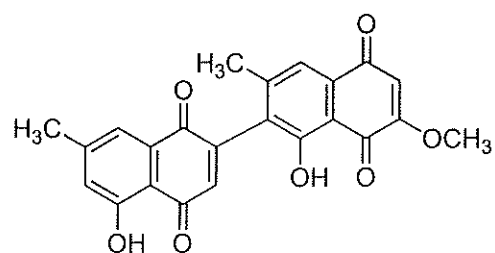
143m: Ethylidene-3,6'-biplumbagin



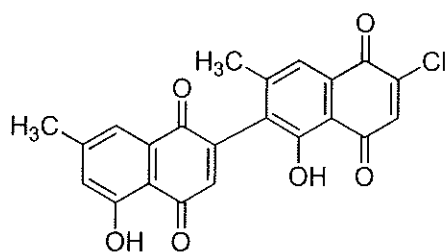
144m: Ethylidene-6,6'-biplumbagin



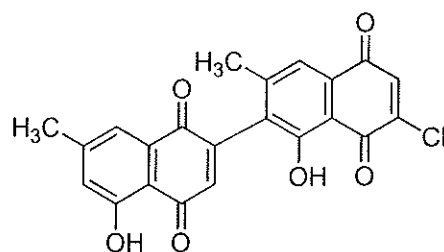
145m: Diospyrin



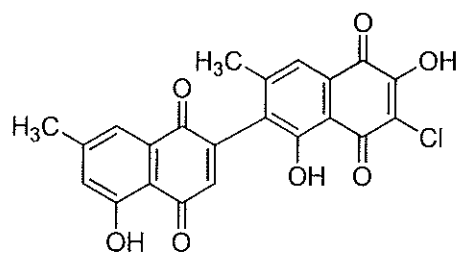
146m: 3'-Methoxydiospyrin



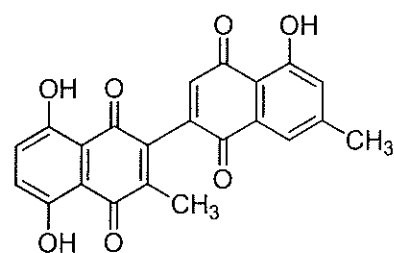
147m: 2'-Chlorodiospyrin



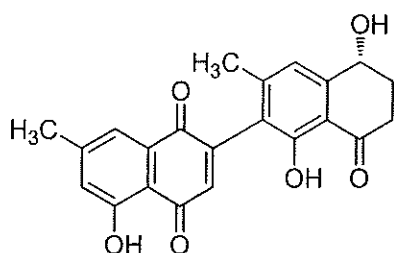
148m: 3'-Chlorodiospyrin



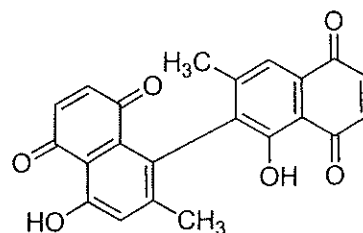
149m: 3'-Chloro-2'-hydroxydiospyrin



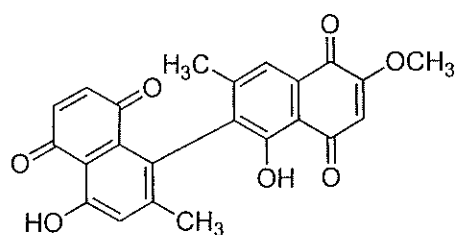
150m: 8'-Hyxydiospyrin



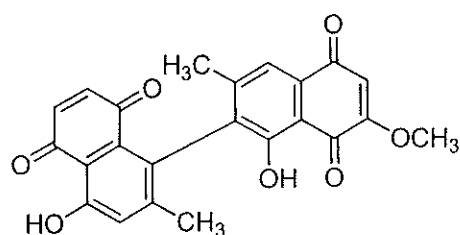
151m: Tetrahydrodiospyrin



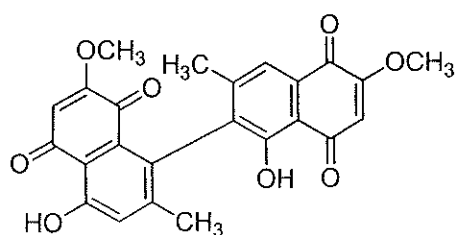
152m: Isodiospyrin



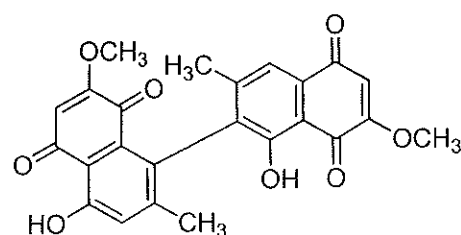
153m: 2'-Methoxy isodiospyrin



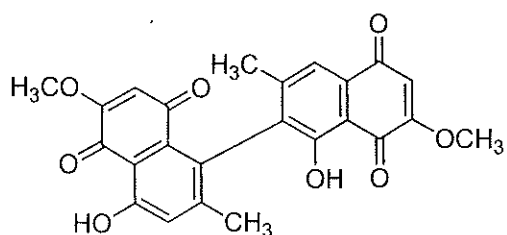
154m: 3'-Methoxy isodiospyrin



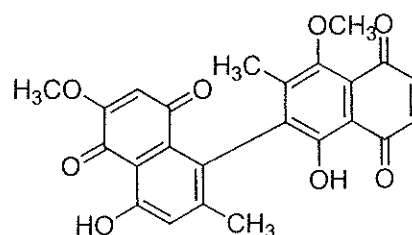
155m: 2,2'-Dimethoxy isodiospyrin



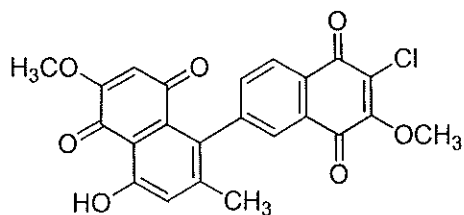
156m: 2,3'-Dimethoxy isodiospyrin



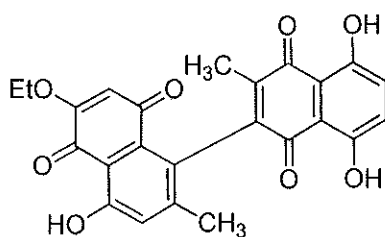
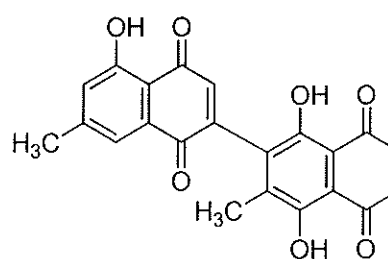
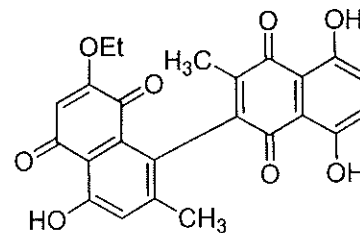
157m: 3,3'-Dimethoxy isodiospyrin



158m: 8'-Hydroxy-3-methoxy isodiospyrin

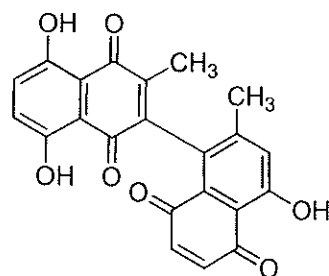


159m: 2'-Chloro-3,3'-dimethoxyisodiospyrin

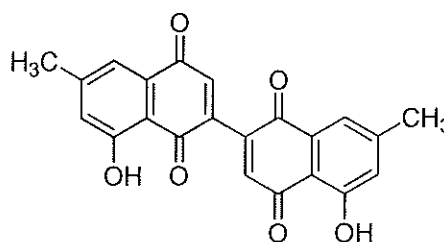


161m: 3-Ethoxy-8'-hydroxyisodiospyrin

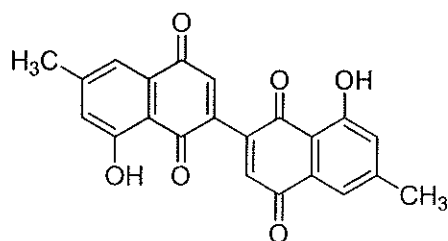
162m: Hydroxyisodiospyrin



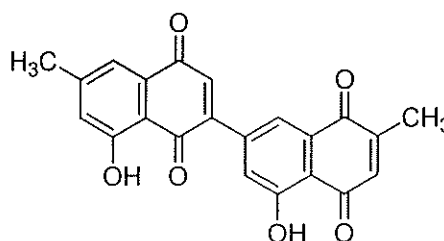
163m: 8'-Hydroxyisodiospyrin



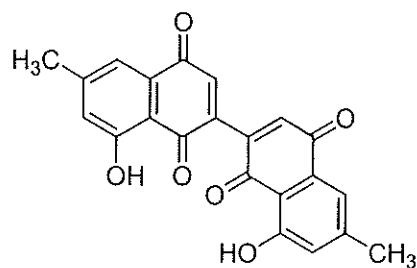
164m: Rotundiquinone



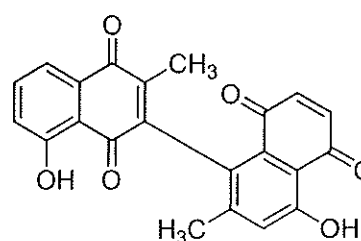
165m: Biramentaceone



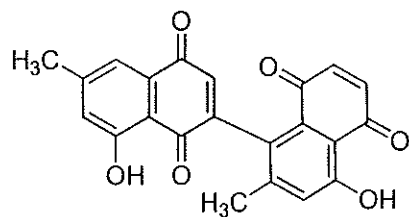
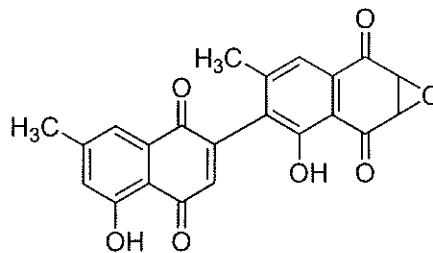
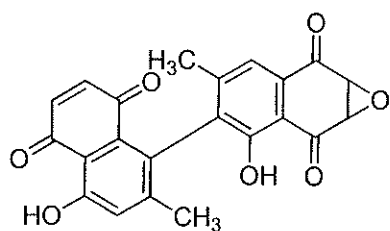
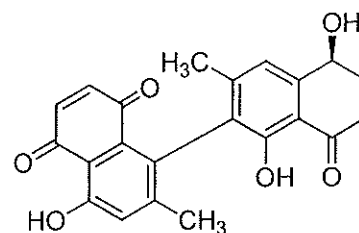
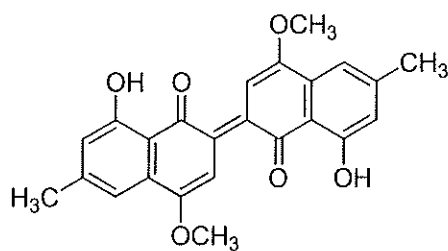
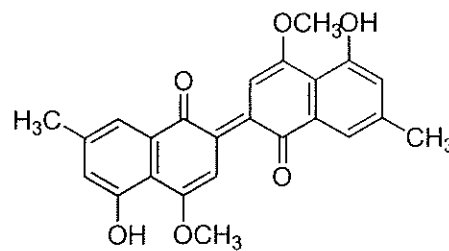
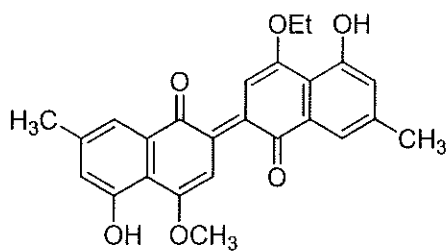
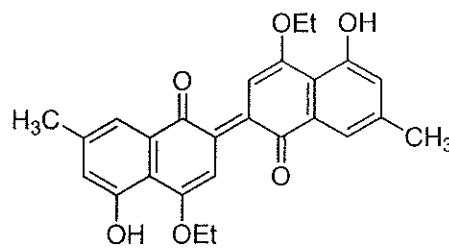
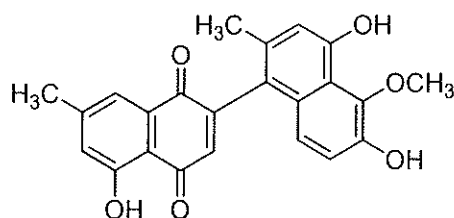
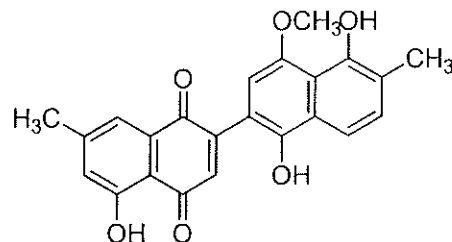
166m: Ehretione

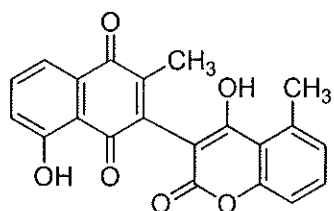
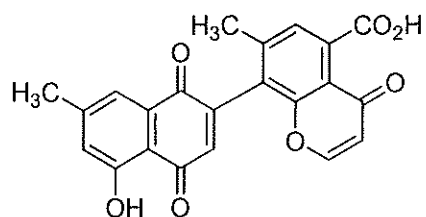
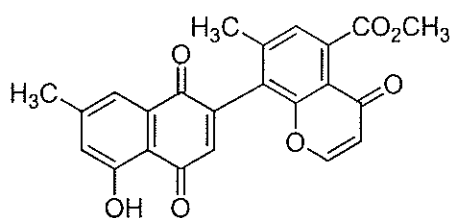
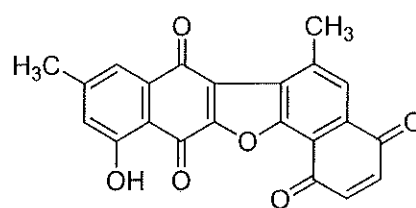
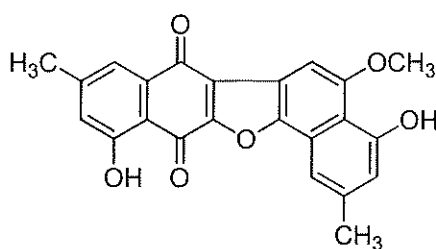
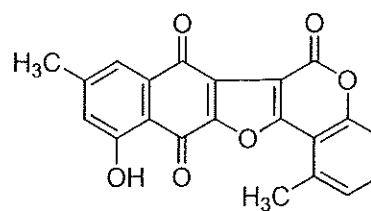
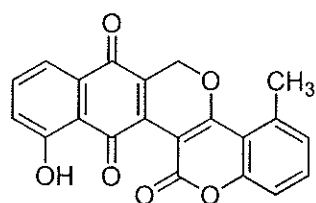
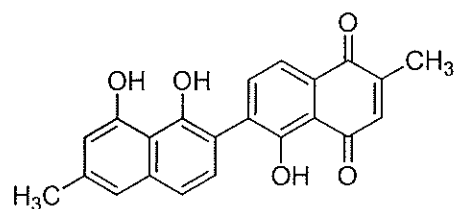
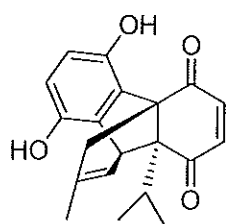
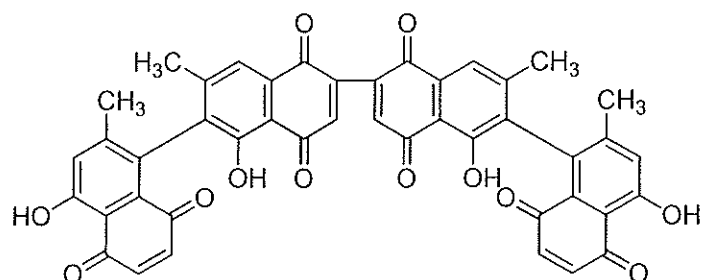


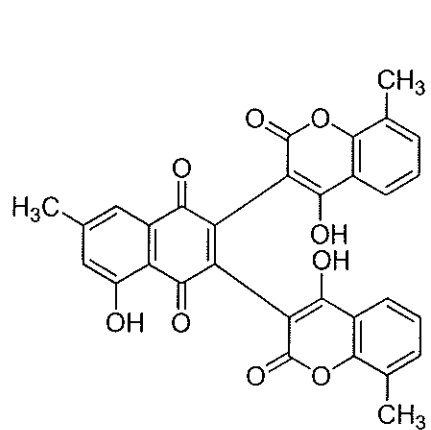
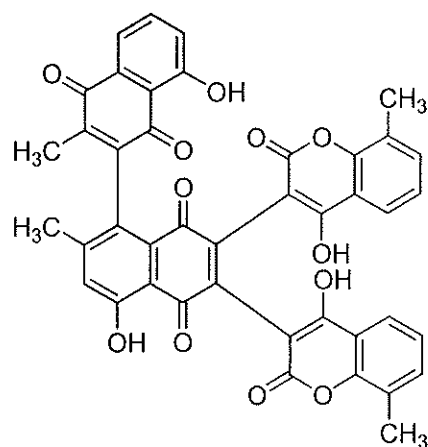
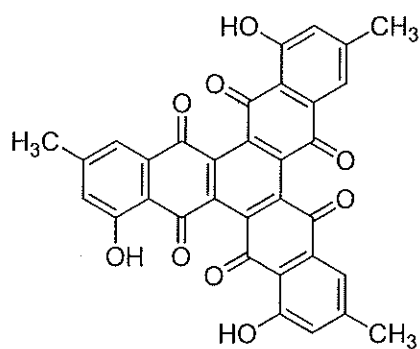
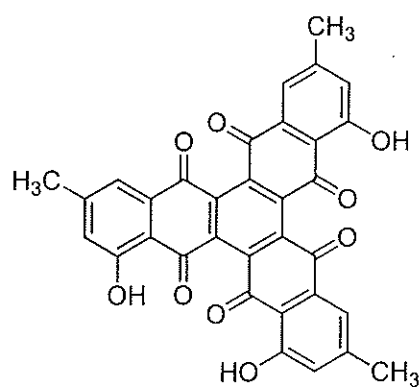
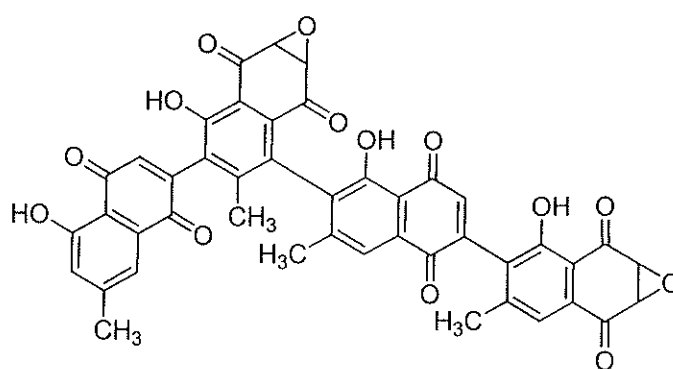
167m: Mamegakinone

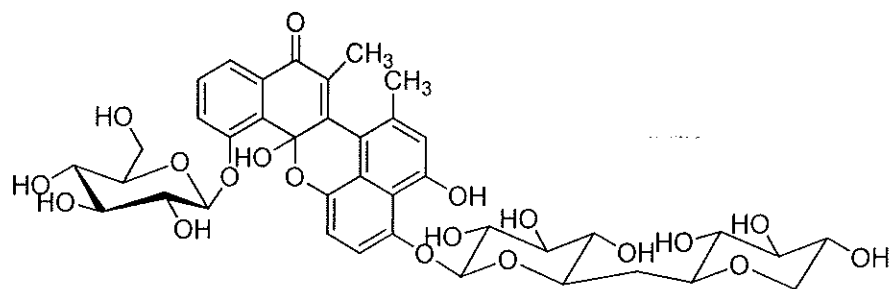


168m: Habibone

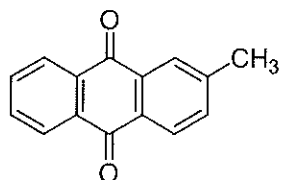
**169m:** Neodiospyrin**170m:** Diosquinone**171m:** Batacanone**172m:** Isodiospyrol A**173m:** Diosindigo A**174m:** Diosindigo B**175m:** Diosindigo B₁**176m:** Diosindigo B₂**177m:** Celebaquinone**178m:** Isocelebaquinone

**179m:** Canaliculatin**180m:** Chromenone acid**181m:** Chromenone ester**182m:** Violet quinone**183m:** Cyclodiospyrin**184m:** Crassiflorone**185m:** Cyclocanaliculatin**186m:** Ebenone**187m:** Microphyllone**188m:** Bisisodiopyrin

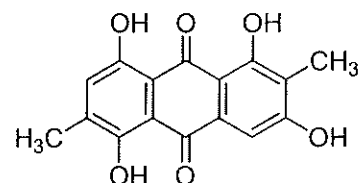
**189m:** Ismailin**190m:** Diospyrone**191m:** Xylopyrin**192m:** Isoxylopyrin**193m:** 6'',8'-Bisdiosquinone



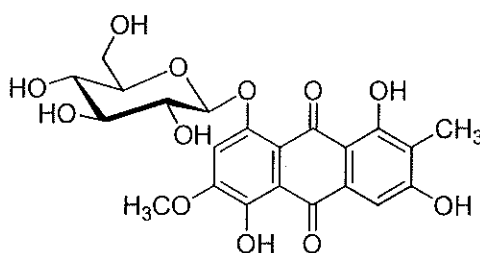
194m: 1',2-Binaphthalen-4-one-2',3-dimethyl-1,8'-epoxy-1,4',5,5',8,8'-hexahydroxy-8-
O- β -glucopyranosyl-5'-O- α -xylopyranosyl(1 \rightarrow 6)- β -glucopyranoside



195m: 2-Methyl anthraquinone

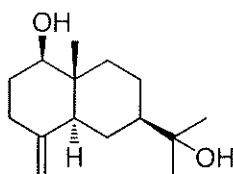


196m: Aglycone



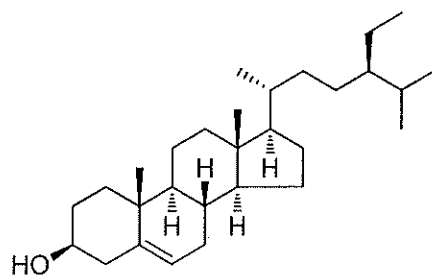
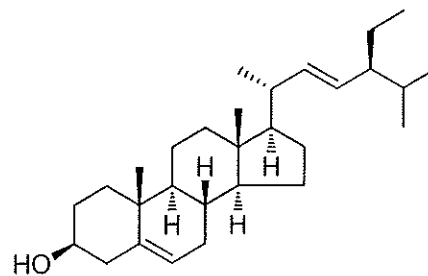
197m: 1,3,5-Trihydroxy-6-methoxy-2-methylanthraquinone 8-O- β -D-glucopyranoside

n: sesquiterpenoid

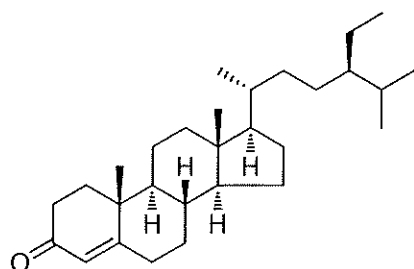


198n: Selin-4(15)-en-1 β ,11-diol

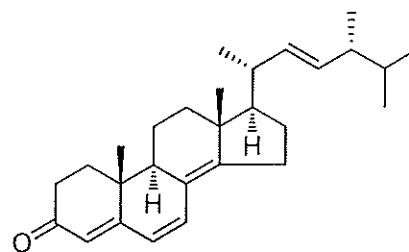
o: steroids

199o: β -Sitosterol

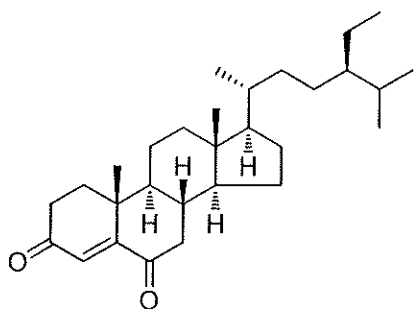
200o: Stigmasterol



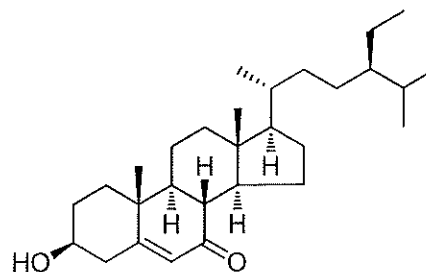
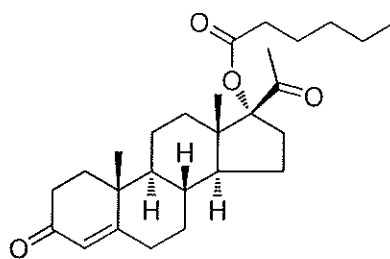
201o: Stigmasta-4-en-3-one



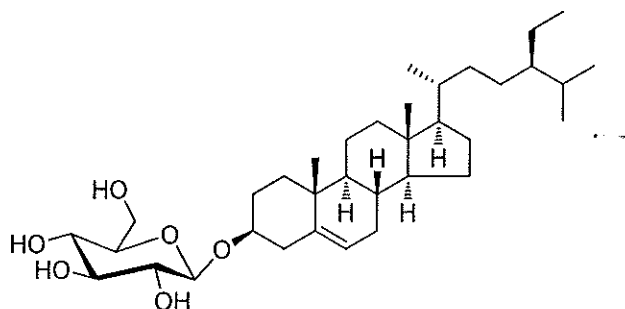
202o: Ergosta-4,6,8(14),22-tetraen-3-one



203o: Stigmast-4-ene-3,6-dione

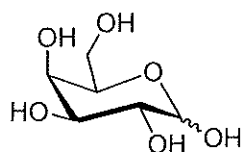
204o: 3 β -Hydroxystigmast-5-en-7-one

205o: Neolutein

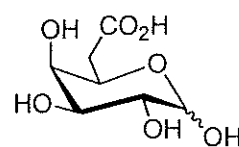


206o: Sitosterol 3-*O*- β -D-glucopyranoside

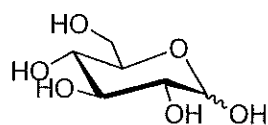
p: sugars



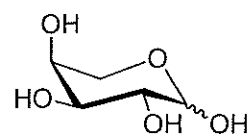
207p: D-Galactose



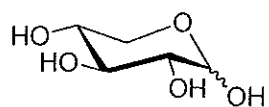
208p: D-Galacturonic acid



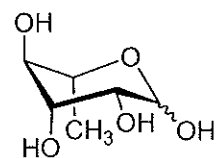
209p: D-Glucose



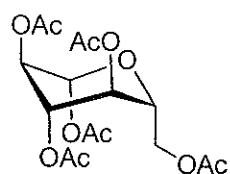
210p: L-Arabinose



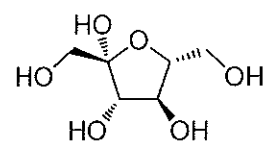
211p: D-Xylose



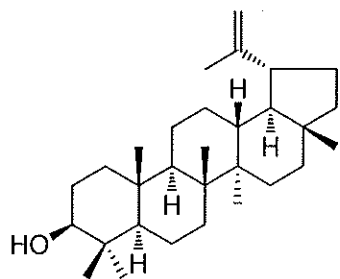
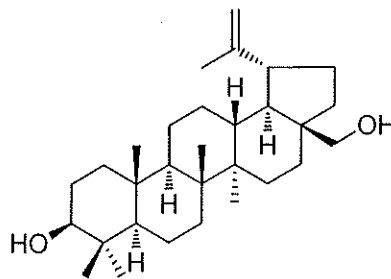
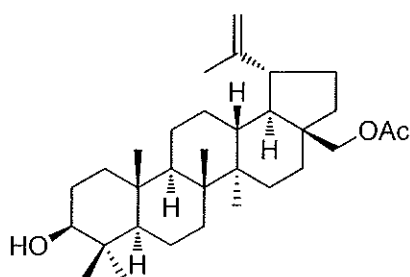
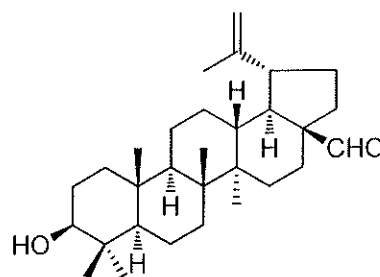
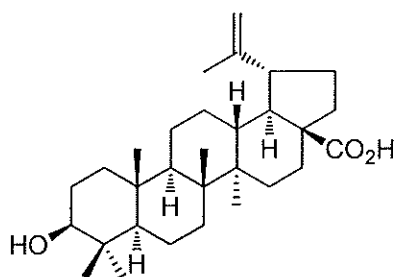
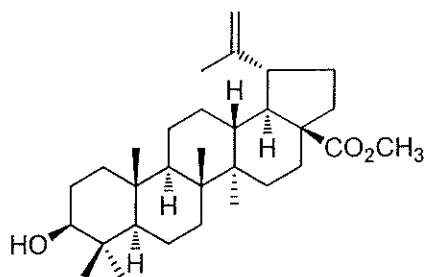
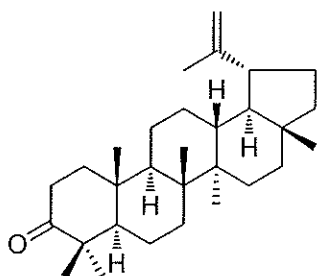
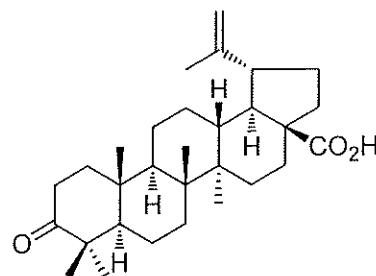
212p: L-Rhamnose

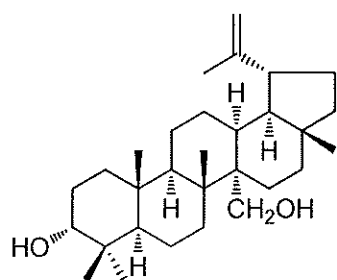


213p: β -D-Glucopyranose pentaacetate

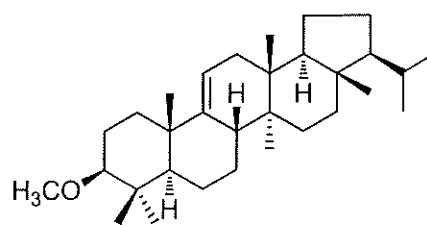


214p: D-Fructose

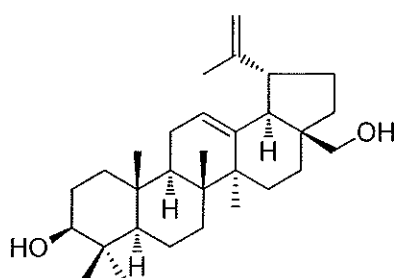
q: triterpenoids**215q: Lupeol****216q: Betulin****217q: Betulin-28-acetate****218q: Betulinaldehyde****219q: Betulinic acid****220q: Betulinic acid methyl ester****221q: Lupenone****222q: 3-Oxo-20(29)-lupen-28-oic acid**



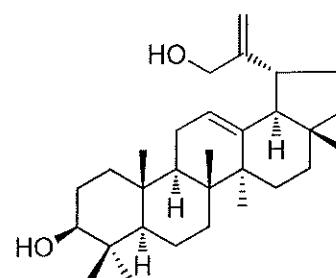
223q: Peregrinol



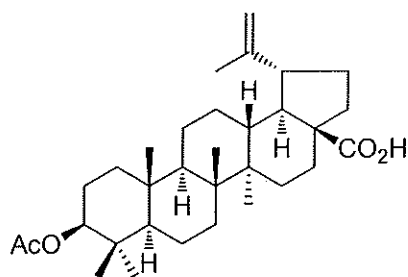
224q: Isoarborinol methyl ether



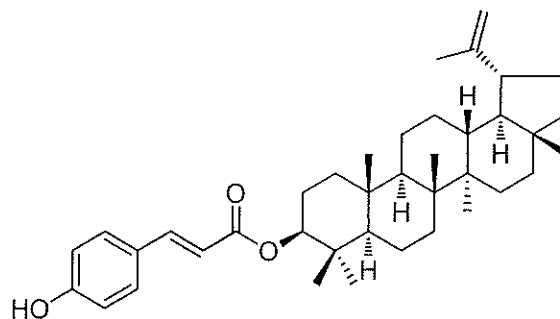
225q: 12,13-Dehydro-20,29-dihydrobetulin



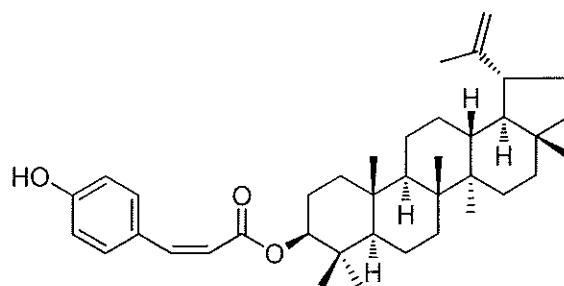
226q: Lup-20(29)-en-3β,30-diol



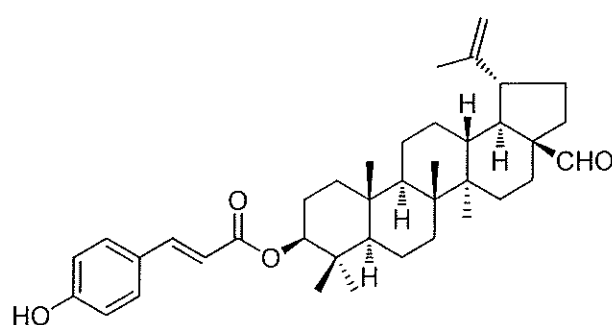
227q: Betulic acid acetate



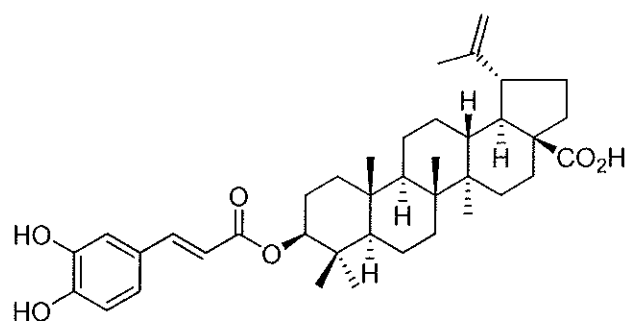
228q: 3-(*E*)-Coumaroyllupeol



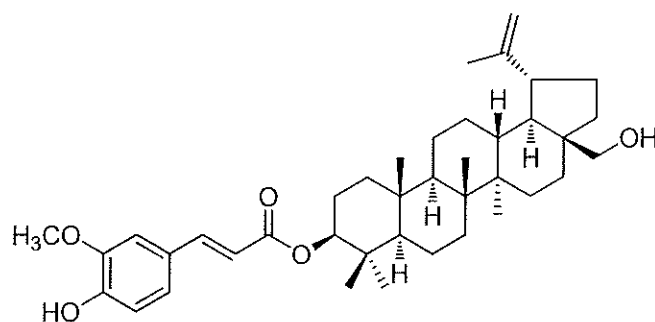
229q: 3-(*Z*)-Coumaroyllupeol



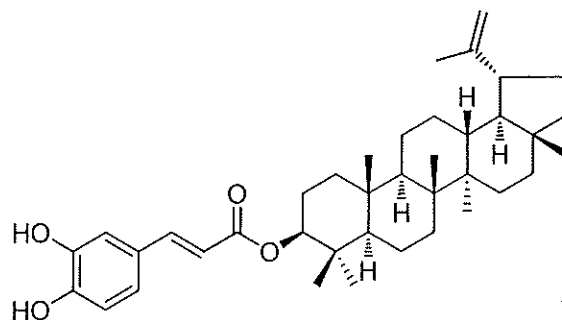
230q: 3-(*E*)-Coumaroylbetulinaldehyde



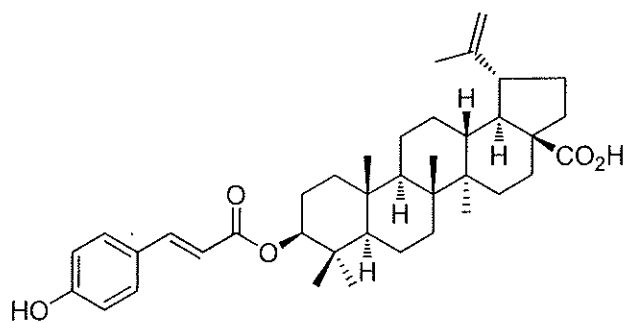
231q: Betulinic acid 3-caffeate



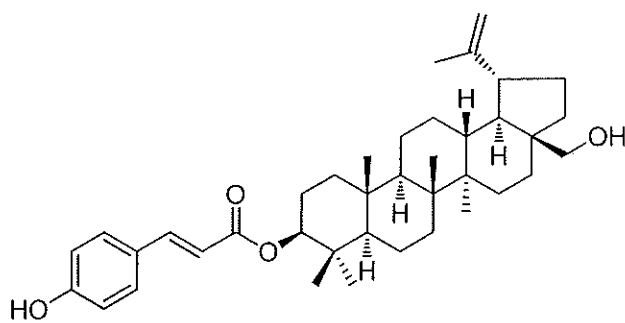
232q: 3-(*E*)-Feruloylbetulin



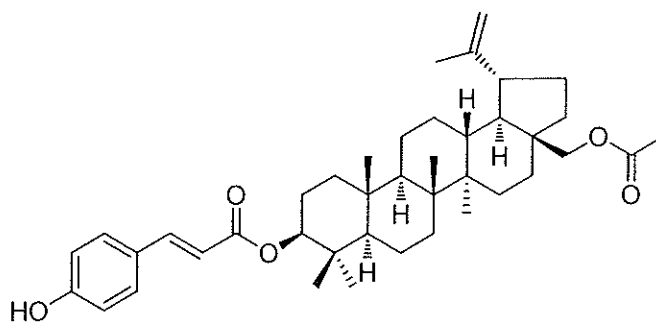
233q: Lupeol caffeate



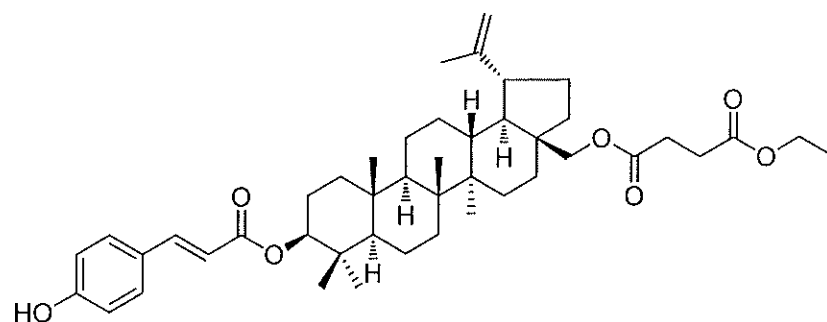
234q: 3-*O*-Betulinic acid *p*-coumarate



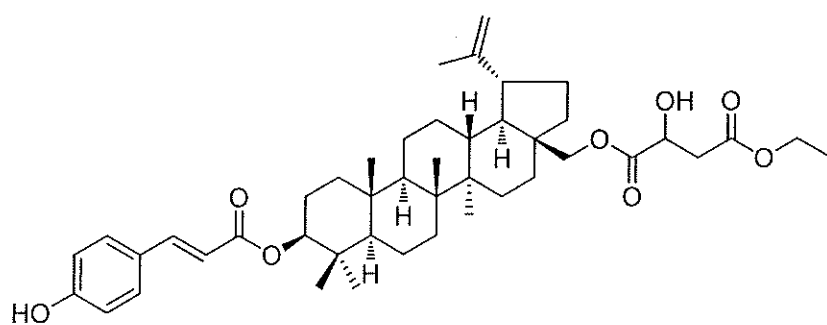
235q: (*E*)-Betulin-3 β -*p*-coumarate



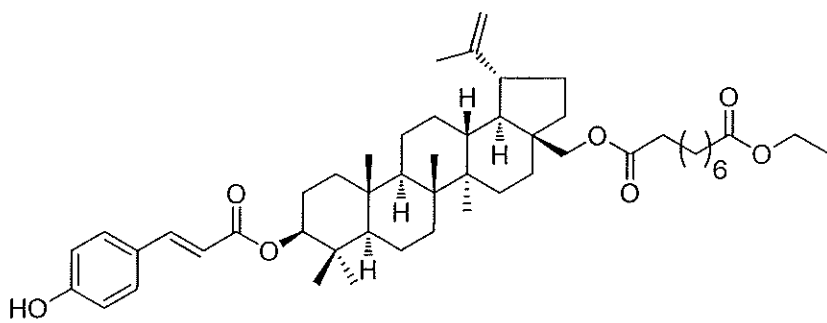
236q: 28-Acetyl-3-(*E*)-coumaroylbetulin



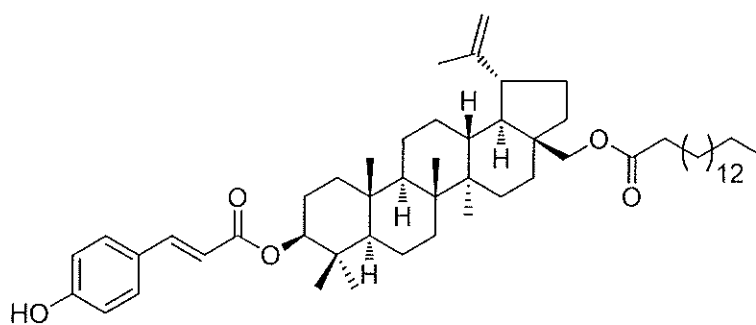
237q: 3-(*E*)-Coumaroylbetulin-28-yl ethyl succinate



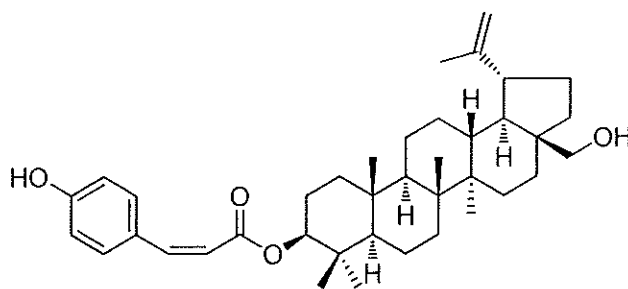
238q: 3-(*E*)-Coumaroylbetulin-28-yl ethyl (2*R*)-2-hydroxysuccinate



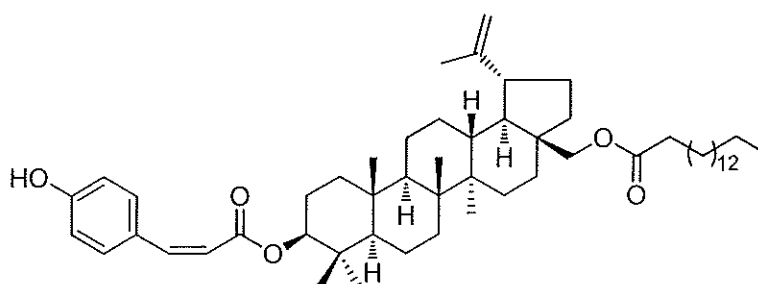
239q: 3-(*E*)-Coumaroylbetulin-28-yl ethyl nonanedioate



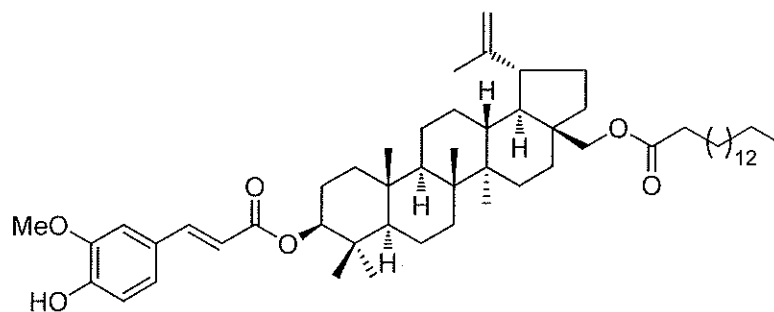
240q: 3-(*E*)-Coumaroyl-28-palmitoylbetulin



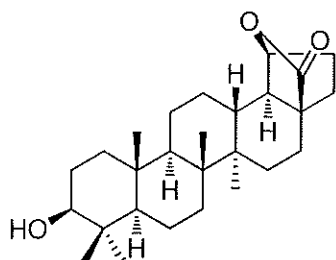
241q: (Z)-Betulin-3 β -*p*-coumarate



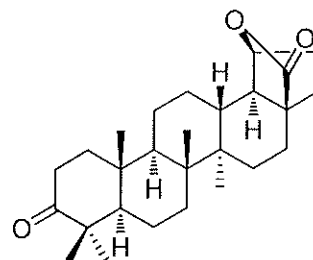
242q: 3-(Z)-Coumaroyl-28-palmitoylbetulin



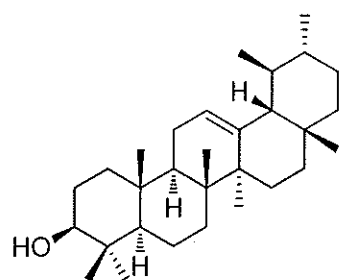
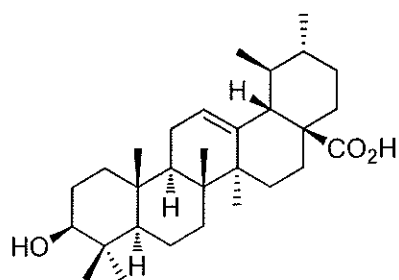
243q: 3-(E)-Feruloyl-28-palmitoylbetulin



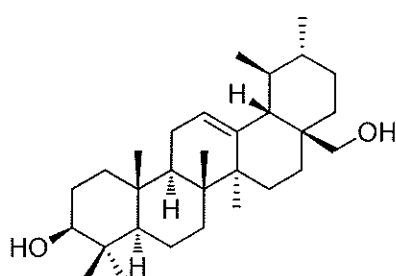
244q: Diospyrolide



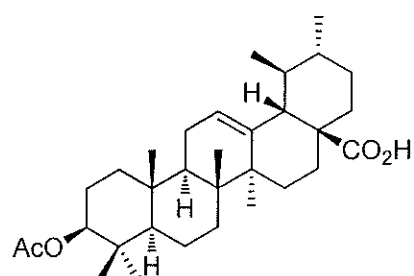
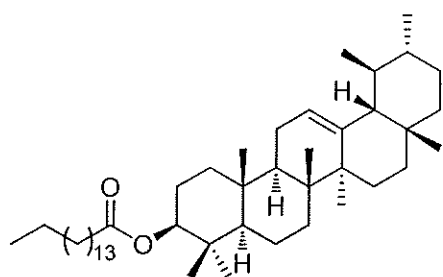
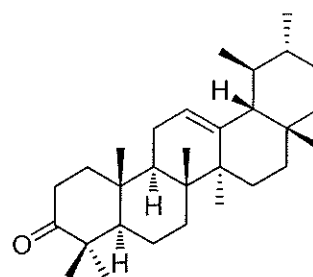
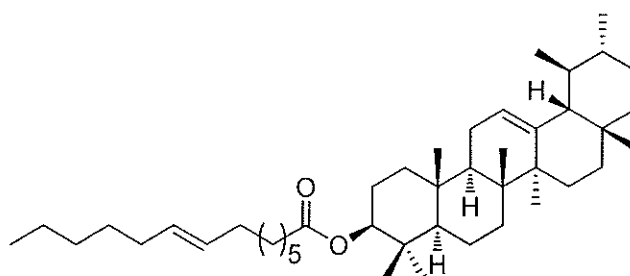
245q: Diospyrolidone

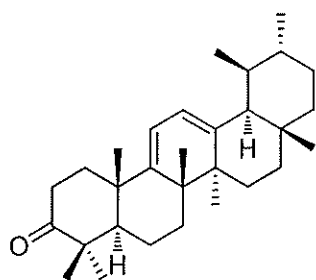
246q: α -Amyrin

247q: Ursolic acid

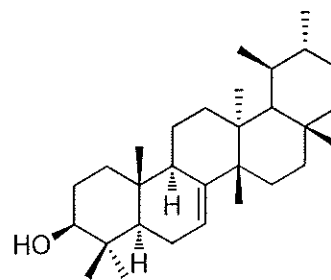


248q: Uvaol

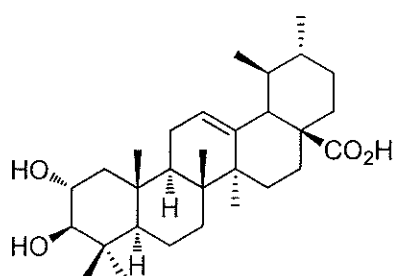
249q: 3 β -Acetoxyurs-12-en-28-oic acid250q: α -Amyrin palmitate251q: α -Amyrenone252q: α -Amyrin palmitoleate



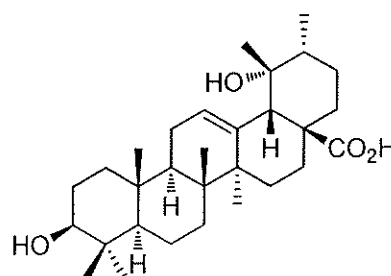
253q: Marsfomosanone



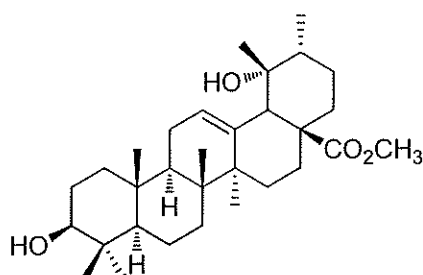
254q: Baurenol



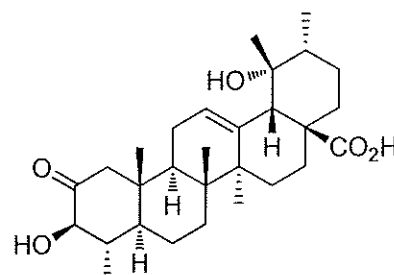
255q: Corsolic acid



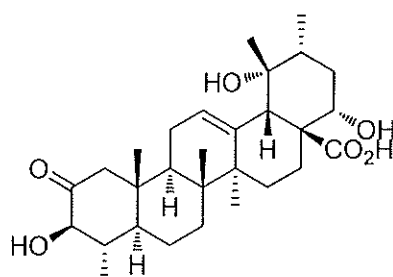
256q: Pomolic acid



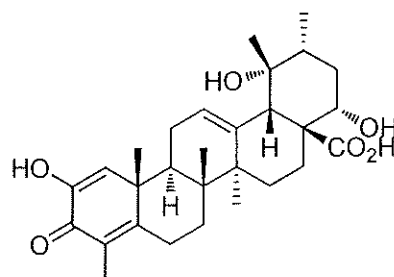
257q: Pomolic acid methyl ester



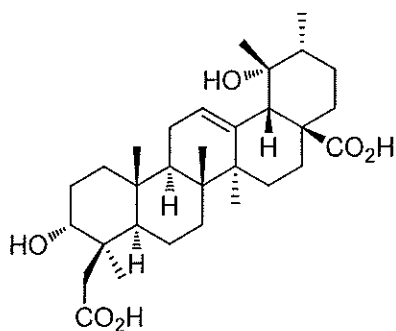
258q: Diospyric acid A



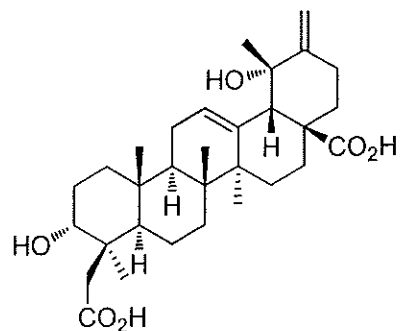
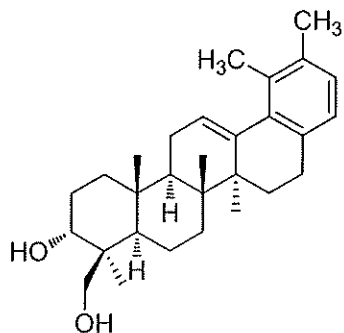
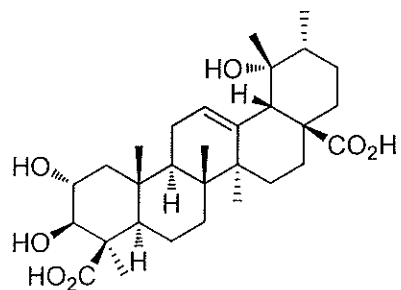
259q: Diospyric acid B



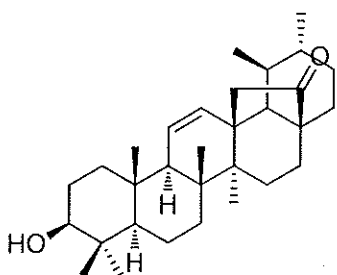
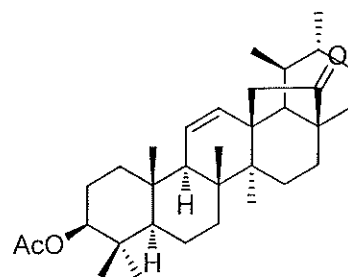
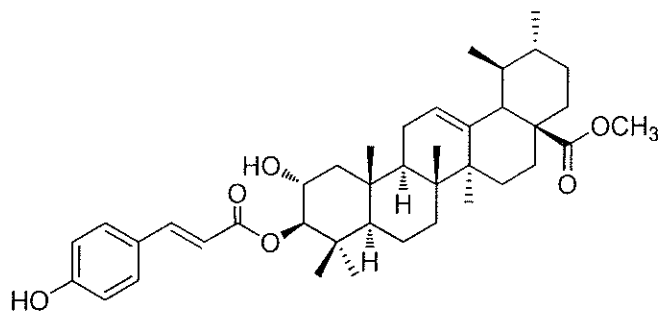
260q: Diospyric acid C



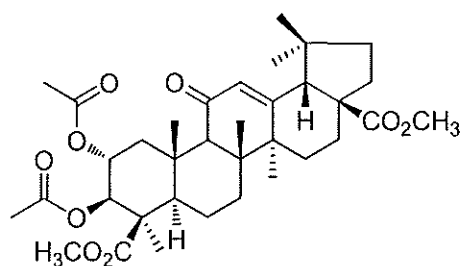
269q: Kakidiol

270q: 3 α ,19 α -Dihydroxyurs-12,20(30)-dien-24,28-dioic acid271q: 3 α ,19 α -Dihydroxyurs-12-en-24,28-dioic acid

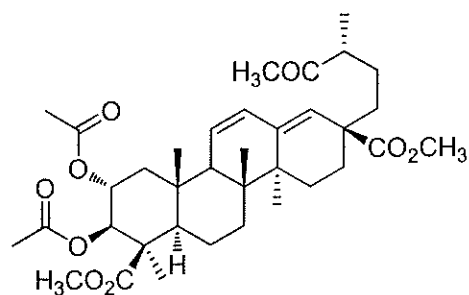
272q: Vismiaefolic acid

273q: 3 β -Hydroxyurs-12-en-28,13-olide274q: 3 β -Acetoxyurs-11-ene-28,13-olide

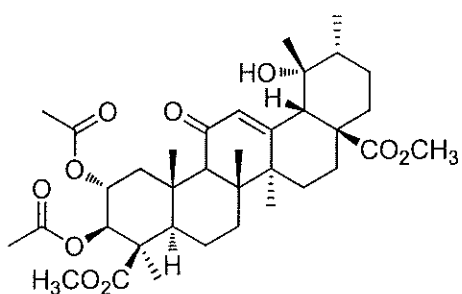
275q: Jacoumaric acid methyl ester



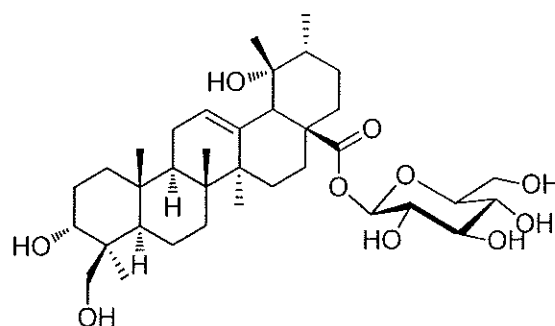
276q: Dimethyl-2 α ,3 β -di-*O*-acetyl-19-*nor*-11-oxoolean-12-en-24,28-dioate



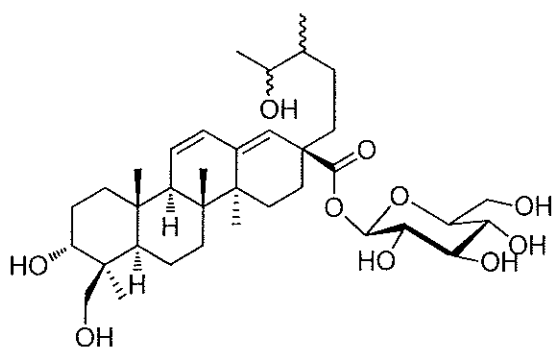
277q: Dimethyl-2 α ,3 β -di-*O*-acetyl-18,19-*seco*-19-oxours-11,13(18)-dien-24,28-dioate



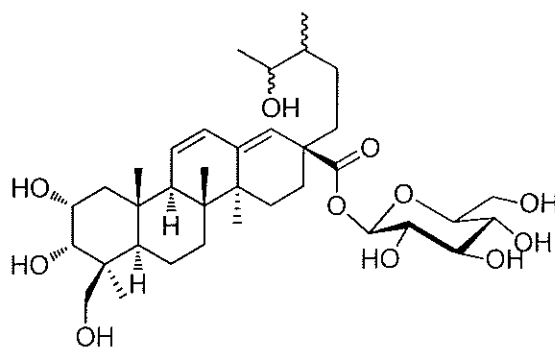
278q: Dimethyl-2 α ,3 β -di-*O*-acetyl-19 α -hydroxy-11-oxours-12-en-24,28-dioate



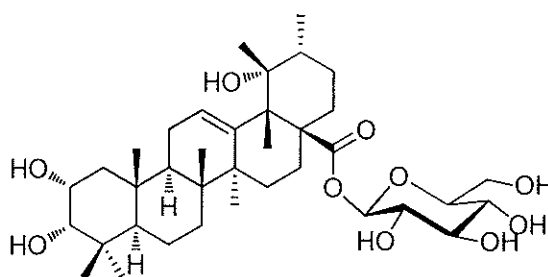
279q: Kakisaponin A



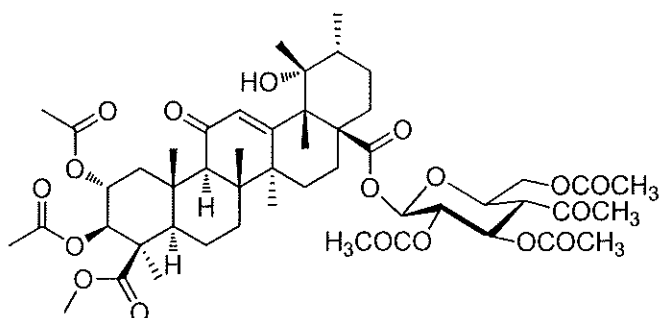
280q: Kakisaponin B



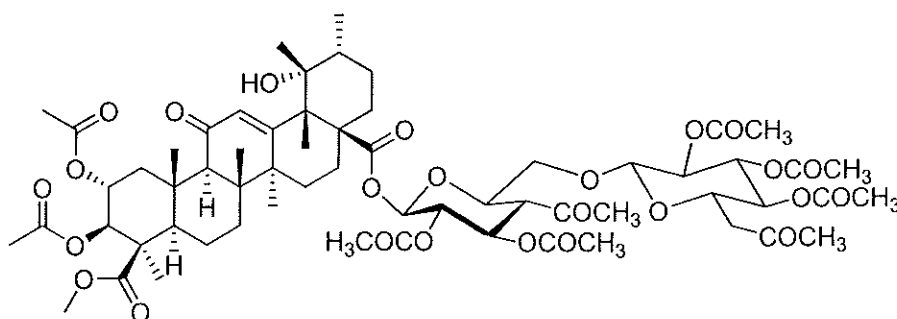
281q: Kakisaponin C



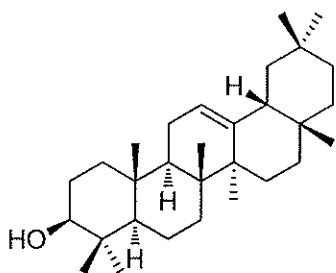
282q: Rosamultin



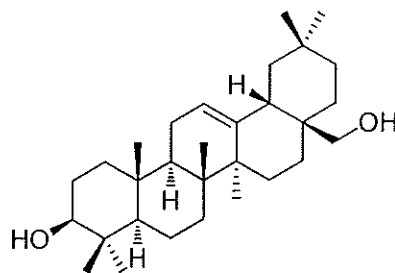
283q: 2 α ,3 β ,2',3',4',6'-Hexa-*O*-acetyl-24-methyl-28-10- β -D-glucopyranosyl-19 α -hydroxyurs-12-en-24,28-dioate



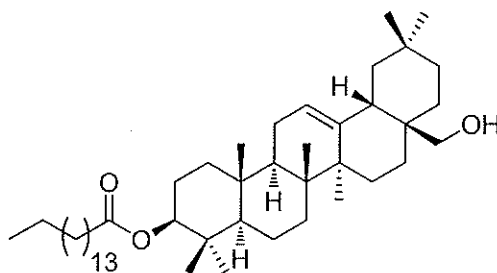
284q: 24-Methyl-2 α ,3 β ,2',3',4',2'',3'',4'',6''-nona-*O*-acetyl-28-1'- β -D-[glucopyranosyl-(1'' \rightarrow 6')-glucopyranosyl]-19 α -hydroxyurs-12-en-24,28-dioate



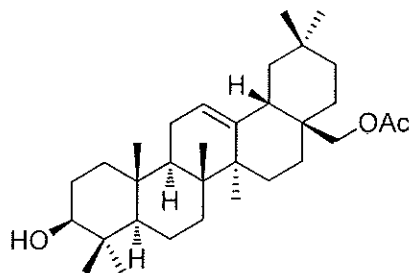
285q: β -Amyrin



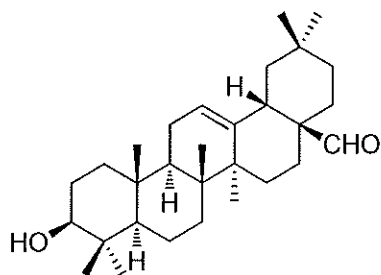
286q: Erythrodiol



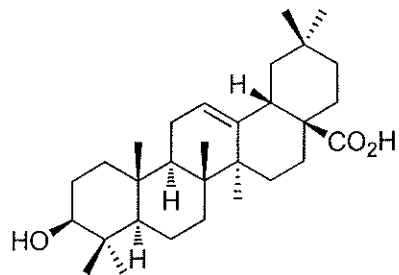
287q: 3-*O*-Palmitoylerythrodiol



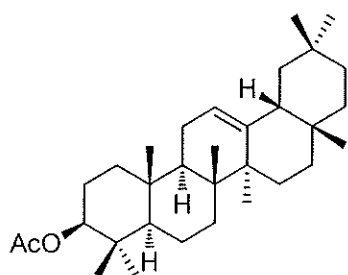
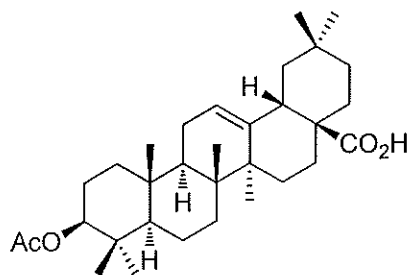
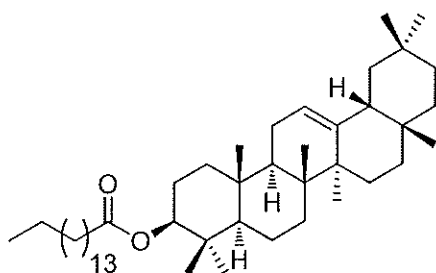
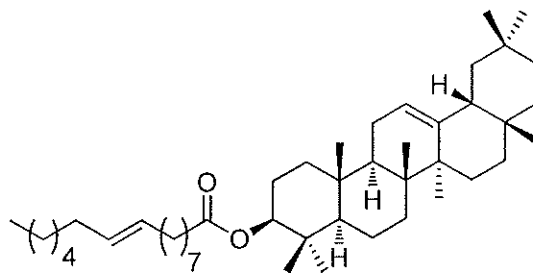
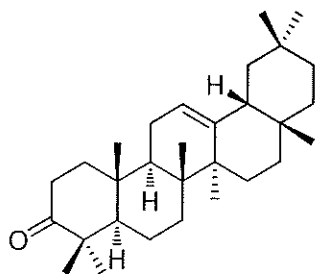
288q: 28-*O*-Acetylerthrodiol



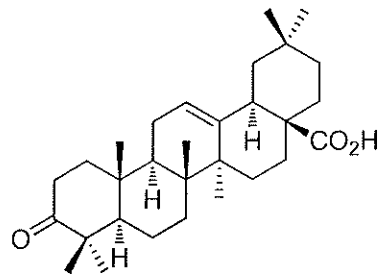
289q: Ursaldehyde



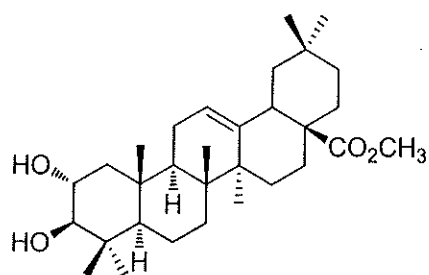
290q: Oleanolic acid

291q: β -Amyrin acetate292q: 3 β -Acetoxyoleanolic acid293q: β -Amyrin palmitate294q: β -Amyrin palmitoleate

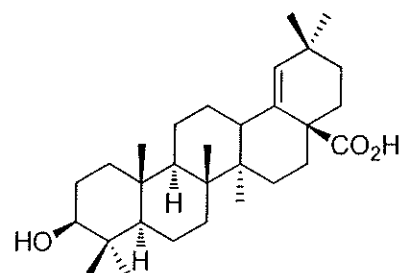
295q: Olean-12-en-3-one



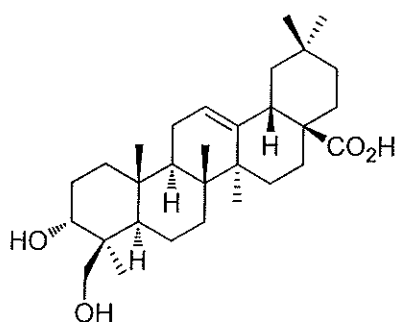
296q: Oleanolic acid



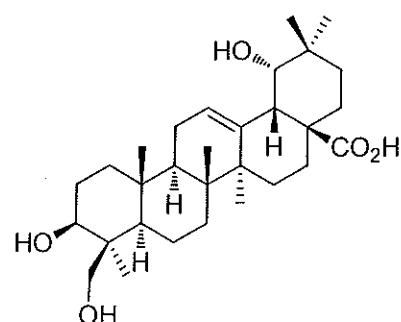
297q: Maslinic acid methyl ester



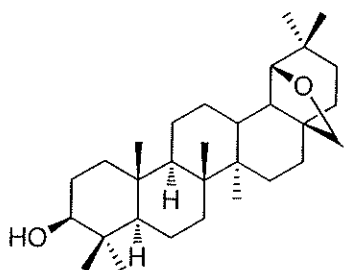
298q: Morolic acid



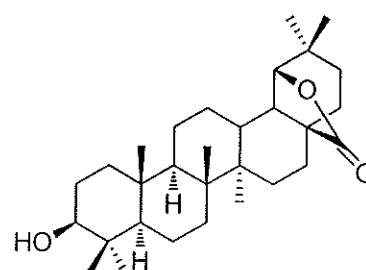
299q: 24-Hydroxy-3-*epi*-oleanolic acid



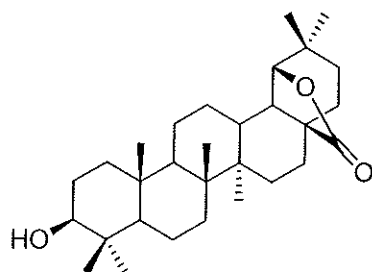
300q: Spathodic acid



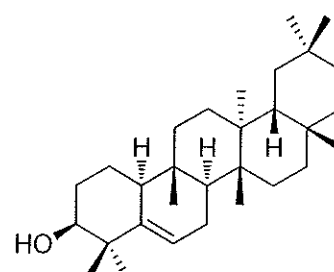
301q: Allobetulin



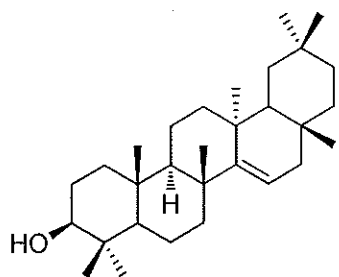
302q: Oxyallobetulin



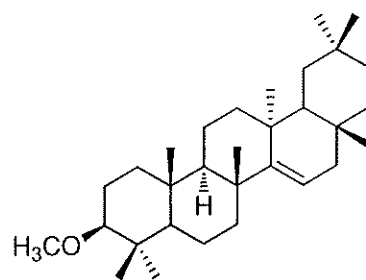
303q: 3 β -Hydroxy-28,19 β -oleanolide



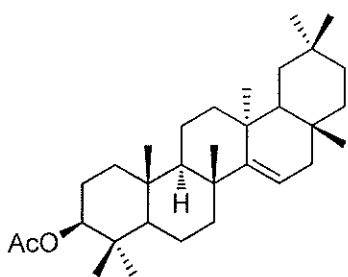
304q: Glutinol



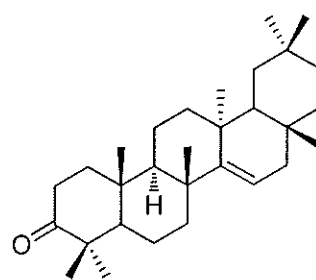
305q: Taraxerol



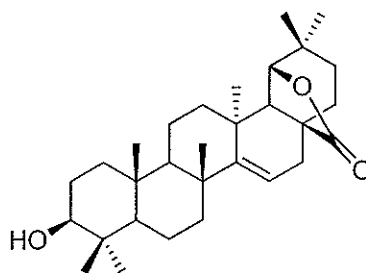
306q: Taraxerol methyl ether



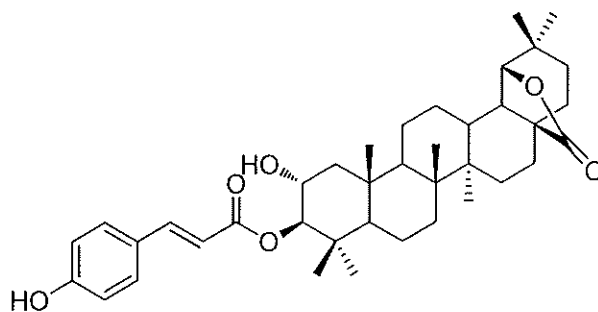
307q: Taraxeryl acetate



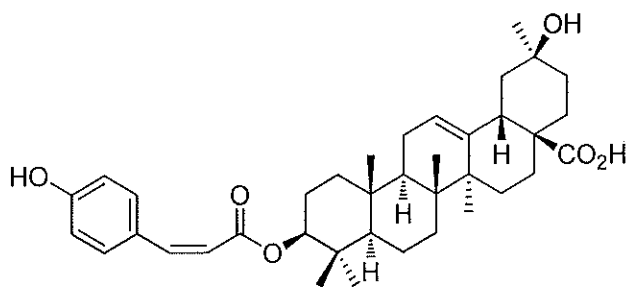
308q: Taraxerone



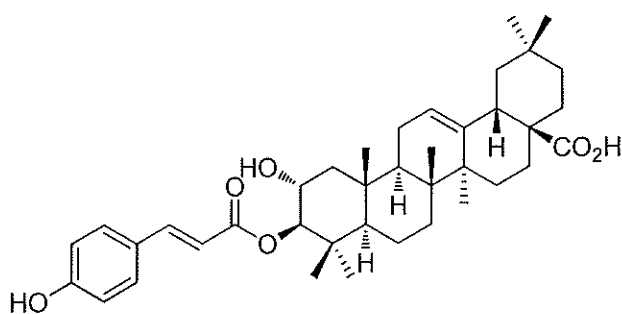
309q: 3β-Hydroxytaraxastan-28, 20β-olide



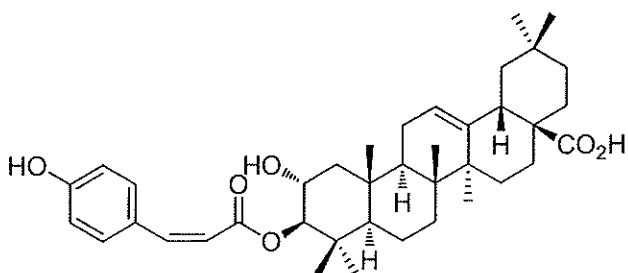
310q: Diospyrosooleanolide



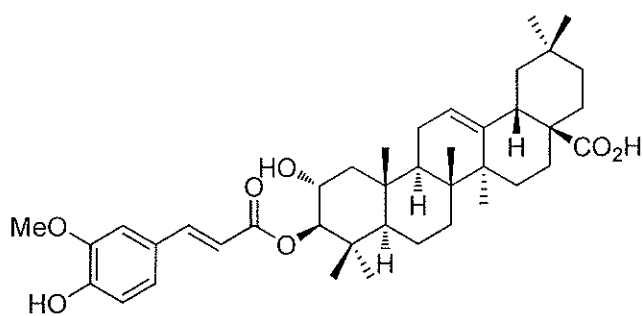
311q: 3β-*O-cis-p*-Coumaroyl-20β-hydroxy-12-ursen-28-oic acid



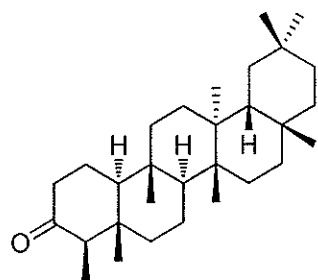
312q: 3β-*O-trans-p*-Coumaroyl-2α-hydroxy-12-ursen-28-oic acid



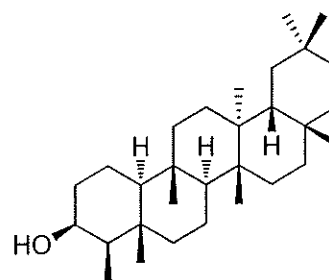
313q: 3β-*O-cis-p*-Coumaroyl-2α-hydroxy-12-ursen-28-oic acid



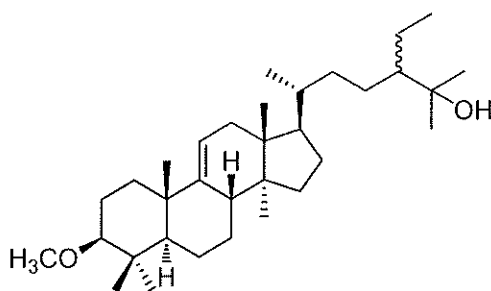
314q: 3β-*O-trans*-Feruloyl-2α-hydroxy-12-ursen-28-oic acid



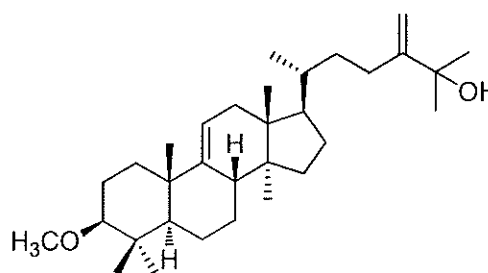
315q: Friedelin



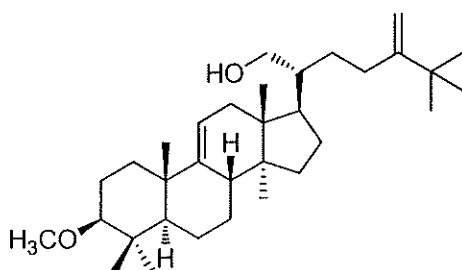
316q: β -Friedelinol



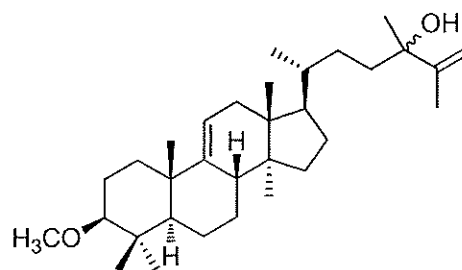
317q: 24-Ethyl-3 β -methoxyelanost-9(11)-en-25-ol



318q: 3 β -Methoxy-24-methylenelanost-9(11)-en-25-ol

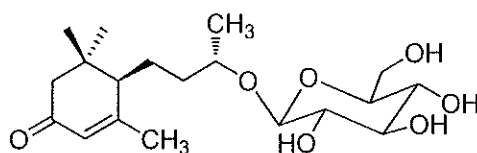


319q: 3 β -Methoxy-25-methyl-24-methylenelanost-9(11)-en-21-ol

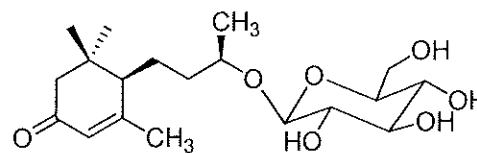


320q: 3 β -Methoxy-24-methyllanosta-9(11),25-dien-24-ol

r: terpenoids

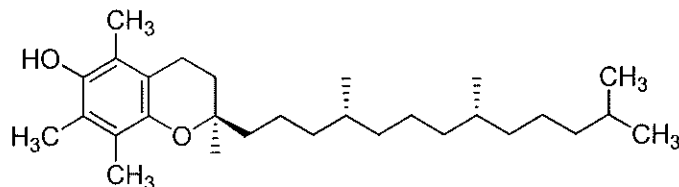


321r: Byzantionoside B



322r: Blumeol C glucoside

s: vitamin



323q: α -Tocopherol

1.2 Chemical constituents from *Premna obtusifolia*

1.2.1 Introduction

The genus *Premna* L. belonging to the family Verbenaceae was established by Linnaeus based on *P. serratifolia*. The genus now contains about 200 species worldwide which are mainly distributed in tropical and subtropical Asia, Africa, Australia and the Pacific Islands. A preliminary study of the genus in Thailand was first undertaken by Fletcher, enumerating 30 species. *Premna obtusifolia*, a plant widely distributed in the southern part of Thailand and locally known as “akkhi thawan thale (อัครคีทวารทะเล)”, has been used in folk medicine to treat fever, headaches, coughs, skin rash, diarrhea, migraine, pneumonia, asthma, and ear-aches (Chopra, 1969; Nandwani et al., 2008).

P. obtusifolia is usually found in the higher parts of the mangrove-occupied areas, often above mean high tide levels. The substratum here is mud or muddy sand that is often harder and drier than in the lower tidal areas. The tree produces serrate yellow green leaves which release a powerful odor upon breaking. The flowers are small and white and organized in clusters. The fruit is a small dark drupe.



Figure 2 Parts of *Premna obtusifolia*

1.2.2 Review of literatures

Chemical constituents isolated from sixteen species of *Premna* genus were summarized in **Table 2**. Information from the Scifinder Scholar copyright in 2012 will be presented and they can be classified into groups as follows: alkaloids, benzenoids, coumarin, diterpenoids, fatty acids, flavonoids, hydrocarbons, iridoids, lignans, phenylethanoids, sesquiterpenoids, steroids, terpenoids, triterpenoids and xanthonnes

Table 2 Compounds from plants of *Premna* genus.

a: alkaloids	f: flavonoids	k: sesquiterpenoid
b: benzenoids	g: hydrocabons	l: steroids
c: coumarin	h: iridoids	m: terpenoids
d: diterpenoids	i: lignans	n: triterpenoids
e: fatty acids	j: phenylethanoids	o: xanthonnes

Plant	part	Compound	Bibliography
<i>P. corymbosa</i>	Stems	Premnoside C, 97h Saccatoside, 98h Premnoside D, 100h 6- α -L-(4"-O-Feruloyl)- rhamnopyranosylcatalpol, 109h 4- <i>epi</i> -Gummadiol-O- β -D- glucopyranoside, 137i Premnafolioside, 140j Verbascoside, 141j Martynoside, 142j (-)-Olivile, 145j Plucheoside D1, 148j	Yuasa <i>et al.</i> , 1993

Table 2 (continued)

Plant	part	Compound	Bibliography
<i>P. corymbosa</i>	Stems	Lyoniresinol 9'- β -D-glucopyranoside, 146j <i>erythro</i> -(4-Hydroxy-3-methoxyphenyl)-2-(4-[2-formyl-(<i>E</i>)-vinyl]-2-methoxyphenoxy)-propan-1,3-diol, 149j <i>threo</i> -(4-Hydroxy-3-methoxyphenyl)-2-(4-[2-formyl-(<i>E</i>)-vinyl]-2-methoxyphenoxy)-propan-1,3-diol, 150j	Yuasa <i>et al.</i> , 1993
	Stem barks	Rutin, 83f Scutellarioside II, 119h Leonurioside A, 147j	Nguyen <i>et al.</i> , 2008
	Flowers	10- <i>O</i> - <i>trans-p</i> -Methoxy cinnamoylcatalpol, 110h Verbascoside, 141j	Pham <i>et al.</i> , 2008
<i>P. crassa</i>	Stem	Stearic acid, 64e Sitosterol, 160l Friedelin, 175n β -Friedelanol, 176n β -	Wei <i>et al.</i> , 1990
<i>P. flavescens</i>	Aerial parts	Quercetin 3- <i>O</i> - α -L-rhamnopyranoside, 80f Kaempferol 3- <i>O</i> - β -D-glucopyranoside, 81f Afzelin, 82f	Trinh <i>et al.</i> , 1998

Table 2 (continued)

Plant	part	Compound	Bibliography
<i>P. fulva</i>	Stem bark	Vanillic acid, 7b Naringenin, 66f β -Sitosterol, 160l β -Daucosterol, 162l Lupenone, 168n Friedelin, 175n β -Friedelanol, 176n <i>p</i> -Hydroxybenzoic acid, 6b Vanillic acid, 7b Naringenin, 66f Apigenin, 67f Vitexin, 85f 4'-Hydroxy-8,3'- dimethoxy-6-acroleinylflavan-3,4-diol, 92f Syringaresinol, 136i	Zeng <i>et al.</i> , 1989, 1990 Chen <i>et al.</i> , 2010
	Stems	Naringenin, 66f Apigenin, 67f Vicenin 2, 86f	Huang <i>et al.</i> , 2009
<i>P. hainanensis</i>	Root	<i>p</i> -Hydroxybenzoic acid, 6b Hexacosic acid, 65e β -Sitosterol, 160l β -Daucosterol, 162l Lupeol, 166n Friedelin, 175n	Dai <i>et al.</i> , 1989
<i>P. herbacea</i>	Roots	Pygmaeotherin, 15c Sugiol, 27d Pygmaeocins B, 43d	Meng <i>et al.</i> , 1988, 1990,

Table 2 (continued)

Plant	part	Compound	Bibliography
<i>P. herbacea</i>	Root nodules	Pygmaeocins C, 44d Pygmaeocin A, 61d 5,6- Didehydropygmaeocin A, 62d Bharangin, 55d	Shihari <i>et al.</i> , 2011
	Roots	11-Hydroxy-5,7,9,13-abietatetraene-2,12-dione, 28d Isobharangin, 29d Fuerstione, 30d 15-Deoxyfuerstione, 31d 3 β -Acetoxifyfuerstione, 32d Neobharangin, 54d Bharangin , 55	Satish <i>et al.</i> , 2011
<i>P. integrifolia</i>	Root bark	Sandaracopimaradiene, 22d 7 α -Hydroxysandaraco pimar-8(14),15-diene, 23d 11 β -Hydroxy-7-ketosandaracopimar-8(14),15-diene, 24d Sandaracopimar-8(14),15-diene,caryophyllen-3-one, 25d Premnenol, 26d 11,14-Dihydroxy-12,16-epoxyabieta-5,8,11,13-tetra ene-7-one, 41d 11,12,16- Trihydroxyabieta-5,8,11,13-tetraen-7-one, 42d Premnaspirodiene, 157k	Rao <i>et al.</i> , 1985, 1987

Table 2 (continued)

Plant	part	Compound	Bibliography
<i>P. integrifolia</i>	Leaves	6 α ,11,12,16-tetrahydroxy-7-oxo-abieta-8,11,13-triene, 40d	Yadav <i>et al.</i> , 2010
	Flowers	Verbascoside, 141 10- <i>O</i> - <i>trans</i> - <i>p</i> -Methoxy cinnamoylcatalpol, 110h Premnacorymboside A, 132h	Nguyen <i>et al.</i> , 2008
<i>P. japonica</i>	Leaves	6- <i>O</i> - α -L-(2''- <i>O</i> -Isoferuloyl, 4''- <i>O</i> -acetyl)rhamnopyranosylcatalpol, 99h 6- <i>O</i> - α -L-(3''- <i>O</i> -Isoferuloyl, 4''- <i>O</i> -acetyl)rhamnopyranosylcatalpol, 101h 6- <i>O</i> - α -L-(4''- <i>O</i> - <i>trans</i> - <i>p</i> -Coumaroyl)rhamnopyranosylcatalpols, 102h 6- <i>O</i> - α -L-(2''- <i>O</i> -Caffeoyl)rhamnopyranosylcatalpol, 103h 6- <i>O</i> - α -L-(3''- <i>O</i> -Caffeoyl)rhamnopyranosylcatalpol, 104h 6- <i>O</i> - α -L-(2''- <i>O</i> - <i>p</i> -Methoxycinnamoyl)rhamnopyranosylcatalpol, 105h 6- <i>O</i> - α -L-(3''- <i>O</i> - <i>p</i> -Methoxycinnamoyl)rhamnopyranosylcatalpol, 106h	Otsuka <i>et al.</i> , 1990, 1991

Table 2 (continued)

Plant	part	Compound	Bibliography
<i>P. japonica</i>	Leaves	Saccatoside, 98h 6- <i>O</i> - α -L-(2''- <i>O</i> - <i>p</i> -Methoxy cinnamoyl-4- <i>O</i> -acetyl)rham nopyrano sylvacatapol, 107h 6- <i>O</i> - α -L-(3''- <i>O</i> - <i>p</i> -Methoxy cinnamoyl-4''- <i>O</i> -acetyl) rhamnopyra nosylvacatapol, 108h	Otsuka <i>et al.</i> , 1990, 1991
<i>P. latifolia</i>	Leaves	Saropeptate, 2a Aurantiamide, 3a Premnalatin, 13b 1,3-Benzodioxole-5-carboxylic acid, 1,2-ethanediyl ester, 14b Vicenin 2, 86f Triacontanol, 93g (+)-Sesamin, 134i β -Daucosterol, 162l	Rao <i>et al.</i> , 1986
	Root bark	Sandaracopimar-15-en-8 β -ol, 16d 11-Ketosandaracopimar-15-en- 18 β -ol, 17d Sandaracopimar-15-en-1 β ,8 β - diol, 18d 15- Sandaracopimaran-1 β ,8 β ,12 β - triol, 19d Nellionol, 33d Anhydronellionol, 34d Dehydronellionol, 35d Ferruginol, 36d	Rao <i>et al.</i> , 1978, 1982, 1984

Table 2 (continued)

Plant	part	Compound	Bibliography
<i>P. latifolia</i>	Root bark	Taxodione, 37d Premnolal, 38d Dehydropremnolal, 39d Premnaspiral, 156k Premnaspirodiene, 157k	Rao <i>et al.</i> , 1978, 1982, 1984
	Stem bark	Latifolionol, 56d Dihydrolatifolionol, 57d Premnalatifolin A, 63d Glucoside-B, 95h Glucoside-C, 96h	Suresh <i>et al.</i> , 2011
<i>P. microphylla</i>	Roots	1-Hydroxy-2,3-methylenedioxy-6-methoxycarbonyl-7-acetyl xanthone, 177o 1,3-Dihydroxy-2-methoxy-6-methoxycarbonyl-7-acetyl xanthone, 178o 6,3'-Dihydroxy-7-methoxy-4',5'-methylenedioxy isoflavone, 88f 6,3'-Dihydroxy-7-methoxy-4',5'-methylenedioxy isoflavone 6- <i>O</i> - β -D-glucopyranoside, 89f 6-3'-Dihydroxy-7-methoxy-4',5'-methylenedioxy isoflavone 6- <i>O</i> - β -D-xylo pyranosyl (1 \rightarrow 6)- β -D-glucopyranoside, 90f 6,3'-Dihydroxy-7-methoxy-4',5'-methylenedioxy isoflavone 6- <i>O</i> - α -L-rhamno pyranoside, 91f	Wang <i>et al.</i> , 2003 Zhong <i>et al.</i> , 2003

Table 2 (continued)

Plant	part	Compound	Bibliography
<i>P. microphylla</i>	Leaves	28- <i>O</i> - α -L-Rhamnopyrano syl(1 \rightarrow 2)- β -D-glucopyrano side tormentic acid ester, 172n Arjunolic acid, 173n Hyptatic acid A, 174n	Zhan <i>et al.</i> , 2009
<i>P. oligotricha</i>	Aerial parts	(5 <i>R</i> ,8 <i>R</i> ,9 <i>S</i> ,10 <i>R</i>)-12-Oxo- <i>ent</i> -3,13 (16)-clerodien-15-oic acid, 58d <i>ent</i> -12-Oxolabda-8,13(16)-dien- 15-oic acid, 59d <i>ent</i> -8 β ,12 α -Epidioxy-12 β - hydroxylabda-9(11),13-dien-15- oic acid, 60d 7 α -Hydroxy-6,11-cyclo farnes- 3(15)-en-2-one, 155k	Habtemariam <i>et al.</i> , 1991, 1993
<i>P. recinosa</i>	Leaves	(+)-1-Hydroxypinoresinol, 135i (+)-Lariciresinol, 138i (-)- <i>seco</i> -Isolariciresinol, 139i	Habtemariam, 1995
<i>P. schimperi</i>	Leaves	(5 <i>R</i> ,8 <i>R</i> ,9 <i>S</i> ,10 <i>R</i>)-12-Oxo- <i>ent</i> -3,13 (16)-clerodien-15-oic acid, 58d	Habtemariam <i>et al.</i> , 1990
<i>P. subscanden</i>	Leaves	10- <i>O</i> - <i>trans</i> - <i>p</i> -Methoxy cinnamoylcatalpol, 110 10- <i>O</i> - <i>cis</i> - <i>p</i> -Methoxy cimmamoylcatalpol, 111h 10- <i>O</i> - <i>trans</i> -Caffeoylcatalpol, 112h 10- <i>O</i> - <i>trans</i> -Isoferuloylcatalpol, 113h	Sudo <i>et al.</i> , 1997, 1998, 1999

Table 2 (continued)

Plant	part	Compound	Bibliography
<i>P. subscanden</i>	Leaves	10- <i>O-trans-p</i> -Methoxy cinnamoyl asystasioside E, 114h 10- <i>O-cis-p</i> -Methoxy cinnamoyl asystasioside E, 115h 10- <i>O-trans-p</i> -Coumaroyl asystasioside E, 116h 10- <i>O-cis-p</i> -Coumaroyl asystasioside E, 117h 10- <i>O-cis-p</i> -Coumaroyl catalpol, 118h Scutellarioside II, 119h 4''-Methoxy- <i>E</i> -globularinin, 120h 4''-Methoxy- <i>Z</i> -globularinin, 121h 4''-Hydroxy- <i>Z</i> -globularinin, 122h 4''-Methoxy- <i>E</i> -globularimin, 123h 4''-Methoxy- <i>Z</i> -globularimin, 124h Premnaodoroside A, 125h Premnaodoroside B, 126h Premnaodoroside C, 127h Premnaodoroside D, 128h Premnaodoroside E, 129h Premnaodoroside F, 130h	Sudo <i>et al.</i> , 1997, 1998, 1999

Table 2 (continued)

Plant	part	Compound	Bibliography
<i>P. subscanden</i>	Leaves	Premnaodoroside G, 131h Premcorymboside A, 132h 4,4'-Dimethoxy- β -truxinic acid catalpol diester, 133h Verbascoside, 141j Premnethanoside A, 143j Premnethanoside B, 144j Decaffeoylacteoside, 151j Benzyl alcohol β -D-(2'-O- β -D- xylopyranosyl)glucopyranoside, 152j Phenethyl alcohol β -D-(2'-O- β - D-glucopyranosyl) glucopyranoside, 153j 7-(3,5-Dihydroxy-1,1,5- trimethylcyclohexylidene)-9- methylprop-8-enyl 9-O- β -D- glucopyranoside, 163m 3-Hydroxy-5,6-epoxy- β -ionol 9- O- β -D-glucopyra noside, 164m Premnaionoside, 165m	Sudo <i>et al.</i> , 1997, 1998, 1999
<i>P. szemaoensis</i>		Linarigenin, 68f 5,4'-Dihydroxy-7-methoxy flavonol, 70f 5,3'-Dihydroxy-7,4'-di methoxyflavonol, 71f 3',4',5-Trihydroxy-3,7-di methoxyflavone, 72f	Li <i>et al.</i> , 2008

Table 2 (continued)

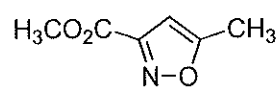
Plant	part	Compound	Bibliography
<i>P. szemaoensis</i>	Leaves	5-Hydroxy-3',4',6,7-tetra methoxyflavone, 73f 3,7,3'-Trimethylquercetin, 75f 5-Hydroxy-7,3',4'-tri methoxy flavonol, 79f	Li <i>et al.</i> , 2008
<i>P. tomentosa</i>	Heart wood	Vicenin 3, 87f	Jyotsna <i>et al.</i> , 1984
	Leaves	Myricetin-3',4',7-trimethyl ether, 77f Premnones A, 45d Premnones B, 46d Premnones C, 47d 5,3'-Dihydroxy-3,7,4',5'-tetra methoxyflavone, 74f 3,7,3'-Trimethylquercetin, 75f 5,3'-Dihydroxy-3,6,7,4',5' pentamethoxyflavone, 76f Chryso splenetin, 78f 2 α -Hydroxyursolic acid, 170n Ursolic acid, 169n 3- <i>epi</i> -Corosolic acid lactone, 171n	Balakrishna <i>et al.</i> , 2003 Chin <i>et al.</i> , 2006
	Roots	4-(4-Methoxyphenyl)-2-butanone, 9b Syranzaldehyde, 10b Acetoxy syranzaldehyde, 11b	Ayinampudi <i>et al.</i> 2012

Table 2 (continued)

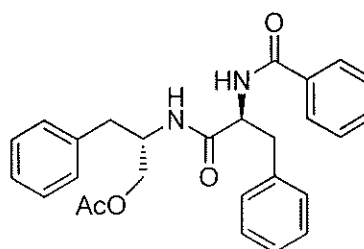
Plant	part	Compound	Bibliography
<i>P. tomentosa</i>	Roots	Coniferaldehyde, 12b Icetexatriene-1, 52d Icetexatriene-2, 53d Lupeol, 166n Betulin, 167n	Ayinampudi <i>et al.</i> 2012
	Stem bark	4-(4-Methoxyphenyl)-2-butanone, 9b Syringaldehyde, 10b Coniferaldehyde, 12b Icetexane-1, 48d Icetexane-2, 49d Icetexatriene-3, 50d Icetexane-4, 51d Lupeol, 166n Betulin, 167n	Hymavathi <i>et al.</i> , 2009

Structures

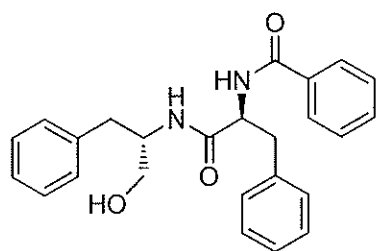
a: alkaloids



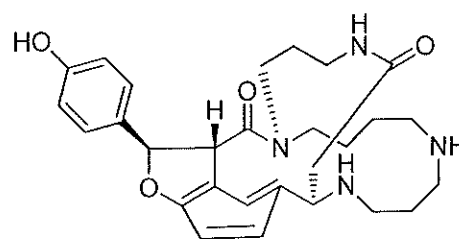
1a: Premnazole



2a: Saropeptate

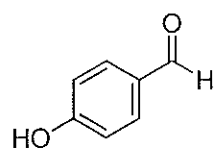


3a: Aurantiamide

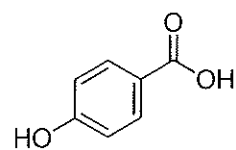
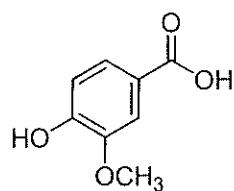


4a: Aphelandrine

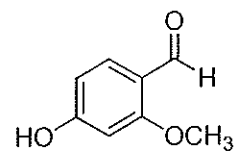
b: benzenoids



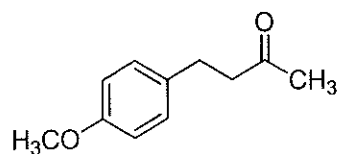
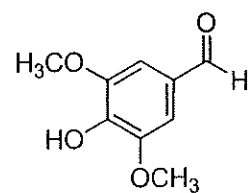
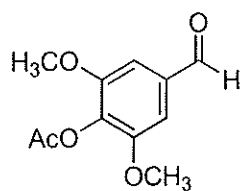
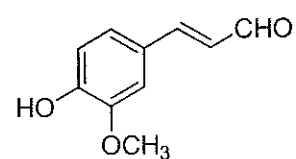
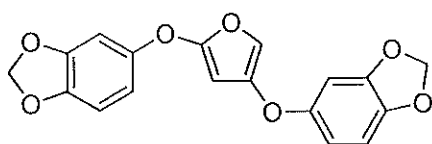
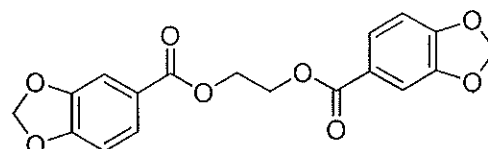
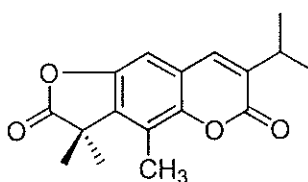
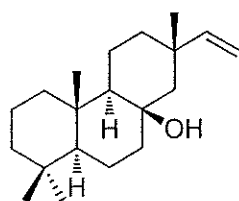
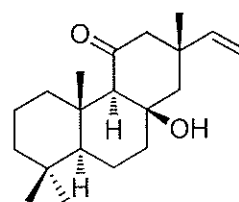
5b: 4-Hydroxybenzaldehyde

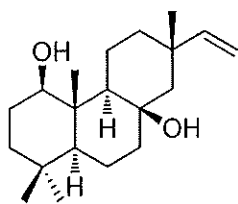
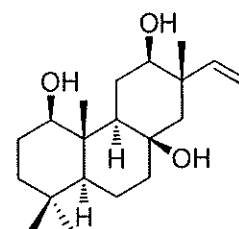
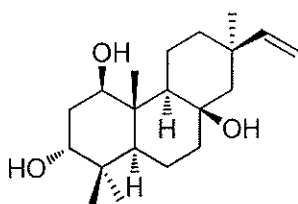
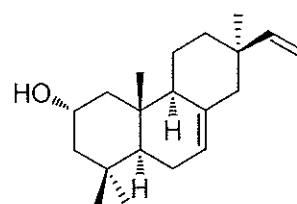
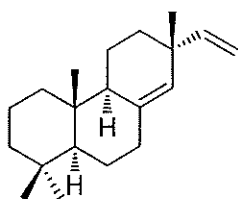
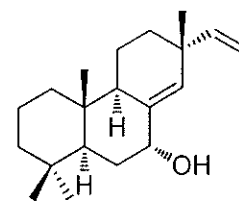
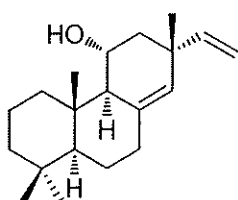
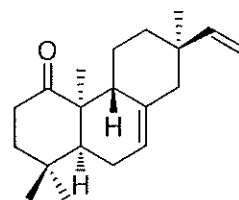
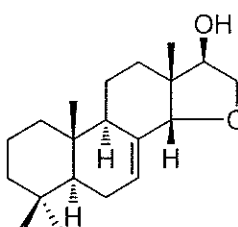
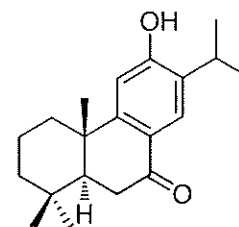
6b: *p*-Hydroxybenzoic acid

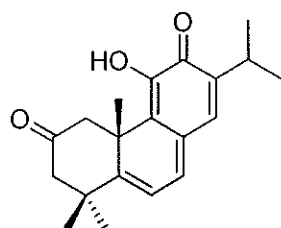
7b: Vanillic acid



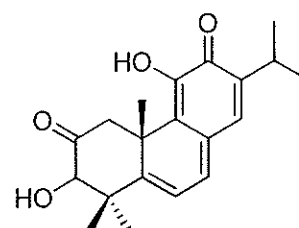
8b: 4-Hydroxy-2-methoxybenzaldehyde

**9b:** 2-(4-Methoxyphenyl)-2-butanone**10b:** Syringaldehyde**11b:** Acetoxy syringaldehyde**12b:** Coniferaldehyde**13b:** Premnalatin**14b:** 1,3-Benzodioxole-5-carboxylic acid, 1,2-ethanediyl ester**c: coumarins****15c:** Pygmaeoherin**d: diterpenoids****16d:** Sandaracopimar-15-en-8β-ol**17d:** 11-Ketosandaracopimar-15-en-18β-ol

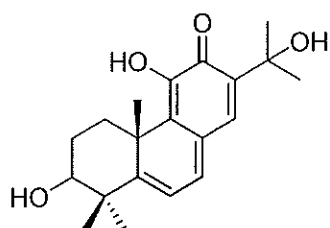
**18d:** Sandaracopimar-15-en-1 β ,8 β -diol**19d:** Sandaracopimaran-1 β ,8 β ,12 β -triol**20d:** 1 β ,3 α ,8 β -Trihydroxy-pimara-15-ene**21d:** 2 α ,19-Dihydroxy-pimara-7,15-diene**22d:** Sandaracopimaradiene**23d:** 7 α -Hydroxysandaracopimar-8(14),15-diene**24d:** 11 β -Hydroxy-7-ketosandaracopimar-8(14),15-diene**25d:** Sandaracopimar-8(14),15-diene, caryophyllen-3-one**26d:** Premnenol**27d:** Sugiol



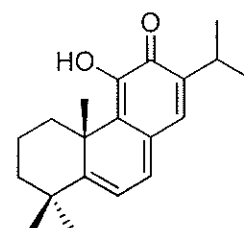
28d: 11-Hydroxy-5,7,9,13-abietatetraene-
2,12-dione



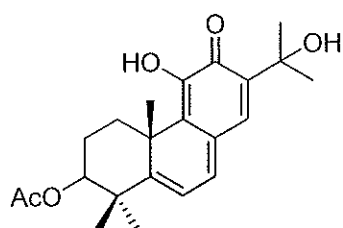
29d: Isobharangin



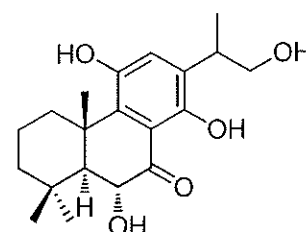
30d: Fuerstione



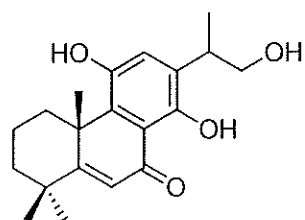
31d: 15-Deoxyfuerstione



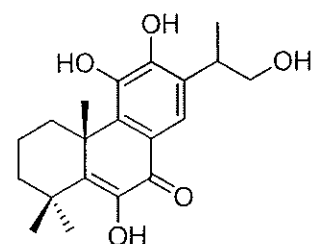
32d: 3 β -Acetoxyfuerstione



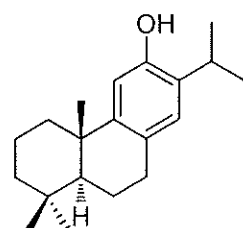
33d: Nellionol



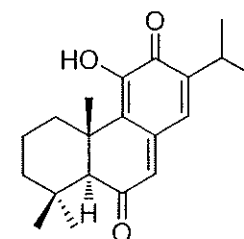
34d: Anhydronelliono



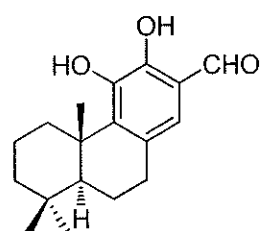
35d: 15-Dehydronellionol



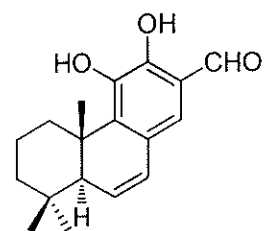
36d: Ferruginol



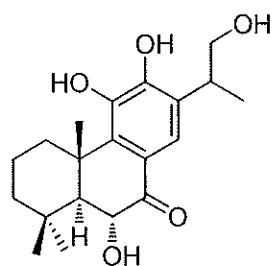
37d: Taxodione



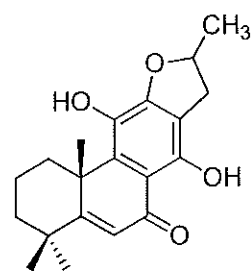
38d: Premnolal



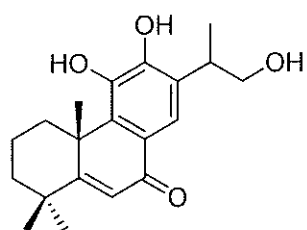
39d: Dehydropremnolal



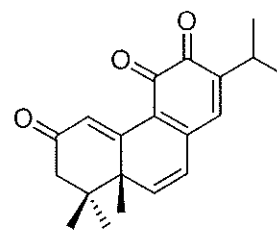
40d: 6 α ,11,12,16-Tetrahydroxy-7-oxo-
abieta-8,11,13-triene



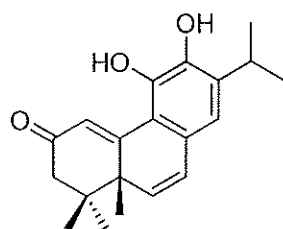
41d: 11,14-Dihydroxy-12,16-
epoxyabieta-5,8,11,13-tetraene-7-one



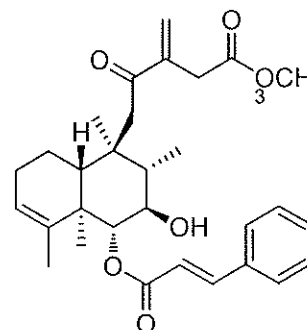
42d: 11,12,16-Trihydroxyabieta-
5,8,11,13-tetraen-7-one



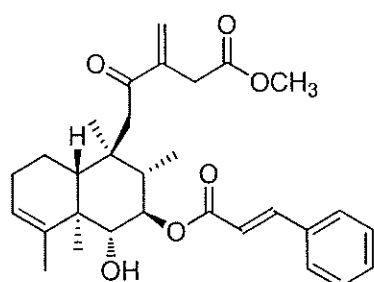
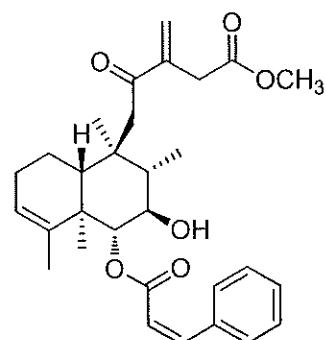
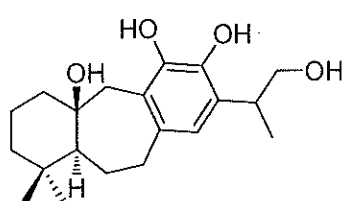
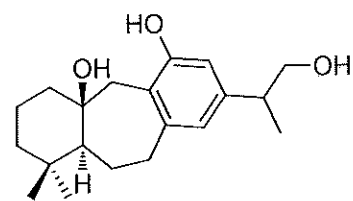
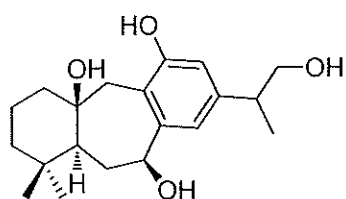
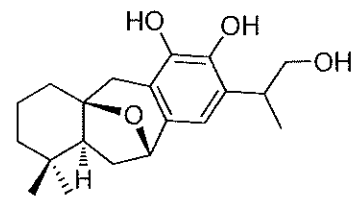
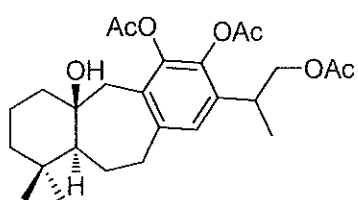
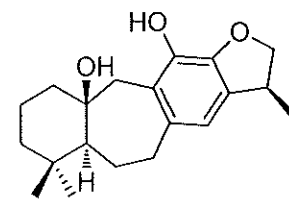
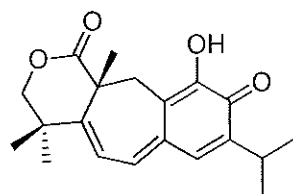
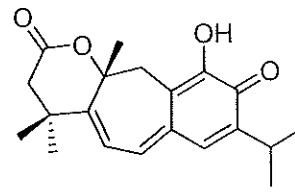
43d: Pygmaecins B

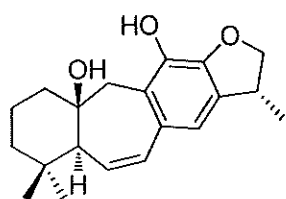


44d: Pygmaecins C

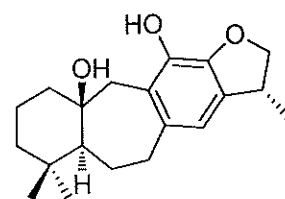


45d: Premnone A

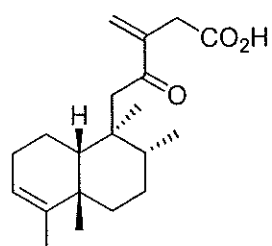
**46d:** Premnone B**47d:** Premnone C**48d:** Icetexane-1**49d:** Icetexane-2**50d:** Icetexatriene-3**51d:** Icetexane-4**52d:** Icetexatriene-1**53d:** Icetexatriene-2**54d:** Neobharangin**55d:** Bharangin



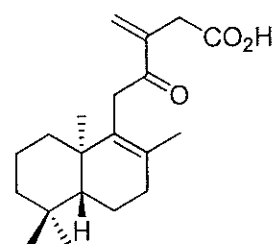
56d: Latifolionol



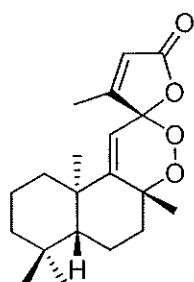
57d: Dihydratatifolionol



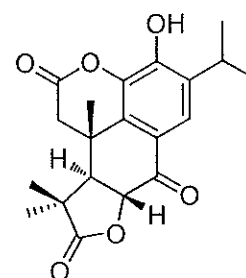
58d: (5*R*,8*R*,9*S*,10*R*)-12-Oxo-*ent*-3,
13(16)-clerodien-15-oic acid



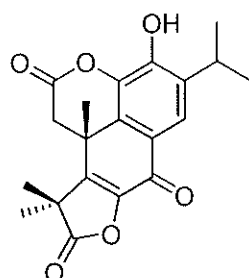
59d: *ent*-12-Oxolabda-8,13(16)-dien-15-
oic acid



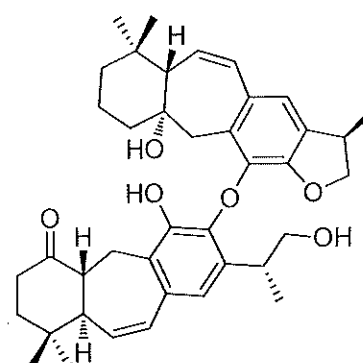
60d: *ent*-8 β ,12 α -Epoxy-12 β -hydroperoxy
labda-9(11),13-dien-15-oic acid



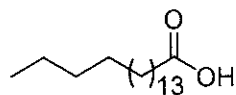
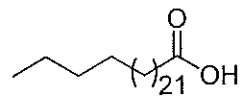
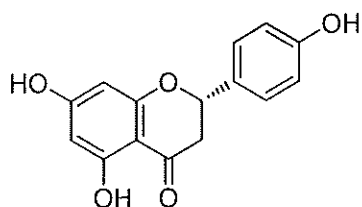
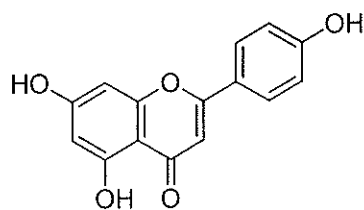
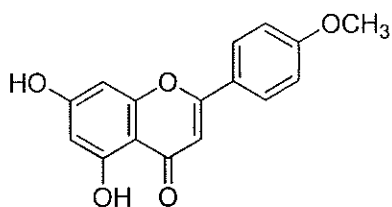
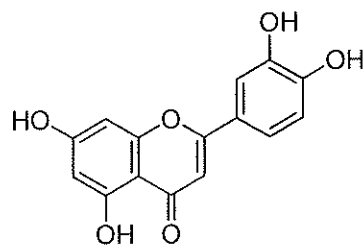
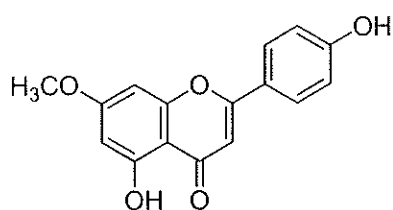
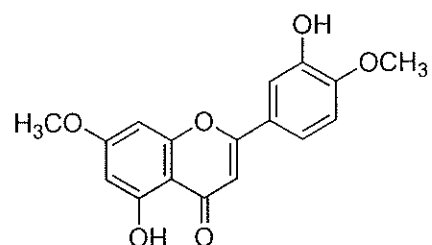
61d: Pygmaecocin A

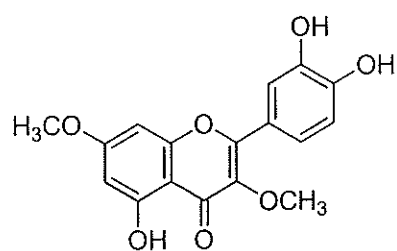


62d: 5,6-Didehydropygmaecocin A

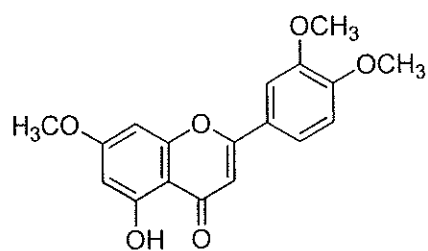


63d: Premnatatifolin A

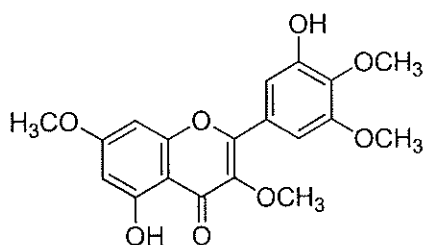
e: fatty acids**64e:** Stearic acid**65e:** Hexacosanoic acid**f: flavonoids****66f:** Naringenin**67f:** Apigenin**68f:** Linarigenin**69f:** Luteolin**70f:** 5,4'-Dihydroxy-7- methoxyflavonol**71f:** 5,3'-Dihydroxy-7,4'-
dimethoxyflavonol



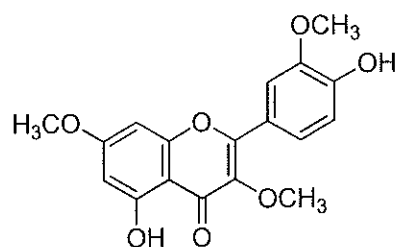
72f: 3',4',5-Trihydroxy-3,7-dimethoxyflavone



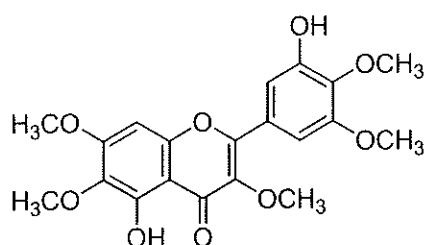
73f: 5-Hydroxy-7,3',4'-trimethoxyflavonol



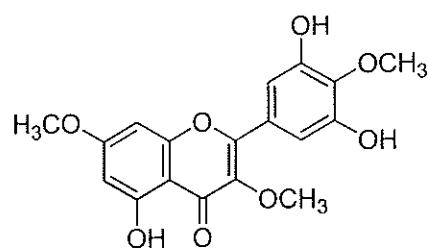
74f: 5,3'-Dihydroxy-3,7,4',5'-tetramethoxyflavone



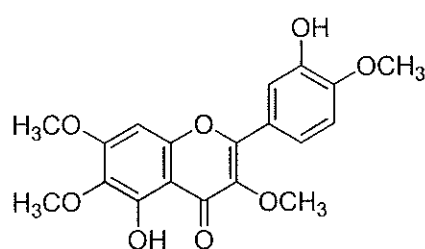
75f: 3,7,3'-Trimethylquercetin



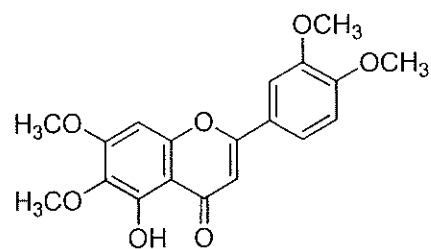
76f: 5,3'-Dihydroxy-3,6,7,4',5'-pentamethoxyflavone



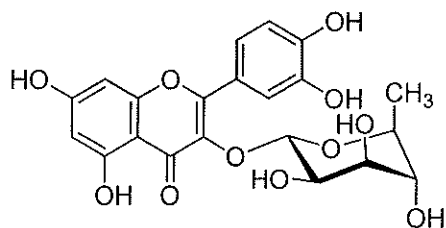
77f: Myricetin-3',4',7-trimethyl ether



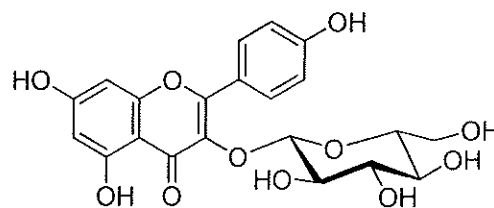
78f: Chryso-splenetin



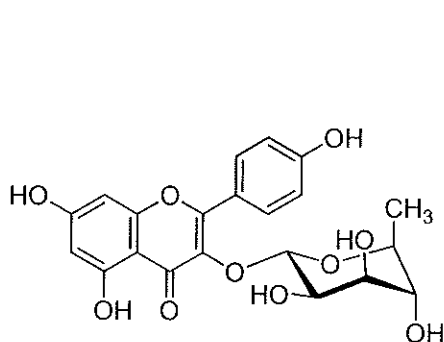
79f: 5-Hydroxy-3',4',6,7-tetramethoxyflavone



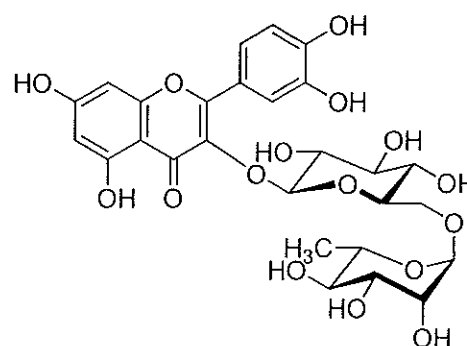
80f: Quercetin 3-*O*- α -L-rhamnopyranoside



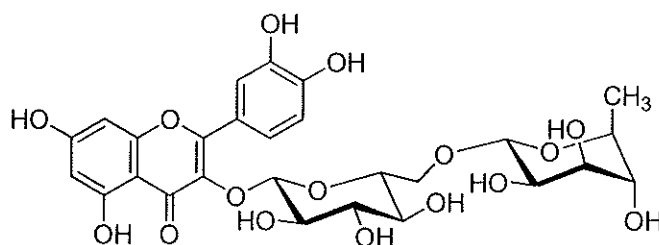
81f: Kaempferol 3-*O*- β -D-glucopyranoside



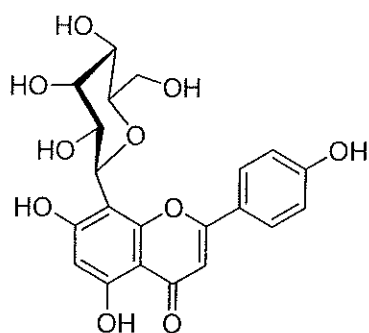
82f: Afzelin



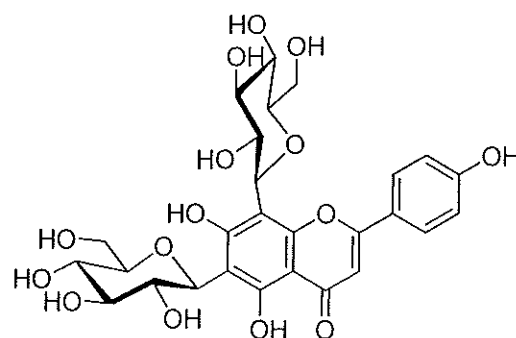
83f: Rutin



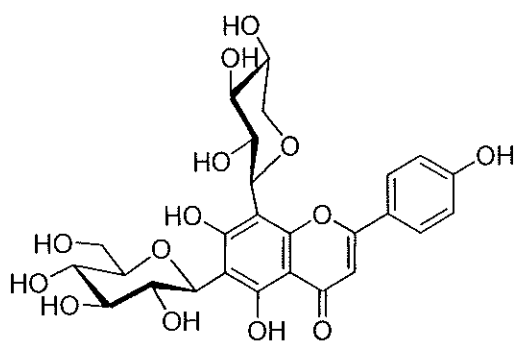
84f: Quercetin 3-rutinoside



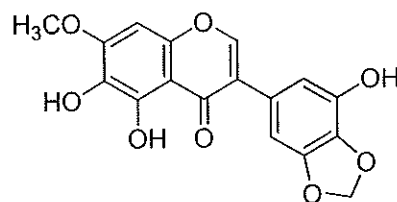
85f: Vitexin



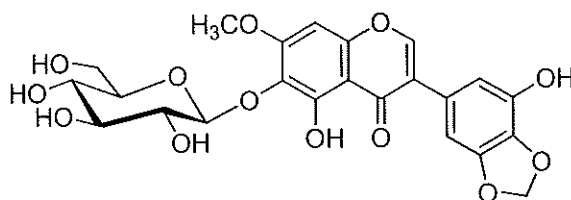
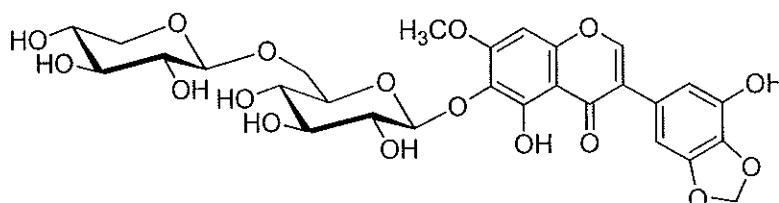
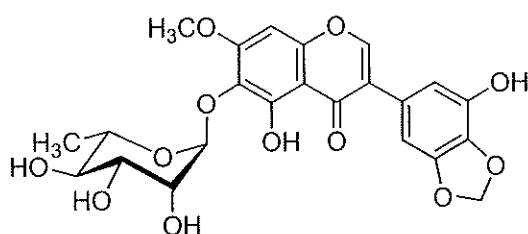
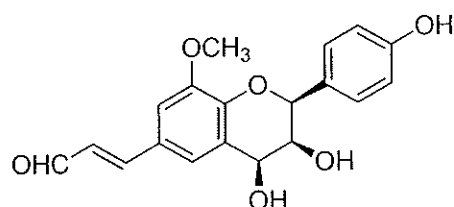
86f: Vicenin 2



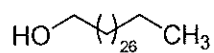
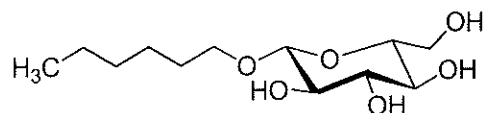
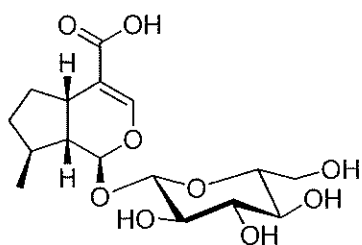
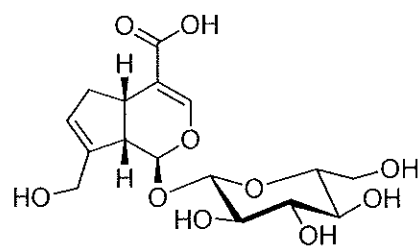
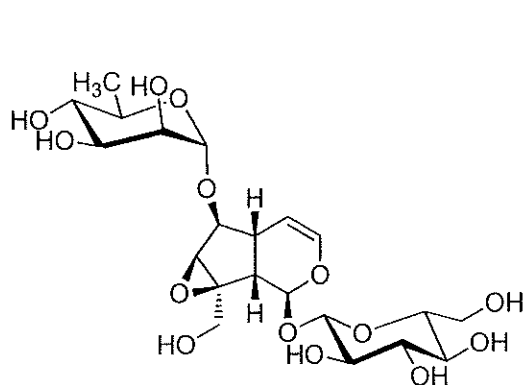
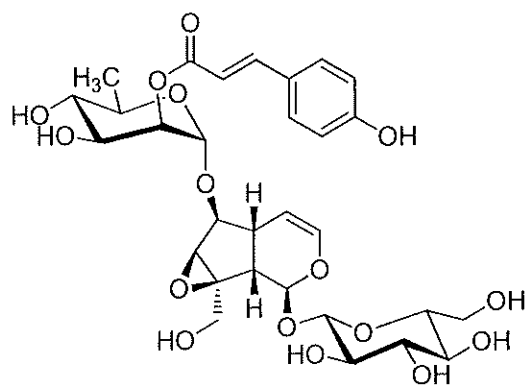
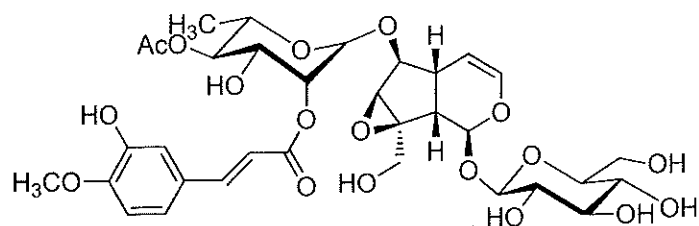
87f: Vicenin 3

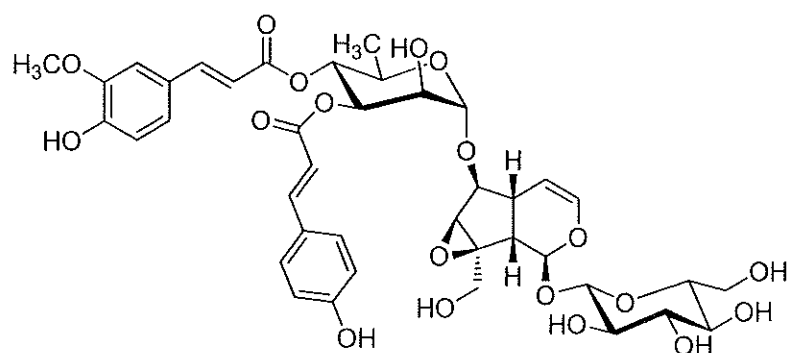


88f: 6,3'-Dihydroxy-7-methoxy-4',5'-methylenedioxyisoflavone

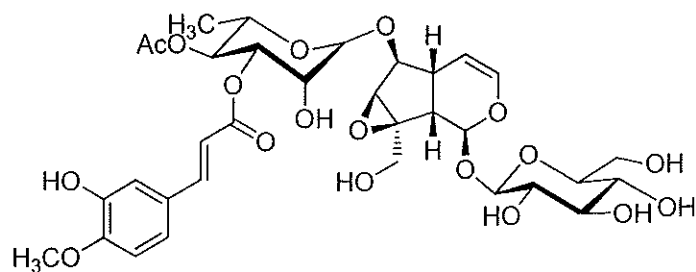
89f: 6,3'-Dihydroxy-7-methoxy-4',5'-methylenedioxyisoflavone 6-O- β -D-glucopyranoside90f: 6,3'-Dihydroxy-7-methoxy-4',5'-methylenedioxyisoflavone 6-O- β -D-xylopyranosyl(1 \rightarrow 6)- β -D-glucopyranoside91f: 6,3'-Dihydroxy-7-methoxy-4',5'-methylenedioxyisoflavone 6-O- α -L-rhamnopyranoside

92f: 4'-Hydroxy-8,3'-dimethoxy-6-acroleinylflavan-3,4-diol

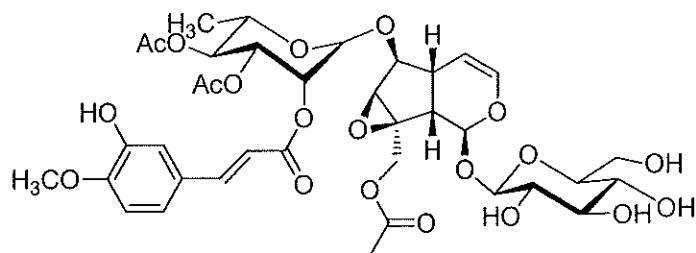
g: hydrocabons**93g:** Triacontanol**94g:** Hexyl glucoside**h: iridoids****95h:** Glucoside-B**96h:** Glucoside-C**97h:** Premnoside C**98h:** Saccatoside**99h:** 6-O-α-L-(2''-O-Isoferuloyl, 4''-O-acetyl)rhamnopyranosylcatalpol



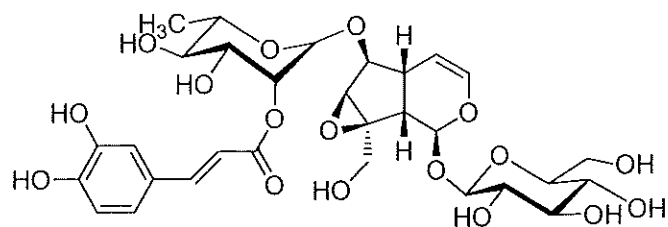
100h: Premnoside D



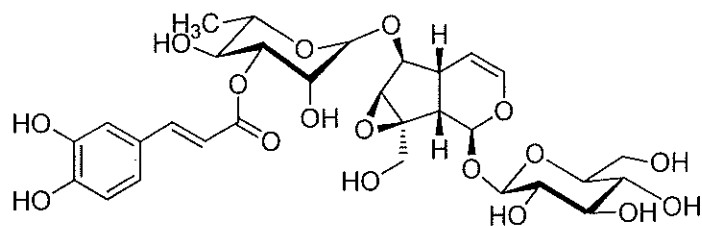
101h: 6-*O*- α -L-(3''-*O*-Isoferuloyl, 4''-*O*-acetyl)rhamnopyranosylcatalpol



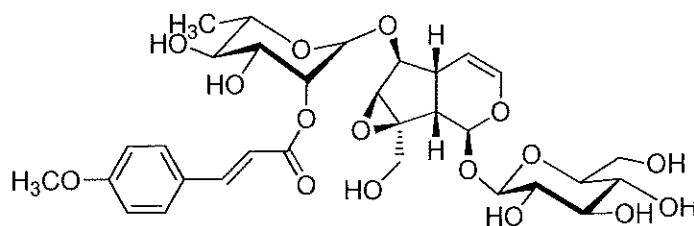
102h: 6-*O*- α -L-(4''-*O*-*trans*-*p*-Coumaroyl)rhamnopyranosylcatapols



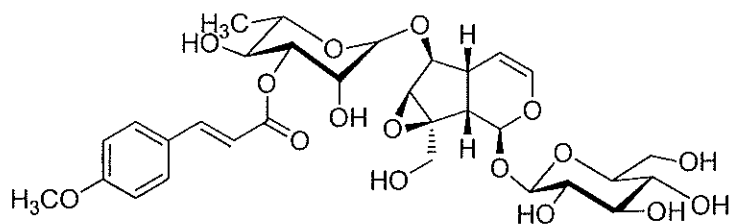
103h: 6-*O*- α -L-(2''-*O*-Caffeoyl)rhamnopyranosylcatapol



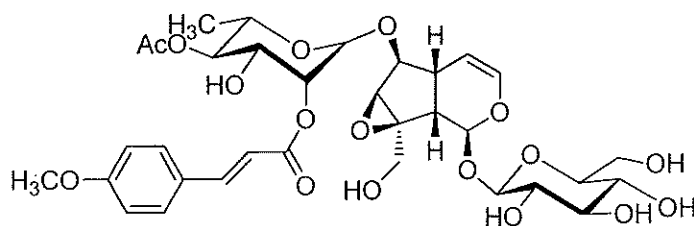
104h: 6-*O*-α-*L*-(3''-*O*-Caffeoyl)rhamnopyranosylcatalpol



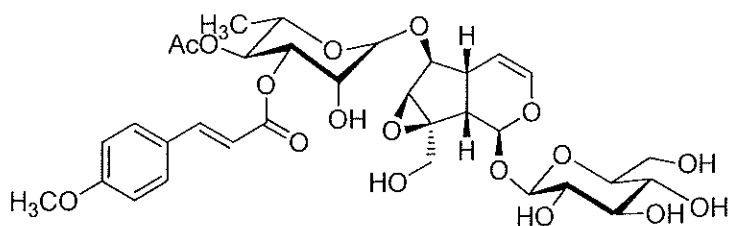
105h: 6-*O*-α-*L*-(2''-*O*-*p*-Methoxycinnamoyl)rhamnopyranosylcatalpol



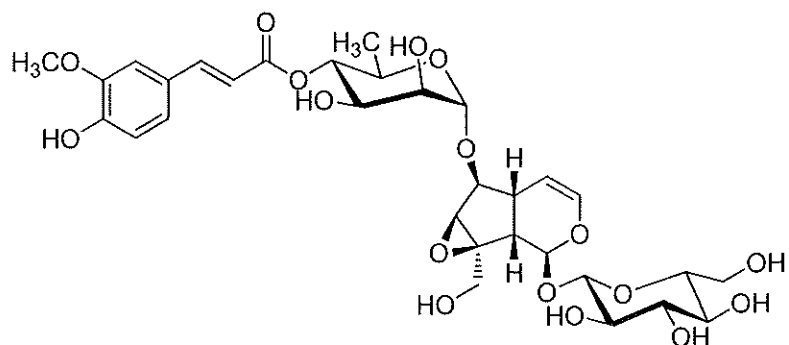
106h: 6-*O*-α-*L*-(3''-*O*-*p*-Methoxycinnamoyl)rhamnopyranosylcatalpol



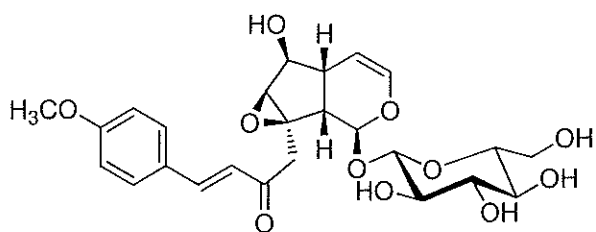
107h: 6-*O*-α-*L*-(2''-*O*-*p*-Methoxycinnamoyl-4-*O*-acetyl)rhamnopyranosylcatalpol



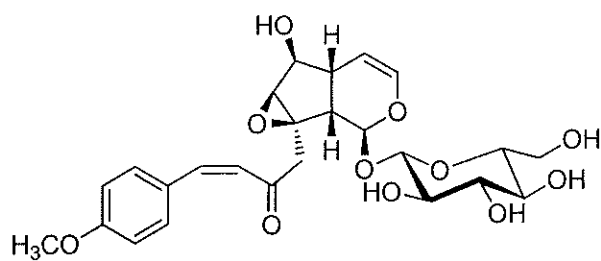
108h: 6-*O*-α-*L*-(3''-*O*-*p*-Methoxycinnamoyl-4''-*O*-acetyl)rhamnopyranosylcatalpol



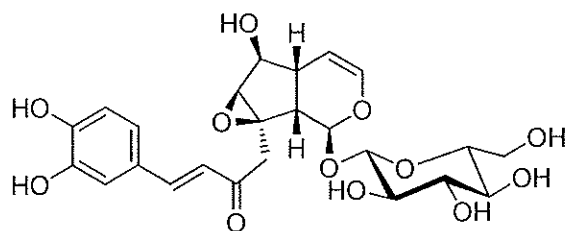
109h: 6- α -L-(4''-O-Feruloyl)-rhamnopyranosylcatalpol



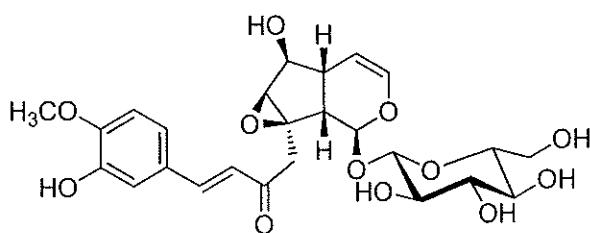
110h: 10-*O*-*trans*-*p*-Methoxycinnamoylcatalpol



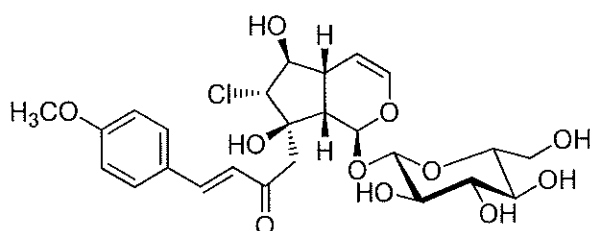
111h: 10-*O*-*cis*-*p*-Methoxycinnamoylcatalpol



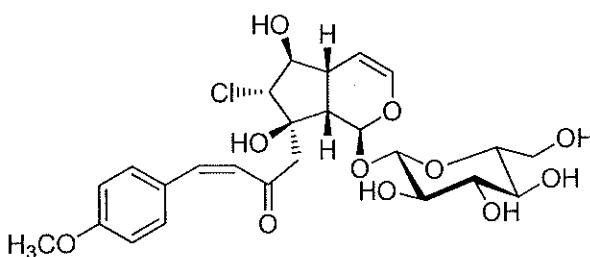
112h: 10-*O*-*trans*-Caffeoylcatalpol



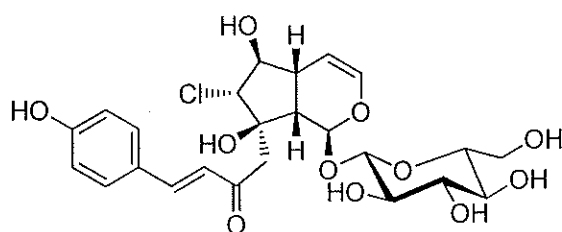
113h: 10-*O*-*trans*-Isoferuloylcatalpol



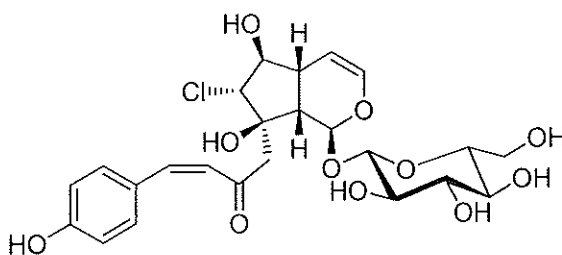
114h: 10-*O*-*trans*-*p*-Methoxycinnamoyl asystasioside E



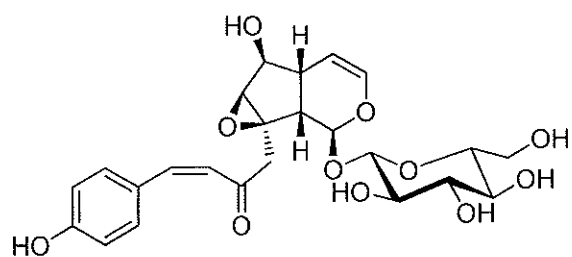
115h: 10-*O*-*cis*-*p*-Methoxycinnamoyl asystasioside E



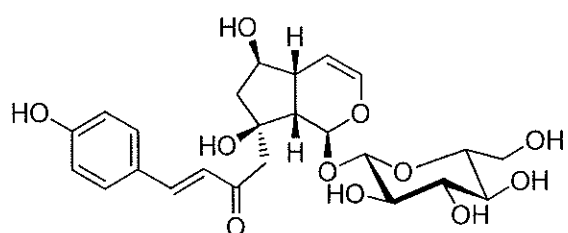
116h: 10-*O*-*trans*-*p*-Coumaroyl asystasioside E



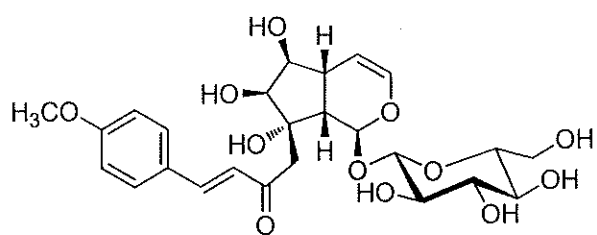
117h: 10-*O*-*sis*-*p*-Coumaroyl asystasioside E



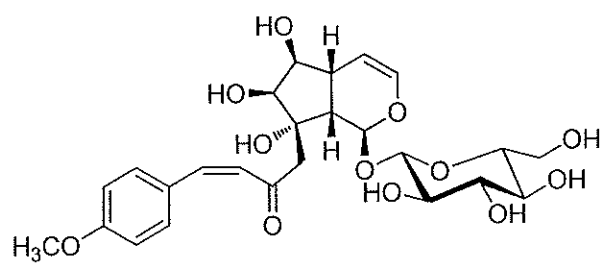
118h: 10-*O*-*cis*-*p*-Coumaroylcatalpol



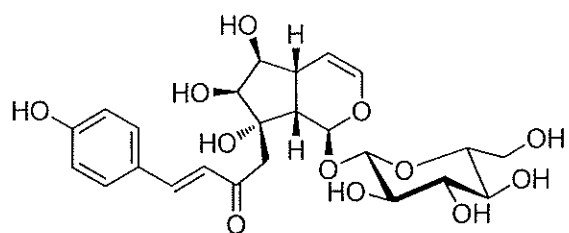
119h: Scutellarioside II



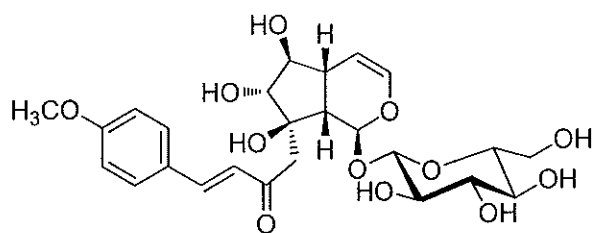
120h: 4''-Methoxy-*E*-globularinin



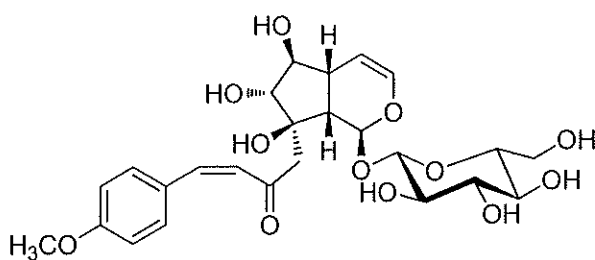
121h: 4''-Methoxy-*Z*-globularinin



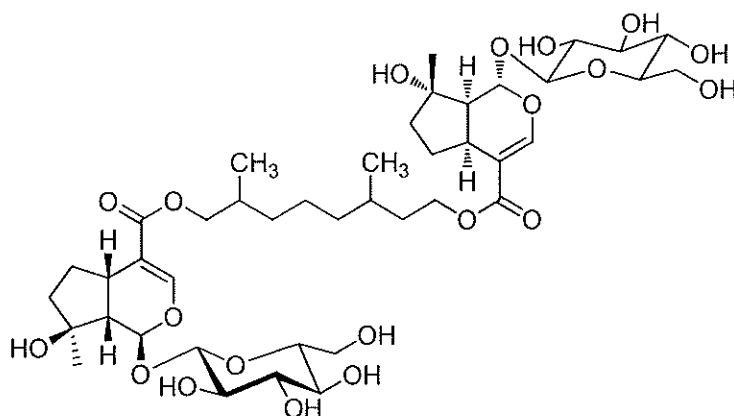
122h: 4''-Hydroxy-*E*-globularinin



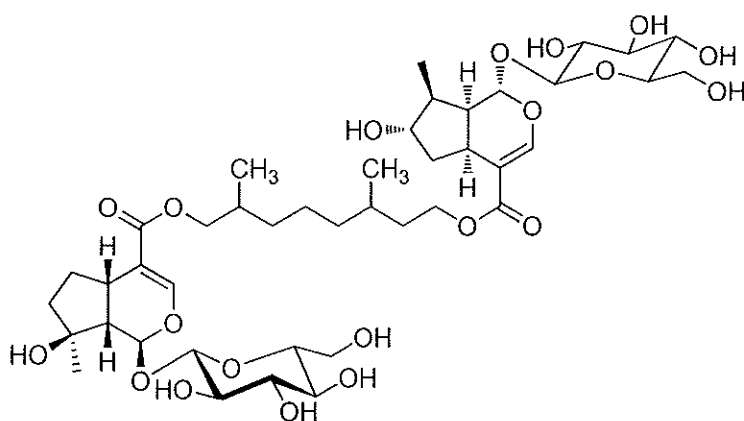
123h: 4''-Methoxy-*E*-globularimin



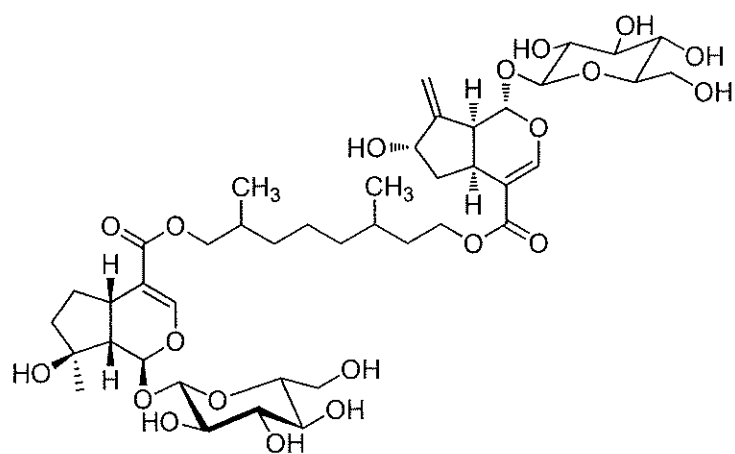
124h: 4''-Methoxy-*Z*-globularimin



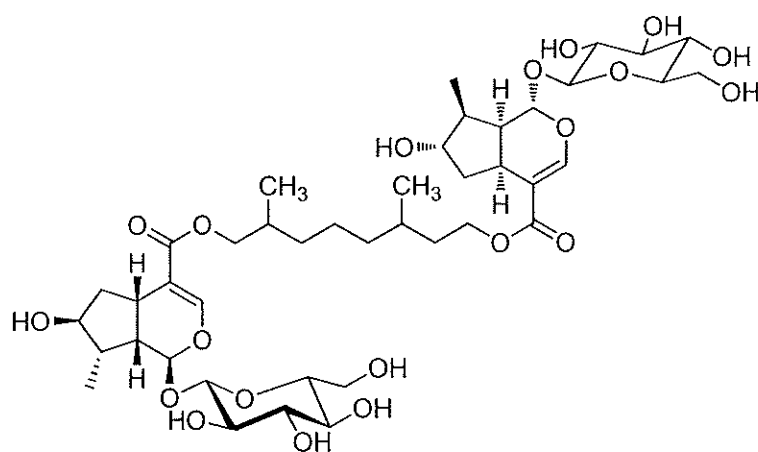
125h: Premnaodoroside A



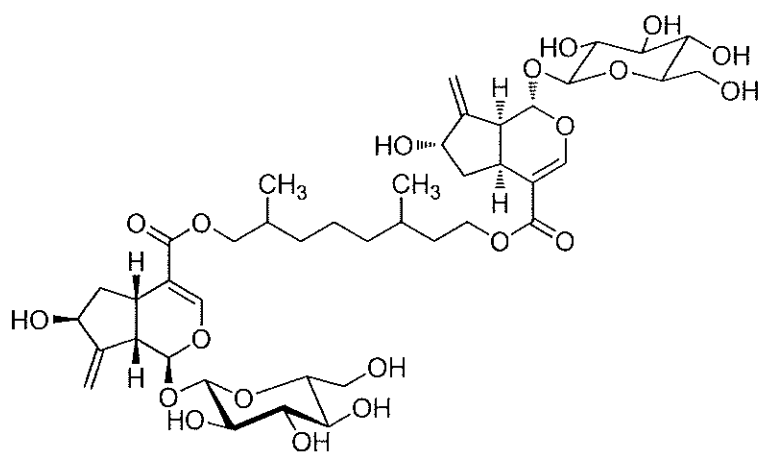
126h: Premnaodoroside B



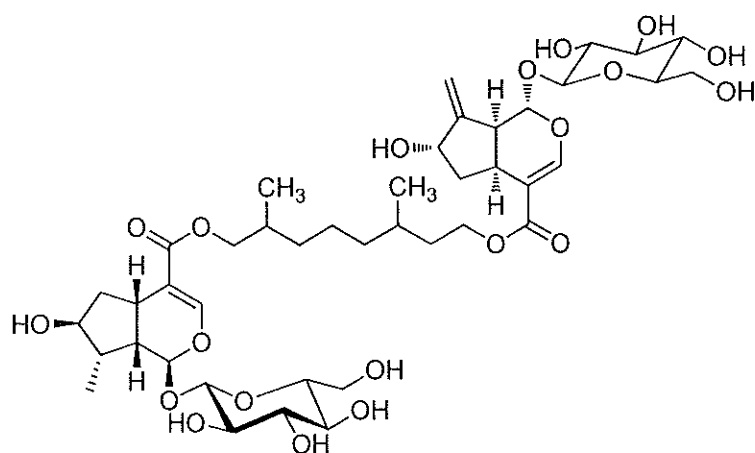
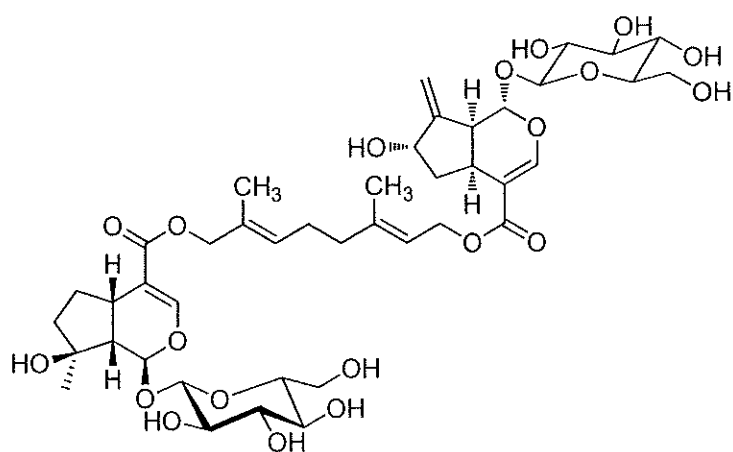
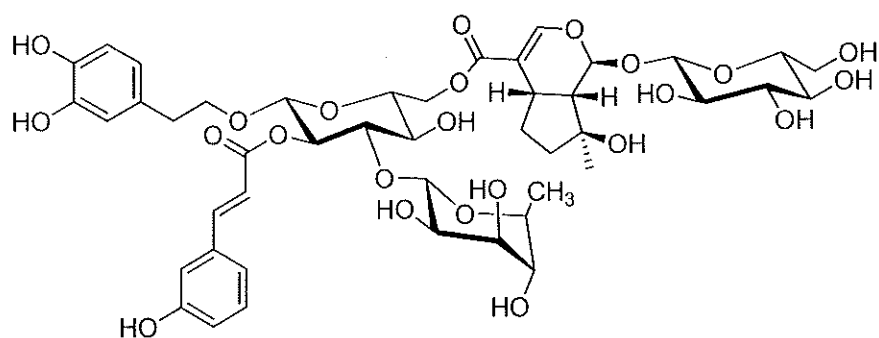
127h: Premnaodoroside C

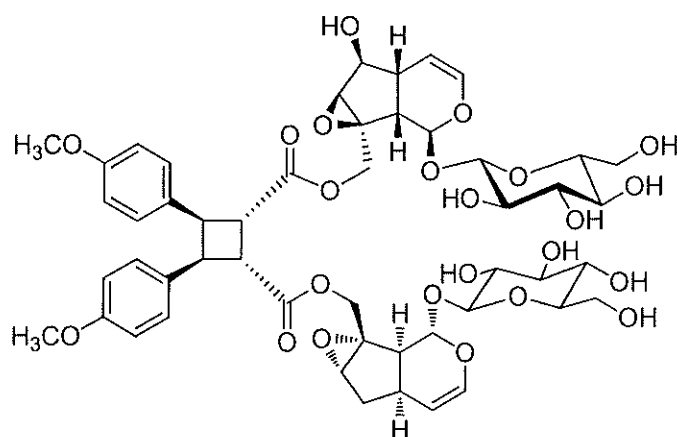


128h: Premnaodoroside D



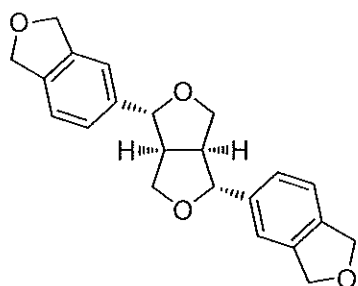
129h: Premnaodoroside E

**130h:** Premnaodoroside F**131h:** Premnaodoroside G**132h:** Premcorymboside A

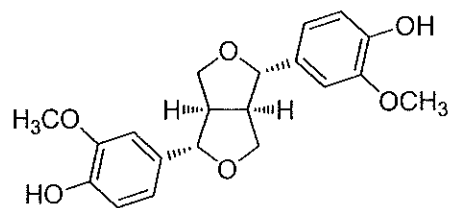


133h: 4,4'-Dimethoxy- β -truxinic acid catalpol diester

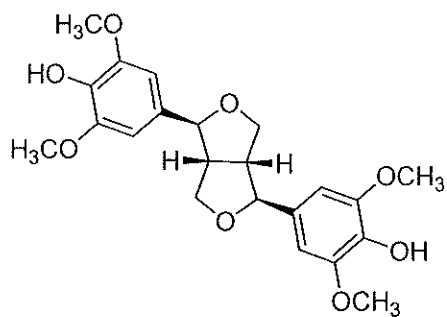
i: lignans



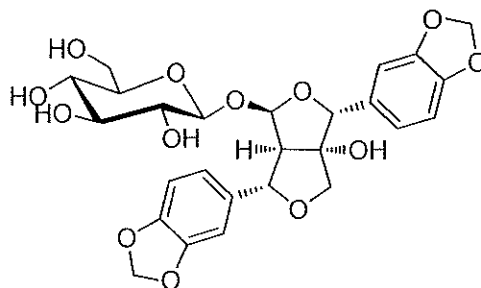
134i: (+)-Sesamin



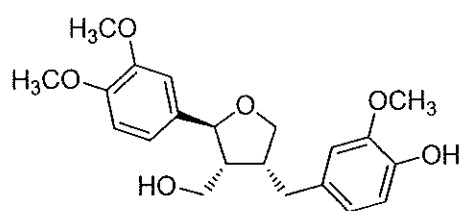
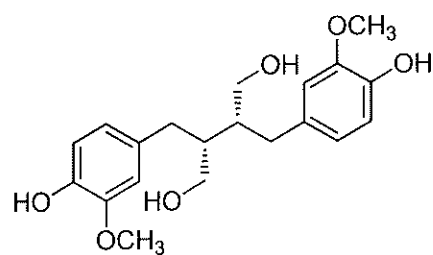
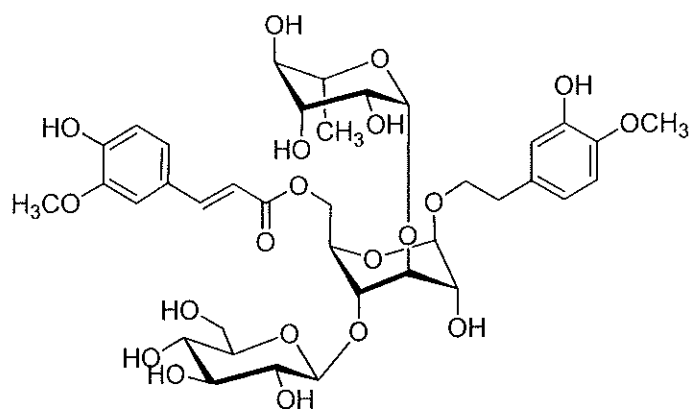
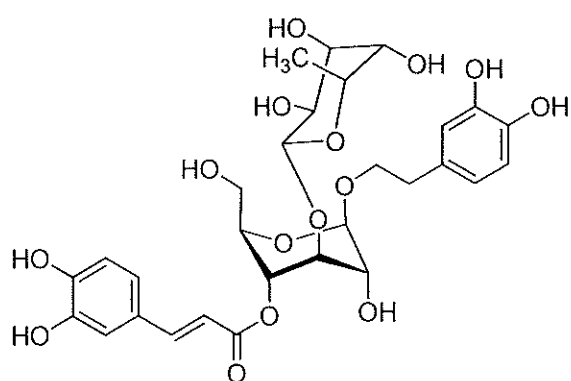
135i: (+)-1-Hydroxypinoresinol

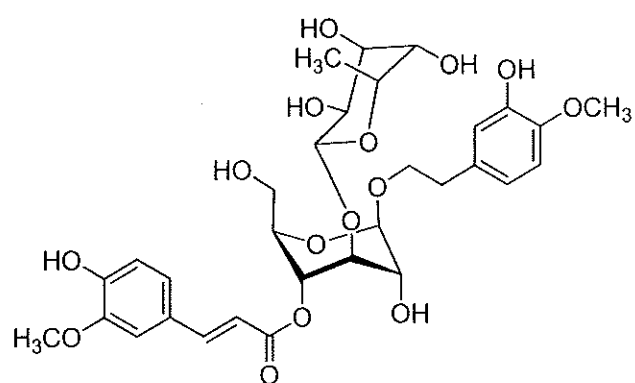
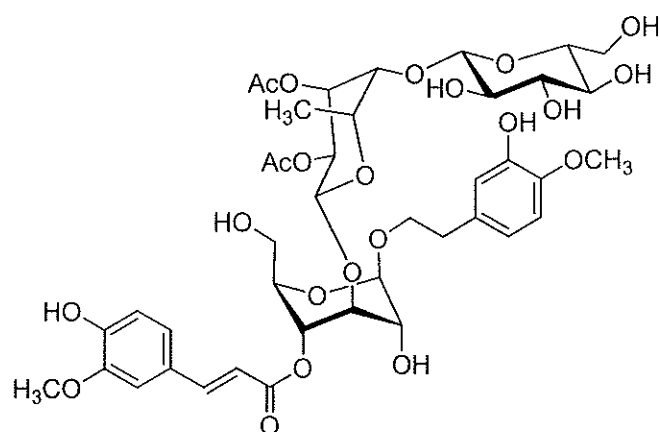
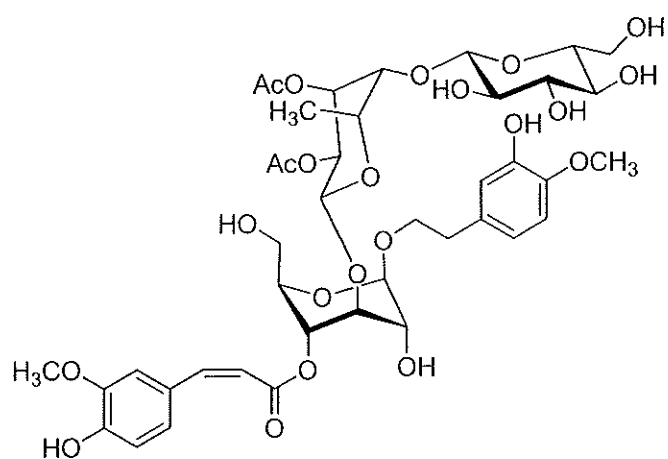


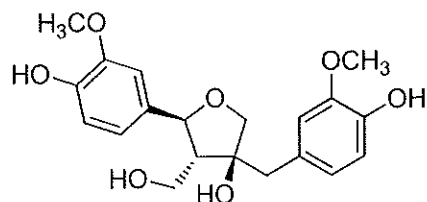
136i: Syringaresinol



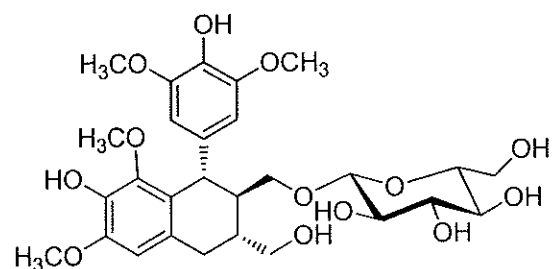
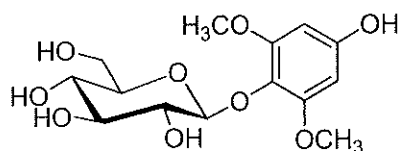
137i: 4-*epi*-Gummadiol-*O*- β -D-glucopyranoside

**138i:** (+)-Lariciresinol**139i:** (-)-*seco*-Isolariciresinol**j: phenylethanoids****140j:** Premnafolioside**141j:** Verbascoside

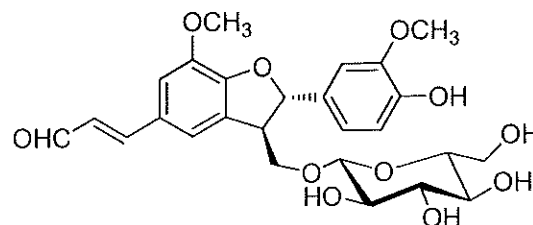
**142j:** Martynoside**143j:** Premnethanoside A**144j:** Premnethanoside B



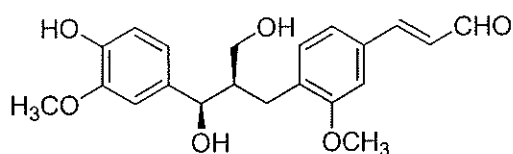
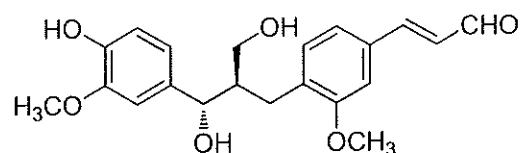
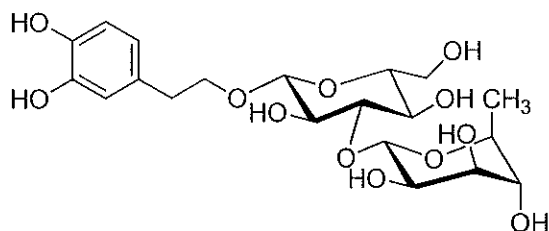
145j: (-)-Olivile

146j: Lyoniresinol 9'- β -D-glucopyranoside

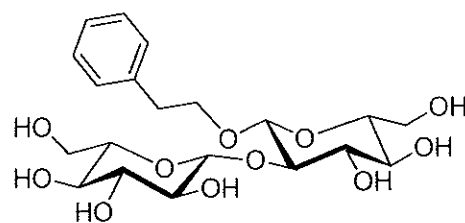
147j: Leonuriside A

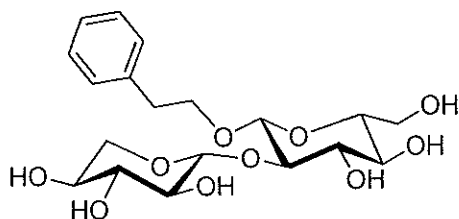


148j: Plucheoside D1

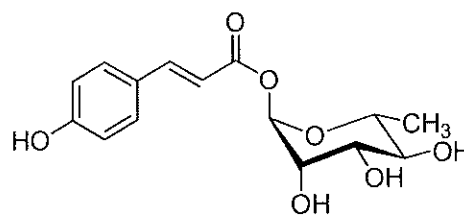
149j: *erythro*-(4-Hydroxy-3-methoxyphenyl)-2-{4-[2-formyl-(*E*)-vinyl]-2-methoxyphenoxy}-propan-1,3-diol150j: *thero*-(4-Hydroxy-3-methoxyphenyl)-2-{4-[2-formyl-(*E*)-vinyl]-2-methoxyphenoxy}-propan-1,3-diol

151j: Decaffeoyllacteoside

152j: Benzyl alcohol β -D-(2'-*O*- β -D-xylopyranosyl)glucopyranoside

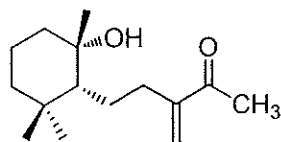


153j: Phenethyl alcohol β -D-(2'-O- β -D-glucopyranosyl)glucopyranoside

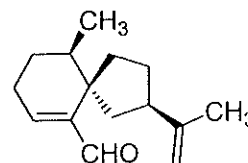


154j: 1-O-*trans-p*-Coumaroyl- α -L-rhamnopyranoside

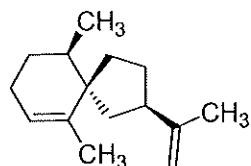
k: sesquiterpenoids



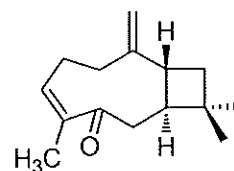
155k: 7 α -Hydroxy-6,11-cyclofarnes-3(15)-en-2-one



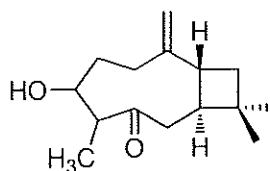
156k: Premnaspical



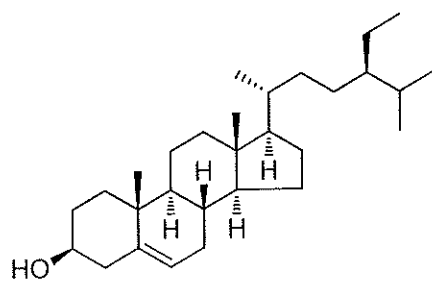
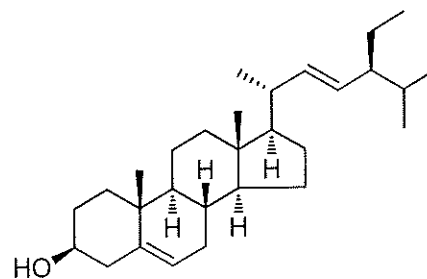
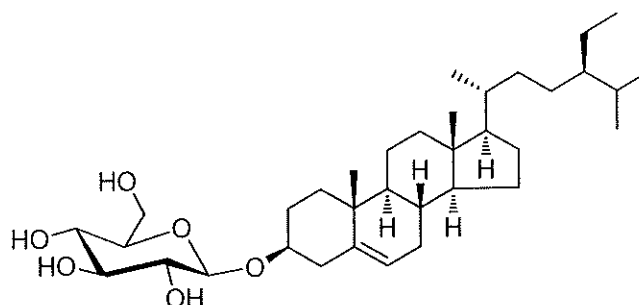
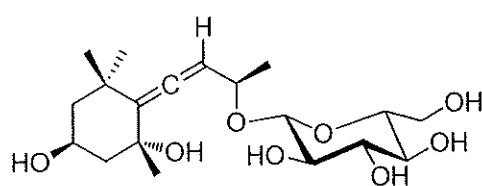
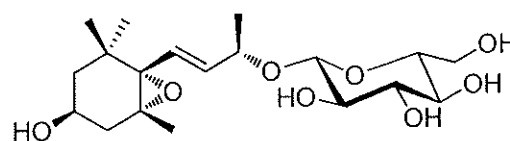
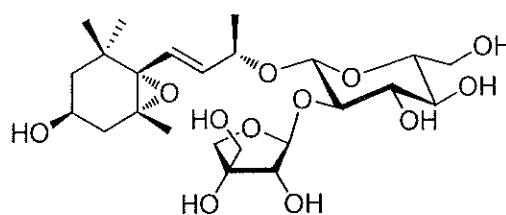
157k: Premnaspirodiene



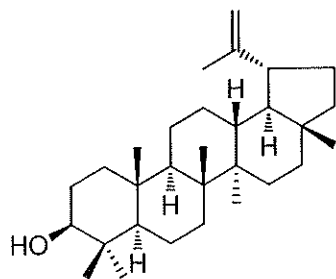
158k: Buddledin C



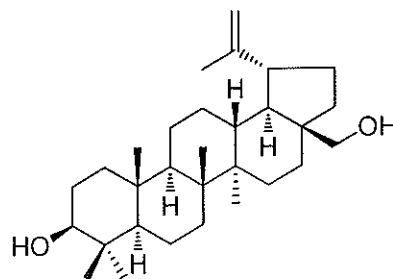
159k: 5-Hydroxy-4,5-dihydrocaryophyllen-3-one

l: steroids**160l:** β -Sitosterol**161l:** Stigmasterol**162l:** β -Daucosterol**m: terpenoids****163m:** 7-(3,5-Dihydroxy-1,1,5-trimethyl cyclohexylidene)-9-methylprop-8-enyl 9-*O*- β -D-glucopyranoside**164m:** 3-Hydroxy-5,6-epoxy- β -ionol-9-*O*- β -D-glucopyranoside**165m:** Premnaionoside

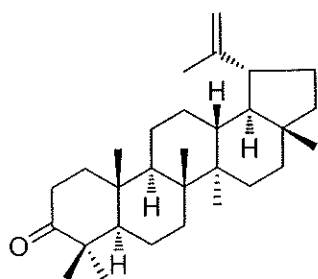
n: triterpenoids



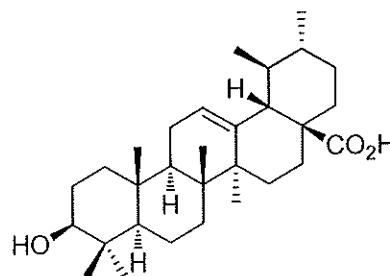
166n: Lupeol



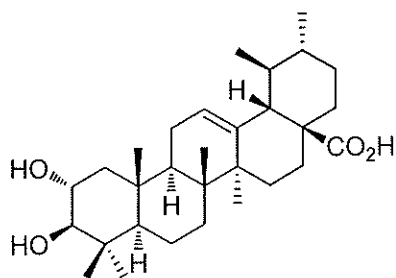
167n: Betulin



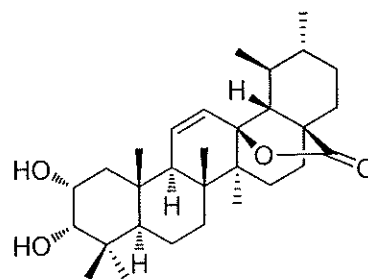
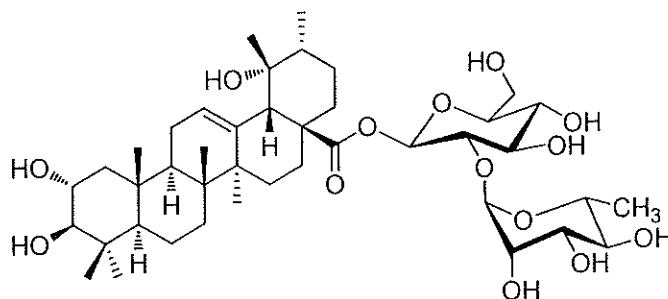
168n: Lupenone

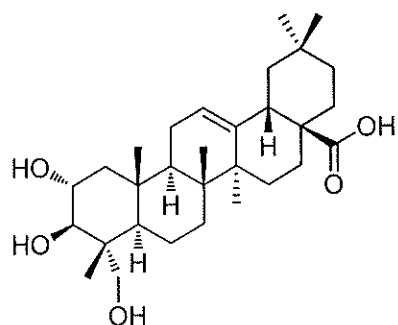


169n: Ursolic acid

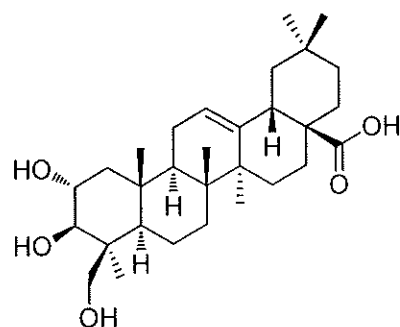


170n: 2α-Hydroxyursolic acid

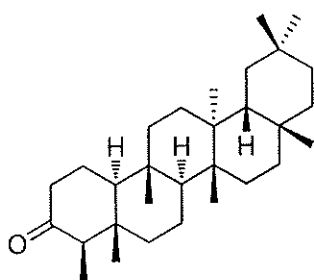
171n: 3-*epi*-Corosolic acid lactone172n: 28-*O*-α-L-Rhamnopyranosyl(1→2)-β-D-glucopyranoside tormentic acid ester



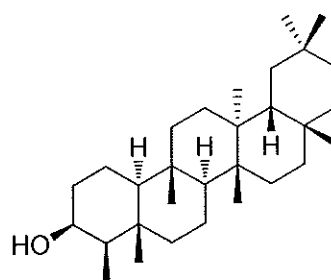
173n: Arjunolic acid



174n: Hyptatic acid A

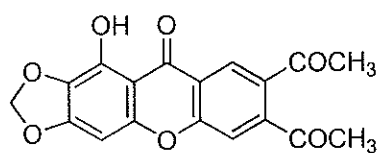


175n: Friedelin

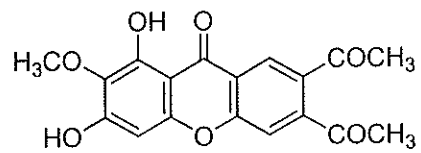


176n: β -Friedelinol

o: xanthenes



177o: 1-Hydroxy-2,3-methylenedioxy-6-methoxycarbonyl-7-acetylxanthone



178o: 1,3-dihydroxy-2-methoxy-6-methoxycarbonyl-7-acetylxanthone

1.3 Objectives

Up to the present, the chemical constituents and biological activities of these plants are of interest. This research involved isolation, purification and structure elucidation of chemical constituents isolated from the roots and fruits of *Diosyros wallichii* and the roots and twigs of *Premna obtusifolia* and also evaluation of pure compounds for antibacterial and cytotoxic activities for *D. wallichii* and anti-inflammatory, and antibacterial activities for *P. obtusifolia*.

CHAPTER 2

EXPERIMENTAL

2.1 Instruments and Chemicals

Melting points were determined on the Fisher-John melting point apparatus. UV spectra were recorded on SPECORD S100 (Analytikjena), UV-160A spectrophotometer (Shimadzu) and principle bands (λ_{\max}) were recorded as wavelengths (nm) and $\log \varepsilon$ in MeOH solution. The optical rotations $[\alpha]_D$ were measured in chloroform and methanol solution at the Sodium D line (590 nm) on a JASCO P-1020 digital polarimeter. The IR spectra were measured with a Perkin-Elmer FTS FT-IR and Shimadzu FTIR-8900 IR spectrophotometer. Single Crystal X-ray diffraction measurements were collected using SMART 1-K CDD diffractometer with monochromated Mo-K α radiation ($\lambda = 0.71073 \text{ \AA}$) using ω -scan mode and SHELXTL for structure solution and refinement. NMR spectra were recorded using 300, 400 and 500 MHz Bruker FTNMR Ultra ShieldTM spectrometers in CDCl₃ with TMS as the internal standard. Chemical shifts are reported in δ (ppm) and coupling constants (J) are expressed in hertz. EI and HREI mass spectra were measured on a Kratos MS 25 RFA spectrometer. Solvents for extraction and chromatography were distilled at their boiling point ranges prior to use except chloroform which was analytical grade reagent. Vacuum liquid chromatography (VLC) and column chromatography (CC) were carried out on silica gel 60H (Merck) and silica gel 100 (Merck), respectively.

2.2 Plant Material

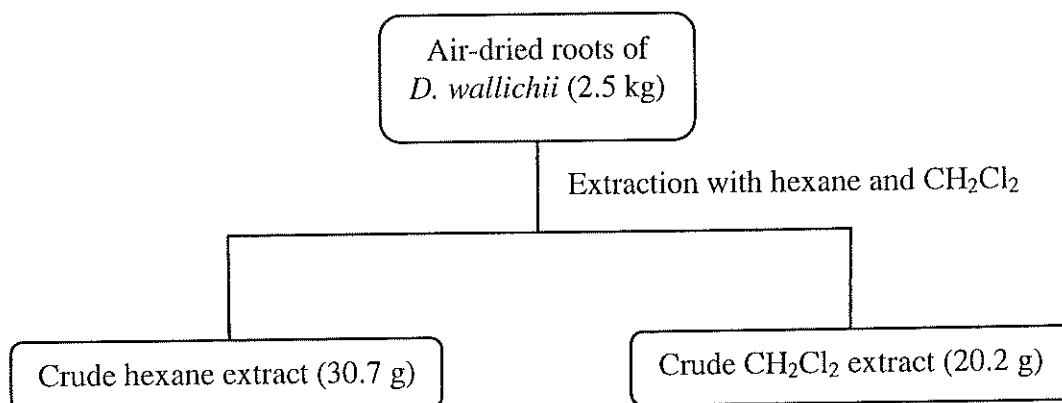
The roots and fruits of *D. wallichii* were collected in December 2008 from Satun Province in the southern part of Thailand. This plant was identified by Prof. Puangpen Sirirugsa and a voucher specimen (No. PSU 0013410) has been deposited at the Herbarium of Department of Biology, Faculty of Science, Prince of Songkla University.

Roots and twigs of *P. obtusifolia* were collected from Satun Province in the southern part of Thailand in 2008 and identified by Assoc. Prof. Dr. Kitichate Sridith, Department of Biology, Faculty of Science, Prince of Songkla University and a voucher specimen (No. PSU 0013409) has been deposited in the Herbarium of the same department.

2.3 Extractions and Isolations

2.3.1 Isolation and chemical investigation of *D. wallichii*

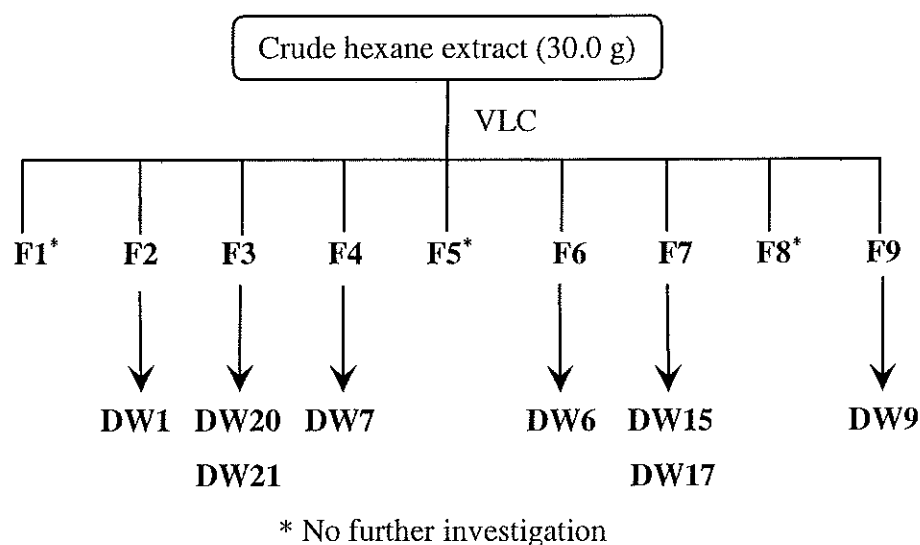
The air-dried and pulverized roots (2.5 kg) were exhaustively extracted with hexane and methylene chloride successively (2 x 10 L for each solvent for one week) at room temperature and evaporated under reduced pressure to provide crude hexane (30.7 g) and CH₂Cl₂ (20.2 g) extracts, respectively. The process of extraction was shown in **Scheme 1**.



Scheme 1 Extraction of the roots of *D. wallichii*.

2.3.1.1 Investigation of the crude hexane extract from the roots of *D. wallichii*

The crude hexane extract (30.0 g) was subjected to vacuum liquid chromatography (VLC) using hexane as eluent and increasing polarity with EtOAc to give nine fractions (F1-F9).



Scheme 2 Isolation of compounds **DW1**, **DW6-DW7**, **DW9**, **DW15**, **DW17** and **DW20-DW21** from the hexane extract.

Fraction F2 (8.8 g) was recrystallized from methylene chloride to give **DW1** (4.3 g).

Fraction F3 (3.7 g) was separated by VLC using EtOAc-hexane (2:8, v/v) as eluting solvent to afford five subfractions (F3a-F3e). Subfraction F3b (2.9 g) was purified by VLC with EtOAc-hexane (1:9, v/v) to afford a mixture of **DW20** and **DW21** (1.7 g).

Fraction F4 (3.5 g) was separated by VLC using EtOAc-hexane (1:9, v/v) as eluting solvent to afford five subfractions (F4a-F4e). Subfraction F4d (762.3 mg) was purified by VLC with EtOAc-hexane (0.5:9.5, v/v) to afford **DW7** (117.2 mg).

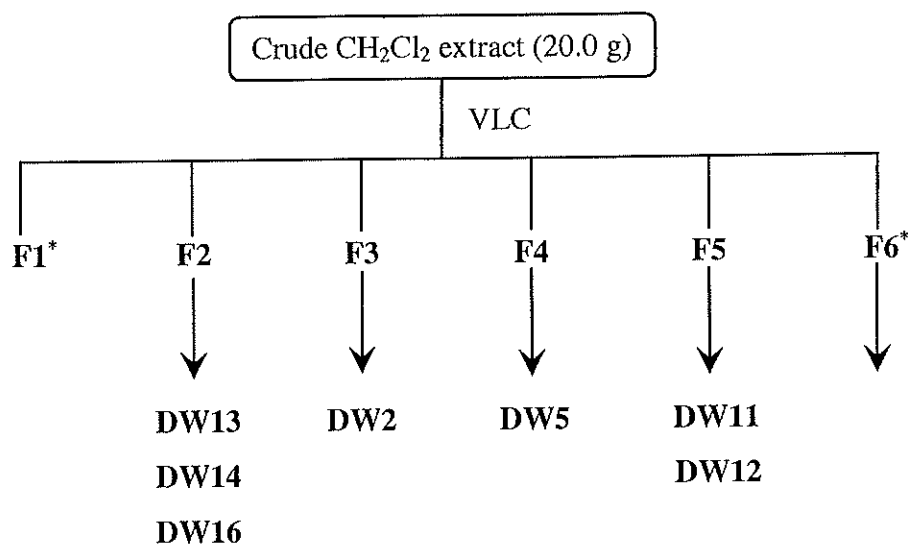
Fraction F6 (1.5 g) was separated by VLC using CH₂Cl₂-hexane (4:6, v/v) as eluting solvent to afford three subfractions (F6a-F6c). Subfraction F6c (428.6 mg) was purified by VLC with EtOAc-hexane (2:8, v/v) to give **DW6** (47.7 mg).

Fraction F7 (6.4 g) was separated by VLC with EtOAc-hexane (3:7, v/v) to afford **DW15** (3.9 g) and **DW17** (509.2 mg).

Fraction F9 (1.3 g) was separated by VLC with EtOAc-CH₂Cl₂ (1:9, v/v) to give **DW9** (156.4 mg).

2.3.1.2 Investigation of the crude CH₂Cl₂ extract from the roots of *D. wallichii*

The CH₂Cl₂ extract (20.2 g) was separated by VLC using hexane as eluent and increasing polarity with EtOAc to give six fractions (F1-F6).



* No further investigation

Scheme 3 Isolation of compounds **DW2**, **DW5**, **DW11-DW14** and **DW16** from the CH₂Cl₂ extract.

Fraction F2 (3.6 g) was separated by VLC with EtOAc-hexane (2:8, v/v) to afford **DW13** (35.4 mg), **DW14** (3.7 g) and **DW16** (25.6 mg).

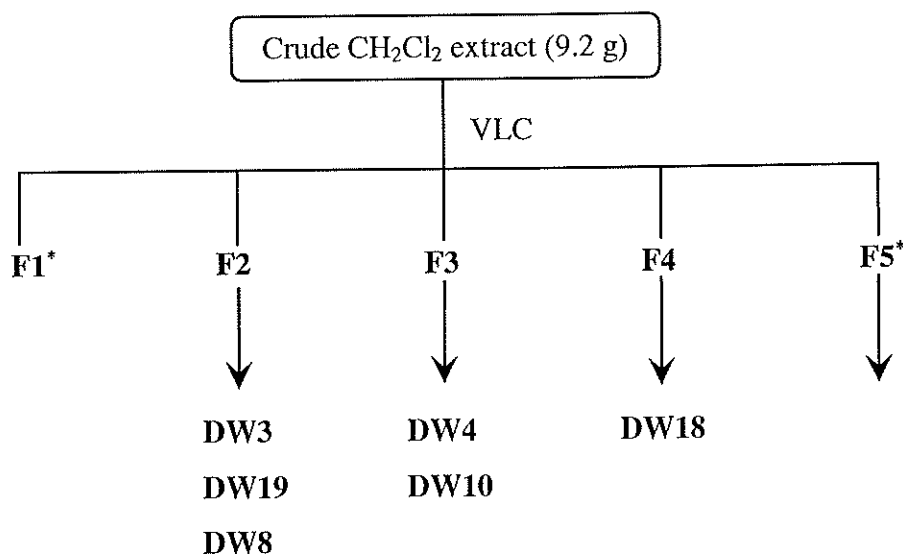
Fraction F3 (1.2 g) was separated by VLC using acetone-hexane (2:9, v/v) as eluting solvent to afford six subfractions (F3a-F3f). Subfraction F3d (352.8 mg) was purified by VLC with EtOAc-hexane (1:9, v/v) to give **DW2** (33.6 mg).

Fraction F4 (612.8 mg) was separated by VLC with Acetone-hexane (1:9, v/v) to afford **DW5** (18.4 mg).

Fraction F5 (2.3 g) was separated by VLC using EtOAc-hexane (3:7, v/v) as eluting solvent to afford four subfractions (F5a-F5d). Subfraction F5c (1.5 g) was separated by VLC using Acetone-hexane (2:8, v/v) as eluting solvent to afford five subfractions (F5c1-F5c5). Subfraction F5c3 (527.2 mg) was purified by VLC with CH₂Cl₂-hexane (4:6, v/v) to give **DW11** (40.4 mg). Subfraction F5c5 (752.3 mg) was purified by VLC with EtOAc-hexane (3:7, v/v) to give **DW12** (32.4 mg).

2.3.1.2 Investigation of the crude CH₂Cl₂ extract from the fresh fruits of *D. wallichii*

The fresh fruits of *Diospyros wallichii* (0.5 kg) were extracted with MeOH (2 x 2 L for one week) at room temperature. The extract was evaporated to dryness and the residue was partitioned between CH₂Cl₂ and H₂O. The CH₂Cl₂ layer was evaporated and the residue (9.2 g) was subjected to VLC using hexane as eluent and increasing polarity with EtOAc to give five fractions (F1-F5).



* No further investigation

Scheme 4 Isolation of compounds **DW3-DW4, DW8, DW10, DW18** and **DW19** from the CH₂Cl₂ extract

Fraction F2 (1.3 g) was separated by VLC using EtOAc-hexane (1:9, v/v) as eluting solvent to afford five subfractions (F2a-F2e). Subfraction F2d (452.2

mg) was purified by VLC with EtOAc-hexane (0.5:9.5, v/v) to give **DW3** (19.5 mg) and **DW19** (11.7 mg). Subfraction F2e (552.3 mg) was separated by VLC using EtOAc-hexane (0.5:9.5, v/v) as eluting solvent to afford two subfractions (F2e1-F2e2). Subfraction F2e2 (359.3 mg) was purified by VLC with CH₂Cl₂-hexane (3:7, v/v) to afford **DW8** (14.7 mg).

Fraction F3 (3.3 g) was separated by VLC using Acetone-hexane (2:8, v/v) as eluting solvent to afford five subfractions (F3a-F4e). Subfraction F3a (528.1 mg) was purified by VLC with EtOAc-hexane (3:7, v/v) to give **DW4** (10.5 mg) and **DW10** (13.4 mg).

Fraction F4 (1.5 g) was separated by VLC with EtOAc-hexane (5:5, v/v) to afford **DW18** (18.9 mg).

Compound DW1, plumbagin: Orange needles; m.p. 77-79 °C; UV (MeOH) λ_{\max} : 209, 264 and 413 nm; IR (thin film) ν_{\max} : 3370, 1665, 1645, 1610, 1595, 875 cm⁻¹; ¹H NMR (CDCl₃, 300 MHz) and ¹³C NMR (CDCl₃, 75 MHz), see Table 3.

Compound DW2, droserone: Orange amorphous powder; m.p. 169-172 °C; UV (MeOH) λ_{\max} : 228, 278 and 400 nm; IR (thin film) ν_{\max} : 3308, 1643, 1625, 1580, 1435, 1395, 1095, 835 cm⁻¹; ¹H NMR (CDCl₃, 300 MHz) and ¹³C NMR (CDCl₃, 75 MHz), see Table 5.

Compound DW3, 2,3-epoxyplumbagin: Pale yellow needles; m.p. 97-99 °C; $[\alpha]_{\text{D}}^{28}$ -17.4 (CHCl₃, *c* 0.50); UV (MeOH) λ_{\max} : 254, 283 and 420 nm; IR (thin film) ν_{\max} : 3407, 1655, 1635, 1614, 1577, 754 cm⁻¹; ¹H NMR (CDCl₃, 300 MHz) and ¹³C NMR (CDCl₃, 75 MHz), see Table 7.

Compound DW4, 2-hydroxymethyl-5-methoxy-1,4-naphthoquinone: Orange powder; m.p. 145-147 °C; UV (MeOH) λ_{\max} : 226, 263 and 414 nm; IR (thin film) ν_{\max} : 3467, 1651, 1632, 1458, 1377, 1284 1065, 980 cm⁻¹; ¹H NMR (CDCl₃, 300 MHz) and ¹³C NMR (CDCl₃, 75 MHz), see Table 9.

Compound DW5, diomuscinone: White amorphous solid; m.p. 93-95 °C; UV (MeOH) λ_{\max} : 212 and 256 nm; IR (thin film) ν_{\max} : 3430, 1640, 1600, 1575, 1490, 1082, 907 cm^{-1} ; ^1H NMR (CDCl_3 , 300 MHz) and ^{13}C NMR (CDCl_3 , 75 MHz), see Table 10.

Compound DW6, isoshinanolone: Colorless oil; $[\alpha]_{\text{D}}^{28} +42.5$ (CHCl_3 , c 1.00); UV (MeOH) λ_{\max} : 217, 259 and 335 nm; IR (thin film) ν_{\max} : 3500, 1634, 1580, 1451, 1406, 1341, 1242, 1090, 980, 755 cm^{-1} ; ^1H NMR (CDCl_3 , 300 MHz) and ^{13}C NMR (CDCl_3 , 75 MHz), see Table 12.

Compound DW7, *epi*-isoshinanolone: Colorless oil; $[\alpha]_{\text{D}}^{28} -42.5$ (CHCl_3 , c 0.70); UV (MeOH) λ_{\max} : 213, 256 and 334 nm; IR (thin film) ν_{\max} : 3465, 1633, 1578, 1455, 1399, 1362, 1240, 1072, 996 cm^{-1} ; ^1H NMR (CDCl_3 , 300 MHz) and ^{13}C NMR (CDCl_3 , 75 MHz), see Table 14.

Compound DW8, maritinone: Red amorphous powder; m.p. 199-201 °C; UV (MeOH) λ_{\max} : 211, 267 and 409 nm; IR (thin film) ν_{\max} : 3489, 1661, 1635, 1615, 1583, 883 cm^{-1} ; ^1H NMR (CDCl_3 , 300 MHz) and ^{13}C NMR (CDCl_3 , 75 MHz); EIMS m/z $[\text{M}]^+$ 374.1 (Calcd for $\text{C}_{22}\text{H}_{14}\text{O}_6$, 374.1), see Table 16.

Compound DW9, 5,5'-dihydroxy-2,2'-dimethyl-7,7'-binaphthalen-1,1',4,4'-tetraone: Red solid; m.p. 250 °C (decomposed); UV (MeOH) λ_{\max} : 210, 270 and 415 nm; IR (thin film) ν_{\max} : 3473, 1664, 1641, 1600, 1418, 1367, 1353, 1261, 774 cm^{-1} ; ^1H NMR (CDCl_3 , 300 MHz) and ^{13}C NMR (CDCl_3 , 75 MHz), see Table 18; HREIMS: m/z $[\text{M}]^+$ 374.0812 (calcd for $\text{C}_{22}\text{H}_{14}\text{O}_6$, 374.0790).

Compound DW10, methylene-3,3'-biplumbagin: Orang needles; m.p. 202-204 °C; UV (MeOH) λ_{\max} : 215, 247, 275 and 410 nm; IR (thin film) ν_{\max} : 3570, 2910, 1655, 1632, 1597, 1455, 1389, 1360, 1290, 1195, 960 cm^{-1} ; ^1H NMR (CDCl_3 , 300 MHz) and ^{13}C NMR (CDCl_3 , 75 MHz); EIMS m/z $[\text{M}]^+$ 388.1 (Calcd for $\text{C}_{23}\text{H}_{16}\text{O}_6$, 388.1), see Table 20.

Compound DW11, 2-hydroxymethyl-1,5-dimethoxynaphthalen-4-ol: White powder; m.p. 63-65 °C; UV (MeOH) λ_{max} : 231 and 291 nm; IR (neat) ν_{max} : 3400, 1633, 1613, 1445, 1387, 1262, 1239, 1072, 996, 755, cm^{-1} ; ^1H NMR (CDCl_3 , 300 MHz) and ^{13}C NMR (CDCl_3 , 75 MHz), see Table 23; HREIMS: m/z $[\text{M}]^{+\bullet}$ 234.0920 (calcd for $\text{C}_{13}\text{H}_{14}\text{O}_4$, 233.9992).

Compound DW12, 2,2'-bis-hydroxymethyl-1,1',5,5'-tetramethoxy-3,3'-binaphthalen-4,4'-diol: White amorphous powder; m.p. 115-117 °C; UV (MeOH) λ_{max} : 228 and 295 nm; IR (neat) ν_{max} : 3389, 1632, 1605, 1455, 1382, 1357, 1244, 1069, 998, 762 cm^{-1} . ^1H NMR (CDCl_3 , 400 MHz) and ^{13}C NMR (CDCl_3 , 100 MHz), see Table 24; HREIMS: m/z $[\text{M}]^{+\bullet}$ 466.1622 (calcd for $\text{C}_{26}\text{H}_{26}\text{O}_8$, 466.1627).

Compound DW13, scopoletin: Yellow oil; UV (MeOH) λ_{max} : 225, 240, 245 and 346 nm; IR (thin film) ν_{max} : 3450, 1725, 1630, 1590, 1450, 1180, 940, 820 cm^{-1} ; ^1H NMR (CDCl_3 , 300 MHz) and ^{13}C NMR (CDCl_3 , 75 MHz), see Table 25.

Compound DW14, lupeol: White solid; m.p. 193-194 °C; $[\alpha]_{\text{D}}^{28} +25.0$ (CHCl_3 , c 0.20); IR (KBr) ν_{max} : 3343, 2945, 1638 cm^{-1} ; ^1H NMR (CDCl_3 , 300 MHz) and ^{13}C NMR (CDCl_3 , 75 MHz), see Table 26.

Compound DW15, lupenone: White solid; m.p. 163-165 °C; $[\alpha]_{\text{D}}^{28} +50.0$ (CHCl_3 , c 0.10); IR (KBr) ν_{max} : 2914, 1704, 1642 cm^{-1} ; ^1H NMR (CDCl_3 , 300 MHz) and ^{13}C NMR (CDCl_3 , 75 MHz), see Table 28.

Compound DW16, betulin: White solid; m.p. 230-231 °C; $[\alpha]_{\text{D}}^{28} +16.7^\circ$ (CHCl_3 , c 0.150); IR (KBr) ν_{max} : 3382, 2942, 1645 cm^{-1} ; ^1H NMR (CDCl_3 , 300 MHz) and ^{13}C NMR (CDCl_3 , 75 MHz), see see Table 30.

Compound DW17, betulinaldehyde: Colorless viscous oil, due to its instability, no IR was obtained. ^1H NMR (CDCl_3 , 300 MHz) and ^{13}C NMR (CDCl_3 , 75 MHz), see Table 32.

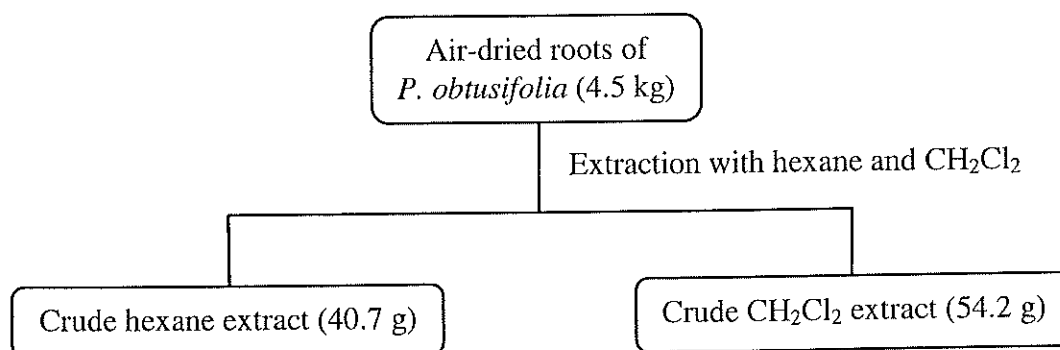
Compound DW18, betulinic acid: White solid; m.p. 279-280 °C; $[\alpha]_D^{28} +15.0$ (CHCl₃, $c = 0.10$); IR ν_{\max} : 3415, 2942, 1686, 1645 cm⁻¹; ¹H NMR (CDCl₃, 300 MHz) and ¹³C NMR (CDCl₃, 75 MHz), see Table 34.

Compound DW19, 3 β ,29-dihydroxyolean-12-en-28-oic acid: White amorphous powder; m.p. 334-336 °C; $[\alpha]_D^{26} +82.0$ (CHCl₃; c 0.10); IR (thin film) ν_{\max} : 3400, 2950, 1695, 1460, 1030 cm⁻¹; ¹H NMR (CDCl₃, 300 MHz) and ¹³C NMR (CDCl₃, 75 MHz), see Table 37.

Compound DW20, β -sitosterol and **DW21**, stigmasterol: White solid; IR (neat) ν_{\max} : 3425, 1642 cm⁻¹; ¹H NMR (CDCl₃, 300 MHz) and ¹³C NMR (CDCl₃, 75 MHz), see Figure 77.

2.3.2 Isolation and Chemical Investigation of *P. obtusifolia*

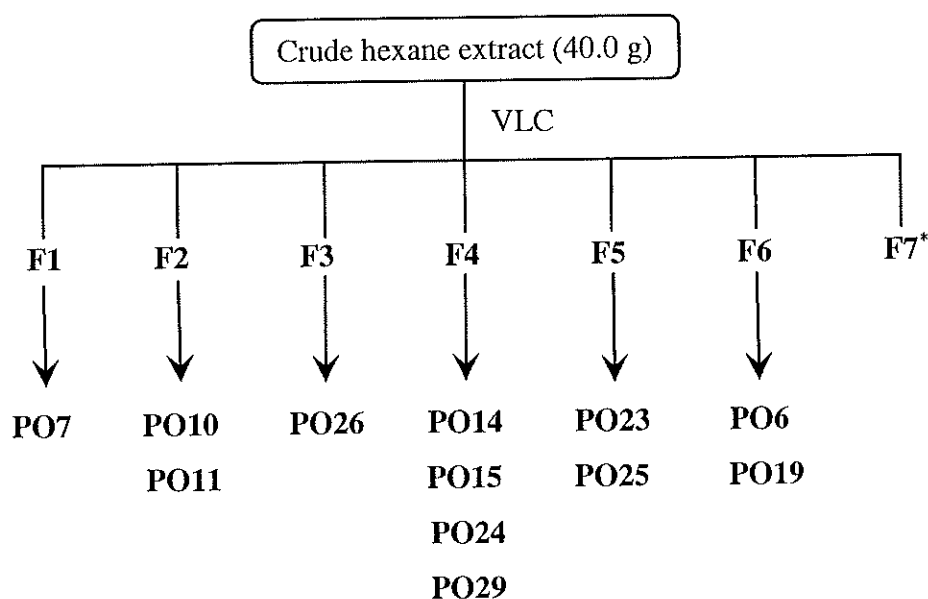
The dried roots of *P. obtusifolia* (4.5 kg) were extracted with hexane and CH₂Cl₂ successively (2 × 10 L for each solvent for one week) at room temperature and evaporated under reduced pressure to provide crude hexane (40.7 g) and CH₂Cl₂ (54.2 g) extracts, respectively. The process of extraction was shown in Scheme 5.



Scheme 5 Extraction of the roots of *P. obtusifolia*.

2.3.2.1 Investigation of the crude hexane extract from the roots of *P. obtusifolia*

The crude hexane extract (40.7 g) was subjected to vacuum liquid chromatography (VLC) using hexane as eluent and increasing polarity with EtOAc to give seven fractions (F1-F7).



* No further investigation

Scheme 6 Isolation of compounds **PO6**, **PO7**, **PO10**, **PO11**, **PO14**, **PO15**, **PO19**, **PO23-PO26** and **PO29** from the hexane extract.

Fraction F1 (3.7 g) was separated by VLC using EtOAc-hexane (0.5:9.5, v/v) as eluting solvent to give three subfractions (F1a-F1c). Subfraction F1a (501.4 mg) was purified by VLC using 100% hexane providing **PO7** (6.4 mg).

Fraction F2 (1.2 g) was separated by VLC using EtOAc-hexane (0.5:9.5, v/v) as eluting solvent to give three subfractions (F2a-F2c). Subfraction F2a (409.2 mg) was purified by VLC using 100% hexane to provide **PO10** (6.1 mg). Subfraction F2c (214.2 mg) was purified by VLC using EtOAc-hexane (1:9, v/v) to afford **PO11** (57.5 mg).

Fraction F3 (4.5 g) was separated by VLC using EtOAc-hexane (1:9, v/v) as eluting solvent to afford seven subfractions (F3a-F3g). Subfraction F3b (728.4 mg) was separated by VLC with CH₂Cl₂-hexane (3:7, v/v) as eluting solvent to afford four subfractions (F3b1-F3b4). Subfraction F3b2 (40.7 mg) was purified by VLC using CH₂Cl₂-hexane (3:7, v/v) to provide **PO26** (3.3 mg).

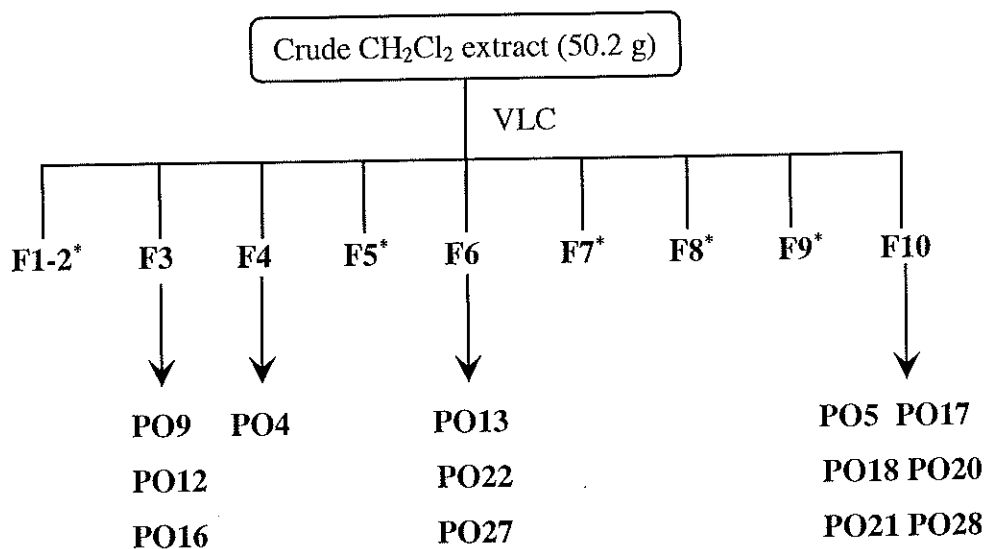
Fraction F4 (9.0 g) was separated by VLC using CH₂Cl₂-hexane (2:8, v/v) as eluting solvent to afford six subfractions (F4a-F4f). Subfraction F4a (5.8 g) was recrystallized from methylene chloride to give **PO15** (95.0 mg). Subfraction F4c (1.4 g) was purified by VLC with EtOAc-hexane (1:9, v/v) to give **PO14** (16.0 mg) and **PO29** (27.2 mg). Subfraction F4e (862.4 mg) was purified by VLC using EtOAc-hexane (1:9, v/v) to provide **PO24** (12.3 mg).

Fraction F5 (3.7 g) was separated by VLC using EtOAc-hexane (0.5:9.5, v/v) as eluting solvent to afford five subfractions (F5a-F5e). Subfraction F5c (726.7 mg) was separated by VLC with EtOAc-hexane (0.5:9.5, v/v) as eluting solvent to give three subfractions (F5c1-F5c3). Subfraction F5c2 (448.1 mg) was purified by VLC using EtOAc-CH₂Cl₂ (0.5:9.5, v/v) to provide **PO25** (35.5 mg) and **PO23** (58.7 mg).

Fraction F6 (15.9 g) was separated by VLC with EtOAc-hexane (1:9, v/v) as eluting solvent to afford six subfractions (F6a-F6f). Subfraction F6d (4.4 g) was separated by VLC using EtOAc-hexane (0.5:9.5, v/v) as eluting solvent to give five subfractions (F6d1-F6d5). Subfraction F6d3 gave **PO19** (18.2 mg) after recrystallization from CH₂Cl₂. Subfraction F6f (1.4 g) was purified by VLC using EtOAc-hexane (0.5:9.5, v/v) to provide **PO6** (5.2 mg).

2.3.2.2 Investigation of the crude CH₂Cl₂ extract from the roots of *P. obtusifolia*

The CH₂Cl₂ extract (50.2 g) was separated by VLC using hexane as eluent and increasing polarity with EtOAc to give ten fractions (F1-F10).



* No further investigation

Scheme 7 Isolation of compounds **PO4**, **PO5**, **PO9**, **PO12**, **PO13**, **PO16-PO18**, **PO20**, **PO21**, **PO22** and **PO27-PO28** from the CH_2Cl_2 extract.

Fraction F3 (7.0 g) was separated by VLC with EtOAc-hexane (0.5:9.5, v/v) as eluting solvent to afford six subfractions (F3a-F3f). Subfraction F3f (1.2 g) was purified by VLC with EtOAc-hexane (2:8, v/v) to provide **PO9** (7.9 mg), **PO16** (16.3 mg) and **PO12** (6.8 mg).

Fraction F4 (1.5 g) was separated by VLC using EtOAc-hexane (1:9, v/v) as eluting solvent to give eight subfractions (F4a-F4h). Subfraction F4c (745.1 mg) was purified by VLC with EtOAc-hexane (1:9, v/v) to provide **PO4** (82.6 mg).

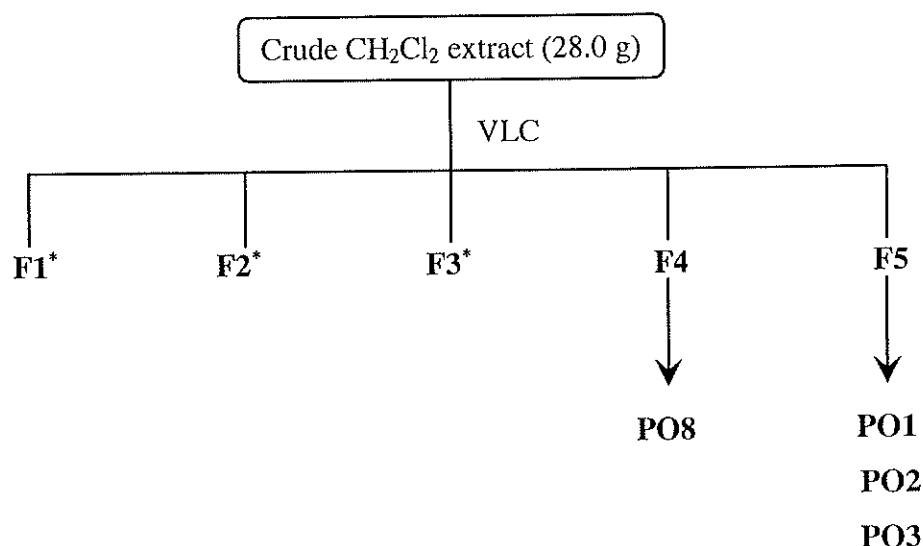
Fraction F6 (6.5 g) was separated by VLC with EtOAc-hexane (0.5:9.5, v/v) as eluting solvent to afford four subfractions (F6a-F6d). Subfraction F6a (1.4 g) was purified by VLC with EtOAc-hexane (1:9, v/v) to give **PO27** (251.7 mg). Subfraction F6c (1.7 g) was purified by VLC with EtOAc-hexane (2:8, v/v) to provide **PO22** (8.3 mg). Subfraction F6d (2.8 g) was recrystallized from methylene chloride to give **PO13** (746.3 mg).

Fraction F10 (20.5 g) was separated by VLC using EtOAc-hexane (3:7, v/v) as eluting solvent to afford ten subfractions (F10a-F10j). Subfraction F10d (4.1 g) was purified by VLC using EtOAc-hexane (3:7, v/v) to provide **PO18** (118.5 mg), **PO17** (15.1 mg) and **PO5** (15.6 mg). Subfraction F10f (4.7 g) was separated by VLC

using EtOAc-hexane (3:7, v/v) as eluting solvent to afford four subfractions (F10f1-F10f4). Subfraction F10f4 (2.2 g) was purified by VLC using EtOAc-hexane (4:6, v/v) to give **PO28** (6.2 mg), **PO20** (147.2 mg) and **PO21** (62.6 mg).

2.3.2.3 Investigation of the crude CH_2Cl_2 extract from the twigs of *P. obtusifolia*

The twigs of *P. obtusifolia* (2.0 kg) were extracted with CH_2Cl_2 (2×2 L for one week) at room temperature and evaporated under reduced pressure to provide crude CH_2Cl_2 extract (28.2 g). The CH_2Cl_2 extract (28.0 g) was subjected to VLC using hexane as eluent and increasing polarity with EtOAc to give five fractions (F1-F5).



* No further investigation

Scheme 8 Isolation of compounds **PO1-PO3** and **PO8** from the CH_2Cl_2 extract.

Fraction F4 (2.8 g) was separated by VLC using EtOAc-hexane (1:9, v/v) as eluting solvent to afford nine subfractions (F4a-F4i). Subfraction F4i (728.2 mg) was purified by VLC with EtOAc-hexane (0.5:9.5, v/v) to give **PO8** (16.4 mg).

Fraction F5 (7.2 g) was separated by VLC using acetone-hexane (2:8, v/v) as eluting solvent to afford five subfractions (F5a-F5e). Subfraction F5a (2.6 g) was purified by VLC with EtOAc-hexane (2:8, v/v) to give **PO1** (12.0 mg) and **PO2**

(13.6 mg). Subfraction F5d (1.4 g) was purified by VLC with EtOAc-hexane (1:9, v/v) to provide **PO3** (35.6 mg).

Compound PO1, isopimara-7,15-dien-1 β ,3 β -diol: White amorphous solid; m.p. 168–170 °C; $[\alpha]_D^{26}$ –18.4 (CHCl₃; *c* 0.59); IR (thin film) ν_{\max} : 3339, 2968, 2876, 1637, 1457, 1366, 1001, 908, 758 cm⁻¹; ¹H NMR (CDCl₃, 300 MHz) and ¹³C NMR (CDCl₃, 75 MHz), see Table 38; HREIMS: *m/z* [M]⁺• 304.2407 (calcd for C₂₀H₃₂O₂, 304.2402).

Compound PO2, isopimara-7,15-dien-1 β ,19-diol: White amorphous solid; m.p. 92–95 °C; $[\alpha]_D^{26}$ –17.5 (CHCl₃; *c* 0.71); IR (thin film) ν_{\max} : 3344, 2927, 2867, 1690, 1637, 1451, 1215, 1084, 1021, 909, 758 cm⁻¹; ¹H NMR (CDCl₃, 300 MHz) and ¹³C NMR (CDCl₃, 75 MHz), see Table 39; HREIMS: *m/z* [M]⁺• 304.2403 (calcd for C₂₀H₃₂O₂, 304.2402).

Compound PO3, 13-*epi*-5,15-rosadien-3 α ,11 β -diol: White amorphous solid; m.p. 78–81 °C; $[\alpha]_D^{26}$ –13.6 (CHCl₃; *c* 0.09); IR (thin film) ν_{\max} : 3409, 2930, 2863, 1615, 1276, 1157, 1114, 1026, 760, 711, 667 cm⁻¹; ¹H NMR (CDCl₃, 300 MHz) and ¹³C NMR (CDCl₃, 75 MHz), see Table 41; HREIMS: *m/z* [M]⁺• 304.2397 (calcd for C₂₀H₃₂O₂, 304.2402).

Compound PO4, abietatrien-1 β -ol: Colorless oil; $[\alpha]_D^{26}$ –51.4 (CHCl₃; *c* 0.15); UV (EtOH) λ_{\max} (log ϵ): 214 (3.99) and 258 (3.05) nm; IR (thin film) ν_{\max} : 3421, 2956, 2969, 1670, 1609, 1495, 1459, 1387, 1217, 1030, 992, 832, 757 cm⁻¹; ¹H NMR (CDCl₃, 300 MHz) and ¹³C NMR (CDCl₃, 75 MHz), see Table 42; HREIMS: *m/z* [M]⁺• 286.2295 (calcd for C₂₀H₃₀O, 286.2297).

Compound PO5, abietatrien-1 β ,12-diol: Colorless oil; $[\alpha]_D^{26}$ –15.7 (CHCl₃; *c* 0.27); UV (EtOH) λ_{\max} (log ϵ): 210 (3.97) and 282 (3.90) nm; IR (thin film) ν_{\max} : 3351, 2958, 1507, 1420, 1216, 1005, 891, 767 cm⁻¹; ¹H NMR (CDCl₃, 400 MHz) and ¹³C

NMR (CDCl₃, 100 MHz), see Table 43; HREIMS: m/z [M]⁺ 302.2254 (calcd for C₂₀H₃₀O₂, 302.2246).

Compound PO6, ferruginol: White powder; m.p. 56-58 °C; $[\alpha]_D^{26}$ +42.7 (CHCl₃; c 0.70); UV (EtOH) λ_{\max} (log ϵ): 213 (4.31) and 258 (3.43) nm; IR (thin film) ν_{\max} : 3605, 2914, 2832, 1587 cm⁻¹; ¹H NMR (CDCl₃, 300 MHz) and ¹³C NMR (CDCl₃, 75 MHz), see Table 45.

Compound PO7, *O*-methyl ferruginol: Colorless oil; $[\alpha]_D^{26}$ +15.0 (CHCl₃; c 0.10); UV (EtOH) λ_{\max} (log ϵ): 210 (4.24) and 253 (3.35) nm; IR (thin film) ν_{\max} : 2978, 2889, 1524 cm⁻¹; ¹H NMR (CDCl₃, 300 MHz) and ¹³C NMR (CDCl₃, 75 MHz), see Table 47.

Compound PO8, lambertic acid: Amorphous solid; m.p. 251-253 °C; $[\alpha]_D^{26}$ +128 (CHCl₃; c 0.07); UV (EtOH) λ_{\max} (log ϵ): 215 (4.37) and 283 (3.89) nm; IR (thin film) ν_{\max} : 3360, 2800, 1694, 1619, 1580, 976, 857 cm⁻¹; ¹H NMR (CDCl₃, 300 MHz) and ¹³C NMR (CDCl₃, 75 MHz), see Table 49.

Compound PO9, sugiol: White amorphous solid; m.p. 292-294 °C; $[\alpha]_D^{26}$ +17.7 (CHCl₃; c 0.11); UV (EtOH) λ_{\max} (log ϵ): 220 (4.29), 233 (4.28) and 286 (3.38) nm; IR (thin film) ν_{\max} : 3224, 2928, 2865, 1648, 1590, 1342, 906, 867 cm⁻¹; ¹H NMR (CDCl₃, 300 MHz) and ¹³C NMR (CDCl₃, 75 MHz), see Table 50.

Compound PO10, royleanone: White amorphous solid; m.p. 179-181 °C; $[\alpha]_D^{26}$ +115.8 (CHCl₃; c 2.87); UV (EtOH) λ_{\max} (log ϵ): 277 (4.28) and 407 (3.38) nm; IR (thin film) ν_{\max} : 3360, 2958, 2927, 1641, 1631, 1603, 1461, 1377, 1252, 959 cm⁻¹; ¹H NMR (CDCl₃, 300 MHz) and ¹³C NMR (CDCl₃, 75 MHz), see Table 52.

Compound PO11, horminone: Orange crystal; m.p. 170-172 °C; $[\alpha]_D^{26}$ -114.0 (CHCl₃; c 0.10); UV (EtOH) λ_{\max} (log ϵ): 218 (3.40), 272 (4.2) and 400 (2.00) nm; IR

(thin film) ν_{\max} : 3358, 2957, 2868, 1649, 1624, 1600, 1455, 1250, 1060, 947 cm^{-1} ; ^1H NMR (CDCl_3 , 300 MHz) and ^{13}C NMR (CDCl_3 , 75 MHz), see Table 54.

Compound PO12, montbretol: Yellow powder; m.p. 201-203 $^{\circ}\text{C}$; $[\alpha]_{\text{D}}^{26} -27$ (CHCl_3 ; c 0.17); UV (EtOH) λ_{\max} (log ϵ): 248 (4.25) and 342 (3.42) nm; IR (thin film) ν_{\max} : 3328, 2932, 1676, 1635, 1504, 1378, 890 cm^{-1} ; ^1H NMR (CDCl_3 , 300 MHz) and ^{13}C NMR (CDCl_3 , 75 MHz), see Table 57.

Compound PO13, 14-deoxycoleon: Colorless crystals; m.p. 279-280 $^{\circ}\text{C}$; $[\alpha]_{\text{D}}^{26} +58.0$ (CHCl_3 ; c 0.10); UV (EtOH) λ_{\max} (log ϵ): 210 (4.70), 287 (3.80), and 345 (3.0) nm; IR (thin film) ν_{\max} : 3400, 3050, 2960, 2880, 1690, 1660, 1560, 1560, 1320, 1140, 750 cm^{-1} ; ^1H NMR (CDCl_3 , 300 MHz) and ^{13}C NMR (CDCl_3 , 75 MHz), see Table 59.

Compound PO14, taxodion: Yellow oil; $[\alpha]_{\text{D}}^{26} +43.9$ (CHCl_3 ; c 2.03); UV (EtOH) λ_{\max} (log ϵ): 231 (4.17), 254 (4.11), 320 (3.58), 333 (3.26) and 400 (2.05) nm; IR (thin film) ν_{\max} : 3530, 2873, 1740, 1643, 1531, 1376, 1288, 912 cm^{-1} ; ^1H NMR (CDCl_3 , 300 MHz) and ^{13}C NMR (CDCl_3 , 75 MHz), see Table 61.

Compound PO15, arucadiol: Orang crystals; m.p. 183-185 $^{\circ}\text{C}$; $[\alpha]_{\text{D}}^{26} +9.9$ (CHCl_3 ; c 1.00); UV (EtOH) λ_{\max} (log ϵ): 228 (4.58), 270 (4.25), 362 (3.54) and 410 (3.65) nm; IR (thin film) ν_{\max} : 3490, 3060, 2970, 2880, 1640, 1590, 1510, 1425, 1040, 870 cm^{-1} ; ^1H NMR (CDCl_3 , 300 MHz) and ^{13}C NMR (CDCl_3 , 75 MHz), see Table 63.

Compound PO16, 12-hydroxy-6,7-secoabieta-8,11,13-triene-6,7-dial: Colorless crystals; m.p. 193-195 $^{\circ}\text{C}$; $[\alpha]_{\text{D}}^{26} +12.8$ (CHCl_3 ; c 0.81); UV (EtOH) λ_{\max} (log ϵ): 218 (4.35), 260 (4.20) and 295 (3.64) nm IR (thin film) ν_{\max} : 3434, 2942, 1710, 1666, 1545, 1472, 2310, 865 cm^{-1} ; ^1H NMR (CDCl_3 , 300 MHz) and ^{13}C NMR (CDCl_3 , 75 MHz), see Table 64.

Compound PO17, salvicanaraldehyde: Colorless oil; $[\alpha]_D^{26} +38.1$ (CHCl₃; *c* 0.91); UV (EtOH) λ_{\max} (log ϵ): 231 (4.55) and 281 (3.70) nm; IR (thin film) ν_{\max} : 3552, 2951, 1685, 1619, 1440, 1098, 879 cm⁻¹; ¹H NMR (CDCl₃, 300 MHz) and ¹³C NMR (CDCl₃, 75 MHz), see Table 66.

Compound PO18, 6 α ,11,12-trihydroxy-7 β ,20-epoxy-8,11,13-abietatriene: White solid; m.p. 199–201 °C; $[\alpha]_D^{24} -21.1$ (CHCl₃; *c* 0.02); UV (EtOH) λ_{\max} (log ϵ): 210 (4.29), 222 (4.28) and 276 (3.38) nm; IR (thin film) ν_{\max} : 3351, 2958, 2871, 1578, 1446, 1297, 1046, 757 cm⁻¹; ¹H NMR (CDCl₃, 400 MHz) and ¹³C NMR (CDCl₃, 100 MHz), see Table 68; HREIMS: *m/z* [M]⁺ 332.1999 (calcd for C₂₀H₂₈O₄, 332.1988).

Compound PO19, 5 α ,11,12-trihydroxy-6-oxa-abieta-8,11,13-trien-7-one: Colorless oil; $[\alpha]_D^{24} +59.3$ (CHCl₃; *c* 0.14); UV (EtOH) λ_{\max} (log ϵ): 218 (4.46), 260 (3.95) and 295 (3.60) nm; IR (thin film) ν_{\max} : 3452, 2961, 2871, 1682, 1621, 1584, 1417, 1236, 1001, 928, 760 cm⁻¹; ¹H NMR (CDCl₃, 300 MHz) and ¹³C NMR (CDCl₃, 75 MHz), see Table 69; HREIMS: *m/z* [M]⁺ 334.1792 (calcd for C₁₉H₂₆O₅, 334.1780).

Compound PO20, 5,6-dihydro-6 α -hydroxysalviasperanol: Amorphous solid; m.p. 188–190 °C; $[\alpha]_D^{26} -8.6$ (CHCl₃; *c* 0.88); UV (EtOH) λ_{\max} (log ϵ): 205 (4.50) and 270 (3.80) nm; IR (thin film) ν_{\max} : 3693, 3604, 3551, 1601, 1539, 1451, 1259, 929 cm⁻¹; ¹H NMR (CDCl₃, 300 MHz) and ¹³C NMR (CDCl₃, 75 MHz), see Table 70.

Compound PO21, salviasperanol: Amorphous solid; m.p. 207–209 °C; $[\alpha]_D^{26} -32.5$ (CHCl₃; *c* 2.10); UV (EtOH) λ_{\max} (log ϵ): 205 (3.13), 275 (4.50) and 280 (4.60) nm; IR (thin film) ν_{\max} : 3500, 3420, 1620, 1260, 855 cm⁻¹; ¹H NMR (CDCl₃, 300 MHz) and ¹³C NMR (CDCl₃, 75 MHz), see Table 72.

Compound PO22, 11,12-dihydroxy-8,11,13-icetexatrien-1-one: Colorless crystals; m.p. 179–182 °C; $[\alpha]_D^{26} +107.5$ (CHCl₃; *c* 0.41); UV (EtOH) λ_{\max} (log ϵ): 219 (4.17), 269 (3.86) and 292 (3.49) nm; IR (thin film) ν_{\max} : 3293, 2958, 1686, 1451, 1286,

1158, 756 cm^{-1} ; ^1H NMR (CDCl_3 , 300 MHz) and ^{13}C NMR (CDCl_3 , 75 MHz), see Table 74.

Compound PO23, 11,12-dihydroxy-6,8,11,13-icetexatetraen-1-one: Colorless crystals; m.p. 176–178 °C; $[\alpha]_{\text{D}}^{26} -182.2$ (CHCl_3 ; c 0.21); UV (EtOH) λ_{max} (log ϵ): 219 (4.17), 269 (3.86) and 292 (3.49) nm; IR (thin film) ν_{max} : 3478, 2959, 2869, 1681, 1629, 1584, 1444, 1306, 759 cm^{-1} ; ^1H NMR (CDCl_3 , 400 MHz) and ^{13}C NMR (CDCl_3 , 100 MHz), see Table 76; HREIMS: m/z $[\text{M}]^{+\bullet}$ 314.1894 (calcd for $\text{C}_{20}\text{H}_{26}\text{O}_3$, 314.1882).

Compound PO24, obtusinone A: Red amorphous solid; m.p. 135–137 °C; $[\alpha]_{\text{D}}^{24} +112.4$ (CHCl_3 ; c 0.21); UV (EtOH) λ_{max} (log ϵ): 223 (5.06), 263 (4.97) and 451 (4.20) nm; IR (thin film) ν_{max} : 3327, 2933, 2871, 1691, 1667, 1654, 1598, 1461, 1263, 927, 755 cm^{-1} ; ^1H NMR (CDCl_3 , 300 MHz) and ^{13}C NMR (CDCl_3 , 75 MHz), see Table 77; HREIMS: m/z $[\text{M}]^{+\bullet}$ 298.1566 (calcd for $\text{C}_{19}\text{H}_{22}\text{O}_3$, 298.1569).

Compound PO25, obtusinone B: Orange amorphous solid; m.p. 89–91 °C; $[\alpha]_{\text{D}}^{24} +14.9$ (CHCl_3 ; c 1.17); UV (EtOH) λ_{max} (log ϵ): 215 (4.04), 272 (4.12) and 352 (3.23) nm; IR (thin film) ν_{max} : 2961, 2871, 1665, 1634, 1602, 1566, 1459, 1345, 1263, 1167, 946, 772 cm^{-1} ; ^1H NMR (CDCl_3 , 400 MHz) ^{13}C NMR (CDCl_3 , 100 MHz), see Table 78; HREIMS: m/z $[\text{M}]^{+\bullet}$ 282.1614 (calcd for $\text{C}_{19}\text{H}_{22}\text{O}_2$, 282.1620).

Compound PO26, obtusinone C: Red amorphous solid; m.p. 104–106 °C; $[\alpha]_{\text{D}}^{24} +57.2$ (CHCl_3 ; c 0.12); UV (EtOH) λ_{max} (log ϵ): 215 (4.23), 285 (4.15), 353 (3.67) and 411 (2.87) nm; IR (thin film) ν_{max} : 3386, 2962, 2851, 1728, 1650, 1628, 1461, 1414, 1090, 765 cm^{-1} ; ^1H NMR (CDCl_3 , 300 MHz) and ^{13}C NMR (CDCl_3 , 75 MHz), see Table 80; HREIMS: m/z $[\text{M}]^{+\bullet}$ 298.1563 (calcd for $\text{C}_{19}\text{H}_{22}\text{O}_3$, 298.1569).

Compound PO27, 4 β ,5 β -dihydroxy-10-*epi*-eudesmane: Colorless oil; $[\alpha]_D^{26}$ -54.0 (CHCl₃; *c* 0.84); IR (thin film) ν_{\max} : 3400, 2942, 1686, 1645 cm⁻¹; ¹H NMR (CDCl₃, 300 MHz) and ¹³C NMR (CDCl₃, 75 MHz), see Table 82.

Compound PO28, 4 β ,10 β -dihydroxyaromadendrane: Colorless prisms; m.p. 138-140 °C; $[\alpha]_D^{26}$ -37.1 (CHCl₃; *c* 0.76); IR (thin film) ν_{\max} : 3396, 2924, 2862, 1456, 1375, 1109 cm⁻¹; ¹H NMR (CDCl₃, 300 MHz) and ¹³C NMR (CDCl₃, 75 MHz), see Table 84.

Compound PO29, spathulenol: Colorless oil; $[\alpha]_D^{25}$ +12 (CHCl₃; *c* 0.15).; IR (thin film) ν_{\max} : 3413, 2945, 1614, 920, 880 cm⁻¹; ¹H NMR (CDCl₃, 300 MHz) and ¹³C NMR (CDCl₃, 75 MHz), see Table 86.

2.4 Bioassays

2.4.1 Cytotoxic assay

The cancer cell lines MCF-7 (human breast adenocarcinoma) were grown in Dulbecco's Modified Eagle Medium: Nutrient Mixture F12 (D-MEM/F12) supplemented with 10% Fetal bovine serum (FBS). Cells were seeded in 96-well (3000 cell/well) and allowed to adhere for 24 h at 37 °C with 5% CO₂ in fully humidified incubator. Then 100 μ l of 25 μ g/ml crude extract or five fold diluted pure compound in medium (final concentration 0.008, 0.04, 0.2, 1, 5 μ g/ml) were dispensed into wells of the cell plates and incubated further for 72 h. After removal of the sample medium, the cells were topped up with 200 μ l D-MEM/F12 medium and incubated. After 72 h. Cells were fixed with cold 40% Trichloroacetic acid and kept at 4 °C for 1 h and washed with tap water. The cells were determined by Sulphorodamine assay. The absorbance was measured at 492 nm using a microplate reader. The results were based on the ability of extracts to inhibit cells growth compared with control (cells in media without extract) and calculated for IC₅₀ using

probit analysis. Camptothecin, which was used as a standard, showed cytotoxic activity at $<0.024 \mu\text{g/ml}$.

2.4.2 Antibacterial assay

The isolated compounds from the roots and fresh fruits of *D. wallichii* and the roots and twigs of *P. obtusifolia* were tested against both Gram-positive and Gram-negative bacteria: *B. subtilis*, *S. aureus*, TISTR517, *E. faecalis* TISTR459, Methicillin-Resistant *S. aureus* (MRSA) ATCC43300, Vancomycin-Resistant *E. faecalis* (VRE) ATCC 51299, *Streptococcus faecalis*, *S. typhi*, *S. sonnei* and *P. aeruginosa*. The microorganisms were obtained from the culture collections, Department of Industrial Biotechnology and Department of Pharmacognosy and Botany, PSU, except for the TISTR and ATCC strains, which were obtained from Pharmaceutical Microbial Research Center (MIRCEN), Bangkok, Thailand. The antibacterial assay employed was the same as described in Boonnak et al.. Vancomycin, which was used as a standard, showed antibacterial activity against Vancomycin-Resistant *E. faecalis* (VRE) ATCC 51299 at $<2.34 \mu\text{g/ml}$.

2.4.3 Anti-inflammatory assay

Inhibitory effects on NO production by murine macrophage-like RAW264.7 cells were evaluated using a modified method from that previously reported (Banskota et al., 2003). Briefly, the RAW264.7 cell line [purchased from Cell Lines Service (CLS)] was cultured in Rosewell Park Memorial Institute (RPMI) medium supplemented with 0.1% sodium bicarbonate and 2 mM glutamine, penicillin G (100 units/ml), streptomycin (100 $\mu\text{g/ml}$) and 10% fetal calf serum (FCS). The cells were harvested with trypsin–ethylenediaminetetraacetic acid (EDTA) and diluted to a suspension in a fresh medium. The cells were seeded in 96-well plates with 1×10^5 cells/well and allowed to adhere for 1 h at 37 °C in a humidified atmosphere containing 5% CO₂. After that the medium was replaced with a fresh medium containing 50 $\mu\text{g/ml}$ of LPS together with the test samples at various concentrations

and was then incubated for 48 h. NO production was determined by measuring the accumulation of nitrite in the culture supernatant using the Griess reagent. Cytotoxicity was determined using the 3-(4,5-dimethyl-2-thiazolyl)-2,5-diphenyl-2H-tetrazolium bromide (MTT) colorimetric method. Briefly, after 48 h incubation with the test samples, MTT solution (10 μ l, 5 mg/ml in phosphate buffer saline (PBS) was added to the wells. After 4 h incubation, the medium was removed, and isopropanol containing 0.04 M HCl was then added to dissolve the formazan production in the cells. The optical density of the formazan solution was measured with a microplate reader at 570 nm. The test compounds were considered to be cytotoxic when the optical density of the sample-treated group was less than 80% of that in the control (vehicle-treated) group. L-NA and caffeic acid phenethyl ester (CAPE) were used as positive controls. The stock solution of each test sample was dissolved in DMSO, and the solution was added to the medium RPMI (final DMSO is 1%). Inhibition (%) was calculated using the following equation and IC₅₀ values were determined graphically (n = 4):

$$\text{Inhibition (\%)} = \frac{A - B}{A - C} \times 100$$

A-C : NO₂⁻ concentration (μ M) [A : LPS (+), sample (-); B : LPS (+), sample(+); C : LPS (-), sample (-)].

The results were expressed as mean \pm standard error means (S.E.M) of four determinations at each concentration for each sample. The IC₅₀ values were calculated using the Microsoft Excel program. Statistical significance was calculated by one-way analysis of variance (ANOVA), followed by Dunnett's test.

2.5 X-ray crystallographic studies of 11,12-dihydroxy-6,8,11,13-icetexatetraen-1-one (PO23) and obtusinone A (PO24)

Crystallographic data were collected at 100.0(1) K with the Oxford Cyrosystem Cobra low-temperature attachment. The data were collected using a Bruker Apex2 CCD diffractometer with a graphite monochromated Mo K α radiation

at a detector distance of 5 cm and with APEX2 software. The collected data were reduced using *SAINT* program, and the empirical absorption corrections were performed using *SADABS* program. The structures were solved by direct methods and refined by least-squares using the *SHELXTL* software package (Spek, 2009). For 11,12-dihydroxy-6,8,11,13-icetexatetraen-1-one (**PO23**), hydroxy H atom was located from the difference map and refined isotropically. The remaining H atoms were placed in calculated positions with (C-H) = 0.93 for aromatic, 0.98 for CH, 0.97 for CH₂ and 0.96 Å^o for CH₃ atoms, after checking their positions in the difference map. The U_{iso} values were constrained to be $1.5U_{\text{eq}}$ of the carrier atoms for methyl H atoms and $1.2U_{\text{eq}}$ for hydroxyl and the other H atoms. Whereas for obtusinone A, all H atoms were located from the difference maps and refined isotropically. The final refinement converged well. Materials for publication were prepared using *SHELXTL* (Spek, 2009) and *PLATON* (Sheldrick, 2008).

Crystal data for 11,12-dihydroxy-6,8,11,13-icetexatetraen-1-one (**PO23**): C₂₀H₂₆O₃, $M=314.41$, $0.53\times 0.43\times 0.11$ mm, monoclinic, $P2_1/n$, $a=9.7176(2)$ Å, $b=14.1949(2)$ Å, $c=12.6935(2)$ Å, $\beta=107.395(1)^\circ$, $D_x=1.250$ Mg m⁻³, $\mu(\text{Mo K}\alpha)=0.082$ mm⁻¹, 28,434 reflection measured, 6246 unique reflections, $R=0.0364$, $R_w=0.0929$.

Crystal data for obtusinone A (**PO24**): C₁₉H₂₂O₃, $M=298.37$, $0.57\times 0.26\times 0.02$ mm, triclinic, $P-1$, $a=7.3596(7)$ Å, $b=8.8950(8)$ Å, $c=12.6014(11)$ Å, $\alpha=97.941(2)^\circ$, $\beta=106.284(2)^\circ$, $\gamma=97.958(2)^\circ$, $D_x=1.286$ Mg m⁻³, $\mu(\text{Mo K}\alpha)=0.086$ mm⁻¹, 16,608 reflection measured, 4479 unique reflections, $R=0.0452$, $R_w=0.1263$.

The crystallographic-information files for 11,12-dihydroxy-6,8,11,13-icetexatetraen-1-one and obtusinone A have been deposited in the Cambridge Crystallographic Data Center as CCDC826321 and CCDC826437, respectively. These data can be obtained free of charge via http://www.ccdc.cam.ac.uk/data_request/cif, or by e-mailing data_request@ccdc.cam.ac.uk, or by contacting the Cambridge Crystallographic Data Centre, 12, Union Road, Cambridge CB2 1EZ, UK; fax: +44 1223 336033.

CHAPTER 3

RESULTS AND DISCUSSION

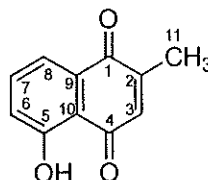
3.1 Structure elucidation of compounds from the roots and fruits of *Diospyros wallichii*

The air-dried and pulverized roots (2.5 kg) of *D. wallichii* were extracted with hexane at room temperature. The solvent was removed under reduced pressure yielding a dark-yellow viscous oil (30.7 g). The residue obtained after hexane extraction was further extracted with CH₂Cl₂ to yield a dark-yellow, resinous extract (20.2 g) after evaporation of the CH₂Cl₂ under vacuum. The hexane and CH₂Cl₂ extracts were subjected to silica gel vacuum liquid chromatography and /or crystallized affording fifteen compounds as two new naphthalene derivatives (**DW11** and **DW12**), one new binaphthoquinone (**DW9**), five known naphthoquinones (**DW1**, **DW2** and **DW5-DW7**), one known coumarin (**DW13**), four known triterpenoids (**DW14-DW17**) and a known mixture of steroids (**DW20** and **DW21**).

The fresh fruits of *Diospyros wallichii* (0.5 kg) were extracted with MeOH at room temperature. The extract was evaporated to dryness and the residue was partitioned between CH₂Cl₂ and H₂O. The CH₂Cl₂ layer was evaporated and the residue (9.2 g) was subjected to silica gel vacuum liquid chromatography and /or crystallization affording six compounds as four known naphthoquinones (**DW3**, **DW4**, **DW8** and **DW10**) and two known triterpenoids (**DW18** and **DW19**).

Their structures were elucidated mainly by 1D and 2D NMR spectroscopic data: ¹H, ¹³C NMR, DEPT 135°, DEPT 90°, HMQC, HMBC and ¹H-¹H COSY. Mass spectra were determined for three new compounds **DW9**, **DW11** and **DW12** and two known compounds **DW8** and **DW10**. The physical data of the known compounds were also compared with the reported values.

3.1.1 Compound DW1



Compound **DW1** was obtained as orange needles, m.p. 77-79 °C. The UV absorption maxima at λ_{max} 209, 264 and 413 nm indicated a highly conjugated system. Its IR spectrum suggested the presence of carbonyl group (1665 and 1645 cm^{-1}), a hydroxyl group (3370 cm^{-1}) and an aromatic group (1595 cm^{-1}). Furthermore, the presence of two carbonyl groups were shown at δ 183.9 and 189.7 in the ^{13}C NMR spectrum. These data indicated that **DW1** should have a *para*-naphthoquinone chromophore (Lin *et al.*, 1989).

The 11 carbon signals were observed in the ^{13}C NMR spectrum of **DW1** (Table 3, Figure 39) which were further classified by DEPT experiments as one methyl (δ_{C} 16.1), four olefinic methine (δ 118.7, 123.7, 134.9 and 135.7), six quaternary olefinic including two carbonyl carbons (δ 114.5, 131.5, 149.2, 160.7, 183.9 and 189.7).

The ^1H NMR spectrum of **DW1** (Table 3, Figure 38) revealed the presence of three adjacent aromatic proton signals at δ 7.06 (dd, $J= 8.4, 1.2$ Hz), 7.46 (t, $J= 8.4$ Hz), and 7.35 (dd, $J= 8.4, 1.2$ Hz) assignable to H-6, H-7 and H-8, respectively. One broad doublet quinoid proton signal at δ 6.63 ($J= 1.5$ Hz) was due to H-3. An upfield doublet quinonoid methyl signal at δ 2.01 ($J= 1.5$ Hz) was attached to the C-2 on quinone ring, while a signal at δ 11.79 was due to the presence of a hydrogen bonded hydroxyl at C-5, whose assignments were based on the HMBC experiments (Table 3, Figure 3). Thus on the basis of its spectroscopic data and comparison of the ^1H and ^{13}C NMR spectral data with the previous report (Khan *et al.*, 1998; Gu *et al.*, 2004; Tangmouo *et al.*, 2005) (Table 4), compound **DW1** was identified as plumbagin.

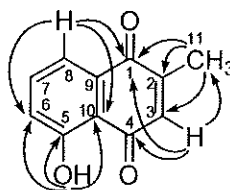


Figure 3 Major HMBC correlations of **DW1**

Table 3 ^1H , ^{13}C NMR, DEPT and HMBC spectral data of compound **DW1**

Position	DEPT	$\delta_{\text{C}}/\text{ppm}$	$\delta_{\text{H}}/\text{ppm}$ (mult., J in Hz)	HMBC
1	CO	183.9		
2	C	149.2		
3	CH	134.9	6.63 br d (1.5)	1, 10, 11
4	CO	189.7		
5	C	160.7		
6	CH	123.7	7.06 dd (8.4, 1.2)	5, 8, 10
7	CH	135.7	7.46 t (8.4)	5, 6, 8, 9
8	CH	118.7	7.35 dd (8.4, 1.2)	1, 6, 10
9	C	131.5		
10	C	114.5		
11	CH ₃	16.1	2.01 d (1.5)	1, 2, 3
5-OH			11.79 s	5, 6, 7, 10

Spectra recorded at 300 (^1H NMR) and 75 (^{13}C NMR) MHz, CDCl_3 .

Table 4 Comparison of ^1H and ^{13}C NMR spectral data of compounds **DW1** and plumbagin

Position	$\delta_{\text{C}}/\text{ppm}$		$\delta_{\text{H}}/\text{ppm}$ (mult., J in Hz)	
	DW1	plumbagin	DW1	plumbagin
1	183.9	183.9		
2	149.2	149.2		
3	134.9	134.9	6.63 br d (1.5)	6.75 q (2.0)
4	189.7	189.6		
5	160.7	160.6		
6	123.7	123.6	7.06 dd (8.4, 1.2)	7.19 dd, (8.0, 2)
7	135.7	135.7	7.46 t (8.4)	7.55 m
8	118.7	118.7	7.35 dd (8.4, 1.2)	7.55 m
9	131.5	131.5		
10	114.5	114.6		
11	16.1	16.1	2.01 d (1.5)	2.15 d, (2)
5-OH			11.79 s	11.90 s

Spectra recorded at 300 (^1H NMR) and 75 (^{13}C NMR) MHz, CDCl_3 .

Table 5 ^1H , ^{13}C NMR, DEPT and HMBC spectral data of compound **DW2** and ^{13}C NMR of droserone (**R**)

Position	DEPT	$\delta_{\text{C}}/\text{ppm}$		$\delta_{\text{H}}/\text{ppm}$ (mult., J in Hz)	HMBC
		R ^a	DW2 ^b		
1	CO	184.5	184.1		
2	C	121.8	121.8		
3	C	152.8	152.7		
4	CO	184.2	184.5		
5	C	161.2	161.1		
6	CH	123.2	123.1	7.19 dd (7.5, 1.8)	5, 8, 10
7	CH	137.5	137.5	7.62 t (7.5)	5, 6, 9
8	CH	119.7	119.6	7.67 dd (7.5, 1.8)	1, 6, 7, 10
9	C	132.7	132.7		
10	C	112.9	112.9		
11	CH ₃	8.8	8.7	2.10 s	1, 2, 3
3-OH				7.24 br s	2, 3, 4
5-OH				11.1 s	5, 6, 7, 10

^a Spectrum recorded at 150 (^{13}C NMR) MHz, CDCl_3 .

^b Spectra recorded at 300 (^1H NMR) and 75 (^{13}C NMR) MHz, CDCl_3 .

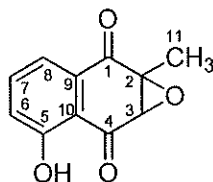
Table 6 Comparison of ^1H NMR spectral data of compounds **DW1**, **DW2** and droserone

Position	$\delta_{\text{H}}/\text{ppm}$ (mult., J in Hz)		
	DW1 ^a	DW2 ^a	droserone ^b
3	6.63 br d (1.5)		
6	7.06 dd (8.4, 1.2)	7.19 dd (7.5, 1.8)	} 7.10–7.70 m
7	7.46 t (8.4)	7.62 t (7.5)	
8	7.35 dd (8.4, 1.2)	7.67 dd (7.5, 1.8)	
11	2.01 d (1.5)	2.10 s	2.10 s
3-OH		7.24 br s	
5-OH	11.79 s	11.1 s	11.03 s

^a Spectra recorded at 300 (^1H NMR) MHz, CDCl_3 .

^b Spectrum recorded at 60 (^1H NMR) MHz, CDCl_3 .

3.1.3 Compound DW3



Compound **DW3** was isolated as pale yellow needles, m.p. 97-99 °C; $[\alpha]_D^{28} -17.4$ (CHCl_3 , c 0.50). The UV and IR spectra were similar to those of **DW1**.

The ^1H and ^{13}C NMR spectral data of **DW3** (Table 7, Figures 42 and 43) were similar to those of **DW1** (Table 3, Figures 38 and 39). However, six olefinic carbons can be found in the ^{13}C NMR spectrum of **DW3**, which indicated the disappearance of one double bond of quinonoid ring. The appearances of oxymethine proton as a singlet at δ 3.80 and an oxymethine carbon at δ 61.3 and an oxyquaternary carbon at δ 61.2 in the ^1H and ^{13}C NMR spectra of **DW3**, suggesting an epoxy moiety. This finding was further supported by HMBC correlations (Table 7, Figure 5) from H-11 (δ 1.75) to C-2 (δ 61.2) and C-3 (δ 61.3). By comparison of the ^1H and ^{13}C NMR spectral data with the previously reported data (Ogihara *et al.*, 1997; Higa *et al.*, 2002) (Table 7 and 8), therefore compound **DW3** was identified as 2,3-epoxyplumbagin.

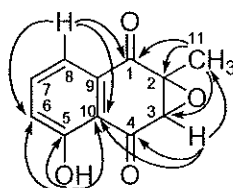


Figure 5 Major HMBC correlations of **DW3**

Table 7 ^1H , ^{13}C NMR, DEPT and HMBC spectral data of compound **DW3** and ^{13}C NMR of 2,3-epoxyplumbagin (**R**)

Position	DEPT	$\delta_{\text{C}}/\text{ppm}$		$\delta_{\text{H}}/\text{ppm}$ (mult., J in Hz)		HMBC
		R ^a	DW3 ^b			
1	CO	190.8	190.8			
2	C	61.2	61.2			
3	CH	61.3	61.3	3.80 s		2, 4, 10, 11
4	CO	196.6	196.6			
5	C	161.4	161.4			
6	CH	124.1	124.1	7.26 dd (8.1, 1.2)		5, 8, 10
7	CH	137.1	137.1	7.64 t (8.1)		5, 9
8	CH	119.8	119.8	7.58 dd (8.1, 1.2)		1, 6, 10
9	C	132.1	132.2			
10	C	114.4	114.4			
11	CH ₃	14.6	14.6	1.75 s		1, 2, 3
5-OH				11.2 s		5, 6, 10

^a Spectrum recorded at 67.8 (^{13}C NMR) MHz, CDCl_3 .

^b Spectra recorded at 300 (^1H NMR) and 75 (^{13}C NMR) MHz, CDCl_3 .

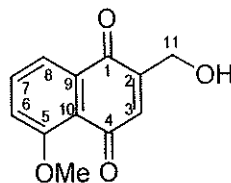
Table 8 Comparison of ^1H NMR spectral data of compounds **DW1**, **DW3** and 2,3-epoxyplumbagin

Position	δ_{H} /ppm (mult., J in Hz)		
	DW1 ^a	DW3 ^a	2,3-epoxyplumbagin ^b
3	6.63 br d (1.5)	3.80 s	3.78 s
6	7.06 dd (8.4, 1.2)	7.26 dd (8.1, 1.2)	} 7.15–7.66 m
7	7.46 t (8.4)	7.64 t (8.1)	
8	7.35 dd (8.4, 1.2)	7.58 dd (8.1, 1.2)	
11	2.01 d (1.5)	1.75 s	1.70 s
5-OH	11.79 s	11.2 s	11.1 s

^a Spectra recorded at 300 (^1H NMR) MHz, CDCl_3 .

^b Spectrum recorded at 90 (^1H NMR) MHz, CDCl_3 .

3.1.4 Compound DW4



Compound **DW4** was isolated as an orange powder, m.p. 145-147 °C. The UV and IR spectra were similar to those of **DW1**.

The ^1H and ^{13}C NMR spectral data of **DW4** (Table 9, Figures 44 and 45) were related to those of **DW1** (Table 3, Figures 38 and 39). The difference in the spectrum of **DW4** was shown as an additional singlet methyl proton signal at δ 4.01 and a methyl carbon signal at δ 56.4 which replaced a hydroxyl group at δ 11.79 in **DW1**, suggesting a methoxyl proton at C-5. Furthermore, the spectrum of **DW4** was shown as the disappearance of a methyl proton at δ 2.01 (H-11) in the ^1H NMR of **DW1** but the appearance of a broad singlet of methylene protons at δ 4.64 in **DW4**, whereas the ^{13}C NMR spectrum of **DW4** displayed a signal of oxymethylene carbon at δ 59.7 instead of a methyl carbon at δ 16.1 as in **DW1**. The location of the methoxyl and oxymethylene groups were confirmed by HMBC experiment (Table 9, Figure 6) in which the methoxyl protons at δ 4.01 showed correlations to C-5 (δ 159.6). Thus, compound **DW4** was identified as 2-hydroxymethyl-5-methoxy-1,4-naphthoquinone, which was previously synthesized by Wurm, 1982. This is the first report of **DW4** from a natural source.

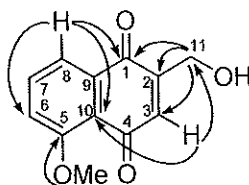


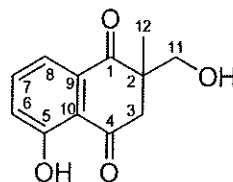
Figure 6 Major HMBC correlations of **DW4**

Table 9 ^1H , ^{13}C NMR, DEPT and HMBC spectral data of compound DW4

Position	DEPT	$\delta_{\text{C}}/\text{ppm}$	$\delta_{\text{H}}/\text{ppm}$ (mult., J in Hz)	HMBC
1	CO	185.6		
2	C	146.7		
3	CH	135.7	6.90 br d (1.6)	1, 2, 10, 11
4	CO	184.4		
5	C	159.6		
6	CH	118.1	7.31 d (8.4)	5, 8, 10
7	CH	134.9	7.67 t (8.4)	5, 6, 9
8	CH	119.1	7.73 d (8.4)	1, 6, 10
9	C	134.2		
10	C	119.7		
11	CH ₂	59.7	4.64 br s	1, 2, 3, 4
5-OCH ₃		56.4	4.01 s	5

Spectra recorded at 300 (^1H NMR) and 75 (^{13}C NMR) MHz, CDCl_3 .

3.1.5 Compound DW5



Compound **DW5** was isolated as a white amorphous solid, m.p. 93-95 °C. The IR and UV spectra were closely related to that of **DW4**.

The ^1H and ^{13}C NMR spectral data of **DW5** (Table 10, Figures 46 and 47) resembled those of **DW4** (Table 9, Figures 44 and 45). The differences were shown in the chemical shifts of the methyl protons which was shown at δ 4.01 in **DW4** but at δ 1.35 in **DW5** and the signal of an aliphatic methine proton at δ 6.90 (br d) in **DW4** was changed to signals of two doublets at δ 2.57 and 3.38 in **DW5**. In addition, two doublets of oxymethylene protons were shown at δ 3.47 and 4.09 (d, $J=10.8$). The location of the methyl group at C-2 was confirmed by HMBC experiment (Table 10, Figures 7) in which the methyl proton at δ 1.35 (H-12) showed correlations to C-2 (δ 50.7), C-1 (δ 200.7), C-3 (δ 46.5) and C-11 (δ 67.7). By comparison of the ^1H and ^{13}C NMR spectral data with the previously reported data (Miyoshi *et al.*, 1984) (Table 10, 11 and 22), therefore compound **DW5** was identified as diomuscinone.

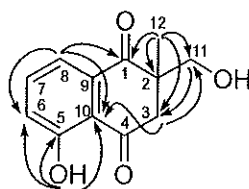


Figure 7 Major HMBC correlations of **DW5**

Table 10 ^1H , ^{13}C NMR, DEPT and HMBC spectral data of compound **DW5** and ^{13}C NMR of diomuscine (**R**)

Position	DEPT	$\delta_{\text{C}}/\text{ppm}$		$\delta_{\text{H}}/\text{ppm}$ (mult., J in Hz)	HMBC
		R ^a	DW5 ^b		
1	CO	200.8	200.7		
2	C	50.5	50.7		
3	CH ₂	46.6	46.5	2.57 d (17.1) 3.38 d (17.1)	1, 2, 10, 11, 12
4	CO	202.8	202.9		
5	C	161.1	161.1		
6	CH	124.0	123.9	7.25 dd (8.4, 1.2)	5, 8, 10
7	CH	136.9	136.9	7.63 t (8.4)	5, 6, 9
8	CH	118.5	117.5	7.53 dd (8.4, 1.2)	1, 6, 10
9	C	134.0	133.9		
10	C	117.5	117.5		
11	CH ₂	67.8	67.7	3.47 d (10.8) 4.09 d (10.8)	1, 3
12	CH ₃	21.4	21.3	1.35 s	1, 2, 3, 11
5-OH				12.00 s	5, 6, 10

^a Spectrum recorded at 90 (^{13}C NMR) MHz, CDCl_3 .

^b Spectra recorded at 300 (^1H NMR) and 75 (^{13}C NMR) MHz, CDCl_3 .

Table 11 Comparison of ^1H NMR spectral data of compounds **DW1**, **DW5** and diomuscinone

Position	$\delta_{\text{H}}/\text{ppm}$ (mult., J in Hz)		
	DW4 ^a	DW5 ^a	diomuscinone ^b
3	6.90 br d (1.6)	2.57 d (17.1)	2.80 d (17.0)
		3.38 d (17.1)	3.43 d (17.0)
6	7.31 d (8.4)	7.25 dd (8.4, 1.2)	7.25–7.4 ^c
7	7.67 t (8.4)	7.63 t (8.4)	7.5–7.8 ^d
8	7.73 d (8.4)	7.53 dd (8.4, 1.2)	7.5–7.8 ^d
11	4.64 br s	3.47 d (10.8)	3.53 d (11.5)
		4.09 d (10.8)	4.06 d (11.5)
12	4.01 s	1.35 s	1.31 s
5-OH		12.00 s	

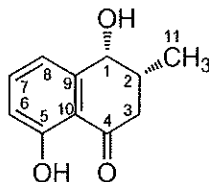
^a Spectra recorded at 300 (^1H NMR) MHz, CDCl_3 .

^b Spectrum recorded at 90 (^1H NMR) MHz, CDCl_3 .

^c Overlapped with the solvent signal.

^d Complex.

3.1.6 Compound DW6



Compound **DW6** was isolated as a colorless oil; $[\alpha]_D^{28} + 42.5$ (CHCl_3 , c 1.00). The IR and UV spectra were closely related to those of **DW1**.

The ^1H and ^{13}C NMR spectral data of **DW6** (Table 12, Figures 48 and 49) were similar to those of **DW1** (Table 3, Figures 38 and 39). However, a carbonyl and olefinic carbons in quinonoid ring were absent in the ^{13}C NMR spectrum of **DW6**, which indicated the reduction of one carbonyl and one double bond of a quinonoid ring in **DW1**. The appearances of a complex coupling system attributing to a methine at δ 2.33 (m, H-2), which was coupled with the methyl at δ 1.11 (d, $J= 6.9$ Hz, H-11), an oxymethine proton at δ 4.63 (br d, $J= 2.7$ Hz, H-1), and two methylene protons at δ 2.47 (dd, $J= 17.7, 4.2$ Hz, H-3a) and 2.77 (dd, $J= 17.7, 10.8$ Hz, H-3b) were observed. This finding was further supported by HMBC correlations (Table 12, Figure 8).

The relative stereochemistry at C-1 and C-2 should be α orientations for both hydroxyl and methyl groups. The *cis*-isomer was established with the aid of the coupling constant ($J= 2.7$ Hz) found for H-1, and by supporting from NOESY cross peak of H-1 and H-2. By comparison of the ^1H and ^{13}C NMR spectral data with the previously reported data (Bringmann *et al.*, 1999, $[\alpha]_D^{25} + 22.2$ (CHCl_3 , c 1.0) (Table 12, 13 and 22), therefore compound **DW6** was identified as isoshinanolone.

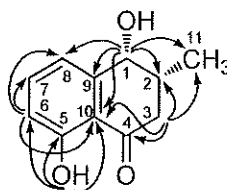


Figure 8 Major HMBC correlations of **DW6**

Table 12 ^1H , ^{13}C NMR, DEPT and HMBC spectral data of compounds **DW6** and ^{13}C NMR of isoshinanolone (**R**)

Position	DEPT	$\delta_{\text{C}}/\text{ppm}$		$\delta_{\text{H}}/\text{ppm}$ (mult., J in Hz)	HMBC
		R ^a	DW6 ^b		
1	CH	71.2	70.7	4.63 br d (2.7)	2, 8, 9, 10, 11
2	CH	34.3	34.3	2.33 m	11
3	CH ₂	40.7	40.6	2.47 dd (17.7, 4.2) 2.77 dd (17.7, 10.8)	1, 2, 4, 10, 11,
4	CO	204.7	205.1		
5	C	162.7	162.3		
6	CH	118.2	117.7	6.86 d (8.1)	6, 7, 8, 10
7	CH	136.9	137.0	7.41 t (8.1)	9
8	CH	118.6	119.0	6.83 d (8.1)	1, 6, 9, 10
9	C	145.0	145.1		
10	C	114.9	114.8		
11	CH ₃	16.1	16.1	1.11 d (6.9)	1, 2, 3
5-OH				12.35 s	5, 6, 10

^a Spectrum recorded at 150.9 (^{13}C NMR) MHz, CDCl_3 .

^b Spectra recorded at 300 (^1H NMR) and 75 (^{13}C NMR) MHz, CDCl_3 .

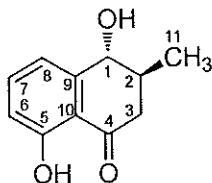
Table 13 Comparison of ^1H NMR spectral data of compounds **DW1**, **DW6** and isoshinanolone

Position	$\delta_{\text{H}}/\text{ppm}$ (mult., J in Hz)		
	DW1 ^a	DW6 ^a	isoshinanolone
1		4.63 br d (2.7)	4.75 d d (2.4)
2		2.33 m	2.44 m
3	6.63 br d (1.5)	2.47 dd (17.7, 4.2)	2.56 ddd (17.7, 4.3, 0.9)
		2.77 dd (17.7, 10.8)	2.87 dd (17.7, 11.0)
6	7.06 dd (8.4, 1.2)	6.83 d (8.1)	6.94 dd (8.5, 1.2)
7	7.46 t (8.4)	7.41 t (8.1)	7.48 dd (8.3, 7.3)
8	7.35 dd (8.4, 1.2)	6.86 d (8.1)	6.92 d (7.3)
11	2.01 d (1.5)	1.11 d (6.9)	1.19 d (6.7)
5-OH	11.79 s	12.35 s	12.42 s

^a Spectra recorded at 300 (^1H NMR) MHz, CDCl_3 .

^b spectrum recorded at 250 (^1H NMR) MHz, CDCl_3 .

3.1.7 Compound DW7



Compound **DW7** was isolated as a colorless oil; $[\alpha]_D^{28} - 42.5$ (CHCl_3 , c 0.70). The IR and UV spectra were closely related to those of **DW6**.

The ^1H and ^{13}C NMR spectral data of **DW7** (Table 14, Figures 50 and 51) were closely resemble to those of **DW6** (Table 12, Figures 48 and 49), except that the coupling constant of H-1 in **DW7** was 8.1 Hz, whereas the coupling constant of H-1 in **DW6** was 2.7 Hz. The coupling constant of H-1 in compound **DW7** was in agreement with the respective coupling pattern (axial-equatorial) of H-1 and H-2, indicating the *trans*-isomer. Thus on the basis of its spectroscopic data and comparison of the ^1H and ^{13}C NMR spectral data with the previous report (Bringmann *et al.*, 1999 (Table 14, 15 and 22), compound **DW7** was identified as *epi*-isoshinanolone, an epimer of isoshinanolone.

Table 14 ^1H , ^{13}C NMR, DEPT and HMBC spectral data of compounds **DW7** and ^{13}C NMR of *epi*-isoshinanolone (**R**)

Position	DEPT	$\delta_{\text{C}}/\text{ppm}$		$\delta_{\text{H}}/\text{ppm}$ (mult., <i>J</i> in Hz)		HMBC
		R ^a	DW7 ^b			
1	CH	73.7	73.6	4.51 d (8.1)		2, 8, 9, 10, 11
2	CH	37.4	38.0	2.27 m		
3	CH ₂	43.4	43.4	2.47 dd (17.1, 10.2)		1, 2, 4, 10, 11, 12
				2.93 dd (17.1, 3.9)		
4	CO	203.6	203.8			
5	C	162.5	162.7			
6	CH	117.3	117.1	6.92 d (8.4)		6, 7, 8, 10
7	CH	137.0	137.0	7.50 t (8.4)		6, 9
8	CH	117.2	117.4	7.12 d (8.4)		1, 6, 9, 10
9	C	145.9	145.8			
10	C	115.3	115.3			
11	CH ₃	17.8	17.4	1.12 d (6.9)		1, 2, 3
				12.38 s		
5-OH						5, 6, 10

^a Spectrum recorded at 50 (^{13}C NMR) MHz, CDCl_3 .

^b Spectra recorded at 300 (^1H NMR) and 75 (^{13}C NMR) MHz, CDCl_3 .

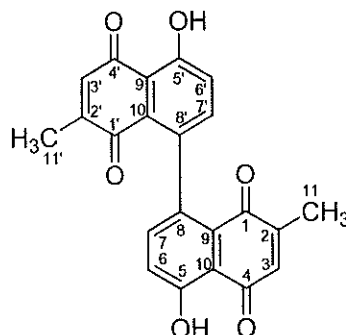
Table 15 Comparison of ^1H NMR spectral data of compounds **DW6**, **DW7** and *epi*-isoshinanolone

Position	δ_{H} /ppm (mult., <i>J</i> in Hz)		
	DW6 ^a	DW7 ^a	<i>epi</i> -isoshinanolone ^b
1	4.63 d (2.7)	4.51 d (8.1)	4.50 d (8.0)
2	2.33 m	2.27 m	2.25 m
3	2.47 dd (17.7, 4.2)	2.47 dd (17.1, 10.2)	2.43 dd (17.0, 10.1)
	2.77 dd (17.7, 10.8)	2.93 dd (17.1, 3.9)	2.91 dd (17.0, 3.8)
6	6.83 d (8.1)	6.92 d (8.4)	7.10 dd (7.6, 1.0)
7	7.41 t (8.1)	7.50 t (8.4)	7.49 t (8.0)
8	6.86 d (8.1)	7.12 d (8.4)	6.90 ddd (8.4, 1.1, 0.6)
11	1.11 d (6.9)	1.12 d (6.9)	1.19 d (6.5)
5-OH	12.35 s	12.38 s	11.74 s

^a Spectra recorded at 300 (^1H NMR) MHz, CDCl_3 .

^b Spectrum recorded at 200 (^1H NMR) MHz, CDCl_3 .

3.1.8 Compound DW8



Compound **DW8** was isolated as a red amorphous powder, m.p. 199-201 °C. Its molecular formula, $C_{22}H_{14}O_6$ ($[M]^+$ 374.1, calcd 374.1), was deduced by EI-MS spectrum. The UV and IR spectra were similar to those of **DW1**.

The 1H and ^{13}C NMR spectral data of **DW8** (Table 16, Figures 52 and 53) were closely resemble to those of **DW1** (Table 3, Figures 38 and 39), except that the ABX system of phenolic ring A was absence, while one pair of *ortho*-coupled aromatic protons at δ 7.21 and 7.29 (d, $J = 8.7$ Hz, H-6 and H-7, respectively) was observed. Thus, the splitting pattern for H-6 and H-7 was simplified due to the absence of H-8, together with the molecular formula, establishing the dimer with linkage at C-8 to C8' and was supported by HMBC correlation (Table 16, Figure 9) of H-6 and H-7 to C-8 (δ 128.2). Thus on the basis of its spectroscopic data and comparison of the 1H and ^{13}C NMR spectral data with the previous report (Gu *et al.*, 2004) (Tables 16, 17 and 22), compound **DW8** was assigned as maritinone.

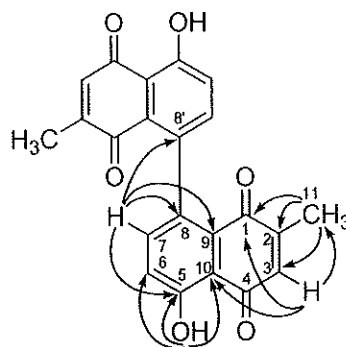


Figure 9 Major HMBC correlations of **DW8**

Table 16 ^1H , ^{13}C NMR, DEPT and HMBC spectral data of compound **DW8** and ^{13}C NMR of Maritinone (**R**)

Position	DEPT	$\delta_{\text{C}}/\text{ppm}$		$\delta_{\text{H}}/\text{ppm}$ (mult., J in Hz)	HMBC
		R ^a	DW8 ^b		
1	CO	185.1	185.2		
2	C	150.0	150.0		
3	CH	134.9	134.9	6.81 q (1.5)	1, 10, 11
4	CO	190.5	190.5		
5	C	161.3	161.3		
6	CH	124.3	124.3	7.21 d (8.7)	5, 8, 10
7	CH	137.9	138.0	7.29 d (8.7)	5, 6, 8, 9
8	C	128.2	128.2		
9	C	135.5	135.6		
10	C	115.4	115.5		
11	CH ₃	16.6	16.6	2.01 d (1.5)	1, 2, 3,
5-OH				12.55 s	5, 6, 7, 10

^a Spectrum recorded 125 (^{13}C NMR) MHz, CDCl_3 .

^b Spectra recorded at 300 (^1H NMR) and 75 (^{13}C NMR) MHz, CDCl_3 .

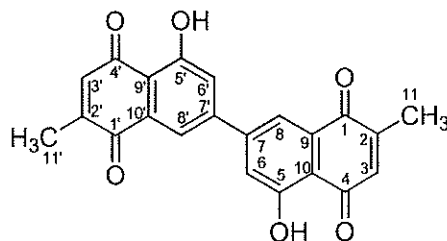
Table 17 Comparison of ^1H NMR spectral data of compounds **DW1**, **DW8** and maritinone

Position	δ_{H} /ppm (mult., J in Hz)		
	DW1 ^a	DW8 ^a	maritinone ^b
3	6.63 br d (1.5)	6.81 q (1.5)	6.81 q (1.5)
6	7.06 dd (8.4, 1.2)	7.21 d (8.7)	7.21 d (8.7)
7	7.46 t (8.4)	7.29 d (8.7)	7.29 d (8.7)
8	7.35 dd (8.4, 1.2)		
11	2.01 d (1.5)	2.01 d (1.5)	2.01 d (1.5)
5-OH	11.79 s	12.55 s	12.67 s

^a Spectra recorded at 500 (^1H NMR) MHz, CDCl_3 .

^b Spectrum recorded at 300 (^1H NMR) MHz, CDCl_3 .

3.1.9 Compound DW9



Compound **DW9** was obtained as a red solid, m.p. 250 °C (decomposed). The HREIMS spectrum showed a molecular ion peak $[M]^+$ at m/z 374.0812, corresponding to the molecular formula of $C_{22}H_{14}O_6$. The UV spectrum exhibited bands (λ_{max} 210, 270 and 415 nm) and the IR spectrum showed absorption bands for hydroxyl (3473 cm^{-1}), carbonyl (1664 cm^{-1}) and aromatic ring (1600 cm^{-1}) typical of the general pattern observed for **DW1**. The ^{13}C and 1H NMR spectral data (Table 18, Figures 54 and 55) revealed only 11 carbon signals and proton signals similar to **DW1** (Table 3, Figures 38 and 39), but the mass spectrum and the molecular formula revealed 22 carbons, thus suggesting that **DW9** is a symmetrical dimer of **DW1**. The 1H NMR spectrum of **DW9** was comparable to that of **DW1** (Table 19) except that there were no clear signals for the *ortho* and *meta*-coupled protons, but the presence of a broad singlet aromatic proton at δ 7.73 (2H, H-6 and H-8). The triplet proton signal of H-7 at δ 7.46 as present in **DW1** was absent in **DW9**, thus suggesting the linkage to be at the 7 to 7' positions and supporting by HMBC correlation (Table 18, Figure 10) of H-6 and H-8 to C-7 (δ 131.2). The structure of **DW9** was thus established to be 5,5'-dihydroxy-2,2'-dimethyl-7,7'-binaphthalen-1,1',4,4'-tetraone, a 7-7'-plumbagin dimer, a new compound (Salae *et al.*, 2010).

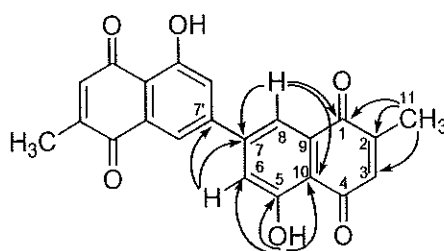


Figure 10 Major HMBC correlations of DW9

Table 18 ^1H , ^{13}C NMR, DEPT and HMBC spectral data of compound DW9

Position	DEPT	$\delta_{\text{C}}/\text{ppm}$	$\delta_{\text{H}}/\text{ppm}$ (mult., J in Hz)	HMBC
1	CO	183.1		
2	C	149.8		
3	CH	135.5	6.85 q (1.5)	10
4	CO	190.4		
5	C	158.9		
6	CH	118.7	7.73 br s	5, 7, 10
7	C	131.2		
8	CH	137.6	7.73 br s	1, 7, 9, 10
9	C	131.9		
10	C	115.3		
11	CH ₃	16.4	2.22 d (1.5)	1, 2, 3
5-OH			12.50 s	5, 7, 10

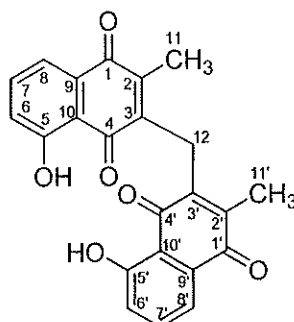
Spectra recorded at 300 (^1H NMR) and 75 (^{13}C NMR) MHz, CDCl_3 .

Table 19 Comparison of ^1H and ^{13}C NMR spectral data of compounds **DW1** and **DW9**

Position	$\delta_{\text{C}}/\text{ppm}$		$\delta_{\text{H}}/\text{ppm}$ (mult., J in Hz)	
	DW1	DW9	DW1	DW9
1	183.9	183.1		
2	149.2	149.8		
3	134.9	135.5	6.63 br d (1.5)	6.85 q (1.5)
4	189.7	190.4		
5	160.7	158.9		
6	123.7	118.7	7.06 dd (8.4, 1.2)	7.73 br s
7	135.7	131.2	7.46 t (8.4)	
8	118.7	137.6	7.35 dd (8.4, 1.2)	7.73 br s
9	131.5	131.9		
10	114.5	115.3		
11	16.1	16.4	2.01 d (1.5)	2.22 d (1.5)
12			11.79 s	12.50 s

Spectra recorded at 300 (^1H NMR) and 75 (^{13}C NMR) MHz, CDCl_3 .

3.1.10 Compound DW10



Compound **DW10** was isolated as orange needles, m.p. 202-204 °C. The UV and IR spectra showed the characteristic signals of **DW1**. The molecular ion (m/z $[M]^+$ 388.1, calcd 388.1) was shown in the EIMS spectrum.

The ^1H and ^{13}C NMR spectral data of **DW10** (Table 20, Figures 56 and 57) were similar to those of **DW1** (Table 3, Figures 38 and 39). The difference in the spectrum of **DW10** was shown as the absence of quinonoid proton at δ 6.63 (br d, H-3) in the ^1H NMR of **DW1** and the NMR spectrum of **DW10** showed a singlet signal of methylene protons at δ_{H} 3.97 (δ_{C} 25.6), thus suggesting a methylene group attached at C-3. The NMR and EIMS spectral data show that **DW10** is a symmetric dimer of **DW1** linked by a methylene bridge. Since no quinonoid proton was observed, the position of the dimeric linkage must be 3-3'. The HMBC experiment (Table 20, Figure 11) showed long-range correlations between the methylene proton to C-2 (δ 149.8), C-3 (δ 135.5) and C-4 (δ 189.3). By comparison of the ^1H and ^{13}C NMR spectral data with the previously reported data (Gunaherath *et al.*, 1988; Higa *et al.*, 2002) (Table 20-22), therefore compound **DW10** was identified as methylene-3,3'-biplumbagin.

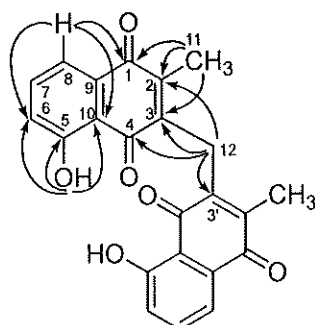


Figure 11 Major HMBC correlations of DW10

Table 20 ^1H , ^{13}C NMR, DEPT and HMBC spectral data of compound DW10

Position	DEPT	$\delta_{\text{C}}/\text{ppm}$	$\delta_{\text{H}}/\text{ppm}$ (mult., J in Hz)	HMBC
1	CO	184.2		
2	C	149.8		
3	C	135.5		
4	CO	189.3		
5	C	161.3		
6	CH	124.0	7.23 dd, (7.8, 1.5)	5, 8, 10
7	CH	136.1	7.59 t, (7.8)	5, 6, 9
8	CH	119.1	7.64 dd, (7.8, 1.5)	1, 6, 10
9	C	132.0		
10	C	114.7		
11	CH ₃	13.4	2.32 s	1, 2, 3, 4
12	CH ₂	25.6	3.97 s	2, 3, 4
5-OH			11.9 s	5, 6, 10

Spectra recorded at 300 (^1H NMR) and 75 (^{13}C NMR) MHz, CDCl_3 .

Table 21 Comparison of ^1H NMR spectral data of compounds **DW1**, **DW10** and methylene-3,3'-biplumbagin (**R**)

Position	$\delta_{\text{H}}/\text{ppm}$ (mult., J in Hz)		
	DW1 ^a	DW10 ^a	R ^b
3	6.63 br d (1.5)		
6	7.06 dd (8.4, 1.2)	7.23 dd, (7.8, 1.5)	7.63–7.13 m
7	7.46 t (8.4)	7.59 t, (7.8)	
8	7.35 dd (8.4, 1.2)	7.64 dd, (7.8, 1.5)	
11	2.01 d (1.5)	2.32 s	2.30 s
12		3.97 s	3.96 s
5-OH	11.79 s	11.90 s	11.93 s

^a Spectra recorded at 300 (^1H NMR) MHz, CDCl_3 .

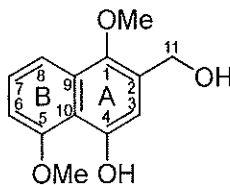
^b Spectrum recorded at 60 (^1H NMR) MHz, CDCl_3 .

Table 22 Comparison of ^{13}C NMR spectral data of compounds **DW1-DW10**

No.	DW1	DW2	DW3	DW4	DW5	DW6	DW7	DW8	DW9	DW10
1	183.9	184.1	190.8	185.6	200.7	70.7	73.6	185.1	183.1	184.2
2	149.2	121.8	61.2	146.7	50.7	34.3	38.0	150.0	149.8	149.8
3	134.9	152.7	61.3	135.7	46.5	40.6	43.4	134.9	135.5	135.5
4	189.7	184.5	196.6	184.4	202.9	205.1	203.8	190.5	190.4	189.3
5	160.7	161.1	161.4	159.6	161.1	162.3	162.7	161.3	158.9	161.3
6	123.7	123.1	124.1	118.1	123.9	117.7	117.1	124.3	118.7	124.0
7	135.7	137.5	137.1	134.9	136.9	137.0	137.0	138.0	131.2	136.1
8	118.7	119.6	119.8	119.1	117.5	119.0	117.4	128.2	137.6	119.1
9	131.5	132.7	132.2	134.2	133.9	145.1	145.8	135.4	131.9	132.0
10	114.5	112.9	114.4	119.7	117.5	114.8	115.3	115.4	115.3	114.7
11	16.1	8.7	14.6	59.7	67.7	16.1	17.4	16.6	16.4	13.4
12					21.3					25.6

Spectra recorded at 75 (^{13}C NMR) MHz, CDCl_3 .

3.1.11 Compound DW11



Compound **DW11** was obtained as white amorphous powder, m.p. 63-65 °C. The molecular formula $C_{13}H_{14}O_4$, on the basis of $[M]^+$ at m/z 234.0920 in the HREIMS suggested seven unsaturations. The UV spectrum exhibited absorption bands at λ_{max} 231 and 291 nm while IR spectrum showed absorption bands for hydroxyl (3400 cm^{-1}) and aromatic ring (1613 cm^{-1}).

The analysis of the ^{13}C NMR spectral data (**Table 23, Figure 59**) of **DW11** through DEPT revealed 13 carbons among which are two methoxyls (δ_{C} 56.1 and 62.3), an oxymethylene (δ_{C} 60.3), four sp^2 methine and six sp^2 quaternary carbons. Of the six sp^2 quaternary carbons, three were linked to oxygen atoms in view of their deshielded chemical shifts at δ_{C} 145.5, 150.7 and 156.3. Since two methoxyl groups were present, the third oxygenated quaternary carbon should link to a hydroxyl group. These data together with seven unsaturations suggested a naphthalene skeleton. The ^1H NMR data (**Table 23, Figure 58**) showed four aromatic proton signals. The first three signals appeared at δ_{H} 6.72 (1H, d, $J= 8.4$ Hz, H-6), 7.30 (1H, t, $J= 8.4$ Hz, H-7) and 7.60 (1H, d, $J= 8.4$ Hz, H-8). The fourth aromatic proton signal appeared as a broad singlet at δ_{H} 6.86 (1H, H-3), hence suggesting a substituent group in ring B and three substituent groups in ring A of a naphthalene skeleton. The two methoxyl protons, a hydroxyl and oxymethylene protons appeared at δ_{H} 3.81, 3.98, 9.13 and 4.78 ppm, respectively. The HMBC experiment (**Table 23, Figure 12**) allowed the assignment of the structure as follow: the methyl singlet of O- CH_3 at δ 3.81 showed correlation with C-1 (δ 145.5) whereas that at δ 3.98 showed correlation with C-5 (δ 156.3), indicating the location of the two O- CH_3 groups at C-1 and C-5, respectively. A methine proton H-3 (δ 6.86) showed clear 3J correlation with oxymethylene carbon C-11 (δ 60.3), the oxyquaternary carbon C-1 (δ 145.5) and C-10 (δ 115.1) and a 2J correlation with an oxyquaternary carbon C-4 (δ 150.7), hence the hydroxymethyl

group was located at C-2 and a hydroxyl group at C-4 of ring A. The NOESY experiment (**Figure 12**) revealed interactions between 1-OCH₃/H₂-11, H₂-11/H-3, 1-OCH₃/H-8, 5-OCH₃/H-6, thus supporting the assigned structure. Compound **DW11** was therefore a new compound and characterized as 2-hydroxymethyl-1,5-dimethoxynaphthalen-4-ol, a reduced and 1-*O*-methylated derivative of compound **DW4** (Salae *et al.*, 2010).

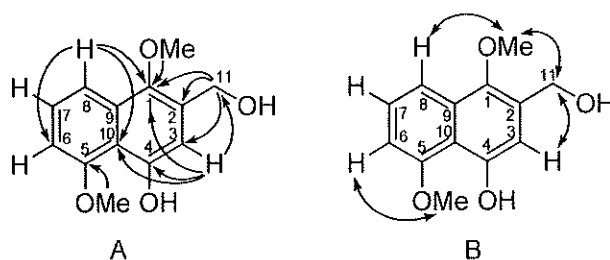


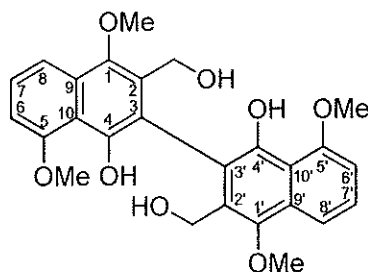
Figure 12 Selected HMBC correlations (A) and NOESY correlations (B) for **DW11**

Table 23 ¹H, ¹³C NMR, DEPT and HMBC spectral data of compounds **DW11**

Position	DEPT	δ_C /ppm	δ_H /ppm (mult., <i>J</i> in Hz)	HMBC
1	C	145.5		
2	C	131.1		
3	CH	109.8	6.86 br s	1, 4, 10, 11
4	C	150.7		
5	C	156.3		
6	CH	104.3	6.72 d (8.4)	5, 8
7	CH	126.1	7.30 t (8.4)	5, 6, 8, 9
8	CH	115.7	7.60 d (8.4)	1, 6, 9, 10
9	C	130.3		
10	C	115.1		
11	CH ₂	60.3	4.78 br s	1, 2, 3
1-OCH ₃		62.3	3.81 s	1
5-OCH ₃		56.1	3.98 s	5
4-OH			9.13 s	

Spectra recorded at 300 (¹H NMR) and 75 (¹³C NMR) MHz, CDCl₃.

3.1.12 Compound DW12



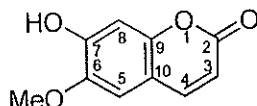
Compound **DW12** was obtained as white amorphous powder, m.p. 115-117 °C. The UV and IR spectra showed the characteristics of **DW11**. The HREIMS spectrum showed a molecular ion peak $[M]^+$ at m/z 466.1622, suggesting a molecular formula of $C_{26}H_{26}O_8$. A comparison of the NMR and mass spectral data between compounds **DW11** and **DW12** (Table 23 and 24, Figures 58, 59, 60 and 61) suggested that **DW12** was a dimer of **DW11** with C_2 symmetry (Table 24). A broad singlet signal of H-3 at δ 6.86 as shown in **DW11** was absent in **DW12**, suggesting the dimeric linkage between C-3 and C-3'. On the basis of these evidences, compound **DW12** was a new compound and identified as 2,2'-bis-hydroxymethyl-1,1',5,5'-tetramethoxy-3,3'-binaphthalen-4,4'-diol (Salae *et al.*, 2010).

Table 24 Comparison of ^1H and ^{13}C NMR spectral data of compounds **DW11** and **DW12**

Position	$\delta_{\text{C}}/\text{ppm}$		$\delta_{\text{H}}/\text{ppm}$ (mult., J in Hz)	
	DW11	DW12	DW11	DW12
1	145.5	147.8		
2	131.1	131.1		
3	109.8	118.1	6.86 br s	
4	150.7	147.2		
5	156.3	156.3		
6	104.3	105.0	6.72 d (8.4)	6.84 d (8.4)
7	126.1	126.7	7.30 t (8.4)	7.40 t (8.4)
8	115.7	116.5	7.60 d (8.4)	7.80 d (8.4)
9	130.3	130.5		
10	115.1	115.6		
11	60.3	58.2	4.78 br s	4.50 d (11.1) 4.56 d (11.1)
1-OCH ₃	62.3	63.4	3.81 s	
5-OCH ₃	56.1	56.2	3.98 s	4.01 s

Spectra recorded at 300 (^1H NMR) and 75 (^{13}C NMR) MHz, CDCl_3 .

3.1.13 Compound DW13



Compound **DW13** was obtained as yellow oil. The UV spectrum showed absorption maxima at 225, 240 and 346 nm and IR spectrum absorption bands at ν_{\max} 3450, 1725, 1630 and 1590 cm^{-1} , suggesting the presence of a hydroxyl, an unsaturated lactone and aromatic ring groups, respectively.

The ^{13}C NMR and DEPT spectral data (**Table 25, Figure 63**) of **DW13** indicated 10 resonances including a methoxy signal at δ 56.3 (OCH_3), a lactone signal at δ 162.1 ($\text{C}=\text{O}$), and eight low-field signals at δ 103.2 (CH), 107.9 (CH), 111.2 (C), 112.6 (CH), 143.8 (CH), 144.8 (C), 150.1 (C), and 150.4 (C). These data indicated that **DW13** contained an unsaturated lactone and a methoxyl group attached to aromatic ring.

In the ^1H NMR spectral data (**Table 25, Figure 62**) of **DW13**, the characteristic signals of a 6,7-disubstituted coumarin were apparent, with two doublets at δ 6.28 (1H, d, $J=9.6$ Hz, H-3) and 7.60 (1H, d, $J=9.6$ Hz, H-4), two aromatic signals at δ 6.86 (1H, s, H-5) and δ 6.88 (1H, s, H-8), and one methoxyl signal at δ 3.93 (3H, s, OCH_3 -6). The location of the methoxy group was assigned to C-6 based on the HMBC correlation between a methoxyl signal at δ 3.93 and C-6 at δ_{C} 144.8 and NOESY cross-peak between OCH_3 -6 (δ_{H} 3.93) and H-5 (δ_{H} 6.86) (**Table 25, Figure 13**). Thus on the basis of its spectroscopic data and comparison of the ^1H and ^{13}C NMR spectral data with the previous report (Razdan *et al.*, 1987) (**Table 25**), compound **DW13** was identified as scopoletin.

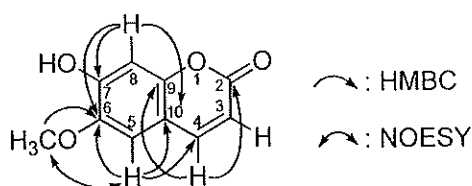


Figure 13 Major HMBC and NOESY correlations of **DW13**

Table 25 ^1H , ^{13}C NMR, DEPT and HMBC spectral data of compound **DW13** and comparison of ^1H and ^{13}C NMR of **DW13** and scopoletin (**R**)

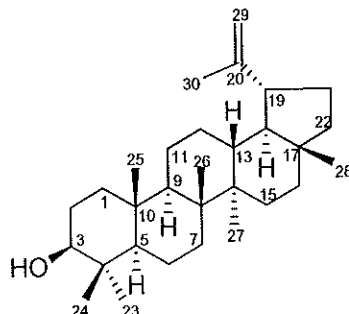
Position	DEPT	$\delta_{\text{C}}/\text{ppm}$		$\delta_{\text{H}}/\text{ppm}$ (mult., J in Hz)		HMBC [*]
		R ^a	DW13 ^b	R ^a	DW13 ^b	
1						
2	CO	160.5	162.1			
3	CH	112.5	112.6	6.26 d (9.4)	6.28 d (9.6)	2, 4, 10
4	CH	142.0	143.8	7.58 d (9.4)	7.60 d (9.6)	2, 5, 9, 10
5	CH	107.5	107.9	6.89 s	6.86 s	4, 6, 7, 10
6	C	143.0	144.8			
7	C	149.5	150.4			
8	CH	102.0	103.2	6.82 s	6.88 s	6, 7, 10
9	C	150.0	150.1			
10	C	110.5	111.2			
6-OCH ₃		55.2	56.3	3.93 s	3.93 s	6

^a Spectra recorded at 400 (^1H NMR) and 100 (^{13}C NMR) MHz, CDCl_3 .

^b Spectra recorded at 300 (^1H NMR) and 75 (^{13}C NMR) MHz, CDCl_3 .

* For **DW13**

3.1.14 Compound DW14



Compound **DW14** was obtained as a white solid, mp. 193-194 °C, $[\alpha]_D^{28} +25.0$ (CHCl₃, *c* 0.20). It exhibited hydroxyl (3343 cm⁻¹) and double bond (1638 cm⁻¹) absorptions in the IR spectrum and gave a purple vanillin-sulfuric acid test indicating a triterpene.

The ¹H NMR spectral data of **DW14** (Table 26, Figure 64) showed characteristic of lupane triterpenoid as seven methyl singlet signals at δ 0.76, 0.79, 0.83, 0.94, 0.97 and 1.03 including one vinylic methyl at δ 1.68, two protons of an isopropenyl moiety at δ 4.68 (1H, d, *J*= 2.1 Hz) and 4.56 (1H, m) and a typical lupane H_β-19 proton at δ 2.38 (dt, *J*= 11.1, 5.7 Hz). An oxymethine proton was shown at δ 3.19 (1H, dd, *J*= 10.8, 5.1 Hz, H-3). The doublet splitting pattern together with a large coupling constant of H-3 with *J*_{ax-ax} = 10.8 Hz and *J*_{ax-aq} = 5.1 Hz indicated an axial (α) orientation of H-3. The ¹³C and DEPT spectral data (Table 26, Figure 65) of **DW14** showed all 30 carbon signals as seven methyl (δ 14.6, 15.4, 16.0, 16.1, 18.0, 19.3 and 28.0), eleven methylene (δ 18.3, 20.9, 25.2, 27.4, 27.5, 29.9, 34.3, 35.6, 38.7, 40.0 and 109.3), six methine (δ 38.1, 48.0, 48.3, 50.5, 55.3 and 79.0) and six quaternary carbons (δ 37.2, 38.9, 40.8, 42.8, 43.0 and 151.0).

The position of the hydroxyl group at C-3 was determined through an HMBC experiment (Table 26, Figure 14) in which the oxymethine proton at δ 3.19 (H-3) showed correlations with C-1 (δ 38.7), C-4 (δ 38.9), C-23 (δ 28.0) and C-24 (δ 15.4). The position of a methine proton at C-19 was determined from HMBC correlation of H-19 (δ 2.38) with C-18 (δ 48.3), C-20 (δ 151.0), C-21 (δ 29.9) and C-

30 (δ 19.3). Thus on the basis of its spectroscopic data and comparison of the ^1H and ^{13}C NMR spectral data with the previous report (Reynolds *et al.*, 1986, $[\alpha]_{\text{D}}^{25} +23.0^\circ$ (EtOH, c 0.50); Burns *et al.*, 2000; Thongdeeying 2005) (Table 26, 27 and 36), compound **DW14** was identified as 3β -lupeol.

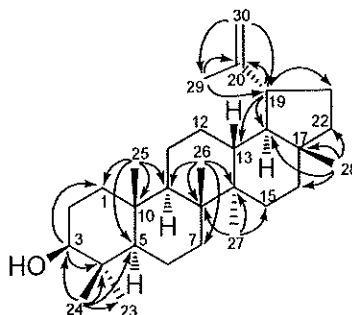


Figure 14 Major HMBC correlations of **DW14**

Table 26 ^1H , ^{13}C NMR, DEPT and HMBC spectral data of compound **DW14** and ^{13}C NMR of lupeol (**R**)

Position	DEPT	$\delta_{\text{C}}/\text{ppm}$		$\delta_{\text{H}}/\text{ppm}$ (mult., J in Hz)	HMBC
		R^b	DW14^c		
1	CH ₂	38.7	38.7	0.91 m ^a	
2	CH ₂	27.4	27.4	1.56 m ^a	
3	CH	79.0	79.0	3.19 dd (10.8, 5.1)	1, 4, 23, 24
4	C	38.8	38.9		
5	CH	55.3	55.3	0.69 m ^a	
6	CH ₂	18.3	18.3	1.40, 1.55 m ^a	
7	CH ₂	34.2	34.3	1.40 m ^a	
8	C	40.8	40.8		
9	CH	50.3	50.5	1.28 m ^a	
10	C	37.1	37.2		
11	CH ₂	20.9	20.9	1.22, 1.45 m ^a	
12	CH ₂	25.1	25.2	1.08 m ^a	
13	CH	38.0	38.1	1.67 m ^a	

Table 26 (continued)

Position	DEPT	δ_C /ppm		δ_H /ppm (mult., <i>J</i> in Hz)		HMBC
		R^b		DW14 ^c		
14	C	42.8	42.8			
15	CH ₂	27.4	27.5	1.56 m ^a		
16	CH ₂	35.6	35.6	1.51 m ^a		
17	C	43.0	43.0			
18	CH	48.3	48.3	1.38 m ^a		
19	CH	48.0	48.0	2.38 dt (11.1, 5.7)		13, 18, 20, 29, 30
20	C	150.9	151.0			
21	CH ₂	29.8	29.9	1.94 m ^a		
22	CH ₂	40.0	40.0	1.20, 1.40 m ^a		
23	CH ₃	28.0	28.0	0.97 s		3, 4, 5, 24
24	CH ₃	15.3	15.4	0.76 s		3, 4, 5, 23
25	CH ₃	16.1	16.1	0.83 s		1, 5, 9, 10
26	CH ₃	15.9	16.0	1.03 s		7, 8, 9, 14
27	CH ₃	14.5	14.6	0.94 s		8, 14, 15
28	CH ₃	18.0	18.0	0.79 s		16, 17, 18, 22
29	CH ₂	109.3	109.3	4.56 m		19, 30
				4.68 d (2.1)		
30	CH ₃	19.3	19.3	1.68 s		19, 30

^a Deduced from HMQC experiment.

^b Spectrum recorded at 125 (¹³C NMR) MHz, CDCl₃.

^c Spectra recorded at 300 (¹H NMR) and 75 (¹³C NMR) MHz, CDCl₃.

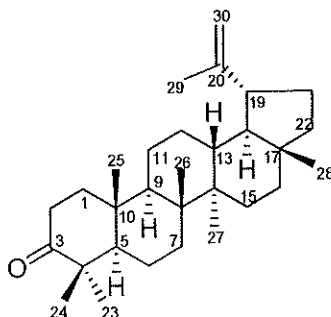
Table 27 Comparison of ^1H NMR spectral data of compounds **DW14** and lupeol

Position	δ_{H} /ppm (mult., <i>J</i> in Hz)	
	DW14 ^a	lupeol ^b
1	0.91 m	0.90, 1.67 m
2	1.56 m	1.56, 1.60 m
3	3.19 dd (10.8, 5.1)	3.18 dd
5	0.69 m	0.68 m
6	1.40, 1.55 m	1.39, 1.51 m
7	1.40 m	1.39 m
9	1.28 m	1.27 m
11	1.22, 1.45 m	1.23, 1.41 m
12	1.08 m	1.07, 1.67 m
13	1.67 m	1.66 m
15	1.56 m	1.00, 1.68 m
16	1.51 m	1.37, 1.47 m
18	1.38 m	1.36 m
19	2.38 dt (11.1, 5.7)	2.38 dt
21	1.94 m	1.94 m
22	1.20, 1.40 m	1.19, 1.38 m
23	0.97 s	0.96 s
24	0.76 s	0.76 s
25	0.83 s	0.83 s
26	1.03 s	1.03 s
27	0.94 s	0.94 s
28	0.79 s	0.78 s
29	4.56 m	4.56 m
	4.68 d (2.1)	4.69 m
30	1.68 s	1.68 s

^a Spectrum recorded at 300 (^1H NMR) MHz, CDCl_3 .

^b Spectrum recorded at 500 (^1H NMR) MHz, CDCl_3 .

3.1.15 Compound DW15



Compound **DW15** was obtained as a white solid, mp. 163-165 °C, $[\alpha]_D^{28} +50.0$ (CHCl₃, *c* 0.10). It exhibited carbonyl (1704 cm⁻¹) and double bond (1642 cm⁻¹) absorptions in the IR spectrum and gave a purple vanillin-sulfuric acid test indicating a triterpene.

The ¹H and ¹³C NMR spectral data (Table 28, Figures 66 and 67) of **DW15** showed signals similar to **DW14** (Table 26, Figures 64 and 65) except that in **DW15** a doublet of doublets signal of a methine proton H-3 disappeared and the carbon signal at C-3 (δ 217.0) was displayed as a carbonyl carbon instead of the oxymethine carbon at δ 79.0 as in **DW14**. The location of the carbonyl group was confirmed by HMBC experiment (Table 28) in which both H₃-24 (δ 1.02) and H₃-23 (δ 1.07) showed long-range correlations with C-3 (δ 217.0), C-4 (δ 46.3) and C-5 (δ 54.3). Thus on the basis of its spectroscopic data and comparison of the ¹H and ¹³C NMR spectral data with the previous report (Razdan *et al.*, 1988, $[\alpha]_D^{25} +50.0$ (CHCl₃, *c* 0.10); Thongdeeying 2005) (Table 28, 29 and 36), compound **DW15** was identified as lupenone.

Table 28 ^1H , ^{13}C NMR, DEPT and HMBC spectral data of compound **DW15** and ^{13}C NMR of lupenone (**R**)

Position	DEPT	$\delta_{\text{C}}/\text{ppm}$		$\delta_{\text{H}}/\text{ppm}$ (mult., J in Hz)	HMBC
		R^{b}	DW15^{c}		
1	CH ₂	39.6	38.6	0.90 m ^a	
2	CH ₂	34.1	33.1	2.49 m ^a	
3	C	217.9	217.0		
4	C	47.2	46.3		
5	CH	55.8	54.3	1.32 m ^a	
6	CH ₂	19.6	18.7	1.45 m ^a	
7	CH ₂	33.5	32.6	0.87, 1.45 m ^a	
8	C	40.7	39.8		
9	CH	49.7	48.8	1.38 m ^a	
10	C	36.8	35.9		
11	CH ₂	21.4	20.5	1.30 m ^a	
12	CH ₂	25.1	24.2	1.68 m ^a	
13	CH	38.1	37.2	1.68 m ^a	
14	C	42.7	41.9		
15	CH ₂	27.4	26.4	0.82 m ^a	
16	CH ₂	35.6	34.5	1.37, 1.50 m ^a	
17	C	42.7	42.0		
18	CH	48.2	47.3	1.38 m ^a	
19	CH	47.8	47.0	2.40 m ^a	18, 20, 21, 29, 30
20	C	150.5	149.8		
21	CH ₂	29.8	28.8	1.26, 1.92 m ^a	
22	CH ₂	39.9	39.0	1.19, 1.41 m ^a	
23	CH ₃	26.6	25.7	1.07 s	3, 4, 5, 24
24	CH ₃	21.0	20.0	1.02 s	3, 4, 5, 23
25	CH ₃	15.8	15.0	0.93 s	5, 9, 10
26	CH ₃	15.4	14.8	1.07 s	7, 8, 9, 14

Table 28 (continued)

Position	DEPT	δ_C /ppm		δ_H /ppm (mult., <i>J</i> in Hz)		HMBC
		R ^b		DW15 ^c		
27	CH ₃	14.4	13.5	0.96 s		14, 15
28	CH ₃	18.0	17.0	0.80 s		17, 18, 22
29	CH ₂	109.2	108.1	4.57 m		19, 30
				4.69 d (2.1)		
30	CH ₃	19.2	18.3	1.68 s		19, 20, 29

^a Deduced from HMQC experiment.

^b Spectrum recorded at 75 (¹³C NMR) MHz, CDCl₃.

^c Spectra recorded at 300 (¹H NMR) and 75 (¹³C NMR) MHz, CDCl₃.

Table 29 Comparison of ¹H NMR spectral data of compounds DW14, DW15 and lupenone

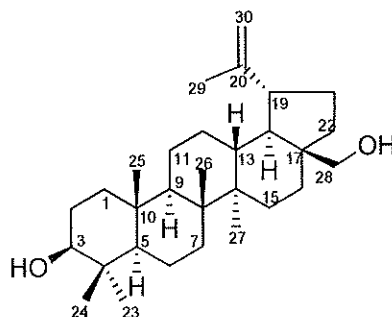
Position	δ_H /ppm (mult., <i>J</i> in Hz)		
	DW14	DW15	lupenone
1	0.91 m	0.90 m	
2	1.56 m	2.49 m	
3	3.19 dd (10.8, 5.1)		
5	0.69 m	1.32 m	
6	1.40, 1.55 m	1.45 m	
7	1.40 m	0.87, 1.45 m	
9	1.28 m	1.38 m	
11	1.22, 1.45 m	1.30 m	
12	1.08 m	1.68 m	
13	1.67 m	1.68 m	
15	1.56 m	0.82 m	
16	1.51 m	1.37, 1.50 m	
18	1.38 m	1.38 m	

Table 29 (continued)

Position	δ_{H} /ppm (mult., <i>J</i> in Hz)		
	DW14	DW15	lupenone
19	2.38 dt (11.1, 5.7)	2.40 m	2.24–252 m
21	1.94 m	1.26, 1.92 m	1.84–1.97 m
22	1.20, 1.40 m	1.19, 1.41 m	
23	0.97 s	1.07 s	1.04 s
24	0.76 s	1.02 s	1.00 s
25	0.83 s	0.93 s	0.90 s
26	1.03 s	1.07 s	1.02 s
27	0.94 s	0.96 s	0.93 s
28	0.79 s	0.80 s	0.77 s
29	4.56 m	4.57 m	4.55 br s
	4.68 d (2.1)	4.69 d (2.1)	4.66 br s
30	1.68 s	1.68 s	1.66 s

Spectra recorded at 300 (^1H NMR) MHz, CDCl_3 .

3.1.16 Compound DW16



Compound **DW16** was obtained as a white solid, m.p. 230-231°C, $[\alpha]_{\text{D}}^{28} +16.7^\circ$ (CHCl_3 , c 0.15). The IR spectrum showed the characteristics of **DW14** and gave a purple vanillin-sulfuric acid test indicating a triterpene.

The ^1H and ^{13}C NMR spectral data of **DW16** (Table 30, Figures 68 and 69) and **DW14** (Table 26, Figures 64 and 65) revealed close structural similarity. The difference in the spectrum of **DW16** was shown as only six singlet signals of methyl groups at δ 0.76, 0.82, 0.97, 0.98, 1.02 and 1.68. In addition, the AB system of oxymethylene protons was shown at δ 3.80 (1H, dd, $J= 10.8, 1.5$ Hz) and 3.33 (1H, dd, $J= 10.8$) which was not observed in **DW14**. On the basis of HMBC experiment (Table 30), the oxymethylene protons (2H-28) showed long-range correlation with C-16 (δ 29.2), C-17 (δ 47.5) and C-22 (δ 34.0), thus the oxymethylene protons were located at C-28 (δ 60.6). This compound was assigned as betulin by comparison of its spectral data (Table 30, 31 and 36) with those reported in the literature (Monago *et al.*, 1984, $[\alpha]_{\text{D}} +19^\circ$ (CHCl_3 , c 0.15); Tinto *et al.*, 1992; Thongdeeying 2005).

Table 30 ^1H , ^{13}C NMR, DEPT and HMBC spectral data of compound **DW16** and ^{13}C NMR of betulin (**R**)

Position	DEPT	$\delta_{\text{C}}/\text{ppm}$		$\delta_{\text{H}}/\text{ppm}$ (mult., J in Hz)	HMBC
		R^b	DW16^c		
1	CH ₂	38.8	38.7	0.90, 1.70 m ^a	
2	CH ₂	27.2	27.4	1.59 m ^a	
3	CH	78.9	79.0	3.19 dd (10.8, 5.1)	1, 4, 23, 24
4	C	38.9	38.9		
5	CH	55.3	55.3	0.68 m ^a	
6	CH ₂	18.3	18.3	1.41 m ^a	
7	CH ₂	34.3	34.2	1.04, 1.40 m ^a	
8	C	40.9	40.9		
9	CH	50.4	50.4	1.27 m ^a	
10	C	37.2	37.2		
11	CH ₂	20.9	20.8	1.28, 1.46 m ^a	
12	CH ₂	25.3	25.2	1.68 m ^a	
13	CH	27.3	37.3	1.67 m ^a	
14	C	42.7	42.7		
15	CH ₂	27.0	27.0	1.11, 1.66 m ^a	
16	CH ₂	29.2	29.2	1.20, 1.98 m ^a	
17	C	47.8	47.5		
18	CH	48.8	48.8	1.60 m ^a	
19	CH	47.8	47.5	2.38 m ^a	18, 20, 21, 29, 30
20	C	150.6	150.5		
21	CH ₂	29.8	29.8	1.91 m ^a	
22	CH ₂	34.0	34.0	1.80, 1.88 m ^a	
23	CH ₃	28.0	28.0	0.97 s	3, 4, 5, 24
24	CH ₃	15.4	15.4	0.76 s	3, 4, 5, 23
25	CH ₃	16.1	16.1	0.82 s	1, 5, 9
26	CH ₃	16.0	16.0	1.02 s	7, 8, 9, 14

Table 30 (continued)

Position	DEPT	δ_C /ppm		δ_H /ppm (mult., <i>J</i> in Hz)		HMBC
		R^b			DW16 ^c	
27	CH ₃	14.8	14.8	0.98 s		8, 13,14, 15
28	CH ₂	60.2	60.6	3.33 d (10.8) 3.80 dd (10.8, 1.5)		16, 17, 22
29	CH ₂	109.6	109.7	4.58 m 4.68 d (2.1)		19, 20, 30
30	CH ₃	19.1	19.1	1.68 s		19, 20, 29

^a Deduced from HMQC experiment.

^b Spectrum recorded at 100 (¹³C NMR) MHz, CDCl₃.

^c Spectra recorded at 300 (¹H NMR) and 75 (¹³C NMR) MHz, CDCl₃.

Table 31 Comparison of ¹H NMR spectral data of compounds DW14, DW16 and betulin

Position	δ_H /ppm (mult., <i>J</i> in Hz)		
	DW14 ^a	DW16 ^a	betulin ^b
1	0.91 m	0.90, 1.70 m	
2	1.56 m	1.59 m	
3	3.19 dd (10.8, 5.1)	3.19 dd (10.8, 5.1)	3.20 dd (10.1, 4.7)
5	0.69 m	0.68 m	
6	1.40, 1.55 m	1.41 m	
7	1.40 m	1.04, 1.40 m	
9	1.28 m	1.27 m	
11	1.22, 1.45 m	1.28, 1.46 m	
12	1.08 m	1.68 m	
13	1.67 m	1.67 m	
15	1.56 m	1.11, 1.66 m	
16	1.51 m	1.20, 1.98 m	

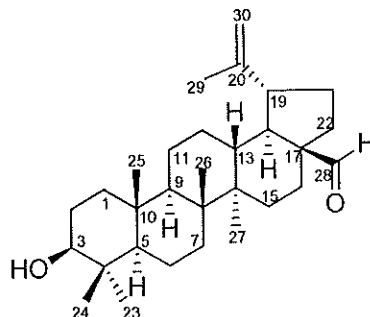
Table 31 (continued)

Position	$\delta_{\text{H}}/\text{ppm}$ (mult., J in Hz)		
	DW14 ^a	DW16 ^a	betulin ^b
18	1.38 m	1.60 m	
19	2.38 dt (11.1, 5.7)	2.38 m	
21	1.94 m	1.91 m	
22	1.20, 1.40 m	1.80, 1.88 m	
23	0.97 s	0.97 s	0.96 s
24	0.76 s	0.76 s	0.76 s
25	0.83 s	0.82 s	0.82 s
26	1.03 s	1.02 s	0.97 s
27	0.94 s	0.98 s	0.98 s
28	0.79 s	3.33 d (10.8)	3.33 d (11.0)
		3.80 dd (10.8, 1.5)	3.79 d (11.0)
29	4.56 m	4.58 m	4.58 m
	4.68 d (2.1)	4.68 d (2.1)	4.68 m
30	1.68 s	1.68 s	1.65 s

^a Spectra recorded at 300 (¹H NMR) MHz, CDCl₃.

^b Spectrum recorded at 400 (¹H NMR) MHz, CDCl₃.

3.1.17 Compound DW17



Compound **DW17** was obtained as a colorless viscous oil. It gave a purple vanillin-sulfuric acid test. Due to its instability, no IR spectrum was obtained.

The ^1H and ^{13}C NMR spectral data (**Table 32, Figures 70 and 71**) of **DW17** were similar to those of **DW14** (**Table 26, Figures 64 and 65**), except that **DW17** had only six methyl singlets at δ 0.75, 0.82, 0.92, 0.96, 0.98 and 1.70 and showed additional signal of aldehydic proton at δ 9.68 (1H, d, $J= 1.5$ Hz). The signal of a methine proton at δ 2.86 (H-19) in **DW17** was shifted more downfield than **DW14** (δ 2.38). On the basis of the HMBC (**Table 32**), the aldehyde group was located at C-28 (δ 206.7) from correlation of H-28 (δ 9.68) with C-17 (δ 59.3) and C-18 (δ 48.1). Compound **DW17** was identified as betulinaldehyde by comparison of its spectral data with those reported in the literature (Macias *et al*, 1994) (**Table 32, 33 and 36**).

Table 32 ^1H , ^{13}C NMR, DEPT and HMBC spectral data of compounds **DW17** and ^{13}C NMR of betulinaldehyde (**R**)

Position	DEPT	$\delta_{\text{C}}/\text{ppm}$		$\delta_{\text{H}}/\text{ppm}$ (mult., J in Hz)		HMBC
		R^b	DW17^c			
1	CH ₂	38.7	38.7	0.91, 1.67 m ^a		
2	CH ₂	27.3	27.4	1.58, 1.66 m ^a		
3	CH	78.9	79.0	3.18 dd (10.8, 5.1)		23, 24
4	C	38.8	38.8			
5	CH	55.5	55.3	0.67 m ^a		
6	CH ₂	18.2	18.3	1.40, 1.55 m ^a		
7	CH ₂	34.3	34.3	1.38, 1.44 m ^a		
8	C	40.8	40.8			
9	CH	50.4	50.5	1.26 m ^a		
10	C	37.1	37.2			
11	CH ₂	20.7	20.7	1.27, 1.46 m ^a		
12	CH ₂	25.5	25.2	1.75 m ^a		
13	CH	38.7	38.7	2.03 m ^a		
14	C	42.5	42.6			
15	CH ₂	29.2	29.3	1.46 m ^a		
16	CH ₂	28.8	28.8	1.17, 2.12 m ^a		14, 17, 20, 28
17	C	59.3	59.3			
18	CH	48.0	48.1	1.73 m ^a		
19	CH	47.5	47.5	2.86 dt (10.8, 5.7)		18, 21, 30
20	C	149.7	149.7			
21	CH ₂	29.8	29.9	1.24, 1.89 m ^a		
22	CH ₂	33.2	33.2	1.34, 1.80 m ^a		
23	CH ₃	27.9	28.0	0.96 s		3, 4, 5, 24
24	CH ₃	15.4	15.3	0.75 s		3, 4, 5, 23
25	CH ₃	15.9	16.1	0.82 s		1, 5, 9, 10
26	CH ₃	16.1	16.0	0.92 s		7, 8, 9, 14

Table 32 (continued)

Position	DEPT	δ_C /ppm		δ_H /ppm (mult., <i>J</i> in Hz)	HMBC
		R^b	DW17 ^c		
27	CH ₃	14.2	14.3	0.98 s	8, 14, 15
28	CHO	205.6	206.7	9.68 d (1.5)	17, 18
29	CH ₂	110.1	110.2	4.63 m 4.76 m	19, 30
30	CH ₃	19.0	19.0	1.70 s	19, 20, 29

^a Deduced from HMQC experiment.

^b Spectrum recorded at 100 (¹³C NMR) MHz, CDCl₃.

^c Spectra recorded at 300 (¹H NMR) and 75 (¹³C NMR) MHz, CDCl₃.

Table 33 Comparison of ¹H NMR spectral data of compounds DW14, DW17 and betulinaldehyde

Position	δ_H /ppm (mult., <i>J</i> in Hz)		
	DW14 ^a	DW17 ^a	betulin ^b
1	0.91 m	0.91, 1.67 m	0.90, 1.65 m
2	1.56 m	1.58, 1.66 m	1.54, 1.59 m
3	3.19 dd (10.8, 5.1)	3.18 dd (10.8, 5.1)	3.17 dd (11.1, 5.0)
5	0.69 m	0.67 m	0.67 m
6	1.40, 1.55 m	1.40, 1.55 m	1.36, 1.55 m
7	1.40 m	1.38, 1.44 m	1.40 m
9	1.28 m	1.26 m	1.28 m
11	1.22, 1.45 m	1.27, 1.46 m	1.24, 1.42 m
12	1.08 m	1.75 m	1.02, 1.74 m
13	1.67 m	2.03 m	2.01 m
15	1.56 m	1.46 m	1.17 m
16	1.51 m	1.17, 2.12 m	1.42, 2.06 m

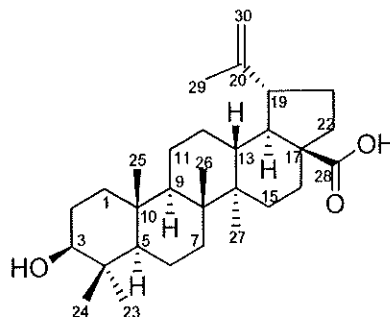
Table 33 (continued)

Position	$\delta_{\text{H}}/\text{ppm}$ (mult., J in Hz)		
	DW14 ^a	DW17 ^a	betulinaldehyde ^b
18	1.38 m	1.73 m	1.71 m
19	2.38 dt (11.1, 5.7)	2.86 dt (10.8, 5.7)	2.85 m
21	1.94 m	1.24, 1.89 m	1.45, 1.87 m
22	1.20, 1.40 m	1.34, 1.80 m	1.33, 1.74 m
23	0.97 s	0.96 s	0.95 s
24	0.76 s	0.75 s	0.74 s
25	0.83 s	0.82 s	0.80 s
26	1.03 s	0.92 s	0.90 s
27	0.94 s	0.98 s	0.96 s
28	0.79 s	9.68 d (1.5)	9.66 d
29	4.56 m	4.63 m	4.62
	4.68 d (2.1)	4.76 m	4.74
30	1.68 s	1.70 s	1.68 s

^a Spectra recorded at 300 (¹H NMR) MHz, CDCl₃.

^b Spectrum recorded at 400 (¹H NMR) MHz, CDCl₃.

3.1.18 Compound DW18



Compound **DW18** was obtained as a white solid, mp. 279-280 °C, $[\alpha]_D^{28} +15.0$ (CHCl₃, *c* 0.10). It exhibited hydroxyl (3415 cm⁻¹) and a carboxyl (1686 cm⁻¹) absorption in the IR spectrum. It also gave a purple vanillin-sulfuric acid test indicating a triterpene.

The ¹H and ¹³C NMR spectral data (Table 34, Figures 72 and 73) of **DW18** were similar to those of **DW14** (Table 26, Figures 64 and 65). The difference in the spectrum of **DW18** was shown as disappearance of a methyl signal at δ_H 0.79 (H₃-28, s, δ_C 18.0) in **DW14** and the appearance of a carboxyl signal at δ_C 179.6 (C-28) in **DW18**. The location of the carboxyl group was confirmed by HMBC experiment (Table 34) in which the methylene proton signals at δ 1.93 (1H, m, H-22a) and 1.40 (1H, m, H-22b) showed correlations with C-17 (δ 55.3), C-18 (δ 48.3) and C-28 (δ 179.6). Thus on the basis of its spectroscopic data and comparison with the previous report (Tinto *et al.*, 1992, $[\alpha]_D^{28} +6.8^\circ$ (pyridine, *c* 2.00); Peng *et al.*, 1998; Thongdeeying 2005) (Table 34-36), compound **DW18** was identified as betulinic acid.

Table 34 ^1H , ^{13}C NMR, DEPT and HMBC spectral data of compounds **DW18** and ^{13}C NMR of betulinic acid (**R**)

Position	DEPT	$\delta_{\text{C}}/\text{ppm}$		$\delta_{\text{H}}/\text{ppm}$ (mult., J in Hz)	HMBC
		R^b	DW18^c		
1	CH ₂	38.5	37.7	0.87, 1.64 m ^a	
2	CH ₂	28.2	26.4	1.55 m ^a	
3	CH	78.1	78.0	3.19 dd (10.8, 5.4)	
4	C	39.4	37.9		
5	CH	55.9	54.4	0.69 m ^a	
6	CH ₂	18.7	17.3	1.35, 1.48 m ^a	
7	CH ₂	34.7	33.3	1.35 m ^a	
8	C	41.0	39.7		
9	CH	50.9	49.5	1.20 m ^a	
10	C	37.5	36.2		
11	CH ₂	21.1	19.8	1.42 m ^a	
12	CH ₂	26.0	24.5	1.67 m ^a	
13	CH	39.2	37.4	2.20 m ^a	
14	C	42.8	41.4		
15	CH ₂	30.2	28.7	1.14, 1.23 m ^a	
16	CH ₂	32.8	31.2	2.22 m ^a	
17	C	56.6	55.3		
18	CH	49.7	48.3	1.55 m ^a	
19	CH	47.7	45.9	3.00 m ^a	18, 20, 21, 29, 30
20	C	151.4	149.4		
21	CH ₂	31.1	29.6	1.89 m ^a	
22	CH ₂	37.4	36.0	1.40, 1.93 m ^a	17, 18, 28
23	CH ₃	28.5	27.0	0.97 s	3, 4, 5, 24
24	CH ₃	16.2	14.3	0.75 s	3, 4, 5, 23
25	CH ₃	16.3	15.1	0.82 s	1, 5, 9, 10
26	CH ₃	16.2	15.0	0.94 s	7, 8, 9, 14

Table 34 (continued)

Position	DEPT	δ_C /ppm		δ_H /ppm (mult., <i>J</i> in Hz)	HMBC
		R^b	DW18 ^c		
27	CH ₃	14.8	13.7	0.98 s	8, 13,14, 15
28	CO	180.0	179.6		
29	CH ₂	109.2	108.7	4.74 br s 4.61 br s	19, 20, 30
30	CH ₃	19.3	18.4	1.69 s	19, 20, 29

^a Deduced from HMQC experiment.

^b Spectrum recorded at 100 (¹³C NMR) MHz, CDCl₃.

^c Spectra recorded at 300 (¹H NMR) and 75 (¹³C NMR) MHz, CDCl₃.

Table 35 Comparison of ¹H NMR spectral data of compounds DW14, DW18 and betulinic acid

Position	δ_H /ppm (mult., <i>J</i> in Hz)		
	DW14	DW18	betulinic acid
1	0.91 m	0.87, 1.64 m	
2	1.56 m	1.55 m	
3	3.19 dd (10.8, 5.1)	3.19 dd (10.8, 5.4)	3.19 dd (10.0, 4.7)
5	0.69 m	0.69 m	
6	1.40, 1.55 m	1.35, 1.48 m	
7	1.40 m	1.35 m	
9	1.28 m	1.20 m	
11	1.22, 1.45 m	1.42 m	
12	1.08 m	1.67 m	
13	1.67 m	2.20 m	
15	1.56 m	1.14, 1.23 m	
16	1.51 m	2.22 m	
18	1.38 m	1.55 m	

Table 35 (continued)

Position	$\delta_{\text{H}}/\text{ppm}$ (mult., J in Hz)		
	DW14	DW18	betulinic acid
19	2.38 dt (11.1, 5.7)	3.00 m	2.99 ddd (11.0, 11.0, 5.5)
21	1.94 m	1.89 m	
22	1.20, 1.40 m	1.40, 1.93 m	
23	0.97 s	0.97 s	0.93 s
24	0.76 s	0.75 s	0.75 s
25	0.83 s	0.82 s	0.82 s
26	1.03 s	0.94 s	0.96 s
27	0.94 s	0.98 s	0.97 s
28	0.79 s		
29	4.56 m	4.61 br s	4.60 d (1.5)
	4.68 d (2.1)	4.74 br s	4.73 d (1.5)
30	1.68 s	1.69 s	1.68 s

Spectra recorded at 300 (^1H NMR) MHz, CDCl_3 .

Table 36 Comparison of ^{13}C NMR spectral data of compounds DW14-DW18

Position	DW14	DW15	DW16	DW17	DW18
1	38.7	38.6	37.7	38.7	38.7
2	27.4	33.1	26.4	27.4	27.4
3	79.0	217.0	78.0	79.0	79.0
4	38.9	46.3	37.9	38.9	38.8
5	55.3	54.3	54.4	55.3	55.3
6	18.3	18.7	17.3	18.3	18.3
7	34.3	32.6	33.3	34.2	34.3
8	40.8	39.8	39.7	40.9	40.8
9	50.5	49.7	49.5	50.4	50.5
10	37.2	36.8	36.2	37.2	37.2

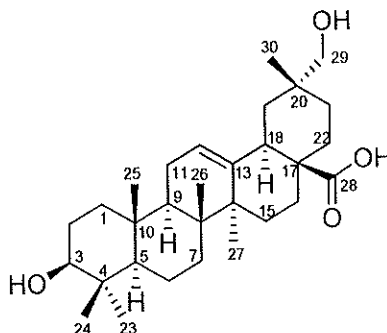
Table 36 (continued)

Position	DW14	DW15	DW16	DW17	DW18
11	20.9	21.4	19.8	20.8	20.7
12	25.2	25.1	24.5	25.2	25.2
13	38.1	38.1	37.4	37.3	38.7
14	42.8	42.7	41.4	42.7	42.6
15	27.5	27.4	28.7	27.0	29.3
16	35.6	35.6	31.2	29.2	28.8
17	43.0	42.7	55.3	47.5	59.3
18	48.3	48.2	48.3	48.8	48.1
19	48.0	47.8	45.9	47.5	47.5
20	151.0	150.5	149.4	150.5	149.7
21	29.9	29.8	29.6	29.8	29.9
22	40.0	39.9	36.0	34.0	33.2
23	28.0	26.6	27.0	28.0	28.0
24	15.4	21.0	14.3	15.4	15.3
25	16.1	15.8	15.1	16.1	16.1
26	16.0	15.4	15.0	16.0	16.0
27	14.6	13.5	13.7	14.8	14.3
28	18.0	17.0	179.6	60.6	206.7
29	109.3	108.1	108.7	109.7	110.2
30	19.3	18.3	18.4	19.1	19.0

Assignments were based on DEPT 90° and DEPT 135° experiments.

Spectra recorded at 75 (¹³C NMR) MHz, CDCl₃.

3.1.19 Compound DW19



Compound **DW19** was isolated as an amorphous powder, m.p. 334-336 °C; $[\alpha]_D^{26} +82.0$ (CHCl_3 ; c 0.10). It exhibited hydroxyl (3400 cm^{-1}) and carbonyl (1695 cm^{-1}) absorptions in the IR spectrum.

The ^{13}C and DEPT spectral data (**Table 37, Figure 75**) of **DW19** showed all 30 carbon signals as six methyl (δ 15.3, 15.4, 17.0, 19.0, 26.0 and 28.0), eleven methylene (δ 18.3, 23.0, 23.4, 27.2, 27.6, 28.8, 31.6, 32.6, 38.4, 40.1, and 74.3), five methine (δ 40.2, 47.6, 55.2, 79.0 and 123.0), seven quaternary carbons (δ 35.7, 37.1, 38.7, 39.3, 41.6, 46.8 and 143.3) and a carboxyl carbon (δ 182.0).

The ^1H NMR spectral data (**Table 37, Figure 74**) of **DW19** showed signals for six tertiary methyl groups at δ_{H} 0.76, 0.77, 0.91, 0.96, 0.98 and 1.14, which correlated in the HMQC experiments with the carbon signals at δ_{C} 15.3, 15.5, 17.0, 19.0, 26.0 and 28.0, respectively. A further feature was the signal at 5.30 (1H, br s) typical of H-12 of oleanene skeleton, which was confirmed by the presence of the signals at δ_{C} 123.0 and 143.3 attributable to C-12 and C-13 in the ^{13}C NMR spectrum (**Table 37, Figures 73**). A signal at δ_{C} 182.0 and the carbon resonances of ring D in the ^{13}C NMR spectrum similar to those of oleanolic acid suggested the occurrence of a free carboxylic group at C-28 position. The presence of one secondary alcoholic function was also deduced from the signal at δ_{H} 3.22 (1H, dd, $J= 10.2, 4.8$ Hz), which correlated in the HMQC spectrum with the carbon resonance at δ_{C} 79.0. This signal is typical of ring A of a 3β -hydroxy substituted oleanolic acid (Maillard *et al.*, 1992). The NMR spectra of **DW19** contained one methyl group less than oleanolic acid and one signal at δ 3.28 (2H, s) in the ^1H NMR spectrum that correlated to δ 74.3 in the

^{13}C NMR spectrum, suggesting that one of the methyl groups of the oleanolic acid was replaced by a hydroxymethyl group. This group was located at C-29 on the basis of HMBC correlations (Table 37, Figure 15) from the methyl at δ 0.96 (CH₃-30) to C-29 (δ 74.3). Compound **DW19** was identified as 3 β ,29-dihydroxyolean-12-en-28-oic acid by comparison of its spectral data with those reported in the literature (Ahmad *et al.*, 1984, $[\alpha]_{\text{D}} +70.4$ (CH₃OH; *c* 0.3); (Table 37).

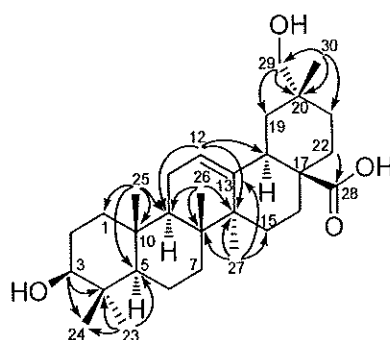


Figure 15 Major HMBC correlations of **DW19**

Table 37 ^1H , ^{13}C NMR, DEPT and HMBC spectral data of compounds **DW19** and ^{13}C NMR of 3 β ,29-dihydroxyolean-12-en-28-oic acid (**R**)

Position	DEPT	$\delta_{\text{C}}/\text{ppm}$		$\delta_{\text{H}}/\text{ppm}$ (mult., <i>J</i> in Hz)	HMBC
		R^b	DW19^c		
1	CH ₂	38.9	38.4	1.13, 1.60 m ^a	
2	CH ₂	28.1	27.2		
3	CH	78.1	79.0	3.22 dd (10.2, 4.8)	23, 24
4	C	39.4	37.1		
5	CH	55.9	55.2	0.71 m ^a	
6	CH ₂	18.8	18.3	1.39, 1.59 m ^a	
7	CH ₂	33.3	32.6	1.30, 1.44 m ^a	
8	C	39.8	39.3		
9	CH	48.2	47.6	1.57 m ^a	

Table 37 (continued)

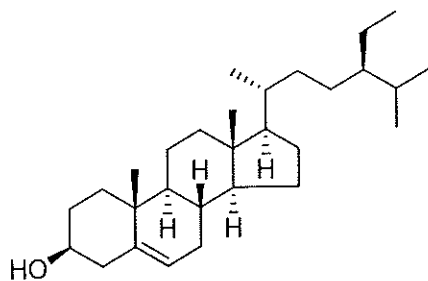
Position	DEPT	δ_C/ppm		δ_H/ppm (mult., J in Hz)	HMBC
		R^b	DW19 ^c		
10	C	37.4	38.7		
11	CH ₂	23.8	23.4	1.65, 1.98 m ^a	
12	CH	122.5	123.0	5.30 br s	9, 14, 18
13	C	144.9	143.3		
14	C	42.2	41.6		
15	CH ₂	28.2	27.6		
16	CH ₂	23.8	23.0	1.63, 1.70 m ^a	
17	C	47.2	46.8		
18	CH	41.4	40.2	1.13 m ^a	
19	CH ₂	41.4	40.1	2.87 dd (13.8, 3.9), 1.70 m	18, 21, 30
20	C	36.6	35.7		
21	CH ₂	29.1	28.8		
22	CH ₂	32.7	31.6	1.62, 1.80 m ^a	28
23	CH ₃	28.8	28.0	0.98 s	3, 4, 5, 24
24	CH ₃	16.5	15.3	0.77 s	3, 4, 5, 23
25	CH ₃	15.5	15.4	0.91 s	1, 5, 9, 10
26	CH ₃	17.4	17.0	0.76 s	8, 9, 14
27	CH ₃	26.2	26.0	1.14 s	8, 13, 14, 15
28	CO	180.2	182.0		
29	CH ₂	73.9	74.3	3.28 s	19, 20, 21, 30
30	CH ₃	19.8	19.0	0.96 s	19, 20, 21, 29

^a Deduced from HMQC experiment.

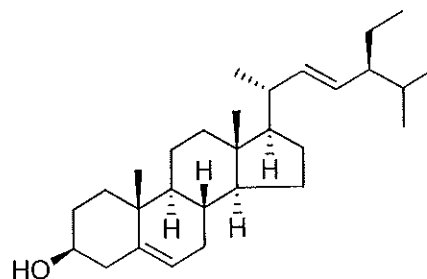
^b Spectrum recorded at 100 (¹³C NMR) MHz, CDCl₃.

^c Spectra recorded at 300 (¹H NMR) and 75 (¹³C NMR) MHz, CDCl₃.

3.1.20 Compounds DW20 and DW21



DW20: β -Sitosterol



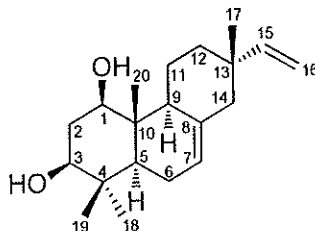
DW21: Stigmasterol

The mixture of **DW20** and **DW21** was isolated as a white solid. Its IR spectrum showed absorption bands at 3425 (hydroxyl) and 1642 cm^{-1} (double bond). The ^1H NMR (**Figure 76**) spectral data contained an oxymethine proton at δ 3.57-3.47 (m), three olefinic protons at δ 5.36-5.34 (d, $J = 5.1$ Hz), 5.16 (dd, $J = 15.1, 8.4$ Hz) and 5.01 (dd, $J = 15.1, 8.4$ Hz). The ^1H NMR data was corresponded to previous reported data of β -sitosterol and stigmasterol. Thus, this mixture was identified as β -sitosterol (**DW20**) and stigmasterol (**DW21**) (Cheenpracha, 2004).

3.2 Structure elucidation of compounds from the roots and twigs of *Premna obtusifolia*

The air-dried roots and twigs of *P. obtusifolia* (4.5 kg) were extracted with hexane and methylene chloride successively at room temperature. The hexane and CH₂Cl₂ extracts were subjected to silica gel vacuum liquid chromatography repeatedly and /or crystallization to give eleven new compounds as two isopimarane diterpenoids (**PO1** and **PO2**), one rosane diterpenoid (**PO3**), four abietane diterpenoids (**PO4**, **PO5**, **PO18** and **PO19**), four icetexane diterpenoids (**PO23-PO26**), together with nineteen known compounds (**PO6**, **PO7**, **PO8-PO15**, **PO16**, **PO17**, **PO20-PO22** and **PO27-PO29**). Their structures were elucidated by spectroscopic analysis, mainly UV, IR, 1D and 2D NMR (¹H, ¹³C, DEPT, COSY, NOESY, HMQC and HMBC) and HREIMS spectroscopic techniques. The known compounds were identified by comparison of their spectroscopic and physical data with those reported in the literature. In addition, the structures of compounds **PO10**, **PO11**, **PO13**, **PO20**, **PO23** and **PO25** were additionally confirmed by X-ray diffraction analysis.

3.2.1 Compound PO1



Compound **PO1** was obtained as a white amorphous solid, m.p. 168–170 °C, $[\alpha]_D^{26} -18.4$ (CHCl_3 ; c 0.59) which exhibited a molecular ion $[\text{M}]^{+\bullet}$ peak at 304.2407 (calcd 304.2402) in the HREIMS corresponding to a molecular formula $\text{C}_{20}\text{H}_{32}\text{O}_2$ with five degrees of unsaturation. The IR spectrum showed strong absorption bands for hydroxyl at 3339 cm^{-1} and double bond at 1637 cm^{-1} .

The combined analysis of the ^{13}C NMR and DEPT spectra of **PO1** (**Table 38**, **Figure 78**) revealed the presence of 20 carbon signals assigned to four methyls, six methylenes, six methines including those of two oxymethines, and two olefinic methine carbons and four quaternary carbons.

The occurrence in the ^1H NMR spectrum of **PO1** (**Table 38**, **Figure 77**) of a vinyl group with three dd resonances at δ_{H} 5.80 ($J = 17.4$ and 10.8 Hz, H-15), δ_{H} 4.92 ($J = 17.4$ and 1.2 Hz, H_b-16) and δ_{H} 4.86 ($J = 10.8$ and 1.2 Hz, H_a-16) and the presence of a broad doublet for an olefinic methine proton at δ_{H} 5.39 ($J = 3.0$ Hz, H-7) and four methyl group singlets suggested a pimarane type skeleton (Wenkert *et al.*, 1972). Two oxymethine carbons resonated at δ_{C} 79.0 (C-1) and 76.1 (C-3). Their positions were deduced from the HMBC correlations (**Table 38**, **Figure 16**) observed between H-1 (δ_{H} 3.55) and C-2 (δ 37.9) and C-10 (δ 41.5) and between H-3 (δ_{H} 3.33) and C-2 (δ 37.9) and C-4 (δ 38.7), respectively. The oxymethine protons H-1 and H-3 both resonated as a doublet of doublets with large and small coupling constants of 12.0 and 4.5 Hz and 12.0 and 4.2 Hz, respectively. The magnitude of these coupling constants suggested the α axial position for both of these protons. These assignments were further supported from NOESY experiments (**Figure 16**). An olefinic methine proton at δ 5.39 (H-7) showed HMBC correlations (**Table 38**) with the carbons at δ

46.7 (C-14), 48.7 (C-5) and 52.4 (C-9) and COSY cross-peak with the methylene protons H₂-6 at δ 1.97-2.04 and 2.03-2.11.

The stereochemistry at C-13 was established by comparison of the ¹³C NMR chemical shifts of C-12, C-13, C-14, C-15, C-16 and C-17 with those of isopimarane diterpenoids (Wenkert *et al.*, 1972; Lago *et al.*, 2000; Passannanti *et al.*, 1984; Rijo *et al.*, 2009): isopimaradiene (Wenkert *et al.*, 1972) establishing an axial position for the Me-17 and an equatorial position for the vinyl group. Compound **PO1** was therefore a new compound which identified as isopimara-7,15-dien-1 β ,3 β -diol (Salae *et al.*, 2012).

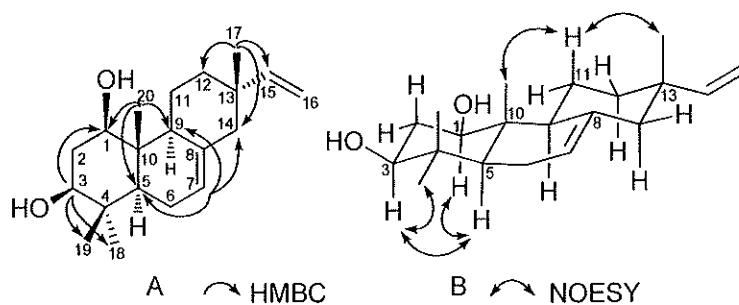


Figure 16 Selected HMBC correlations (A) and NOESY correlations (B) for **PO1**

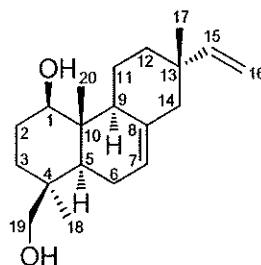
Table 38 ^1H , ^{13}C NMR, DEPT and HMBC spectral data of compound **PO1**

Position	DEPT	$\delta_{\text{C}}/\text{ppm}$	$\delta_{\text{H}}/\text{ppm}$ (mult., J in Hz)	HMBC
1	CH	79.0	3.55 dd (12.0, 4.5)	2, 3, 9, 10, 20
2	CH ₂	37.9	1.71 q (12.0) 1.80–1.90 m ^a	1, 3, 4, 10
3	CH	76.1	3.33 dd (12.0, 4.2)	1, 2, 4, 18, 19
4	C	38.7		
5	CH	48.7	1.02 dd (11.7, 4.8)	4, 7, 9, 10, 18, 19, 20
6	CH ₂	22.6	1.97–2.04 m ^a 2.03–2.11 m ^a	5, 7, 8, 10
7	CH	121.2	5.39 br d (3.0)	5, 6, 9, 14
8	C	136.1		
9	CH	52.4	1.81–1.91 m ^a	
10	C	41.5		
11	CH ₂	23.9	1.37–1.53 m ^a 2.10–2.21 m ^a	8, 9, 12, 14, 17
12	CH ₂	36.5	1.33–1.53 m ^a	9, 11, 13, 14, 17
13	C	36.8		
14	CH ₂	46.7	1.91 d (15.3) 1.98 d (15.3)	9, 12, 13, 17
15	CH	150.3	5.80 dd (17.4, 10.8)	12, 13, 14, 17
16	CH ₂	109.2	4.86 dd (10.8, 1.2) 4.92 dd (17.4, 1.2)	13, 15
17	CH ₃	21.5	0.87 s	12, 13, 14, 15
18	CH ₃	28.3	0.98 s	3, 4, 5, 19
19	CH ₃	15.7	0.88 s	3, 4, 5, 18
20	CH ₃	8.3	0.89 s	1, 5, 9, 10

^a Deduced from HMQC experiment.

^c Spectra recorded at 300 (^1H NMR) and 75 (^{13}C NMR) MHz, CDCl_3 .

3.2.2 Compound PO2



Compound **PO2** was also obtained as a white amorphous solid, m.p. 92–95 °C, $[\alpha]_D^{26} -17.5$ (CHCl_3 ; c 0.71). The HREIMS showed a molecular ion $[M]^{+\bullet}$ peak at m/z 304.2403 (calcd 304.2402) consistent with the molecular formula $\text{C}_{20}\text{H}_{32}\text{O}_2$ and like **PO1** implied five degrees of unsaturation. The IR spectrum proved the existence of hydroxyl (3344 cm^{-1}) and double bond (1637 cm^{-1}).

The ^1H and ^{13}C NMR spectroscopic data of **PO2** (Table 39, Figures 79 and 80) indicated that **PO2** had the same isopimarane diterpene skeleton as **PO1** (Table 38, Figures 77 and 78). Compound **PO2**, however, showed the presence of an AB system (δ_{H} 3.40 and 3.84 (d, $J = 10.8\text{ Hz}$, $\text{H}_2\text{-19}$)) for a hydroxymethyl group attached to the quaternary carbon C-4, instead of the singlet for the C-19 protons at δ_{H} 0.88 in the ^1H NMR spectrum of compound **PO1** and the signal of an oxymethine proton at δ_{H} 3.33 (H-3) in **PO1** was replaced by multiplet signals of methylene protons at δ 1.00–1.16 and 1.84–1.97 in **PO2**. The ^{13}C NMR and DEPT spectra confirmed the presence of oxymethylene at δ_{C} 64.2 and the methylene at δ_{C} 33.1. This finding was further confirmed by the HMBC correlations from $\text{H}_3\text{-18}$ (δ 0.95) to C-19 (δ 64.2) and C-3 (δ 33.1).

The stereochemistry at the stereogenic centers was consistent with that of **PO1** based on the analysis of the NOESY experiment. The location of the primary alcohol at C-19 was found to be β -oriented due to NOESY cross-peak between $\text{H}_3\text{-19}/\text{H}_3\text{-20}$. Compound **PO2** was therefore a new compound which elucidated as isopimara-7,15-dien-1 β ,19-diol (Salae *et al.*, 2012).

Table 39 ^1H , ^{13}C NMR, DEPT and HMBC spectral data of compound **PO2**

Position	DEPT	$\delta_{\text{C}}/\text{ppm}$	$\delta_{\text{H}}/\text{ppm}$ (mult., J in Hz)	HMBC
1	CH	81.4	3.45 dd (11.1, 5.1)	2, 3, 9, 10, 20
2	CH ₂	28.7	1.53–1.67 m ^a	
3	CH ₂	33.1	1.00–1.16 m ^a 1.84–1.97 m ^a	
4	C	37.8		
5	CH	51.3	1.20–1.32 m ^a	4, 6, 7, 10, 18, 20
6	CH ₂	22.6	1.90–2.04 m ^a	
7	CH	121.4	5.37 br s	5, 9
8	C	136.3		
9	CH	52.6	1.87–1.96 m ^a	1, 5, 7, 8, 12
10	C	41.2		
11	CH ₂	23.9	1.37–1.45 m ^a 2.13–2.27 m ^a	
12	CH ₂	36.7	1.35–1.51 m ^a	
13	C	36.5		
14	CH ₂	46.8	1.83–2.04 m ^a	
15	CH	150.4	5.80 dd (17.7, 10.8)	12, 13, 14, 17
16	CH ₂	109.1	4.85 dd (10.8, 1.2) 4.91 dd (17.7, 1.2)	13, 15
17	CH ₃	21.4	0.87 s	12, 13, 14, 15
18	CH ₃	26.6	0.95 s	3, 4, 5, 19
19	CH ₂	64.2	3.40 d (10.8) 3.84 d (10.8)	3, 4, 5, 18
20	CH ₃	9.5	0.87 s	3, 4, 18

^a Deduced from HMQC experiment.

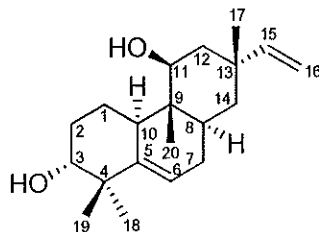
Spectra recorded at 300 (^1H NMR) and 75 (^{13}C NMR) MHz, CDCl_3 .

Table 40 Comparison of ^1H and ^{13}C NMR spectral data of compounds **PO1** and **PO2**

Position	$\delta_{\text{C}}/\text{ppm}$		$\delta_{\text{H}}/\text{ppm}$ (mult., J in Hz)	
	PO1	PO2	PO1	PO2
1	79.0	81.4	3.55 dd (12.0, 4.5)	3.45 dd (11.1, 5.1)
2	37.9	28.7	1.71 q (12.0) 1.80–1.90 m	1.53–1.67 m
3	76.1	33.1	3.33 dd (12.0, 4.2)	1.00–1.16 m 1.84–1.97 m
4	38.7	37.8		
5	48.7	51.3	1.02 dd (11.7, 4.8)	1.20–1.32 m
6	22.6	22.6	1.97–2.04 m 2.03–2.11 m	1.90–2.04 m
7	121.2	121.4	5.39 br d (3.0)	5.37 br s
8	136.1	136.3		
9	52.4	52.6	1.81–1.91 m	1.87–1.96 m
10	41.5	41.2		
11	23.9	23.9	1.37–1.53 m 2.10–2.21 m	1.37–1.45 m 2.13–2.27 m
12	36.5	36.7	1.33–1.53 m	1.35–1.51 m
13	36.8	36.5		
14	46.7	46.8	1.91 d (15.3) 1.98 d (15.3)	1.83–2.04 m
15	150.3	150.4	5.80 dd (17.4, 10.8)	5.80 dd (17.7, 10.8)
16	109.2	109.1	4.86 dd (10.8, 1.2) 4.92 dd (17.4, 1.2)	4.85 dd (10.8, 1.2) 4.91 dd (17.7, 1.2)
17	21.5	21.4	0.87 s	0.87 s
18	28.3	26.6	0.98 s	0.95 s
19	15.7	64.2	0.88 s	3.40 d (10.8), 3.84 d (10.8)
20	8.3	9.5	0.89 s	0.87 s

Spectra recorded at 300 (^1H NMR) and 75 (^{13}C NMR) MHz, CDCl_3 .

3.2.3 Compound PO3



Compound **PO3** was isolated as white amorphous solid, m.p. 78–81 °C, $[\alpha]_D^{26} -13.6$ (CHCl_3 ; c 0.09). Its molecular formula $\text{C}_{20}\text{H}_{32}\text{O}_2$ was established by the HREIMS which exhibited a molecular ion $[\text{M}]^{+\bullet}$ peak at m/z 304.2397 (calcd 304.2402) suggesting five degrees of unsaturation. The IR spectrum showed absorption bands for hydroxyl (3409 cm^{-1}) and double bond (1615 cm^{-1}).

The ^1H NMR spectrum of **PO3** (Table 41, Figure 81) displayed four tertiary methyl groups (δ_{H} 1.12, 0.97, 0.95 and 0.69) and four olefinic protons of a vinyl group (δ_{H} 5.75, 5.02 and 5.00), a trisubstituted double bond (δ_{H} 5.56) and two oxymethine protons (δ_{H} 3.60 and 3.21). The ^{13}C NMR spectrum (Table 41, Figure 82) revealed the presence of 20 carbons including two oxymethine (δ_{C} 77.9 and 77.0), a vinyl group (δ_{C} 146.4 and 112.1), a trisubstituted double bond (δ_{C} 145.8 and 117.9) and four methyl groups (δ_{C} 31.3, 24.6, 21.0 and 6.3). Pimarane, isopimarane and rosane skeletons have four angular methyl groups and can be differentiated by the relative stereochemistry at C-3 and the position of the methyl at C-20. Rosanes arise from migration of the C-10 methyl group of pimaranes to the C-9 position and occurs in both enantiomeric series (Santos *et al.*, 2006).

The placement of a methyl group at C-9 in a rosane skeleton for **PO3** was established from the HMBC correlations (Table 41, Figure 17) of CH_3 -20 at δ 0.69 to the carbons at δ 36.6 (C-8), 40.1 (C-9), 45.9 (C-10) and 77.9 (C-11), and of an oxymethine at δ 3.60 (H-11) to the carbons at δ 6.3 (C-20), 36.6 (C-8), 37.7 (C-13) and 45.9 (C-10). This also established the hydroxyl group at C-11. Furthermore the correlations of H-3 at δ 3.21 to the carbons at δ 21.0 (C-19), 24.6 (C-18), 27.4 (C-1), 42.1 (C-4) and 145.8 (C-5), of an olefinic methine at δ 5.56 (H-6) to the carbons at δ

29.3 (C-7), 36.6 (C-8), 42.1 (C-4) and 45.9 (C-10), of the methyl group at δ 0.97 (CH₃-17) to the carbons at δ 37.7 (C-13), 39.4 (C-14), 43.3 (C-12) and 146.4 (C-15) allowed the placement of another hydroxyl group at C-3 and double bonds at C-5/C-6 and C-15/C-16, respectively.

The stereochemistry of **PO3** was determined by a NOESY experiment (**Figure 17**) in which the key correlations are as follows: CH₃-20/H-1 β and H-12 β ; H-12 β /CH₃-17; CH₃-18/H-10; H-10/H-11; H-3/H-1 β ; H-11/H-10 and H-12 α . These data were in accordance with the β -orientations of CH₃-20, CH₃-17, and H-3 and the α -orientations of H-10, H-11 and CH₃-18. It was notable that in a previously isolated 11 β -hydroxy-rosa-5,15-diene, that Me-17 and Me-20 had a *trans* stereochemical relationship (Geis *et al.*, 2000) whereas this relationship was *cis* in compound **PO3**. Further, the configuration at C-13 in **PO3** is the same as that in compounds **PO1** and **PO2**. Therefore, the structure of **PO3** is represented as 13-*epi*-5,15-rosadien-3 α ,11 β -diol, a new compound (Salae *et al.*, 2012).

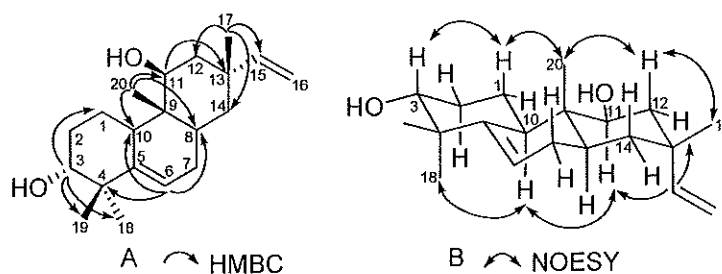


Figure 17 Selected HMBC correlations (A) and NOESY correlations (B) for **PO3**

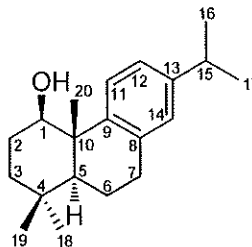
Table 41 ^1H , ^{13}C NMR and HMBC spectral data of compound **PO3**

Position	DEPT	$\delta_{\text{C}}/\text{ppm}$	$\delta_{\text{H}}/\text{ppm}$ (mult., J in Hz)	HMBC
1	CH ₂	27.4	1.10 qd (13.2, 3.6) 2.43 dq (13.2, 3.6)	2, 3, 5, 9, 10
2	CH ₂	30.7	1.49–1.66 m ^a 1.74–1.82 m ^a	1, 3, 4, 10
3	CH	77.0	3.21 dd (11.7, 4.5)	1, 2, 4, 18, 19
4	C	42.1		
5	C	145.8		
6	CH	117.9	5.56 td (4.5, 2.1)	4, 7, 8, 10
7	CH ₂	29.3	1.69–1.78 m ^a	6, 8, 9, 14
8	CH	36.6	1.26–1.37 m ^a	7, 9, 10, 13
9	C	40.1		
10	CH	45.9	2.11 br d (13.2)	
11	CH	77.9	3.60 dd (12.0, 4.2)	8, 9, 10, 12, 13, 20
12	CH ₂	43.3	1.43 t (12.0) 1.66 ddd (12.0, 4.2, 2.1)	9, 11, 13, 14, 15, 17
13	C	37.7		
14	CH ₂	39.4	1.18–1.29 m ^a 1.30–1.41 m ^a	7, 8, 9, 12, 13, 15, 17
15	CH	146.4	5.75 dd (17.4, 11.1)	12, 13, 14, 17
16	CH ₂	112.1	5.00 dd (17.4, 1.2) 5.02 dd (11.1, 1.2)	13, 15, 17
17	CH ₃	31.3	0.97 s	12, 13, 14, 15
18	CH ₃	24.6	1.12 s	3, 4, 5, 19
19	CH ₃	21.0	0.95 s	3, 4, 5, 18
20	CH ₃	6.3	0.69 s	8, 9, 10, 11

^a Deduced from HMQC experiment.

Spectra recorded at 300 (^1H NMR) and 75 (^{13}C NMR) MHz, CDCl_3 .

3.2.4 Compound PO4



Compound **PO4** was isolated as a colorless oil with $[\alpha]_D^{26} -51.4$ (CHCl_3 ; c 0.15). The molecular formula was determined to be $\text{C}_{20}\text{H}_{30}\text{O}$ from a molecular ion $[\text{M}]^{+\bullet}$ peak at m/z 286.2295 (calcd 286.2297) in HREIMS, implying six degrees of unsaturation. The IR spectrum showed absorption bands for hydroxyl (3421 cm^{-1}) and aromatic (1670 cm^{-1}). The presence of an aromatic ring was supported by the UV spectrum at λ_{max} 214 and 258 nm.

The ^{13}C NMR and DEPT spectra of **PO4** (Table 42, Figure 84) indicated 20 carbon signals, of five methyls, four methylenes, six methines and five quaternary, suggesting that **PO4** should contain three rings. The ^{13}C NMR spectra indicated the presence of six aromatic carbons (δ 146.9, 146.0, 135.5, 126.9, 126.7 and 123.9) and one oxymethine (δ 77.6).

Examination of the ^1H NMR spectrum of **PO4** (Table 42, Figure 83) and ^1H - ^1H COSY spectrum indicated the presence of an isopropyl group as evidenced from two methyl doublets at δ_{H} 1.21 (d, $J=7.2$ Hz, H_3 -16 and H_3 -17) which were coupled to a methine proton at δ 2.80 (sept, $J=7.2$ Hz, H-15), two *ortho*-coupled aromatic protons at δ 8.07 (d, $J=8.4$ Hz, H-11) and δ 6.97 (br d, $J=8.4$ Hz, H-12), and an aromatic singlet signal at δ 6.87 (s, H-14). The spectrum also showed two geminal methyl protons at δ_{H} 0.89 (s, H_3 -18) and δ_{H} 0.92 (s, H_3 -19) and tertiary methyl protons at δ_{H} 1.21 (s, H_3 -20). In addition, an oxymethine proton was displayed at δ 3.85 (dd, $J=9.9$ and 6.0 Hz, H-1). This combination of signals suggested an abietane skeleton comparable to that of abietatrien-3 β -ol (Urones *et al.*, 1988) except for the position of an oxymethine in ring A of **PO4**. The hydroxyl group was suggested to be at C-1 from the downfield shift of C-10 (δ 43.6 in **PO4** vs. δ 37.4 in

abietatrien-3 β -ol), and this was confirmed by the HMBC correlations (Table 42, Figure 18) of the methyl protons CH₃-20 at δ 1.21 to C-1 (δ 77.6).

The relative stereochemistry of an oxymethine H-1 was assigned as α -axial from a doublet of doublets signal with $J= 9.9$ and 6.0 Hz and from the NOESY experiment (Figure 18) which showed cross-peaks between H-5, H-1, Me-18 and H-7 α . Compound 4 was a new compound and assigned as abietatrien-1 β -ol (Salae *et al.*, 2012).

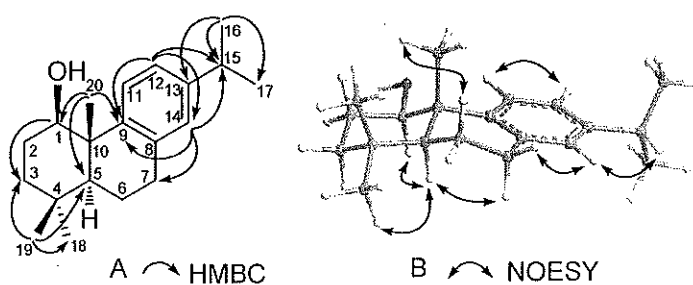


Figure 18 Selected HMBC correlations (A) and NOESY correlations (B) for PO4

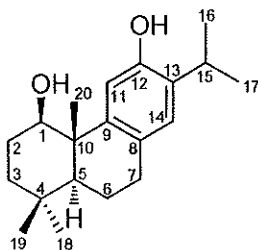
Table 42 ^1H , ^{13}C NMR, DEPT and HMBC spectral data of compound PO4

Position	DEPT	$\delta_{\text{C}}/\text{ppm}$	$\delta_{\text{H}}/\text{ppm}$ (mult., J in Hz)	HMBC
1	CH	77.6	3.85 dd (9.9, 6.0)	2, 3, 9, 10, 20
2	CH ₂	30.2	1.65–1.73 m ^a 1.74–1.84 m ^a	1, 3, 10
3	CH ₂	39.8	1.30 ddd (13.2, 12.3, 5.7) 1.45 td (13.2, 3.6)	1, 2, 4, 5, 18, 19
4	C	33.4		
5	CH	49.6	1.26 dd (11.4, 4.5)	1, 3, 7, 10, 18, 19, 20
6	CH ₂	19.2	1.78–1.85 m ^a 1.87–1.95 m ^a	4, 5, 7, 8, 10
7	CH ₂	29.8	2.70–2.85 m ^a 2.92 ddd (17.1, 7.5, 3.6)	5, 6, 8, 9, 14
8	C	135.5		
9	C	146.9		
10	C	43.6		
11	CH	126.9	8.07 d (8.4)	8, 10, 12, 13, 20
12	CH	123.9	6.97 br d (8.4)	8, 9, 14, 15
13	C	146.0		
14	CH	126.7	6.87 s	7, 9, 11, 12, 15
15	CH	33.5	2.80 sept (7.2)	12, 13, 14, 16, 17
16	CH ₃	24.1	1.21 d (7.2)	13, 15, 17
17	CH ₃	24.1	1.21 d (7.2)	13, 15, 16
18	CH ₃	32.8	0.89 s	3, 4, 5, 19
19	CH ₃	21.3	0.92 s	3, 4, 5, 18
20	CH ₃	17.4	1.21 s	1, 5, 9, 10

^a Deduced from HMQC experiment.

Spectra recorded at 300 (^1H NMR) and 75 (^{13}C NMR) MHz, CDCl_3 .

3.2.5 Compound PO5



Compound **PO5** was obtained as a colorless oil with $[\alpha]_D^{26} -15.7$ (CHCl_3 ; c 0.27). Its molecular formula $\text{C}_{20}\text{H}_{30}\text{O}_2$ was determined from a molecular ion $[\text{M}]^{+\bullet}$ peak at m/z 302.2254 (calcd 302.2246) in the HREIMS, indicating an increment of one oxygen atom from **PO4**. The IR spectrum indicated the existence of hydroxyl (3351 cm^{-1}) and aromatic (1507 cm^{-1}) groups.

The ^1H and ^{13}C NMR spectral data of **PO5** (Tables 43, Figure 85 and 86) were similar to those of **PO4** (Tables 42 and 44, Figure 83 and 84), except for differences in the substitution pattern of the phenyl ring in **PO5**, in which two *para* protons were shown at δ 7.72 (s, H-11) and δ 6.81 (s, H-14) instead of *ortho*-coupled protons at δ 8.07 and 6.97 and a singlet at δ 6.87 as in **PO4**. The ^{13}C NMR and DEPT experiments also proved the presence of an additional oxyquaternary carbon at δ_{C} 151.0 in **PO5**, which was associated with the absence of the ^1H NMR signal of H-12 at δ 6.97 (br d) as in **PO4**. This finding was further supported by HMBC correlations (Tables 43) from H-14 (δ 6.81), and H-15 (δ 3.20) to C-12 (δ 151.0). The foregoing spectral data and literature survey provided evidence of **PO5** as a ferruginol derivative (Harrison *et al.*, 1987).

The relative configuration of H-1 in **PO5** was suggested to be α -oriented as in **PO4**. Thus, compound **PO5** was a new compound and identified as 1 β -hydroxyferruginol (abietatrien-1 β ,12-diol) (Salae *et al.*, 2012).

Table 43 ^1H , ^{13}C NMR, DEPT and HMBC spectral data of compound **PO5**

Position	DEPT	$\delta_{\text{C}}/\text{ppm}$	$\delta_{\text{H}}/\text{ppm}$ (mult., J in Hz)	HMBC
1	CH	78.2	3.80 dd (10.4, 4.8)	9, 10, 20
2	CH ₂	30.1	1.65–1.85 m ^a	1, 3, 10
3	CH ₂	39.7	1.35 dd (13.2, 3.6) 1.48 td (13.2, 3.6)	1, 2, 4, 5, 18, 19
4	C	33.3		
5	CH	49.8	1.26 dd (12.4, 3.2)	1, 4, 7, 10, 18, 19, 20
6	CH ₂	19.2	1.70–1.90 m ^a	4, 5, 7, 8, 10
7	CH ₂	29.6	2.65–2.76 m ^a 2.84 ddd (16.4, 7.2, 2.4)	5, 6, 8, 9
8	C	127.3		
9	C	147.0		
10	C	43.4		
11	CH	113.7	7.72 s	8, 9, 10, 12, 13
12	C	151.0		
13	C	132.4		
14	CH	126.3	6.81 s	7, 9, 11, 12, 15
15	CH	26.6	3.20 sept (6.8)	12, 13, 14, 16, 17
16	CH ₃	22.6	1.22 d (6.8)	13, 15, 17
17	CH ₃	22.7	1.21 d (6.8)	13, 15, 16
18	CH ₃	32.7	0.91 s	3, 4, 5, 19
19	CH ₃	21.3	0.91 s	3, 4, 5, 18
20	CH ₃	17.8	1.21 s	1, 5, 9, 10

^a Deduced from HMQC experiment.

Spectra recorded at 400 (^1H NMR) and 100 (^{13}C NMR) MHz, CDCl_3 .

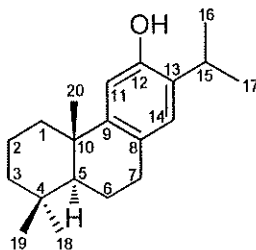
Table 44 Comparison of ^1H and ^{13}C NMR spectral data of compounds **PO4** and **PO5**

Position	$\delta_{\text{C}}/\text{ppm}$		$\delta_{\text{H}}/\text{ppm}$ (mult., J in Hz)	
	PO4 ^a	PO5 ^b	PO4 ^a	PO5 ^b
1	77.6	78.2	3.85 dd (9.9, 6.0)	3.80 dd (10.4, 4.8)
2	30.2	30.1	1.65–1.73 m 1.74–1.84 m	1.65–1.85 m
3	39.8	39.7	1.30 ddd (13.2, 12.3, 5.7) 1.45 td (13.2, 3.6)	1.35 dd (13.2, 3.6) 1.48 td (13.2, 3.6)
4	33.4	33.3		
5	49.6	49.8	1.26 dd (11.4, 4.5)	1.26 dd (12.4, 3.2)
6	19.2	19.2	1.78–1.85 m 1.87–1.95 m	1.70–1.90 m
7	29.8	29.6	2.70–2.85 m 2.92 ddd (17.1, 7.5, 3.6)	2.65–2.76 m 2.84 ddd (16.4, 7.2, 2.4)
8	135.5	127.3		
9	146.9	147.0		
10	43.6	43.4		
11	126.9	113.7	8.07 d (8.4)	7.72 s
12	123.9	151.0	6.97 br d (8.4)	
13	146.0	132.4		
14	126.7	126.3	6.87 s	6.81 s
15	33.5	26.6	2.80 sept (7.2)	3.20 sept (6.8)
16	24.1	22.6	1.21 d (7.2)	1.22 d (6.8)
17	24.1	22.7	1.21 d (7.2)	1.21 d (6.8)
18	32.8	32.7	0.89 s	0.91 s
19	21.3	21.3	0.92 s	0.91 s
20	17.4	17.8	1.21 s	1.21 s

^a Spectra recorded at 300 (^1H NMR) and 75 (^{13}C NMR) MHz, CDCl_3 .

^b Spectra recorded at 400 (^1H NMR) and 100 (^{13}C NMR) MHz, CDCl_3 .

3.2.6 Compound PO6



Compound **PO6** was isolated as a white solid, m.p. 56-58 °C, $[\alpha]_D^{26} +42.7$ (CHCl_3 ; c 0.70). The UV and IR spectrum showed absorption bands similar to those of **PO5**.

The ^1H and ^{13}C NMR spectral data of **PO6** (Table 45, Figures 87 and 88) were similar to those of **PO5** (Table 43, Figure 85 and 86). The difference in the spectrum of **PO6** was shown as the disappearance of an oxymethine proton at δ 3.80 (H-1) in the ^1H NMR of **PO5** and the ^{13}C NMR spectrum of **PO6** displayed a signal of methylene carbon at δ 38.8 instead of an oxymethine carbon at δ 78.2, thus suggesting a methylene group at C-1. This finding was further confirmed by the HMBC correlations (Table 45, Figure 19) from H_3 -20 (δ 1.15) to C-1 (δ 38.8). By comparison of the ^1H and ^{13}C NMR spectral data with the previously reported data [Tezuka et al., 1998; Lee *et al.*, 2005; Ryu *et al.*, 2010, $[\alpha]_D^{24} +51.7$ (MeOH; c 0.50)] (Table 46), therefore compound **PO6** was identified as ferruginol.

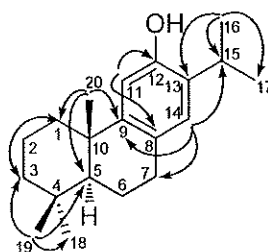


Figure 19 Selected HMBC correlations for **PO6**

Table 45 ^1H , ^{13}C NMR, DEPT and HMBC spectral data of compound **PO6** and ^{13}C NMR of ferruginol (**R**)

Position	DEPT	$\delta_{\text{C}}/\text{ppm}$		$\delta_{\text{H}}/\text{ppm}$ (mult., <i>J</i> in Hz)	HMBC
		R ^b	PO6 ^c		
1	CH ₂	38.8	38.8	1.37 dd (12.6, 3.6) 2.23 br d (12.6)	2, 3, 5, 10, 20
2	CH ₂	19.2	19.2	1.30–1.48 m ^a 1.50–1.90 m ^a	1, 3, 4, 10
3	CH ₂	41.7	41.7	1.20 m, 1.46 m ^a	1, 2, 4, 5, 18, 19
4	C	33.4	33.4		
5	CH	50.3	50.3	1.29 dd (12.3, 2.4)	1, 3, 7, 9, 19, 20
6	CH ₂	19.3	19.3	1.30–1.48 m ^a 1.50–1.90 m ^a	4, 5, 7, 8, 10
7	CH ₂	29.7	29.7	2.70–2.90 m ^a	5, 6, 8, 9, 14
8	C	127.3	127.3		
9	C	146.8	146.8		
10	C	37.5	37.5		
11	CH	110.9	111.0	6.62 s	8, 10, 12
12	C	150.6	150.6		
13	C	131.3	131.4		
14	CH	126.6	126.6	6.83 s	7, 8, 9, 12, 13, 15
15	CH	26.8	26.8	3.11 sept (6.9)	12, 13, 14, 16, 17
16	CH ₃	22.7	22.7	1.23 d (6.9)	13, 15, 17
17	CH ₃	22.5	22.6	1.21 d (6.9)	13, 15, 16
18	CH ₃	33.3	33.3	0.93 s	3, 4, 5, 19
19	CH ₃	21.6	21.6	0.90 s	3, 4, 5, 18
20	CH ₃	24.7	24.8	1.15 s	1, 5, 9, 10
12-OH				4.73 s	

^a Deduced from HMQC experiment, ^b Spectrum recorded at 125 (^{13}C NMR) MHz, CDCl_3 . ^c Spectra recorded at 300 (^1H NMR) and 75 (^{13}C NMR) MHz, CDCl_3 .

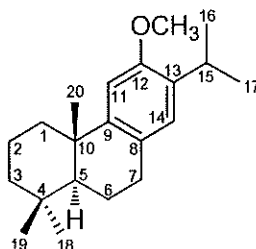
Table 46 Comparison of ^1H NMR spectral data of compounds **PO5**, **PO6** and ferruginol

Position	δ_{H} /ppm (mult., J in Hz)		
	PO5 ^a	PO6 ^a	ferruginol ^b
1	3.80 dd (10.4, 4.8)	1.37 dd (12.6, 3.6)	1.37 td (13.5, 3.5)
		2.23 br d (12.6)	2.15 dtd (13.5, 3.5, 1.5)
2	1.65–1.85 m	1.30–1.48 m	1.58 dq (13.5, 3.5)
		1.50–1.90 m	1.72 qt (13.5, 3.5)
3	1.35 dd (13.2, 3.6) 1.48 td (13.2, 3.6)	1.20 m	1.20 td (13.5, 3.5)
		1.46 m	1.46 dtd (13.5, 3.5, 1.5)
5	1.26 dd (12.4, 3.2)	1.29 dd (12.3, 2.4)	1.31 dd (12.5, 2.0)
6	1.70–1.90 m	1.30–1.48 m	1.66 dddd (13.5, 12.7, 11.0, 7.0)
		1.50–1.90 m	1.85 ddt (13.5, 7.5, 2.0)
		2.70–2.70 m	2.76 ddd (16.5, 11.0, 7.5)
7	2.65–2.76 m 2.84 ddd (16.4, 7.2, 2.4)	2.70–2.70 m	2.85 ddd (16.7, 7.0, 2.0)
		6.62 s	6.61 s
11	7.72 s	6.62 s	6.61 s
14	6.81 s	6.83 s	6.81 s
15	3.20 sept (6.8)	3.11 sept (6.9)	3.11 sept (7.0)
16	1.22 d (6.8)	1.23 d (6.9)	1.22 d (7.0)
17	1.21 d (6.8)	1.21 d (6.9)	1.24 d (7.0)
18	0.91 s	0.93 s	0.93 s
19	0.91 s	0.90 s	0.91 s
20	1.21 s	1.15 s	1.16 s
12-OH		4.73 br s	4.60 br s

^a Spectra recorded at 300 (^1H NMR) MHz, CDCl_3 .

^b Spectrum recorded at 500 (^1H NMR) MHz, CDCl_3 .

3.2.7 Compound PO7



Compound **PO7** was isolated as a colorless oil with $[\alpha]_{\text{D}}^{26} +15.0$ (CHCl_3 ; c 0.10). The UV and IR spectrum showed absorption bands similar to those of **PO6**.

The ^1H and ^{13}C NMR spectral data of **PO7** (Table 47, Figures 89 and 90) were related to those of **PO6** (Table 45, Figures 87 and 88). The difference in the spectrum of **PO7** was shown as an additional singlet methyl proton signal at δ 3.80 and a methyl carbon signal at δ 55.6 replaced a hydroxyl group at δ 4.73 in **PO6**, thus suggesting a methoxyl proton at C-12. The location of the methoxyl group was confirmed by HMBC experiment (Table 47) in which the methoxyl protons at δ 3.80 showed correlations to C-12 (δ 155.0). By comparison of the ^1H and ^{13}C NMR spectral data with the previously reported data (kato *et al.*, 2007) (Table 48), therefore compound **PO7** was identified as *O*-methyl ferruginol.

Table 47 ^1H , ^{13}C NMR, DEPT and HMBC spectral data of compound **PO7** and ^{13}C NMR of *O*-methyl ferruginol (**R**)

Position	DEPT	$\delta_{\text{C}}/\text{ppm}$		$\delta_{\text{H}}/\text{ppm}$ (mult., <i>J</i> in Hz)		HMBC
		R^b		PO7^c		
1	CH ₂	38.9	38.9	1.43 m ^a		2, 3, 5, 10, 20
				2.24 br d (12.3)		
2	CH ₂	19.2	19.2	1.60–1.90 m ^a		
3	CH ₂	41.7	41.7	1.22 m ^a		1, 2, 4, 5, 18, 19
				1.48 m ^a		
4	C	33.5	33.5			
5	CH	50.5	50.5	1.33 dd (12.3, 2.4)		1, 3, 7, 9, 19, 20
6	CH ₂	19.4	19.4	1.60–1.90 m ^a		
7	CH ₂	29.8	29.8	2.71–2.90 m ^a		5, 6, 8, 9, 14
8	C	126.9	126.9			
9	C	148.1	148.1			
10	C	37.9	37.9			
11	CH	106.6	106.6	6.72 s		8, 12, 13
12	C	155.0	155.0			
13	C	134.3	134.3			
14	CH	126.4	126.4	6.83 s		7, 9, 12, 15
15	CH	26.5	26.5	3.21 sept (6.9)		12, 13, 14, 16, 17
16	CH ₃	22.7	22.7	1.19 d (6.9)		13, 15, 17
17	CH ₃	22.9	22.9	1.17 d (6.9)		13, 15, 16
18	CH ₃	33.3	33.3	0.94 s		3, 4, 5, 19
19	CH ₃	21.6	21.6	0.92 s		3, 4, 5, 18
20	CH ₃	24.8	24.8	1.20 s		1, 5, 9, 10
12-OCH ₃		55.6	55.6	3.80 s		12

^a Deduced from HMQC experiment.

^b Spectrum recorded at 100 (^{13}C NMR) MHz, CDCl_3 .

^c Spectra recorded at 300 (^1H) and 75 (^{13}C NMR) MHz, CDCl_3 .

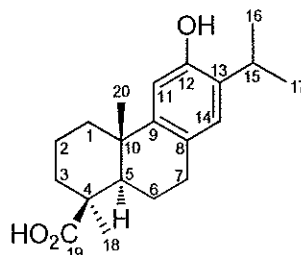
Table 48 Comparison of ^1H NMR spectral data of compounds **PO6**, **PO7** and *O*-methyl ferruginol

Position	δ_{H} /ppm (mult., <i>J</i> in Hz)		
	PO6 ^a	PO7 ^a	<i>O</i> -methyl ferruginol ^b
1	1.37 dd (12.6, 3.6)	1.43 m	1.32–1.51 m
	2.23 br d (12.6)	2.24 br d (12.3)	2.23–2.27 m
2	1.30–1.48 m	1.60–1.90 m	1.58–1.78 m
	1.50–1.90 m		
3	1.20 m, 1.46 m	1.22 m	1.15–1.25 m
		1.48 m	1.32–1.51 m
5	1.29 dd (12.3, 2.4)	1.33 dd (12.3, 2.4)	1.32–1.51 m
6	1.30–1.48 m	1.60–1.90 m	1.83–1.89
	1.50–1.90 m		
7	2.70–2.79 m	2.71–2.90 m	2.73–2.89 m
	2.80–2.90 m		
11	6.62 s	6.72 s	6.48 s
14	6.83 s	6.83 s	6.72 s
15	3.11 sept (6.9)	3.21 sept (6.9)	3.21 sept (7.0)
16	1.23 d (6.9)	1.19 d (6.9)	1.19 d (7.0)
17	1.21 d (6.9)	1.17 d (6.9)	1.19 d (7.0)
18	0.93 s	0.94 s	0.94 s
19	0.90 s	0.92 s	0.92 s
20	1.15 s	1.20 s	1.17 s
12-OH	4.73 s		
12-OCH ₃		3.80 s	3.79 s

^a Spectra recorded at 300 (^1H NMR) MHz, CDCl_3 .

^b Spectrum recorded at 400 (^1H NMR) MHz, CDCl_3 .

3.2.8 Compound PO8



Compound **PO8** was isolated as a white amorphous solid, mp. 251-253 °C, $[\alpha]_D^{26} +128$ (CHCl₃; *c* 0.07). It exhibited hydroxyl (3360 cm⁻¹), carbonyl (1694 cm⁻¹) and double bond (1619 cm⁻¹) absorptions in the IR spectrum. The UV spectrum showed absorption bands similar to those of **PO6**.

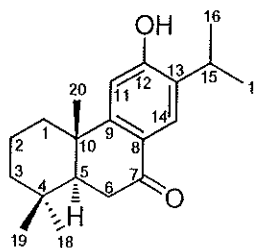
The ¹H and ¹³C NMR spectral data (Table 49, Figures 91 and 92) of **PO8** were comparable to those of **PO6** (Table 45, Figures 87 and 88). The difference in the spectrum of **PO8** was shown as disappearance of a methyl signal at δ_H 0.90 (H₃-19, s, δ_C 21.6) in **PO6** and the appearance of a carboxyl signal at δ_C 182.0 (C-19) in **PO8**. The location of the carboxyl group was confirmed by HMBC experiment (Table 49) in which the methyl proton signal at δ 1.31 (1H, s, H-18) showed correlations with C-19 (δ 182.0), C-3 (δ 37.4), C-4 (δ 43.7) and C-5 (δ 52.7). Thus on the basis of its spectroscopic data and comparison with the previous report (Campello *et al.*, 1975; Cambie *et al.*, 1983), compound **PO8** was identified as lambertic acid.

Table 49 ^1H , ^{13}C NMR, DEPT and HMBC spectral data of compound **PO8**

Position	DEPT	δ_{C} /ppm	δ_{H} /ppm (multiplicity, J /Hz)	HMBC
1	CH ₂	39.3	1.40 dd (13.2, 3.9) 2.17 m	3, 5, 10, 20
2	CH ₂	19.9	1.61 m 2.01 m	1, 3
3	CH ₂	37.4	1.10 m 2.26 m	1, 4, 5
4	C	43.7		
5	CH	52.7	1.53 dd (12.3 1.5)	4, 6, 7, 10, 19, 20
6	CH ₂	21.1		
7	CH ₂	31.2	2.70 m 2.82 m	5, 6, 8, 9, 14
8	C	127.2		
9	C	146.4		
10	C	38.2		
11	CH	111.8	6.63 s	8, 10, 12
12	C	150.9		
13	C	131.9		
14	CH	126.5	6.82 s	7, 9, 12, 15
15	CH	26.7	3.12 sept (6.9)	12, 13, 14, 16, 17
16	CH ₃	22.5	1.23 d (6.9)	13, 15, 17
17	CH ₃	22.6	1.22 d (6.9)	13, 15, 16
18	CH ₃	28.7	1.31 s	3, 4, 5, 19
19	CO ₂ H	182.0		
20	CH ₃	23.1	1.10 s	1, 5, 9, 10
12-OH			2.20–2.80 br	

Spectra recorded at 300 (^1H NMR) and 75 (^{13}C NMR) MHz, CDCl₃.

3.2.9 Compound PO9



Compound **PO9** was obtained as a white amorphous solid, m.p. 292-294 °C, $[\alpha]_D^{26} +17.7$ (CHCl_3 ; c 0.11). Its UV and IR spectra showed absorptions for hydroxyl, a conjugated carbonyl, and a conjugated aromatic functional groups.

The ^1H and ^{13}C NMR spectral data of **PO9** (Table 50, Figures 93 and 94) were similar to those that of **PO6** (Table 45, Figures 87 and 88). The presence of an isopropyl group followed from two doublets of methyl proton signals at δ 1.27 and 1.24 (each 3H, H₃-16 and H₃-17, respectively) and a septet methine proton signal at δ 3.15 (H-15). Three singlet methyl proton signals were at δ 0.92 (H-18), 0.99 (H-19), and 1.22 (H-20). Other signals were a separate methylene doublet of doublets proton signals at δ 2.58 and 2.69 (H-6), two singlet aromatic methine proton signals at δ 6.70 (H-11) and 7.91 (H-14). When compared to compound **PO6**, an additional carbonyl group was observed at δ 198.5 in the ^{13}C NMR spectrum of **PO9** and the only downfield aromatic methine proton signal was shown at δ 7.91 (H-14), which suggested the presence of a keto group instead of a methylene group at C-7, which was confirmed by the HMBC experiment (Table 50) from H-14 (δ 7.91) and H-5 (δ 1.85) to C-7 (δ 198.5). By comparison of the ^1H and ^{13}C NMR spectral data with the previously reported data [Ara *et al.*, 1988; Benjamin, 2003; Kolak *et al.*, 2005; Marcos *et al.*, 2010, $[\alpha]_D^{24} +51.7$ (CDCl_3 ; c 0.1)] (Table 51), compound **PO9** was identified as sugiol.

Table 50 ^1H , ^{13}C NMR, DEPT and HMBC spectral data of compound **PO9** and ^{13}C NMR of sugiol (**R**)

Position	DEPT	$\delta_{\text{C}}/\text{ppm}$		$\delta_{\text{H}}/\text{ppm}$ (mult., J in Hz)	HMBC
		R^b	PO9^c		
1	CH ₂	37.3	37.9	1.50 m ^a 2.20 br d (12.6)	2, 3, 5, 10
2	CH ₂	18.4	18.9	1.68 m ^a 1.77 tt (13.5, 3.3)	1, 3, 4, 10
3	CH ₂	40.9	41.4	1.26 m ^a 1.53 dd (12.6, 3.3)	1, 4
4	C	32.7	33.3		
5	CH	49.2	49.5	1.85 dd (12.9, 4.5)	1, 4, 7, 9, 10, 19, 20
6	CH ₂	35.4	36.1	2.58 dd (18.0, 12.9) 2.69 dd (18.0, 4.5)	4, 5, 7, 8, 10
7	CO	199.2	198.5		
8	C	122.4	124.7		
9	C	156.3	156.4		
10	C	37.4	37.9		
11	CH	109.0	110.1	6.70 s	8, 9, 10, 12, 13
12	C	160.3	158.1		
13	C	133.0	132.6		
14	CH	125.6	126.6	7.91 s	7, 9, 12, 15
15	CH	26.1	26.8	3.15 sept (6.9)	12, 13, 14, 16, 17
16	CH ₃	21.8	22.3	1.27 d (6.9)	13, 15, 17
17	CH ₃	21.6	22.4	1.24 d (6.9)	13, 15, 16
18	CH ₃	31.9	32.6	0.92 s	3, 4, 5, 19
19	CH ₃	20.7	21.4	0.99 s	3, 4, 5, 18
20	CH ₃	22.5	23.2	1.22 s	1, 5, 9, 10
12-OH				5.60 br s	

^a Deduced from HMQC experiment, ^b Spectrum recorded at 125 (^{13}C NMR) MHz, CDCl_3 . ^c Spectra recorded at 300 (^1H NMR) and 75 (^{13}C NMR) MHz, CDCl_3 .

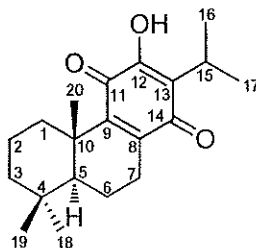
Table 51 Comparison of ^1H NMR spectral data of compounds **PO6**, **PO9** and sugiol

Position	δ_{H} /ppm (mult., J in Hz)		
	PO6 ^a	PO9 ^a	sugiol ^b
1	1.37 dd (12.6, 3.6)	1.50 m	1.56 m
	2.23 br d (12.6)	2.20 br d (12.6)	2.25 br dt (13.0, 2.0)
2	1.30–1.48 m	1.68 m	
	1.50–1.90 m	1.77 tt (13.5, 3.3)	
3	1.20 m, 1.46 m	1.26 m	
		1.53 dd (12.6, 3.3)	
5	1.29 dd (12.3, 2.4)	1.85 dd (12.9, 4.5)	
6	1.30–1.48 m	2.58 dd (18.0, 12.9)	2.52 dd (17.5, 13.5)
	1.50–1.90 m	2.69 dd (18.0, 4.5)	2.64 dd (17.5, 3.5)
7	2.70–2.79 m		
	2.80–2.90 m		
11	6.62 s	6.70 s	6.70 s
14	6.83 s	7.91 s	7.87 s
15	3.11 sept (6.9)	3.15 sept (6.9)	3.20 sept (7.0)
16	1.23 d (6.9)	1.27 d (6.9)	1.22 d (7.0)
17	1.21 d (6.9)	1.24 d (6.9)	1.22 d (7.0)
18	0.93 s	0.92 s	0.95 s
19	0.90 s	0.99 s	0.95 s
20	1.15 s	1.22 s	1.22 s
12-OH	4.73 s	5.60 br s	

^a Spectra recorded at 300 (^1H NMR) MHz, CDCl_3 .

^b Spectrum recorded at 400 (^1H NMR) MHz, CDCl_3 .

3.2.10 Compound PO10



Compound **PO10** was obtained as a white amorphous solid, m.p. 179–181 °C, $[\alpha]_{\text{D}}^{26} +115.8$ (CHCl_3 ; c 2.87). Its IR spectrum showed hydroxyl (3360 cm^{-1}) and carbonyl (1641 and 1631 cm^{-1}) and the UV absorptions at λ_{max} 277 and 407 nm suggested the presence of a *para*-benzoquinone element.

The ^{13}C NMR spectrum and DEPT experiment of **PO10** (Table 52, Figures 95 and 96) indicated that **PO10** has a total of 20 carbons, which is consistent with a diterpene skeleton. Two new signals of carbonyl carbons appeared at δ 183.4 (C-11) and 187.5 (C-14). In addition, in the ^1H NMR spectrum, two singlet signals for the olefinic methine protons at δ 6.62 and 6.83 of **PO6** were disappeared and the downfield protons H_2 -7 (δ 2.33, ddd, $J=20.7, 11.4, 7.2$ Hz and 2.71 ddd, $J=20.7, 5.2, 1.2$) were shown in **PO10** indicating the existence of a *para*-benzoquinone group. This finding was further confirmed by the HMBC correlations (Table 52, Figure 20) from H_2 -7 (δ 2.33 and 2.71) to C-14 (δ 187.5) and 12-OH (δ 7.23 to C-11 (δ 183.4). Thus on the basis of its spectroscopic data and comparison of the ^1H and ^{13}C NMR spectral data with the previous report [Tezuka *et al.*, 1998; Benjamin Rodrigues 2003; kolak *et al.*, 2005, $[\alpha]_{\text{D}}^{26} +129.6$ (CHCl_3 ; c 0.1)] (Table 53), compound **PO10** was assigned as royleanone. X-ray crystallographic analysis of **PO10** (Hoong-Kun *et al.*, 2011) was also carried out and gave ORTEP drawing as shown in Figure 21.

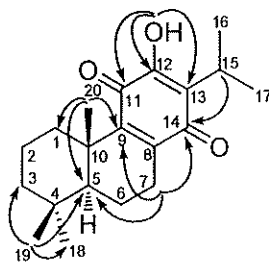


Figure 20 Selected HMBC correlations of **PO10**

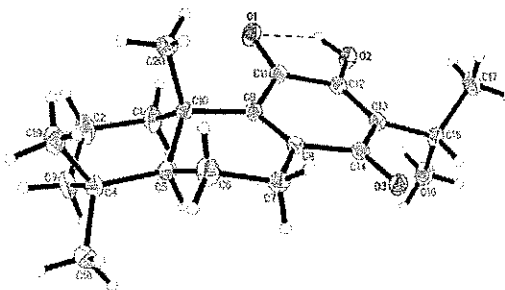


Figure 21 *ORTEP* drawing of **PO10**

Table 52 ^1H , ^{13}C NMR, DEPT and HMBC spectral data of compound **PO10** and ^{13}C NMR of royleanone (**R**)

Position	DEPT	$\delta_{\text{C}}/\text{ppm}$		$\delta_{\text{H}}/\text{ppm}$ (mult., J in Hz)	HMBC
		R ^b	PO10 ^c		
1	CH ₂	36.2	36.3	1.15 m ^a , 2.75 m ^a	2, 3, 10
2	CH ₂	18.9	18.9	1.51 m ^a 1.72 tt (13.8, 3.3)	1, 3, 4, 10
3	CH ₂	41.3	41.3	1.21 m ^a , 1.46 m ^a	1, 2, 4, 18, 19
4	C	33.4	33.5		
5	CH	51.7	51.7	1.10 m ^a	4, 7, 9, 10, 18, 20
6	CH ₂	17.4	17.4	1.38 m ^a 1.86 dd (13.2, 7.2)	4, 5, 7, 8, 10
7	CH ₂	26.7	26.7	2.33 ddd (20.7, 11.4, 7.2) 2.71 ddd (20.7, 5.2, 1.2)	5, 6, 8, 9, 14
8	C	146.0	146.0		
9	C	146.5	146.5		
10	C	38.4	38.4		
11	CO	183.4	183.4		
12	C	150.5	150.5		
13	C	123.7	123.7		
14	CO	187.5	187.5		
15	CH	24.1	24.1	3.15 sept (6.9)	12, 13, 14, 16, 17
16	CH ₃	19.9	19.8	1.21 d (6.9)	13, 15, 17
17	CH ₃	20.0	19.9	1.20 d (6.9)	13, 15, 16
18	CH ₃	33.5	33.4	0.93 s	3, 4, 5, 19
19	CH ₃	21.8	21.7	0.90 s	3, 4, 5, 18
20	CH ₃	20.0	20.1	1.25 s	1, 5, 9, 10
12-OH				7.23 s	11, 12, 13

^a Deduced from HMQC experiment.

^b Spectrum recorded at 100 (^{13}C NMR) MHz, CDCl_3 .

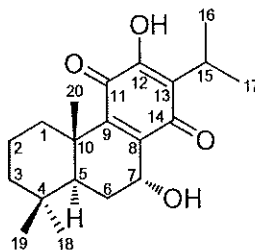
^c Spectra recorded at 300 (^1H NMR) and 75 (^{13}C NMR) MHz, CDCl_3 .

Table 53 Comparison of ^1H NMR spectral data of compounds **PO6**, **PO10** and royleanone

Position	δ_{H} /ppm (mult., <i>J</i> in Hz)		
	PO6 ^a	PO10 ^a	royleanone ^b
1	1.37 dd (12.6, 3.6)	1.15 m	1.12 td (13.5, 3.5)
	2.23 br d (12.6)	2.75 m	2.75 ddt (13.5, 3.5, 1.5)
2	1.30–1.48 m	1.51 m	1.53 dq (13.5, 3.5)
	1.50–1.90 m	1.72 tt (13.8, 3.3)	1.72 qt (13.5, 3.5)
3	1.20 m, 1.46 m	1.21 m	1.20 m
		1.46 m	1.46 dtd (13.5, 3.5, 1.5)
5	1.29 dd (12.3, 2.4)	1.10 m	1.10 dd (12.5, 1.5)
6	1.30–1.48 m	1.38 m	1.38 dddd (13.5, 12.5,
	1.50–1.90 m	1.86 dd (13.2, 7.2)	11.5, 6.0)
			1.87 ddt (13.5, 7.5, 1.5)
7	2.70–2.79 m	2.33 ddd (20.7, 11.4,	2.34 ddd (21.0, 11.5,
	2.80–2.90 m	7.2)	7.5)
		2.71 ddd (20.7, 5.2, 1.2)	2.71 ddd (21.0, 6.0, 1.5)
11	6.62 s		
14	6.83 s		
15	3.11 sept (6.9)	3.15 sept (6.9)	3.15 sept (7.0)
16	1.23 d (6.9)	1.21 d (6.9)	1.21 d (7.0)
17	1.21 d (6.9)	1.20 d (6.9)	1.20 d (7.0)
18	0.93 s	0.93 s	0.93 s
19	0.90 s	0.90 s	0.90 s
20	1.15 s	1.25 s	1.25 s
12-OH	4.73 s	7.23 s	7.23 s

^a Spectra recorded at 300 (^1H NMR) MHz, CDCl_3 .^b Spectrum recorded at 400 (^1H NMR) MHz, CDCl_3 .

3.2.11 Compound PO11



Compound **PO11** was obtained as orange crystals, m.p. 170-172 °C, $[\alpha]_D^{26} -114.0$ (CHCl₃; *c* 0.10). The UV and IR spectrum were closely related to that of **PO10**.

The ¹H and ¹³C NMR spectral data of **PO11** (Table 54, Figures 97 and 98) resembled those of **PO10** (Table 52, Figures 95 and 96), except that an additional oxymethine proton signal at δ 4.72 (*J*= 4.8, 1.5 Hz) was observed in **PO11**. The linkage position for the oxymethine proton at C-7 was established by HMBC correlation (Table 54) to C-5, C-6, C-8, C-9 and C-14, and the configuration of hydroxyl group was determined to be α due to absence of cross peak between H-7 (δ_H 4.72) and H-5 (δ_H 1.53) in the NOESY experiment. Thus on the basis of its spectroscopic data and comparison of the ¹H and ¹³C NMR spectral data with the previous report [Tezuka *et al.*, 1998; Benjamin Rodrigues 2003, $[\alpha]_D^{26} -128.2$ (CHCl₃; *c* 0.1)] (Table 55), compound **PO11** was assigned as horminone. X-ray crystallographic analysis of **PO11** (Abdul Razak *et al.*, 2010) was also carried out and gave ORTEP drawing as shown in Figure 22.

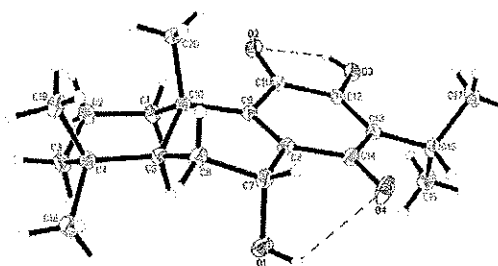


Figure 22 ORTEP drawing of **PO11**

Table 54 ^1H , ^{13}C NMR, DEPT and HMBC spectral data of compound **PO11** and ^{13}C NMR of horminone (**R**)

Position	DEPT	$\delta_{\text{C}}/\text{ppm}$		$\delta_{\text{H}}/\text{ppm}$ (mult., J in Hz)		HMBC
		R^b	PO11^c			
1	CH ₂	35.8	35.7	1.19 m ^a 2.70 m ^a		3, 5, 10, 20
2	CH ₂	18.9	18.8	1.50 m ^a 1.74 m ^a		1, 3, 4, 10
3	CH ₂	41.1	41.1	1.23 m ^a 1.48 m ^a		1, 2, 4, 5, 18, 19
4	C	33.0	33.0			
5	CH	45.7	45.7	1.53 m ^a		1, 3, 4, 6, 7, 10
6	CH ₂	25.8	25.7	1.59 m ^a 1.96 d (12.6)		4, 5, 7, 8, 10
7	CH	63.2	63.2	4.72 dd (4.8, 1.5)		5, 6, 8, 9, 14
8	C	143.2	143.1			
9	C	147.8	147.8			
10	C	39.1	39.1			
11	CO	183.9	183.9			
12	C	151.1	151.2			
13	C	124.2	124.0			
14	CO	189.1	189.1			
15	CH	24.0	24.0	3.16 sept (6.9)		12, 13, 14, 16, 17
16	CH ₃	19.8	19.8	1.20 d (6.9)		13, 15, 17
17	CH ₃	19.9	19.9	1.19 d (6.9)		13, 15, 16
18	CH ₃	33.1	33.1	0.99 s		3, 4, 5, 19
19	CH ₃	21.7	21.2	0.90 s		3, 4, 5, 18
20	CH ₃	18.4	18.4	1.25 s		1, 5, 9, 10
12-OH				7.39 s		11, 12, 13

^a Deduced from HMQC experiment, ^b Spectrum recorded at 125 (^{13}C NMR) MHz, CDCl_3 . ^c Spectra recorded at 300 (^1H NMR) and 75 (^{13}C NMR) MHz, CDCl_3 .

Table 55 Comparison of ^1H NMR spectral data of compounds **PO10**, **PO11** and royleanone

Position	$\delta_{\text{H}}/\text{ppm}$ (mult., J in Hz)		
	PO10 ^a	PO11 ^a	royleanone ^b
1	1.15 m	1.19 m	1.18 td (13.5, 3.5)
	2.75 m	2.70 m	2.70 ddt (13.5, 3.5, 1.5)
2	1.51 m	1.50 m	1.47 dtd (13.5, 3.5, 1.5)
	1.72 tt (13.8, 3.3)	1.74 m	1.73 qt (13.5, 3.5)
3	1.21 m	1.23 m	1.25 dt (13.5, 3.5)
	1.46 m	1.48 m	1.56 dt (13.5, 3.5)
5	1.10 m	1.53 m	1.54 br d (13.5)
6	1.38 m	1.59 m	1.61 td (13.5, 4.5)
	1.86 dd (13.2, 7.2)	1.96 d (12.6)	1.97 br d (13.5)
7	2.33 ddd (20.7, 11.4, 7.2)	4.72 dd (4.8, 1.5)	4.73 br d (4.5)
	2.71 ddd (20.7, 5.2, 1.2)		
15	3.15 sept (6.9)	3.16 sept (6.9)	3.16 sept (7.0)
16	1.21 d (6.9)	1.20 d (6.9)	1.21 d (7.0)
17	1.20 d (6.9)	1.19 d (6.9)	1.22 d (7.0)
18	0.93 s	0.99 s	0.98 s
19	0.90 s	0.90 s	0.90 s
20	1.25 s	1.25 s	1.21 s
12-OH	7.23 s	7.39 s	7.33 br s

^a Spectra recorded at 300 (^1H NMR) MHz, CDCl_3 .

^b Spectrum recorded at 400 (^1H NMR) MHz, CDCl_3 .

Table 56 Comparison of ^{13}C NMR spectral data of compounds **PO4-PO9**

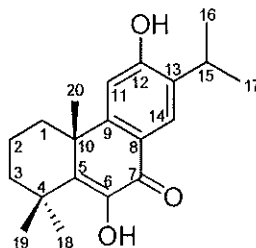
Position	PO4 ^a	PO5 ^b	PO6 ^a	PO7 ^a	PO8 ^a	PO9 ^a	PO10 ^a	PO11 ^a
1	77.6	78.2	38.8	38.9	39.3	37.9	36.3	35.7
2	30.2	30.1	19.2	19.2	19.9	18.9	18.9	18.8
3	39.8	39.7	41.7	41.7	37.4	41.4	41.3	41.1
4	33.4	33.3	33.4	33.5	43.7	33.3	33.5	33.0
5	49.6	49.8	50.3	50.5	52.7	49.5	51.7	45.7
6	19.2	19.2	19.3	19.4	21.1	36.1	17.4	25.7
7	29.8	29.6	29.7	29.8	31.2	198.5	26.7	63.2
8	135.5	127.3	127.3	126.9	127.2	124.7	146.0	143.1
9	146.9	147.0	146.8	148.1	146.4	156.4	146.5	147.8
10	43.6	43.4	37.5	37.9	38.2	37.9	38.4	39.1
11	126.9	113.7	111.0	106.6	111.8	110.1	183.4	183.9
12	123.9	151.0	150.6	155.0	150.9	158.1	150.5	151.2
13	146.0	132.4	131.4	134.3	131.9	132.6	123.7	124.0
14	126.7	126.3	126.6	126.4	126.5	126.6	187.5	189.1
15	33.5	26.6	26.8	26.5	26.7	26.8	24.1	24.0
16	24.1	26.6	22.6	22.7	22.5	22.3	19.8	19.8
17	24.1	22.7	22.7	22.9	22.6	22.4	19.9	19.9
18	32.8	32.7	33.3	33.3	28.7	32.6	33.4	33.1
19	21.3	21.3	21.6	21.6	182.0	21.4	21.7	21.2
20	17.4	17.8	24.8	24.8	23.1	23.2	20.1	18.4

Assignments were based on DEPT 90° and DEPT 135° experiments.

^a Spectrum recorded at 75 (^{13}C NMR) MHz, CDCl_3 .

^b Spectrum recorded at 100 (^{13}C NMR) MHz, CDCl_3 .

3.2.12 Compound PO12



Compound **PO12** was isolated as a yellow powder, m.p. 201-203 °C, $[\alpha]_D^{26} -27$ (CHCl₃; *c* 0.17). The UV absorption maxima at λ_{\max} 248 and 342 nm indicated an aromatic system. The IR spectrum confirmed the presence of the aromatic system (1635 and 1504 cm⁻¹), conjugated carbonyl (1676 cm⁻¹), and hydroxyl (3328 cm⁻¹) groups.

The ¹³C NMR and DEPT spectral data of **PO12** (Table 57, Figure 100) indicated 20 resonances including a conjugated carbonyl signal at δ 179.7 (C=O) and eight low-field signals at δ 111.4 (CH), 120.9 (C), 125.6 (CH), 133.8 (C), 141.1 (C), 143.8 (C), 154.9 (C), and 157.7 (C). These data suggested that **PO12** contained a carbonyl, a double bond, and a phenyl groups.

The ¹H NMR spectral data of **PO12** (Table 57, Figure 99) were similar to those of **PO9** (Table 50, Figures 93 and 94), except for the absence of the aliphatic methine proton (H-5) and methylene protons AX signals in **PO9**. Thus, compound **PO12** was deduced to be a 5,6-dehydrogenated derivative of **PO9**. In addition, the singlet signal at δ 7.16 was deduced to be a hydroxyl group at C-6. The double bond and hydroxyl group were assigned to C-5 and C-6 by HMBC correlations (Table 57) of CH₃-20/C-5 (δ_C 141.1), CH₃-18 and 19/C-5 (δ_C 141.1), and OH-6/C-6 (δ_C 143.8). Thus on the basis of its spectroscopic data and comparison of the ¹H and ¹³C NMR spectral data with the previous report (Su *et al.*, 1994, $[\alpha]_D^{26} -8.5$ (CHCl₃; *c* 0.9) (Table 57 and 58), compound **PO12** was assigned as montbretrol.

Table 57 ^1H , ^{13}C NMR, DEPT and HMBC spectral data of compound **PO12** and ^{13}C NMR of montbretrol (**R**)

Position	DEPT	$\delta_{\text{C}}/\text{ppm}$		$\delta_{\text{H}}/\text{ppm}$ (mult., J in Hz)	HMBC
		R ^b	PO12 ^c		
1	CH ₂	33.6	33.6	1.78 m ^a 2.28 m ^a	2, 3, 10, 20
2	CH ₂	17.6	17.6	1.77 m ^a 1.93 m ^a	1, 3, 4, 10
3	CH ₂	37.9	37.9	1.47 m ^a 1.94 m ^a	1, 2, 4, 18, 19
4	C	35.9	35.9		
5	C	141.1	141.1		
6	C	143.7	143.8		
7	CO	179.7	179.7		
8	C	120.9	120.9		
9	C	154.9	154.9		
10	C	40.3	40.3		
11	CH	111.4	111.4	6.90 s	8, 9, 10, 13
12	C	157.7	157.7		
13	C	133.8	133.8		
14	CH	125.6	125.6	8.02 s	7, 9, 12, 15
15	CH	26.9	26.9	3.19 sept (6.8)	12, 13, 14, 16, 17
16	CH ₃	22.3	22.3	1.31 d (6.8)	13, 15, 17
17	CH ₃	22.5	22.5	1.28 d (6.8)	13, 15, 16
18	CH ₃	28.2	28.2	1.45 s	3, 4, 5, 19
19	CH ₃	27.5	27.6	1.45 s	3, 4, 5, 18
20	CH ₃	35.1	35.1	1.50 s	1, 5, 9, 10
12-OH				5.85 s	11, 12, 13

^a Deduced from HMQC experiment.

^b Spectrum recorded at 75 (^{13}C NMR) MHz, CDCl_3 .

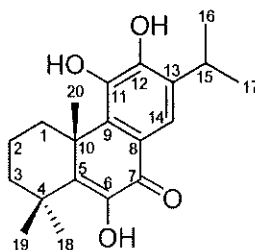
^c Spectra recorded at 300 (^1H NMR) and 75 (^{13}C NMR) MHz, CDCl_3 .

Table 58 Comparison of ^1H NMR spectral data of compounds **PO9**, **PO12** and montbretrol

Position	$\delta_{\text{H}}/\text{ppm}$ (mult., J in Hz)		
	PO9	PO12	montbretrol
1	1.50 m ^a	1.78 m	
	2.20 br d (12.6)	2.28 m	
2	1.68 m ^a	1.77 m	
	1.77 tt (13.5, 3.3)	1.93 m	
3	1.26 m ^a	1.47 m	
	1.53 dd (12.6, 3.3)	1.94 m	
5	1.85 dd (12.9, 4.5)		
6	2.58 dd (18.0, 12.9)		
	2.69 dd (18.0, 4.5)		
11	6.70 s	6.90 s	6.82 s
14	7.91 s	8.02 s	7.99 s
15	3.15 sept (6.9)	3.19 sept (6.8)	3.16 sept (7.0)
16	1.27 d (6.9)	1.31 d (6.8)	1.25 d (7.0)
17	1.24 d (6.9)	1.28 d (6.8)	1.28 d (7.0)
18	0.92 s	1.45 s	1.41 s
19	0.99 s	1.45 s	1.41 s
20	1.22 s	1.50 s	1.46
6-OH		7.16 s	
12-OH	5.60 br s	5.85 s	

Spectra recorded at 300 (^1H NMR) MHz, CDCl_3 .

3.2.13 Compound PO13



Compound **PO13** was obtained as colorless crystals, m.p. 279-280 °C; $[\alpha]_D^{26} +58.0$ (CHCl₃; *c* 0.10). The UV and IR spectrum were closely related to that of **PO12**.

The ¹H and ¹³C NMR spectral data of **PO13** (Table 59, Figures 101 and 102) were resemble to those of **PO12** (Table 57, Figures 99 and 100). The difference in the spectrum of **PO7** was shown as the absence of a singlet olefinic methine proton signal at δ 6.72 and the presence of a downfield proton signal at δ 3.05 (H-1 β , m), which suggested the presence of a hydroxyl group at C-11. By comparison of the ¹H and ¹³C NMR spectral data with the previously reported data (Topcu *et al.*, 1996; Benjamin Rodrigues 2003; Fraga *et al.*, 2005) (Table 59 and 60), therefore compound **PO13** was identified as 14-deoxycoleon. X-ray crystallographic analysis of **PO13** (Salae *et al.*, 2009) was also carried out and gave ORTEP drawing as shown in Figure 23.

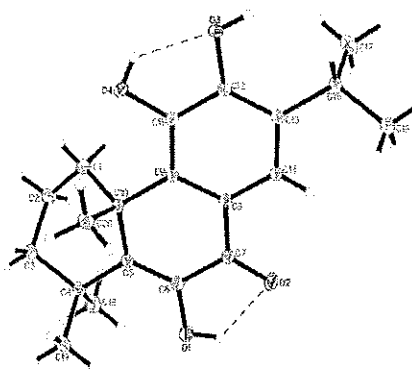


Figure 23 ORTEP drawing of PO13

Table 59 ^1H , ^{13}C NMR, DEPT and HMBC spectral data of compound **PO13** and ^{13}C NMR of 14-deoxycoleon (**R**)

Position	DEPT	$\delta_{\text{C}}/\text{ppm}$		$\delta_{\text{H}}/\text{ppm}$ (mult., J in Hz)		HMBC
		R ^b	PO13 ^c			
1	CH ₂	30.3	29.7	1.68 m ^a 3.05 m ^a		2, 3, 5, 10, 20
2	CH ₂	17.8	17.7	1.64 m ^a 1.88 m ^a		1, 3, 4, 10
3	CH ₂	36.3	36.4	1.40 dd (5.7, 3.3) 2.04 dt (18.3, 5.7)		1, 2, 4, 18, 19
4	C	36.4	36.5			
5	C	143.2	144.7			
6	C	140.7	142.6			
7	CO	179.8	180.4			
8	C	120.1	120.5			
9	C	138.1	138.5			
10	C	40.6	41.0			
11	C	142.9	141.8			
12	C	145.3	146.6			
13	C	132.6	134.0			
14	CH	116.4	116.2	7.70 s		7, 9, 12, 15
15	CH	27.0	26.9	3.20 sept (6.9)		12, 13, 14, 16, 17
16	CH ₃	22.3	22.7	1.23 d (6.9)		13, 15, 17
17	CH ₃	22.5	22.4	1.25 d (6.9)		13, 15, 16
18	CH ₃	27.3	27.9	1.45 s		3, 4, 5, 19
19	CH ₃	27.9	27.2	1.45 s		3, 4, 5, 18
20	CH ₃	27.9	27.5	1.67 s		1, 5, 9, 10
6-OH				7.15 s		5, 6, 7

^a Deduced from HMQC experiment.

^b Spectrum recorded at 125 (^{13}C NMR) MHz, CDCl_3 .

^c Spectra recorded at 300 (^1H NMR) and 75 (^{13}C NMR) MHz, CDCl_3 .

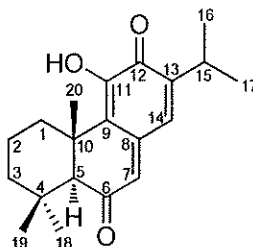
Table 60 Comparison of ^1H NMR spectral data of compounds **PO12**, **PO13** and 14-deoxycoleon (**R**)

Position	$\delta_{\text{H}}/\text{ppm}$ (mult., J in Hz)		
	PO12 ^a	PO13 ^a	14-deoxycoleon ^b
1	1.78 m	1.68 m	1.71 m
	2.28 m	3.05 m	2.93 m
2	1.77 m	1.64 m	1.61 m
	1.93 m	1.88 m	1.86 m
3	1.47 m	1.40 dd (5.7, 3.3)	1.41 m
	1.94 m	2.04 dt (18.3, 5.7)	2.01 td (13.0, 5.0)
11	6.90 s		
14	8.02 s	7.70 s	7.70 s
15	3.19 sept (6.8)	3.20 sept (6.9)	3.04 sept (6.8)
16	1.31 d (6.8)	1.23 d (6.9)	1.27 d (6.8)
17	1.28 d (6.8)	1.25 d (6.9)	1.30 d (6.8)
18	1.45 s	1.45 s	1.43 s
19	1.45 s	1.45 s	1.44 s
20	1.50 s	1.67 s	1.67 s
6-OH	7.16 s	7.15 s	7.09 s
12-OH	5.85 s		

^a Spectra recorded at 300 (^1H NMR) MHz, CDCl_3 .

^b Spectrum recorded at 500 (^1H NMR) MHz, CDCl_3 .

3.2.14 Compound PO14



Compound **PO14** was isolated as a yellow oil, $[\alpha]_{\text{D}}^{26} +43.9$ (CHCl_3 ; c 2.03). The IR spectrum had bands for hydroxyl (3530 cm^{-1}), a conjugate carbonyl (1740 and 1643 cm^{-1}) and a double bond (1531 cm^{-1}) groups which was confirmed by the UV absorption maxima at λ_{max} 206, 320, 333 and 400 nm.

The ^{13}C NMR and DEPT spectral data of **PO14** (Table 61, Figure 104) displayed five methyl, three methylene, four methine, and eight quaternary carbons including two carbonyl signals at δ 181.7 and 201.1 ($\text{C}=\text{O}$), five low-field signals at δ 125.3 (C), 134.0 (CH), 136.1 (CH), 139.9 (C), 145.0 (C), and 145.3 (C).

The ^1H NMR spectral data of **PO14** (Table 61, Figure 103) revealed three singlets at δ 1.27 \times 2 and 1.12, indicating the presence of three methyl groups at C-18, C-19 and C-20 and two methyl doublets at δ 1.18 and 1.16 (each 3H, d, $J=6.8$ Hz, H-16 and H-17), together with a methine signal at δ 3.07 (1H, sept, $J=6.8$ Hz, H-15), showing the presence of an isopropyl group, thus suggested that **PO14** was an abietane-type diterpene. Downfield signals were observed at δ 6.21 (1H, s, H-7) and 6.89 (1H, s, H-14) and an exchangeable enol proton at δ 7.58 (H-11). The signal at δ 2.60 was assigned to be H-5, which exhibited HMBC correlations (Table 61) with C-1 (δ_{C} 37.0), C-3 (δ_{C} 42.5), C-4 (δ_{C} 32.8), C-9 (δ_{C} 125.3), C-10 (δ_{C} 42.9), C-18 (δ_{C} 33.2) and C-19 (δ_{C} 22.1). The HMBC correlations (Table 61) of OH/C-9 (δ_{C} 125.3), C-11 (δ_{C} 145.3) and C-12 (δ_{C} 181.7), and H-20/C-1 (δ_{C} 37.0), C-5 (δ_{C} 63.0), C-9 (δ_{C} 125.3) and C-10 (δ_{C} 42.9) confirmed the hydroxyl group at C-11. The proton H-15 has HMBC correlations with δ_{C} 181.7 and 136.1 [resonating with δ 6.89 (s)], and therefore they were assigned to be C-12 and C-14, respectively. Two singlet olefinic protons at δ 6.21 and 6.89 exhibited the NOESY correlations, and thus δ 6.21 is at C-

7. Thus on the basis of its spectroscopic data and comparison of the ^1H and ^{13}C NMR spectral data with the previous report (Kupchan *et al.*, 1968; Tezuka *et al.*, 1998, $[\alpha]_{\text{D}}^{26} +38.9$ (CHCl_3 ; c 0.1); Benjamin Rodriguez, 2003) (**Table 61** and **62**), compound **PO14** was identified as taxodione.

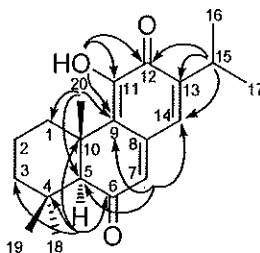


Figure 24 Major selected HMBC correlations of **PO14**

Table 61 ^1H , ^{13}C NMR, DEPT and HMBC spectral data of compound **PO14** and ^{13}C NMR of taxodione (**R**)

Position	DEPT	$\delta_{\text{C}}/\text{ppm}$		$\delta_{\text{H}}/\text{ppm}$ (mult., J in Hz)		HMBC
		R^b		PO14^c		
1	CH ₂	37.1	37.0	1.72 m ^a		2, 3, 5, 10, 20
				2.94 m ^a		
2	CH ₂	18.6	18.5	1.58 m ^a		1, 3, 4, 10
				1.75 m ^a		
3	CH ₂	42.6	42.5	1.16 m ^a		1, 2, 4, 18, 19
				1.42 m ^a		
4	C	32.9	32.8			
5	CH	63.1	63.0	2.60 s		1, 4, 6, 9, 18, 19
6	CO	201.0	201.1			
7	CH	134.0	134.0	6.21 s		5, 9, 14
8	C	140.0	139.9			
9	C	125.7	125.3			
10	C	42.9	42.9			
11	C	145.0	145.3			
12	CO	181.7	181.7			
13	C	145.4	145.0			
14	CH	136.2	136.1	6.89 s		7, 8, 9, 12, 15
15	CH	27.2	27.1	3.07 sept (6.8)		12, 13, 14, 16, 17
16	CH ₃	21.3	21.8	1.18 d (6.8)		13, 15, 17
17	CH ₃	21.6	21.6	1.16 d (6.8)		13, 15, 16
18	CH ₃	33.3	33.2	1.27 s		3, 4, 5, 19
19	CH ₃	22.1	22.1	1.27 s		3, 4, 5, 18
20	CH ₃	21.9	21.2	1.12 s		1, 5, 9, 10
11-OH				7.58 s		9, 11, 12

^a Deduced from HMQC experiment.

^b Spectrum recorded at 100 (^{13}C NMR) MHz, CDCl_3 .

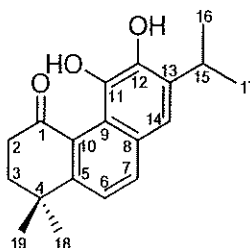
^c Spectra recorded at 400 (^1H NMR) and 100 (^{13}C NMR) MHz, CDCl_3 .

Table 62 Comparison of ^1H NMR spectral data of compounds **PO14** and taxodione

Position	$\delta_{\text{H}}/\text{ppm}$ (mult., J in Hz)	
	PO14	taxodione
1	1.72 m	1.75 m
	2.94 m	2.94 m
2	1.58 m	1.59 dq (13.5, 3.5)
	1.75 m	1.71 qt (13.5, 3.5)
3	1.16 m	1.20 m
	1.42 m	1.41 dtd (13.5, 3.5, 1.5)
5	2.60 s	2.60 s
7	6.21 s	6.21 s
14	6.89 s	6.88 s
15	3.07 sept (6.8)	3.07 sept (7.0)
16	1.18 d (6.8)	1.18 d (7.0)
17	1.16 d (6.8)	1.16 d (7.0)
18	1.27 s	1.12 s
19	1.27 s	1.27 s
20	1.12 s	1.27 s
11-OH	7.58 s	7.57 s

Spectra recorded at 300 (^1H NMR) MHz, CDCl_3 .

3.2.15 Compound PO15



Compound **PO15** was obtained as orange crystals, m.p. 183-185 °C, $[\alpha]_D^{26} +9.9$ (CHCl₃; *c* 1.00). The IR spectrum showed bands for hydroxyl (3490 cm⁻¹), a carbonyl (1640 cm⁻¹) and for a double bond (1590 cm⁻¹) groups and the UV absorption maxima at λ_{\max} 270, 362 and 410 nm indicating the presence of an aromatic system.

The ¹H NMR spectral data of **PO15** (Table 63, Figure 105) showed the existence of signals for an isopropyl group (δ 1.21, 6H, d, *J*= 6.8 Hz and δ 3.26, septet, *J*= 6.8 Hz) as well as two methyl groups as a singlet at δ 1.13 (6H). Signals for two protons with an AX pattern were found at δ 6.62 (d, *J*= 12.0 Hz, H-6) and δ 7.34 (d, *J*= 12.0 Hz, H-7), a geminal dimethyl group at δ 1.13 (s, 6H, H-18 and H-19, respectively) and two methylene groups at δ 2.42 (t, *J*= 6.6 Hz, H-2) and δ 1.87 (t, *J*= 6.6 Hz, H-3) were observed. Another aromatic proton at δ 6.77 (s, H-14) and one hydrogen bonded phenolic functions at δ 6.38 (s, OH-11).

The 19 carbon signals observed in the ¹³C NMR and DEPT spectral data of **PO15** (Table 63, Figure 106) showed the presence of a carbonyl group at δ 200.5, ten olefinic carbons at δ 117.6 (CH), 121.9 (C), 124.1 (CH), 127.7 (C), 128.2 (C), 132.4 (C), 138.2 (CH), 140.0 (CH), 145.6 (C), 156.8 (C), suggesting that **PO15** contained two rings and a norditerpenoid structure. Careful analysis of the 1D and 2D NMR spectra indicated that **PO15** could be ascribed to a 20-norabietane diterpenoid by the absence of the characteristic methyl (CH₃-20) for a simple abietane diterpenoid. This finding was further confirmed by the HMBC correlations (Table

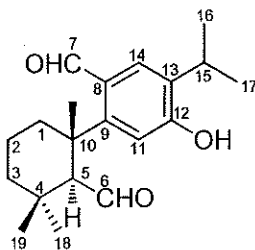
63). Compound **PO15** was identified as arucadiol by comparison of its spectral data with those reported in the literature (Michavila *et al.*, 1986).

Table 63 ^1H , ^{13}C NMR, DEPT and HMBC spectral data of compound **PO15**

Position	DEPT	$\delta_{\text{C}}/\text{ppm}$	$\delta_{\text{H}}/\text{ppm}$ (mult., J in Hz)	HMBC
1	CO	200.5		
2	CH ₂	36.6	2.42 t (6.6)	1, 3, 4, 10
3	CH ₂	33.4	1.87 t (6.6)	1, 4, 5, 18, 19
4	C	35.0		
5	C	156.8		
6	CH	124.1	6.62 d (12.0)	4, 5, 7, 8, 10
7	CH	140.0	7.34 d (12.0)	5, 8, 9, 14
8	C	127.7		
9	C	121.9		
10	C	128.2		
11	C	138.2		
12	C	145.6		
13	C	132.4		
14	CH	117.6	6.77 s	7, 9, 12, 15
15	CH	27.3	3.26 sept (6.9)	12, 13, 14, 16, 17
16	CH ₃	22.5	1.21 d (6.9)	13, 15, 17
17	CH ₃	22.5	1.21 d (6.9)	13, 15, 16
18	CH ₃	27.2	1.13 s	3, 4, 5, 19
19	CH ₃	27.2	1.13 s	3, 4, 5, 18
11-OH			6.38 s	11, 12, 13

Spectra recorded at 400 (^1H NMR) and 100 (^{13}C NMR) MHz, CDCl_3 .

3.2.16 Compound PO16



Compound **PO16** was isolated as colorless crystals, m.p. 193-195 °C, $[\alpha]_{\text{D}}^{26} +12.8$ (CHCl_3 ; c 0.81). The IR spectrum showed absorption bands at 3434 cm^{-1} for hydroxyl group, 1710 cm^{-1} and 1666 cm^{-1} for carbonyl groups, 1545 cm^{-1} for aromatic groups and the UV absorption maxima at λ_{max} 218, 260 and 295 nm which indicated the presence of an aromatic system.

The ^1H NMR spectral data of **PO16** (Table 64, Figure 107) showed two aromatic proton singlets at δ 7.00 and 7.84, an isopropyl moiety with a doublet for two methyls at δ 1.26 and 1.27 ($J= 6.9$ Hz) and a septet for a proton at δ 3.22, three singlet quaternary methyl groups at δ 0.71, 1.03 and 1.50, a doublet aliphatic methine proton at δ 3.16, and two aldehyde protons at δ 9.86 (d, $J= 4.2$ Hz) and 10.44 (s). Its ^{13}C NMR and DEPT spectral data (Table 64, Figure 108) exhibited five methyls, three methylenes, four methines, six quaternary carbons and two aldehyde carbons. The HMBC correlations (Table 64) for the C-6 aldehyde at δ 206.9 with the H-5 proton in the aliphatic methine proton at δ 3.16, and the C-7 aldehyde at δ 192.1 with the H-14 aromatic proton at δ 7.84, suggested that **PO16** must possess a 6,7-*seco*-abietane skeleton. The relative stereochemistry at C-5 position was determined from the NOESY spectrum. Since the methyl group at C-10 could be assigned with a β -configuration for biogenetic reasons and no correlation between this methyl group and the proton at C-5 was observed, H-5 was determined to have an α -configuration. Thus on the basis of its spectroscopic data and comparison of the ^1H and ^{13}C NMR spectral data with the previous report (Kuo *et al.*, 2001, $[\alpha]_{\text{D}}^{26} +20.0$ (CHCl_3 ; c 1.2); Katoh *et al.*, 2007) (Table 65), compound **PO16** was assigned as 12-hydroxy-6,7-*seco*abieta-8,11,13-triene-6,7-dial.

Table 64 ^1H , ^{13}C NMR, DEPT and HMBC spectral data of compound **PO16** and ^{13}C NMR of 12-hydroxy-6,7-secoabieta-8,11,13-triene-6,7-dial (**R**)

Position	DEPT	$\delta_{\text{C}}/\text{ppm}$		$\delta_{\text{H}}/\text{ppm}$ (mult., J in Hz)		HMBC
		R^b	PO16			
1	CH ₂	37.4	37.4	1.55–1.80 m ^a	2.31 m ^a	3, 5, 9, 10, 20
2	CH ₂	19.3	19.3	1.60–1.80 m ^a		1, 3, 4, 10
3	CH ₂	37.6	37.7	1.55–1.80 m ^a		1, 2, 4, 18, 19
4	C	33.5	33.4			
5	CH	64.6	64.5	3.16 d (4.2)		1, 3, 4, 6, 10, 18, 19
6	CHO	206.2	206.9	9.86 d (4.2)		
7	CHO	192.6	192.1	10.44 s		8, 9, 14
8	C	127.9	127.3			
9	C	151.1	151.0			
10	C	40.4	40.5			
11	CH	114.8	115.0	7.00 s		8, 9, 10, 13
12	C	157.9	158.4			
13	C	132.4	132.4			
14	CH	134.6	135.0	7.84 s		7, 8, 9, 12, 15
15	CH	26.7	26.7	3.22 sept (6.9)		12, 13, 14, 16, 17
16	CH ₃	22.2	22.2	1.26 d (6.9)		13, 15, 17
17	CH ₃	22.2	22.2	1.27 d (6.9)		13, 15, 16
18	CH ₃	30.6	30.7	0.71 s		3, 4, 5, 19
19	CH ₃	27.4	27.3	1.03 s		3, 4, 5, 18
20	CH ₃	28.1	28.0	1.50 s		1, 5, 9, 10
12-OH				7.13 br s		

^a Deduced from HMQC experiment.

^b Spectrum recorded at 100 (^{13}C NMR) MHz, CDCl_3 .

^c Spectra recorded at 300 (^1H NMR) and 75 (^{13}C NMR) MHz, CDCl_3 .

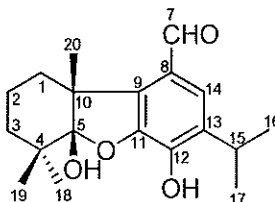
Table 65 Comparison of ^1H NMR spectral data of compounds **PO16** and 12-hydroxy-6,7-secoabieta-8,11,13-triene-6,7-dial

Position	δ_{H} /ppm (mult., <i>J</i> in Hz)	
	PO16 ^a	12-hydroxy-6,7-secoabieta-8,11,13-triene-6,7-dial ^b
1	1.55–1.80 m 2.31 m	1.50–1.83 m 2.28–2.34 m
2	1.60–1.80 m	1.50–1.83 m
3	1.55–1.80 m	1.50–1.83 m
5	3.16 d (4.2)	3.13 d (3.8)
6	9.86 d (4.2)	9.86 d (3.8)
7	10.44 s	10.47 s
11	7.00 s	6.96 s
14	7.84 s	7.84 s
15	3.22 sept (6.9)	3.18 sept (7.0)
16	1.26 d (6.9)	1.26 d (6.9)
17	1.27 d (6.9)	1.27 d (6.9)
18	0.71 s	0.70 s
19	1.03 s	1.01 s
20	1.50 s	1.50 s
12-OH	7.13 br s	7.57 s

^a Spectrum recorded at 300 (^1H NMR) MHz, CDCl_3 .

^b Spectrum recorded at 400 (^1H NMR) MHz, CDCl_3 .

3.2.17 Compound PO17



Compound **PO17** was isolated as a colorless oil with $[\alpha]_D^{26} +38.1$ (CHCl_3 ; c 0.91). The UV and IR spectra were closely related to those of **PO16**. The ^{13}C NMR and DEPT spectral data of **PO17** (Table 66, Figure 110) showed 19 carbons made up of five methyls, three methylenes, three methines, and eight quaternary carbons and one aldehyde carbon (δ_{C} 190.2). The ^1H and ^{13}C NMR spectroscopic data (Table 66, Figures 109 and 110) of **PO17** were resembled to those of **PO16** (Table 64, Figure 107 and 108). The difference in the spectrum of **PO17** was the absence of a doublet of an aldehydic proton signal at δ 9.86 in the ^1H NMR of **PO16** and the ^{13}C NMR spectrum of **PO17** displayed of a carbon at δ 114.8, suggesting a hemiacetal group and thus the ether linkage to tertiary hydroxyl group at C-5. The linkage position for the hemiacetal was established as C-5 by HMBC correlations (Table 66, Figures 25) for the CH_3 -18, CH_3 -19 and CH_3 -20 to C-5 (Table 66). By comparison of the ^1H and ^{13}C NMR spectral data with the previously reported data (Luis *et al.*, 1993) (Table 67), therefore compound **PO17** was identified as salvicanaraldehyde.

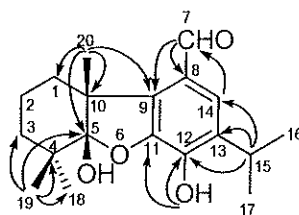


Figure 25 Major selected HMBC correlations of **PO17**

Table 66 ^1H , ^{13}C NMR, DEPT and HMBC spectral data of compound **PO17** and ^{13}C NMR of salvicanaraldehyde (**R**)

Position	DEPT	$\delta_{\text{C}}/\text{ppm}$		$\delta_{\text{H}}/\text{ppm}$ (mult., J in Hz)	HMBC
		R ^b		PO17 ^c	
1	CH ₂	39.4	39.7	1.42 m ^a 2.25 m ^a	2, 3
2	CH ₂	17.6	17.6	1.30–1.70 m ^a	
3	CH ₂	37.5	37.4	1.30–1.70 m ^a	
4	C	37.8	37.9		
5	C	115.0	114.8		
6					
7	CHO	189.7	190.2	10.02 s	8, 9
8	C	134.6	125.8		
9	C	126.7	137.7		
10	C	51.3	51.1		
11	C	137.6	143.0		
12	C	144.2	144.1		
13	C	142.0	134.6		
14	CH	125.0	124.2	7.31 s	7, 9, 13, 15
15	CH	30.1	27.1	3.27 sept (6.8)	12, 13, 14, 16, 17
16	CH ₃	19.3	22.4	1.26 d (6.8)	13, 15, 17
17	CH ₃	22.4	22.4	1.25 d (6.8)	13, 15, 16
18	CH ₃	26.4	26.2	1.24 s	3, 4, 5, 19
19	CH ₃	24.5	24.5	1.21 s	3, 4, 5, 18
20	CH ₃	17.7	19.7	1.72 s	1, 5, 9, 10
12-OH				5.61 br s	12, 13

^a Deduced from HMQC experiment.

^b Spectrum recorded at 50 (^{13}C NMR) MHz, C_6D_6 .

^c Spectra recorded at 400 (^1H NMR) and 100 (^{13}C NMR) MHz, CDCl_3 .

Table 67 Comparison of ^1H NMR spectral data of compounds **PO16**, **PO17** and salvicanaraldehyde

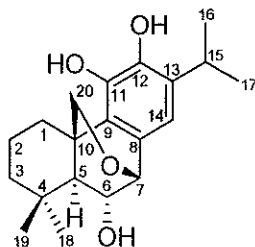
Position	δ_{H} /ppm (mult., J in Hz)		
	PO16 ^a	PO17 ^b	salvicanaraldehyde ^c
1	1.50–1.83 m	1.42 m	2.22 m
	2.28–2.34 m	2.25 m	
2	1.50–1.83 m	1.30–1.70 m	
3	1.50–1.83 m	1.30–1.70 m	
5	3.13 d (3.8)		
6	9.86 d (3.8)		
7	10.47 s	10.02 s	10.04 s
11	6.96 s		
14	7.84 s	7.31 s	7.32 s
15	3.18 sept (7.0)	3.27 sept (6.8)	3.28 hept
16	1.26 d (6.9)	1.26 d (6.8)	1.27 d
17	1.27 d (6.9)	1.25 d (6.8)	1.27 d
18	0.70 s	1.24 s	1.27 s
19	1.01 s	1.21 s	1.27 s
20	1.50 s	1.72 s	1.67 s
12-OH	7.57 s	5.61 br s	5.48 s

^a Spectrum recorded at 300 (^1H NMR) MHz, CDCl_3

^b Spectrum recorded at 400 (^1H NMR) MHz, CDCl_3 .

^c Spectrum recorded at 200 (^1H NMR) MHz, CDCl_3 .

3.2.18 Compound PO18



Compound **PO18** was obtained as a white solid, m.p. 199–201 °C; $[\alpha]_D^{24} -21.1$ (CHCl_3 ; c 0.02). The molecular formula $\text{C}_{20}\text{H}_{28}\text{O}_4$ was determined by HREIMS (calcd 332.1988, found 332.1999 $[\text{M}]^{+\bullet}$), requiring seven degrees of unsaturation. The UV absorption (λ_{max} 210 and 276 nm) indicated an aromatic ring while the IR (3351 and 1578 cm^{-1}) spectrum indicated hydroxyl and aromatic groups, respectively. The spectral data indicated that **PO18** possessed an abietane type skeleton.

The ^{13}C NMR spectral data (**Table 68**, **Figure 112**) revealed 20 carbon signals identified as four methyls (δ_{C} 22.2, 22.7($\times 2$) and 33.5), four methylenes (δ_{C} 18.8, 29.8, 41.3 and 66.9), five methines (δ_{C} 26.9, 56.3, 68.9, 73.8 and 115.9) and seven quaternary carbons (δ_{C} 33.5, 41.2, 127.8, 128.3, 133.3, 139.9 and 142.1). A singlet at δ 6.65 in the ^1H NMR spectrum was ascribed to the aromatic H-14. The characteristic signals of an isopropyl group bound to an aromatic ring, as well as two broad singlets exchangeable with D_2O corresponding to the hydroxy phenolic groups at C-11 and C-12 positions were also observed in the ^1H NMR spectrum (**Table 68**, **Figures 111**), whose data suggested a penta-substituted aromatic ring. Two methyl singlets at δ_{H} 0.97 and 1.06 were ascribed to the C-18 and C-19 methyl groups. The angular methyl group (C-20) frequently found in abietane-type diterpenes was not observed. Instead doublets for two nonequivalent geminal protons were evident at δ_{H} 4.20 and 2.89 ($J = 8.4\text{ Hz}$, H₂-20). A doublet at δ_{H} 4.46 ($J = 4.0\text{ Hz}$, H-7) was observed, the chemical shift of the latter suggested its connection to a hydroxyl group. The etheral function must be cyclic as indicated by its molecular formula and two ^{13}C NMR signals due to two oxygenated sp^3 carbons at δ 66.9 (C-20) and δ 73.8 (C-

7). The proton H-7 was coupled with a proton resonanced as a triplet at δ 3.98 ($J= 4.0$ Hz, H-6; δ_c 68.9) whose chemical shift of the latter suggested a connection to a hydroxyl group. The proton H-6 was also coupled with H-5 (δ 1.04, d, $J= 4.0$ Hz). The coupling constants 4.0 Hz of H-6, H-5, H-7 were in agreement with that of 16-hydroxyisorosmanol (Luis *et al.*, 1993) ($J= 4.4$ Hz) indicated for H-7. NOESY experiments also supported these assignments (**Figure 25**). The NMR data suggested that **PO18** was similar in structure to 6-*epi*-demethylesquirolin D, (Esquivel *et al.*, 1995) with **PO18** however, having a C-20 methylene group rather than a C-20 oxymethine carbon as found in the latter known compound. Therefore, compound **PO18** was a new compound and characterized as 6 α ,11,12-trihydroxy-7 β ,20-epoxy-8,11,13-abietatriene (Salae *et al.*, 2012).

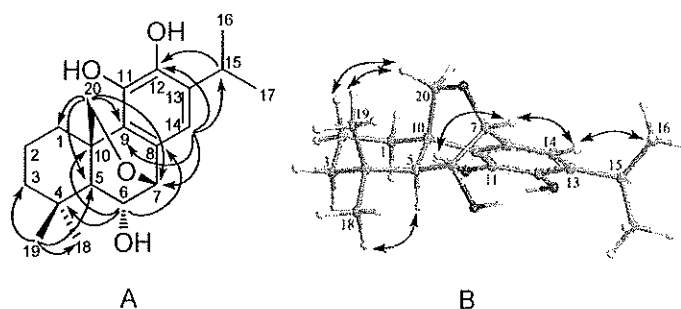


Figure 26 Selected HMBC correlations (A) and NOESY correlations (B) for **PO18**

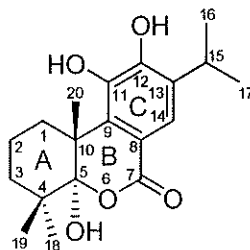
Table 68 ^1H , ^{13}C NMR, DEPT and HMBC spectral data of compound **PO18**

Position	DEPT	$\delta_{\text{C}}/\text{ppm}$	$\delta_{\text{H}}/\text{ppm}$ (mult., J in Hz)	HMBC
1	CH_2	29.8	2.09 br d (13.6) 2.60 td (13.6, 4.8)	3, 5, 10, 20
2	CH_2	18.8	1.50–1.60 m ^a	2, 3, 9, 10, 20
3	CH_2	41.3	1.20–1.25 m ^a 1.45–1.55 m ^a	1, 4, 5, 18
4	C	33.5		
5	CH	56.3	1.04 d (4.0)	3, 4, 6, 10, 18, 19, 20
6	CH	68.9	3.98 t (4.0)	4, 7, 8
7	CH	73.8	4.46 d (4.0)	5, 6, 9, 14, 20
8	C	127.8		
9	C	128.3		
10	C	41.2		
11	C	139.9		
12	C	142.1		
13	C	133.3		
14	CH	115.9	6.65 s	7, 9, 10, 11, 12, 15
15	CH	26.9	3.09 sept (6.8)	12, 13, 14, 16, 17
16	CH_3	27.7	1.16 d (6.8)	13, 15, 17
17	CH_3	22.7	1.17 d (6.8)	13, 15, 16
18	CH_3	33.5	0.97 s	3, 4, 5, 19
19	CH_3	22.2	1.06 s	3, 4, 5, 18
20a	CH_2	66.9	2.89 d (8.4) 4.02 d (8.4)	1, 5, 7, 9, 10
11-OH			6.33 s	9, 11, 12
12-OH			6.86 s	

^a Deduced from HMQC experiment.

Spectra recorded at 300 (^1H NMR) and 75 (^{13}C NMR) MHz, CDCl_3 .

3.2.19 Compound PO19



Compound **PO19** was isolated as a colorless oil with $[\alpha]_D^{24} +59.3$ (CHCl_3 ; c 0.14). Its molecular formula, $\text{C}_{19}\text{H}_{26}\text{O}_5$ was established by HREIMS (calcd 334.1780, found 334.1792 $[\text{M}]^{+}$), with seven degrees of unsaturation. The IR spectrum showed a conjugated carbonyl (1682 cm^{-1}) and hydroxyl (3452 cm^{-1}) groups. The maximum absorption bands at λ_{max} 218, 260 and 295 nm in the UV spectrum indicated the presence of aromatic and conjugated carbonyl groups.

The ^{13}C NMR spectral data of **PO19** (Table 69, Figure 114) revealed 19 carbon signals which were sorted by a DEPT experiment into five methyls (δ 17.5, 22.3, 22.4, 24.4 and 26.3), three methylenes (δ 17.6, 37.9 and 38.3), two methines (δ 27.1 and 123.3), three tetrasubstituted sp^3 carbons (δ 37.6, 51.3 and 114.9), five tetrasubstituted sp^2 carbons (δ 118.0, 134.0, 137.2, 143.0 and 143.2) and a lactone carbonyl (δ 172.1).

The ^1H and ^{13}C NMR spectroscopic data of **PO19** (Table 69, Figures 113 and 114) were similar to those of **PO18** (Table 68, Figures 111 and 112) for the signals corresponding to the A and C rings. The major differences were the NMR signals corresponding to the ring B of **PO19**. The molecular formula of **PO19** and the presence of a lactone carbonyl carbon at δ 172.1 suggested a 6,7-*seco*-abietane skeleton. This was supported by the HMBC correlations (Table 69, Figures 27) of H-14 at δ 7.49 to the carbons at δ 27.1 (C-15), 51.3 (C-10), 137.2 (C-9), 143.2 (C-12) and 172.1 (C-7). Furthermore the HMBC correlations of CH_3 -20 at δ 1.26 with the carbons at δ 38.3 (C-1), 51.3 (C-10), 114.9 (C-5) and 137.2 (C-9) placed an OH at C-5. The structure of **PO19** was closely related to cupresol (Jolad *et al.*, 1984) except for

the presence of a hydroxyl group at C-11 in ring C of **PO19** instead of an aromatic proton and 5β -OH in cupresol (Jolad *et al.*, 1984).

The relative stereochemistry of a tertiary hydroxyl at C-5 in **PO19** should be α -oriented indicating a *trans*-junction for the A and B rings because the methyl protons of **PO19** at C-18 were shifted more downfield than cupresol (δ 1.21 vs. δ 0.69). Thus, compound **PO19** was a new compound and characterized as $5\alpha,11,12$ -trihydroxy-6-oxa-abieta-8,11,13-trien-7-one (Salae *et al.*, 2012).

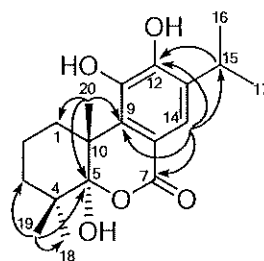


Figure 27 Major selected HMBC correlations of **PO19**

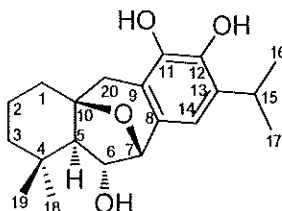
Table 69 ^1H , ^{13}C NMR, DEPT and HMBC spectral data of compound **PO19**

Position	DEPT	$\delta_{\text{C}}/\text{ppm}$	$\delta_{\text{H}}/\text{ppm}$ (mult., J in Hz)	HMBC
1a	CH_2	38.3	1.40–1.50 m ^a 2.46 br d (12.6)	
2	CH_2	17.6	1.50–1.55 m ^a	
3	CH_2	37.9	1.37–1.49 m ^a	
4	C	37.6		
5	C	114.9		
6				
7	CO	172.1		
8	C	118.0		
9	C	137.2		
10	C	51.3		
11	C	143.0		
12	C	143.2		
13	C	134.0		
14	CH	123.3	7.49 s	7, 9, 10, 12, 15
15	CH	27.1	3.25 sept (7.2)	12, 13, 14, 16, 17
16	CH_3	22.4	1.25 d (7.2)	13, 15, 17
17	CH_3	22.3	1.25 d (7.2)	13, 15, 16
18	CH_3	24.4	1.21 s	3, 4, 5, 19
19	CH_3	26.3	1.24 s	3, 4, 5, 18
20	CH_3	17.5	1.26 s	1, 5, 9, 10

^a Deduced from HMQC experiment

Spectra recorded at 400 (^1H NMR) and 100 (^{13}C NMR) MHz, CDCl_3 .

3.2.20 Compound PO20



Compound **PO20** was isolated as an amorphous solid, m.p. 188-190 °C, $[\alpha]_D^{26} -8.6$ (CHCl_3 ; c 0.88). The IR spectrum displayed the absorption bands due to aromatic ring (1601 and 1539 cm^{-1}) and hydroxyl groups (3693 and 3604 cm^{-1}). The UV spectrum showed the absorption maxima at λ_{max} 205 and 270 nm, indicative of a simple phenolic ring.

The ^1H NMR spectrum of **PO20** (Table 70, Figure 115) showed signals for an isopropyl group (δ 1.16, 6H, d, $J= 6.8$ Hz and δ 3.14, septet, $J= 6.8$ Hz) as well as two methyl groups as a singlet at δ 0.91 and 0.92. The H-7, H-6 and H-5 protons appeared at δ 4.57 (d, $J= 6.4$ Hz, H-7), 4.17 (t, $J= 6.4$ Hz, H-6) and 1.26 (d, $J= 6.4$ Hz, H-5), as detected by a ^1H - ^1H COSY experiment. One sharp singlet proton at δ 6.47 was assigned as an aromatic proton at C-14. Finally, an AB system at δ 2.41 and 2.68 (d, $J=16.4$ Hz) suggested the methylene protons at C-20 in **PO20**.

The ^{13}C NMR and DEPT spectral data of **PO20** (Table 70, Figure 116) showed four methyls, four methylenes, five methines (including an olefinic one and two oxygenated ones), and seven quaternary carbons (including six olefinic ones and an oxyquaternary one). Considering the structures of the compounds previously isolated from this genus, along with showing a clearly AB system at δ 2.41 and 2.68 ($J= 16.4$ Hz) characteristic of the C-20 methylene protons of an icetexane skeleton (Esquivel *et al.*, 1995), **PO20** could be ascribed to be an icetexane or abietane diterpenoid (Rasool *et al.*, 1991; Fraga *et al.*, 1986; Hasegawa *et al.*, 1985). Careful analysis of the 1D and 2D NMR spectra indicated that **PO20** could be ascribed to be an icetexane diterpenoid by the absence of the characteristic quaternary carbon (C-10) and a methyl group (Me-20) for a simple abietane diterpenoid. A comparison of the ^1H and ^{13}C NMR spectral data of **PO20** with those of brussonol (Fraga *et al.*, 2005)

indicated that they were strikingly similar except that the presence of a triplet at δ 4.17 ($J= 6.4$ Hz) was assigned to H-6, geminal to the secondary hydroxyl group in **PO20**. The hydroxyl group was located at C-6 by HMBC correlation (Table 70, Figures 28)

The relative stereochemistry at C-6 should be an α orientation for hydroxyl group because the *trans* fusion depicted in **PO20** was established with the aid of the coupling constant ($J= 6.4$ Hz) found for H-6, and by comparison with related compound **PO18**. Thus on the basis of its spectroscopic data and comparison of the ^1H and ^{13}C NMR spectral data with the previous report [Esquivel *et al.*, 1995, $[\alpha]_{\text{D}}^{26} -20.0$ (CHCl_3 ; c 0.1)] (Table 70 and 71), compound **PO20** was assigned as 5,6-dihydro-6 α -hydroxysalviasperanol. X-ray crystallographic analysis of **PO20** (Asik *et al.*, 2010) was also carried out and gave ORTEP drawing as shown in Figure 29.

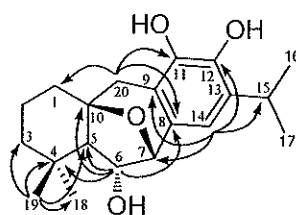


Figure 28 Major selected HMBC correlations of **PO20**

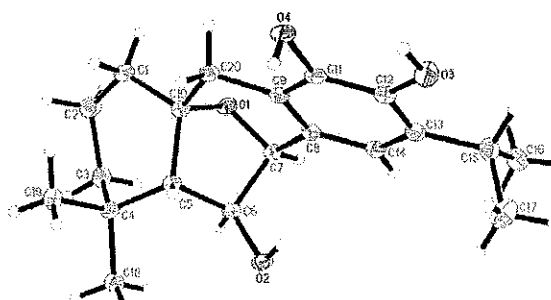


Figure 29 ORTEP drawing of **PO20**

Table 70 ^1H , ^{13}C NMR, DEPT and HMBC spectral data of compound **PO20** and ^{13}C NMR of 5,6-dihydro-6 α -hydroxysalviasperanol (**R**)

Position	DEPT	$\delta_{\text{C}}/\text{ppm}$		$\delta_{\text{H}}/\text{ppm}$ (mult., J in Hz)	HMBC
		R ^b	PO20 ^c		
1	CH ₂	29.6	29.5	1.45–1.60 m ^a 1.70–1.80 m ^a	
2	CH ₂	15.2	15.1	1.70–1.80 m ^a	
3	CH ₂	30.0	30.3	1.45–1.60 m ^a	
4	C	31.3	31.2		
5	CH	58.1	57.4	1.26 d (6.4)	3, 6, 7, 10, 18, 20
6	CH	77.9	77.9	4.17 t (6.4)	4, 5, 7, 8
7	CH	78.4	78.2	4.57 d (6.4)	5, 8, 9, 10, 14
8	C	126.6	126.2		
9	C	117.3	117.6		
10	C	80.5	80.9		
11	C	142.3	142.7		
12	C	140.6	141.4		
13	C	132.3	133.0		
14	CH	115.7	115.6	6.47 s	7, 9, 12, 15
15	CH	27.2	26.9	3.14 sept (6.8)	12, 13, 14, 16, 17
16	CH ₃	22.6	22.6	1.16 d (6.8)	13, 15, 17
17	CH ₃	22.6	22.7	1.16 d (6.8)	13, 15, 16
18	CH ₃	30.1	29.9	0.91 s	3, 4, 5, 19
19	CH ₃	22.8	22.8	0.92 s	3, 4, 5, 18
20	CH ₂	30.4	39.9	2.41 d (16.4) 2.68 d (16.4)	1, 5, 8, 9, 10, 11

^a Deduced from HMQC experiment.

^b Spectrum recorded at 50 (^{13}C NMR) MHz, CDCl_3 .

^c Spectra recorded at 400 (^1H NMR) and 100 (^{13}C NMR) MHz, CDCl_3 .

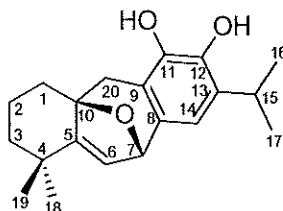
Table 71 Comparison of ^1H NMR spectral data of compounds **PO20** and 5,6-dihydro-6 α -hydroxysalviasperanol

Position	δ_{H} /ppm (mult., J in Hz)	
	PO20 ^a	5,6-dihydro-6 α -hydroxysalviasperanol ^b
1	1.45–1.60 m	
	1.70–1.80 m	
2	1.70–1.80 m	
3	1.45–1.60 m	
5	1.26 d (6.4)	
6	4.17 t (6.4)	4.30 t (6.2)
7	4.57 d (6.4)	4.72 d (6.2)
14	6.47 s	6.54 s
15	3.14 sept (6.8)	3.12 sept (6.8)
16	1.16 d (6.8)	1.24 d (6.8)
17	1.16 d (6.8)	1.23 d (6.8)
18	0.91 s	1.03 s
19	0.92 s	1.01 s
20	2.41 d (16.4)	2.43 d (16.0)
	2.68 d (16.4)	2.76 d (16.0)

^a Spectrum recorded at 400 (^1H NMR) MHz, CDCl_3 .

^b Spectrum recorded at 200 (^1H NMR) MHz, CDCl_3 .

3.2.21 Compound PO21



Compound **PO21** was isolated as an amorphous solid, m.p. 207-209 °C, $[\alpha]_{\text{D}}^{26} -32.5$ (CHCl_3 ; c 2.10). The IR and UV spectral data were closely related to that of **PO20**.

The close similarity of the ^1H and ^{13}C NMR spectral data of **PO21** (Table 72, Figures 117 and 118) to that of an icetexane diterpene, compound **PO20** (Table 70, Figures 115 and 116), indicated that **PO21** has the same 7,10-hemiketalic icetexane skeleton as **PO20**. Analysis of the HMQC and HMBC spectra supported this structure. However, instead of the hydroxy group as in **PO20**, a doublet, observed in the ^1H NMR spectrum of **PO21** at δ 6.03 ($J= 2.0$ Hz) was assigned to the olefinic proton at C-6. The ^{13}C NMR and DEPT experiments also proved the presence of two additional sp^2 carbon atoms at δ 149.1 (C-5) and δ 128.2 (C-6) in **PO21**, which was associated with the absence of the ^1H NMR signal of H-5 at δ 1.26 and 4.17 as in **PO20**. This finding was further supported by HMBC correlations (Table 72) from CH_3 -18, CH_3 -19, CH_2 -20 and H-7 to C-5 (δ 149.1). By comparison of the ^1H and ^{13}C NMR spectral data with the previously reported data [Esquivel *et al.*, 1995, $[\alpha]_{\text{D}}^{26} -31.5$ (CHCl_3 ; c 0.2)] (Table 73), therefore compound **PO21** was identified as salviasperanol.

Table 72 ^1H , ^{13}C NMR, DEPT and HMBC spectral data of compound **PO21** and ^{13}C NMR of salviasperanol (**R**)

Position	DEPT	$\delta_{\text{C}}/\text{ppm}$		$\delta_{\text{H}}/\text{ppm}$ (mult., J in Hz)	HMBC
		R^{b}		PO21 ^c	
1	CH ₂	38.6	38.5	1.77 m ^a 2.13 m ^a	3, 5, 10, 20
2	CH ₂	19.0	18.9	1.78 m ^a	
3	CH ₂	40.0	40.0	1.35 m ^a 1.58 m ^a	
4	C	33.6	33.6		
5	C	149.5	149.1		
6	CH	128.3	128.2	6.03 d (2.0)	4, 5, 7, 10
7	CH	79.9	80.5	5.08 d (2.0)	5, 6, 8, 9, 10, 14
8	C	131.4	130.5		
9	C	117.0	117.4		
10	C	83.8	84.0		
11	C	142.6	143.0		
12	C	139.9	141.1		
13	C	131.0	131.9		
14	CH	112.1	111.8	6.41 s	7, 9, 12, 13, 15
15	CH	27.0	26.8	3.20 sept (6.8)	12, 13, 14, 16, 17
16	CH ₃	22.4	22.3	1.25 d (6.8)	13, 15, 17
17	CH ₃	22.8	22.6	1.17 d (6.8)	13, 15, 16
18	CH ₃	29.9	29.6	1.01 s	3, 4, 5, 19
19	CH ₃	27.7	27.3	1.12 s	3, 4, 5, 18
20	CH ₂	30.2	30.5	2.64 d (16.8) 2.98 d (16.8)	1, 5, 8, 9, 10, 11

^a Deduced from HMQC experiment.

^b Spectrum recorded at 50 (^{13}C NMR) MHz, CDCl_3 .

^c Spectra recorded at 400 (^1H NMR) and 100 (^{13}C NMR) MHz, CDCl_3 .

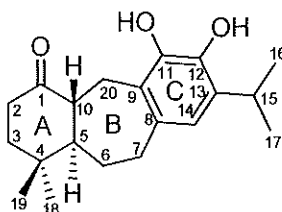
Table 73 Comparison of ^1H NMR spectral data of compounds **PO20**, **PO21** and salviasperanol

Position	δ_{H} /ppm (mult., J in Hz)		
	PO20 ^a	PO21 ^a	salviasperanol ^b
1	1.45–1.60 m	1.77 m	
	1.70–1.80 m	2.13 m	
2	1.70–1.80 m	1.78 m	
3	1.45–1.60 m	1.35 m	
		1.58 m	
5	1.26 d (6.4)		
6	4.17 t (6.4)	6.03 d (2.0)	6.04 dd (2.1, 0.8)
7	4.57 d (6.4)	5.08 d (2.0)	5.07 d (2.1)
14	6.47 s	6.41 s	6.43 s
15	3.14 sept (6.8)	3.20 sept (6.8)	3.08 sept (6.8)
16	1.16 d (6.8)	1.25 d (6.8)	1.24 d (6.8)
17	1.16 d (6.8)	1.17 d (6.8)	1.30 d (6.8)
18	0.91 s	1.01 s	1.02 s
19	0.92 s	1.12 s	1.12 s
20	2.41 d (16.4)	2.64 d (16.8)	2.65 d (16.5)
	2.68 d (16.4)	2.98 d (16.8)	2.88 d (16.5)

^a Spectra recorded at 400 (^1H NMR) MHz, CDCl_3 .

^b Spectrum recorded at 200 (^1H NMR) MHz, CDCl_3 .

3.2.22 Compound PO22



Compound **PO22** was isolated as colorless crystals, m.p. 179-182 °C, $[\alpha]_D^{26} +107.5$ (CHCl₃; *c* 0.41). The IR spectrum displayed the absorption bands due to carbonyl (1686 cm⁻¹) and hydroxyl groups (3293 cm⁻¹). The UV spectrum was closely related to that of **PO20**.

The ¹H NMR spectral data of **PO22** (Table 74, Figure 119) displayed signals for an isopropyl group as two methyl doublets at δ 1.23 and 1.20 ($J = 6.9$ Hz, CH₃-16 and CH₃-17) and a septet at δ 3.23 ($J = 6.9$ Hz, H-15). Signals for two tertiary methyl groups were evident as two singlets at δ 1.08 (CH₃-18) and 0.91 (CH₃-19). In addition, two methine protons were shown as resonances at δ 1.14 (1H, m, H-5) and 2.70 (1H, dd, $J = 12.0, 6.6$ Hz, H-10) while the methylene protons were displayed at δ 3.15 (1H, d, $J = 14.4$ Hz, H-20a), 2.60 (1H, dd, $J = 14.4, 6.6$ Hz, H-20b), δ 2.27 (1H, ddd, $J = 13.5, 4.5, 2.7$ Hz, H-2a), δ 2.53 (1H, dt, $J = 13.5, 6.3$ Hz, H-2b), δ 1.54 (1H, dt, $J = 13.5, 4.5$ Hz, H-3a), δ 1.70 (1H, ddd, $J = 13.5, 6.3, 2.7$ Hz, H-3b), δ 1.57 (1H, m, H-6a), δ 1.91 (1H, dddd, $J = 16.5, 6.0, 5.7, 2.7$ Hz, H-6b), δ 2.60 (1H, m, H-7a), and δ 2.99 (1H, ddd, $J = 15.6, 10.5, 5.7$ Hz, H-7b).

The ¹³C NMR and DEPT spectral data of **PO22** (Table 74, Figure 120) displayed 20 carbon signals in which contained four methyls, five methylenes, four methines (including one olefinic carbon), and seven quaternary carbons (including five olefinic ones and a carbonyl one). A ketone carbon signal at δ 217.2 was also observed. These data indicated an icetexane diterpene skeleton similar to that of rosmaridiphrenol (Houlihan et al., 1984) except for the location of carbonyl in **PO22** was attached to cyclohexane in ring A. This finding was further supported by HMBC correlations (Table 75).

The relative stereochemistry of **PO22** was deduced by analysis of its NOESY spectrum. Correlations from Me-19 to H-10 and Me-18 to H-5 revealed that H-10 and H-5 were in β and α configuration, respectively. By comparison of the ^1H and ^{13}C NMR spectral data with the previously reported data [Pertino *et al.*, 2010, $[\alpha]_{\text{D}}^{26} +23$ (CHCl_3 ; c 0.2)] (**Table 75**), therefore compound **PO22** was identified as 11,12-dihydroxy-8,11,13-icetexatrien-1-one.

Table 74 ^1H , ^{13}C NMR, DEPT and HMBC spectral data of compound **PO22** (300 (^1H NMR) and 75 (^{13}C NMR) MHz, CDCl_3)^b and ^{13}C NMR of 11,12-dihydroxy-8,11,13-icetexatrien-1-one (100 MHz, CDCl_3)^a

Position	DEPT	$\delta_{\text{C}}/\text{ppm}$		$\delta_{\text{H}}/\text{ppm}$ (mult., <i>J</i> in Hz)	HMBC
		R^{a}	PO22^b		
1	CO	217.2	217.2		
2	CH ₂	38.4	38.5	2.27 ddd (13.5, 4.5, 2.7) 2.53 td (13.5, 6.3)	1, 3, 4, 10
3	CH ₂	42.2	42.2	1.54 td (13.5, 4.5) 1.70 ddd (13.5, 6.3, 2.7)	1, 2, 4, 4, 18, 19
4	C	33.6	33.6		
5	CH	48.9	48.9	1.14 m	4, 6, 10, 18, 19
6	CH ₂	24.5	24.5	1.57 m 1.91 dddd (16.5, 6.0, 5.7, 2.7)	4, 7, 8, 10
7	CH ₂	30.3	30.4	2.60 m 2.99 ddd (15.6, 10.5, 5.7)	6, 8, 9, 14
8	C	130.3	130.4		
9	C	122.8	120.7		
10	CH	49.5	49.5	2.70 dd (12.0, 6.6)	1, 4, 5, 6, 9, 20
11	C	141.8	140.1		
12	C	142.6	141.8		
13	C	131.7	131.8		
14	CH	117.7	117.9	6.47 s	7, 9, 12, 13, 15
15	CH	27.1	27.2	3.23 sept (6.9)	12, 14, 16, 17
16	CH ₃	22.1	22.1	1.23 d (6.9)	13, 15, 17
17	CH ₃	22.9	22.9	1.20 d (6.9)	13, 15, 16
18	CH ₃	19.9	19.9	1.08 s	3, 4, 5, 19
19	CH ₃	28.9	29.0	0.91 s	3, 4, 5, 18
20	CH ₂	22.7	22.7	2.60 dd (14.4, 6.6) 3.15 d (14.4)	1, 8, 9, 10, 11
11-OH				7.96 br s	
12-OH				5.76 s	11, 12, 13

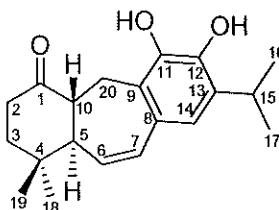
Table 75 Comparison of ^1H spectrum data of compounds **PO22** and 11,12-dihydroxy-8,11,13-icetexatrien-1-one (**R**)

Position	$\delta_{\text{H}}/\text{ppm}$ (mult., J in Hz)	
	PO22 ^b	R ^a
2	2.27 ddd (13.5, 4.5, 2.7)	2.22 ddd (14.1, 4.3, 2.8)
	2.53 td (13.5, 6.3)	2.52 ddd (14.1, 14.1, 6.3)
3	1.54 td (13.5, 4.5)	1.54 ddd (14.1, 13.1, 4.3)
	1.70 ddd (13.5, 6.3, 2.7)	1.69 ddd (14.1, 13.1, 4.3)
5	1.14 m	1.13 ddd (13.9, 11.9, 2)
6	1.57 m, 1.91 dddd (16.5, 6.0, 5.7, 2.7)	1.52 m
		1.91 m
7	2.60 m, 2.99 ddd (15.6, 10.5, 5.7)	2.68 m
		2.98 ddd
10	2.70 dd (12.0, 6.6)	2.70 m
14	6.47 s	6.47 s
15	3.23 sept (6.9)	3.23 dq (6.8, 6.8)
16	1.23 d (6.9)	1.23 d (6.8)
17	1.20 d (6.9)	1.20 d (6.8)
18	1.08 s	1.07 s
19	0.91 s	0.90 s
20	2.60 dd (14.4, 6.6)	2.58 d (14.0)
	3.15 d (14.4)	3.14 d (14.0)
11-OH	7.96 br s	
12-OH	5.76 s	

^a Spectra recorded at 400 (^1H NMR) MHz, CDCl_3 .

^b Spectrum recorded at 300 (^1H NMR) MHz, CDCl_3 .

3.2.23 Compound PO23



Compound **PO23** was isolated as colorless crystals after recrystallization from CH_2Cl_2 , m.p. 176–178 °C, $[\alpha]_{\text{D}}^{24} -182.2$ (CHCl_3 ; c 2.93). A molecular formula $\text{C}_{20}\text{H}_{26}\text{O}_3$ was determined by HREIMS (calcd 314.1882, found 314.1894 $[\text{M}]^{+\bullet}$), implying eight degrees of unsaturation. The UV spectrum of **PO23** showed absorption maxima at λ_{max} 219, 269, and 292 nm, indicating the presence of a conjugated system. Its IR spectrum showed absorption bands at 3478, 1681, and 1629 cm^{-1} suggested the presence of hydroxyl, carbonyl, and aromatic functional groups in the molecule. The subsequent X-ray structure (**Figure 31**) showed an icetexane-type diterpenoid skeleton whose structure could be derived from abietane (Simmons *et al.*, 2009). The structure was also established from analysis of its spectroscopic data.

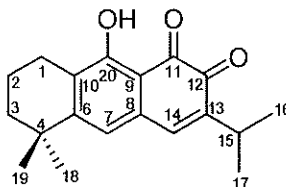
The ^1H NMR spectral data of **PO23** (**Table 76**, **Figure 121**) displayed signals for an isopropyl group as two methyl doublets at δ 1.21 ($J = 6.8$ Hz, CH_3 -16 and CH_3 -17) and a septet at δ 3.27 ($J = 6.8$ Hz, H-15). Signals for two tertiary methyl groups were evident as two singlets at δ 0.90 (CH_3 -18) and 1.24 (CH_3 -19). Furthermore two methine protons were shown as resonances at δ 1.90 (1H, ddd, $J = 13.6, 6.0, 1.6$ Hz, H-5) and 3.31 (1H, dd, $J = 13.6, 6.0$ Hz, H-10) while three olefinic methine protons were displayed at δ 5.90 (1H, dd, $J = 10.4, 6.0$ Hz, H-6), 6.57 (s, H-14) and 6.62 (1H, dd, $J = 10.4, 6.0$ Hz, H-7), whose assignments were based on the HMBC experiments (**Table 76**, **Figures 30**). A ketone carbon signal at δ 216.6 was also observed. These data indicated an icetexane diterpene skeleton similar to that of 11,12-dihydroxy-8,11,13-icetexatrien-1-one (**PO22**) except for the replacement of $-\text{CH}_2-\text{CH}_2-$ in the heptacyclic of **PO22** by $-\text{CH}=\text{CH}-$ moiety in **PO23**. The placement of a double bond at C-6 and C-7 was confirmed by the HMBC experiment (**Table 76**, **Figure 30**). The NOESY spectrum showed the correlations between CH_3 -18/H-5, H-

Table 76 ^1H , ^{13}C NMR, DEPT and HMBC spectral data of compound PO23

Position	DEPT	$\delta_{\text{C}}/\text{ppm}$	$\delta_{\text{H}}/\text{ppm}$ (mult., J in Hz)	HMBC
1	CO	216.6		
2	CH ₂	38.2	2.33 ddd (13.6, 4.8, 2.0) 2.53 td (13.6, 6.4)	1, 3, 4, 10
3	CH ₂	41.5	1.52 td (13.6, 4.8) 1.75 ddd (13.6, 6.4, 2.0)	1, 2, 4, 5, 18, 19
4	C	32.6		
5	CH	51.6	1.90 ddd (13.6, 6.0, 1.6)	1, 3, 7, 10, 18, 19, 20
6	CH	129.0	5.90 dd (10.4, 6.0)	4, 5, 8, 9, 10
7	CH	131.3	6.62 dd (10.4, 6.0)	5, 8, 9, 14
8	C	130.1		
9	C	122.7		
10	CH	60.1	3.31 dd (13.6, 6.0)	1, 4, 5, 6, 9, 20
11	C	140.5		
12	C	142.6		
13	C	132.1		
14	CH	117.7	6.57 s	7, 9, 12, 15
15	CH	27.1	3.27 sept (6.8)	12, 13, 14, 16, 17
16	CH ₃	22.7	1.21 d (6.8)	13, 15, 17
17	CH ₃	22.3	1.21 d (6.8)	13, 15, 16
18	CH ₃	29.2	0.90 s	3, 4, 5, 19
19	CH ₃	19.9	1.24 s	3, 4, 5, 18
20	CH ₂	24.3	2.30 dd (14.0, 6.8) 3.03 d (14.0)	1, 5, 8, 9, 10, 11
11-OH			8.01 s	9, 11, 12
12-OH			6.00 s	11, 12, 13

Spectra recorded at 400 (^1H NMR) and 100 (^{13}C NMR) MHz, CDCl_3 .

3.2.24 Compound PO24



Compound **PO24** was isolated as a red amorphous solid, m.p. 135–137 °C; $[\alpha]_D^{24} +112.4$ (CHCl₃; *c* 0.21), which was further recrystallized from hexane/CH₂Cl₂ to yield orange single crystals. A molecular formula C₁₉H₂₂O₃ was implied by HREIMS (calcd 298.1569, found 298.1566 [M]⁺⁺). Strong absorption bands for a hydroxyl (3327 cm⁻¹), a quinoid carbonyl (1691 and 1667 cm⁻¹) and an aromatic (1654 and 1598 cm⁻¹) groups were shown in the IR spectrum, while the absorption bands (223, 263 and 451 nm) in the UV spectrum indicated quinone group. Signals for two carbonyl groups (δ_C 180.9 and 181.8) were evident from the ¹³C NMR spectrum. The X-ray data of **PO24** (Figure 33) showed a linear tricyclic of cyclohexane-*ortho*-naphthoquinone skeleton.

The 19 carbon signals were observed in the ¹³C NMR spectrum of **PO24** (Table 77, Figure 124) which were further classified by DEPT experiments as four methyl, three methylene, two olefinic methine, one methine, six quaternary olefinic, two carbonyl, and one quaternary carbons.

The ¹H NMR spectrum of **PO24** (Table 77, Figure 123) showed signals for two methyls at δ 1.29, (s, CH₃-18 and CH₃-19), an isopropyl moiety (δ 1.16, d, *J* = 6.9 Hz, CH₃-16 and CH₃-17) and δ 3.06, 1H, sept, *J* = 6.9 Hz, H-15), two singlets of the olefinic methine protons at δ 7.06 and 6.80 (s, H-14 and H-7, respectively), and a chelated hydroxyl proton (δ 12.50, s). The COSY spectrum showed cross-peaks between methylene protons: H₂-2 (δ 1.65-1.75, 1.77-1.89) and H₂-1 (δ 2.67)/H₂-3 (δ 1.60-1.75). On the basis of the above spectroscopic and X-ray crystallographic data, compound **PO24** was a new compound and designated as obtusinone A (Salae *et al.*, 2012).

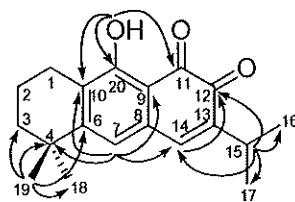


Figure 32 Major selected HMBC correlations of **PO24**

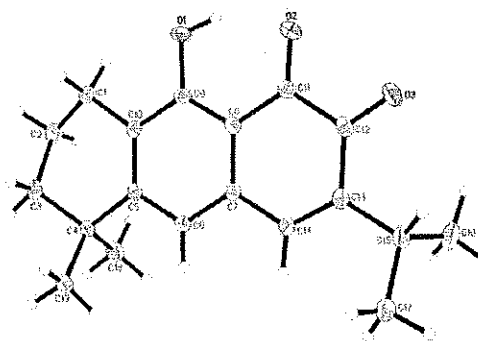


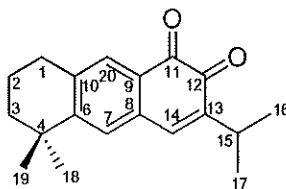
Figure 33 ORTEP drawing of **PO24**

Table 77 ^1H , ^{13}C NMR, DEPT and HMBC spectral data of compound **PO24**

Position	DEPT	$\delta_{\text{C}}/\text{ppm}$	$\delta_{\text{H}}/\text{ppm}$ (mult., J in Hz)	HMBC
1	CH ₂	23.1	2.67 t (6.3)	2, 3, 5, 8, 9, 10
2	CH ₂	18.2	1.65–1.75 m 1.77–1.89 m	1, 3, 4, 10
3	CH ₂	38.0	1.60–1.75 m	1, 2, 4, 5, 18, 19
4	C	34.8		
5				
6	C	158.0		
7	CH	121.0	6.80 s	4, 5, 8, 9, 10, 11, 14
8	C	131.8		
9	C	111.1		
10	C	128.8		
11	CO	181.8		
12	CO	180.9		
13	C	145.0		
14	CH	138.4	7.06 s	6, 7, 8, 9, 12, 13, 15
15	CH	26.9	3.06 sept (6.9)	12, 13, 14, 16, 17
16	CH ₃	21.6	1.16 d (6.9)	13, 15, 17
17	CH ₃	21.6	1.16 d (6.9)	13, 15, 16
18	CH ₃	30.5	1.29 s	3, 4, 5, 19
19	CH ₃	30.5	1.29 s	3, 4, 5, 18
20	C	165.2		
20-OH			12.50 s	5, 8, 9, 10, 11

Spectra recorded at 300 (^1H NMR) and 75 (^{13}C NMR) MHz, CDCl_3 .

3.2.25 Compound PO25



Compound **PO25** was also isolated as an orange amorphous solid, m.p. 89–91 °C, $[\alpha]_D^{24} +14.9$ (CHCl₃; *c* 1.17). The HREIMS of **PO25** showed a molecular ion [M]⁺ peak at *m/z* 282.1614 (calcd 282.1620), consistent with the molecular formula C₁₉H₂₂O₂ with nine degrees of unsaturation similar to that of **PO24**. The UV and IR spectra were similar to those of **PO24**. The ¹H and ¹³C NMR spectral data (Table 78, Figures 125 and 126) of **PO25** were very similar to those of **PO24** (Table 77 and 79, Figures 123 and 124) except for the presence of a singlet signal of an aromatic methine proton at δ 7.72 in **PO25** instead of a chelated hydroxyl proton at δ 12.50 as in **PO24**. This aromatic methine proton showed HMBC correlations (Table 78, Figures 34) with δ 34.6 (C-4), δ 155.0 (C-6), δ 133.0 (C-8) and δ 179.6 (C-11) which supported its location at C-20. Thus, **PO25** was a new compound and designated as obtusinone B (Salae *et al.*, 2012).

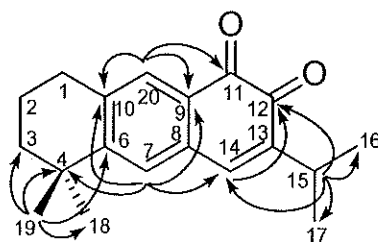


Figure 34 Major selected HMBC correlations of **PO25**

Table 78 ^1H , ^{13}C NMR, DEPT and HMBC spectral data of compound **PO25**

Position	DEPT	$\delta_{\text{C}}/\text{ppm}$	$\delta_{\text{H}}/\text{ppm}$ (mult., J in Hz)	HMBC
1	CH ₂	30.4	2.78 t (6.4)	2, 3, 5, 9, 10
2	CH ₂	19.1	1.75–1.85 m	1, 3, 4, 10
3	CH ₂	38.5	1.65–1.71 m	1, 2, 4, 5, 18, 19
4	C	34.6		
5				
6	C	155.0		
7	CH	128.0	7.22 s	4, 8, 10, 11
8	C	133.0		
9	C	127.7		
10	C	138.6		
11	CO	179.6		
12	CO	181.2		
13	C	145.2		
14	CH	139.1	7.13 s	6, 8, 12, 15
15	CH	26.9	3.05 sept (6.8)	12, 13, 14, 16, 17
16	CH ₃	21.6	1.16 d (6.8)	13, 15, 17
17	CH ₃	21.6	1.16 d (6.8)	13, 15, 16
18	CH ₃	31.3	1.32 s	3, 4, 5, 19
19	CH ₃	31.3	1.32 s	3, 4, 5, 18
20	CH	131.2	7.72 s	4, 6, 7, 11

Spectra recorded at 400 (^1H NMR) and 100 (^{13}C NMR) MHz, CDCl_3 .

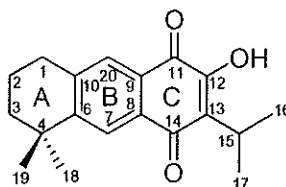
Table 79 Comparison of ^1H and ^{13}C NMR spectral data of compounds **PO24** and **PO25**

Position	$\delta_{\text{C}}/\text{ppm}$		$\delta_{\text{H}}/\text{ppm}$ (mult., J in Hz)	
	PO24 ^a	PO25 ^b	PO24 ^a	PO25 ^b
1	23.1	30.4	2.67 t (6.3)	2.78 t (6.4)
2	18.2	19.1	1.65–1.75 m 1.77–1.89 m	1.75–1.85 m
3	38.0	38.5	1.60–1.75 m	1.65–1.71 m
4	34.8	34.6		
5				
6	158.0	155.0		
7	121.0	128.0	6.80 s	7.22 s
8	131.8	133.0		
9	111.1	127.7		
10	128.8	138.6		
11	181.8	179.6		
12	180.9	181.2		
13	145.0	145.2		
14	138.4	139.1	7.06 s	7.13 s
15	26.9	26.9	3.06 sept (6.9)	3.05 sept (6.8)
16	21.6	21.6	1.16 d (6.9)	1.16 d (6.8)
17	21.6	21.6	1.16 d (6.9)	1.16 d (6.8)
18	30.5	31.3	1.29 s	1.32 s
19	30.5	31.3	1.29 s	1.32 s
20	165.2	131.2		7.72 s
20-OH			12.50 s	

^a Spectra recorded at 300 (^1H NMR) and 75 (^{13}C NMR) MHz, CDCl_3 .

^b Spectra recorded at 400 (^1H NMR) and 100 (^{13}C NMR) MHz, CDCl_3 .

3.2.26 Compound PO26



Compound **PO26** was obtained as a red amorphous solid, m.p. 104–106 °C, $[\alpha]_D^{24} +57.2$ (CHCl_3 ; c 0.12). The molecular formula $\text{C}_{19}\text{H}_{22}\text{O}_3$ as determined by the HREIMS (calcd 298.1569, found 298.1563 $[\text{M}]^{+*}$) indicating nine degrees of unsaturation. The IR spectrum of **PO26** exhibited bands for carbonyl (1728 and 1650 cm^{-1}), hydroxyl (3386 cm^{-1}) and aromatic (1628 cm^{-1}) groups. Furthermore, the presence of two carbonyl groups at δ 184.8 and 181.8 in the ^{13}C NMR spectrum and the UV absorption maxima at λ_{max} 215, 285, 353 and 411 nm indicated that **PO26** should have a *para*-naphthoquinone chromophore (Lin *et al.*, 1989).

The ^1H and ^{13}C NMR spectral data of **PO26** (Table 80, Figures 127 and 128) were comparable to those of **PO25** (Table 78 and 81, Figures 125 and 126) except for the differences in ring C in which that of **PO25** was an *ortho*-quinonoid but that of **PO26** was a *para*-quinonoid. A singlet signal of an aromatic methine proton H-14 at δ_{H} 7.13; δ_{C} 139.1 shown in **PO25** was replaced by a hydroxyl signal at δ 7.41 in **PO26** whose location at C-12 was suggested from the HMBC correlations (Table 80, Figures 35) of H-15 at δ 3.40 with the carbons at δ 128.4 (C-13), 152.7 (C-12) and 184.8 (C-14). Furthermore an aromatic proton H-7 which appeared at δ 7.22 in **PO25** was shifted more downfield in **PO26** to δ 8.06 supporting a carbonyl group at

C-14. Based on all of the spectroscopic evidence, the structure of **PO26** was a new compound and characterized as obtusinone C (Salae *et al.*, 2012).

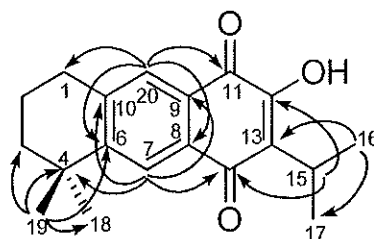


Figure 35 Major selected HMBC correlations of **PO26**

Table 80 ^1H , ^{13}C NMR, DEPT and HMBC spectral data of compound **PO26**

Position	DEPT	$\delta_{\text{C}}/\text{ppm}$	$\delta_{\text{H}}/\text{ppm}$ (mult., J in Hz)	HMBC
1	CH ₂	30.8	2.86 t (6.3)	2, 3, 5, 9, 10
2	CH ₂	19.1	1.80–1.85 m	1, 3, 4, 10
3	CH ₂	38.6	1.65–1.75 m	1, 2, 4, 5, 18, 19
4	C	34.9		
5				
6	C	154.1		
7	CH	125.7	8.06 s	1, 4, 7, 8, 10, 11, 14
8	C	131.1		
9	C	126.3		
10	C	141.9		
11	CO	181.8		
12	C	152.7		
13	C	128.4		
14	CO	184.8		
15	CH	24.6	3.40 sept (7.2)	12, 13, 14, 16, 17
16	CH ₃	19.9	1.30 d (7.2)	13, 15, 17
17	CH ₃	19.9	1.30 d (7.2)	13, 15, 16
18	CH ₃	31.3	1.33 s	3, 4, 5, 19
19	CH ₃	31.3	1.33 s	3, 4, 5, 18
20	CH	127.0	7.72 s	1, 5, 7, 11, 14
12-OH			7.41 s	11, 12, 13

Spectra recorded at 300 (^1H NMR) and 75 (^{13}C NMR) MHz, CDCl_3 .

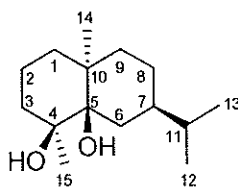
Table 81 Comparison of ^1H and ^{13}C NMR spectral data of compounds **PO25** and **PO26**

Position	$\delta_{\text{C}}/\text{ppm}$		$\delta_{\text{H}}/\text{ppm}$ (mult., J in Hz)	
	PO25 ^a	PO26 ^b	PO25 ^a	PO26 ^b
1	30.4	30.8	2.78 t (6.4)	2.86 t (6.3)
2	19.1	19.1	1.75–1.85 m	1.80–1.85 m
3	38.5	38.6	1.65–1.71 m	1.65–1.75 m
4	34.6	34.9		
5				
6	155.0	154.1		
7	128.0	125.7	7.22 s	8.06 s
8	133.0	131.1		
9	127.7	126.3		
10	138.6	141.9		
11	179.6	181.8		
12	181.2	152.7		
13	145.2	128.4		
14	139.1	184.8	7.13 s	
15	26.9	24.6	3.05 sept (6.8)	3.40 sept (7.2)
16	21.6	19.9	1.16 d (6.8)	1.30 d (7.2)
17	21.6	19.9	1.16 d (6.8)	1.30 d (7.2)
18	31.3	31.3	1.32 s	1.33 s
19	31.3	31.3	1.32 s	1.33 s
20	131.2	127.0	7.72 s	7.72 s
12-OH				7.41 s

^a Spectra recorded at 400 (^1H NMR) and 100 (^{13}C NMR) MHz, CDCl_3 .

^b Spectra recorded at 300 (^1H NMR) and 75 (^{13}C NMR) MHz, CDCl_3 .

3.2.27 Compound PO27



Compound **PO27** was isolated as a colorless oil, $[\alpha]_D^{26} -54.0$. Its IR spectrum showed an absorption band at 3400 cm^{-1} , indicating the presence of hydroxyl groups.

The ^{13}C NMR and DEPT spectra indicated that **PO27** (**Table 82**, **Figure 130**) contained 15 resonances including two methine, six methylene, four methyl carbons as well as three quaternary carbons. Two oxygenated quaternary carbon signals at δ 74.6 and 78.6 in the ^{13}C NMR spectrum indicated the presence of two tertiary hydroxyl groups. The ^1H and ^{13}C NMR spectra of **PO27** suggested an eudesmane framework with oxygenated function at C-4 (δ_{C} 74.6) and C-5 (δ_{C} 78.6). Analysis of the ^1H NMR spectrum of **PO7** (**Table 82**, **Figure 129**) suggested an isopropyl [δ 0.92 (3H, d, $J = 6.9$ Hz, H-12), 0.89 (3H, d, $J = 6.9$ Hz, H-13), 2.02 (1H, dq, $J = 10.5, 6.9, 6.9$ Hz, H-11)], two methyl [δ 1.01 (3H, s, H-14), 1.27 (3H, s, H-15)]. The above-mentioned ^1H and ^{13}C NMR spectra of **PO27** showed a close similarity to those of dihydrokongol (Eduardo *et al.*, 1979). However, the methine carbon signal at δ 51.7 of C-5 in dihydrokongol was absent in the ^{13}C NMR spectrum of **PO27**. Instead, an oxyquaternary carbon signal appearing at δ 78.6 was observed. This suggested that **PO27** was a 5-hydroxyl derivative of dihydrokongol. This conclusion was confirmed by HMBC experiment (**Table 82**, **Figure 36**). The relative configuration of **PO27** was derived from NOESY correlation of H-14/H-6 α , H-14/H-15 and 6 α /7 α (**Figure 36**). Thus on the basis of its spectroscopic data and comparison of the ^1H and ^{13}C NMR spectral data with the previous report (Jakupovic *et al.*, 1992) (**Table 82** and **83**), compound **PO27** was identified as 4 β ,5 β -dihydroxy-10-*epi*-eudesmane.

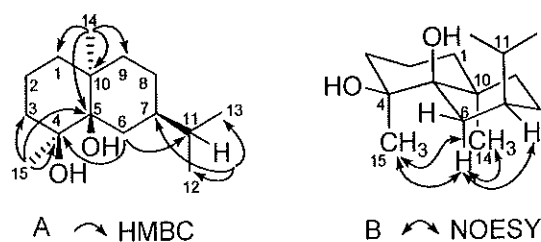


Figure 36 Selected HMBC correlations (A) and NOESY correlations (B) for **PO27**

Table 82 ^1H , ^{13}C NMR, DEPT and HMBC spectral data of compound **PO27** and ^{13}C NMR of 4 β ,5 β -dihydroxy-10-*epi*-eudesmane (**R**)

Position	DEPT	$\delta_{\text{C}}/\text{ppm}$		$\delta_{\text{H}}/\text{ppm}$ (mult., J in Hz)	HMBC
		R ^b	PO12 ^c		
1	CH ₂	33.7	33.7	1.53–1.68 m ^a	
2	CH ₂	19.2	19.2	1.44–1.66 m ^a	
3	CH ₂	37.0	37.0	1.88, 1.45 m ^a	
4	C	74.6	74.6		
5	C	78.8	78.6		
6	CH ₂	26.0	26.1	1.87, 1.65 m ^a	
7	CH	40.5	40.7	1.34 m ^a	
8	CH ₂	22.4	22.4	1.81, 1.65 m ^a	
9	CH ₂	34.7	34.7	1.87, 0.90 m ^a	
10	C	37.6	37.5		
11	CH	29.3	29.7	2.02 dq (10.5, 6.9, 6.9)	7, 8, 12, 13
12	CH ₃	21.9	21.9	0.92 d (6.9)	7, 11, 13
13	CH ₃	22.9	22.9	0.89 d (6.9)	7, 11, 12
14	CH ₃	22.7	22.7	1.01 s	3, 4, 5
15	CH ₃	24.0	24.0	1.27 s	1, 5, 9, 10

^a Deduced from HMQC experiment.

^b Spectrum recorded at 100 (^{13}C NMR) MHz, CDCl_3 .

^c Spectra recorded at 300 (^1H NMR) and 75 (^{13}C NMR) MHz, CDCl_3 .

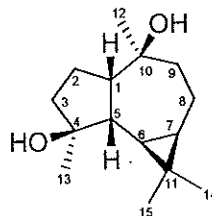
Table 83 Comparison of ^1H NMR spectral data of compounds **PO27** and 4 β ,5 β -dihydroxy-10-*epi*-eudesmane

Position	$\delta_{\text{H}}/\text{ppm}$ (mult., J in Hz)	
	PO27 ^a	4 β ,5 β -dihydroxy-10- <i>epi</i> -eudesmane ^b
1	1.53–1.68 m 0.97 m	1.48–1.67m 0.97 m
2	1.44–1.66 m	1.48–1.67m
3	1.88 m 1.45 m	1.86 br ddd 1.45 m
6	1.87 m 1.65 m	1.89 ddd (15, 2, 0.5) 1.66 dd (15, 6.5)
7	1.34 m	1.34 m
8	1.81 m 1.65 m	1.71 dddd 1.62 m
9	1.87 m 0.90 m	1.86 br ddd (14, 13, 3.5) 0.88 ddd
11	2.02 dqq (10.5, 6.9, 6.9)	2.01 dqq (10.5, 7, 7)
12	0.92 d (6.9)	0.93 d (7)
13	0.89 d (6.9)	0.89 d (7)
14	1.01 s	1.01 s
15	1.27 s	1.27 s

^a Spectra recorded at 300 (^1H NMR) MHz, CDCl_3 .

^b Spectra recorded at 400 (^1H NMR) MHz, CDCl_3 .

3.2.28 Compound PO28



Compound **PO28** was isolated as an optically active colorless prism with m.p. 138–140 °C, $[\alpha]_D^{26} -37.1$ (CHCl_3 ; c 0.76). The IR spectrum indicated the presence of hydroxyl group (3396 cm^{-1}). Analysis the ^{13}C NMR and DEPT spectra indicated that **PO28** (Table 84, Figure 132) contained 15 resonances including four methyl, four methylene, four methine and three quaternary carbons including two oxygenated quaternary carbon signals (δ_{C} 75.0 and 80.3).

The ^1H NMR spectrum of **PO28** (Table 84, Figure 131) showed two methine protons [δ 0.42 (1H, dd, $J= 10.8, 9.6$ Hz, H-6), 0.64 (1H, ddd, $J= 11.2, 9.6, 6.4$ Hz, H-7)] and two methyl groups [δ 1.04 (6H, s, H-14 and H-15)], characteristic for the presence of a cyclic propane in the aromadendrane skeleton (Vlakhov *et al.*, 1967). The coupling constant ($J= 9.6$ Hz) between H-6 and H-7 suggested that H-6 and H-7 were *cis* form (Bohlmann *et al.*, 1983). Furthermore, two methine protons at δ 1.49–1.88 (1H, m, H-1), 1.20 (1H, m, H-5), four methylenes [δ 1.49–1.88 (6H, m, H-2, H-3 and H-9), 0.89 (2H, m, H-8)] and two methyls [δ 1.17 (3H, s, H-12), 1.25 (3H, s, H-13)] were also observed. The HMBC experiment (Table 84, Figure 37) showed correlations between H-12 (δ 1.17) and C-10 (δ 75.0) and H-13 (δ 1.25) and C-4 (δ 80.3), suggesting the presence of a tertiary hydroxyl group. According to the above data, the structure of **PO28** is similar to aromadendrane-4 α , 10 β -diol, which was previously isolated from *Brasilia sickie* by Bohlmann *et al.* However, the NOESY experiment (Figure 37) indicated that the relative stereochemistry of hydroxyl groups at C-4 and C-10 both had β -orientations. Thus on the basis of its spectroscopic data and comparison of the ^1H and ^{13}C NMR spectral data with the previous report [Wu *et*

al., 2000, $[\alpha]_D^{25} -20.2$ (CHCl₃; *c* 0.24)] (Table 84 and 85), compound **PO28** was identified as 4 β ,10 β -dihydroxy aromadendrane.

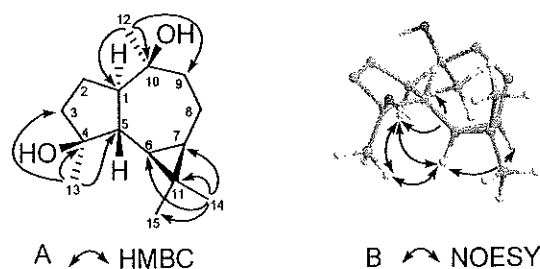


Figure 37 Selected HMBC correlations (A) and NOESY correlations (B) for **PO28**

Table 84 ¹H, ¹³C NMR, DEPT and HMBC spectral data of compound **PO28** and ¹³C NMR of 4 β ,10 β -dihydroxy aromadendrane (**R**)

Position	DEPT	δ_C /ppm		δ_H /ppm (mult., <i>J</i> in Hz)	HMBC
		R ^a	PO28 ^b		
1	CH	56.4	56.4	1.49–1.88 m ^a	
2	CH ₂	23.8	23.7	1.49–1.88 m ^a	
3	CH ₂	41.1	41.1	1.49–1.88 m ^a	
4	C	80.3	80.3		
5	CH	48.4	48.4	1.20 m ^a	
6	CH	28.3	28.3	0.42 dd (10.8, 9.6)	4, 15
7	CH	26.6	26.6	0.64 ddd (11.2, 9.6, 6.4)	5, 15
8	CH ₂	20.1	20.1	0.89 m ^a	
9	CH ₂	44.4	44.4	1.49–1.88 m ^a	
10	C	75.0	75.0		
11	C	19.5	19.5		
12	CH ₃	20.3	20.3	1.17 s	1, 9, 10
13	CH ₃	23.4	24.5	1.25 s	3, 4, 5
14	CH ₃	16.4	16.4	1.04 s	6, 7, 11, 15
15	CH ₃	28.6	28.6	1.04 s	6, 7, 11, 14

^a Deduced from HMQC experiment.

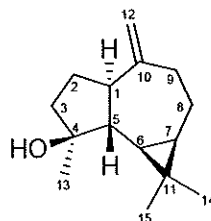
Spectra recorded at 400 (¹H NMR) and 100 (¹³C NMR) MHz, CDCl₃.

Table 85 Comparison of ^1H NMR spectral data of compounds **PO28** and 4 β ,10 β -dihydroxy aromadendrane

Position	δ_{H} /ppm (mult., J in Hz)	
	PO28	4 β ,10 β -dihydroxy aromadendrane
1	1.49–1.88 m	1.50–1.90 m
2	1.49–1.88 m	1.50–1.90 m
3	1.49–1.88 m	1.50–1.90 m
5	1.20 m	1.18 dd (10.7, 10.7)
6	0.42 dd (10.8, 9.6)	0.40 dd (10.7, 9.6)
7	0.64 ddd (11.2, 9.6, 6.4)	0.62 ddd (11.0, 9.6, 6.0)
8	0.89 m	0.88 m
9	1.49–1.88 m	1.50–1.90 m
12		1.15 s
13	1.17 s	1.23 s
14	1.25 s	1.01 s
15	1.04 s	1.01 s

Spectra recorded at 400 (^1H NMR) MHz, CDCl_3 .

3.2.29 Compound PO29



Compound **PO29** was isolated as an optically active colorless oil with $[\alpha]_{\text{D}}^{25} +12$ (CHCl_3 ; c 0.15). The IR spectrum indicated the presence of hydroxyl group (3413 cm^{-1}) and double bond (1614 cm^{-1}). The ^1H and ^{13}C NMR spectral data of **PO29** (Table 86, Figures 133 and 134) were very similar to those of **PO28** (Table 84, Figures 131 and 132) except for the presence of two singlet signals of two olefinic protons due to terminal methylene at δ 4.66 (1H, s, H-12a) and 4.68 (1H, s, H-12b) in **PO29** instead of methyl protons at δ 1.17 (H_3 -12) as in **PO28**. This finding was further confirmed by the HMBC correlations (Table 86) from H-9 (δ 2.42) to C-10 (δ 153.4) and C-12 (δ 106.3). By comparison of the ^1H and ^{13}C NMR spectral data with the previously reported data [Iwabuchi *et al.*, 1989, $[\alpha]_{\text{D}}^{22} +5.3$ (CHCl_3 ; c 3.70)] (Table 87), therefore compound **PO29** was identified as spathulenol.

Table 86 ^1H , ^{13}C NMR, DEPT and HMBC spectral data of compound **PO29** and ^{13}C NMR of spathulenol (**R**)

Position	DEPT	$\delta_{\text{C}}/\text{ppm}$		$\delta_{\text{H}}/\text{ppm}$ (mult., J in Hz)	HMBC
		R ^b	PO29 ^c		
1	CH	53.4	53.4	2.22 m ^a	5, 9
2	CH ₂	26.8	26.7	1.58, 1.85 m ^a	
3	CH ₂	41.8	41.7	1.55, 1.78 m ^a	
4	C	153.5	153.4		
5	CH	54.5	54.2	1.31 m ^a	
6	CH	30.0	29.9	0.46 dd (11.1, 9.6)	3, 7, 8, 11, 15
7	CH	27.7	27.5	0.70 m ^a	6, 11, 15
8	CH ₂	24.9	24.7	1.01, 2.00 m ^a	
9	CH ₂	39.0	38.8	2.42 dd (13.3, 6.1) 2.02 m ^a	1, 7, 8, 10, 12
10	C	80.9	80.8		
11	C	20.3	20.2		
12	CH ₂	106.3	106.3	4.66 br s 4.68 br s	1, 9, 10
13	CH ₃	26.1	26.0	1.28 s	3, 4, 5
14	CH ₃	16.4	16.3	1.03 s	6, 7, 11, 15
15	CH ₃	28.7	28.6	1.05 s	6, 7, 11, 14

^a Deduced from HMQC experiment.

^b Spectra recorded at 100 (^{13}C NMR) MHz, CDCl_3 .

^c Spectra recorded at 300 (^1H NMR) and 75 (^{13}C NMR) MHz, CDCl_3 .

Table 87 Comparison of ^1H NMR spectral data of compounds **PO29** and spathulenol

Position	$\delta_{\text{H}}/\text{ppm}$ (mult., J in Hz)	
	PO29 ^a	spathulenol ^b
1	2.22 m	
2	1.58, 1.85 m	
3	1.55, 1.78 m	
5	1.31 m	
6	0.46 dd (11.1, 9.6)	0.47 dd (11.4, 9.5)
7	0.70 m	0.71 ddd (11.4, 9.4, 5.9)
8	1.01, 2.00 m	
9	2.42 dd (13.3, 6.1)	2.42 m
	2.02 m	
12	4.66 br s	4.67 br s
	4.68 br s	4.69 br s
13	1.28 s	1.28 s
14	1.03 s	1.04 s
15	1.05 s	1.06 s

^a Spectra recorded at 300 (^1H NMR) MHz, CDCl_3 .

^b Spectra recorded at 400 (^1H NMR) MHz, CDCl_3 .

3.3 Biological activities of the isolated compounds from *D. wallichii* and *P. obtusifolia*

In this research, the isolated compounds from the roots and fresh fruits of *D. wallichii* and the roots and twigs of *P. obtusifolia* were tested for antibacterial activities against both Gram-positive bacteria: *B. subtilis*, *S. aureus*, TISTR517, *E. faecalis* TISTR459, Methicillin-Resistant *S. aureus* (MRSA) ATCC43300, Vancomycin-Resistant *E. faecalis* (VRE) ATCC 51299, *Streptococcus faecalis*, and Gram-negative bacteria: *S. typhi*, *S. sonnei* and *P. aeruginosa* (Table 88, 89, 90 and 91). The roots and twigs of *P. obtusifolia* were also tested for anti-inflammatory activity against LPS-induced NO production in RAW264.7 cell line (Table 92). In addition, the roots and fresh fruits of *D. wallichii* were also tested for cytotoxic activity against MCF-7 human cancer cell line. (Table 89)

3.3.1 Activity of isolated compounds from *D. wallichii* on antibacterial and cytotoxic activities

The antibacterial activities of naphthalene derivatives DW1-DW6, DW8, DW9, DW11 and DW12 were reported in Table 88. Compound DW1 showed significant antibacterial activity against *B. subtilis* and *E. faecalis*, but moderate activity against MRSA, VRE and *S. sonnei*. Compounds DW4 and DW5 exhibited moderate antibacterial activity against *B. subtilis* and *S. sonnei*, while compound DW1 also exhibited moderate antibacterial activity against *E. faecalis* and MRSA. Antifungal activity against *C. albicans* of all compounds was inactive. In addition, the cytotoxicity against MCF-7 cell line of compounds DW1-DW6, DW8, DW9, DW11 and DW12 was also evaluated. All compounds except compound DW6 were active. Compounds DW8 and DW9 exhibited better activity than the rest of the tested compounds with respective IC₅₀ values of 0.06 and 0.09 µg/ml. Structure-activity relationships for cytotoxic activity against MCF-7 human cancer cell line should be indicated as a binaphthoquinone skeleton was necessary for increasing the activity: mononaphthoquinone skeleton of compound DW1 was less active with the IC₅₀ value

of 0.46 μM , while binaphthoquinone skeleton of compound **DW8** and **DW9** were most active with respective IC_{50} values of 0.06 and 0.09 μM .

Table 88 Antibacterial activities against gram-positive bacteria of compounds **DW1**-**DW6**, **DW8**, **DW9**, **DW11** and **DW12** from *D. wallichii*

Compounds	Antibacterial activities (MIC, $\mu\text{g/mL}$)				
	<i>B. subtilis</i>	<i>S. aureus</i>	<i>E. faecalis</i>	<i>MRSA</i>	<i>VRE</i>
DW1	4.68	37.5	4.68	9.37	9.37
DW2	150	>300	300	>300	150
DW3	75	150	75	18.75	75
DW4	9.37	37.5	9.37	9.37	37.5
DW5	9.37	75	18.75	18.75	37.5
DW6	300	>300	300	>300	>300
DW8	150	>300	150	>300	>300
DW9	150	>300	300	150	300
DW11	75	300	150	150	150
DW12	>300	>300	>300	>300	>300
Vancomycin*	<2.34	<2.34	<2.34	<2.34	<2.34

* Standard drug.

Table 89 Antibacterial activities against gram-negative bacteria and cytotoxic against MCF-7 cell line of compounds DW1-DW6, DW8, DW9, DW11 and DW12 from *D. wallichii*

Compounds	Antibacterial activities (MIC, µg/mL)			Cytotoxic activity
	<i>S. typhi</i>	<i>S. sonnei</i>	<i>P. aeruginosa</i>	MCF-7 ^a (IC ₅₀ , µg/mL)
DW1	37.5	9.37	150	0.46
DW2	>300	150	>300	0.29
DW3	300	75	300	0.35
DW4	37.5	9.37	>300	0.80
DW5	75	9.37	300	0.86
DW6	>300	300	>300	9.57
DW8	>300	>300	>300	0.06
DW9	>300	150	>300	0.09
DW11	300	150	>300	0.78
DW12				0.51
Camptothecin*				<0.024
Vancomycin*	<2.34	<2.34	<2.34	<2.34

* Standard drug.

^a Human breast adenocarcinoma cell line.

3.3.2 Activity of isolated compounds from *P. obtusifolia* on antibacterial and anti-inflammatory activities

The antibacterial activities of the compounds **PO4**, **PO11**, **PO13**, **PO15-PO23-PO25** and **PO27** are reported in **Table 90** and **91**. Compound **PO13** showed significant antibacterial activity against *B. subtilis*, *S. aureus*, *E. faecalis*, MRSA, VRE, *S. typhi* and *S. sonnei* but weak activity against *P. aeruginosa*. Compound **PO21** showed significant antibacterial activity against *S. sonnei* but moderate activity against *B. subtilis*, *E. faecalis*, MRSA and VRE while compound **PO20** also exhibited moderate antibacterial activity against MRSA. All compounds were found to be inactive against *C. albicans*. In addition the crude hexane and CH_2Cl_2 extracts exhibited potent inhibitory activity against LPS-induced NO production in RAW264.7 cell lines with IC_{50} values of 4.3 and 6.1 $\mu\text{g/ml}$, respectively. Therefore some isolated compounds were evaluated for their anti-NO activity, the results of which are shown in **Table 92**. Compound **PO24** ($\text{IC}_{50} = 1.7 \mu\text{M}$) possessed the highest activity followed by compounds **PO13**, **PO14** and **PO25** ($\text{IC}_{50} = 6.1, 7.8$ and $6.2 \mu\text{M}$, respectively) whereas other compounds exhibited moderate and mild activities. The inhibitory activities of most isolates were much stronger than that of NO synthase inhibitor (Tewtrakul et al., 2009) L-Nitroarginine (L-NA), $\text{IC}_{50} = 61.8 \mu\text{M}$ except for compounds **PO19** and **PO27** which showed weaker activity ($\text{IC}_{50} = >100 \mu\text{M}$). Compound **PO24** also showed higher inhibitory activity than caffeic acid phenethyl ester (CAPE) ($\text{IC}_{50} = 5.2 \mu\text{M}$). Structure-activity relationships for anti-inflammatory activity should be suggested as a hydroxyl group on an *ortho*-naphthoquinone skeleton was necessary for increasing the activity: compound **PO24** with a hydroxyl group was strongly active ($\text{IC}_{50} = 1.7 \mu\text{M}$), whereas compound **PO25** was less active ($\text{IC}_{50} = 6.2 \mu\text{M}$).

Table 90 Antibacterial activities against gram-positive bacteria of compounds **PO4**, **PO11**, **PO13**, **PO15-PO21**, **PO23-PO25** and **PO27** from *P.obtusifolia*

Compounds	Antibacterial activities (MIC, µg/mL)				
	<i>B. subtilis</i>	<i>S. aureus</i>	<i>E. faecalis</i>	<i>MRSA</i>	<i>VRE</i>
PO4	300	300	300	300	300
PO11	300	>300	300	>300	>300
PO13	4.68	2.34	4.68	2.34	2.34
PO15	>300	>300	>300	>300	>300
PO16	300	300	300	300	300
PO17	300	150	300	150	150
PO18	37.5	37.5	37.5	37.5	37.5
PO19	>300	>300	>300	>300	>300
PO20	37.5	75	75	9.37	75
PO21	9.37	18.75	9.37	9.37	9.37
PO23	75	75	75	75	75
PO24	150	75	75	37.5	37.5
PO25	75	75	75	37.5	75
PO27	150	>300	150	300	300
Vancomycin*	<2.34	<2.34	<2.34	<2.34	<2.34

* Standard drug.

Table 91 Antibacterial activities against gram-negative bacteria of compounds **PO4**, **PO11**, **PO13**, **PO15-PO21**, **PO23-PO25** and **PO27** from *P. obtusifolia*

Compounds	Antibacterial activities (MIC, µg/mL)		
	<i>S. typhi</i>	<i>S. sonnei</i>	<i>P. aeruginosa</i>
PO4	300	300	300
PO11	>300	300	>300
PO13	2.46	4.68	150
PO15	>300	>300	>300
PO16	300	300	300
PO17	150	150	>300
PO18	150	37.5	150
PO19	>300	>300	>300
PO20	75	18.75	>300
PO21	37.5	2.34	>300
PO23	75	37.5	150
PO24	75	75	>300
PO25	75	75	>300
PO27	>300	75	>300
Vancomycin*	<2.34	<2.34	<2.34

* Standard drug.

Table 92 Inhibitory effects on NO production^f of compounds **PO3-PO7**, **PO11-PO15**, **PO17-PO25**, **PO27** and **PO28** from *P. obtusifolia*

NO.	% Inhibition at various concentrations (μM)					IC ₅₀ (μM)
	0	3	10	30	100	
PO3	0.0±8.8		13.8±0.5	16.5±1.2	51.6±1.1 ^b	98.1
PO4	0.0±5.4		0.9±1.2	34.5±0.6 ^b	95.3±2.5 ^{b,d}	36.8
PO5	0.0±5.4		11.7±2.2	66.5±2.6 ^b	102.3±0.5 ^{b,d}	23.9
PO7	0.0±5.4		7.9±1.5	13.5±1.5 ^a	80.0±1.2 ^{b,d}	65.9
PO11	0.0±5.4		-27.0±1.2	10.1±1.9	98.4±0.3 ^{b,d}	47.1
PO12	0.0±5.4		-7.0±1.7	7.0±1.2	77.9±1.4 ^{b,d}	59.2
PO13	0.0±5.4	9.1±2.8	96.4±0.6 ^{b,d}	98.9±1.6 ^{b,d}	99.6±1.0 ^{b,d}	6.1
PO14	0.0±6.1	5.7±1.1	70.3±1.4 ^b	99.8±1.5 ^{b,d}	99.8±1.5 ^{b,d}	7.8
PO15	0.0±5.4		-5.4±0.9	59.7±1.1 ^b	94.1±3.6 ^{b,d}	31.3
PO17	0.0±6.1		2.7±1.5	25.9±1.4 ^b	96.9±0.5 ^{b,d}	37.8
PO18	0.0±5.4		-7.6±0.7	-0.7±1.4 ^b	79.9±1.7 ^b	73.6
PO19	0.0±6.1		3.8±1.0	4.4±1.0	35.5±0.6 ^b	>100
PO20	0.0±6.1		6.9±0.9	33.2±1.0 ^b	96.0±1.1 ^{b,d}	35.0
PO21	0.0±6.1		6.9±0.9	52.8±0.9 ^b	96.9±1.1 ^{b,d}	29.3
PO22	0.0±6.1		6.9±1.3	59.4±1.1 ^b	97.6±1.0 ^{b,d}	27.6
PO23	0.0±8.8		13.4±1.0	48.8±2.0 ^b	94.7±1.3 ^{b,d}	29.1
PO24^c	0.0±6.1	79.2±1.9 ^{b,d}	99.3±1.5 ^{b,d}	99.8±1.4 ^{b,d}	100.5±1.4 ^{b,d}	1.7
PO25	0.0±6.1	7.6±1.5	94.6±1.1 ^{b,d}	97.1±0.7 ^{b,d}	99.1±0.7 ^{b,d}	6.2
PO27	0.0±8.8		-20.9±1.9	9.1±0.8	51.0±1.2 ^b	>100
PO28	0.0±8.8		11.4±0.5	17.9±0.9	54.5±0.9 ^b	73.6
L-NA	0.0±9.9	11.7±4.6	20.2±0.2	34.7±0.4 ^a	71.6±1.2 ^b	61.8
CAPE	0.0±9.9	30.7±3.2 ^a	68.6±3.4 ^b	98.7±1.2 ^{b,d}	98.9±2.1 ^{b,d}	5.6

Statistical significance, ^a $p < 0.05$, ^b $p < 0.001$.

^c Each value represents mean \pm S.E.M. of four determinations.

^d Cytotoxic effect was observed.

^e Only **PO24** exhibited on NO production with 25.8±1.3 μM (% Inhibition at various concentrations of 1 μM . L-NA= L-Nitroarginine, CAPE= Caffeic acid phenethyl ester.

CHAPTER 4

CONCLUSION

A new binaphthoquinone, named 5,5'-dihydroxy-2,2'-dimethyl-7,7'-binaphthalen-1,1',4,4'-tetraone (**DW9**), and two new naphthalene derivatives, named 2-hydroxymethyl-1,5-dimethoxynaphthalen-4-ol (**DW11**) and 2,2'-bis-hydroxymethyl-1,1',5,5'-tetramethoxy-3,3'-binaphthalen-4,4'-diol (**DW12**), were isolated from the roots and fruits of *D. wallichii*, together with eighteen known compounds including nine naphthoquinones: plumbagin (**DW1**), droserone (**DW2**), 2,3-epoxyplumbagin (**DW3**), 2-hydroxymethyl-5-methoxy-1,4-naphthoquinone (**DW4**), diomuscione (**DW5**), isoshinanolone (**DW6**) *epi*-isoshinanolone Maritinone (**DW8**) and methylene-3,3'-biplumbagin (**DW10**), one coumarin: scopoletin (**DW13**), six triterpenoids: lupeol (**DW14**), lupenone (**DW15**), betulin (**DW16**), betulinaldehyde (**DW17**), betulinic acid (**DW18**) and 3 β ,29-dihydroxyolean-12-en-28-oic acid (**DW19**), and a mixture of steroids: β -sitosterol (**DW20**) and stigmasterol (**DW21**). The structures of the new compounds were elucidated by spectroscopic analysis, mainly 1D and 2D NMR techniques (^1H , ^{13}C , COSY, NOESY, HMQC and HMBC) and of the known compounds by comparison of their physical, UV, IR, ^1H and ^{13}C NMR data with those of published compounds. Antibacterial and cytotoxic activities of the isolates were also evaluated. It was found that **DW1** possessed the most potent antibacterial activities against *B. subtilis* and *E. faecalis*, but moderate activity against MRSA, VRE and *S. sonnei*. Compounds **DW4** and **DW5** exhibited moderate antibacterial activity against *B. subtilis* and *S. sonnei*, while compound **DW1** also exhibited moderate antibacterial activity against *E. faecalis* and MRSA. Compounds **DW8** and **DW9** exhibited better activity than the rest of the tested compounds with respective IC₅₀ values of 0.06 and 0.09 $\mu\text{g/ml}$. Structure-activity relationships for cytotoxic activity against MCF-7 human cancer cell line should be indicated as a binaphthoquinone skeleton was necessary for increasing the activity: mononaphthoquinone skeleton of compound **DW1** was less active with the IC₅₀ value

of 0.46 μM , while binaphthoquinone skeleton of compound **DW8** and **DW9** were most active with respective IC_{50} values of 0.06 and 0.09 μM .

From the roots and twigs of *P. obtusifolia* were isolated eleven new compounds as two isopimarane diterpenoids, named isopimara-7,15-dien-1 β ,3 β -diol (**PO1**) and isopimara-7,15-dien-1 β ,19-diol (**PO2**), one rosane diterpenoid named 13-*epi*-5,15-rosadien-3 α ,11 β -diol (**PO3**), four abietane diterpenoids, named abietatrien-1 β -ol (**PO4**), 1 β -hydroxyferruginol (**PO5**), 6 α ,11,12-trihydroxy-7 β ,20-epoxy-8,11,13-abietatriene (**PO18**) and 5 α ,11,12-trihydroxy-6-oxa-abieta-8,11,13-trien-7-one (**PO19**), and four icetexane diterpenoids, named 11,12-dihydroxy-6,8,11,13-icetexatetraen-1-one (**PO23**) and obtusinone A-C (**PO24-PO26**) along with eighteen known compounds including sixteen abietane-type diterpenoids: ferruginol (**PO6**), *O*-methyl ferruginol (**PO7**), lambertic acid (**PO8**), sugiol (**PO9**), royleanone (**PO10**), horminone (**PO11**), montbretrol (**PO12**), 14-deoxycoleon (**PO13**), taxodione (**PO14**), arucadiol (**PO15**), 12-hydroxy-6,7-secoabieta-8,11,13-triene-6,7-dial (**PO16**), salvicanaraldehyde (**PO17**), three icetexane-type diterpenoids: 5,6-dihydro-6 α -hydroxysalviasperanol (**PO20**), salviasperanol (**PO21**) and 11,12-dihydroxy-8,11,13-icetexatrien-1-one (**PO22**), and three sesquiterpenoids: 4 β ,5 β -dihydroxy-10-*epi*-eudesmane (**PO27**), 4 β ,10 β -dihydroxy aromadendrane (**PO28**) and spathulenol (**PO29**). In addition, the structures of **PO10**, **PO11**, **PO13**, **PO20**, **PO22** and **PO25** were additionally confirmed by X-ray diffraction analysis. Antibacterial and anti-inflammatory activities of the isolates were also evaluated. Compound **PO13** showed significant antibacterial activities against *B. subtilis*, *S. aureus*, *E. faecalis*, MRSA, VRE, *S. typhi* and *S. sonnei* but weak activity against *P. aeruginosa*. Compound **PO21** showed significant antibacterial activities against *S. sonnei* but moderate activity against *B. subtilis*, *E. faecalis*, MRSA and VRE while compound **PO20** also exhibited moderate antibacterial activity against MRSA. All compounds were found to be inactive against *C. albicans*. Compound **PO24** (IC_{50} = 1.7 μM) possessed the highest anti-inflammatory activity followed by compounds **PO13**, **PO14** and **PO25** (IC_{50} = 6.1, 7.8 and 6.2 μM , respectively) whereas other compounds exhibited moderate and mild activities. The inhibitory activities of most isolates were much stronger than that of NO synthase inhibitor (Tewtrakul et al., 2009) L-Nitroarginine (L-NA), IC_{50} = 61.8

μM except for compounds **PO19** and **PO27** which showed weaker activity ($\text{IC}_{50} = >100 \mu\text{M}$). Compound **PO24** also showed higher inhibitory activity than caffeic acid phenylester (CAPE) ($\text{IC}_{50} = 5.2 \mu\text{M}$). Structure-activity relationships for anti-inflammatory activity should be suggested as a hydroxyl group on an *ortho*-naphthoquinone skeleton was necessary for increasing the activity: compound **PO24** with a hydroxyl group was strongly active ($\text{IC}_{50} = 1.7 \mu\text{M}$), whereas compound **PO25** was less active ($\text{IC}_{50} = 6.2 \mu\text{M}$).

REFERENCE

- Abdul Razak, I.; Salae, A. W.; Chantrapromma, S.; Karalai, C.; Hoong-Kun, F. 2010. Redetermination and absolute configuration of 7 α -hydroxyroyleanone, *Acta Cryst.*, E66, o1566–o1567.
- Ahmad, V. U.; Bano, N.; Bano, S. 1984. Officigenin, a new sapogenin of *Guaiacum officinale*, *J. Nat. Prod.*, 47, 977–982.
- Akak, C. M.; Djama, C. M.; Nkengfack, A. E.; Tu, P. F.; Lei, L. D. 2010. New coumarin glycosides from the leaves of *Diospyros crassiflora* (Hiern), *Fitoterapia*, 81, 873–877.
- Alake, L. B. 1994. Antibacterial activity of diosquinone isolated from *Diospyros tricolor*, *Planta Med.*, 60, 477.
- Alves, A. C.; Costa, M. A. C.; Paul, M. I. 1983. Naphthaquinones of *Diospyros batocana*. *Planta Med.*, 47, 121–124.
- Ara, I.; Siddiqui, B S.; Faizi, S.; Siddiqui, S. 1988. Tricyclic diterpenoids from the stem bark of *Azadirachta indica*, *J. Nat. Prod.*, 51, 1054–1061.
- Asik, S. I. J.; Abdul Razak, I.; Salae, A. W.; Chantrapromma, S.; Hoong Kun, F. 2010. 6 α -Hydroxy-5,6-dihydrosalviasperanol, *Acta Cryst.*, E66, o2899.
- Auamcharoen, W.; Kijjoa, A.; Chandrapatya, A.; Pinto, M. M.; Silva, A. M. S.; Naengchomng, W.; Herz, W. 2009. A new tetralone from *Diospyros cauliflora*, *Biochem. Syst. Ecol.*, 37, 690–692.

- Ayinampudi, S. R.; Domala, R.; Merugu, R.; Bathula, S.; Janaswamy, M. R. 2012. New icetexane diterpenes with intestinal α -glucosidase inhibitory and free-radical scavenging activity isolated from *Premna tomentosa* roots, *Fitoterapia*, 83, 88–92.
- Balakrishna, K.; Sukumar, E.; Vasanth, S.; Patra, A. 2003. Myricetin-3',4',7-trimethyl ether from the leaves of *Premna tomentosa*, *J. Indian Chem. Soc.*, 80, 792.
- Barik, B. R.; Bhowmik, T.; Dey, A. K.; Patra, A.; Chatterjee, A.; Joy, S.; Susan, T.; Alam, M.; Kundu, A. B. 1992. Premnazole, an isoxazole alkaloid of *Premna integrifolia* and *Gmelina arborea* with anti-inflammatory activity, *Fitoterapia*, 63, 295–299.
- Banskota, A. H.; Tezuka, Y.; Nguyen, N. T.; Awale, S.; Nobukawa, T.; Kadota, S. 2003. DPPH Radical Scavenging and Nitric Oxide Inhibitory Activities of the Constituents from the Wood of *Taxus yunnanensis*, *Planta Med.*, 69, 500–505.
- Bhaumik, T.; Dey, A. K.; Das, P. C.; Mukhopadhyay, A. K.; Chatterjee, M. A. 1981. Triterpenes of *Diospyros peregrina* Gurke: partial syntheses of olean-9(11),12-dien-3-one and ursan-9(11),12-dien-3-one (marsformosanone), *Indian J. Chem., Sect. B: Org. Chem. Incl. Med. Chem.*, 20B, 664–668.
- Boonnak, N.; Karalai, C.; Chantrapromma, S.; Ponglimanont, C.; Hoong-Kun, F.; Kanjana-Opas, A.; Chantrapromma, K.; Kato, S. 2009. Anti-Pseudomonas aeruginosa xanthenes from the resin and green fruits of *Cratoxylum cochinchinense*, *Tetrahedron*, 65, 3003–3013.
- Bringmann, G.; Munchbach, M.; Messer, K.; Koppler, D.; Michel, M.; Schupp, O.; Wenzel, M.; Louis, A. M. 1999. *Cis*- and *trans*-isoshinanolone from *Dioncophyllum thollonii*: absolute configuration of two "known", wide-spread natural products, *Phytochemistry*, 51, 693–699.

- Bringmann, G.; Rischer, H.; Wohlfarth, M.; Schlauer, J.; Assi, L. A. 2000. Droserone from cell cultures of *Triphyophyllum peltatum* (Dioncophyllaceae) and its biosynthetic origin, *Phytochemistry*, 53, 339–343.
- Brown, A. G.; Thomson, R. H. 1965. Naphthaldehydes from *Diospyros ebenum*, *J. Chem. Soc.*, (Aug.), 4292–4295.
- Burns, D.; Reynolds, W. F.; Buchanan, G.; Reese, P. B.; Enriquez, R. G. 2000. Assignment of ^1H and ^{13}C spectra and investigation of hindered side-chain rotation in lupeol derivatives, *Magn. Reson. Chem.*, 38, 488–493.
- Cambie, R. C.; Cox, R. E.; Croft, K. D.; Sidwell, D. 1983. Phenolic diterpenoids of some podocarpa, *Phytochemistry*, 22, 1163–1166.
- Campello, J. D. P.; Fonseca, S. F.; Chang, C.-H.; Wenkert, E. 1975. Terpenes of *Podocarpus lambertius*, *Phytochemistry*, 14, 243–248.
- Chang C. I.; Chen C. R.; Chiu H. L.; Kuo C. L.; Kuo Y. H. 2009. Chemical constituents from the stems of *Diospyros maritima*, *Molecules* (Basel, Switzerland), 14, 5281–5288.
- Chang, C. I.; Kuo, Y. H. 1998. Three new lupane-type triterpenes from *Diospyros maritima*, *Chem. Pharm. Bull.*, 46, 1627–1629.
- Chang, C. I.; Kuo, Y. H. 1999. Two new lupane-type triterpenes from *Diospyros maritima*, *J. Nat. Prod.*, 62, 309–310.
- Chang, C. I.; Huan, S. L.; Kuo, Y. H. 2007. Two new naphthoquinones from the stem of *Diospyros maritima*, *J. Asian Nat. Prod. Res.*, 9, 153–158.

- Chauhan, J. S.; Kumari, G. 1980. Nonadecan-7-ol-2-one, an aliphatic ketol from *Diospyros peregrina*, *Phytochemistry*, 19, 2637–2638.
- Chauhan, J. S.; Saraswat, M.; Kumari, G. 1979. Structure of a new dihydroflavonol glycoside from *Diospyros peregrina* roots, *Planta Med.*, 35, 373–375.
- Chen, C. C.; Yu, H. J.; Huang, Y. L. 1992. The constituents of the bark of *Diospyros eriantha*, *Zhonghua Yaoxue Zazhi*, 44, 229–233.
- Chen, C. C.; Yu, H. J.; Ou, J. C.; Pan, T. M. 1994. Constituents of the heartwood of *Diospyros eriantha*, *J. Chin. Chem. Soc. (Taipei, Taiwan)*, 41, 195–198.
- Chen, C. R.; Cheng, C. W.; Pan, M. H.; Liao, Y. W.; Tzeng, C. Y.; Chang, C. I. 2007. Lanostane-type triterpenoids from *Diospyros discolor*, *Chem. Pharm. Bull.*, 55, 908–911.
- Chen, G.; Wei, S. H.; Huang, J.; Sun, J. 2009. A novel C-glycosylflavone from the leaves of *Diospyros kaki*, *J. Asian Nat. Prod. Res.*, 11, 502–506.
- Chen, G.; Wang, Z. Q.; Jia, J. M. 2009. Three minor novel triterpenoids from the leaves of *Diospyros kaki*, *Chem. Pharm. Bull.*, 57, 532–535.
- Chen, H. C.; Lin, Y. M.; Shih, T. S.; Chen, F. C. 1987. Constituents of the heartwood of *Morris persimmon* (II), *Taiwan Kexue*, 41, 46–52.
- Chen, G.; Xue, J.; Xu, S. X.; Zhang, R. Q. 2007. Chemical constituents of the leaves of *Diospyros kaki* and their cytotoxic effects, *J. Asian Nat. Prod. Res.*, 9, 347–353.

- Chen, G.; Xu, S. X.; Wang, H. Z.; Zhang, R. Q. 2005. Kakispyrol, a new biphenyl derivative from the leaves of *Diospyros kaki*, *J. Asian Nat. Prod. Res.*, 7, 265–268.
- Chen, G. Y.; Dai, C. Y.; Wang, T. S.; Jiang, C. W.; Han, C. R.; Song, X. P. 2010. A new flavonol from the stem-bark of *Premna fulva*, *ARKIVOC* (Gainesville, FL, United States), 2, 179–185.
- Chin, Y. W.; Jones, W. P.; Mi, Q.; Rachman, I.; Riswan, S.; Kardono, L. B. S.; Chai, H. B.; Farnsworth, N. R.; Cordell, G. A.; Swanson, S. M. 2006. Cytotoxic clerodane diterpenoids from the leaves of *Premna tomentosa*, *Phytochemistry*, 67, 1243–1248.
- Chivandi, E.; Erlwanger, K. H.; Davidson, B. C. 2009. Lipid content and fatty acid profile of the fruit seeds of *Diospyros mespiliformis*, *Int. J. Integr. Biol.*, 5, 121–124.
- Chopra, R.N. 1969. *Drug of India*, orient Longman Ltd., Chennai, India.
- Costa, M. A. C.; Alves, A. C.; Seabra, R. M.; Andrade, P. B. 1998. Naphthoquinones of *Diospyros chamaethamnus*, *Planta Med.*, 64, 391.
- Dai, C.; Xu, L.; Zhang, X.; Chen, G. 2010. Chemical constituents from the root of *Premna hainanensis*, *Hainan Shifan Daxue Xuebao, Ziran Kexueban*, 23, 66–67.
- Daood, H. G.; Biacs, P.; Czinkotai, B.; Hoschke, A. 1992. Chromatographic investigation of carotenoids, sugars and organic acids from *Diospyros kaki* fruits, *Food Chem.*, 45, 151–155.

- Dasgupta, B.; Sinha, N. K.; Pandey, V. B.; Ray, A. B. 1984. Major alkaloid and flavonoid of *Premna integrifolia*, *Planta Med.*, 50, 281.
- Dinda, B.; Bhattacharya, A.; De, U. C.; Arima, S.; Takayanagi, H.; Harigaya, Y. 2006. Antimicrobial C-glucoside from aerial parts of *Diospyros nigra*, *Chem.Pharm. Bull.*, 54, 679–681.
- Esquivel, B.; Flores, M.; Hernandez-Ortega, S.; Toscano, R. A.; Ramamoorthy, T. P. 1995. Abietane and icetexane diterpenoids from the roots of *Salvia aspera*, *Phytochemistry*, 39, 139–143.
- Fraga, B. M.; Diaz, C. E.; Guadano, A.; Gonzalez-Coloma, A. 2005. Diterpenes from *Salvia broussonetii* transformed roots and their insecticidal activity, *J. Agric. Food Chem.*, 53, 5200–5206.
- Fraga B. M.; Gonzalez A. G.; Herrera J. R.; Luis J. G.; Ravelo A. G. 1986. Diterpenes from the roots of *Salvia canariensis*, *Phytochemistry*, 25, 269–271.
- Ganapaty, S.; Steve, T. P.; Fotso, S.; Laatsch, H. 2004. Antitermitic quinones from *Diospyros sylvatica*, *Phytochemistry*, 65, 1265–1271.
- Ganapaty, S.; Thomas, P. S.; Karagianis, G.; Waterman, P. G.; Brun, R. 2006. Antiprotozoal and cytotoxic naphthalene derivatives from *Diospyros assimilis*. *Phytochemistry*, 67, 1950–1956.
- Ganapaty, S.; Thomas, P. S.; Mallika, B. N.; Balaji, S.; Karagianis, G.; Waterman, P. G. 2005. Dimeric naphthoquinones from *Diospyros discolor*, *Biochem. Syst. Ecol.*, 33, 313–315.
- Geis, W.; Becker, H. 2000. Sesqui- and diterpenes from the liverwort *Gackstroemia decipiens*, *Phytochemistry*, 53, 247–252.

- Guerreiro, E.; Kavka, J.; Giordano, O S.; Gros, E. G. 1979. Sesquiterpenoids and flavonoids from *Flourensia oolepis*, *Phytochemistry*, 18, 1235–1237.
- Gu, J. Q.; Graf, T. N.; Lee, D.; Chai, H. B.; Mi, Q.; Kardono, L. B. S.; Setyowati, F. M.; Ismail, R.; Riswan, S.; Farnsworth, N. R. (2004). Cytotoxic and antimicrobial constituents of the bark of *Diospyros maritima* collected in two geographical locations in Indonesia, *J. Nat. Prod.*, 67, 1156–1161.
- Gunaherath, G. M. K. B.; Gunatilaka, A. A. L. 1988. Structure of a new naphthoquinone from *Plumbago zeylanica*, *J. Chem. Soc. Perkin Trans 1*, 1, 407–410.
- Gunaherath, G. M. K. B.; Gunatilaka, A. A. L.; Sultanbawa, M. U. S.; Balasubramaniam, S. 1983. 1,2(3)-Tetrahydro-3,3'-biplumbagin: a naphthalenone and other constituents from *Plumbago zeylanica*, *Phytochemistry*, 22, 1245–1247.
- Gupta, R. K.; Dhar, M. M. 1969. Naphthoic acid derivatives from *Diospyros ebenum*, *Phytochemistry*, 8, 789–790.
- Habtemariam, S. 1995. Cytotoxicity of diterpenes from *Premna schimperi* and *Premna oligotricha*, *Planta Medica*, 61, 368–369.
- Habtemariam, S.; Gray, A. I.; Halbert, G. W.; Waterman, P. G. 1990. A novel antibacterial diterpene from *Premna schimperi*, *Planta Med.*, 56, 187–189.
- Haq, Q. N.; Hannan, A. 1984. Studies of carbohydrates from the fruits of *Diospyros discolor*, Willd, *Bangladesh J. Sci. Ind. Res.*, 19, 46–52.

- Harper, S. H.; Kemp, A. D.; Tannock, J. 1970. Methoxynaphthaldehydes as constituents of the heartwood of *Diospyros quiloensis* and their synthesis by the Stobbe condensation, *J. Chem. Soc.*, 4, 626–636.
- Hasegawa S.; Kojima T.; Hirose Y. 1985. Terpenoids from the seed of *Chamaecyparis pisifera*: The structures of six diterpenoids, *Phytochemistry*, 24, 1545–1551.
- Higa, M. 1988. A new binaphthoquinone from *Diospyros maritima* Blume, *Chem. Pharm. Bull.*, 36, 3234–3236.
- Higa, M.; Himeno, K.; Yogi, S.; Hokama, K. 1987. A new brominated naphthoquinone from *Diospyros maritima* Blume, *Chem. Pharm. Bull.*, 35, 4366–4367.
- Higa, M.; Noha, N.; Yokaryo, H.; Ogihara, K.; Yogi, S. 2002. Three new naphthoquinone derivatives from *Diospyros maritima* Blume, *Chem. Pharm. Bull.*, 50, 590–593.
- Higa, M.; Ogihara, K.; Yogi, S. 1998. Bioactive naphthoquinone derivatives from *Diospyros maritima* BLUME, *Chem. Pharm. Bull.*, 46, 1189–1193.
- Hoong-Kun, F.; Chantrapromma, S.; Salae, A. W; Abdul Razak, I. Karalai, C. 2011. Redetermined structure, intermolecular interactions and absolute configuration of royleanone, *Acta Cryst.*, E67, o1032–o1033.
- Huang, Q; Chen, L.; Lin, C.; Li, G.; Wei, T.; Wei, W. 2009. Flavonoids in *Premna fulva* craib and their anti-oxidative activities in vitro, *Shizhen Guoyi Guoyao*, 20, 2706–2708.

- Houlihan, C. M.; Ho, C. T.; Chang, S. S. 1984. Elucidation of the chemical structure of a novel antioxidant, rosmaridiphenol, isolated from *rosemary*, *J. Am. Oil Chem. Soc.*, 61, 1036–1039.
- Hu, J. F.; Garo, E.; Goering, M. G.; Pasmore, M.; Yoo, H. D.; Esser, T.; Sestrich, J.; Cremin, P. A.; Hough, G. W.; Perrone, P.; Lee, Y. S. L.; Le, N. T.; O'Neil-Johnson, M.; Costerton, J. W.; Eldridge, G. R. 2006. Bacterial biofilm inhibitors from *Diospyros dendo*, *J. Nat. Prod.*, 69, 118–120.
- Hymavathi, A.; Suresh, B. K.; Naidu, V. G. M.; Rama, K. S.; Diwan, P. V.; Madhusudana, R. J. 2009. Bioactivity-guided isolation of cytotoxic constituents from stem-bark of *Premna tomentosa*, *Bioorg. Med. Chem. Lett.*, 19, 5727–5731.
- Iwabuchi, H.; Yoshikura, M.; Kamisako, W. 1989. Studies on the sesquiterpenoids of *Panax ginseng* C. A. Meyer. III, *Chem. Pharm. Bull.*, 37, 509–510.
- Jain, N.; Yadava, R. N. 1997. Furano-(2",3",7,8)-3',5'-dimethoxy-5-hydroxyflavone: a new furanoflavone from the fruits of *Diospyros peregrina* Gurka, *Asian J. Chem.*, 9, 442–444.
- Jain, N.; Yadava, R. N. 1994. Peregrinol, a lupane type triterpene from the fruits of *Diospyros peregrina*, *Phytochemistry*, 35, 1070–1072.
- Jakupovic, J.; Ganzer, U.; Pritschow, P.; Lehmann, L.; Bohlmann, F.; King, R. M. 1992. Sesquiterpene lactones and other constituents from *Ursinia* species, *Phytochemistry*, 31, 863–880.
- Jeffreys, J. A. D.; Bin Zakaria, M.; Waterman, P. G.; Zhong, S. 1983. A new class of natural product: homologs of juglone bearing 4-hydroxy-5-methylcoumarin-3-yl units from *Diospyros* species, *Tetrahedron Lett.*, 24, 1085–1088.

- Jolad, S. D.; Hoffmann, J. J.; Schram, K. H.; Cole, J. R.; Bates, R. B.; Tempesta, M. 1984. A New Diterpene From *Cupressus goveniana* var. *Abramasiana*: 5 β -Hydroxy-6-Oxasugiol (Cupresol), *J. Nat. Prod.*, 47, 983–987.
- Jyotsna, D.; Sarma, P. N.; Srimannarayana, G.; Rao, A. V. S. 1984. Di-C-glycosyl flavone from *Premna tomentosa*, *Curr. Sci.*, 53, 573–576.
- Karl, S. 1935. The carotenoids of *Diospyros* fruits, *Biochem. J.*, 29, 1779–1782.
- Katoh, T.; Akagi, T.; Noguchi, C.; Kajimoto, T.; Node, M.; Tanaka, R.; Nishizawa, M.; Ohtsu, H.; Suzuki, N.; Saito, K. 2007. Synthesis of DL-standishinal and its related compounds for the studies on structure-activity relationship of inhibitory activity against aromatase, *Bioorg. Med. Chem.*, 15, 2736–2748.
- Khan, M. R.; Kishimba, M. A.; Locksley, H. 1987. Constituents of the root and stem barks of *Diospyros verrucosa*, *Planta Med.*, 53, 498.
- Khan, M. R.; Kishimba, M. A.; Locksley, H. 1989. Naphthoquinones from the root and stem barks of *Diospyros usambarensis*, *Planta Med.*, 55, 581.
- Khan, M. R.; Rwekika, E. 1998. A binaphthoquinone from *Diospyros greeniwayi*, *Phytochemistry*, 49, 2501–2503.
- Khan, M. R.; Rwekika, E. 1999. 6",8'-Bisdiosquinone from *Diospyros mafiensis*, *Phytochemistry*, 50, 143–146.
- Khan, M. R.; Timi, D. 1999. Constituents of the root and stem barks, leaves and fruits of *Diospyros hallierii*, *Fitoterapia*, 70, 320–321.
- Khan, M. R.; Timi, D. 1999. Constituents of the root and stem barks of *Diospyros villosiuscula*, *Fitoterapia*, 70, 209–211.

- Kolak, U.; Topcu, G.; Birteksoz, S.; Otuk, G.; Ulubelen, A. 2005. Terpenoids and steroids from the roots of *Salvia blepharochlaena*, Turk. J. Chem., 29, 177–186.
- Kuo, Y. H.; Chang, C. I.; Kuo, Y. H. 1997. A novel trisnorlupane, diospyrolide, from *Diospyros maritima*, Chem. Pharm. Bull., 45, 1221–1222.
- Kuo, Y. H.; Chang, C. I.; Kuo, Y. H. 1997. Triterpenes from *Diospyros maritima*, Phytochemistry, 46, 1135–1137.
- Kuo, Y. H.; Chang, C. I.; Li, S. Y.; Chou, C. J.; Chen, C. F.; Kuo, Y. H.; Lee, K. H. 1997. Cytotoxic constituents from the stems of *Diospyros maritima*, Planta Med., 63, 363–365.
- Kuo, Y. H.; Chang, C. I. 2000. Six new compounds from the heartwood of *Diospyros maritima*, Chem. Pharm. Bull., 48, 1211–1214.
- Kuo, Y. H.; Chen, C. H. 2001. A novel 7(6→2)abeoabietane-type diterpene, obtusanal, from the heartwood of *Chamaecyparis obtusa* var. *formosana*, Tetrahedron Lett., 42, 2985–2986.
- Kuo, Y. H.; Huang, S. L.; Chang, C. I. 1998. A phenolic and an aliphatic lactone from *Diospyros maritima*, Phytochemistry, 49, 2505–2507.
- Kuo, Y. H.; Li, S. Y.; Shen, C. C.; Yang, L. M.; Huang, H. C.; Liao, W. B.; Chang, C. I.; Kuo, Y. H.; Chen, C. F. 1997. Cytotoxic constituents from the fruit of *Diospyros ferrea*, Chinese Pharm. J. (Taipei), 49, 207–216.
- Kupchan, S. M.; Karim, A.; Marcks, C. 1968. Taxodione and taxodone, two novel diterpenoid quinone methide tumor inhibitors from *Taxodium distichum*, J. Am. Chem. Soc., 90, 5923–5924.

- Kuroyanagi, M.; Yoshihira, K.; Natori, S. 1971. Naphthoquinone derivatives from the Ebenaceae. III. Shinanolone from *Diospyros japonica*, Chem. Pharm. Bull., 19, 2314–2317.
- Lago, J. H. G.; Brochini, C. B.; Roque, N. F. (2000) Terpenes from leaves of *Guarea macrophylla* (Meliaceae), Phytochemistry, 55, 727–731.
- Lee, S. Y.; Choi, D. Y.; Woo, E. R. 2005. Inhibition of osteoclast differentiation by tanshinones from the root of *Salvia miltiorrhiza* Bunge, Arch. Pharmacol Res., 28, 909–913.
- Lillie, T. J.; Musgrave, O. C.; Skoyles, D. 1976. Ehretione, a bisnaphthoquinone derived from plumbagin and 7-methyljuglone, J. Chem. Soc., Perkin Trans. 1, 23, 2546.
- Lillie, T. J.; Musgrave, O. C.; Skoyles, D. 1976. New diospyrin derivatives from *Diospyros montana* Roxb, J. Chem. Soc., Perkin Trans. 1, 20, 2155–2161.
- Lin, L.-Z.; Blasko, G.; Cordell, G. A. 1989. Diterpenes of *Salvia prionitis*, Phytochemistry, 28, 177–181.
- Li, Q.; Shen, Y.; Li, P. 2008. Flavonoids in the leaves of *Premna szemaoensis* Pei, Zhongguo Yaoxue Zazhi (Beijing, China), 43, 417–419.
- Li, X. C.; van der Bijl, P.; Wu, C. D. 1998. Binaphthalenone glycosides from African Chewing Sticks, *Diospyros lycioides*, J. Nat. Prod., 61, 817–820.
- Loizzo, M. R.; Said, A.; Tundis, R.; Hawas, U. W.; Rashed, K.; Menichini, F.; Frega, N. G.; Menichini, F. 2009. Antioxidant and antiproliferative activity of *Diospyros lotus* L. extract and isolated compounds, Plant Food Hum. Nutr., 64, 264–270.

- Luis, J. G.; Grillo, T. A. 1993. New diterpenes from *Salvia munzii*: chemical and biogenetic aspects, *Tetrahedron*, 49, 6277–6284.
- Macias, F. A.; Simonet, A. M.; Esteban, M. D. 1994. Potential allelopathic lupane triterpenes from bioactive fractions of *Melilotus messanensis*, *Phytochemistry*, 36, 1369–1379.
- Ma, C. Y.; Musoke, S. F.; Tan, G. T.; Sydara, K.; Bouamanivong, S.; Southavong, B.; Soejarto, D. D.; Fong, H. H. S.; Zhang, H. J. 2008. Study of antimalarial activity of chemical constituents from *Diospyros quaesita*, *Chem. Biodivers.*, 5, 2442–2448.
- Maiti, B. C.; Musgrave, O. C. 1990. Macassaric acid, an *O*-methoxycarbonylcinnamic acid from macassar ebony, *J. Chem. Soc., Perkin Trans. 1*, 2, 307–310.
- Maiti, B. C.; Musgrave, O. C. 1986. New naphthoquinones and binaphthylquinones from Macassar ebony, *J. Chem. Soc., Perkin Trans. 1*, 4, 675–681.
- Mallavadhani, U. V.; Mahapatra, A. 2005. A new aurone and two rare metabolites from the leaves of *Diospyros melanoxylon*, *Nat. Prod. Res.*, 19, 91–97.
- Mallavadhani, U. V.; Panda, A. K.; Rao, Y. R. 2001. *Diospyros melanoxylon* leaves: a rich source of pentacyclic triterpenes, *Pharm. Biol. (Lisse, Netherlands)*, 39, 20–24.
- Mallavadhani, U. V.; Panda, A. K.; Rao, Y. R. 1998. Triterpene acids from *Diospyros melanoxylon*, *Biochem. Syst. Ecol.*, 26, 941–942.
- Marcos, I. S.; Beneitez, A.; Moro, R. F.; Basabe, P.; Diez, D.; Urones, J. G. 2010. Lateral lithiation in terpenes: synthesis of (+)-ferruginol and (+)-sugiol, *Tetrahedron*, 66, 7773–7780.

- Meng, Q.; Chen, W. 1988. Pygmaeoherin: a novel coumarin from *Pygmaeopremna herbacea*, *Planta Med.*, 54, 48–49.
- Meng, Q.; Hesse, M. 1990. New 20(10 → 5)abeo-diterpenoids from *Pygmaeopremna herbacea*, *Helv. Chim. Acta*, 73, 455–459.
- Meng, Q.; Zhu, N.; Chen, W. 1988. A diterpenoid with a new carbon skeleton from *Pygmaeopremna herbacea*, *Phytochemistry*, 27, 1151–1152.
- Michavila, A.; Torre, M. C. D. L.; Rodriguez, B. 1986. 20-Nor-abietane and rearranged abietane diterpenoids from the root of *Salvia argentea*, *Phytochemistry*, 25, 1935–1937.
- Miyoshi, E.; Shizuri, Y.; Yamamura, S. 1984. Isolation and structure of diomuscinone and diomuscipulone from *Dionaea muscipula*, *Phytochemistry*, 23, 2385–2387.
- Monaco, P.; Previtiera, L. 1984. Isoprenoids from the leaves of *Quercus suber*, *J. Nat. Prod.* 47, 673–676.
- Mongkolsuk, S.; Starwonvivat, C. 1965. 3-Methylnaphthalene-1,8-diol from *Diospyros mollis*, *J. Chem. Soc.*, (Feb.), 1533.
- Musgrave, O. C.; Skoyles, D. 1970. 2,2'-Binaphthyl-1,1'-quinone from *Diospyros buxifolia*, *J. Chem. Soc., Chem. Commun.*, 21, 1461.
- Nandwani, D.; Calvo, J. A.; Tenorio, J.; Calvo, F.; Manglona, L. 2008. Medicinal plants and traditional knowledge in the Northern Mariana Islands., *J. Appl. Biosci.*, 8, 323–320.

- Nareeboon, P.; Kraus, W.; Beifuss, U.; Conrad, J.; Klaiber, I.; Sutthivaiyakit, S. 2006. Novel 24-nor-, 24-nor-2,3-seco-, and 3,24-dinor-2,4-seco-ursane triterpenes from *Diospyros decandra*: evidences for ring A biosynthetic transformations, *Tetrahedron*, 62, 5519–5526.
- Nguyen, T. B. H.; Pham, T. K.; Chau, V. M.; Nguyen, P. T.; Phan, V. K. 2009. Premnaodoroside A and 10-*O*-trans-*p*-methoxycinnamoylcatalpol, two iridoid glycoside derivatives from the leaves of *Premna integrifolia* L, *Tap Chi Hoa Hoc*, 47, 230–235.
- Nguyen, T. B. H.; Pham, T. K.; Chau, V. M.; Nguyen, X. C.; Nguyen, P. T.; Phan, V. K. 2008. Study on the chemical constituents of *Premna integrifolia* L, *Nat. Prod. Commun.*, 3, 1449–1452.
- Nguyen, T. B. H.; Pham, T. K.; Ngo, T. L.; Phan, V. K. 2008. Rutin, scutellarioside II and leonuriside A from *Premna corymbosa* Rottl. ex Willd, *Tap Chi Duoc Hoc*, 48, 32–36.
- Ogihara, K.; Yamashiro, R.; Higa, M; Yogi, S. 1997. Preparation of naphthoquinone derivatives from plumbagin and their ichthyotoxicity, *Chem. Pharm. Bull.*, 45, 437–445.
- Otsuka, H.; Kubo, N.; Sasaki, Y.; Yamasaki, K.; Takeda, Y.; Seki, T. 1991. Iridoid diglycoside monoacyl esters from stems of *Premna japonica*, *Phytochemistry*, 30, 1917–1920.
- Otsuka, H.; Sasaki, Y.; Kubo, N.; Yamasaki, K.; Takeda, Y.; Seki, T. 1991. Isolation and structure elucidation of mono- and diacyl-iridoid diglycosides from leaves of *Premna japonica*, *J. Nat. Prod.*, 54, 547–53.

- Paknikar, S. K.; Fondekar, K. P. Pai; Kirtany, J. K.; Natori, S. 1996. 4-Hydroxy-5-methylcoumarin derivatives from *Diospyros kaki* Thunb and *D. kaki* var. *sylvestris* Makino; structure and synthesis of 11-methylgerberinol, *Phytochemistry*, 41, 931–933.
- Paphassarang, S.; Becchi, M.; Raynaud, J. 1984. A new diospyrol glycoside from *Diospyros mollis* Griff, *Tetrahedron Lett.*, 25, 523–526.
- Pardhasaradhi, M.; Krishnakumari, L. 1979. Tetrahydrodiospyrin: a reduced binaphthoquinone from the bark of *Diospyros Montana*, *Phytochemistry*, 18, 684–685.
- Passannanti, S.; Paternostro, M.; Piozzi, F. 1984. Diterpenes from the Genus *Amaracus*, *J. Nat. Prod.*, 47, 885–889.
- Peng, C.; Bodenhausen, G.; Qiu, S.; Fong, H. H. S.; Farnsworth, N. R.; Yuan, S.; Zheng, C. 1998. Computer-assisted structure elucidation: application of CISOC-SES to the resonance assignment and structure generation of betulinic acid, *Magn. Reson. Chem.*, 36, 267–278.
- Pertino, M. W.; Schmeda-Hirschmann, G. 2010. The corrected structure of rosmaridiphenol, a bioactive diterpene from *Rosmarinus officinalis*, *Planta Med.*, 76, 629–632.
- Pham, T. K.; Nguyen, T. B. H.; Phan, V. K. 2008. 10-*O*-trans-p-methoxycinnamoylcatalpol and verbascoside from *Premna corymbosa* Rottl. ex Willd, *Tap Chi Duoc Hoc*, 48, 36–39.
- Prajoubklang, A.; Sirithunyalug, B.; Charoenchai, P.; Suvannakad, R.; Sriubolmas, N.; Piyamongkol, S.; Kongsaree, P.; Kittakoop, P. 2005. Bioactive deoxypreussomerins and dimeric naphthoquinones from *Diospyros ehretioides*

fruits: Deoxypreussomerins may not be plant metabolites but may be from fungal epiphytes or endophytes, *Chem. Biodivers.*, 2, 1358–1367.

Ragasa, C. Y.; Puno, M. R. A.; Sengson, J. M. A. P.; Shen, C. C.; Rideout, J. A.; Raga, D. D. 2009. Bioactive triterpenes from *Diospyros blancoi* (sic), *Nat. Prod. Res.*, 23, 1252–1258.

Rao, C. B.; Krishna, P. G.; Devi, P. A.; Raju, G. V. S.; Chari, V. M. 1986. Structure of premnoside A from *Premna latifolia* Roxb. (var. *cuneata*), *Indian J. Chem., Sect. B: Org. Chem. Incl. Med. Chem.*, 25B, 100–101.

Rao, C. B.; Krishna, P. G.; Suseela, K. 1985. New isoprenoids from the root barks of *Premna integrifolia* Linn. and *P. latifolia* var. *mollissima*, *Indian J. Chem., Sect. B: Org. Chem. Incl. Med. Chem.*, 24B, 403–407.

Rao, C. B.; Raju, G. V. S.; Krishna, P. G.; Chari, V. M. 1982. Constituents of root bark of *Premna latifolia* var. *cuneata*, *Indian J. Chem., Sect. B: Org. Chem. Incl. Med. Chem.*, 21B, 294–298.

Rao, C. B.; Raju, G. V. S.; Krishna, P. G. 1982. Spirosesquiterpenes from *Premna latifolia* Roxb. and var. *cuneata*, *Indian J. Chem., Sect. B: Org. Chem. Incl. Med. Chem.*, 21B, 267–268.

Rao, C. B.; Rao, T. N. 1978. Premnolal, a new aromatic bisnorditerpene from *Premna latifolia* Roxb, *Curr. Sci.*, 47, 498–499.

Rao, C. B.; Rao, T. N. 1978. Some new hydroxy sandaracopimar-15-enes from *Premna latifolia* Roxb, *Curr. Sci.*, 47, 577–578.

- Rao, C. B.; Suseela, K.; Raju, G. V. S. 1984. Pimaradienols from *Premna latifolia* var. *mollissima*, Indian J. Chem., Sect. B: Org. Chem. Incl. Med. Chem., 23B, 177–179.
- Rao, P. V. S.; Aruna, G. D.; Raju, G. V. S.; Trimurtulu, G.; Rao, C. B. 1987. Phenolic diterpenoids from root bark of *Premna integrifolia* Linn, Indian J. Chem., Sect. B: Org. Chem. Incl. Med. Chem., 26B, 191–192.
- Rasool, N.; Ahmad, V. U.; Malik, A. 1991. Terpenoids from *Pentatropis spiralis*, Phytochemistry, 30, 1331–1332.
- Rauf, A.; Ahmad, M. S.; Osman, S. M. 1987. 8-Hydroxyoctadec-10(Z)-enoic acid in *Diospyros montana* seed oil, Indian J. Chem., Sect. B: Org. Chem. Incl. Med. Chem., 26B, 283.
- Razdan, T. K.; Harkar, S.; Qadri, B.; Qurishi, M. A.; Khuroo, M. A. 1988. Lupene derivatives from *Skimmia laureola*, Phytochemistry, 27, 1890–1982.
- Razdan, T. K.; Qadri, B.; Harkar, S.; Waight, E. S. 1987. Chromones and coumarins from *Skimmia laureola*, Phytochemistry, 26, 2063–2069.
- Recio, M. C.; Giner, R. M.; Manez, S.; Gueho, J.; Julien, H. R.; Hostettmann, K.; Rios, J. L. 1995. Investigations on the steroidal anti-inflammatory activity of triterpenoids from *Diospyros leucomelas*, Planta Med., 61, 9–12.
- Richomme, P.; Papillon, B.; Cabalion, P.; Bruneton, J. 1991. Naphthoquinones of *Diospyros samoensis*, Pharm. Acta Helv., 66, 88–89.
- Rijo, P.; Simoes, M. F.; Duarte, A.; Rodriguez, B. 2009. Isopimarane diterpenoids from *Aeollanthus rydingianus* and their antimicrobial activity, Phytochemistry, 70, 1161–1165.

- Rodriguez, B. 2003. ^1H and ^{13}C NMR spectral assignments of some natural abietane diterpenoids, *Magn. Reson. Chem.*, 41, 741–746.
- Ryu, Y. B.; Jeong, H. J.; Kim, Jang H.; Kim, Y. M.; Park, J. Y.; Kim, D.; Naguyen, T. T. H.; Park, S. J.; Chang, J. S.; Park, K. H. 2010. Biflavonoids from *Torreya nucifera* displaying SARS-CoV 3CLpro inhibition, *Bioorg. Med. Chem. Lett.*, 18, 7940–7947.
- Said, A.; Hawas, U. W.; Nofal, S. M.; Rashed, K.; Huefner, A. 2009. Pharmacochemical studies on the aqueous methanolic extract of *Diospyros lotus* leaves, *Res. J. Phytochem.*, 3, 1–12.
- Salae, A. W.; Chantrapromma, S.; Hoong Kun, F.; Karalai, C. 2009. 6-Hydroxysalvinolone, *Acta Cryst.*, E65, o2379–o2380.
- Salae, A. W.; Karalai, C.; Ponglimanont, C.; Kanjana-Opas, A.; Yuenyongsawad, S. 2010. Naphthalene derivatives from *Diospyros wallichii*, *Can. J. Chem.*, 88, 922–927.
- Salae, A. W.; Rodjun, A.; Karalai, C.; Ponglimanont, C.; Chantrapromma, S.; Kanjana-Opas, A.; Tewtrakul, S.; Hoong-Kun, F. 2012. Potential anti-inflammatory diterpenes from *Premna obtusifolia*, *Tetrahedron*, 68, 819–829.
- Sankaram, A. V. B.; Narayana Reddy, V. V.; Sidhu, G. S. 1981. A pentacyclic quinone and diosindigo B from the heartwood of *Diospyros melanoxylon*, *Phytochemistry*, 20, 1093–1096.
- Sankaram, A. V. B.; Reddy, V. V. N. 1984. Structure of ebenone, a possible biogenetic precursor of elliptinone, from *Diospyros ebenum*, *Phytochemistry*, 23, 2039–2042.

- Santos, C. C.; Lima, M. A. S.; Filho, R. B.; Silveira, E. R. 2006. Diterpenes from *Erythroxylum barbatum*, J. Braz. Chem. Soc., 17, 1304–1308.
- Satish, K.; Vishnuvardhan, M. V. P. S.; Lakshma, N. V.; Srihari, G.; Subrahamanyam, M.; Prabhakar, R. T.; Ramakrishna, S.; Ravikumar, K.; Sridhar, B.; Murthy, M. M. 2011. Cytotoxic diterpenoid quinonemethides from the roots of *Pygmacopremna herbacea*, Bioorg. Med. Chem. Lett., 21, 4581–4584.
- Sharma, K.; Gupta, R. K. 1985. Constituents of *Diospyros ebenum* stem bark, Fitoterapia, 56, 366–367.
- Sheldrick, G. M. 2008. A short history of SHELX, Acta Cryst., A64, 112–122.
- Sidhu, G. S.; Sankaram, A. V. B.; Mahmood Ali, S. 1968. Naphthoquinones and naphthols from the heartwood of *Diospyros melanoxylon*, Indian J. Chem., 6, 681–691.
- Sidhu, G. S.; Sankaram, A. V. B.; Mahmood Ali, S. 1973. New binaphthoquinone from the heartwood of *Diospyros melanoxylon*, Indian J. Chem., 11, 507–508.
- Sidhu, G. S.; Prasad, K. K. 1967. (-)-Isodiospyrin, a novel binaphthoquinone showing atropisomerism, and other extractives from *Diospyros chloroxylon*, Tetrahedron Lett., 30, 2905–2910.
- Simmons, E. M.; Sarpong, R. 2009. Structure, biosynthetic relationships and chemical synthesis of the icetexane diterpenoids, Nat. Prod. Rep., 26, 1195–1217.
- Singh, M.; Prakash, L. 1988. Chemical investigation of persimmon (*Diospyros malanonilau*) heartwood, Herba Pol., 34, 159–160.

- Spek, A. L. 2009. Structure validation in chemical crystallography, *Acta Cryst.*, D65, 148–155.
- Srihari, G.; Vishnuvardhan, M. V. P. S.; Satish, K.; Subrahamanyam, M.; Raju, T. V.; Prabakar, T.; Murthy, M. M. 2011. Two new diterpenoids from the root nodules of *Pygmacopremna herbacea* (Roxb.) Moldenke, *Phytochemistry Lett.*, 4, 109–112.
- Srivastava, S. K.; Pitre, S. (1985). A new anthraquinone glycoside from the stem bark of *Diospyros discolor*, *Planta Med.*, 6, 537–538.
- Sudo, H.; Ide, T.; Otsuka, H.; Hirata, E.; Takushi, A.; Takeda, Y. 1998. Iridoid glucosides with different acyl moieties from globularinin and globularimin from leaves of *Premna subscandens*, *Phytochemistry*, 49, 783–786.
- Sudo, H.; Ide, T.; Otsuka, H.; Hirata, E.; Takushi, A.; Takeda, Y. 1997. 10-*O*-acylated iridoid glucosides from leaves of *Premna subscandens*, *Phytochemistry*, 46, 1231–1236.
- Sudo, H.; Kijima, K.; Otsuka, H.; Ide, T.; Hirata, E.; Takeda, Y.; Isaji, M.; Kurashina, Y. 1999. A collagen network formation effector from leaves of *Premna subscandens*, *Chem. Pharm. Bull.*, 47, 1341–1343.
- Sudo, H.; Takushi, A.; Hirata, E.; Ide, T.; Otsuka, H.; Takeda, Y. 1999. Premnaodorosides D-G: acyclic monoterpenediols iridoid glucoside diesters from leaves of *Premna subscandens*, *Phytochemistry*, 52, 1495–1499.
- Sudo, H.; Takushi, A.; Ide, T.; Otsuka, H.; Hirata, E.; Takeda, Y. 1997. Premnethanosides A and B: phenylethanoids from leaves of *Premna subscandens*, *Phytochemistry*, 46, 1147–1150.

- Suresh, G.; Babu, K. S.; Rao, M. S. A.; Rao, V. R. S.; Yadav, P. A.; Nayak, V. L.; Ramakrishna, S. 2011. Premnalatifolin A, a novel dimeric diterpene from *Premna latifolia* Roxb, *Tetrahedron Lett.*, 52, 5016–5019.
- Sutthivaiyakit, S.; Pakakatsama, P.; Kraus, W.; Vogler, B. 1995. Constituents of *Diospyros rhodocalyx*, *Planta Med.*, 61, 295.
- Sutthivaiyakit, S.; Seeka, C.; Kritwinyu, T.; Pisutchareonpong, S.; Chimnoi, N. 2012. 19-nor-11-Oxooleanan-12-ene and 18,19-seco-19-oxours-11,13(18)-diene triterpenes from *Diospyros decandra* bark, *Tetrahedron Lett.*, 53, 1713–1716.
- Su, W. C.; Fang, J. M.; Cheng, Y. S. 1994. Abietanes and kauranes from leaves of *Cryptomeria japonica*, *Phytochemistry*, 35, 1279–1284.
- Tangmouo, J. G.; Ho, R.; Lannang, A. M.; Komguem, J.; Lontsi, A. T.; Lontsi, D.; Hostettmann, K. 2009. Norbergenin derivatives from the stem bark of *Diospyros sanza-minika* (Ebenaceae) and their radical scavenging activity, *Phytochemistry Lett.*, 2, 192–195.
- Tangmouo, J. G.; Lontsi, D.; Ngounou, F. N.; Kuete, V.; Meli, A. L.; Manfouo, R. N.; Kamdem, H. W.; Tane, P.; Beng, V. P.; Sondengam, B. L. 2005. Diospyrone, a new coumarinylbinaphthoquinone from *Diospyros canaliculata* (Ebenaceae): Structure and antimicrobial activity, *Bull. Chem. Soc. Ethiopia*, 19, 81–88.
- Tangmouo, J. G.; Meli, A. L.; Komguem, J.; Kuete, V.; Ngounou, F. N.; Lontsi, D.; Beng, V. P.; Choudhary, M. I.; Sondengam, B. L. 2006. Crassiflorone, a new naphthoquinone from *Diospyros crassiflora* (Hien), *Tetrahedron Lett.*, 47, 3067–3070.

- Thanakijcharoenpath, W.; Theanphong, O. 2007. Triterpenoids from the stem of *Diospyros glandulosa*, Thai J. Pharm. Sci., 31, 1–8.
- Tewtrakul, S.; Cheenpracha, S.; Karalai, C. 2009. Nitric oxide inhibitory principles from *Derris trifoliata* stems, Phytomedicine, 16, 568–572.
- Tezuka, Y.; Kasimu, R.; Li, J. X.; Basnet, P.; Tanaka, K.; Namba, T.; Kadota, S. 1998. Constituents of roots of *Salvia deserta* Schang. (Xinjiang-Danshen), Chem. Pharm. Bull., 46, 107–112.
- Thongdeeying, P. 2005. Chemical constituents from the leaves of *Ceriops decandra* (Giff.) Ding Hou. Master of Science Thesis in Organic Chemistry, Prince of Songkla University, 31–59.
- Thuong, P. T.; Lee, C. H.; Dao, T. T.; Nguyen, P. H.; Kim, W. G.; Lee, S. J.; Oh, W. K. 2008. Triterpenoids from the Leaves of *Diospyros kaki* (Persimmon) and Their Inhibitory Effects on Protein Tyrosine Phosphatase 1B, J. Nat. Prod., 71, 1775–1778.
- Tinto, W. F.; Blair, L. C.; Alli, A. 1992. Lupane triterpenoids of *Salacia cordata*, J. Nat. Prod., 55, 395–398.
- Topcu, G.; Ulubelen, A. 1996. Abietane and rearranged abietane diterpenes from *Salvia montbretii*, J. Nat. Prod., 59, 734–737.
- Trinh, T. T.; Tran, V. S.; Ripperger, H.; Adam, G. 1998. Flavonol glycosides from *Premna flavescens*, Tap Chi Hoa Hoc, 36, 49–52.
- Urones, J. G.; Marcos, I. S.; Ferreras, J. F.; Barcala, P. B. 1988. Terpenoids from *Nepeta tuberosa* subsp. *reticulata* (II), Phytochemistry, 27, 523–526.

- Utsunomiya, N.; Subhadrabandhu, S.; Yonemori, K.; Oshida, M.; Kanzaki, S.; Nakatsubo, F.; Sugiura, A. 1998. *Diospyros* species in Thailand: their distribution, fruit morphology and uses. *Economic Botany*, 52, 343.
- Vlakhov, R.; Holub, M.; Ognyanov, I; Herout, V. 1967. Sesquiterpenic hydrocarbons from the essential oil of *Mentha piperita* of Bulgarian origin, Collect. Czech. Chem. Comm., 32, 808–821.
- Wang, X.; Habib, E.; Leon, F.; Radwan, M. M.; Tabanca, N.; Gao, J.; Wedge, D. E.; Cutler, S. J. 2011. Antifungal metabolites from the roots of *Diospyros virginiana* by overpressure layer chromatography, Chem. Biodivers., 8, 2331–2340.
- Wang, D. Y.; Xu, S. Y. 2003. Two new xanthenes from *Premna microphylla*, Nat. Prod. Res., 17, 75–77.
- Wei, S.; Si, S.; Xu, X.; Pu, Q.; Pannell, L. K.; Highet, R. J. 1991. Studies on the chemical constituents of *Premna fulva*, Planta Med., 57, 93–94.
- Wenkert, E.; Buckwalter, B. L. 1972. Carbon-13 nuclear magnetic resonance spectroscopy of naturally occurring substances. X. Pimaradienes, J. Am. Chem. Soc., 94, 4367–4369.
- Wurm, G. 1982. 2-Methyl-5-hydroxy-1,4-naphthoquinone, Ger. Offen., DE 3035279 A1 19820401.
- Wu, T. S.; Chan, Y. Y.; Leu, Y. L. 2000. The constituents of the root and stem of *Aristolochia heterophylla* hemsl, Chem. Pharm. Bull., 48, 357–361.
- Yadav, D.; Tiwari, N.; Gupta, M. M. 2010. Diterpenoids from *Premna integrifolia*, Phytochemistry Lett., 3, 143–147.

- Yan, X. Z.; Kuo, Y. H.; Lee, T. J.; Shih, T. S.; Chen, C. H.; McPhail, D. R.; McPhail, A. T.; Lee, K. H. 1989. Cytotoxic components of *Diospyros morrisiana*. *Phytochemistry*, 28, 1541–1543.
- Yoshihira, K.; Tezuka, M.; Natori, S. 1971. Naphthoquinone derivatives from the Ebenaceae. II. Isodiospyrin, bisidiospyrin, and mamegakinone from *Diospyros lotus* and *D. morrisiana*, *Chem. Pharm. Bull.*, 19, 2308–2313.
- Yuasa, K.; Ide, T.; Otsuka, H.; Takeda, Y. 1993. Premnafolioside, a new phenylethanoid, and other phenolic compounds from stems of *Premna corymbosa* var. *obtusifolia*, *J. Nat. Prod.*, 56, 1695–1699.
- Zakaria, M. B. 1989. 4-Hydroxy-5-methylcoumarin from *Diospyros ismailii*, *Planta Med.*, 55, 204.
- Zhan, Z. J.; Tang, L.; Shan, W. G. 2009. A new triterpene glycoside from *Premna microphylla*, *Chem. Nat. Compd.*, 45, 197–199.
- Zhan Z. J.; Yue J M. 2003. New glyceroglycolipid and ceramide from *Premna microphylla*, *Lipids*, 38, 1299–1303.
- Zheng, Q.; Liu, C.; Liu, L. 1989. The constituents from petroleum ether fraction of the stem bark of *Premna fulva* Craib, *Zhongguo Yaoke Daxue Xuebao*, 20, 94–96.
- Zheng, Q.; Liu, C.; Meng, B. 1990. Constituents from ethyl acetate fraction of the stem bark of yellow hairy *premna* (*Premna fulva*), *Zhongcaoyao*, 21, 200–202.

APPENDIX

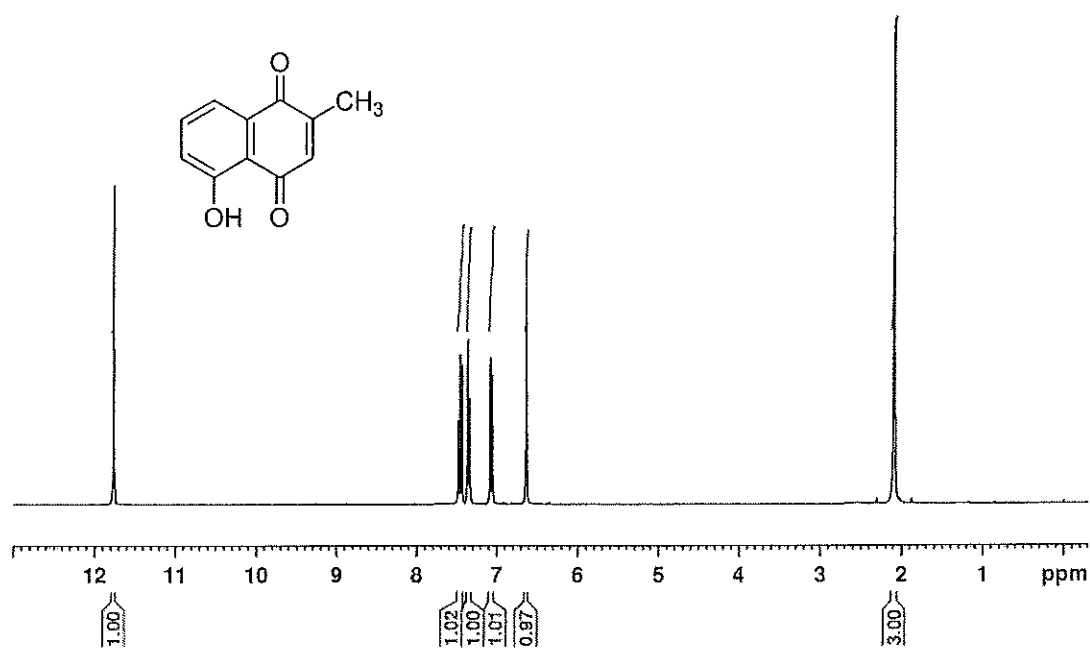


Figure 38 ¹H NMR (300 MHz) (CDCl₃) spectrum of compound DW1

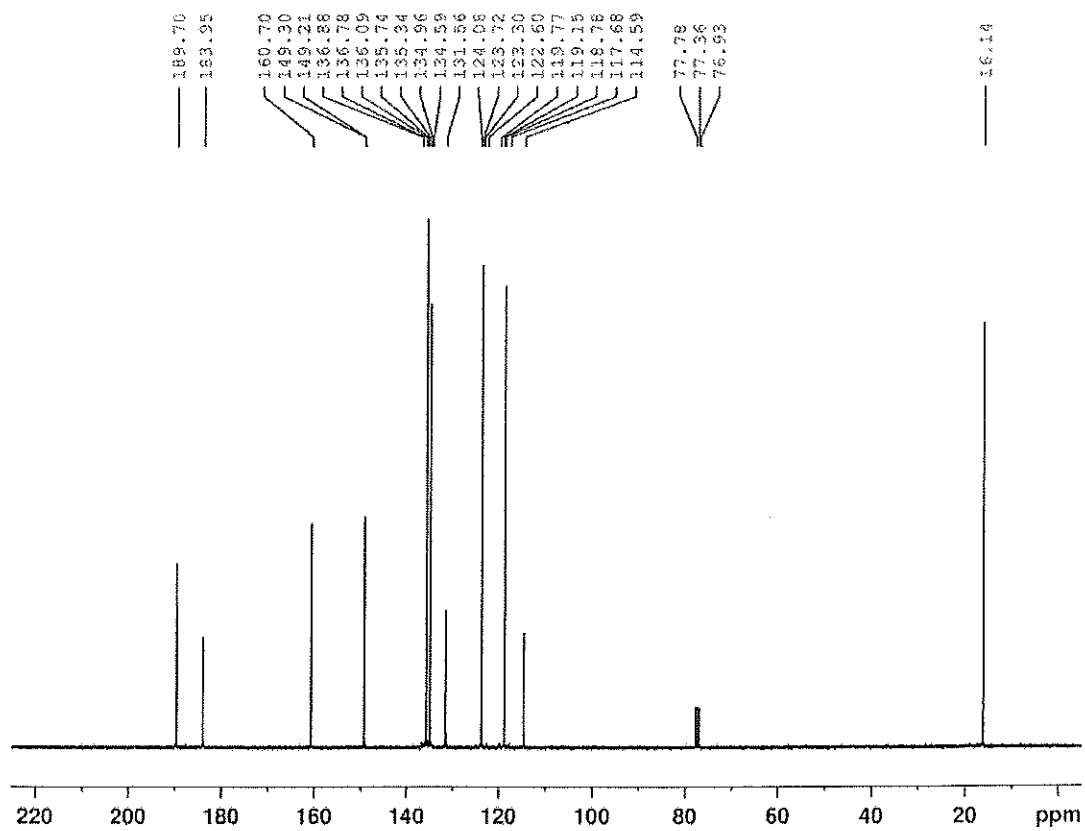


Figure 39 ¹³C NMR (75 MHz) (CDCl₃) spectrum of compound DW1

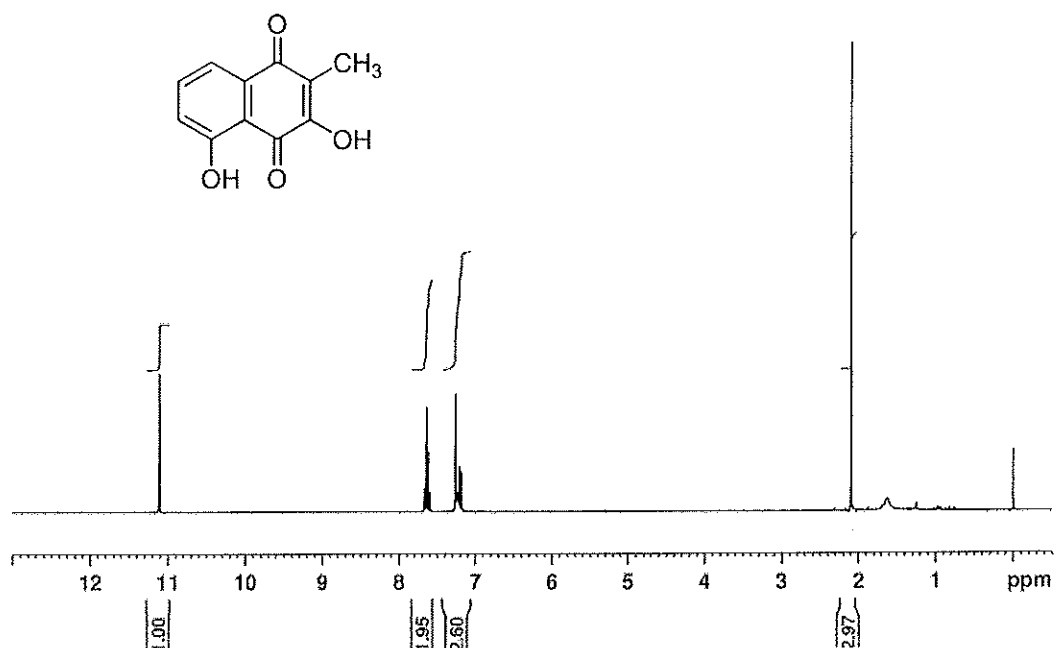


Figure 40 ^1H NMR (300 MHz) (CDCl_3) spectrum of compound DW2

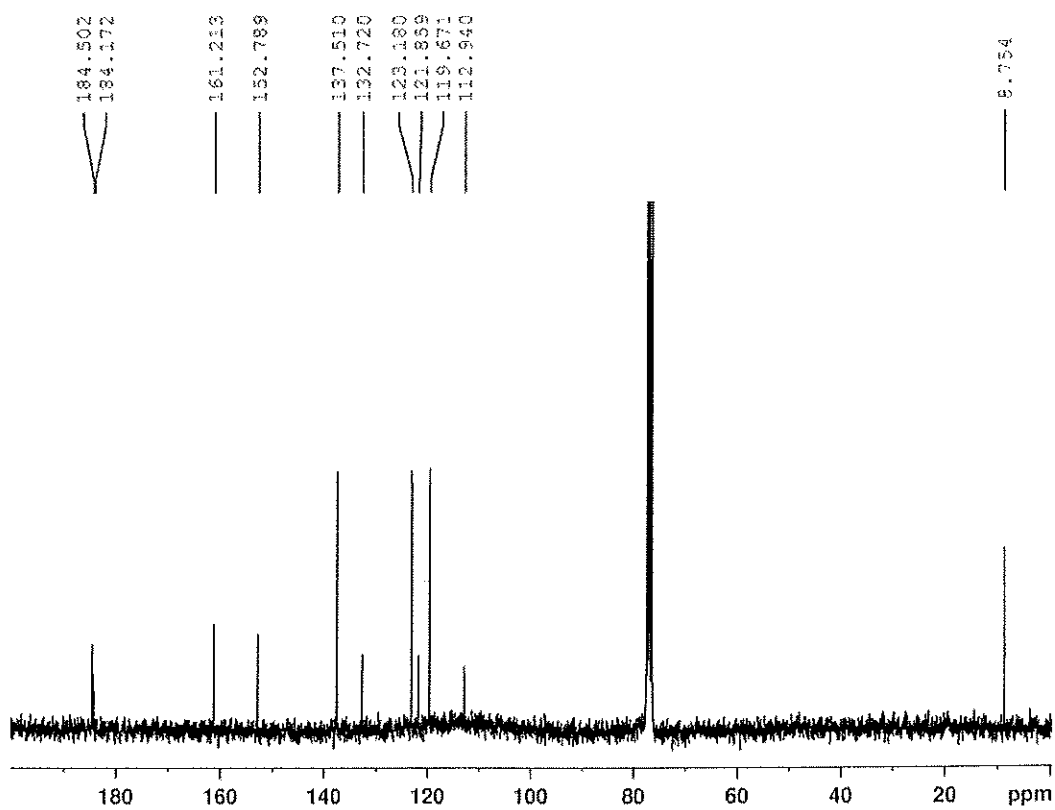


Figure 41 ^{13}C NMR (75 MHz) (CDCl_3) spectrum of compound DW2

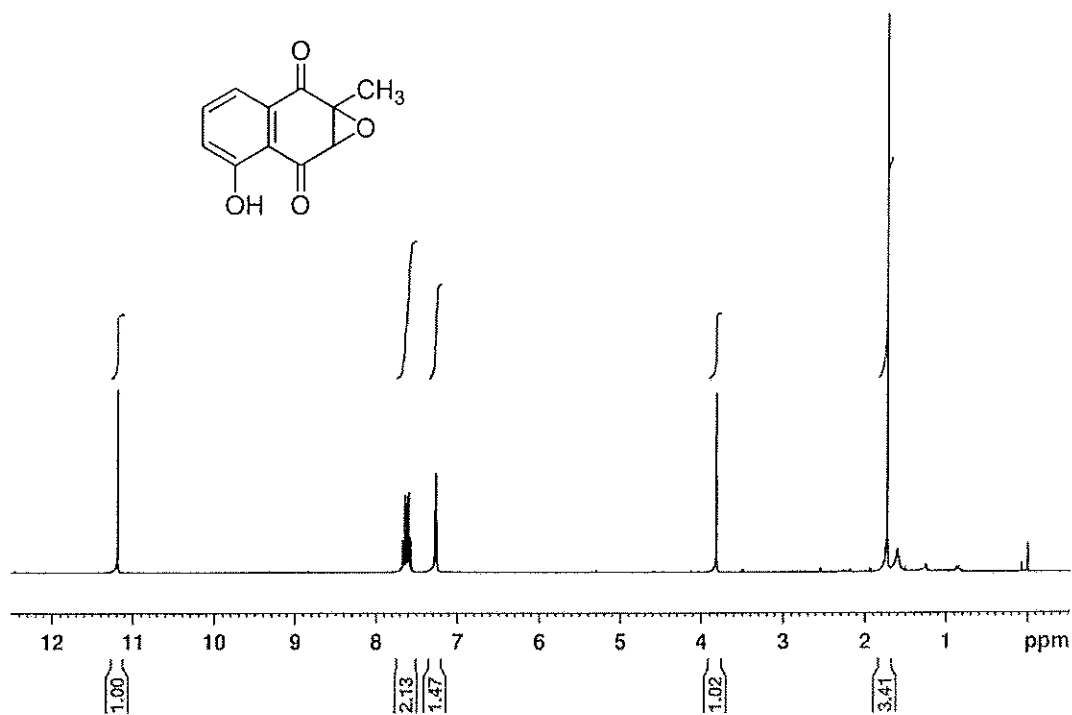


Figure 42 $^1\text{H NMR}$ (300 MHz) (CDCl_3) spectrum of compound DW3

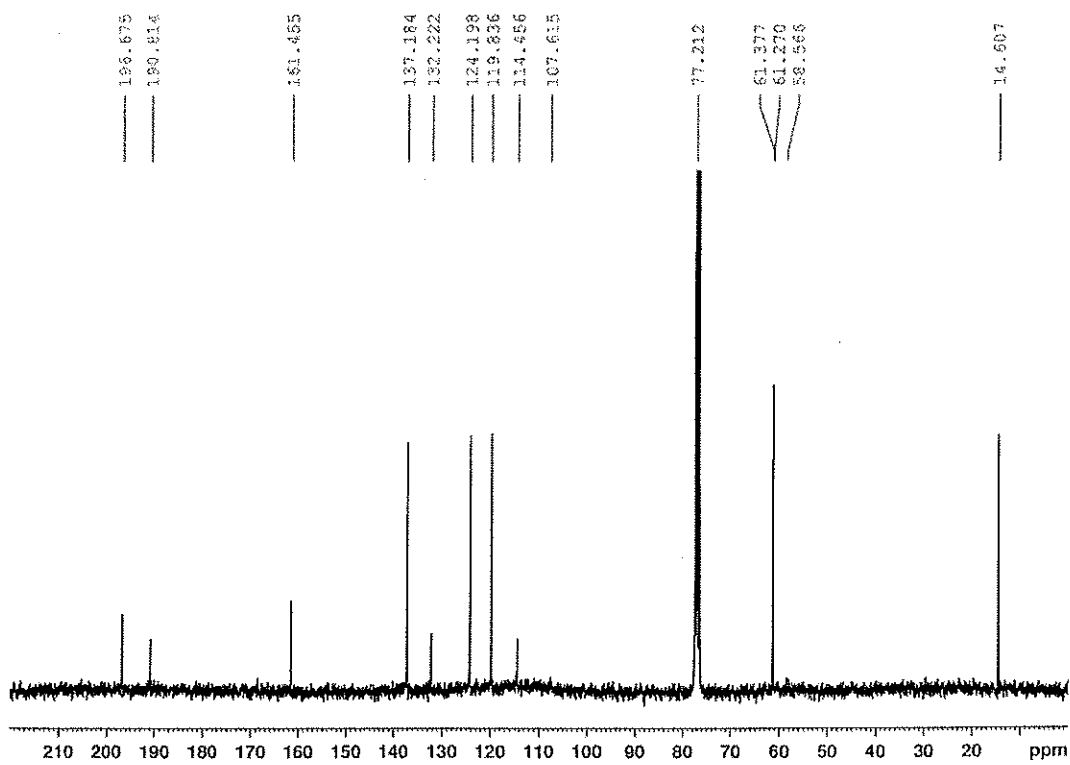


Figure 43 $^{13}\text{C NMR}$ (75 MHz) (CDCl_3) spectrum of compound DW3

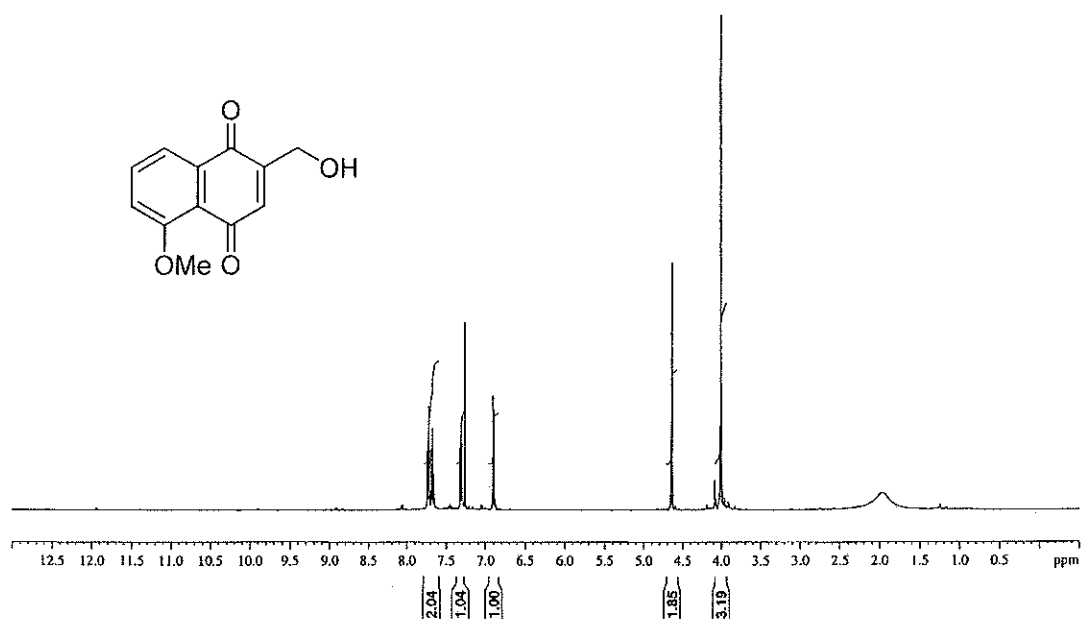


Figure 44 $^1\text{H NMR}$ (400 MHz) (CDCl_3) spectrum of compound DW4

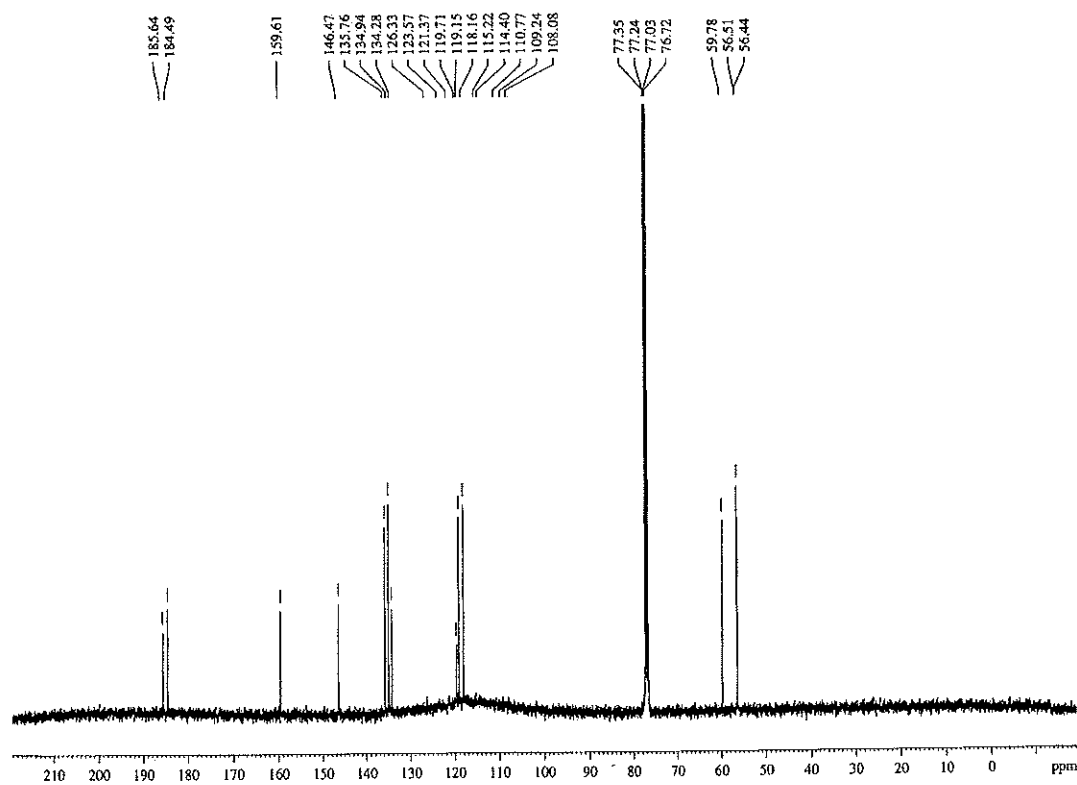
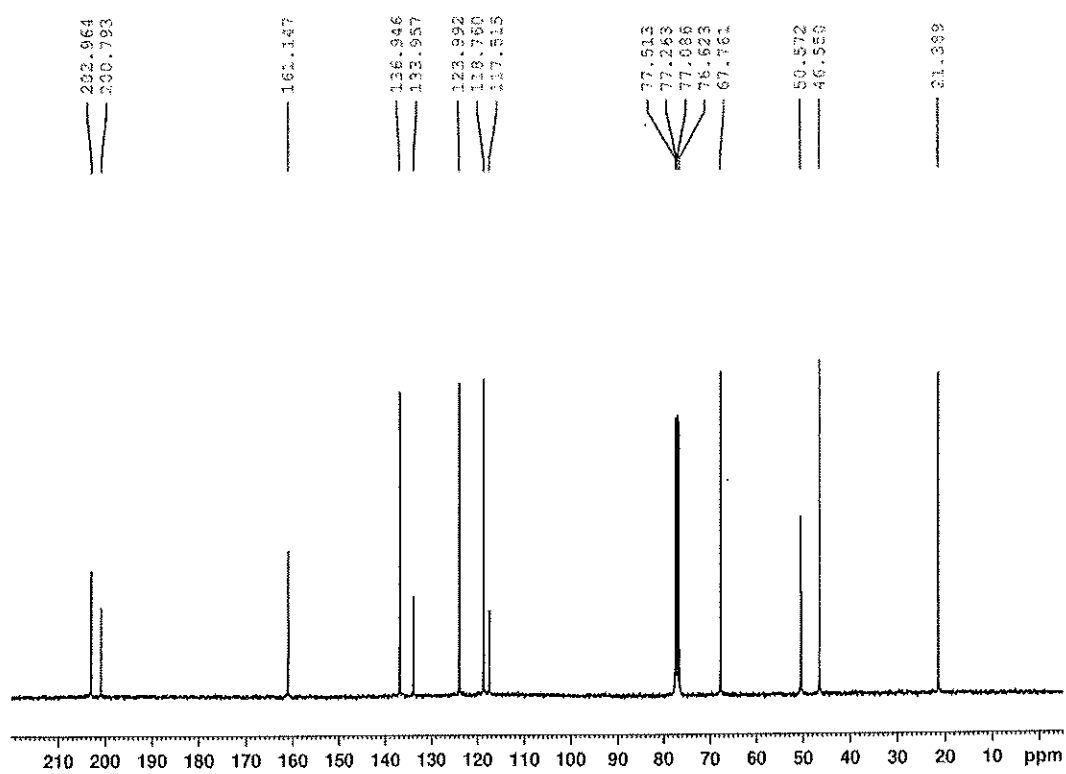
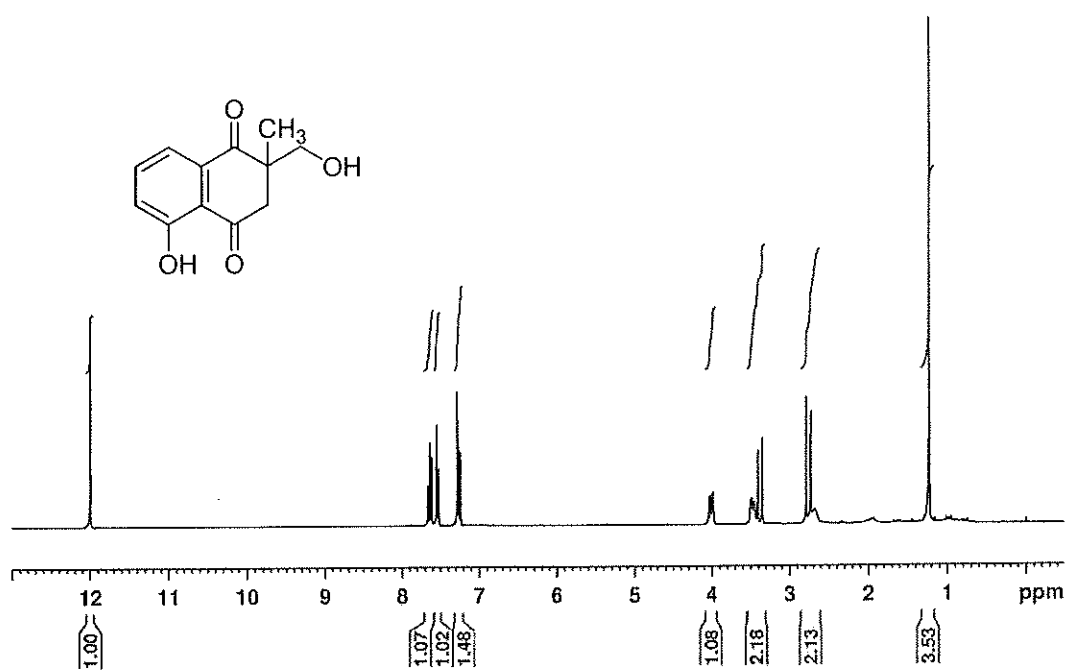


Figure 45 $^{13}\text{C NMR}$ (100 MHz) (CDCl_3) spectrum of compound DW4



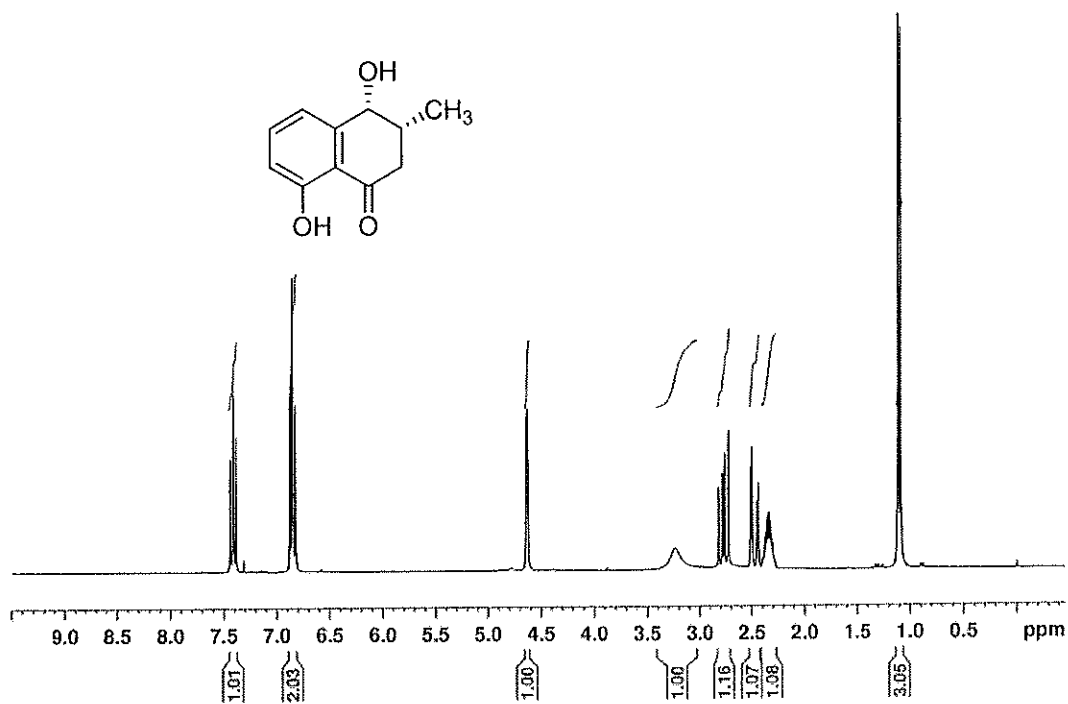


Figure 48 $^1\text{H NMR}$ (300 MHz) (CDCl_3) spectrum of compound DW5

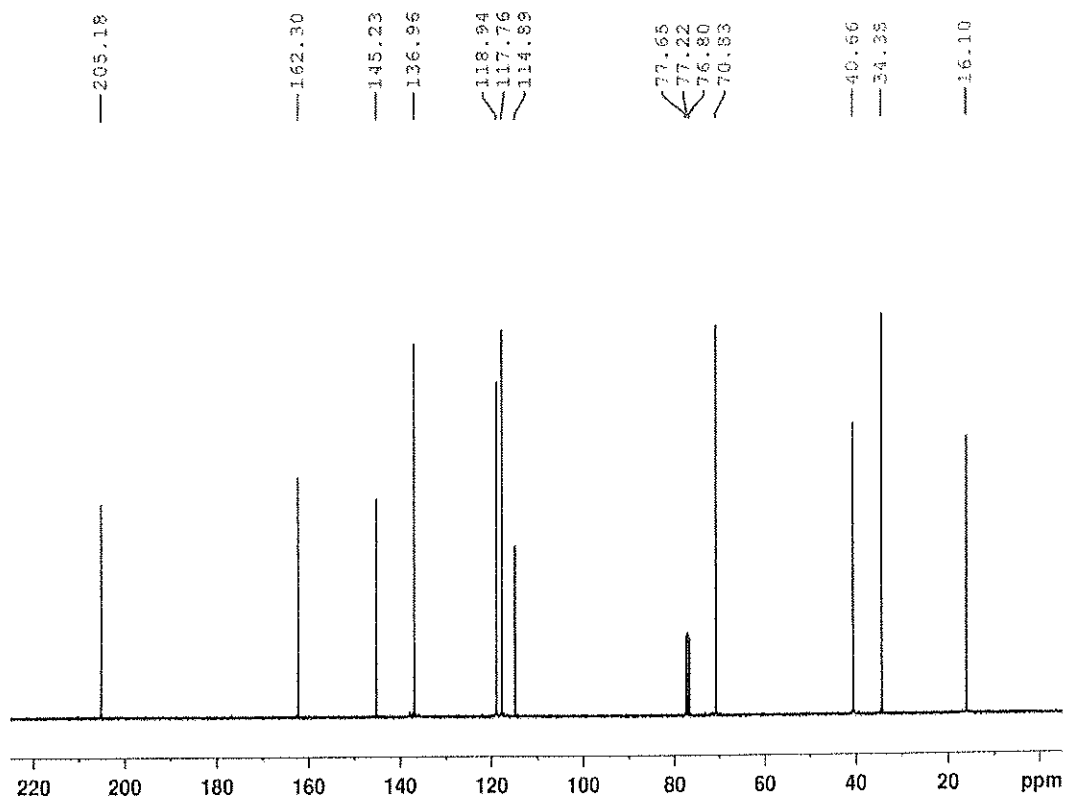


Figure 49 $^{13}\text{C NMR}$ (75 MHz) (CDCl_3) spectrum of compound DW5

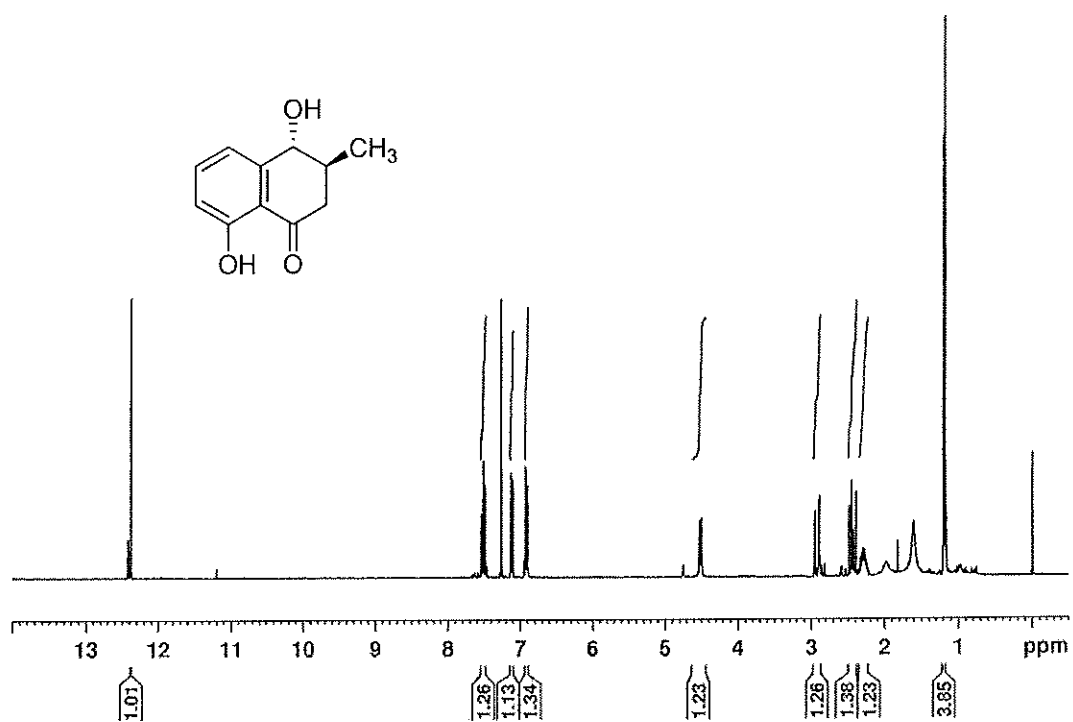


Figure 50 ¹H NMR (300 MHz) (CDCl₃) spectrum of compound DW7

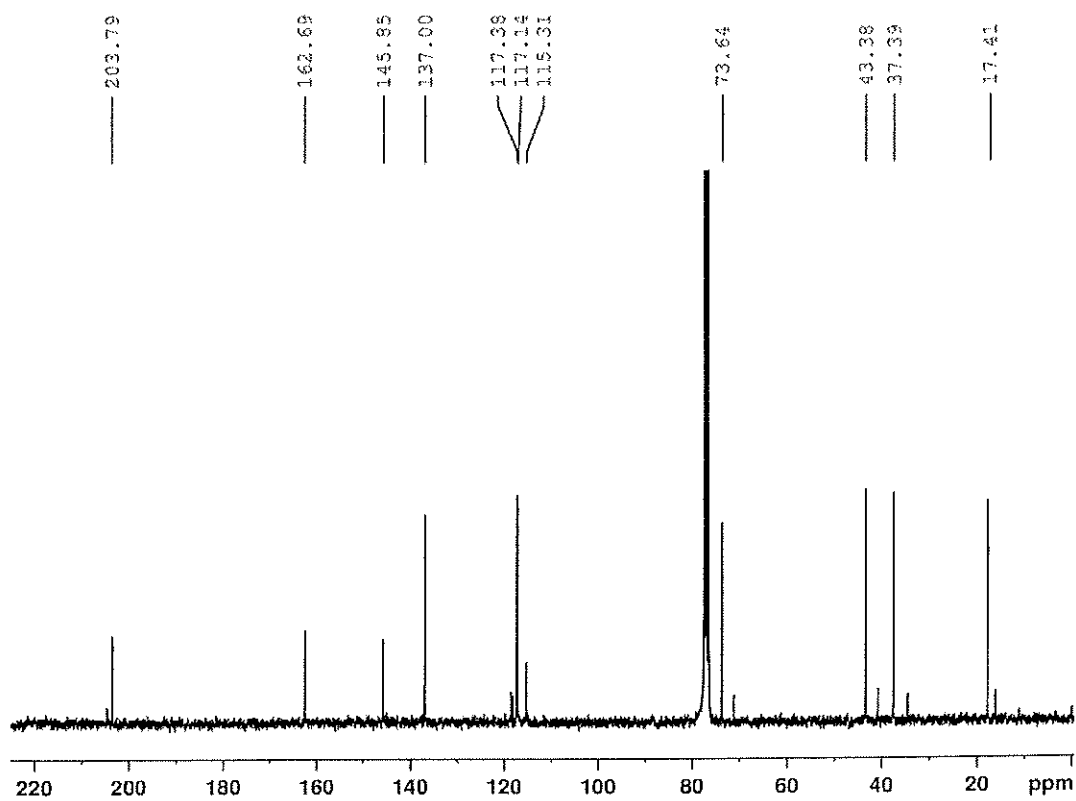


Figure 51 ¹³C NMR (75 MHz) (CDCl₃) spectrum of compound DW7

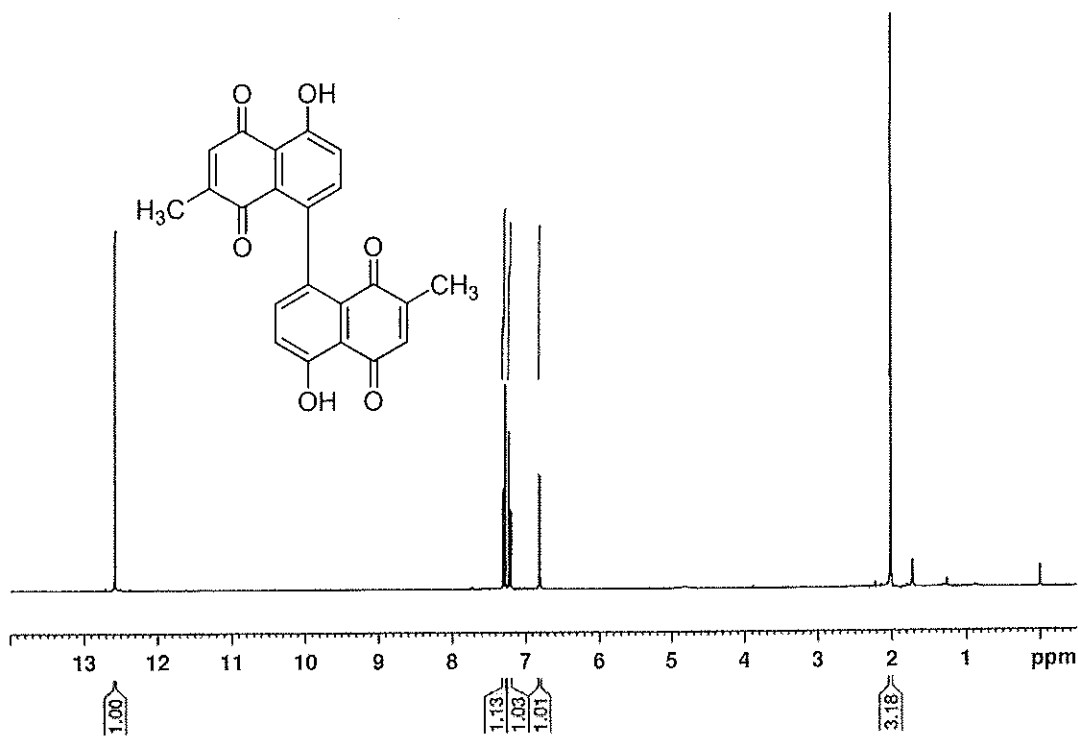


Figure 52 ^1H NMR (300 MHz) (CDCl_3) spectrum of compound DW8



Figure 53 ^{13}C NMR (75 MHz) (CDCl_3) spectrum of compound DW8

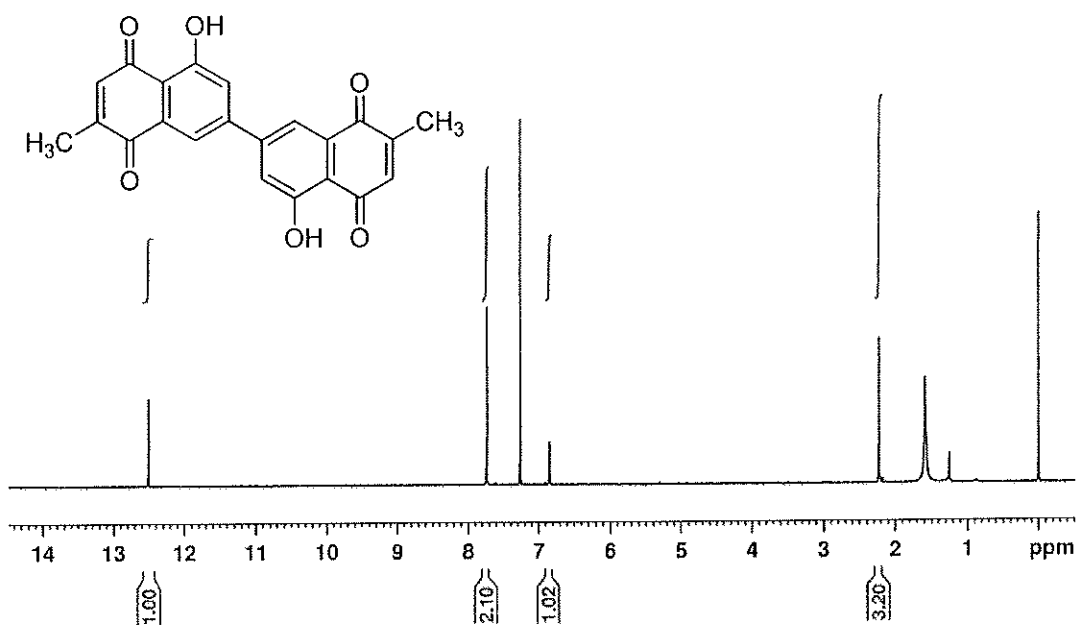


Figure 54 ^1H NMR (300 MHz) (CDCl_3) spectrum of compound DW9

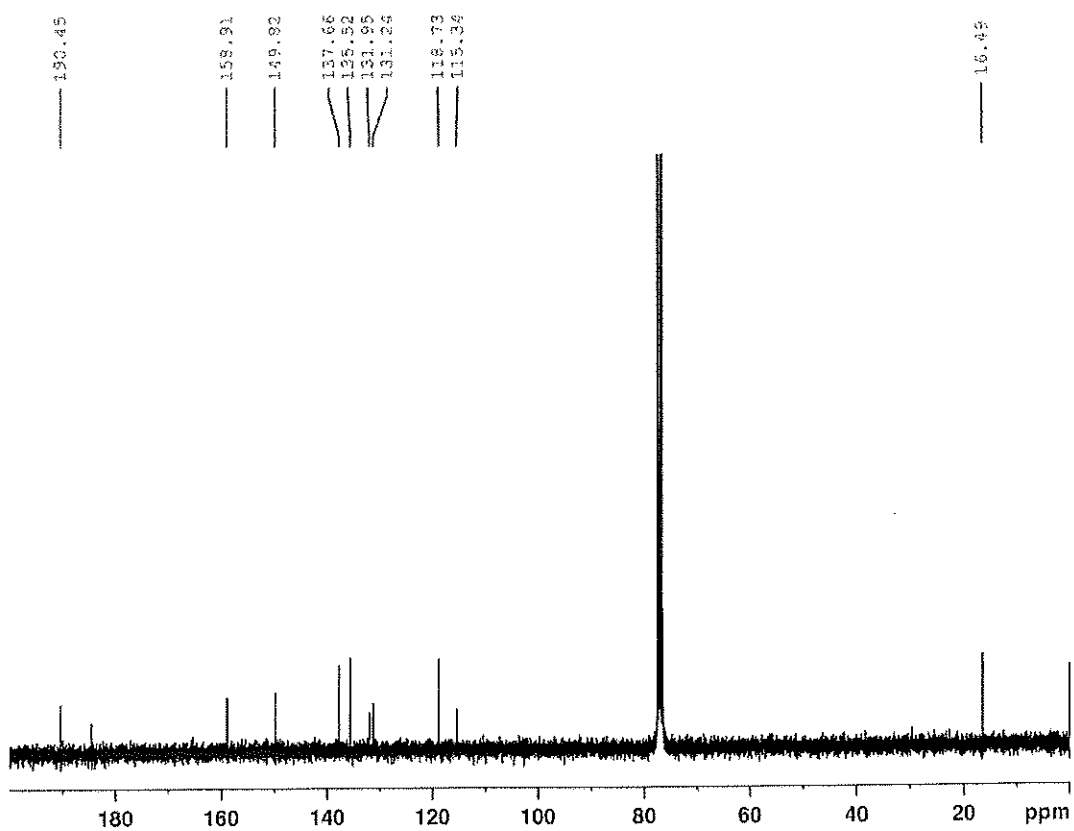
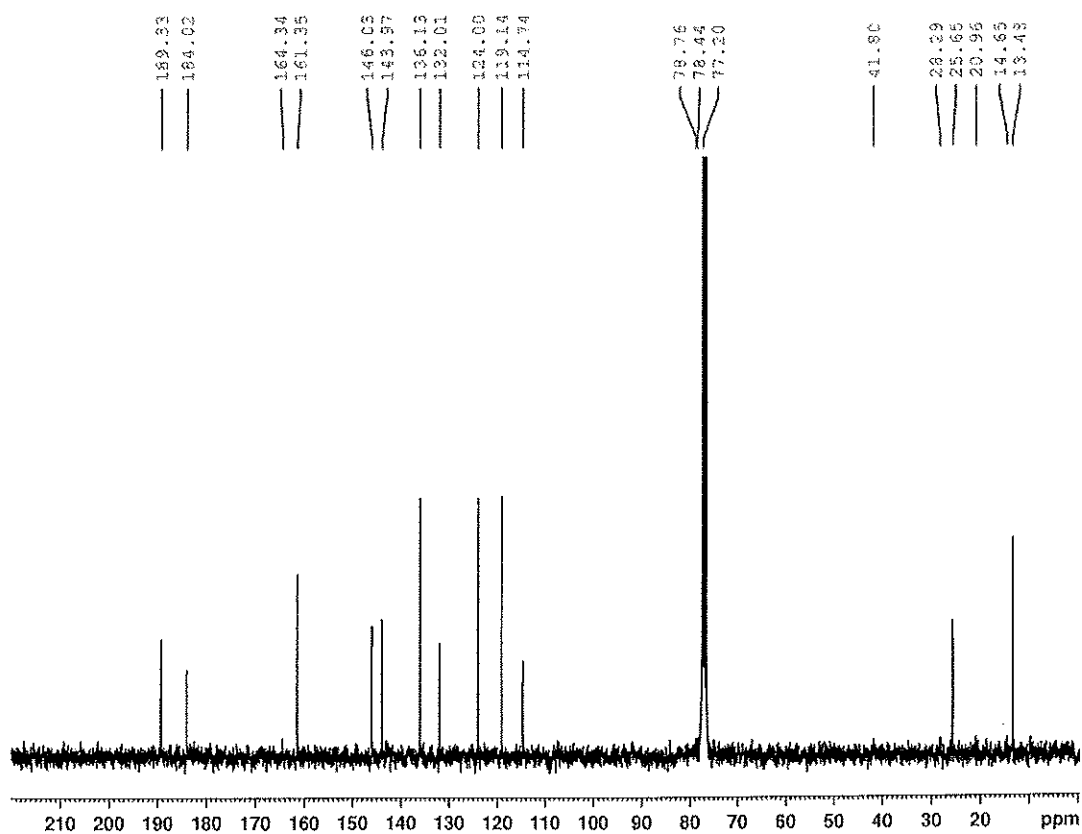
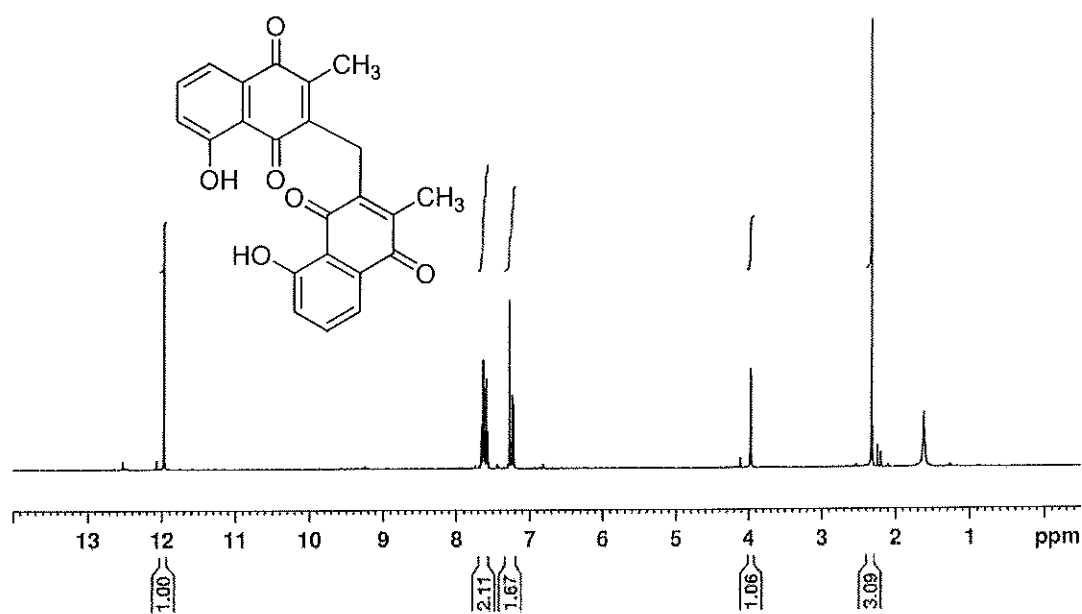


Figure 55 ^{13}C NMR (75 MHz) (CDCl_3) spectrum of compound DW9



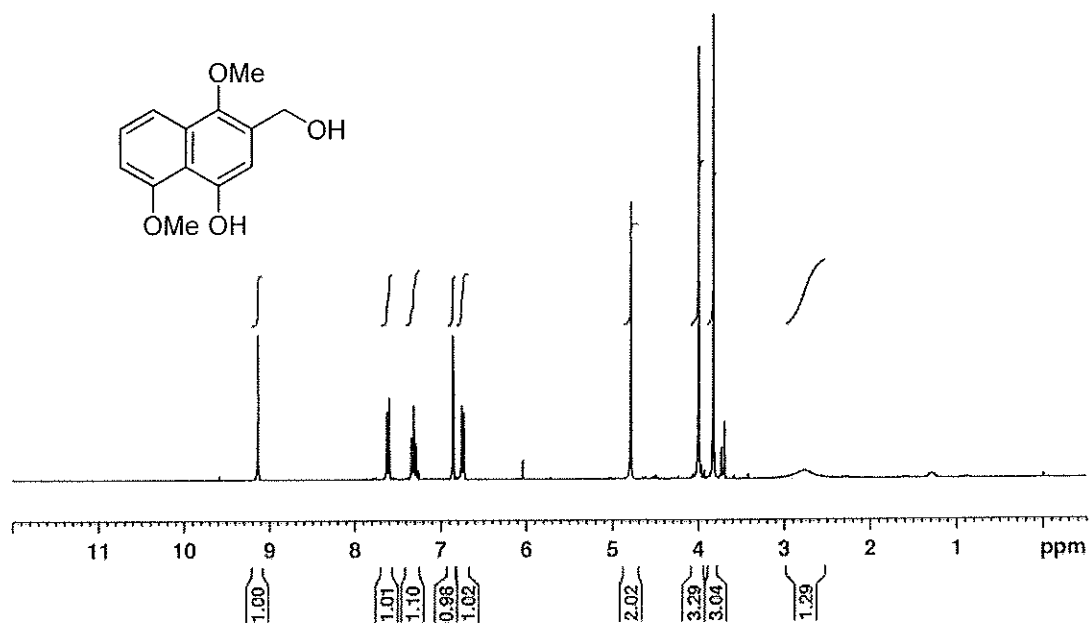


Figure 58 $^1\text{H NMR}$ (400 MHz) (CDCl_3) spectrum of compound DW11

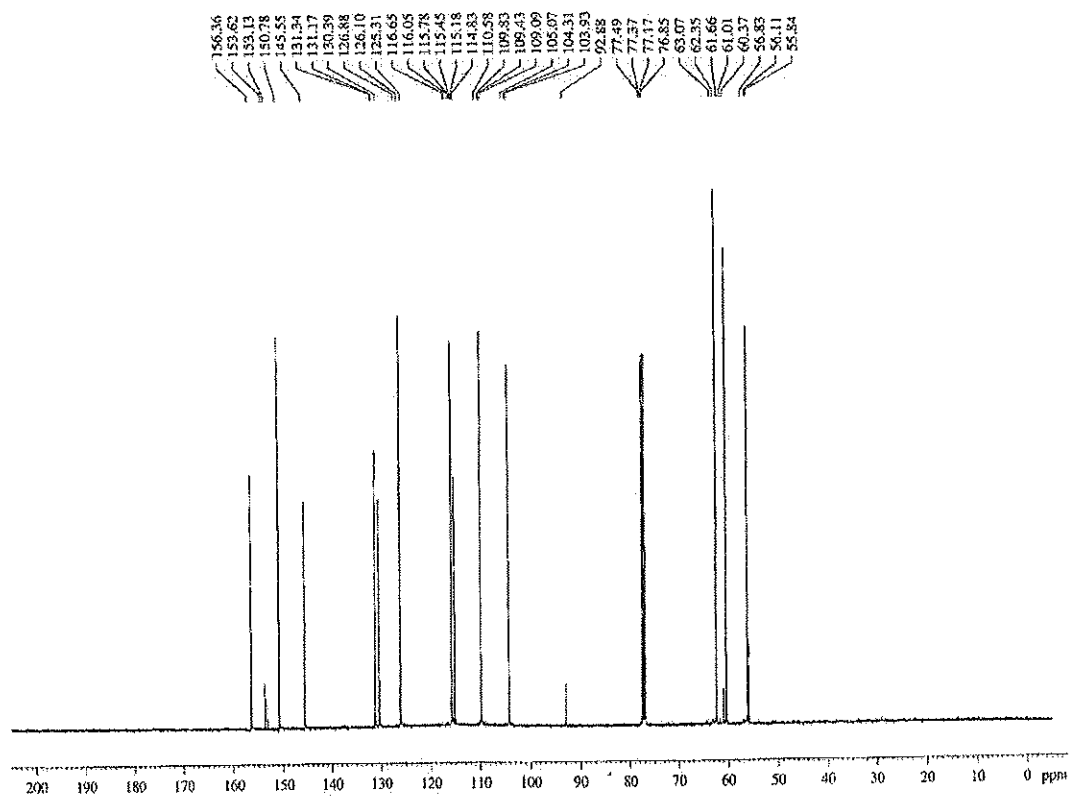


Figure 59 $^{13}\text{C NMR}$ (100 MHz) (CDCl_3) spectrum of compound DW11

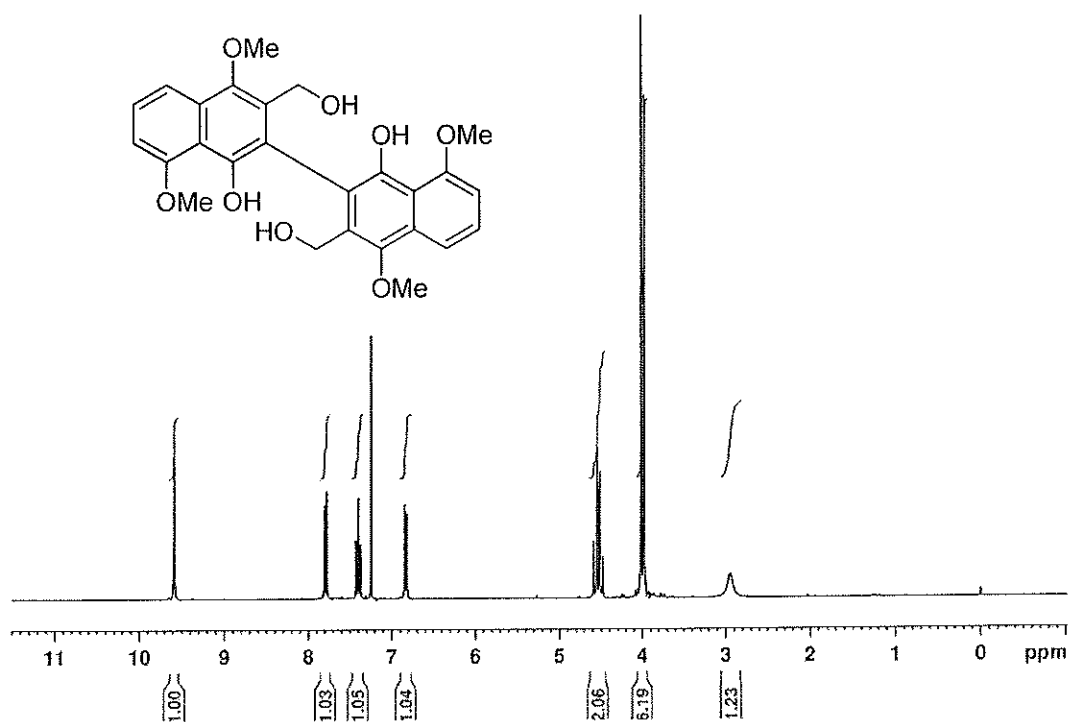


Figure 60 ^1H NMR (300 MHz) (CDCl_3) spectrum of compound DW12

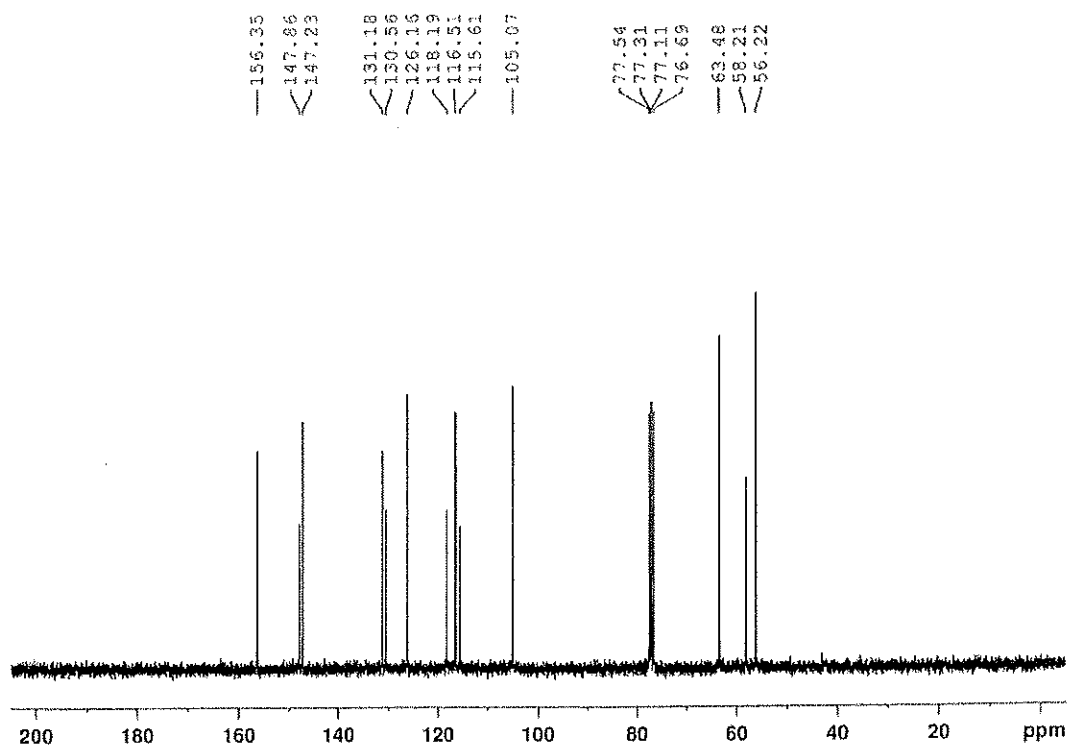


Figure 61 ^{13}C NMR (75 MHz) (CDCl_3) spectrum of compound DW12

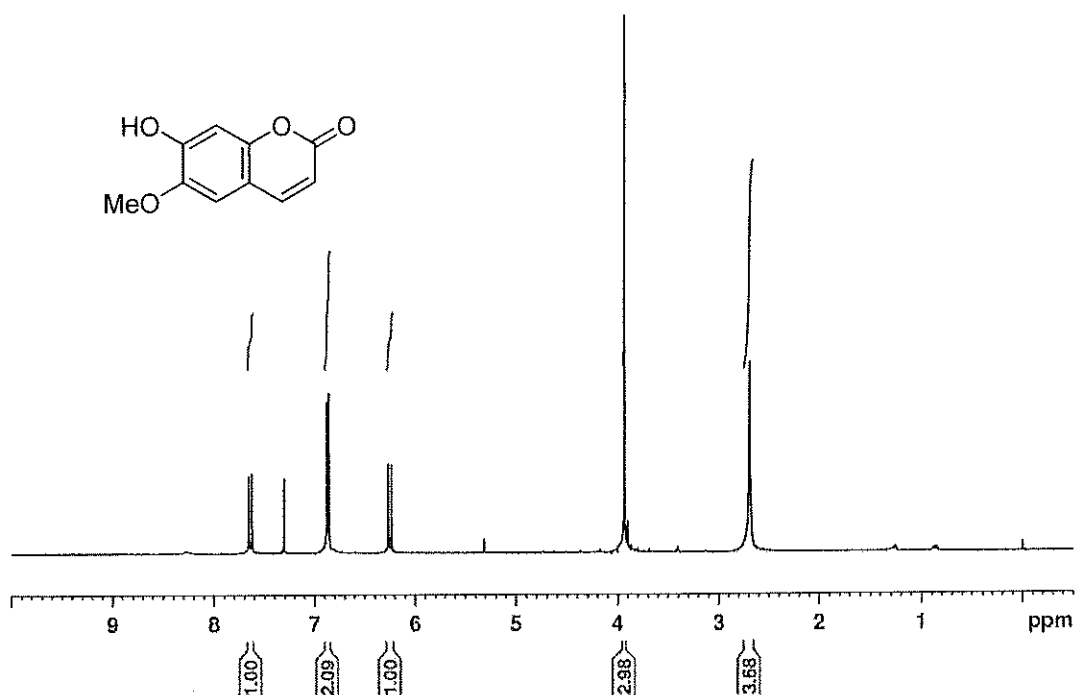


Figure 62 $^1\text{H NMR}$ (300 MHz) (CDCl_3) spectrum of compound DW13

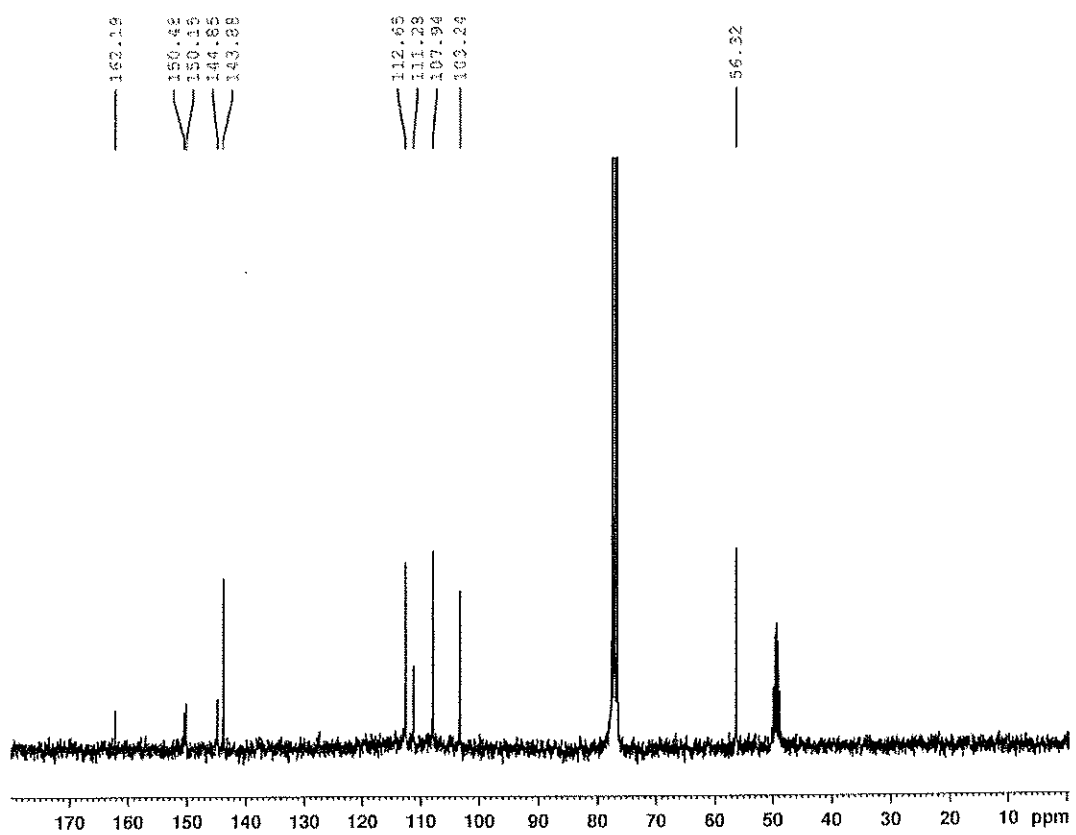


Figure 63 $^{13}\text{C NMR}$ (75 MHz) (CDCl_3) spectrum of compound DW1

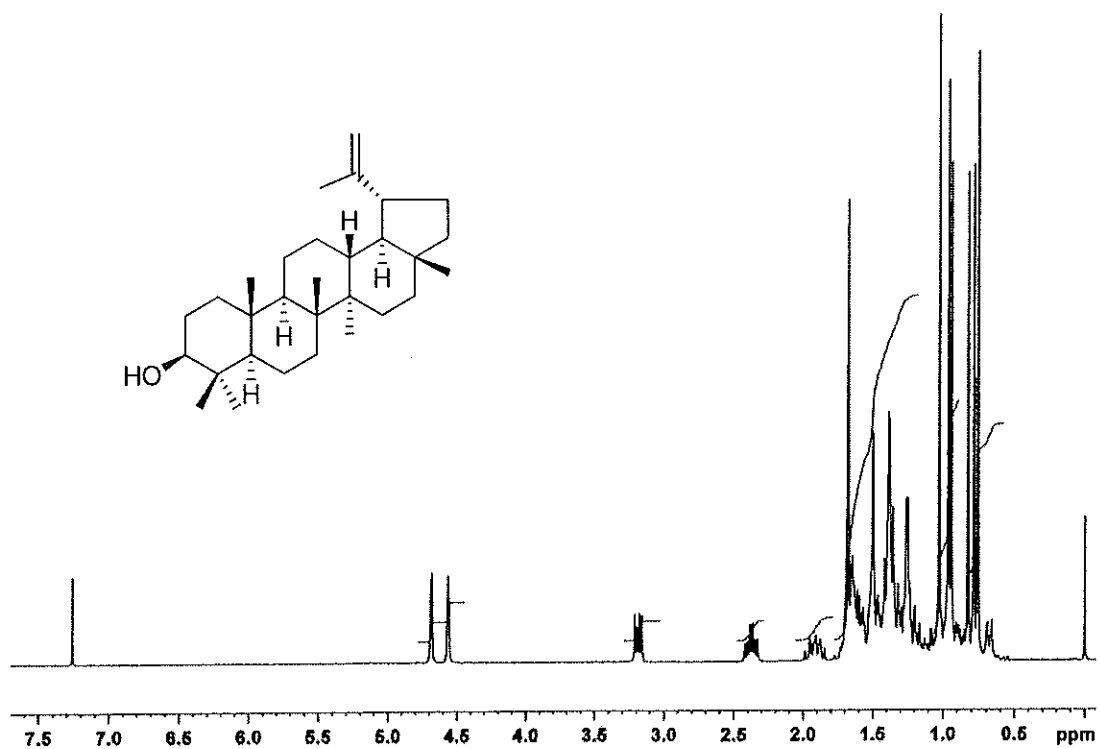


Figure 64 ^1H NMR (300 MHz) (CDCl_3) spectrum of compound DW14

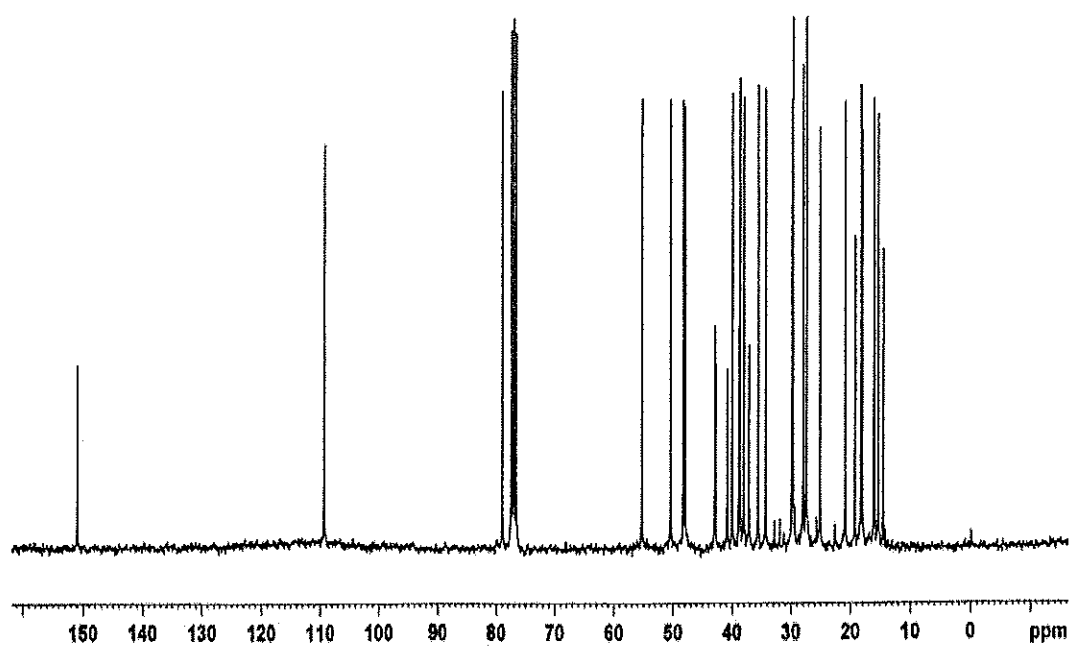


Figure 65 ^{13}C NMR (75 MHz) (CDCl_3) spectrum of compound DW14

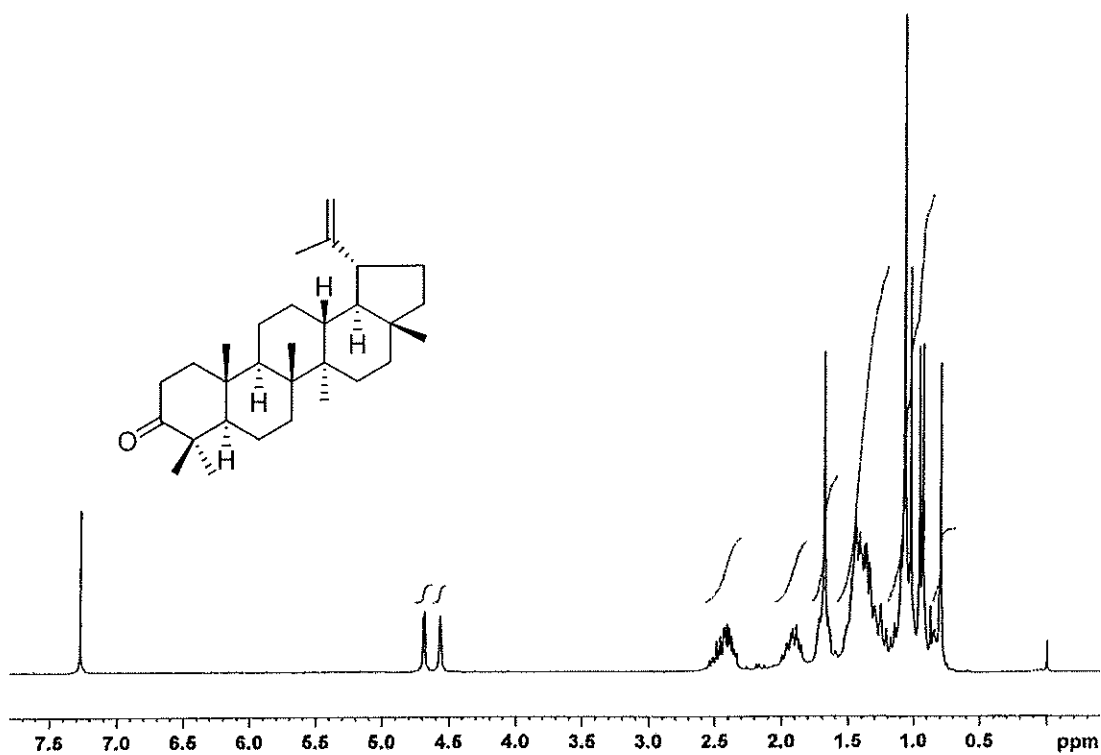


Figure 66 ^1H NMR (300 MHz) (CDCl_3) spectrum of compound DW15

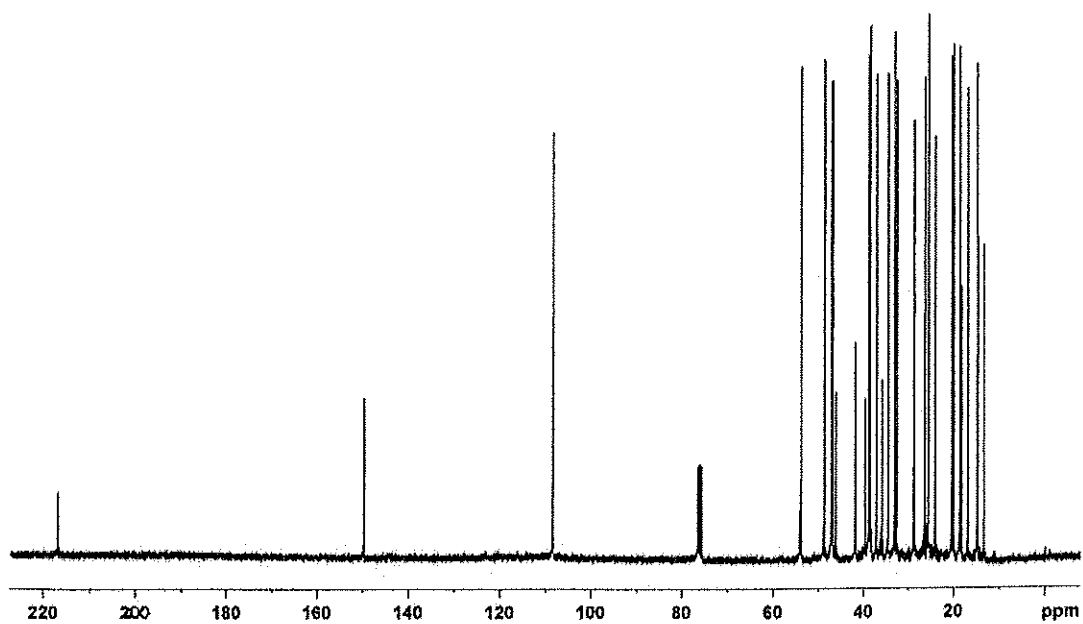


Figure 67 ^{13}C NMR (75 MHz) (CDCl_3) spectrum of compound DW15

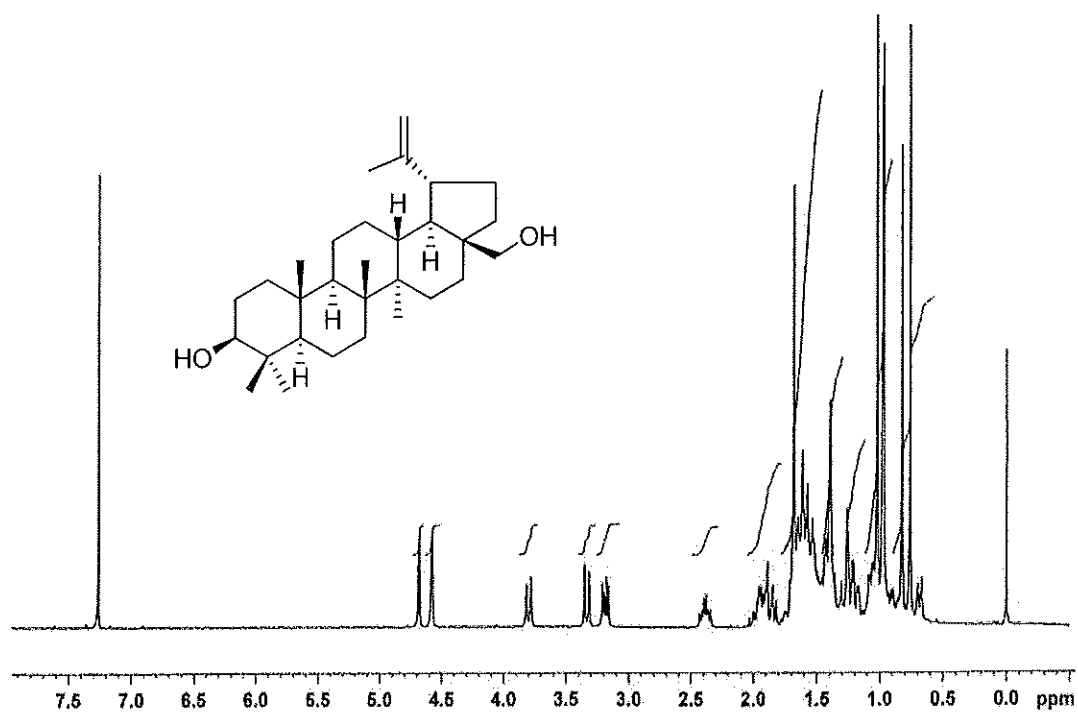


Figure 68 ^1H NMR (300 MHz) (CDCl_3) spectrum of compound DW16

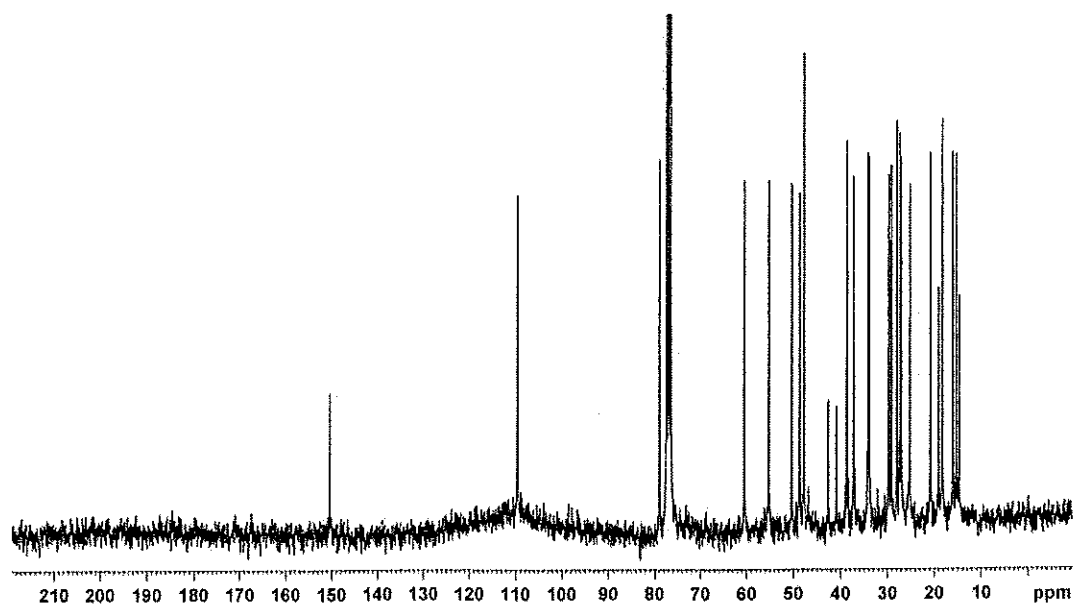


Figure 69 ^{13}C NMR (75 MHz) (CDCl_3) spectrum of compound DW16

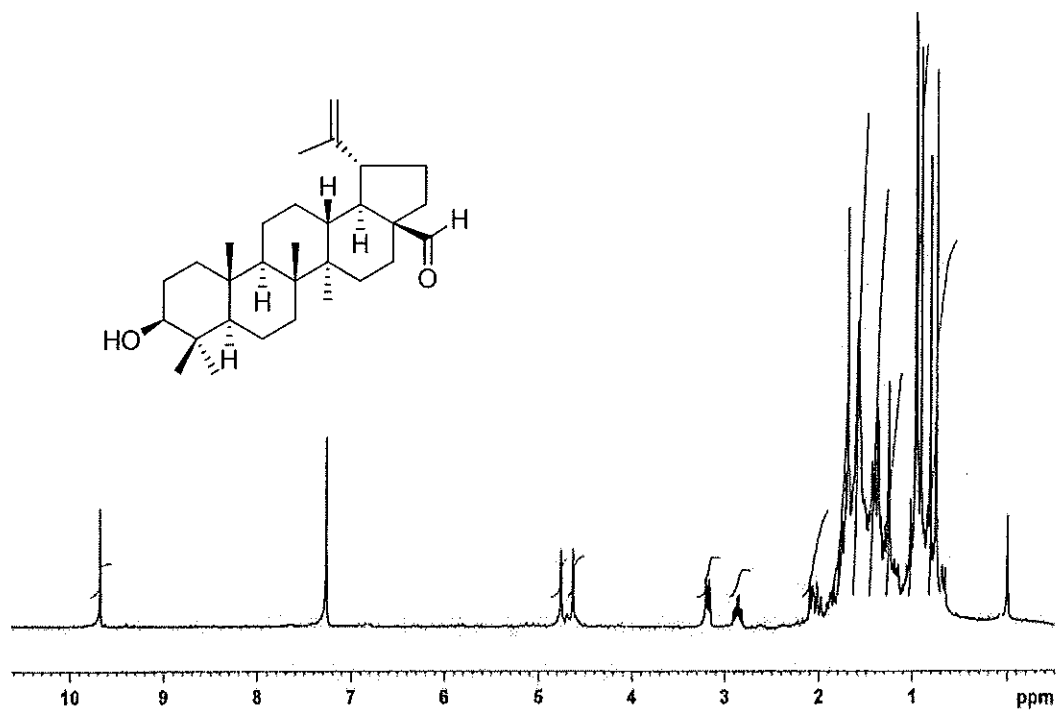


Figure 70 ^1H NMR (300 MHz) (CDCl_3) spectrum of compound DW17

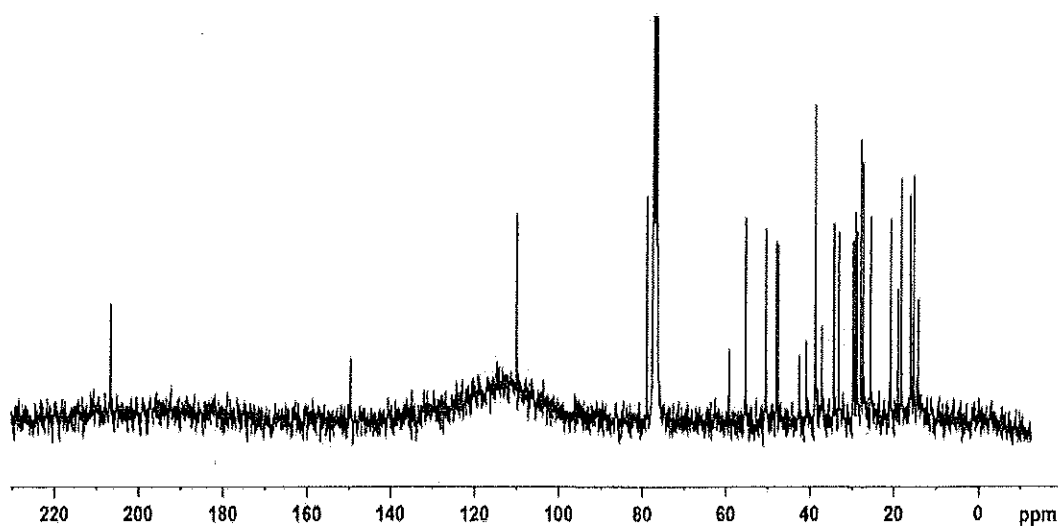


Figure 71 ^{13}C NMR (75 MHz) (CDCl_3) spectrum of compound DW17

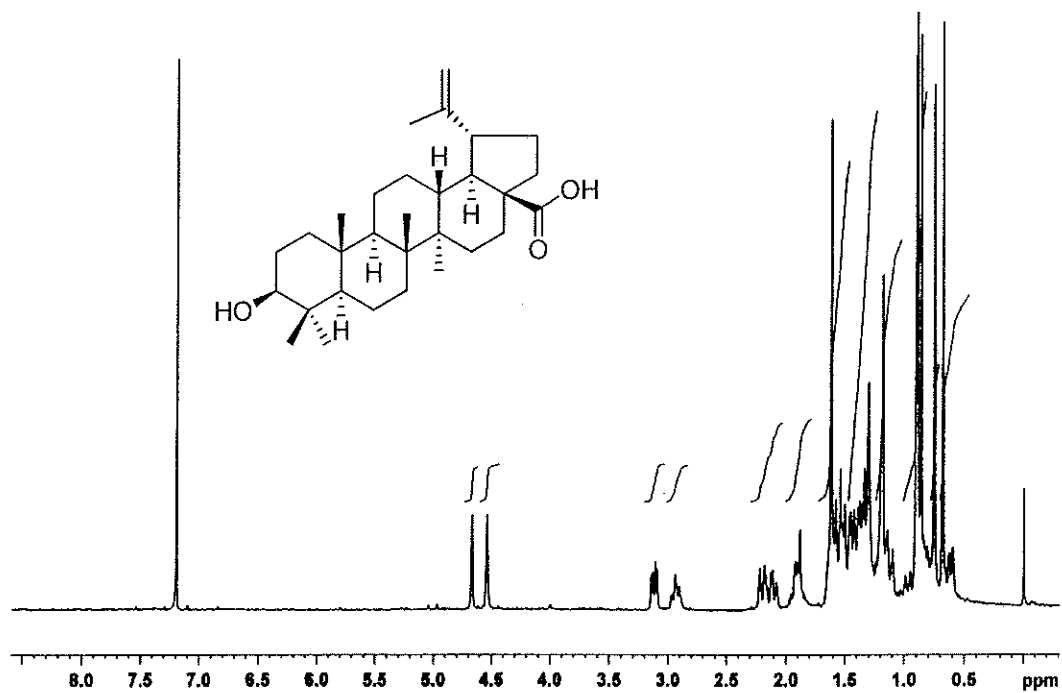


Figure 72 ^1H NMR (300 MHz) ($\text{CDCl}_3+\text{CD}_3\text{OD}$) spectrum of compound DW18

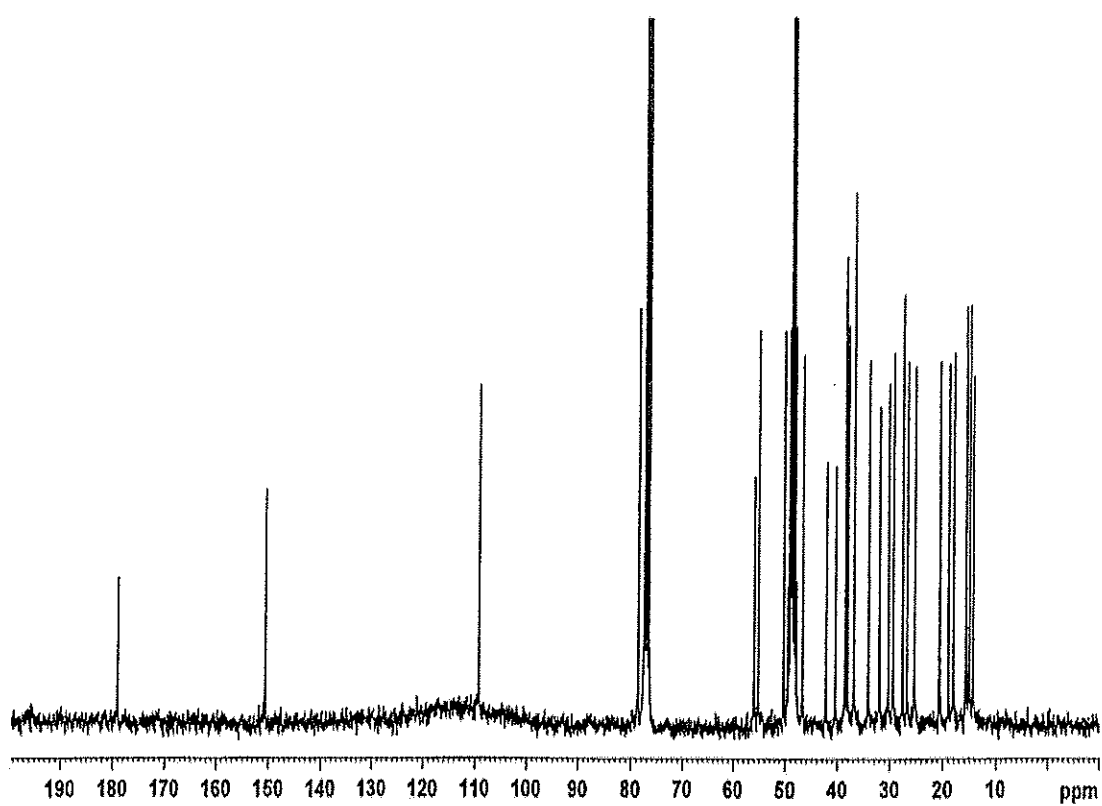


Figure 73 ^{13}C NMR (75 MHz) ($\text{CDCl}_3+\text{CD}_3\text{OH}$) spectrum of compound DW18

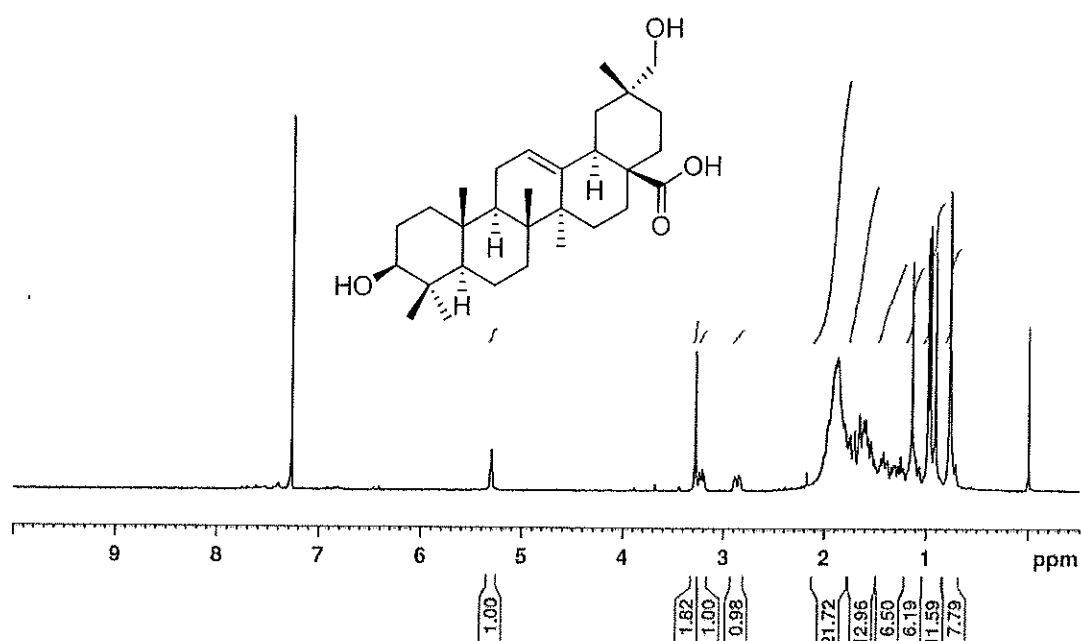


Figure 74 $^1\text{H NMR}$ (300 MHz) (CDCl_3) spectrum of compound DW19

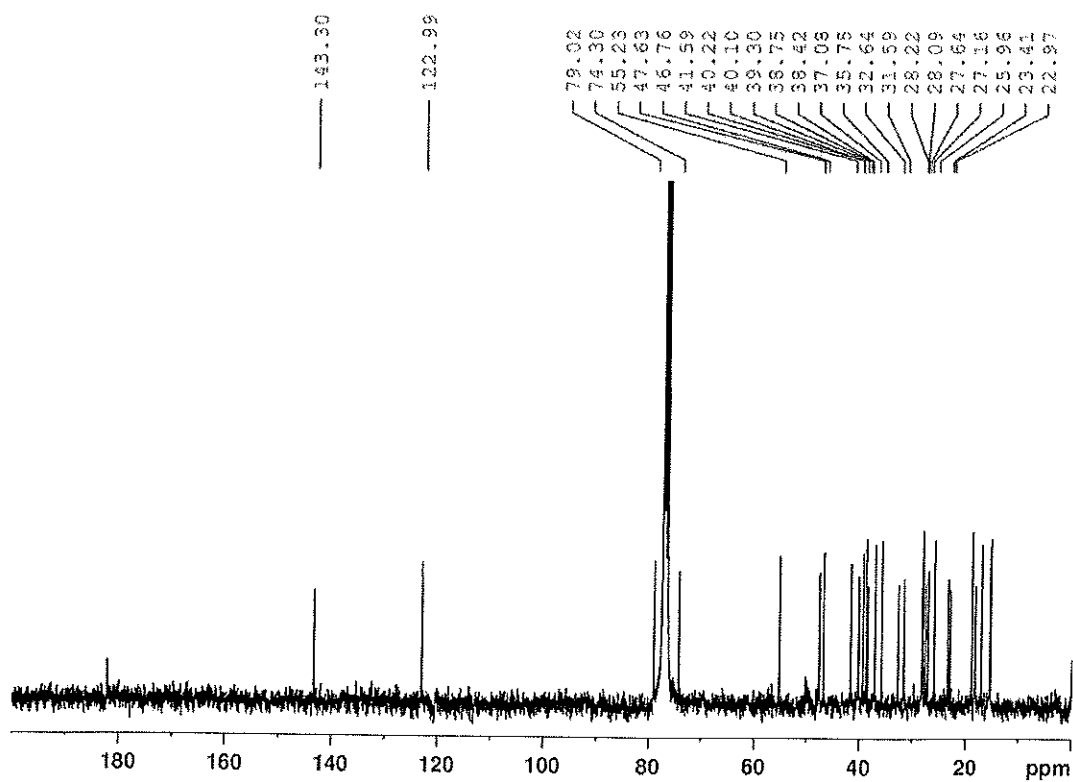
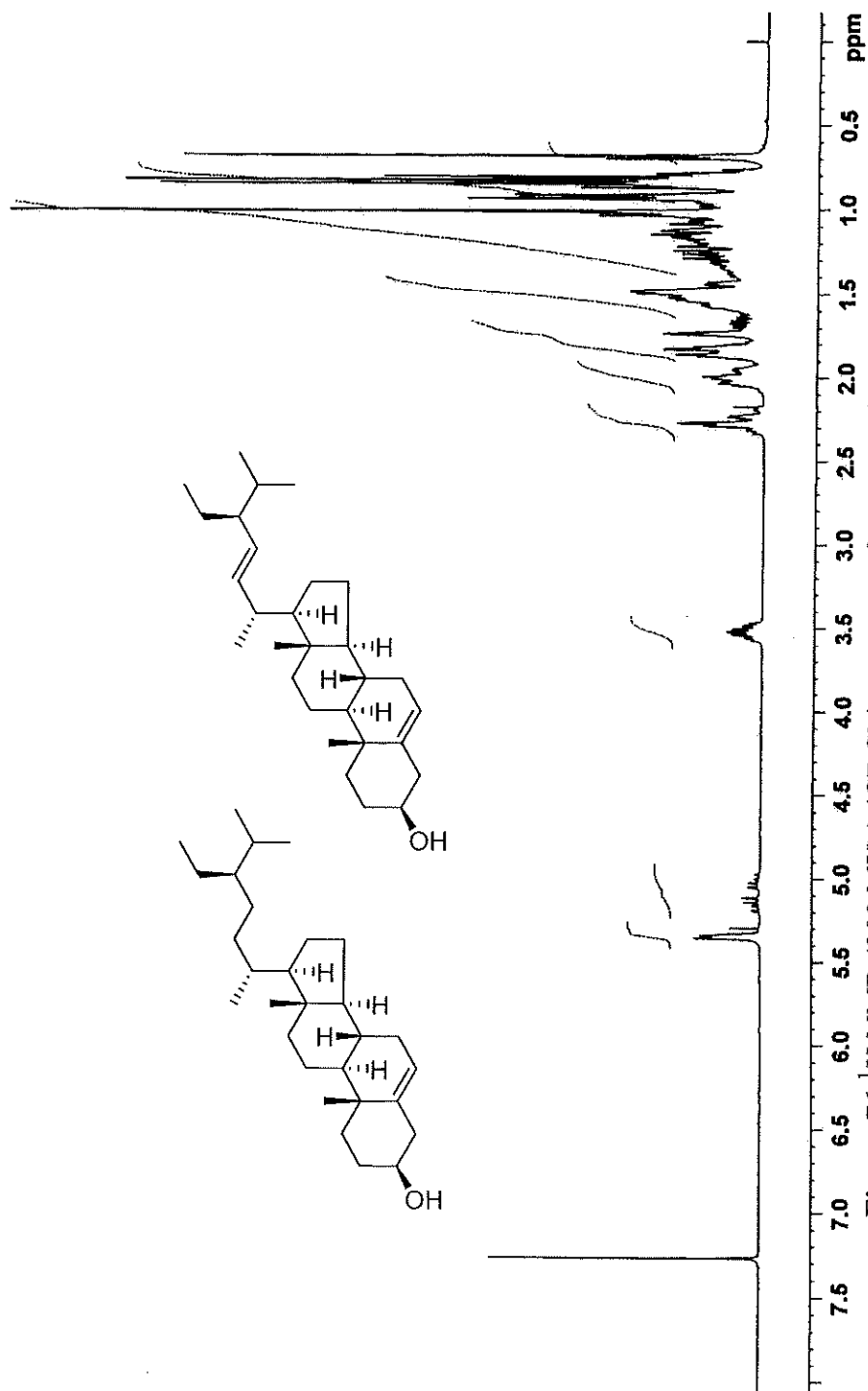


Figure 75 $^{13}\text{C NMR}$ (75 MHz) (CDCl_3) spectrum of compound DW19



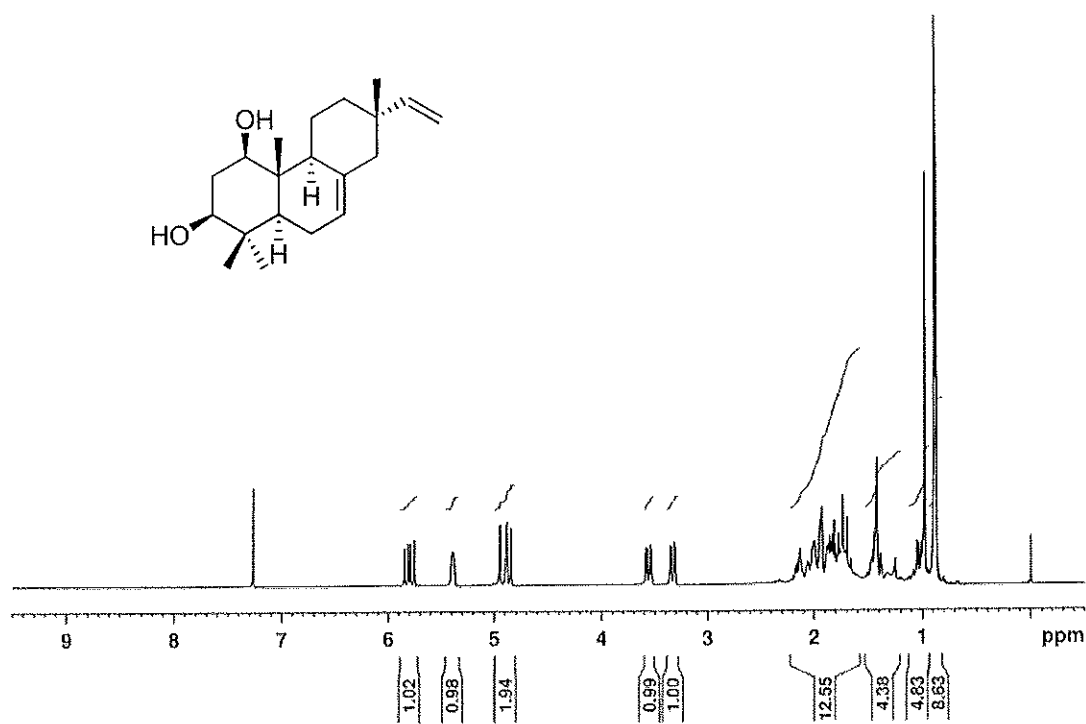


Figure 77 ^1H NMR (300 MHz) (CDCl_3) spectrum of compound PO1

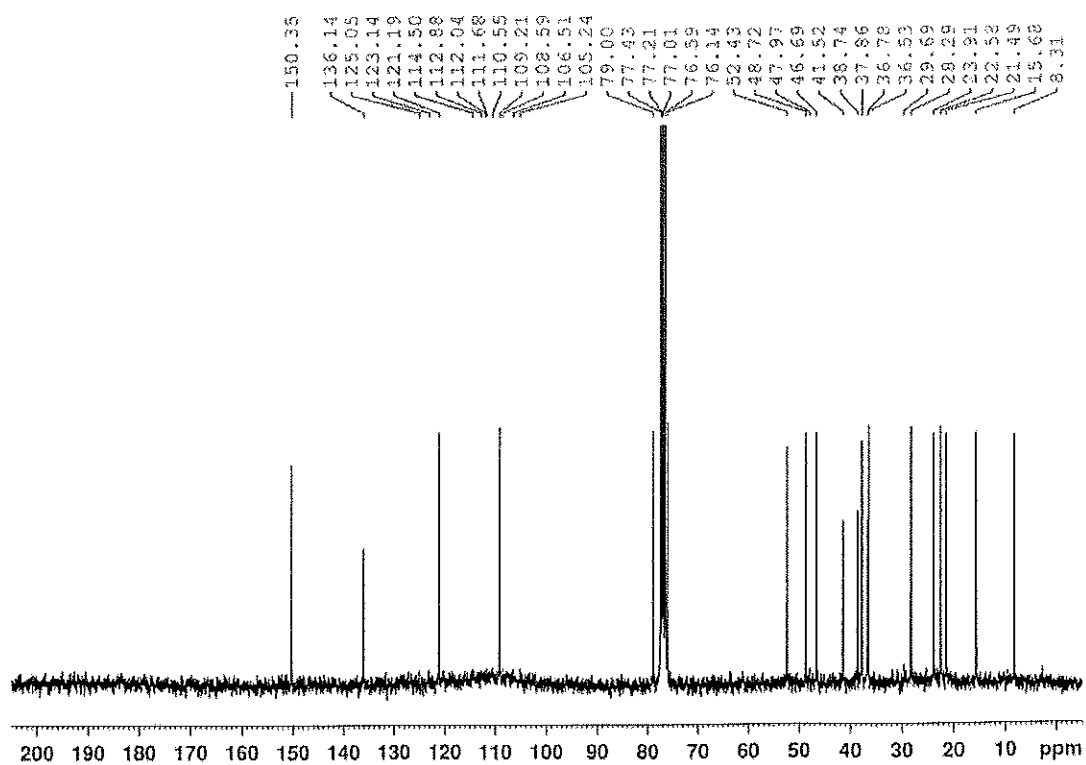


Figure 78 ^{13}C NMR (75 MHz) (CDCl_3) spectrum of compound PO1

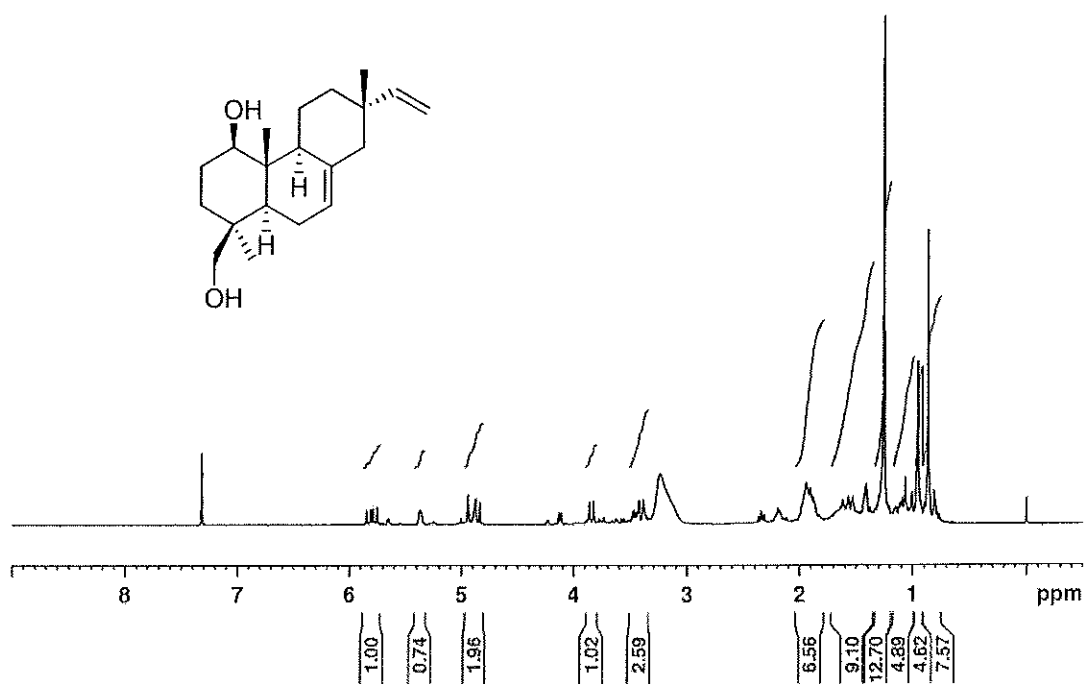


Figure 79 ^1H NMR (300 MHz) ($\text{CDCl}_3+\text{CD}_3\text{OD}$) spectrum of compound PO2

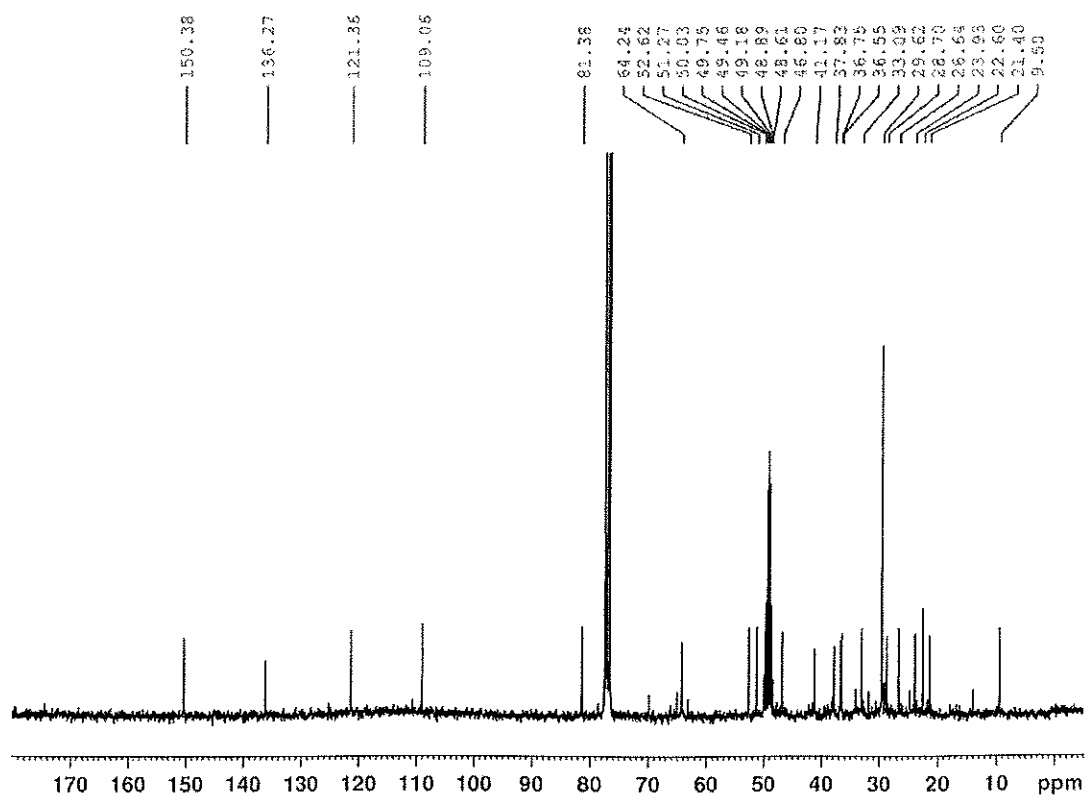


Figure 80 ^{13}C NMR (75 MHz) ($\text{CDCl}_3+\text{CD}_3\text{OD}$) spectrum of compound PO2

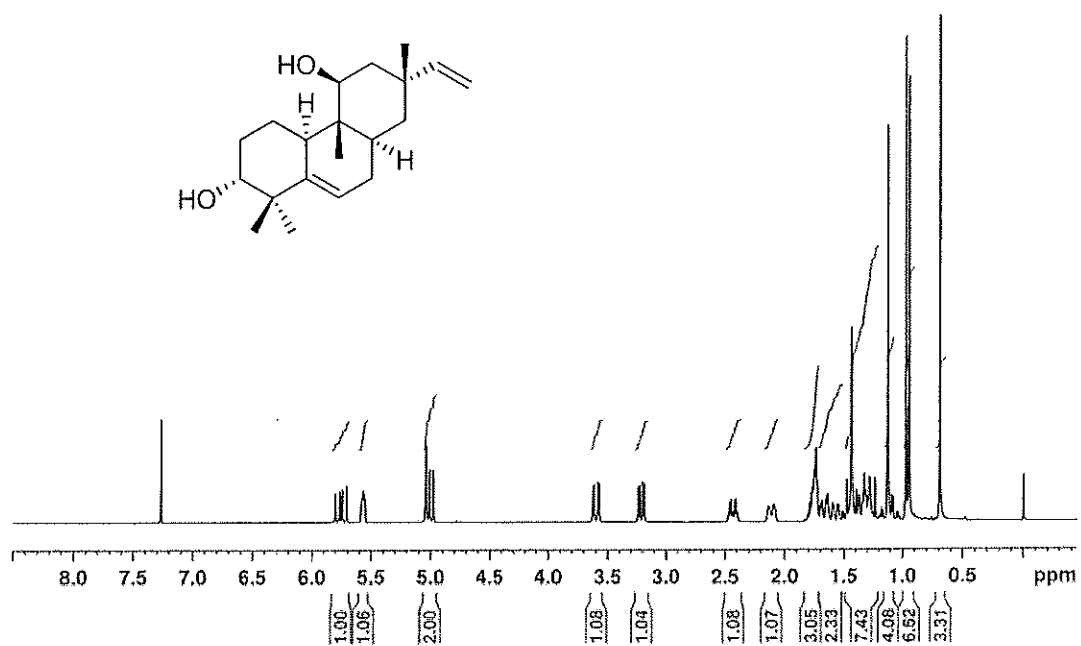


Figure 81 $^1\text{H NMR}$ (300 MHz) (CDCl_3) spectrum of compound PO3

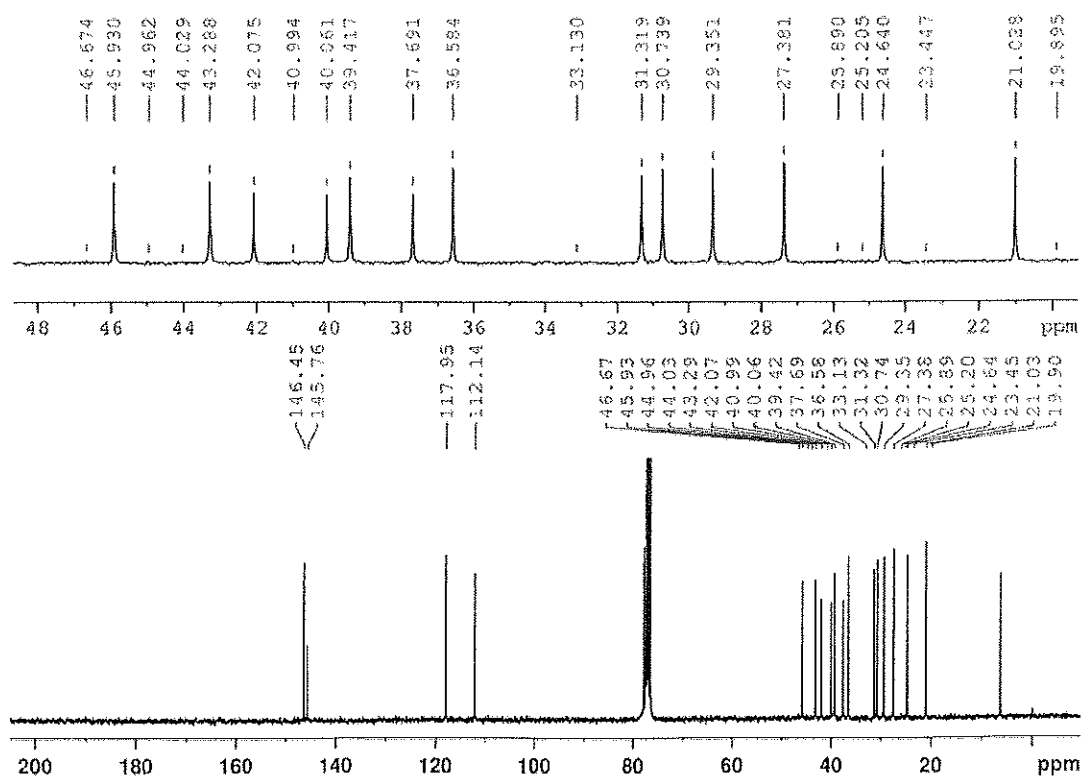


Figure 82 $^{13}\text{C NMR}$ (75 MHz) (CDCl_3) spectrum of compound PO3

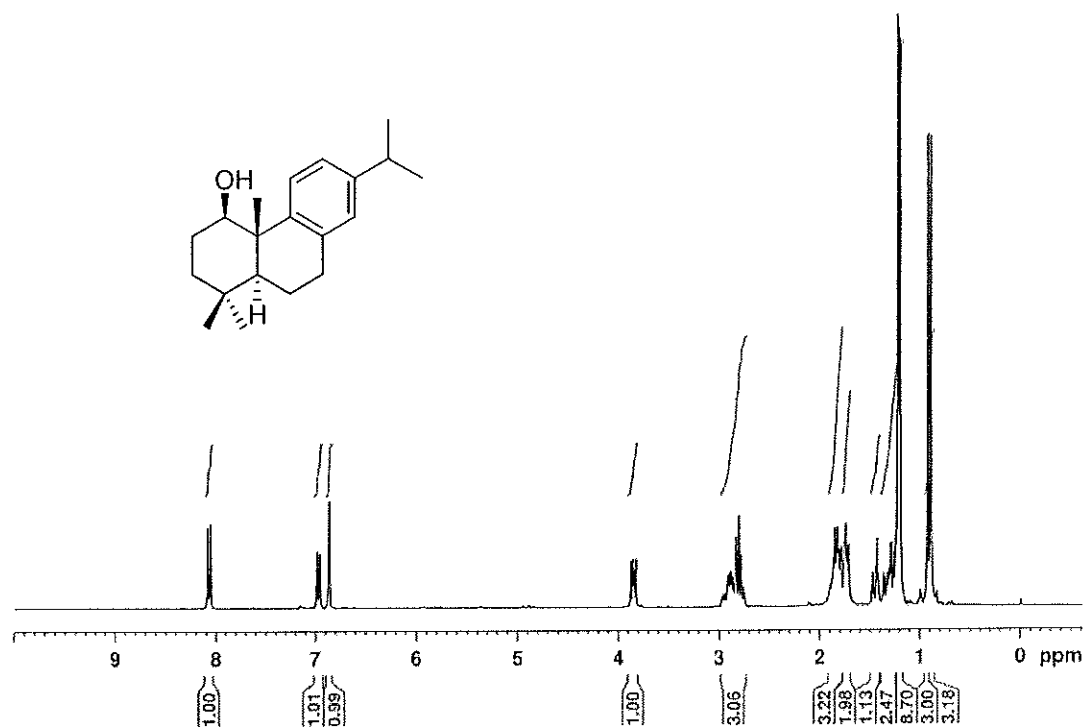


Figure 83 ¹H NMR (300 MHz) (CDCl₃) spectrum of compound PO4

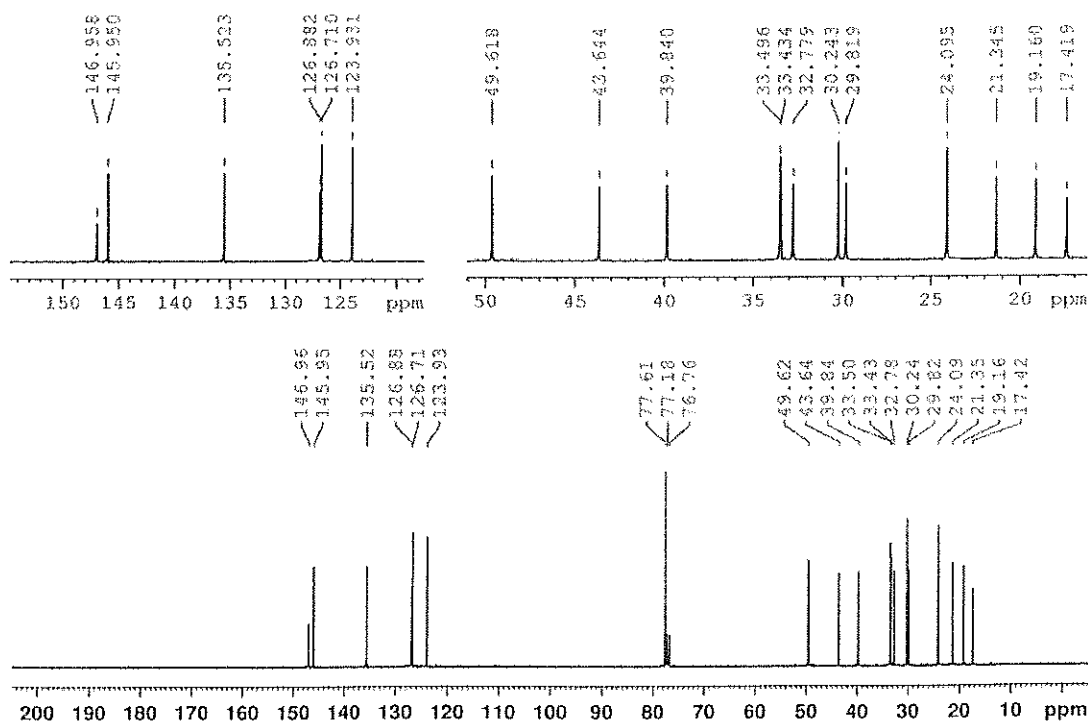


Figure 84 ¹³C NMR (75 MHz) (CDCl₃) spectrum of compound PO4

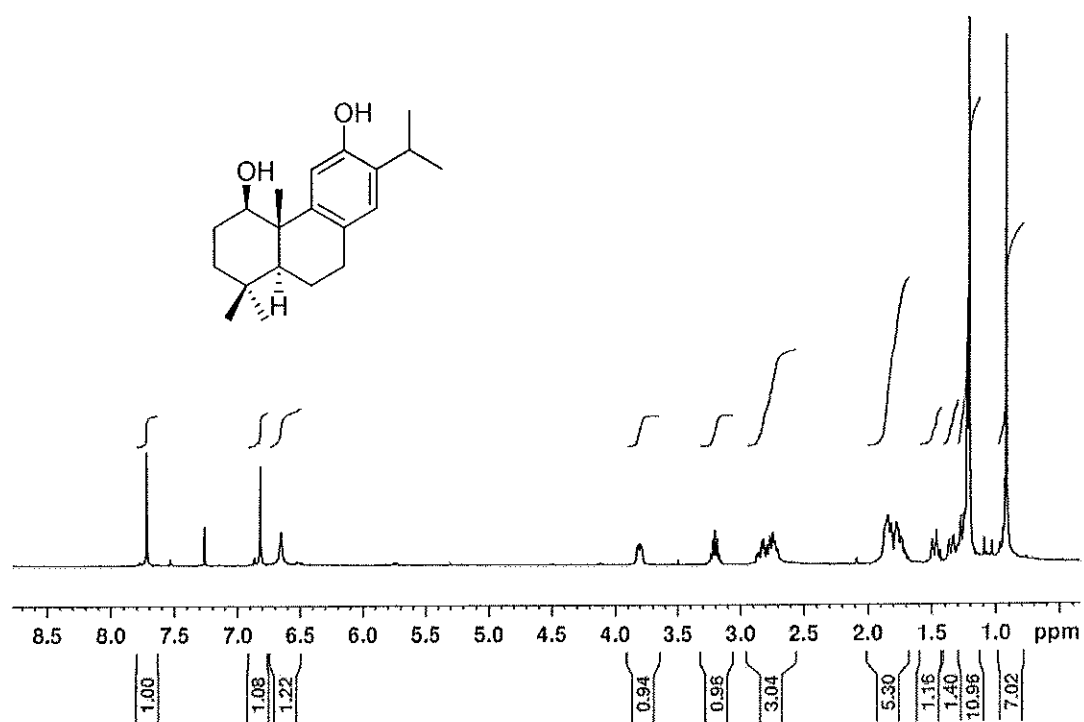


Figure 85 ^1H NMR (400 MHz) (CDCl_3) spectrum of compound PO5

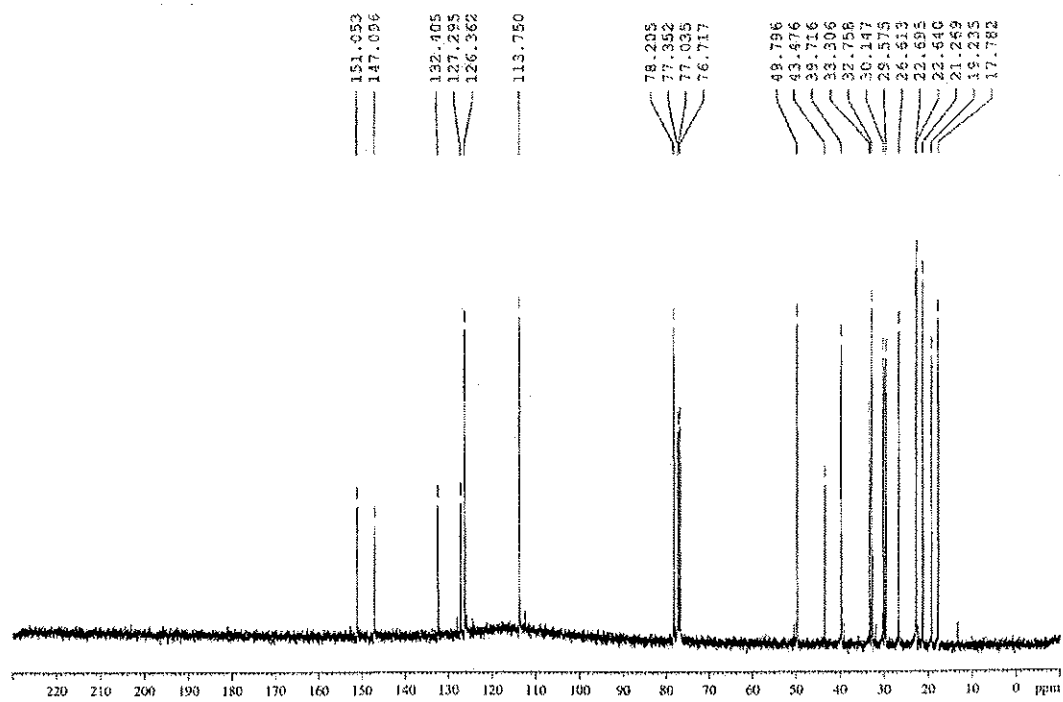


Figure 86 ^{13}C NMR (100 MHz) (CDCl_3) spectrum of compound PO5

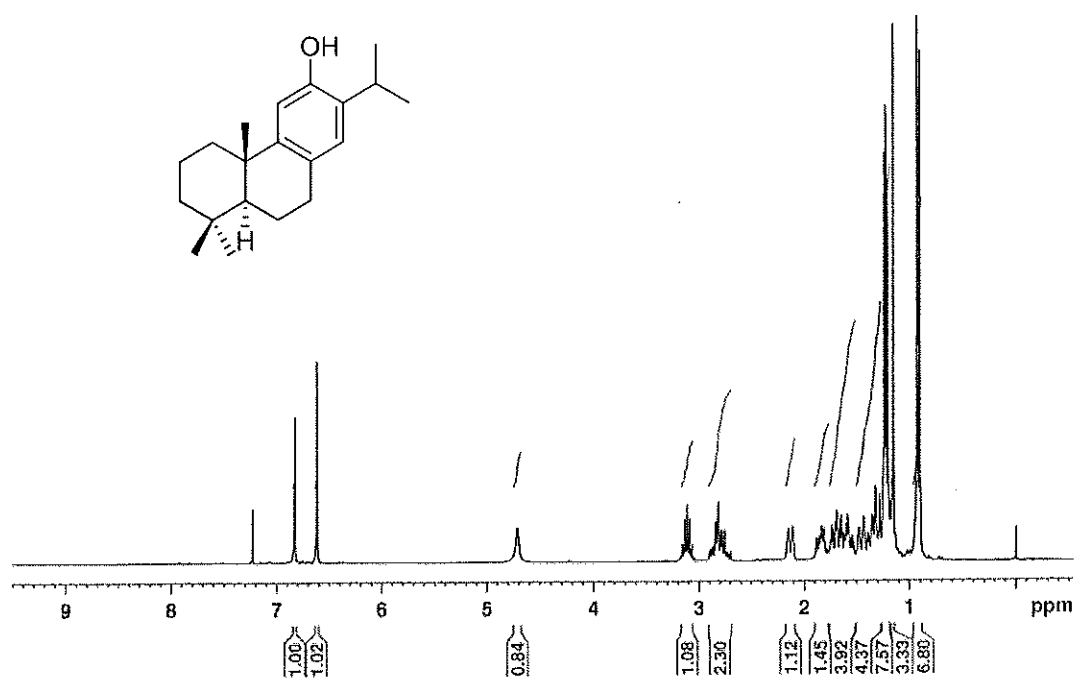


Figure 87 ^1H NMR (300 MHz) (CDCl_3) spectrum of compound PO6

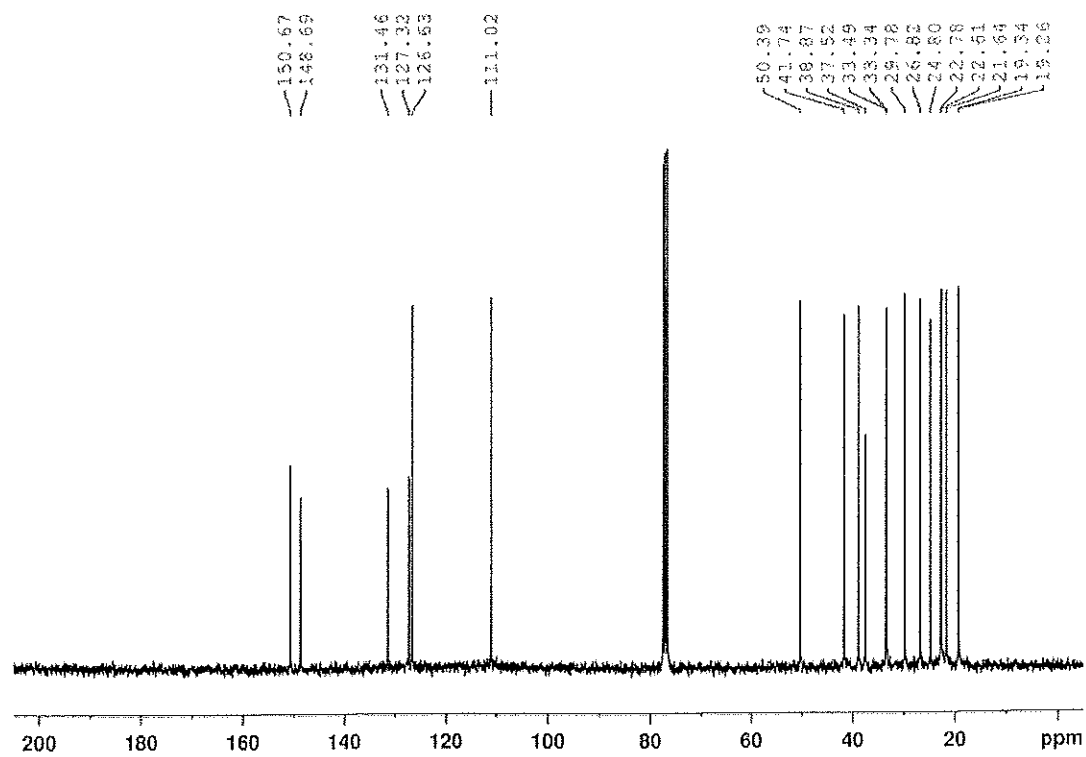


Figure 88 ^{13}C NMR (75 MHz) (CDCl_3) spectrum of compound PO6

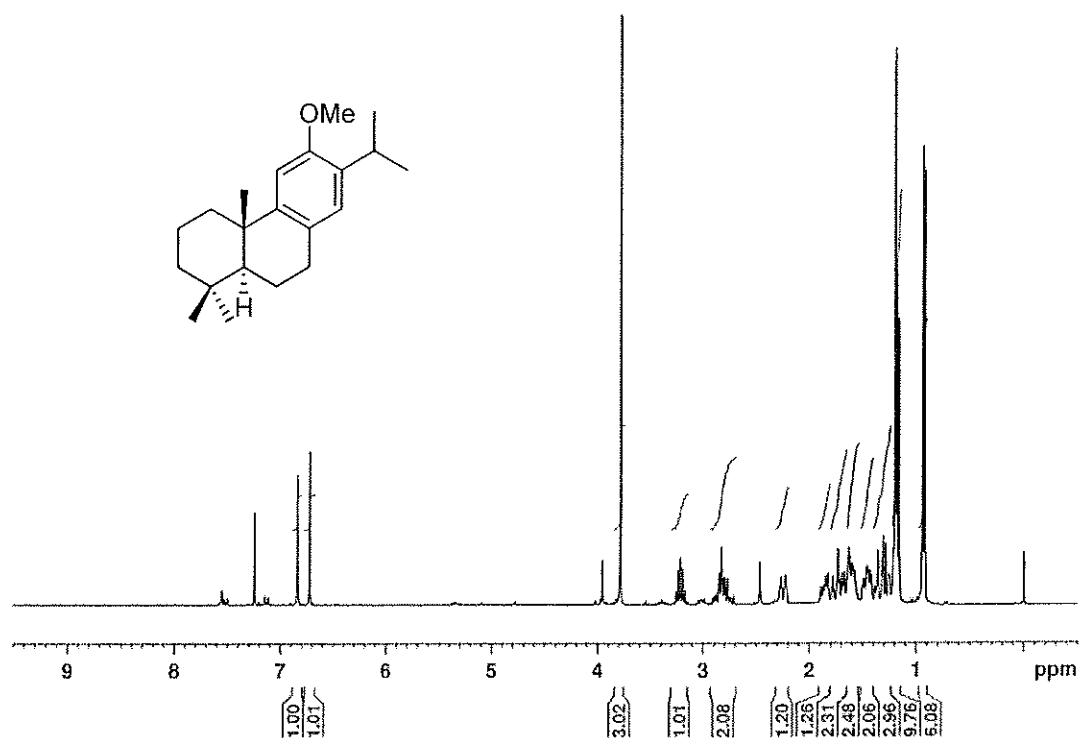


Figure 89 ^1H NMR (300 MHz) (CDCl_3) spectrum of compound PO7

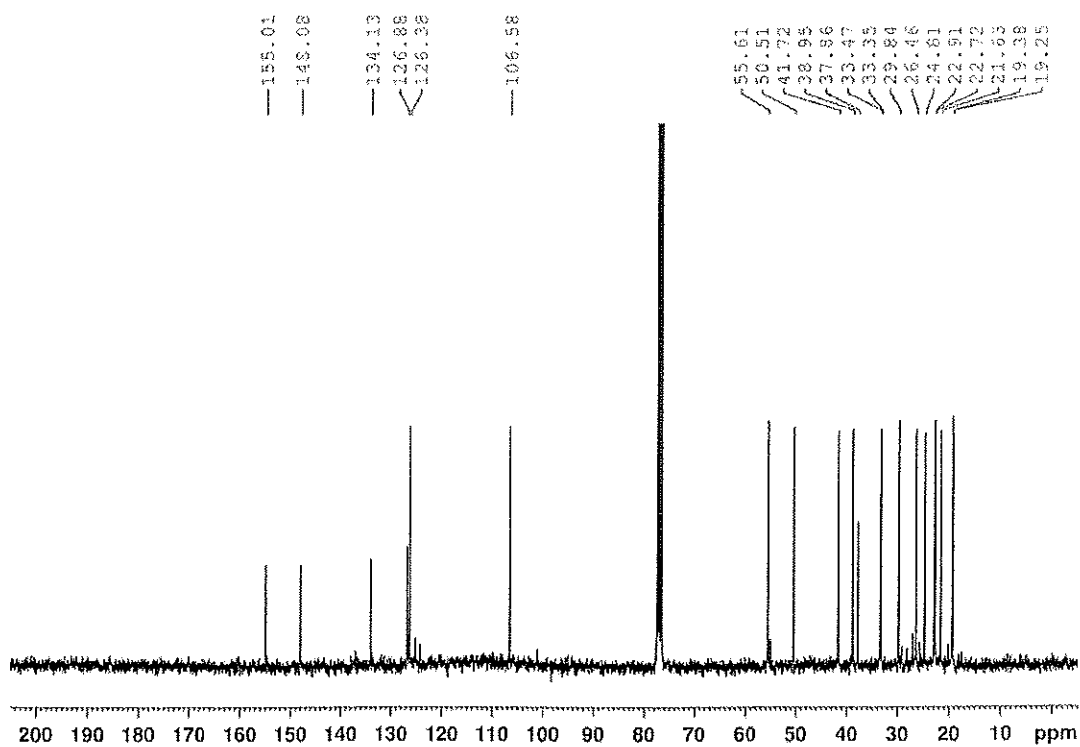


Figure 90 ^{13}C NMR (75 MHz) (CDCl_3) spectrum of compound PO7

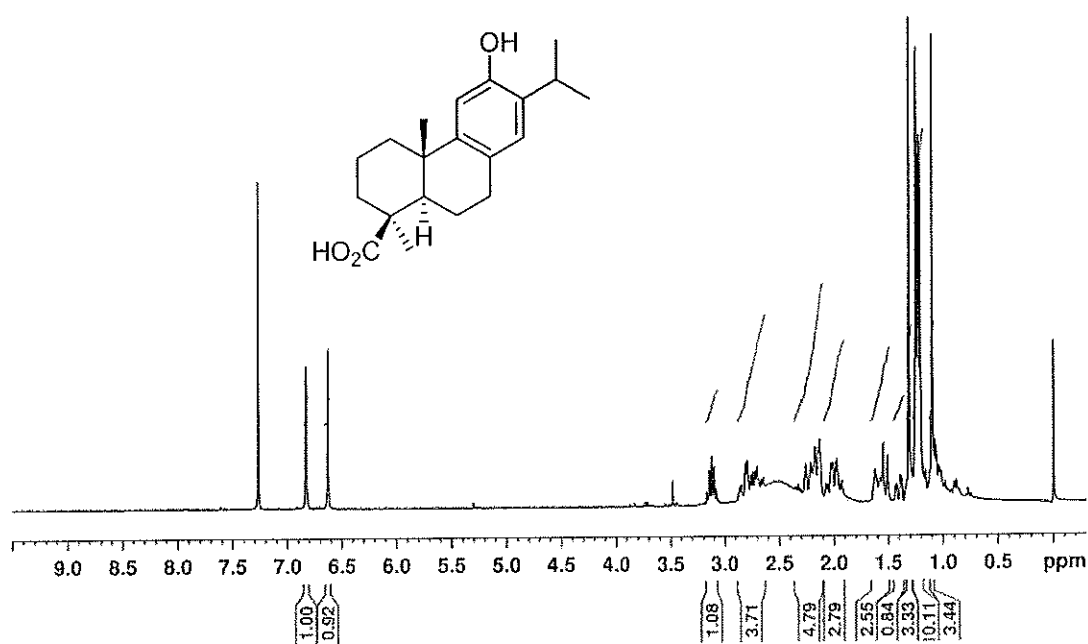


Figure 91 ^1H NMR (300 MHz) (CDCl₃+CD₃OD) spectrum of compound PO8

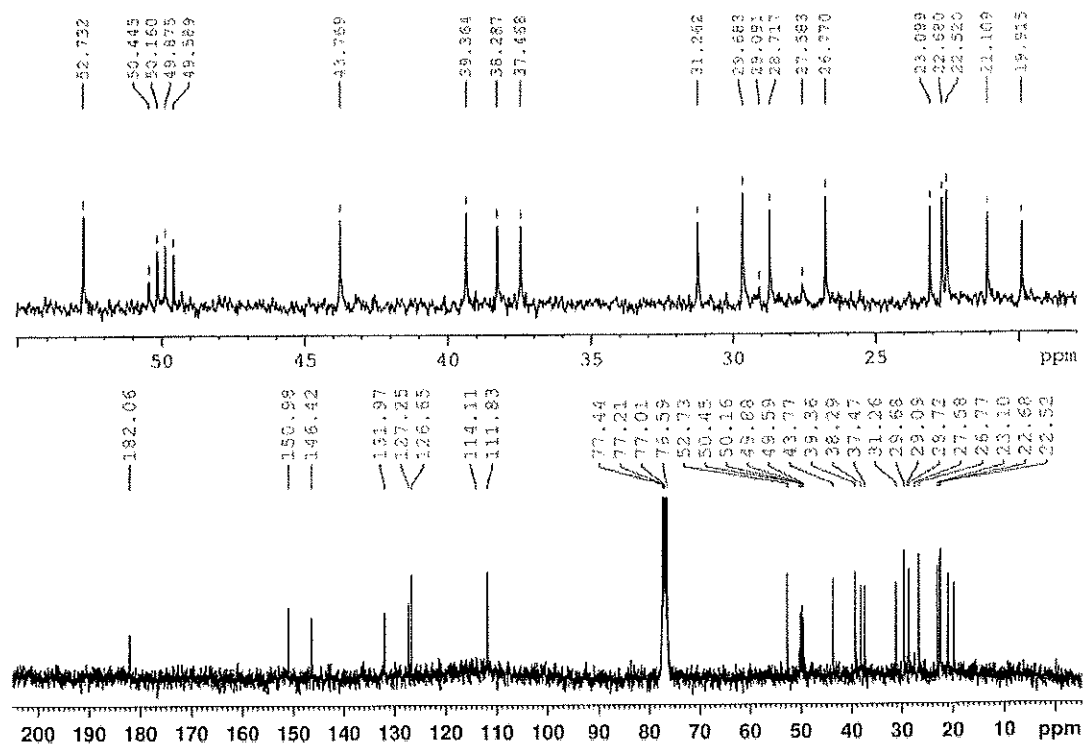


Figure 92 ^{13}C NMR (75 MHz) (CDCl₃+CD₃CD) spectrum of compound PO8

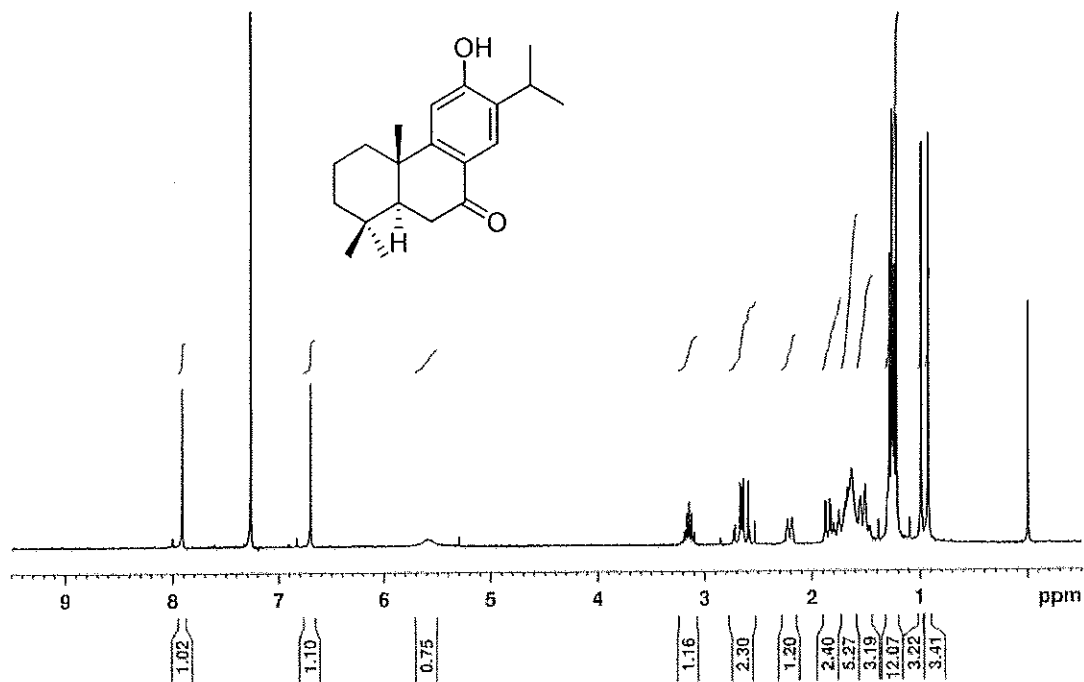


Figure 93 ^1H NMR (300 MHz) (CDCl_3) spectrum of compound PO9

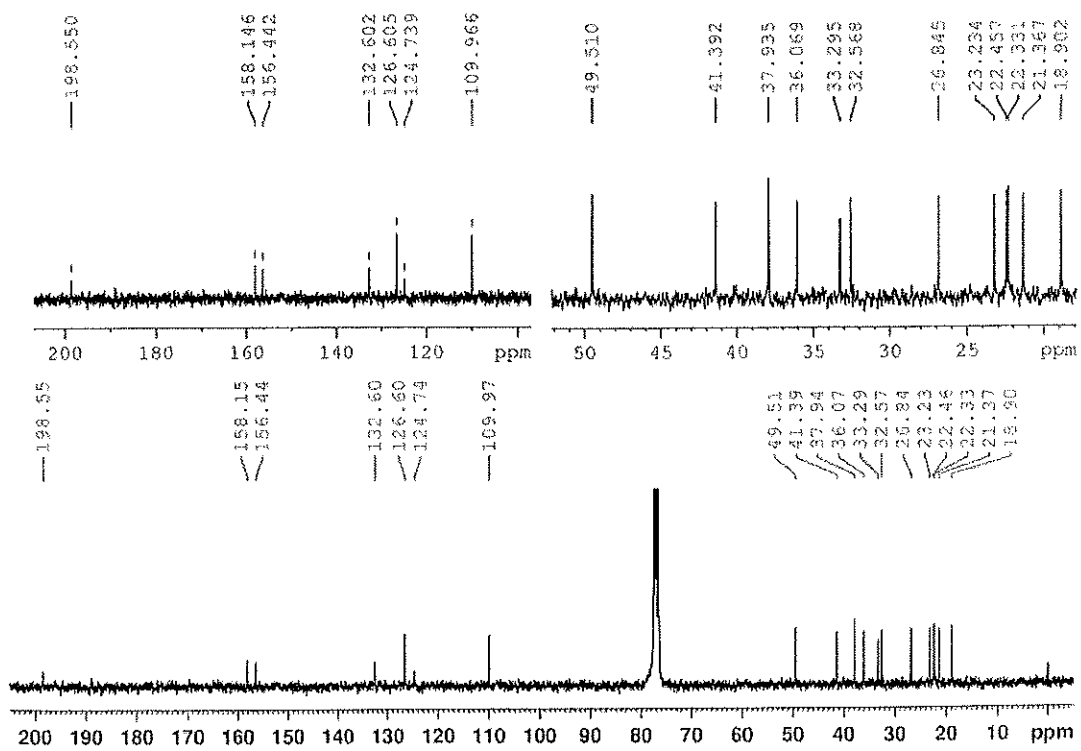


Figure 94 ^{13}C NMR (75 MHz) (CDCl_3) spectrum of compound PO9



Figure 95 $^1\text{H NMR}$ (300 MHz) (CDCl_3) spectrum of compound PO10

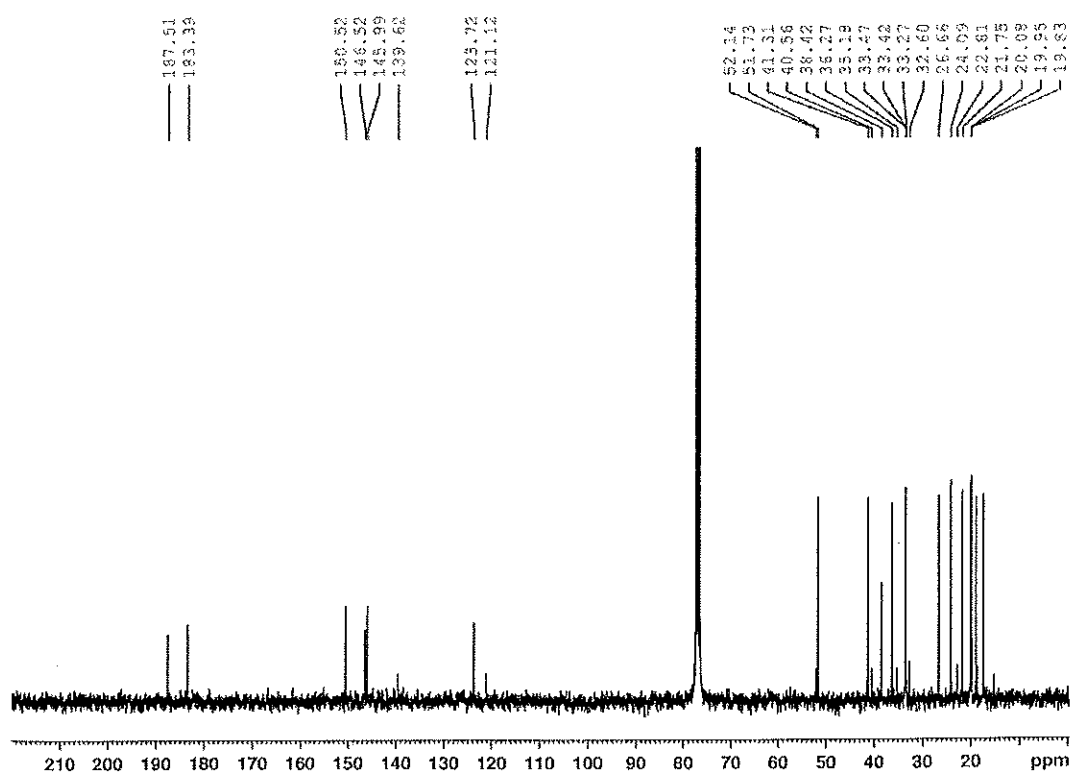


Figure 96 $^{13}\text{C NMR}$ (75 MHz) (CDCl_3) spectrum of compound PO10

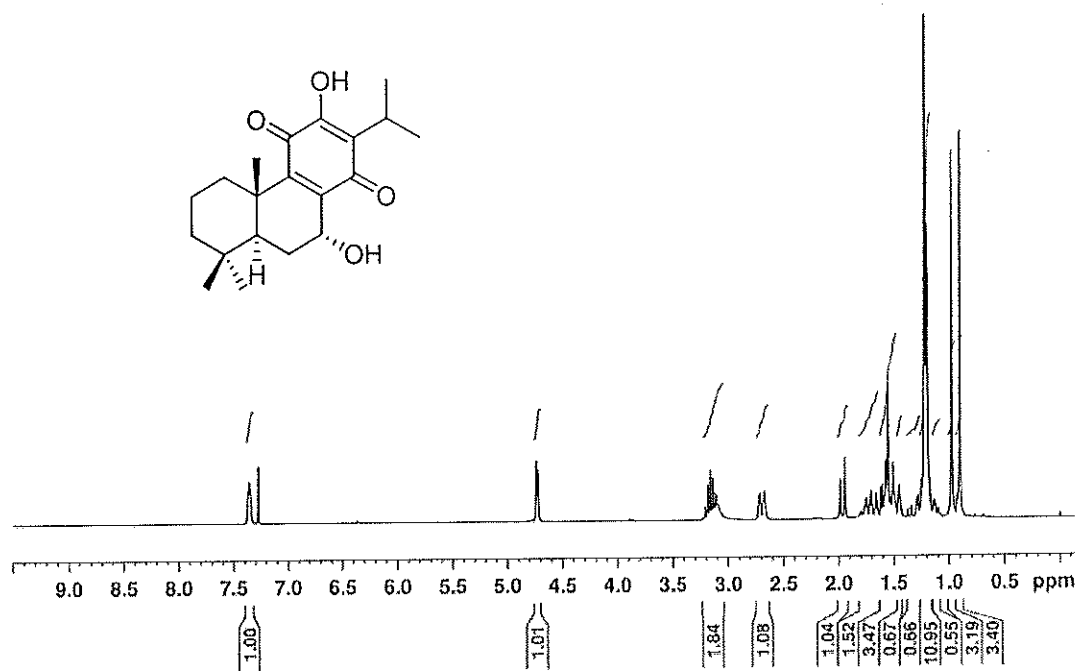


Figure 97 $^1\text{H NMR}$ (300 MHz) (CDCl_3) spectrum of compound PO11

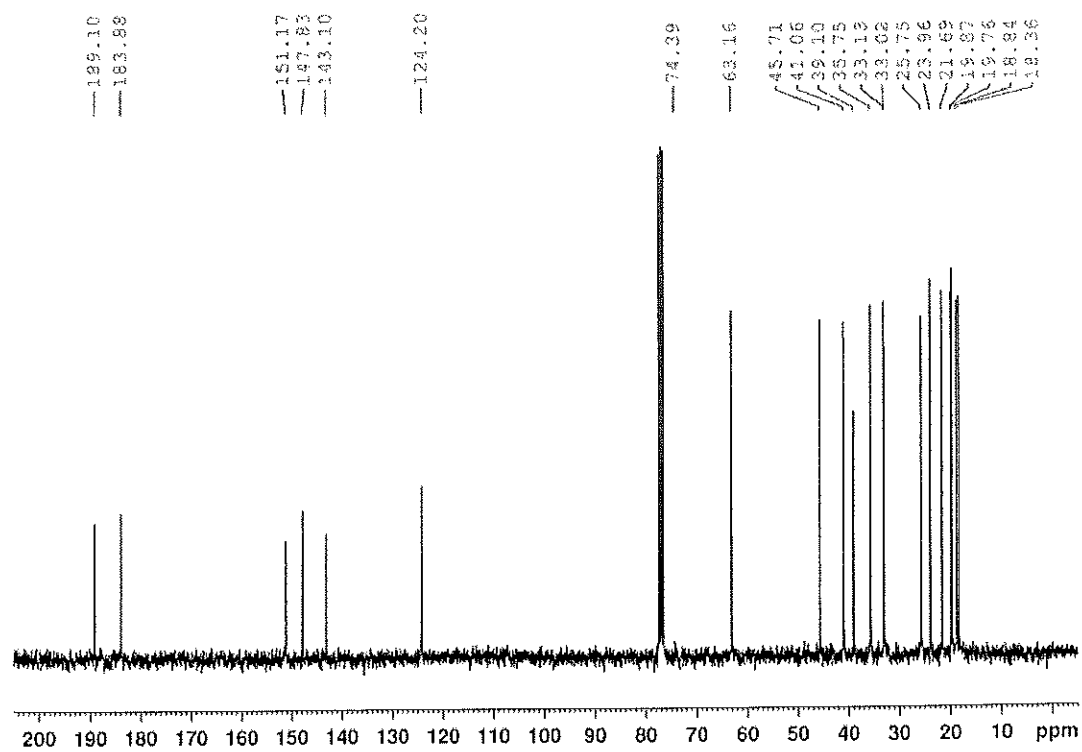


Figure 98 $^{13}\text{C NMR}$ (75 MHz) (CDCl_3) spectrum of compound PO11

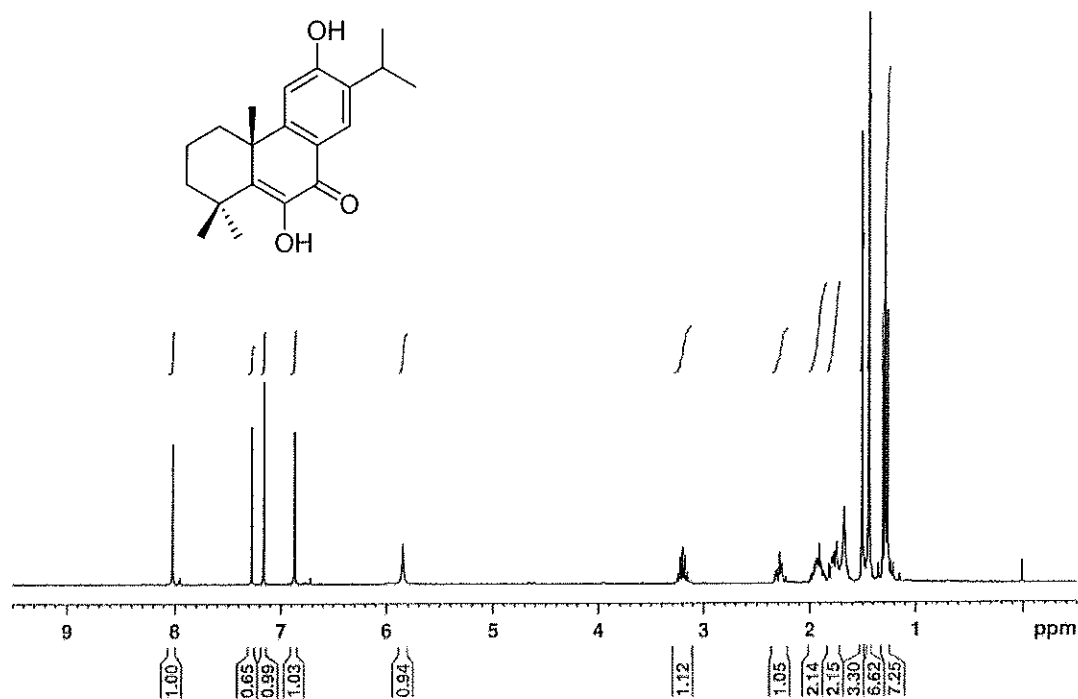


Figure 99 ¹H NMR (300 MHz) (CDCl₃) spectrum of compound PO12

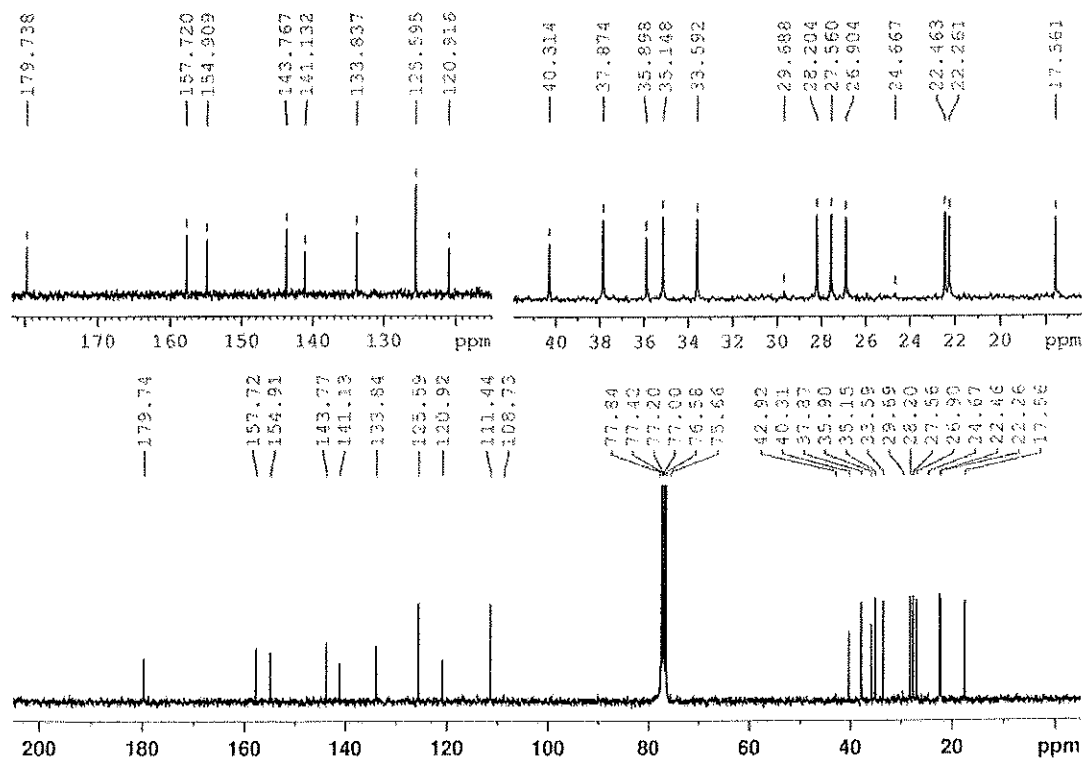


Figure 100 ¹³C NMR (75 MHz) (CDCl₃) spectrum of compound PO12

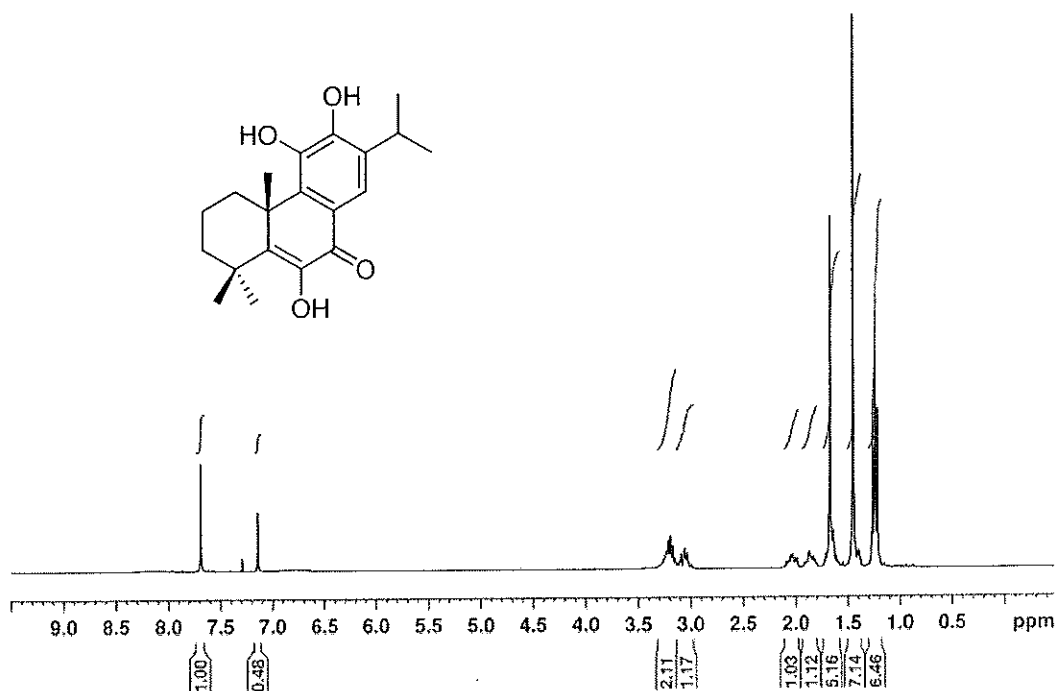


Figure 101 ^1H NMR (300 MHz) ($\text{CDCl}_3 + \text{CD}_3\text{CD}$) spectrum of compound PO13

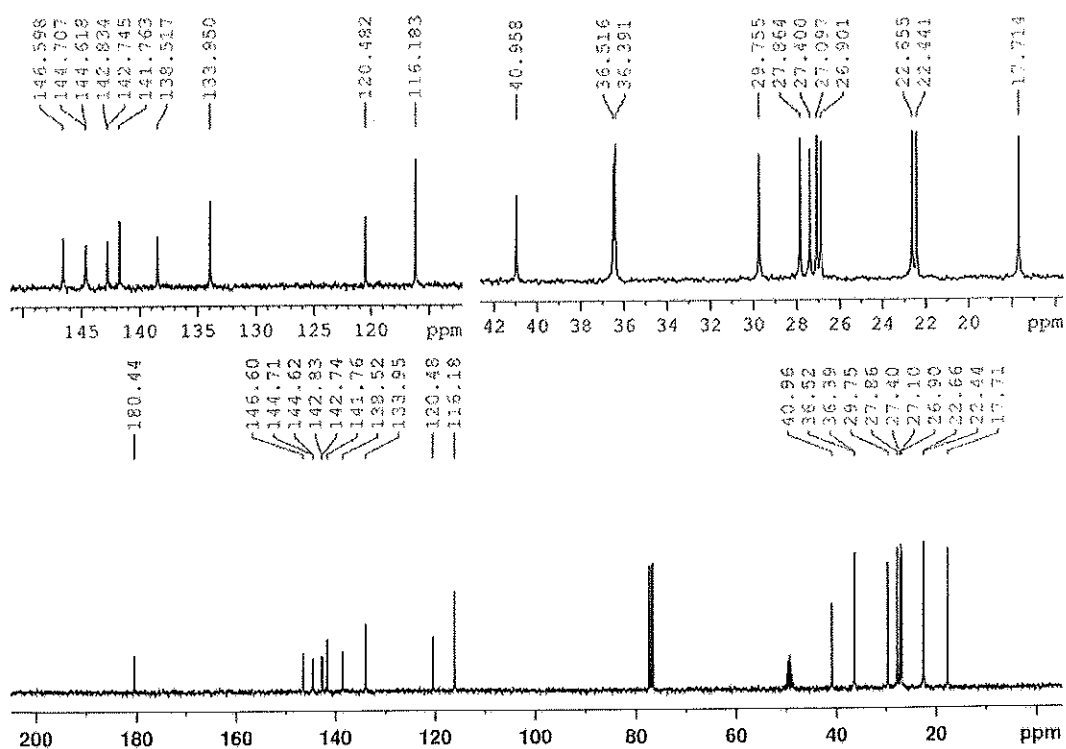


Figure 102 ^{13}C NMR (75 MHz) ($\text{CDCl}_3 + \text{CD}_3\text{CD}$) spectrum of compound PO13

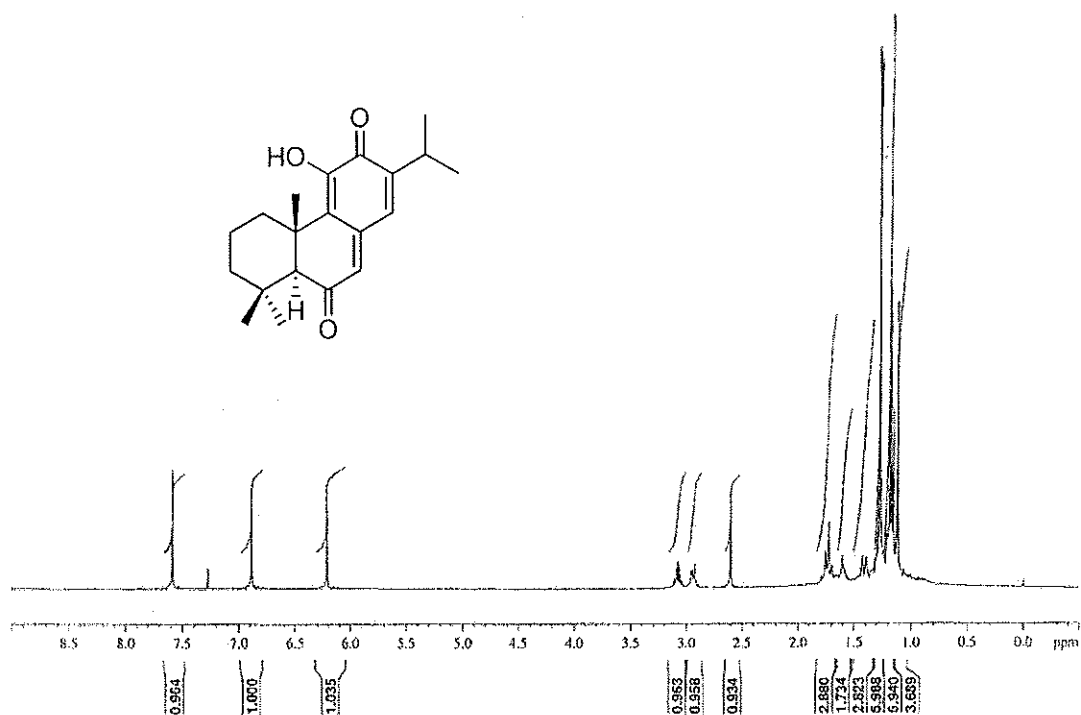


Figure 103 ^1H NMR (400 MHz) (CDCl_3) spectrum of compound PO14

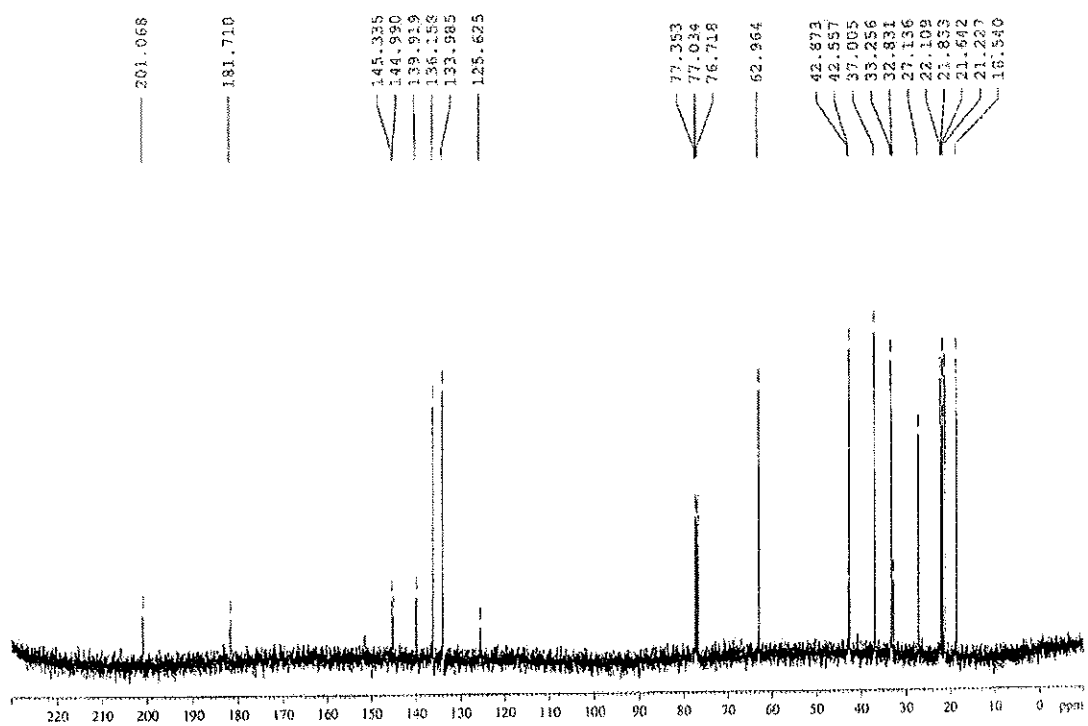


Figure 104 ^{13}C NMR (100 MHz) (CDCl_3) spectrum of compound PO14

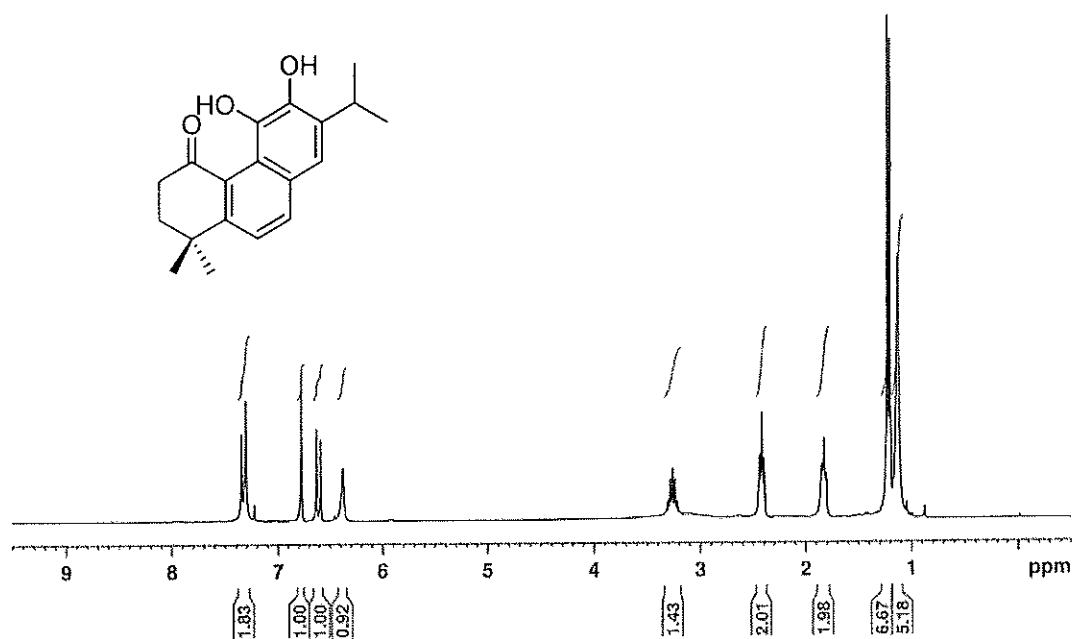


Figure 105 $^1\text{H NMR}$ (300 MHz) (CDCl_3) spectrum of compound PO15

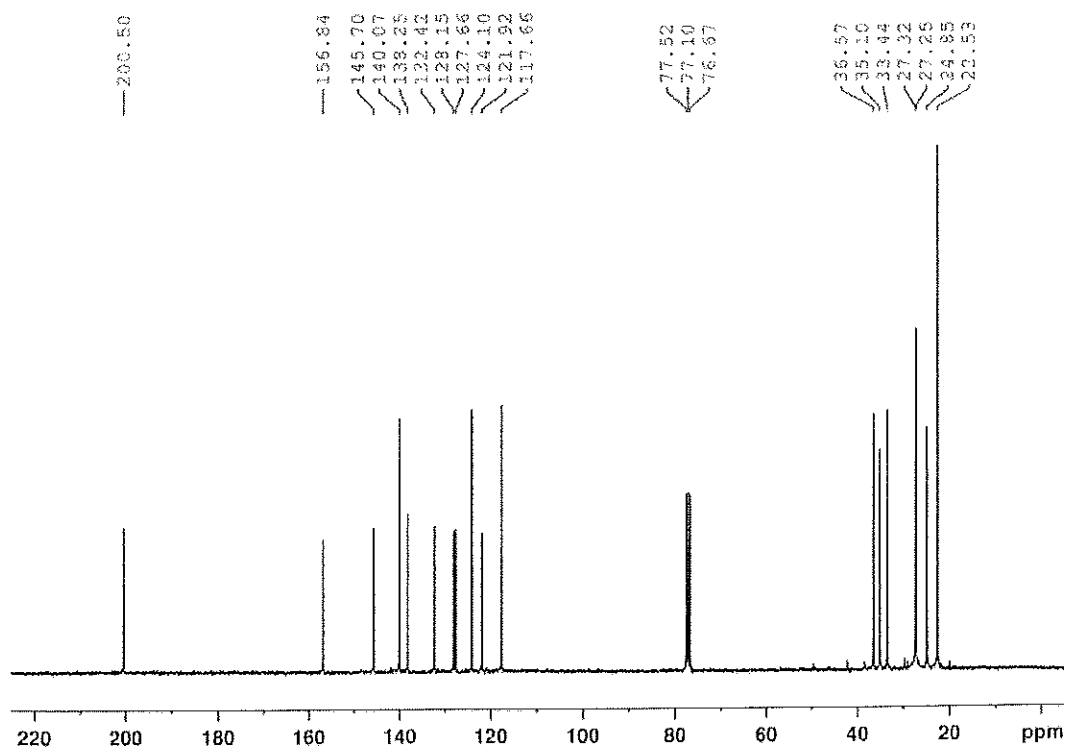


Figure 106 $^{13}\text{C NMR}$ (75 MHz) (CDCl_3) spectrum of compound PO15

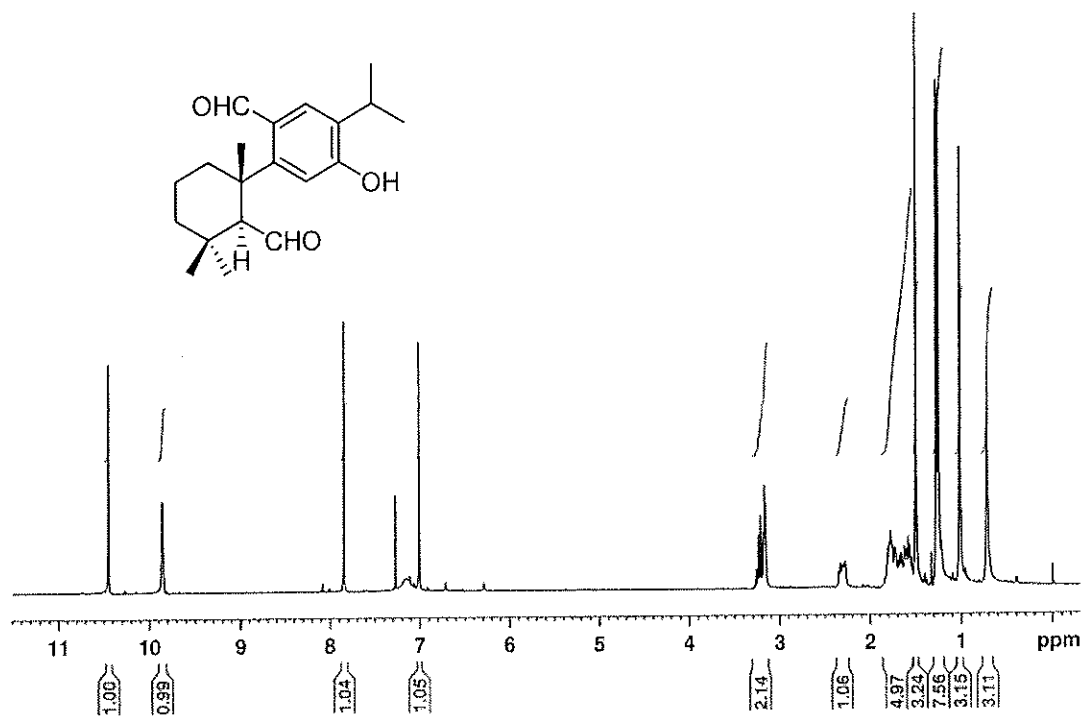


Figure 107 ^1H NMR (300 MHz) (CDCl_3) spectrum of compound **PO16**

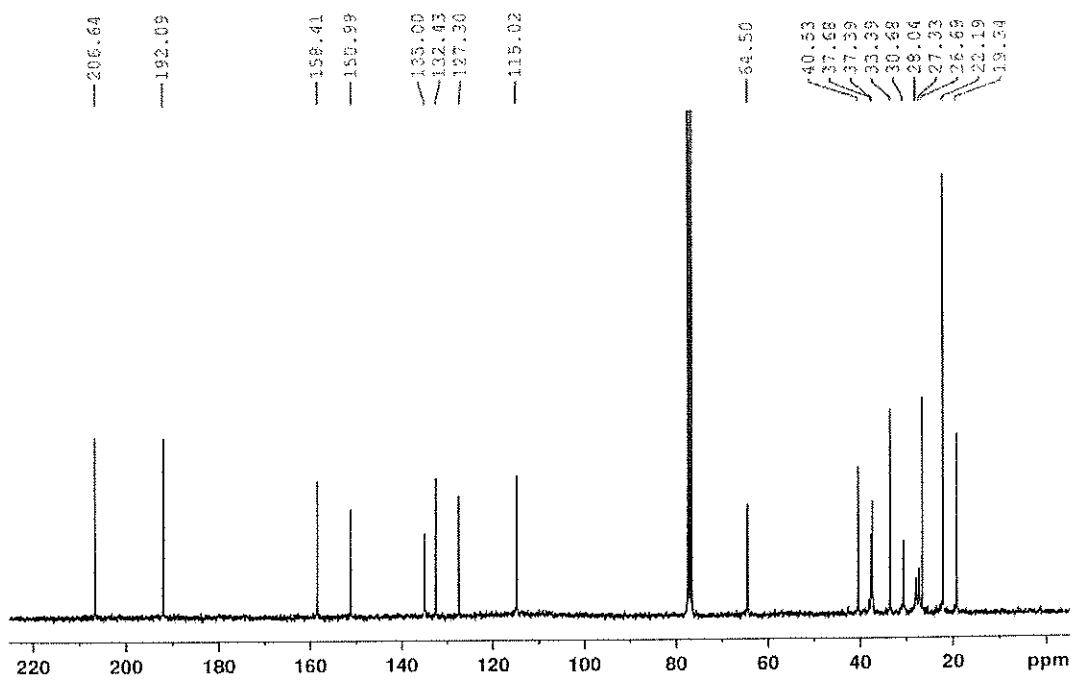


Figure 108 ^{13}C NMR (75 MHz) (CDCl_3) spectrum of compound **PO16**

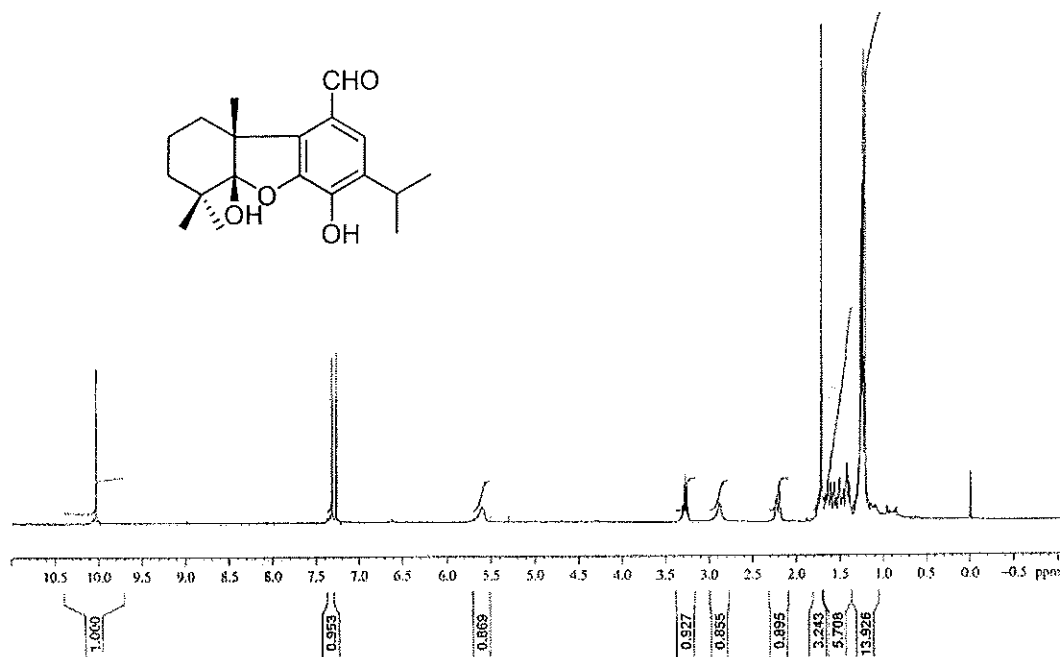


Figure 109 $^1\text{H NMR}$ (400 MHz) (CDCl_3) spectrum of compound PO17

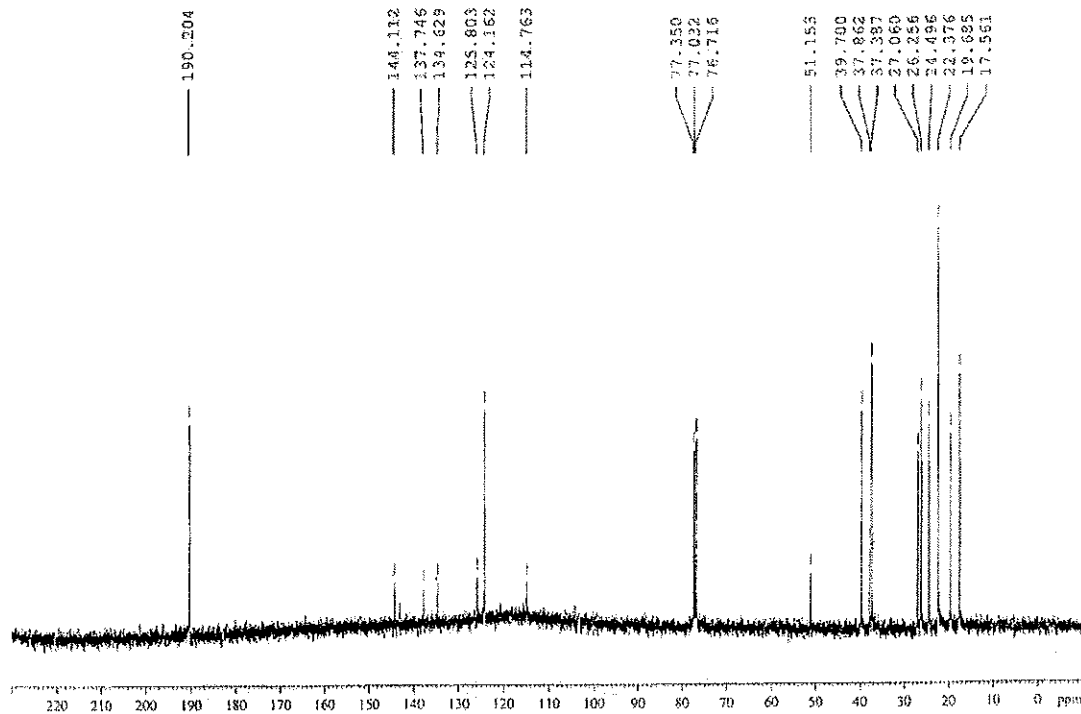


Figure 110 $^{13}\text{C NMR}$ (100 MHz) (CDCl_3) spectrum of compound PO17

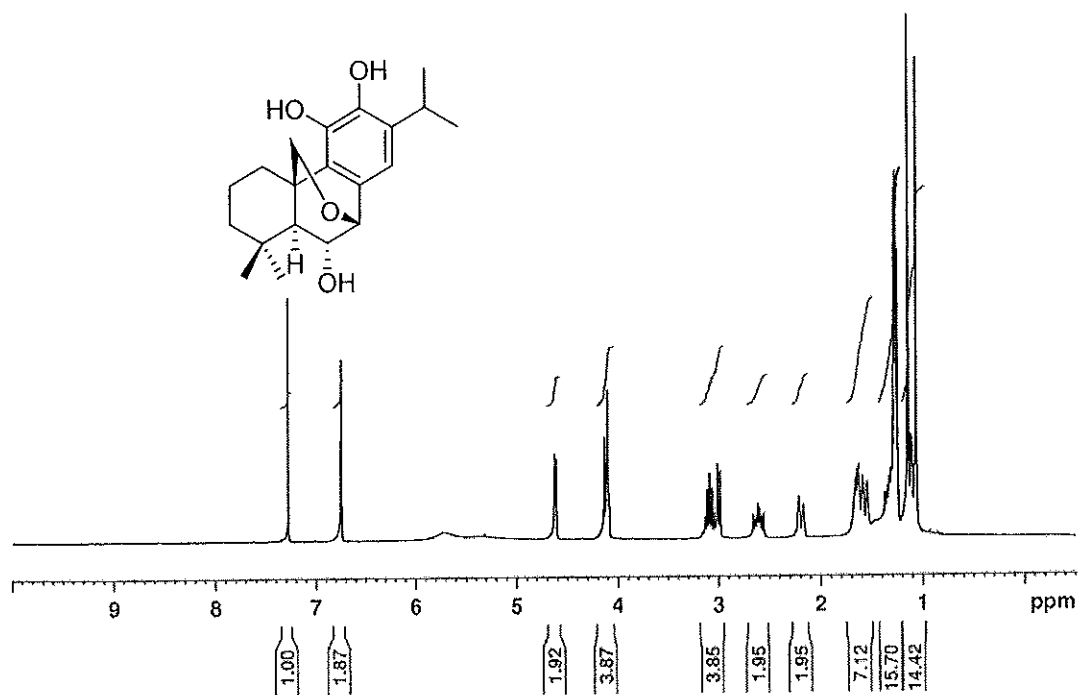


Figure 111 $^1\text{H NMR}$ (400 MHz) ($\text{CDCl}_3 + \text{CD}_3\text{OD}$) spectrum of compound PO18

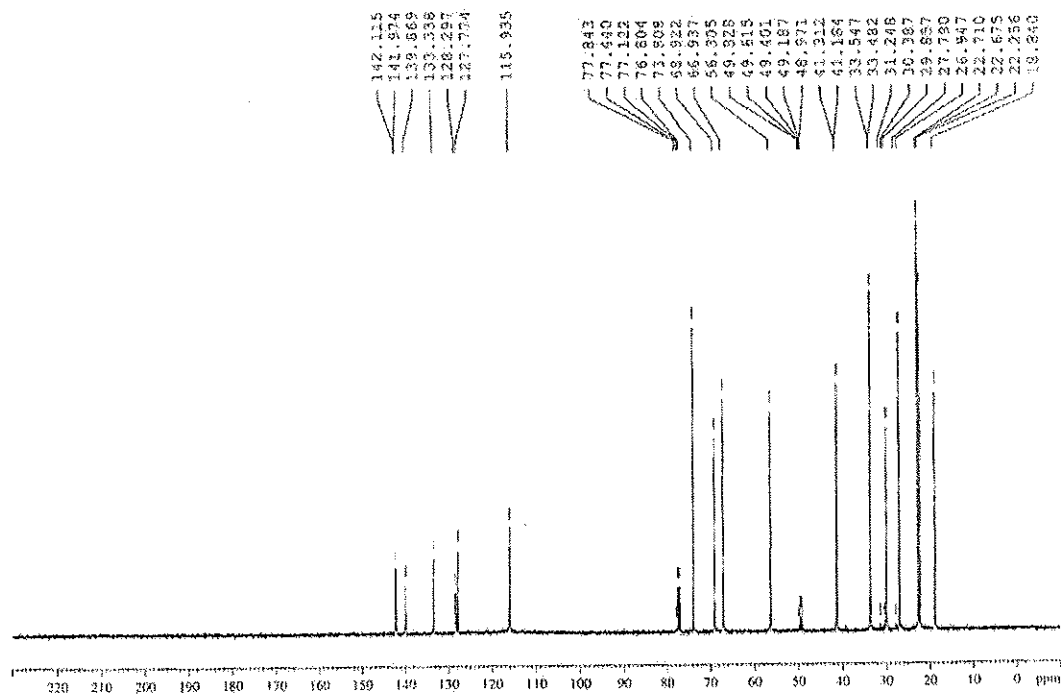
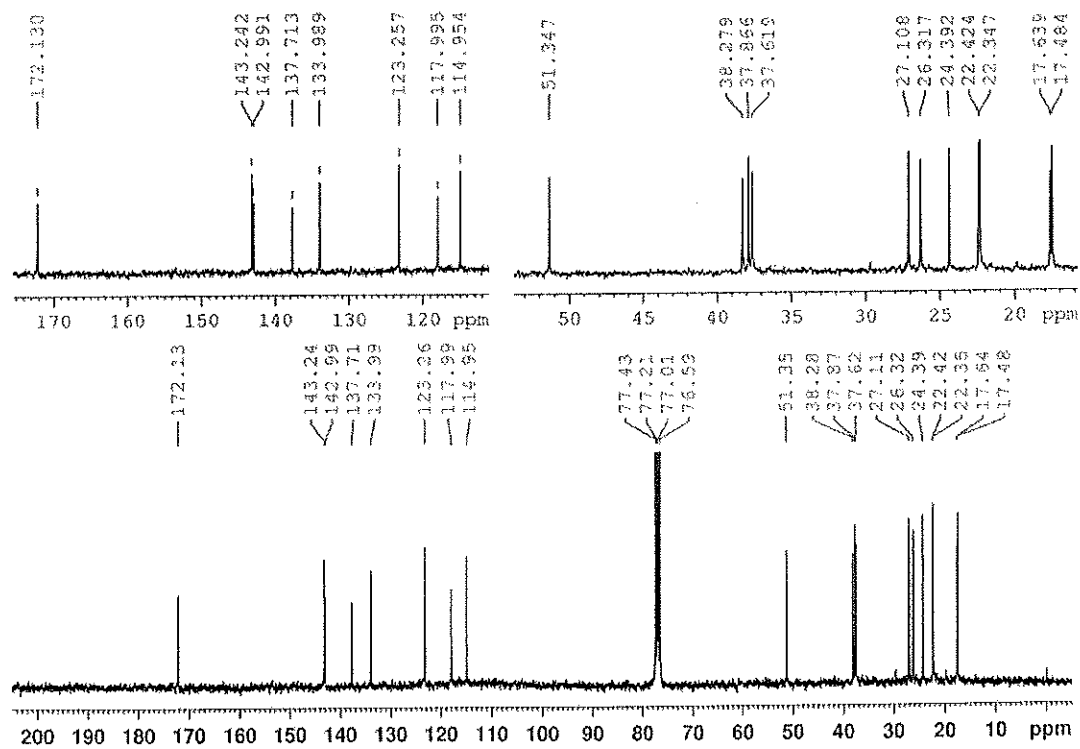
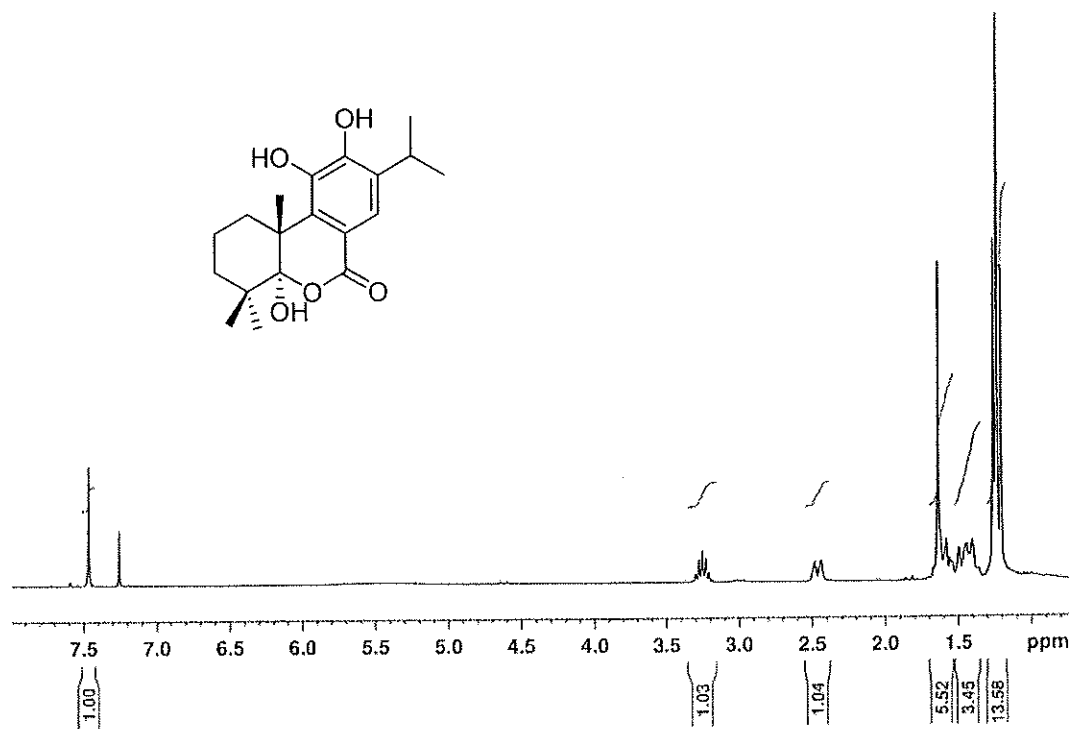


Figure 112 $^{13}\text{C NMR}$ (100 MHz) ($\text{CDCl}_3 + \text{CD}_3\text{OD}$) spectrum of compound PO18



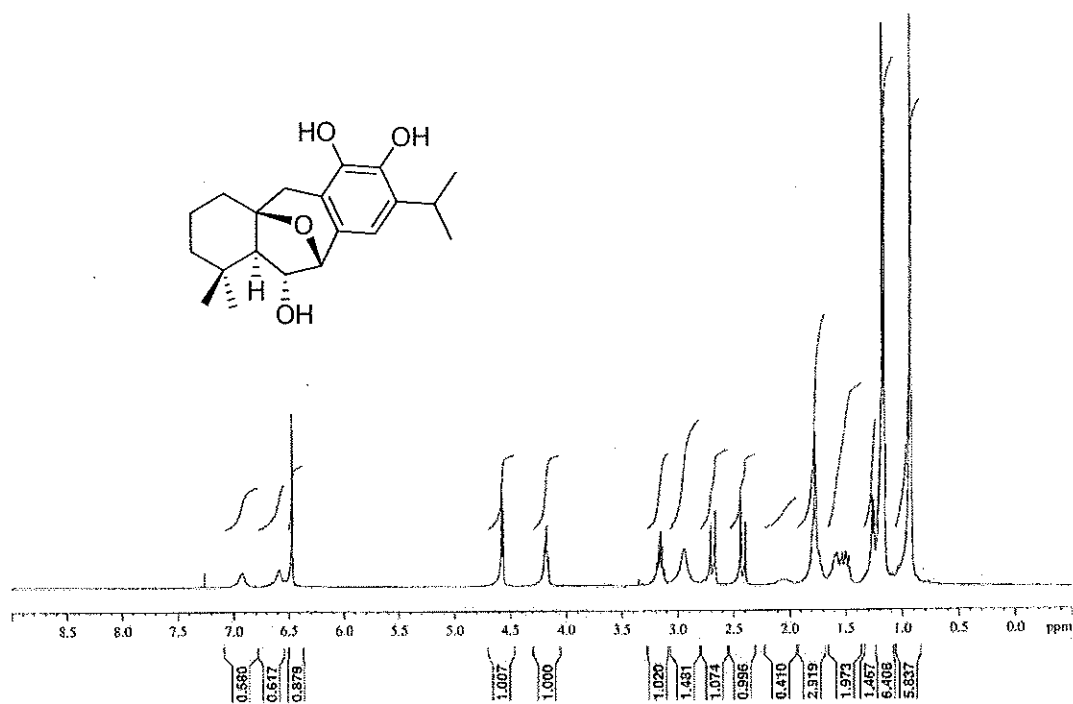


Figure 115 $^1\text{H NMR}$ (400 MHz) ($\text{CDCl}_3+\text{CD}_3\text{OD}$) spectrum of compound PO20

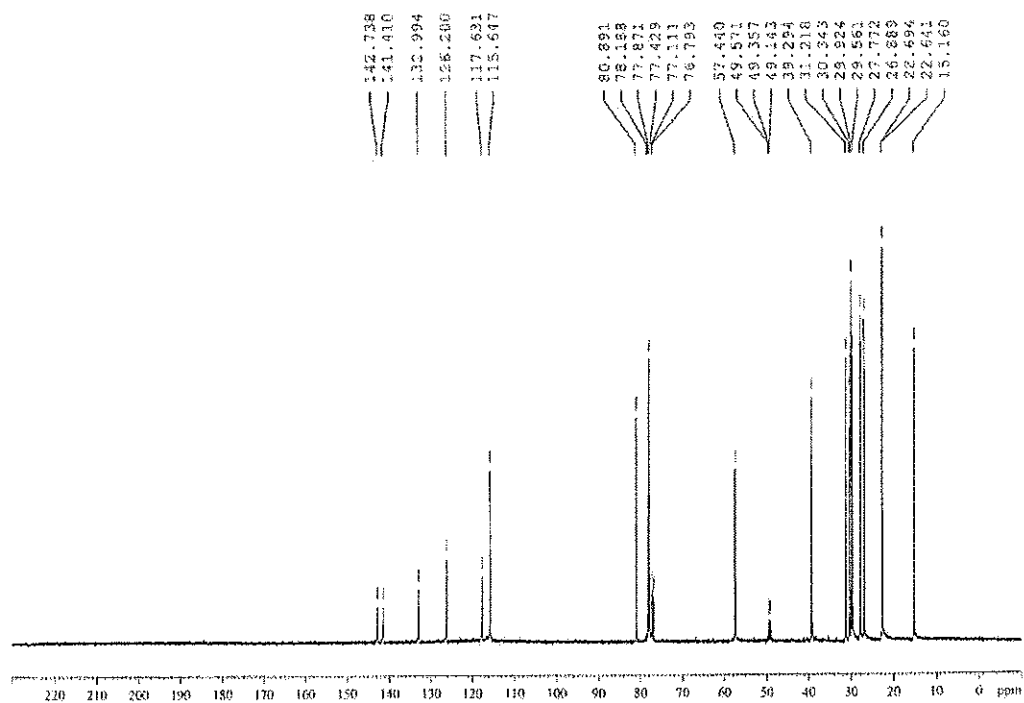


Figure 116 $^{13}\text{C NMR}$ (100 MHz) ($\text{CDCl}_3+\text{CD}_3\text{OD}$) spectrum of compound PO20

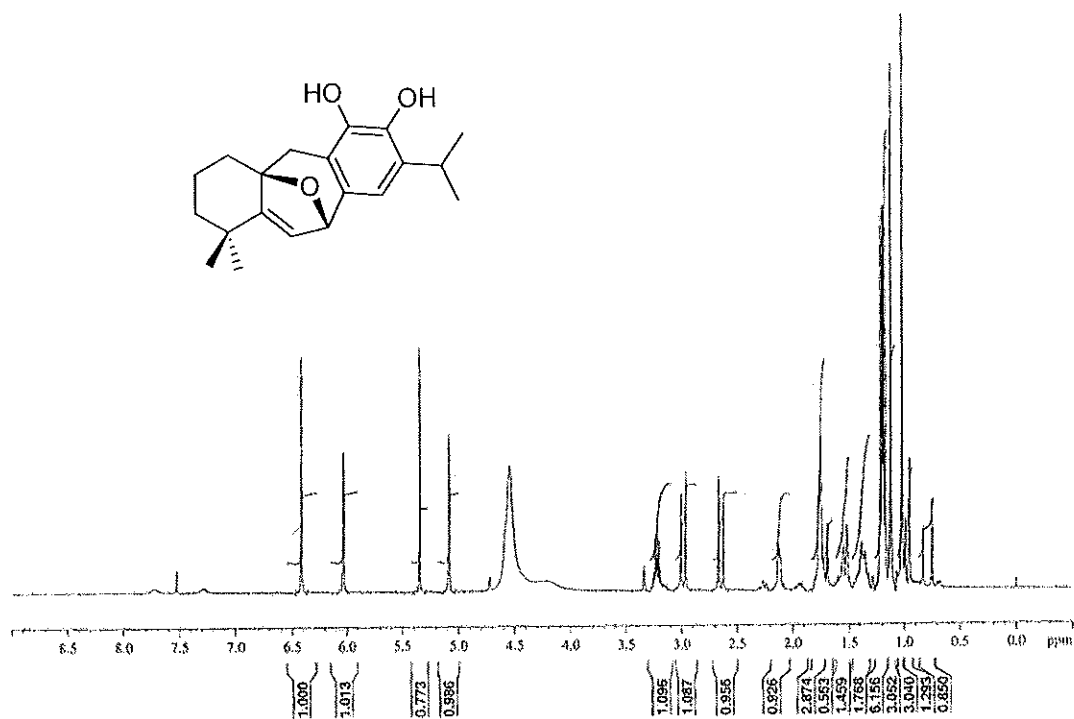


Figure 117 ¹H NMR (400 MHz) (CDCl₃+CD₃OD) spectrum of compound PO21

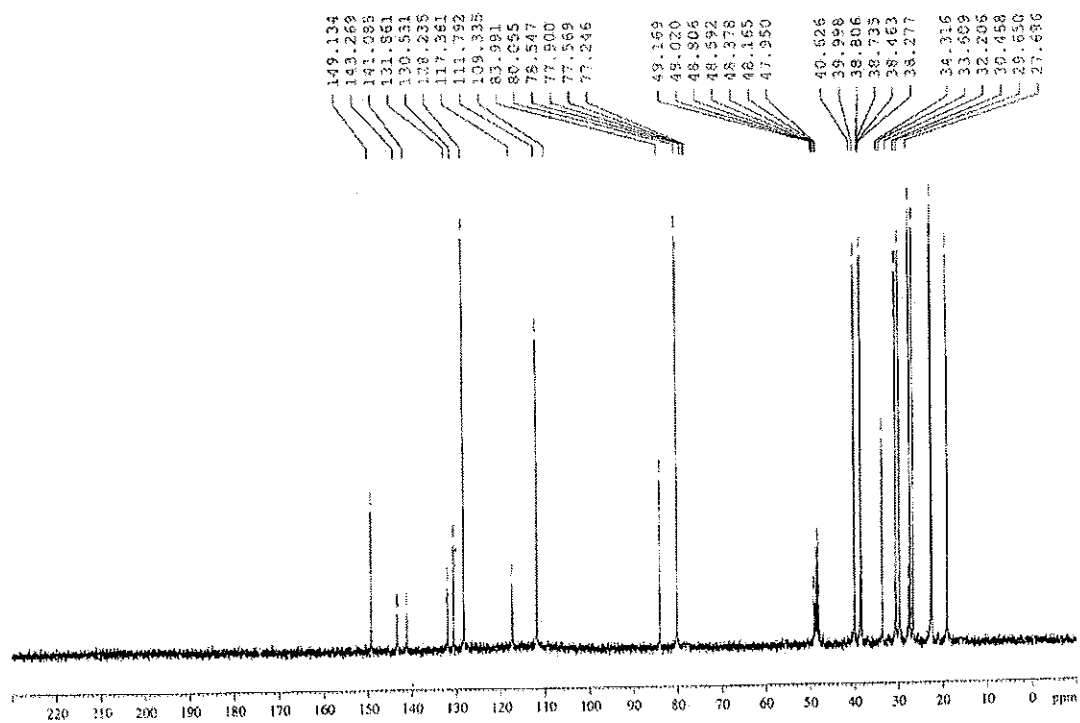


Figure 118 ¹³C NMR (100 MHz) (CDCl₃+CD₃OD) spectrum of compound PO21

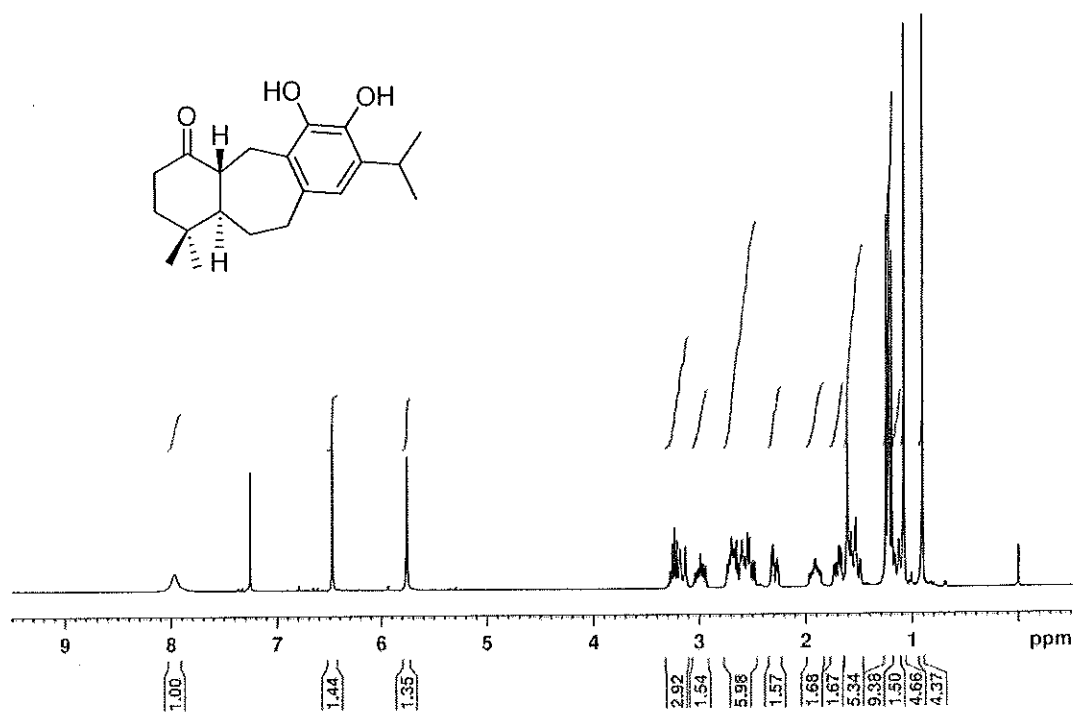


Figure 119 ^1H NMR (300 MHz) (CDCl_3) spectrum of compound PO22

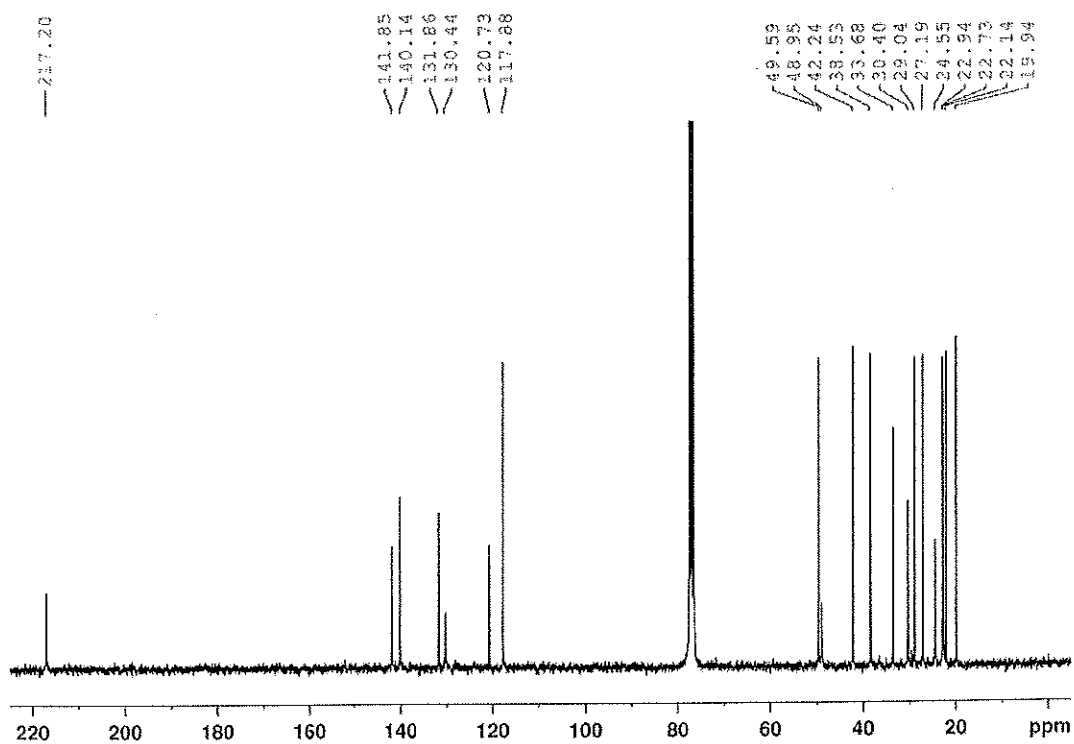


Figure 120 ^{13}C NMR (75 MHz) (CDCl_3) spectrum of compound PO22

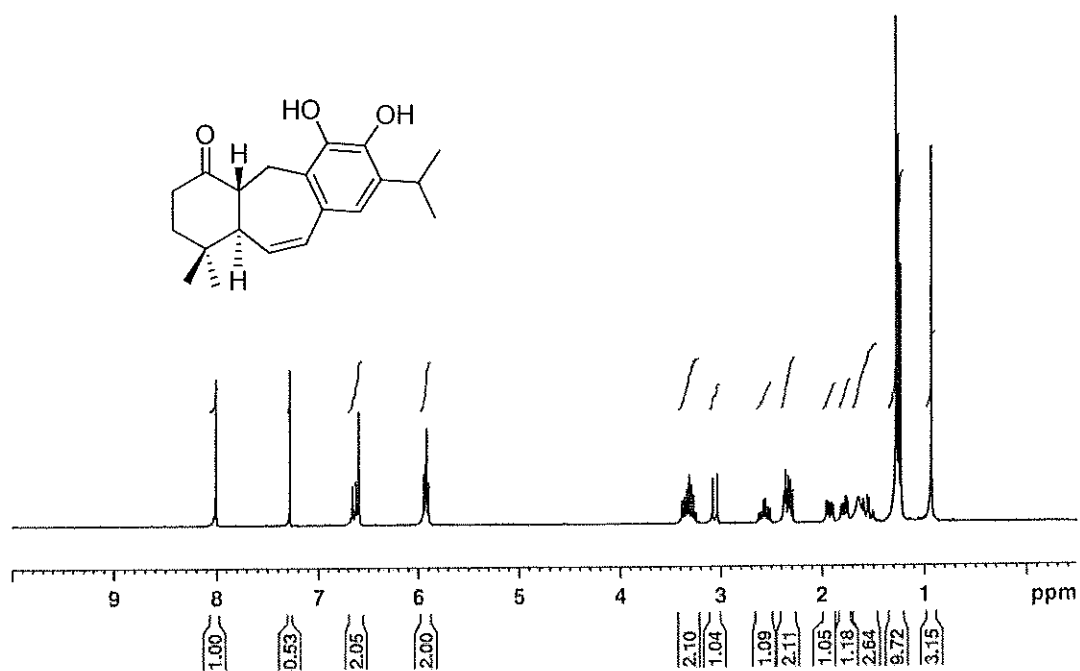


Figure 121 $^1\text{H NMR}$ (400 MHz) (CDCl_3) spectrum of compound PO23

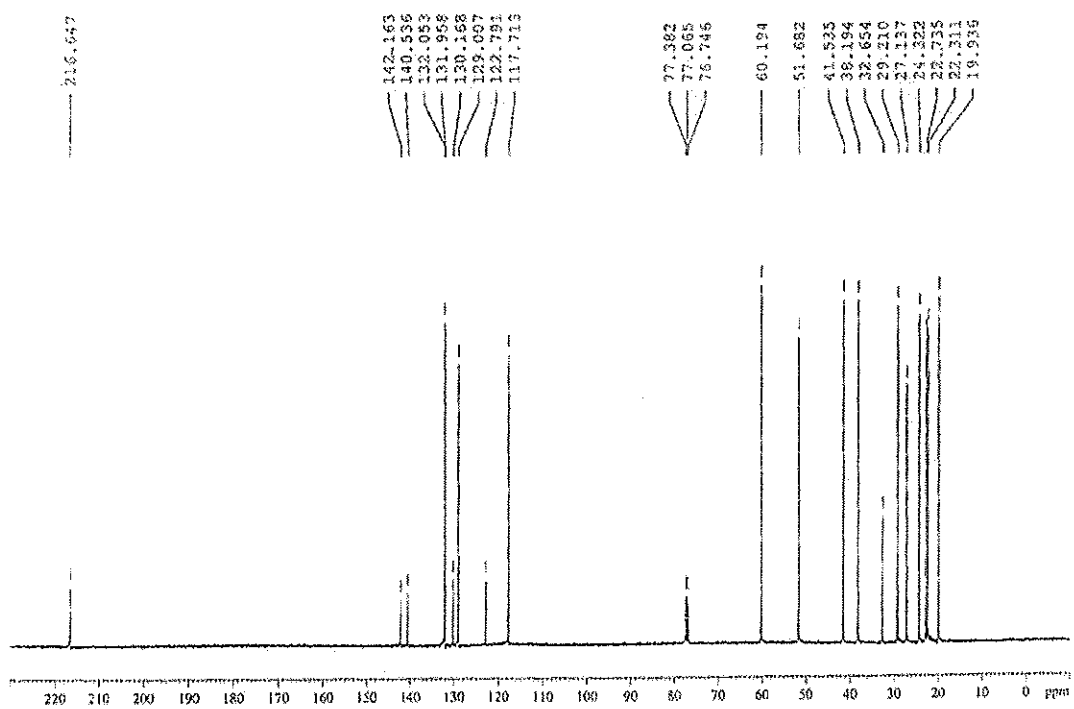


Figure 122 $^{13}\text{C NMR}$ (100 MHz) (CDCl_3) spectrum of compound PO23

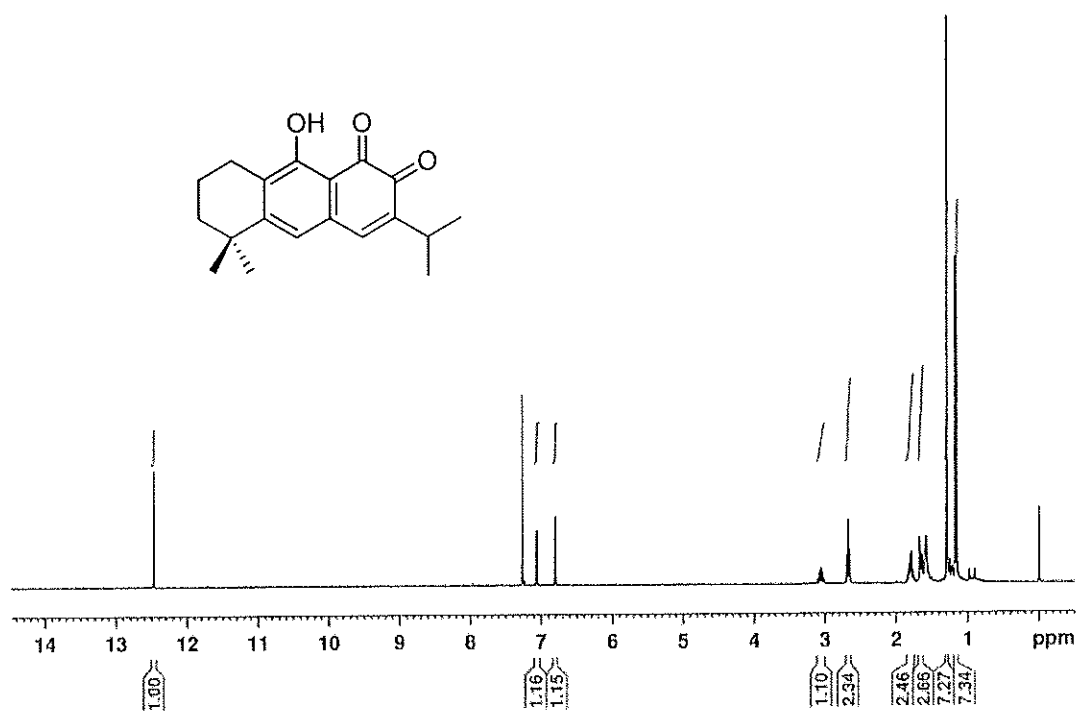


Figure 123 ^1H NMR (300 MHz) (CDCl_3) spectrum of compound PO24

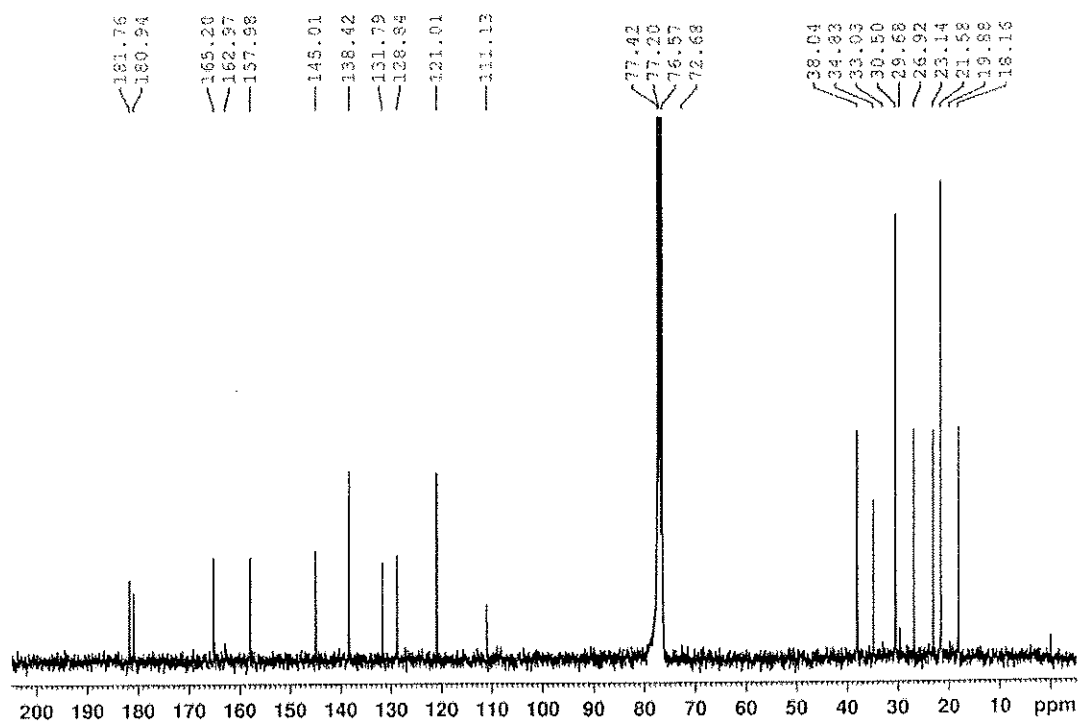


Figure 124 ^{13}C NMR (75 MHz) (CDCl_3) spectrum of compound PO24

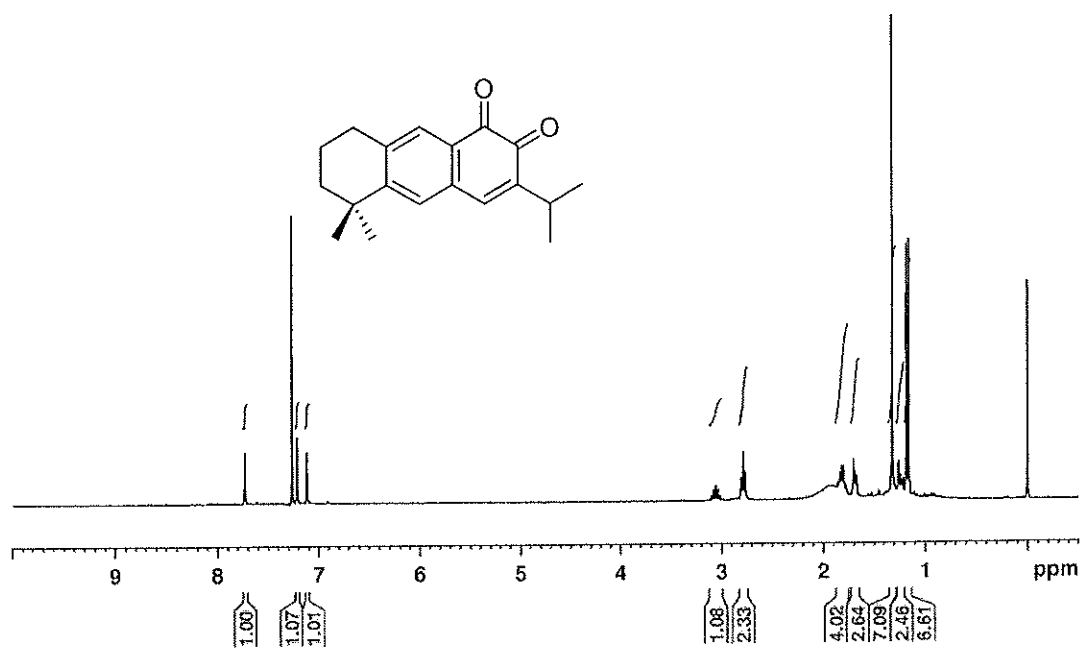


Figure 125 $^1\text{H NMR}$ (400 MHz) (CDCl_3) spectrum of compound PO25

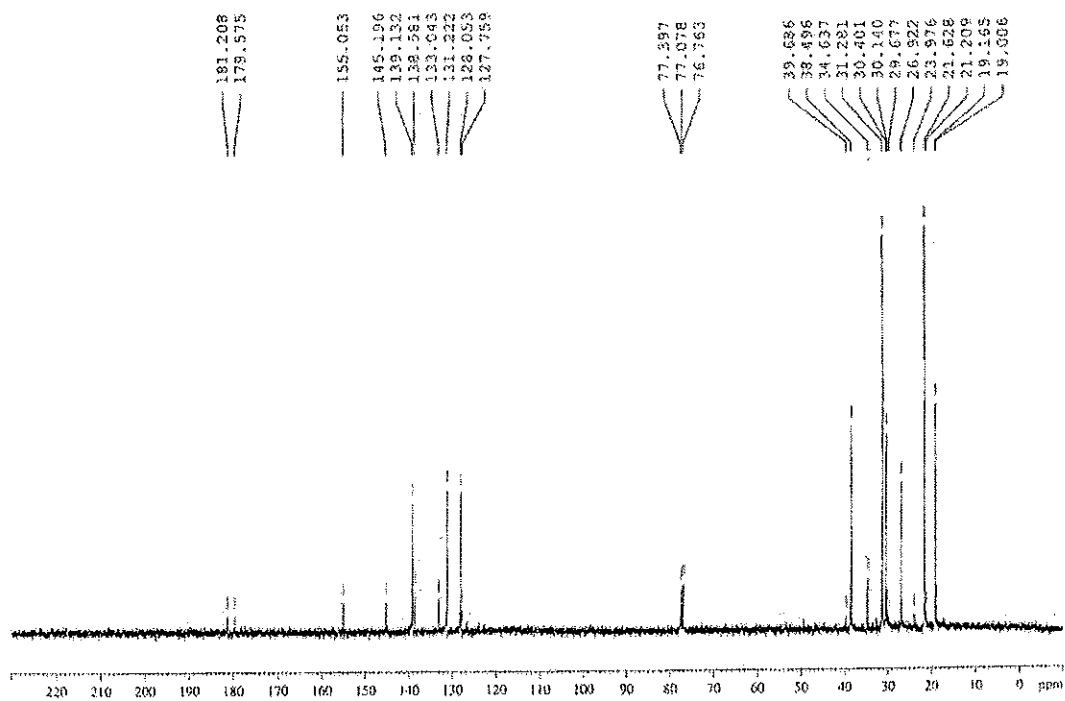


Figure 126 $^{13}\text{C NMR}$ (100 MHz) (CDCl_3) spectrum of compound PO25

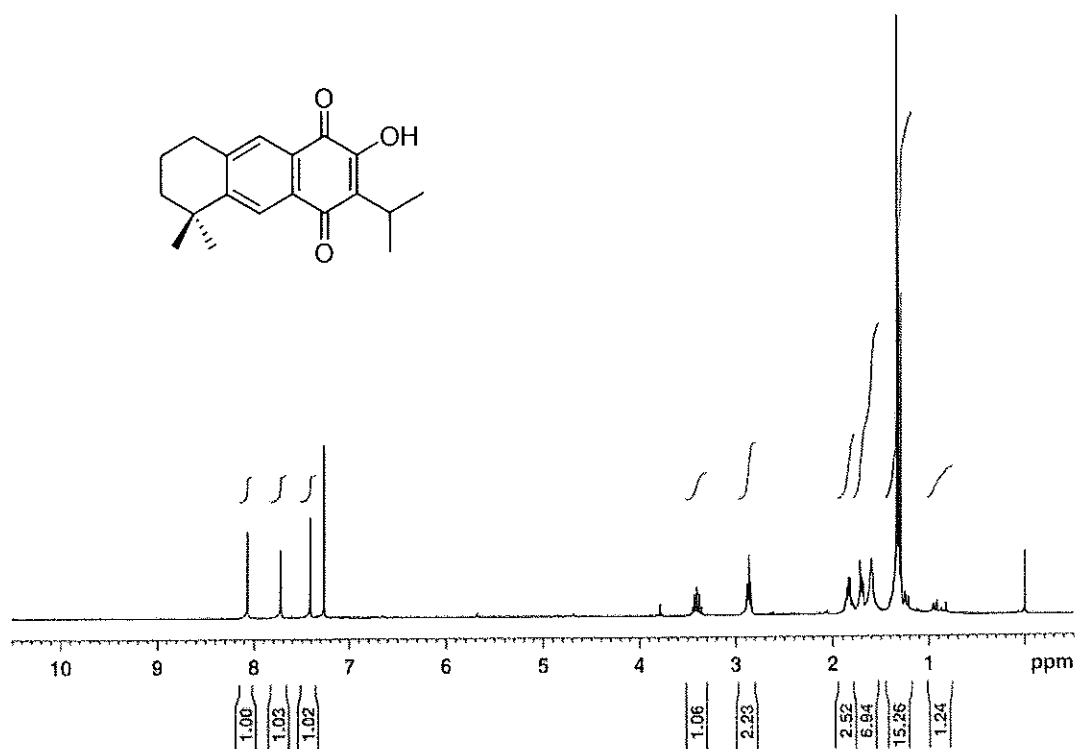


Figure 127 ¹H NMR (300 MHz) (CDCl₃) spectrum of compound PO26

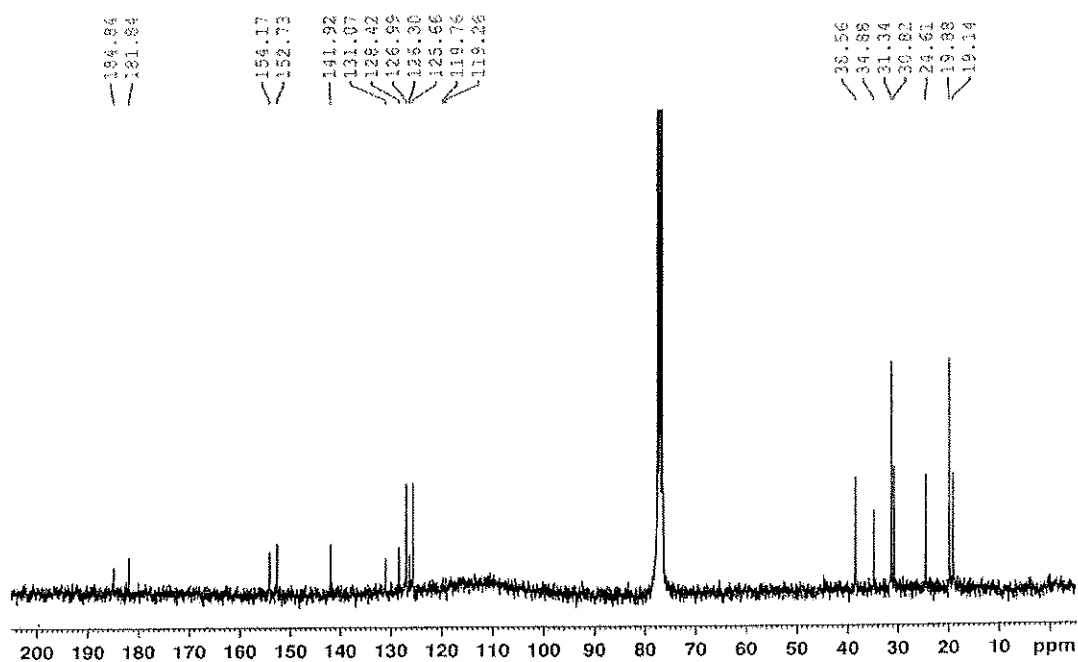


Figure 128 ¹³C NMR (75 MHz) (CDCl₃) spectrum of compound PO26

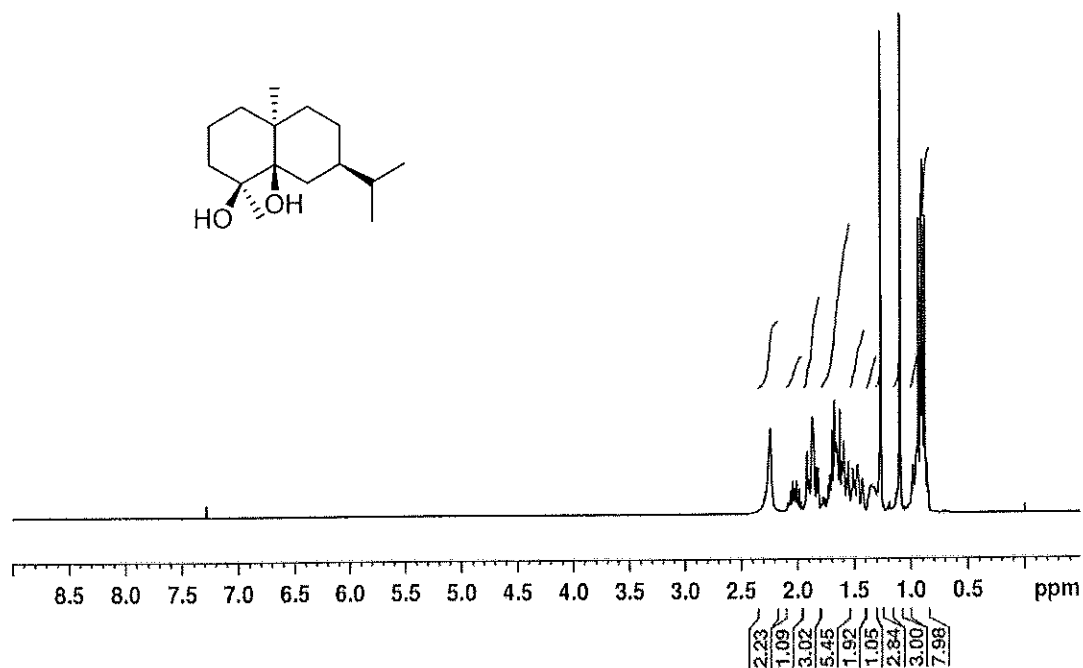


Figure 129 ^1H NMR (300 MHz) (CDCl_3) spectrum of compound PO27

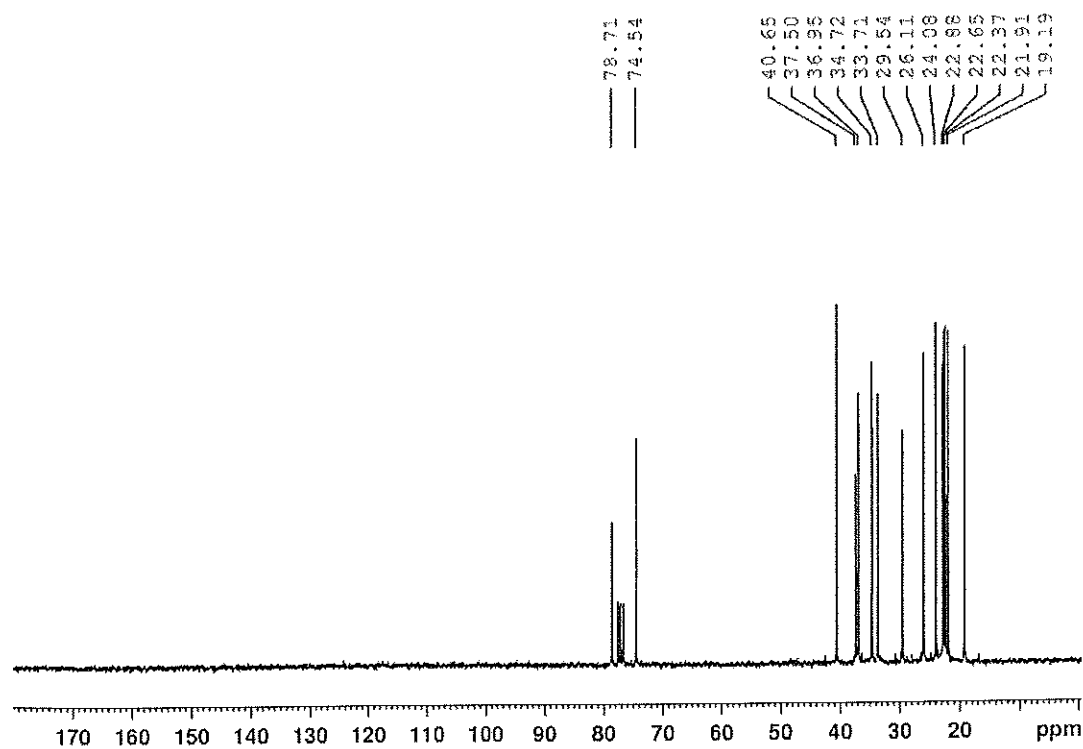


Figure 130 ^{13}C NMR (75 MHz) (CDCl_3) spectrum of compound PO27

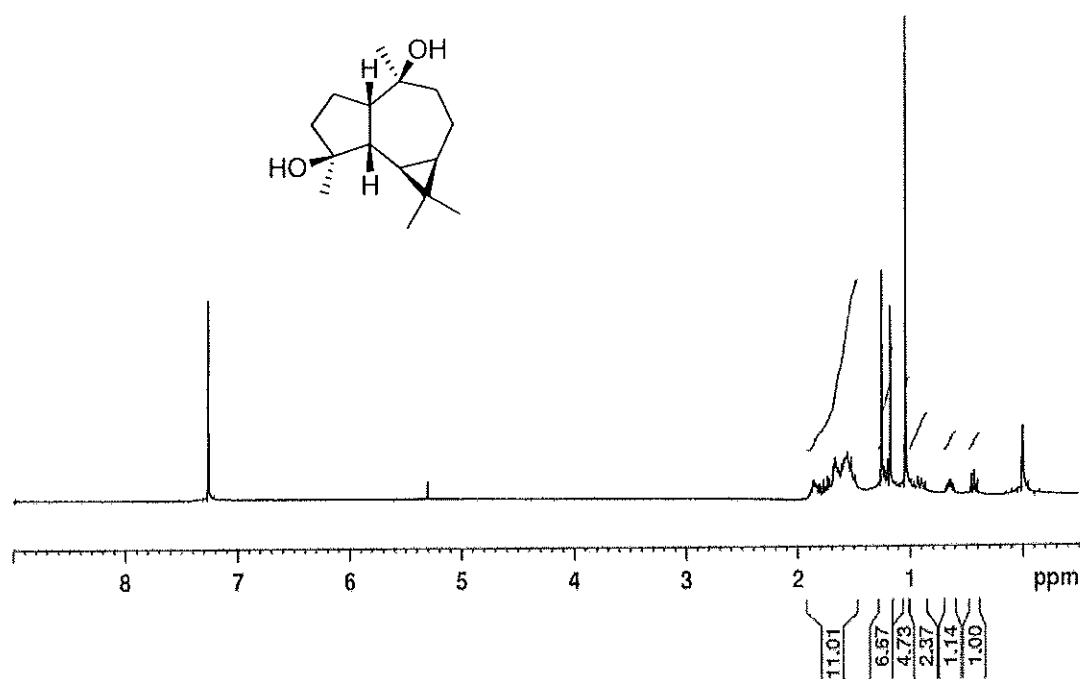


Figure 131 ^1H NMR (300 MHz) (CDCl_3) spectrum of compound PO28

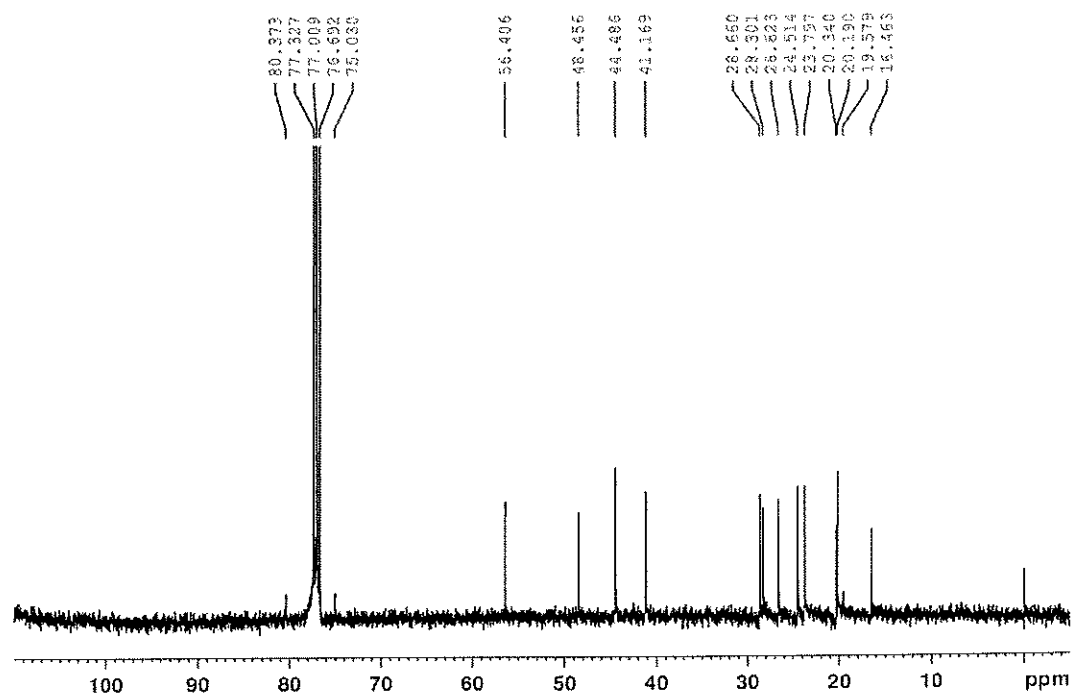
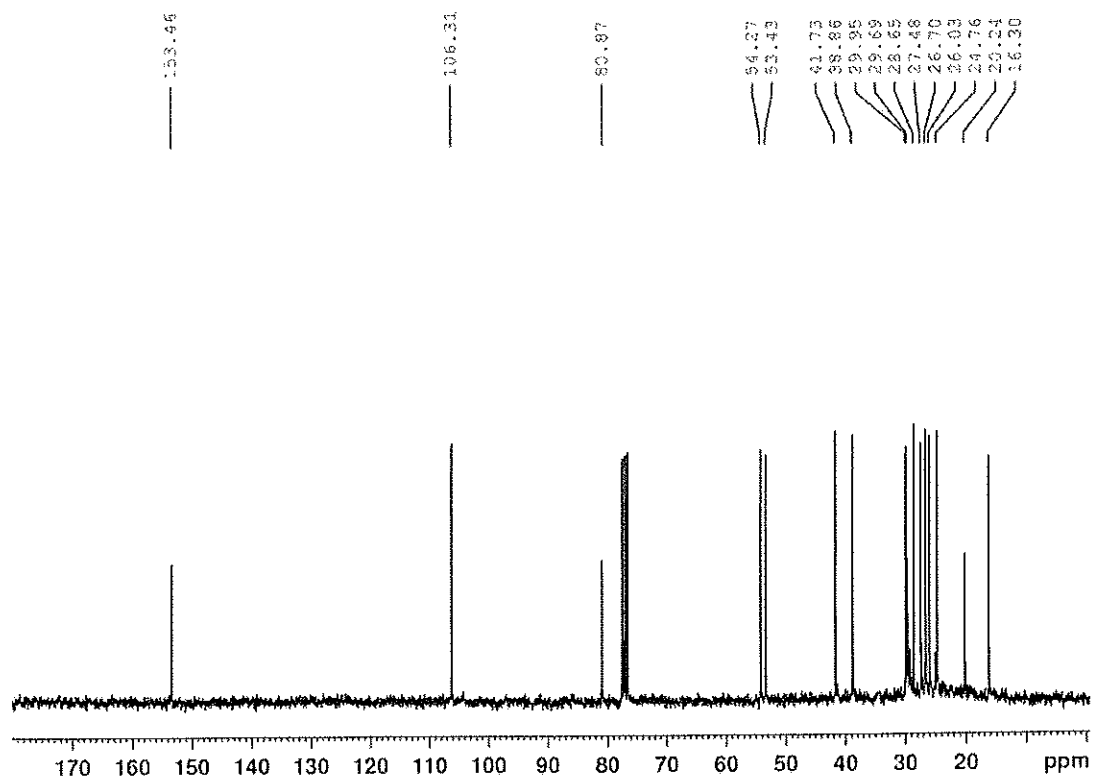
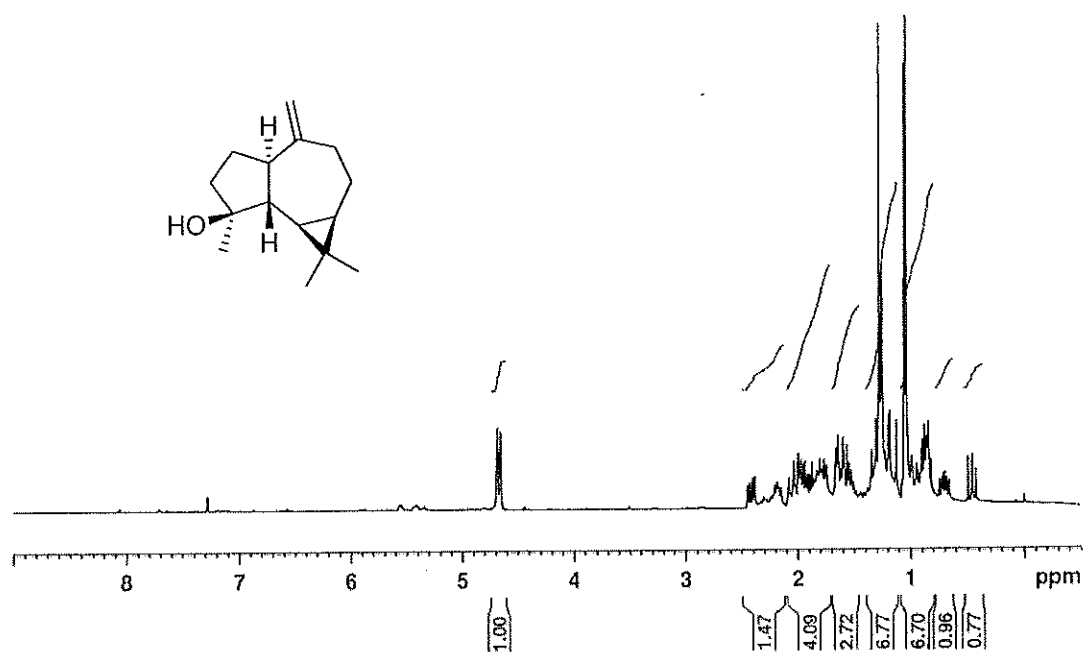


Figure 132 ^{13}C NMR (75 MHz) (CDCl_3) spectrum of compound PO28



VITAE

Name Mr. Abdulwahab Salae

Student ID 5010230030

Educational Attainment

Degree	Name of Institution	Year of Graduation
B. Sc. (Chemistry)	Rajabhat Phuket University	2003
M. Sc. (Organic Chemistry)	Prince of Songkla University	2007

Scholarship Awards during Enrolment

1. The Center for Innovation in Chemistry, (PERCH-CIC), Commission on Higher Education, Ministry of Education
2. The Thesis Research Fund through the Graduate School, Prince of Songkla University

List of Publication and Proceeding

Publications

Salae, A. W.; Chantrapromma, S.; Hoong Kun, F.; Karalai, C. 2009. 6-Hydroxysalvinolone, *Acta Cryst.*, E65, o2379–o2380.

Salae, A. W.; Karalai, C.; Ponglimanont, C.; Kanjana-Opas, A.; Yuenyongsawad, S. 2010. Naphthalene derivatives from *Diospyros wallichii*, *Can. J. Chem.*, 88, 922–927.

Salae, A. W.; Rodjun, A.; Karalai, C.; Ponglimanont, C.; Chantrapromma, S.; Kanjana-Opas, A.; Tewtrakul, S.; Hoong-Kun, F. 2012. Potential anti-inflammatory diterpenes from *Premna obtusifolia*, *Tetrahedron*, 68, 819–829.

Proceedings

Salae, A. W.; Karalai, C.; Ponglimanont, 2008. Chemical constituents from the roots of *Diospyros wallichii*. The 6th Regional IMT-GT UNINET Conference. The Gurney Resort Hotel & Residences, Penang, Malaysia. 28-30 August 2008. (oral presentation)

- Salae, A. W.;** Karalai, C.; Ponglimanont, 2008. "Naphthoquinones and lupine-type triterpenoids from the roots of *Diospyros wallichii*". The 34th Congress on Science and Technology of Thailand, Queen Sirikit National Convention Center, Bangkok, Thailand, October 31- November 2, 2008. (poster presentation)
- Salae, A. W.;** Karalai, C.; Ponglimanont, 2009. "Chemical constituents from the roots of *Diospyros wallichii*", PERCH Conference VI. Jomtein Palm Beach Resort, Pattaya, Chonburi, Thailand, 3-6 May, 2009. (poster presentation)
- Salae, A. W.;** Karalai, C.; Ponglimanont, 2011. "Diterpenoids from the roots of *Premna obtusifolia*", PERCH Conference VII. Jomtein Palm Beach Resort, Pattaya, Chonburi, Thailand, 4-7 May, 2011. (poster presentation)